TUBERCULOSIS AND NON-TUBERCULOUS MYCOBACTERIA INFECTIONS: CONTROL, DIAGNOSIS AND TREATMENT

EDITED BY: Onya Opota, Emmanuelle Cambau, Delia Goletti, Jesica Mazza-Stalder, Miguel Viveiros and Miguel Santin

PUBLISHED IN: Frontiers in Microbiology, Frontiers in Public Health and Frontiers in Medicine

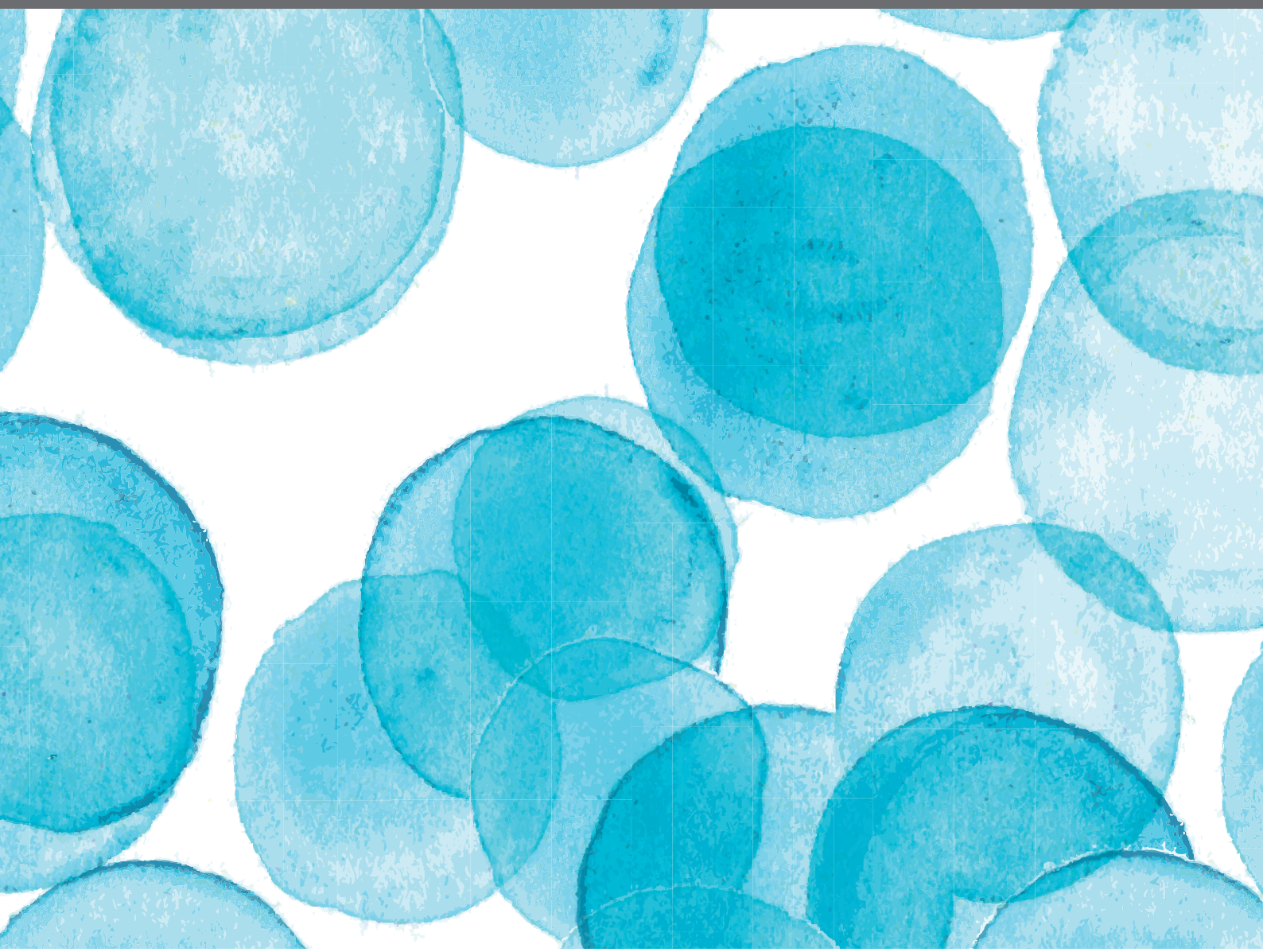

frontiers Research Topics

frontiers

ISSN 1664-8714
ISBN 978-2-88971-904-4
DOI 10.3389/978-2-88971-904-4

About Frontiers

Frontiers is more than just an open-access publisher of scholarly articles: it is a pioneering approach to the world of academia, radically improving the way scholarly research is managed. The grand vision of Frontiers is a world where all people have an equal opportunity to seek, share and generate knowledge. Frontiers provides immediate and permanent online open access to all its publications, but this alone is not enough to realize our grand goals.

Frontiers Journal Series

The Frontiers Journal Series is a multi-tier and interdisciplinary set of open-access, online journals, promising a paradigm shift from the current review, selection and dissemination processes in academic publishing. All Frontiers journals are driven by researchers for researchers; therefore, they constitute a service to the scholarly community. At the same time, the Frontiers Journal Series operates on a revolutionary invention, the tiered publishing system, initially addressing specific communities of scholars, and gradually climbing up to broader public understanding, thus serving the interests of the lay society, too.

Dedication to Quality

Each Frontiers article is a landmark of the highest quality, thanks to genuinely collaborative interactions between authors and review editors, who include some of the world's best academicians. Research must be certified by peers before entering a stream of knowledge that may eventually reach the public - and shape society; therefore, Frontiers only applies the most rigorous and unbiased reviews.
Frontiers revolutionizes research publishing by freely delivering the most outstanding research, evaluated with no bias from both the academic and social point of view. By applying the most advanced information technologies, Frontiers is catapulting scholarly publishing into a new generation.

What are Frontiers Research Topics?

Frontiers Research Topics are very popular trademarks of the Frontiers Journals Series: they are collections of at least ten articles, all centered on a particular subject. With their unique mix of varied contributions from Original Research to Review Articles, Frontiers Research Topics unify the most influential researchers, the latest key findings and historical advances in a hot research area! Find out more on how to host your own Frontiers Research Topic or contribute to one as an author by contacting the Frontiers Editorial Office: frontiersin.org/about/contact

TUBERCULOSIS AND NON-TUBERCULOUS MYCOBACTERIA INFECTIONS: CONTROL, DIAGNOSIS AND TREATMENT

Topic Editors:
Onya Opota, University of Lausanne, Switzerland
Emmanuelle Cambau, Hôpital Lariboisière, France
Delia Goletti, National Institute for Infectious Diseases Lazzaro Spallanzani (IRCCS), Italy
Jesica Mazza-Stalder, Centre Hospitalier Universitaire Vaudois (CHUV), Switzerland
Miguel Viveiros, New University of Lisbon, Portugal
Miguel Santin, Bellvitge University Hospital, Spain

Citation: Opota, O., Cambau, E., Goletti, D., Mazza-Stalder, J., Viveiros, M., Santin, M., eds. (2021). Tuberculosis and Non-Tuberculous Mycobacteria Infections: Control, Diagnosis and Treatment. Lausanne: Frontiers Media SA. doi: 10.3389/978-2-88971-904-4

Table of Contents

frontiers in Public Health

EDITORIAL
published: 28 October 2021
doi: 10.3389/fpubh.2021.666187

Editorial: Tuberculosis and Non-tuberculous Mycobacteria Infections: Control, Diagnosis and Treatment

Onya Opota[1]*, *Jesica Mazza-Stalder*[2], *Miguel Viveiros*[3], *Emmanuelle Cambau*[4], *Miguel Santin*[5] *and Delia Goletti*[6]

[1] *Institute of Microbiology, University of Lausanne and Lausanne University Hospital, Lausanne, Switzerland,* [2] *Respiratory Medicine Department, University of Lausanne and Lausanne University Hospital, Lausanne, Switzerland,* [3] *Global Health and Tropical Medicine, GHTM, Instituto de Higiene e Medicina Tropical, IHMT, Universidade Nova de Lisboa, UNL, Lisbon, Portugal,* [4] *UMR1147 IAME, Inserm, Université de Paris, APHP-GHU Nord, Service de Mycobactériologie Spécialisée et de Référence, Centre National de Référence des Mycobactéries et de la Résistance des Mycobactéries aux Antituberculeux (CNR-MyRMA), Paris, France,* [5] *Service of Infectious Diseases, Tuberculosis Unit, Bellvitge University Hospital-IDIBELL, University of Barcelona, Barcelona, Spain,* [6] *Translational Research Unit, National Institute for Infectious Diseases L. Spallanzani-IRCCS, Rome, Italy*

Keywords: ***Mycobacterium tuberculosis*, tuberculosis, multidrug resistant, whole genome sequencing, tuberculosis treatment, minimal inhibition concentration, microbiota, non-tuberculous mycobacteria**

OPEN ACCESS

Edited by:
Marc Jean Struelens, Université libre de Bruxelles, Belgium

Reviewed by:
Vanessa Mathys, Sciensano, Belgium

***Correspondence:**
Onya Opota
onya.opota@chuv.ch

Specialty section:
This article was submitted to Infectious Diseases - Surveillance, Prevention and Treatment, a section of the journal Frontiers in Public Health

Received: *09 February 2021*
Accepted: *29 September 2021*
Published: *28 October 2021*

Citation:
Opota O, Mazza-Stalder J, Viveiros M, Cambau E, Santin M and Goletti D (2021) Editorial: Tuberculosis and Non-tuberculous Mycobacteria Infections: Control, Diagnosis and Treatment. Front. Public Health 9:666187. doi: 10.3389/fpubh.2021.666187

Editorial on the Research Topic

Tuberculosis and Non-tuberculous Mycobacteria Infections: Control, Diagnosis and Treatment

Tuberculosis (TB), is one of the top 10 causes of death worldwide (WHO). According to the last Global TB report from the World Health Organization, 10 million persons were estimated to have had TB in 2019 worldwide, causing about 1.6 million deaths. Tuberculosis has not only a dramatic impact on the quality of life for the patients, but also has raised many socio-economic issues at a community level, especially in medium and high burden regions, such as India, China, and Indonesia.

In 2014, WHO adopted the "End TB strategy" which aimed to reduce TB deaths by 90% between 2015 and 2030, to prevent new cases by 80% during the same period and to decrease the socio-economic impact of the disease at a family level. Even though tuberculosis global incidence has decreased significantly, efforts still need to be made to reach these goals.

Non-tuberculous mycobacteria (NTM), in contrast to *Mycobacterium tuberculosis*, are bacteria widely spread in the environment and can be found in a broad range of ecosystems such as soils and water, including drinking water systems. NTM are opportunistic pathogens associated with both pulmonary and extrapulmonary infections.

This Research Topic collected articles addressing: (i) TB and NTMs associated diseases, diagnostic, control, and public health, (ii) mycobacterial genomics, (iii) and antimycobacterial drugs and resistance.

Efforts have been made to present the latest technical and scientific approaches for resistance prediction and mutation ranking in *M. tuberculosis*. This included the use of multi-label random forest models from whole genome sequences to rank and identify important mutations for better prediction of first-line drugs resistance (Kouchaki et al.). According to the major advances achieved in the last years, diagnostic and epidemiological approaches based on genomics have dramatically

increased. Whole genome sequencing (WGS) is widely used to identify clusters of transmission of *M. tuberculosis* in different settings like in Ghana, where WGS analysis was used to resolve clusters and explored the spatial distribution of confirmed recent transmission events (Asare et al.). WGS was useful in detecting unsuspected outbreaks as well as to better understand the dynamic of *M. tuberculosis* lineages (Outhred et al.). Different approaches are now available for rapid and accurate drug susceptibility testing including phenotypic and molecular methods based on DNA sequencing. This latter approach has shown its added value for early identification of resistance to anti-TB drugs, including ethambutol (Li et al.; Wan et al.).

Finally, the study of *M. tuberculosis* wild-type MIC distributions addressed the possibility of re-evaluating the critical concentration of anti-TB drugs and pharmacodynamics or optimizing the drug dosage (Dusthackeer et al.). In the endeavor of TB treatment and anti-TB drugs discovery, a new competitive inhibitor of D-alanine–D-alanine ligase A (DdlA) (IMB-0283) that is more potent than the classical D-cycloserine (DCS) has been identified *via* high-throughput screening (Meng et al.). The MIC of IMB-0283 for the standard and clinical drug-resistant *M. tuberculosis* strains ranged from 0.25 to 4.00 μg/mL, whereas that of DCS was 16 μg/mL. This new inhibitor revealed to have lower cytotoxicity and to be more efficacious *in vivo* than DCS, a still important second line antituberculosis drug. Alongside, and in view of the urgent need of more efficacious and less toxic second line antituberculosis drugs, the potential of the recently described cephalosporins, selectively active against non-replicating *Mycobacterium tuberculosis* forms, has been reported. Using alkyne analogs of these cephalosporins and an activity-based protein profiling, over 30 new protein binders were identified related to mycobacterial survival in a non-replicative state and inhibiting the cell by collective action on multiple targets (Lopez Quezada et al.). Improvement of anti-TB regimen, including regimen for the treatment of multidrug-resistant tuberculosis is paramount as such treatment have been shown to have long-term effects on gut microbiota (Wang et al.).

Regarding the treatment of NTM infections, a retrospective analysis focusing on *Mycobacterium abscessus* pulmonary infection reported that among 244 patients, only 110 patients met the criteria for treatment, and the outcomes of treatment were mostly unsatisfactory, particularly among patients suffering from *Mycobacterium abscessus subsp. abscessus* lung disease (Chen et al.). The administration of amikacin, imipenem, linezolid, and tigecycline correlated with increased treatment success. Genomics were also now established as a powerful tool to refine and complete the systematics and classification of NTMs as shown for the *M. kansasii* complex and subtypes reclassified using a three-pronged computational strategy based on the alignment fraction-average nucleotide identity, genome-to-genome distance, and core-genome phylogeny combined with five canonical taxonomic markers (16S rRNA, *hsp*65, *rpo*B, *tuf* genes, and 16S-23S rRNA intergenic spacer region; Jagielski et al.). A study on another clinical important NTM, the *M. avium* complex (MAC) determined the impact of using two different culture media used for MAC drug susceptibility testing. MIC determination using the microdilution method for antibiotics used in the treatment of MAC infections has a clear clinical relevance and accuracy for determining the resistance levels of this important group of NTM (Jaffré et al.). The raise of the medical importance of NTM due to the increasing number of immune-compromised hosts (solid organ transplant recipients and oncologic patients among others) highlighted the importance of a better understanding of the source of contamination and measures to reduce exposure to these sources (Norton et al.; Lecorche et al.).

Major advances have been made in the field of TB and NTM relying on many new technological opportunities, new approaches and new paradigms. This led to a better understanding of these pathogens as well as in improvement of patients care and disease control. Regarding patients care, the importance of multidisciplinary approaches taking into account medico-socio-economic considerations was highlighted (Mazza-Stalder et al.; Pujol-Cruells and Vilaplana). Interestingly, this Research Topic also highlighted the inhomogeneity of practices among Europe for the management of TB (Méchaï et al.). Efforts need to be intensified in parallel with increased translational collaboration to guarantee the application and rapid sharing of new discoveries.

AUTHOR CONTRIBUTIONS

OO, JM-S, MV, EC, MS, and DG contributed to the redaction of the manuscript. All authors contributed to the article and approved the submitted version.

ACKNOWLEDGMENTS

The editors thank all the authors for the amazing work grouped in this Research Topic and all the scientists that achieved the reviewing of these manuscripts. The study was partially funded by the Italian Ministry of health, Ricerca corrente, linea 4.

Conflict of Interest: The authors declare that the research was conducted in the absence of any commercial or financial relationships that could be construed as a potential conflict of interest.

Publisher's Note: All claims expressed in this article are solely those of the authors and do not necessarily represent those of their affiliated organizations, or those of the publisher, the editors and the reviewers. Any product that may be evaluated in this article, or claim that may be made by its manufacturer, is not guaranteed or endorsed by the publisher.

frontiers in Medicine

ORIGINAL RESEARCH
published: 21 June 2019
doi: 10.3389/fmed.2019.00135

Improvement in Tuberculosis Outcomes With a Combined Medical and Social Approach

Jesica Mazza-Stalder[1,2], Emilie Chevallier[1], Onya Opota[3], Ana Carreira[1], Katia Jaton[3], Eric Masserey[4], Jean Pierre Zellweger[5] and Laurent Pierre Nicod[1]*

[1] Pulmonary Division, Lausanne University Hospital, University of Lausanne, Lausanne, Switzerland, [2] Vaud Lung Association, Lausanne, Switzerland, [3] Institute of Microbiology, Lausanne University Hospital, University of Lausanne, Lausanne, Switzerland, [4] Public Health Department, Lausanne, Switzerland, [5] Swiss Lung Association, TB Competence Center, Bern, Switzerland

Setting: Studies performed locally in Switzerland in the late eighties reported unsatisfactory treatment outcomes. Better outcomes were observed since the introduction of directly observed therapy (DOT) in the late nineties and improvement in social support in recent years.

Design: retrospective study of treatment outcomes for all tuberculosis (TB) patients notified in Vaud County (VD), Switzerland, between, 1st of January 2010 and 31st of December of 2014.

Results: 375 patients were notified in VD during the study period. The global outcome was successful in 90.1% of patients (338/375). In 183 culture and PCR positive pulmonary TB, the documented cure rate was 57.9% (106/183), and the treatment completion was 59/183 (32.2%), i.e., a treatment success of 90.2%. DOT was applied globally in 234/375 (62.4%) and in 64/67 of the asylum seekers (AS) (95.5%) followed at the dispensary. Treatment outcomes were successful in 60/67 (89.6%) AS.

Discussion: Improvements in tuberculosis outcomes resulted not only from the introduction of DOT in VD in the nineties but also from a change in the management, with increased attention to the social problems faced by the migrants.

Conclusion: A combined medical and social approach of TB care in VD improved treatment outcomes.

Keywords: tuberculosis outcomes, treatment adherence, tuberculosis in Switzerland, directly-observed therapy, tuberculosis social approach

OPEN ACCESS

Edited by:
Konrad E. Bloch, University Hospital Zürich, Switzerland

Reviewed by:
Otto Dagobert Schoch, Kantonsspital St. Gallen, Switzerland
Carolin Steinack, University Hospital Zürich, Switzerland

****Correspondence:***
Jesica Mazza-Stalder
jesica.mazza-stalder@chuv.ch

Specialty section:
This article was submitted to Pulmonary Medicine, a section of the journal Frontiers in Medicine

Received: *06 December 2018*
Accepted: *30 May 2019*
Published: *21 June 2019*

Citation:
Mazza-Stalder J, Chevallier E, Opota O, Carreira A, Jaton K, Masserey E, Zellweger JP and Nicod LP (2019) Improvement in Tuberculosis Outcomes With a Combined Medical and Social Approach. Front. Med. 6:135. doi: 10.3389/fmed.2019.00135

INTRODUCTION

In Switzerland in 2017, 554 cases of TB were notified to the Swiss Federal Office of Public Health (SFOPH), resulting in a notification rate of 6.5 cases per 100,000 population (1); this rate is fairly stable. Of these TB patients ∼23%, are from Swiss origin and around 77% are from foreign-origin, asylum seekers (AS) account for 34% of the foreign-born patients. Among others, the efficient management of TB, as detailed in the END TB strategy of the WHO, implies rapid diagnosis, high cure rate, and avoidance of failure, relapses, and interruptions before the scheduled end of treatment (2, 3). To guarantee that TB cases are rapidly diagnosed, access to health care must be

universally offered, and avoid stigmatization (4). Adherence is essential for treatment completion, TB prevention and care, and thus one of the major determinants of treatment outcomes (5). In Switzerland, studies performed in the late eighties described unsatisfactory treatment outcomes with a success rate in VD County not exceeding 70% in patients with complete documentation (63% if patients without documentation are included) (6). A countrywide survey revealed better results but confirmed that the success rate among some subgroups of foreign-born patients, for instance undocumented migrants, was below the expected range (7). Local studies demonstrated that the provision of directly observed therapy (DOT) and a better training of the health care workers caring for TB patients had an important impact on the cure rate. Since then, VD County invested more resources in the management of TB. Our aim is to present the integrated medical and social approach implemented in VD County for the management of TB, and the current outcomes.

METHODS

Description of the Cantonal Tuberculosis Health Care System

VD County has a population of 794,000 inhabitants with 33% of foreign-born residents and notifies around 65 cases of TB per year. TB patients are mostly followed by specialists at the TB clinic (TB dispensary or DAT) of the University Hospital of Lausanne. TB notification to the cantonal health authority is mandatory in Switzerland. The physician in charge of the patient declares the new TB cases to the Cantonal health officer who transfers the information to the SFOPH. Diagnostic laboratories, independently, also notify to the cantonal health authority all new strains of *M. tuberculosis* identified. The TB nurses from the Lung association (a Non Governmental Organisation caring for patients with chronic respiratory diseases) carry out contact investigations if ordered by the cantonal health officer. A medical advisor (a lung specialist) works at both the Lung association and the TB dispensary (DAT) and is available for questions regarding TB diagnosis, treatment, follow up, and contact tracing. Notification of the issue of treatment is requested by SFOPH since 2016 for all TB patients.

Study Population, Data Collection, and Ethics Approval

All TB patients notified in VD County between, 1st of January 2010 and 31st of December of 2014 were eligible for inclusion in our study. Patient's data were obtained using the VD Lung Association records and the electronic medical records at the DAT. A common excel table was elaborated to analyze the data. End of treatment notification results forms for pulmonary culture positive patient were obtained, missing information was obtained directly from medical doctors in charge of the patients (mostly lung or infectious disease specialists) or from the final reports on the electronic medical records of the Hospital. We collected data on age, nationality, type of TB (pulmonary [PTB] or extra-pulmonary [EPTB]), new or retreatment cases, legal resident status, tuberculosis resistance pattern, and follow-up 2 years after the end of treatment. Authorization was obtained from the Ethics Committee of VD County *(CER-VD 2017-02300)* to review the clinical records and publish the analyzed data. Written informed consent was not required. All patient identifiable information was anonymized.

Outcomes

Treatment outcomes were defined according to the WHO 2013 revised definitions (8). Successful outcomes included cure (documented with bacteriological conversion in culture positive pulmonary TB) and treatment completion (treatment completed without bacteriological confirmation). Unsatisfactory outcomes included treatment failure, lost to follow up and deaths (deaths due to TB or not due to TB). Potentially unsatisfactory outcomes included "transferred out" cases for whom the treatment outcome was unknown.

Microbiology

Acid fast bacilli detection was achieved through a fluorescent auramine-thiazine red staining according to international guidelines (9). Detection of *M. tuberculosis* complex was achieved either using a real-time PCR targeting the IS6110 on the molecular diagnostic platform of our laboratory of microbiology

TABLE 1 | Social enablers applied at the DAT to facilitate adherence.

Examples of enablers and incentives applied at the dispensary (DAT)
Improvements at the DAT
Increasing the number of nursing staff
Better training of the nurses (organized at a national level by the Swiss Lung Association)
Hiring a Social Worker (since 2011)
Close collaboration between the nurses of the Vaud Lung Association and the DAT
Extended opening hours at the DAT (Monday to Friday 8 to 18 h, weekend open pharmacy and lung specialist on call)
Missed appointments /Reschedule of appointments
Improvements in the patient's care
Increasing use of systematic DOT in migrants and vulnerable population
Working on psychosocial aspects in close collaboration with psychiatrics and social assistants if needed or centers for alcohol or drug abuse/combined Methadone with anti-tuberculous drugs in DOT
Facilitators of adherence (food vouchers, ticket transport or taxis when needed, closer housing, clothing when needed)
Patient education (explaining the disease and the improvement while on treatment, tobacco prevention, and intervention for smoking cessation)
Financial support (by the cantonal Public Health authorities) applied when necessary
Improvements in communication
Nurses speaking different languages/ Hiring translators
Empathy, skills in community medicine, addressing TB related-stigma issues, discussing fears of deportation, and reassuring the patients
Monthly team meetings regrouping nurses, lung and infectious disease specialists, cantonal medical officer, social assistant, health workers working at shelters for migrants
Avoidance of deportation while on treatment (paper work with cantonal and federal migration and following the national law on epidemics)

TABLE 2 | Patient's demographics.

	N	(%)
Gender		
Male	233	(62)
Female	142	(38)
Total	375	(100)
Origin		
Switzerland	87	(23.2)
Africa	99	(26.4)
Europe	61	(16.2)
Eastern Europe	59	(15.7)
Eastern Mediterranean	20	(5.3)
Americas	18	(4.8)
Southeast Asia	15	(4)
Western Pacific	10	(2.7)
Southwest Asia	5	(1.4)
Central Asia	1	(0.3)
Total	375	100

TABLE 3 | Sites of disease.

Site of disease	*N*	(%)
Pulmonary (PTB)	222	(59.2)
Extra-pulmonary (EPTB)	103	(27.4)
Both PTB+EPTB	50	(13.4)
Total	375	(100)
EPTB sites		
Extra thoracic lymph nodes	38	(24.8)
Pleural	37	(24.2)
Mediastinal lymph nodes	23	(15)
Disseminated	17	(11.2)
Bone and Spinal TB	16	(10.5)
Abdominal TB	6	(3.9)
Genitourinary tract	4	(2.6)
Cutaneous	4	(2.6)
SNC	4	(2.6)
Uveitis	2	(1.3)
Pharyngeal	2	(1.3)
Total	153	(100)

P, Pulmonary; EP, Extra pulmonary; TB, Tuberculosis.

(10) or using the Xpert MTB/RIF (11). Mycobacterial culture and drug susceptibility test for first-line drugs were achieved in Mycobacteria Growth Indicator Tube. Drug sensitivity testing for second-line anti-TB drugs for MDR- and XDR-TB was performed at the National Reference Center for Tuberculosis (Zurich, Switzerland).

Treatment Administration

Whenever possible, and at least for all patients recently arrived in Switzerland and during the intensive phase, the treatment was administered under DOT, supervised by nurses, be it by a daily visit to the DAT or to a pharmacy close to the living place or in the social environment of the patient. For well-integrated patients with stable living place and no risk of unexpected moving out of the region, the treatment during the continuation phase may have been under self-administration or by collecting the treatment in the pharmacy once a week (with a pill organizer).

TABLE 4 | Microbiological findings.

Microbiology	***N*/total**	(%)
Culture		
Positive (all included)	268/375	(71.5)
Negative (all included)	94/375	(25)
Not done	11/375	(2.9)
Unknown	2/375	(0.6)
Culture and/or PCR		
Positive (all included)	281/375	(74.9)
Positive PTB	183/222	(82.4)
Positive PTB + EPTB	41/50	(82)
Positive EPTB (only)	80/103	(77.7)
Negative PTB	94/375	(25.1)
Negative EPTB	23/103	(22.3)
Negative PTB+EPTB	9/50	(18)

TB, Tuberculosis; P, Pulmonary; EP, Extra-pulmonary.

Social Support

Every patient with TB diagnosed in the County received a visit from a social worker during the isolation in hospital or within the first 2 weeks of treatment if the patient was at home. Enablers to adherence such as psychosocial, social or financial support were deployed when appropriate as suggested by European standards of tuberculosis care (12–14). Housing closer to the hospital was whenever possible obtained thanks to the networking between the social services and the different structures that provide housing for migrants (15). Interventions to assist and motivate the patients such as providing extra food vouchers, clothes or assistance to travel, were offered, when necessary. Missed appointments were re-scheduled systematically to avoid interruptions while on treatment as proposed by others (16). In case of drug dependency, methadone programs were combined together with TB treatment and DOT (17). Patients missing one DOT appointment received a telephone call or a reminder letter in order to re-establish contact with the TB clinic. To exchange information on DOT, contact tracing, social and financial enablers to improve treatment adherence, we organized monthly meetings with all the different actors of TB care. Enablers and facilitators of treatment adherence are listed in **Table 1**.

RESULTS

Between January 2010 and December 2014, 375 patients were notified in VD, with a male predominance of 62.1%. The mean age was 38 years (range 1–98) for the whole group and 67 years (3–98) in Swiss patients. There were 288 foreign-born

patients (77%) mainly Africans (26.4%), Western Europeans (16.2%), Eastern Europeans (15.7%), and 87 Swiss patients. TB was diagnosed for the first time in 269 patients (72%), 44 patients (12%) had been treated previously and no information on previous treatment was available for 62 patients (17%). Pulmonary tuberculosis (PTB) alone affected 222 patients (59.2%), extra-pulmonary-TB (EPTB) was diagnosed in 103 patients (27. 4%), and both PTB and EPTB was diagnosed in 50 patients (13.4%). Detailed patient's characteristics is reported in **Table 2** and sites of disease (PTB and EPTB) in **Table 3**.

Microbiological Findings

Cultures were performed in 362 patients (96.5%), not done in 11 patients (3%), and information was missing for 2 patients (0.5%). Among all patients (PTB+ EPTB) culture was positive in 268/375 (71.5%). In patients with PTB only the culture and/or PCR was positive in 183/222 (82.4%) and for EPTB only patients we obtained 80/103 (77.6%) positive samples. We excluded from the analysis the culture positive among the group of PTB+EPTB ($n = 41$) because we couldn't differentiate the site from which the culture was positive. Among all the TB strains, 265 were *M. tuberculosis* (98.9%) and 3 were *M. bovis* (1.1%). Complete microbiological data is reported in **Table 4**.

Treatment Outcomes

Globally, treatment was successfully completed in 338 patients (90.1%). Among 183 patients with culture or PCR positive PTB (excluding PTB+EPTB), including 10 MDR-TB, the documented cure rate was 106 (57.9%) and the treatment completion was 59 (32.2%), i.e., a global treatment success of 90.2% ($n = 165$). Among 50 patients with PTB+EPTB tuberculosis, the outcome was successful in 44 (88%). Among 103 patients with EPTB, the treatment completion was 95 (92.2%) (**Figure 1**).

Overall (PTB+EPTB) treatment success among all AS was 79/89 (87.6%). Most AS in VD County were treated at the DAT 67/89 (75.2%) 95.5% of them on DOT (64/67) with a treatment success of 60/67 (89.6%). DOT was applied in 234/375 (62.4%) of our entire study population. We observed no treatment failure. However, 19 patients had unsatisfactory outcomes (5.1%) and 18 potentially unsatisfactory outcomes (4.8%). Among these, we counted 7 persons lost to follow up (1.8%), 12 deaths (3.2%), and 18 transfers while on treatment (4.8%) (**Table 5**). Within the lost to follow up we counted 7 patients that were part of a very mobile population including 5 AS (2 Georgians, 3 Africans) and 2 foreign-born Europeans (Romanians). Among the 12 that died, 6 died from TB, and 6 died due to comorbidities. Among them 10 patients were Swiss (mean age 69 (49–89), the other two were foreign-born (mean age 52 (23–80). The 23-year-old patient that died while on treatment was an XDR-TB patient who died for causes other than TB. In two elderly Swiss patients (mean age 85) TB was not suspected before death and was diagnosed and notified only after an autopsy. Transmission of TB to health care workers occurred from these 2 undiagnosed patients, one to a nurse and one to a pathologist. Treatment outcomes in DOT vs non DOT is shown in **Table 6**. Outcomes by categories are shown in **Table 7**.

Follow-Up Visits After Treatment

We followed 178 patients for up to 2 years, 84.2% of these patients were followed at the DAT or at the university hospital in other units (pediatrics and infectious diseases). Relapses were observed

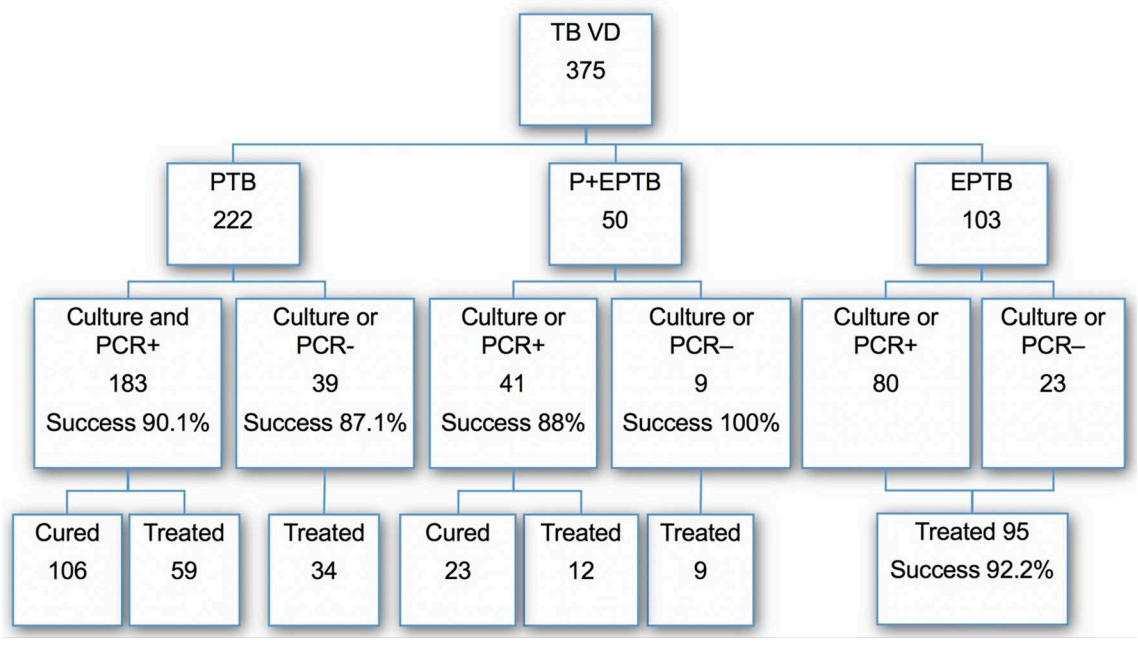

FIGURE 1 | Distribution of TB cases, bacteriological results, and outcome of treatment in each category.

in 2 patients, both during the first year after the end of treatment. No relapse was observed after the first year.

DISCUSSION

This retrospective study assessed TB treatment outcomes among patients in VD County during the period 2010–2014, and showed a global success rate of 90.1%. In culture positive pulmonary patients, the cure rate was similar (90.2%). Our success rate is comparable to studies performed at our institution after the implementation of DOT in the late nineties (88.9%) and with publications from St. Gallen in eastern Switzerland (87.5%) (18, 19). Our results are much superior to the historical results of 70% of treatment outcomes previously published by our own institution by Coulon et al. (6). In this study, and other local studies (20) treatment interruptions were more common among migrants and vulnerable populations because of change in place of living, deportation out of the country or disappearance in illegality for migrants not granted refugee status, and because of a high rate of non-adherence despite good access to health care in Switzerland. Adherence is one of the major determinants of treatment success (5). Among the measures considered for improving the adherence to TB therapy and the cure rate, the DOT is considered as one of the most crucial, since the seminal publication by Weis demonstrating that DOT contributed to the decrease in relapse and acquisition of drug resistance (21). Further studies supported the role of DOT as a method for improving the success rate of TB treatment (22). Recently, several other studies and analysis have questioned this dogma and demonstrated that DOT may not be the only element of success in TB treatment, but that the whole organization of patient care is contributing to the success (23, 24). The experience in our institution seems to confirm this, as the improvement in the cure rate resulted not only from the introduction of DOT in Lausanne in the nineties but also from a change in the management, with better training of specialized nurses, improvements in communication by hiring translators, re-organization of the appointment schedules, and above all increasing the attention to the social problems faced by the migrants and vulnerable populations (19). Indeed, since the nineties, a reinforcement of the existing personnel at the TB clinic was assured in VD County with extended opening hours as recommended in treatment guidelines (14, 25) and the social aspects were better considered with the inclusion of a social worker in the staff. Since most of the treatment interruptions in the late eighties occurred among AS followed outside the TB clinic by general practitioners lacking the necessary structure to take care of difficult social situations, in later years, we tried to follow this particularly vulnerable population at the DAT. We found that 75.2% of the AS were followed at the DAT and a DOT strategy was applied in 95.5% of them. Among the entire study population DOT was applied in 62.4%. As other programs showed before, we found that regulatory interventions (search for missing patient by police order) were rarely needed and were only applied in case of disappearance of infectious patients (26). Furthermore, thanks to an agreement between the SFOPH and the State Secretariat for Migration, migrants with TB, even those who are not granted asylum status, are no longer deported from the country during the treatment against their will, thus avoiding disappearance in illegality and treatment interruptions.

Like other groups we observed diagnostics delay among elderly people. Most of the deaths were among Swiss elderly patients. Atypical forms of Tb presentation among older patients and lack of suspicion of TB by doctors in elderly patients are well known (27). Diagnostic TB delays has been confirmed by a recent study conducted in Switzerland (28). In our study 2 very old Swiss patients (mean age 85) living in nursing

TABLE 5 | Treatment outcomes.

Outcomes	N/total	(%)
Successful outcomes	338/375	(90.1)
Successful (overall PTB+EPTB)	338/375	(90.1)
Successful outcomes in culture or PCR positive PTB	165/183	(92.2)
Cured only PTB culture and/or PCR positive	106/183	(59.9)
Completed without bacteriological confirmation (PTB)	59/183	(32.2)
Successful outcomes in EPTB (completed)	95/103	(90.2)
Successful outcomes in AS (all included)	79/89	(88.8)
Successful outcomes in AS follow at DAT	60/67	(89.6)
Successful outcomes (PTB+EPTB) in Swiss patients	76/87	(87.3)
Unsuccessful Outcomes	19/375	(5.1)
Lost to follow-up	7/375	(1.8)
Failure	0/375	(0)
Deaths	12/375	(3.2)
Causes of death		
Deaths due to TB	12/6	(50)
Deaths due to causes other than TB (comorbidities)	12/6	(50)
Deaths in Swiss patients	12/10	(83.3)
Death in foreign patients	10/2	(16.7)
List of comorbidities		
Chronic Obstructive Pulmonary Disease	6/1	(16.6)
Heart failure	6/1	(16.6)
Immunosuppression/HIV	6/1	(16.6)
Immunosuppression /Anti-TNF therapy	6/1	(16.6)
Malignancy	6/2	(33.6)
Potentially unsuccessful outcomes	18/375	(4.8)
Transfer-out without knowledge of outcome	18/375	(4.8)

Tt, Treatment; TB, tuberculosis; P, pulmonary; EP, extra-pulmonary; AS, Asylum seekers.

TABLE 6 | Outcomes DOT vs. no DOT.

Outcome	DOT ($n = 234$)	No DOT ($n = 141$)	Total DOT + no DOT ($n = 375$)
Cured	117	25	142
Treatment completed	104	92	196
Successful	221 (94.4%)	117 (82.9%)	338 (90.1%)
Transfer	8	10	18
Death	2	10	12
Lost to follow-up	3	4	7

TABLE 7 | Outcomes by categories.

Outcome	Female gender	Male gender	Mean age	PTB	P+EPTB	EPTB	Both (P+EP)	Swiss origin	Foreign -born	Asylum seekers
Treatment success	134 (94%)	204 (87.5%)	42.0	199 (89.6%)	44 (88%)	95 (97%)	338 (90.1%)	76 (87.3%)	262 (90.9%)	79/89 (89%)
Unsuccessful treatment	8 (6%)	29 (12.5%)	49.8	23 (10.4%)	6 (12%)	8 (3%)	37 (9.9%)	11 (12.7%)	26 (9.1%)	10/89 (11%)
Total	142	233	–	222	50	103	375	87	288	89

homes were only diagnosed after death (autopsy). This finding underlines, as described by others, a real underappreciated problem with undiagnosed TB cases among older people with potential transmission in the community and particularly to health care workers (29).

Relapses were rare in our study group with only 2 patients in the year following the end of treatment.

This retrospective study has limitations, as we could not analyze prospectively if the improvements of outcomes and adherence were due to the health care and social interventions deployed among the most vulnerable populations. Another limitation of this study is that we described an observational cohort from a single center in comparison with a historical cohort only but without a control group, and that the role of each different components that helped improving the tuberculosis care (DOT vs. social support) could not be assessed properly in a prospective way. The strengths are the relatively high number of patients included in the analysis, the quality control of the daily work in the center and the good treatment outcomes obtained.

In summary, this study shows an improvement in treatment outcomes in VD County with a global success rate of 90.1% overpassing the expectations of 85% requested by the WHO. The patient-centered approach of TB care in VD County provides social protection with a high-quality standard of TB care and a scale-up compared to previous published outcomes.

ETHICS STATEMENT

Commission cantonale d'Ethique sur la Recherche sur l'ê tre humain. CER-VD Project Number 2017-02300.

AUTHOR CONTRIBUTIONS

JM-S: design of the study, data collection and analysis, manuscript redaction. EC: data collection, manuscript revision. OO and JZ: data analysis and manuscript revision. KJ, EM, and LN: manuscript revision. All authors listed have made a substantial, direct and intellectual contribution to the work, and approved it for publication.

ACKNOWLEDGMENTS

We thank particularly the nurses of the Lung Association of VD County, the nurses and social worker of the DAT and the members of the Laboratory of Molecular Diagnostic and Tuberculosis of the Lausanne University Hospital.

REFERENCES

1. *Tuberculosis in Switzerland-Revised Edition*. (2019). Available online at: https://www.tbinfo.ch/fileadmin/user_upload/1wissenszentrum/Publikationen/Handbuch_Tuberkulose/Handbuch_TB_FR_29_03_19.pdf
2. Lonnroth K, Migliori GB, Abubakar I, D'Ambrosio L, de Vries G, Diel R, et al. Towards tuberculosis elimination: an action framework for low-incidence countries. *Eur Respir J.* (2015) 45:928–52. doi: 10.1183/09031936.00214014
3. Uplekar M, Weil D, Lonnroth K, Jaramillo E, Lienhardt C, Dias HM, et al. WHO's new end TB strategy. *Lancet.* (2015) 385:1799–801. doi: 10.1016/S0140-6736(15)60570-0
4. Lonnroth K, Mor Z, Erkens C, Bruchfeld J, Nathavitharana RR, van der Werf MJ, Lange C, Tuberculosis in migrants in low-incidence countries: epidemiology and intervention entry points. *Int J Tuberc Lung Dis.* (2017) 21:624–37. doi: 10.5588/ijtld.16.0845
5. Sumartojo E, When tuberculosis treatment fails. A social behavioral account of patient adherence. *Am Rev Respir Dis.* (1993) 147:1311–20. doi: 10.1164/ajrccm/147.5.1311
6. Zellweger JP, Coulon P, Outcome of patients treated for tuberculosis in Vaud County, Switzerland. *Int J Tuberc Lung Dis.* (1998) 2:372–7.
7. Helbling P, Medinger C, Altpeter E, Raeber PA, Beeli D, Zellweger JP. Outcome of treatment of pulmonary tuberculosis in Switzerland in 1996. *Swiss Med Wkly.* (2002) 132:517–22. Available online at: https://smw.ch_2002_10045
8. World Health Organization. *Definitions and Reporting Framework for Tuberculosis-—2013 Revision*, Geneva (2013).
9. International Union Against Tuberculosis and Lung Disease. *International Union Against Tuberculosis and Lung Disease*. Technical guide: Sputum examination for tuberculosis by direct microscopy in low-income countries (2000). Available online at: https://www.medbox.org/laboratory-technologies/technical-guide-sputum-examination-for-tuberculosis-by-direct-microscopy-in-low-income-countries/preview?q=
10. Greub G, Sahli R, Brouillet R, Jaton K. Ten years of R&D and full automation in molecular diagnosis. *Future Microbiol.* (2016) 11:403–25. doi: 10.2217/fmb.15.152
11. Opota O, Senn L, Prod'hom G, Mazza-Stalder J, Tissot F, Greub G, et al. Added value of molecular assay Xpert MTB/RIF compared to sputum smear microscopy to assess the risk of tuberculosis transmission in a low-prevalence country. *Clin Microbiol Infect.* (2016) 22:613–9. doi: 10.1016/j.cmi.2016.04.010
12. Volmink J, Matchaba P, Garner P. Directly observed therapy and treatment adherence. *Lancet.* (2000) 355:1345–50. doi: 10.1016/S0140-6736(00)02124-3
13. Munro SA, Lewin SA, Smith HJ, Engel ME, Fretheim A, Volmink J. Patient adherence to tuberculosis treatment: a systematic review of qualitative research. *PLoS Med.* (2007) 4: e238. doi: 10.1371/journal.pmed.0040238
14. Migliori GB, Zellweger JP, Abubakar I, Ibraim E, Caminero JA, De Vries G, et al. European union standards for tuberculosis care. *Eur Respir J.* (2012) 39:807–19. doi: 10.1183/09031936.00203811
15. Nahid P, Dorman SE, Alipanah N, Barry PM, Brozek JL, Cattamanchi A, et al. Official American thoracic society/centers for disease control and

prevention/infectious diseases society of America clinical practice guidelines: treatment of drug-susceptible tuberculosis. *Clin Infect Dis.* (2016) 63:e147–95. doi: 10.1093/cid/ciw376
16. Lutge EE, Wiysonge CS, Knight SE, Volmink J. Material incentives and enablers in the management of tuberculosis. *Cochrane Database Syst Rev.* (2012) 1:CD007952. doi: 10.1002/14651858.CD007952.pub2
17. Morozova O, Dvoryak S, Altice FL. Methadone treatment improves tuberculosis treatment among hospitalized opioid dependent patients in Ukraine. *Int J Drug Policy.* (2013) 24:e91–8. doi: 10.1016/j.drugpo.2013.09.001
18. Guglielmi S, Barben J, Horn L, Schoch OD. Administrative monitoring of tuberculosis treatment in Switzerland. *Int J Tuberc Lung Dis.* (2006) 10:1236–40.
19. Deruaz J, Zellweger JP. Directly observed therapy for tuberculosis in a low prevalence region: first experience at the Tuberculosis Dispensary in Lausanne. *Swiss Med Wkly*. (2004) 134:552–8. doi: 10.4414/smw.2004.10643
20. Rose N, Shang H, Pfyffer GE, Brandli O. [Tuberculosis therapy in canton Zurich 1991–1993: what are the causes for recurrence and therapy failure?]. *Schweiz Med Wochenschr*. (1996) 126:2059–67.
21. Weis SE, Slocum PC, Blais FX, King B, Nunn M, Matney B, et al. The effect of directly observed therapy on the rates of drug resistance and relapse in tuberculosis. *N Engl J Med.* (1994) 330:1179–84. doi: 10.1056/NEJM199404283301702
22. Moonan PK, Quitugua TN, Pogoda JM, Woo G, Drewyer G, Sahbazian B, et al. Does directly observed therapy (DOT) reduce drug resistant tuberculosis? *BMC Public Health.* (2011) 11:19. doi: 10.1186/1471-2458-11-19
23. Volmink J, Garner P. Directly observed therapy for treating tuberculosis. *Cochr Database Systemat Rev*. (2007) 4:CD003343. doi: 10.1002/14651858.CD003343.pub3
24. Pasipanodya JG, Gumbo T. A meta-analysis of self-administered vs. directly observed therapy effect on microbiologic failure, relapse, and acquired drug resistance in tuberculosis patients. *Clin Infect Dis.* (2013) 57:21–31. doi: 10.1093/cid/cit167
25. Garner P, Smith H, Munro S, Volmink J. Promoting adherence to tuberculosis treatment. *Bull World Health Organ.* (2007) 85:404–6. doi: 10.2471/BLT.06.035568
26. Gasner MR, Maw KL, Feldman GE, Fujiwara PI, Frieden TR. The use of legal action in New York City to ensure treatment of tuberculosis. *N Engl J Med.* (1999) 340:359–66. doi: 10.1056/NEJM199902043400506
27. Rajagopalan S. Tuberculosis and aging: a global health problem. *Clin Infect Dis.* (2001) 33:1034–9. doi: 10.1086/322671
28. Christian Auer SK, Zuske M, Schindler C, Wyss K, Blum J, Bosch-Capblanch X, et al. Health-seeking behaviour and treatment delay in patients with pulmonary tuberculosis in Switzerland: some slip through the net. *Swiss Med Wkly.* (2018) 148:w14659. doi: 10.4414/smw.2018.14659
29. Rieder HL, Kelly GD, Bloch AB, Cauthen GM, Snider DE Jr. Tuberculosis diagnosed at death in the United States. *Chest.* (1991) 100:678–81. doi: 10.1378/chest.100.3.678

Conflict of Interest Statement: The authors declare that the research was conducted in the absence of any commercial or financial relationships that could be construed as a potential conflict of interest.

frontiers in Microbiology

ORIGINAL RESEARCH
published: 23 August 2019
doi: 10.3389/fmicb.2019.01977

Clinical Efficacy and Adverse Effects of Antibiotics Used to Treat *Mycobacterium abscessus* Pulmonary Disease

Jianhui Chen[1,2†], Lan Zhao[1†], Yanhua Mao[1†], Meiping Ye[1], Qi Guo[1,2], Yongjie Zhang[1,2], Liyun Xu[1], Zhemin Zhang[1], Bing Li[1] and Haiqing Chu[1,3*]*

[1] Department of Respiratory Medicine, Shanghai Pulmonary Hospital, Tongji University School of Medicine, Shanghai, China, [2] Tongji University School of Medicine, Shanghai, China, [3] Shanghai Key Laboratory of Tuberculosis, Shanghai Pulmonary Hospital, Tongji University School of Medicine, Shanghai, China

OPEN ACCESS

Edited by:
Jesica Mazza-Stalder, Lausanne University Hospital (CHUV), Switzerland

Reviewed by:
Oriol Manuel, Lausanne University Hospital (CHUV), Switzerland
Amit Kaushik, Johns Hopkins University, United States

***Correspondence:**
Bing Li
libing044162@163.com
Haiqing Chu
chu_haiqing@126.com

[†] These authors have contributed equally to this work

Specialty section:
This article was submitted to Antimicrobials, Resistance and Chemotherapy, a section of the journal Frontiers in Microbiology

Received: 19 May 2019
Accepted: 12 August 2019
Published: 23 August 2019

Citation:
Chen J, Zhao L, Mao Y, Ye M, Guo Q, Zhang Y, Xu L, Zhang Z, Li B and Chu H (2019) Clinical Efficacy and Adverse Effects of Antibiotics Used to Treat Mycobacterium abscessus Pulmonary Disease. Front. Microbiol. 10:1977. doi: 10.3389/fmicb.2019.01977

Treatment of *Mycobacterium abscessus* pulmonary infection requires long-term administration of multiple antibiotics. Little is known, however, about the impact of each antibiotic on treatment outcomes. A retrospective analysis was conducted to evaluate the efficacy and adverse effects of antibiotics administered in 244 cases of *M. abscessus* pulmonary disease. Only 110 (45.1%) patients met the criteria for treatment success. The efficacy of treating *M. abscessus* pulmonary disease continues to be unsatisfactory especially for infections involving *M. abscessus* subsp. *abscessus*. Treatment with drug combinations that included amikacin [adjusted odds ratio (AOR), 3.275; 95% confidence interval (CI), 1.221–8.788], imipenem (AOR, 2.078; 95% CI, 1.151–3.753), linezolid (AOR, 2.231; 95% CI, 1.078–4.616), or tigecycline (AOR, 2.040; 95% CI, 1.079–3.857) was successful. Adverse side effects affected the majority of patients (192/244, 78.7%). Severe effects that resulted in treatment modification included: gastrointestinal distress (29/60, 48.3%) mostly caused by tigecycline, ototoxicity (14/60, 23.3%) caused by amikacin; and myelosuppression (6/60, 10%) caused mainly by linezolid. In conclusion, the success rate of treatment of *M. abscessus* pulmonary disease is still unsatisfactory. The administration of amikacin, imipenem, linezolid, and tigecycline correlated with increased treatment success. Adverse side effects are common due to long-term, combination antibiotic therapy. Ototoxicity, gastrointestinal distress, and myelosuppression are the most severe.

Keywords: *Mycobacterium abscessus*, pulmonary disease, drug, efficacy, adverse effect

INTRODUCTION

The incidence of pulmonary infections caused by non-tuberculous mycobacteria (NTM) has increased dramatically worldwide in recent years (Hoefsloot et al., 2013; Lin et al., 2018; Lee et al., 2019). Among them, *Mycobacterium abscessus* (*M. abscessus*) infections are the most difficult to manage (Nessar et al., 2012; Griffith, 2019). *M. abscessus* infections, which are even refractory to combined, long-term antibiotic therapy, often result in mortality.

Mycobacterium abscessus treatment is challenging, albeit effective treatment options are evolving. In 2007, the American Thoracic Society (ATS)/Infectious Disease Society of America (IDSA) introduced a clarithromycin-based multidrug therapy with amikacin plus cefoxitin or imipenem administered parenterally (Griffith et al., 2007). In 2017, the British Thoracic Society guidelines recommended a revision in antibiotic therapy that consisted of intravenous amikacin, tigecycline, and imipenem with a macrolide, e.g., clarithromycin, for the initial treatment phase (Haworth et al., 2017). This was followed by a continuation phase composed of nebulized amikacin and a macrolide in combination with additional oral antibiotics. It was further recommended that selection of a specific agent should consider the antibiotic susceptibility of the isolate and the antibiotic tolerance of the patient.

Patients with pulmonary disease due to *M. abscessus* infection require long-term treatment with multiple antibiotics. Little is known about the impact of each antibiotic on treatment outcomes. Recently, the NTM International Network released a consensus statement defining the treatment outcomes of NTM pulmonary disease, allowing for a better evaluation of the efficacy of each antibiotic used in clinical studies (van Ingen et al., 2018). Using these criteria, Kwak et al. (2019) conducted an excellent meta-analysis of 14 studies with detailed individual patient data. Patients treated with drug combinations that included azithromycin, amikacin, or imipenem exhibited better outcomes, emphasizing the import of different therapeutic approaches. However, two important antibiotics specifically recommended in the 2017 British Thoracic Society guidelines, i.e., linezolid and tigecycline, were not used or were administered in very few cases. Moreover, despite identifying the antibiotics most effective, the adverse effects of these antibiotics were not considered.

We previously reported a series of studies demonstrating the antibiotic susceptibility of clinical *M. abscessus* isolates and the treatment outcomes of patients diagnosed with *M. abscessus* pulmonary disease (Li B. et al., 2017, 2018; Guo et al., 2018; Ye et al., 2019). A number of cases accumulated during the course of these studies dealt with the long-term treatment with antibiotics, including linezolid and tigecycline; the adverse effects of antibiotic treatment were well documented. The retrospective analysis reported herein was undertaken to evaluate the efficacy and adverse effect of a variety of antibiotics used to treat *M. abscessus* pulmonary disease. The results of this analysis should facilitate therapeutic choices in clinical practice.

MATERIALS AND METHODS

Study Population

A retrospective review was conducted of the medical records of all patients entering Shanghai Pulmonary Hospital between January 2012 and December 2017 with *M. abscessus* lung disease. Participating patients were followed-up on a regular basis; sputum culture and chest CT examination were performed once a month and once every 3 months, respectively. The inclusion criteria were: (1) age $>$ 16 years; (2) having undergone initial diagnosis and treatment at the Shanghai Pulmonary Hospital in accordance with the 2007 ATS/IDSA Guidelines or the 2017 British Thoracic Society Guidelines; and (3) follow-up period lasting $>$12 months. Exclusion criteria were: (1) age $<$ 16 years; (2) co-infection with active tuberculosis or another NTM; (3) refusal to sign informed consent form; and (4) AIDS. Notably, patients with cystic fibrosis were never found and are essentially non-existent in Asia. A detailed, patient enrollment flow chart is shown in **Figure 1**. This study was approved by the Ethics Committees of Shanghai Pulmonary Hospital and Tongji University School of Medicine, ethics number K17-150. All participants signed informed consent forms before enrollment.

Collection, Identification, and Preservation of Bacteria

All clinical *M. abscessus* isolates used in this study were preserved in the Clinical Microbiology Laboratory of Shanghai Pulmonary Hospital. Shanghai Pulmonary Hospital is one of the designated treatment centers for tuberculosis and NTM in China, attracting NTM cases nationwide. *M. abscessus* isolates were obtained from sputum and bronchoalveolar lavage fluid. The detailed process of *M. abscessus* identification was described previously by us using *rpoB*, *erm*(41), and *PRA-hsp65* genes to identify and differentiate *abscessus*, *massiliense*, and *bolletii* subspecies (Guo et al., 2018). *M. abscessus* subsp. *bolletii* is extremely rare and, therefore, was excluded. Identified isolates, stored at −80°C, were recovered for microbiology and molecular biology studies.

Genotype Analysis

Genomic information of *rpoB*, *erm*(41), and *PRA-hsp65* genes for 182 isolates was obtained by whole genome sequencing, which was available at DDBJ/ENA/GenBank under the BioProject PRJNA448987, PRJNA398137, and PRJNA488058. The genotype of the remaining isolates was determined by PCR and sequencing the *rpoB*, *erm*(41), and *PRA-hsp65* genes.

Treatment Regimen

All patients were treated with antibiotics recommended by the ATS/IDSA or the British Thoracic Society guidelines (Griffith et al., 2007; Haworth et al., 2017). Clarithromycin, azithromycin, amikacin, tigecycline, linezolid, imipenem, meropenem, cefoxitin, ciprofloxacin, moxifloxacin, doxycycline, minocycline, and levofloxacin (among the most common antibiotics used to treat *M. abscessus* infections) were included in the analysis. These antibiotics were selected based upon: drug susceptibility, adverse side effects, medical history, economic considerations, and the ease with which the regimens could be modified during the course of treatment.

Treatment Efficacy and Adverse Drug Effects

Treatment outcomes were defined in accordance with the NTM International Network consensus statement (van Ingen et al., 2018); a microbiological cure was considered successful treatment. Since all patients enrolled in the current study were simultaneously or sequentially treated with more than one drug, analysis of the direct response to a single drug was

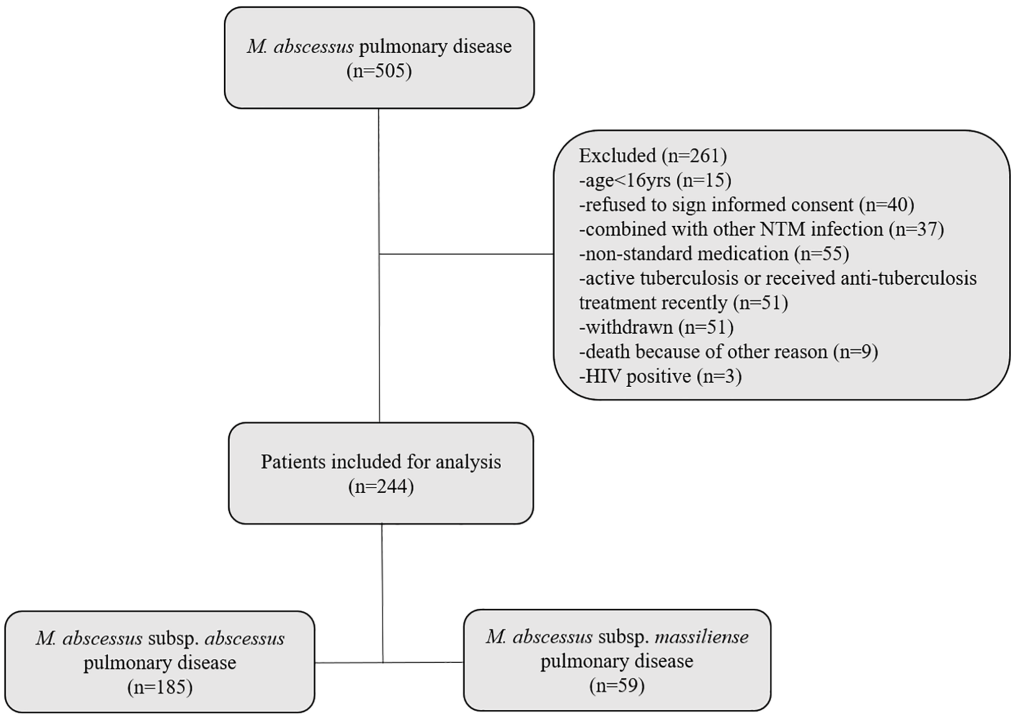

FIGURE 1 | Flow diagram of the study. Two hundred forty-four pulmonary disease patients, who conformed to the inclusion criteria, were enrolled. One hundred eighty-five patients were infected with *M. abscessus* subsp. *abscessus*; 59 patients were infected with *M. abscessus* subsp. *massiliense*.

impossible. Rather, the efficacy of individual drugs was assessed based upon a comparison of the frequency of drug usage in successfully versus unsuccessfully treated patients (Kwak et al., 2019). Evaluation of chest images and symptoms was determined by the treating physician. Adverse drug effects and the drugs responsible were identified by referring to the medical records and confirmed by the diminution or elimination of symptoms following drug cessation.

Statistical Analysis

Statistical analysis was conducted using SPSS version 20 (IBM Corporation, Chicago, IL, United States). Group comparisons for continuous data were performed using Mann–Whitney *U*-test. Group comparisons of proportions were made using Pearson's chi-squared test or Fisher's exact test. Multivariable logistic regression was used to confirm the association of specific drug use with treatment success; symptomatic and radiographic improvement; and adjusting for age, sex, BMI, and radiographic features. Statistical significance was set at a two-sided p-value of <0.05.

RESULTS

Patient Characteristics

Two hundred and forty-four patients who conformed to the recruitment criteria were enrolled. Among them, 75.8% of the patients were infected with *M. abscessus* subsp. *abscessus*; 24.2% were infected with *M. abscessus* subsp. *massiliense* (**Table 1**). Patients experiencing *M. abscessus* pulmonary disease were 73.0% female and had relatively low body mass indices. Most of the patients had comorbidities consisting of prior TB/NTM infection or bronchiectasis. The main symptoms were cough and sputum production. The proportion of pulmonary disease patients infected with *M. abscessus* subsp. *abscessus* exhibited more fibrocavitary and less nodular bronchiectasis in chest images relative to patients infected with *M. abscessus* subsp. *massiliense*.

Treatment Outcomes and Modalities

Only 45.1% of total patients (110/244) met the criteria for treatment success (**Table 2**). Significantly greater success was observed among patients infected with *M. abscessus* subsp. *massiliense* [81.4% (48/59)] compared to those infected with subsp. *abscessus* [33.5% (62/185)]. Clarithromycin used in drug regiments to treat patients infected with *M. abscessus* subsp. *abscessus* was more commonly associated with treatment failure than treatment success (85.4 vs. 71.0%, respectively). Treatments that included a different macrolide (azithromycin), on the other hand, achieved significantly greater success (37.1%) than failure (19.5%). These differences were not found upon analysis of the entire study population or patients infected with *M. abscessus* subsp. *massiliense*. Treatment with drug combinations that included amikacin, imipenem, linezolid, or tigecycline also exhibited far greater success than failure in treating the

TABLE 1 | Baseline patient characteristics[a].

	Total (*n* = 244)	*M. abscessus* subsp. *abscessus* pulmonary disease (*n* = 185)	*M. abscessus* subsp. *massiliense* pulmonary disease (*n* = 59)	*P*-value
Median age (years)	56.0(49.0, 65.8)[b]	56(49.0, 66.0)[b]	54.0(48.0, 63.0)[b]	0.207
Sex, male	66(27.0)	53(28.6)	13(22.0)	0.319
Body mass index (kg/m^2)	19.6(18.6, 20.5)[b]	19.7(18.6, 20.5)[b]	19.4(18.6, 20.6)[b]	0.536
Respiratory comorbidities				
Prior TB/NTM[c]	127(52.0)	92(49.7)	35(59.3)	0.199
Bronchiectasis	208(85.2)	154(83.2)	54(91.5)	0.118
COPD[c]	16(6.6)	13(7.0)	3(5.1)	0.768
Cor pulmonale	12(4.9)	10(5.4)	2(3.4)	0.736
Asthma	15(6.1)	12(6.5)	3(5.1)	1.000
Main respiratory symptoms				
Cough	201(82.4)	153(87.4)	48(81.4)	0.246
Sputum	206(84.4)	158(85.4)	48(81.4)	0.455
Hemoptysis	59(24.2)	47(25.4)	12(20.3)	0.429
Shortness of breath	75(30.7)	54(29.2)	21(35.6)	0.353
Chest pain	48(19.7)	38(20.5)	10(16.9)	0.546
Radiographic features				**<0.001**
Fibrocavitary	61(25.0)	57(30.8)	4(6.8)	
Nodular bronchiectatic	171(70.1)	116(62.7)	55(93.2)	
Indeterminate	12(4.9)	12(6.5)	0(0)	

[a]*Data are the medians (interquartile range) or numbers (percentage).* [b]*Range.* [c]*TB, tuberculosis; NTM, non-tuberculous mycobacterium; COPD, chronic obstructive pulmonary disease.*

entire patient population, as well as treating those patients infected with *M. abscessus* subsp. *abscessus*. Drug combinations that included these same four antibiotics did not exert the same beneficial effects on patients infected with *M. abscessus* subsp. *massiliense*.

The duration of treatment was significantly shorter for the total population of patient who were successfully treated versus patients who failed treatment. Similarly, the treatment duration was substantially shorter for *M. abscessus* subsp. *abscessus* infected patients who were successfully treated. Successfully treated patients infected with *M. abscessus* subsp. *massiliense* exhibited the same trend, but failed to achieve statistical significance. Efficacy of treatment modalities with respect to symptomatic and raidiographic improvement has also been made and similar outcome profiles are obtained (**Supplementary Tables 1, 2**).

Effects of Individual Drugs on Treatment Outcomes

Multiple logistic regression analysis (adjusted for age, gender, BMI, and radiographic findings) indicated that azithromycin was clinically superior to clarithromycin in treating patients infected with *M. abscessus* subsp. *abscessus* (**Table 3**). The superiority of azithromycin was not observed in treating the total patient population or patients infected with *M. abscessus* subsp. *massiliense*. Amikacin, imipenem, linezolid, and tigecycline were also associated with success in treating the entire patient population, as well as those patients infected with *M. abscessus* subsp. *abscessus*. Notably, amikacin was the only drug showing clinical efficacy in treating *M. abscessus* subsp. *massiliense* infected patients in our study. The association of each drug with symptomatic and radiographic improvements was also subjected to multivariable logistic regression analysis (**Supplementary Tables 3, 4**).

Adverse Effects of Antibiotics

One hundred and ninety-two of the 244 patients enrolled in the study experienced 319 adverse events caused by therapeutic intervention (**Table 4**). The most frequent adverse events were gastrointestinal complaints that included nausea, vomiting, diarrhea, and abdominal pain. Hematologic toxicity and nephrotoxicity were the next most frequent events documented. Most of these were mild, tolerable, and did not result in disability or death. Serious adverse reactions, however, occurred in 60 (24.6%) patients resulting in a discontinuation or modification of the treatment regimen. Notably, severe myelosuppression was mainly a consequence of linezolid treatment. Gastrointestinal side effects were most often due to tigecycline; amikacin caused most cases of serious ototoxicity and nephrotoxicity. Fortunately, all severe side effects disappeared or were remarkably alleviated after changes in the treatment regimen.

DISCUSSION

The study reported here evaluated the efficacy and adverse effects of different antibiotics used in combination to treat patients with pulmonary disease caused by *M. abscessus*. A variety of antibiotics recommended by the British Thoracic Society

TABLE 2 | Comparison of treatment modalities: success versus failure[a].

Antibiotic	*M. abscessus* pulmonary disease				*M. abscessus* subsp. *abscessus* pulmonary disease				*M. abscessus* subsp. *massiliense* pulmonary disease			
	Total (*n* = 244)	Success (*n* = 110)	Failure (*n* = 134)	*P*-value	Total (*n* = 185)	Success (*n* = 62)	Failure (*n* = 123)	*P*-value	Total (*n* = 59)	Success (*n* = 48)	Failure (*n* = 11)	*P*-value
Clarithromycin	199	86(78.2)	113(84.3)	0.218	149	44(71.0)	105(85.4)	0.020	50	42(87.5)	8(72.7)	0.347
Azithromycin	61	32(29.1)	29(21.6)	0.181	47	23(37.1)	24(19.5)	0.010	14	9(18.8)	5(45.5)	0.110
Amikacin	218	104(94.5)	114(85.1)	0.017	166	60(96.8)	106(86.2)	0.025	52	44(91.7)	8(72.7)	0.112
Imipenem	67	39(35.5)	28(20.9)	0.011	47	22(35.5)	25(20.3)	0.025	20	17(35.4)	3(27.3)	0.734
Meropenem	13	7(6.4)	6(4.5)	0.514	10	5(8.1)	5(4.1)	0.256	3	2(4.2)	1(9.1)	0.468
Cefoxitin	144	65(59.1)	79(59.0)	0.983	110	38(61.3)	72(58.5)	0.719	34	27(56.2)	7(63.6)	0.745
Linezolid[b]	38	24(21.8)	14(10.4)	0.015	27	15(24.2)	12(9.8)	0.009	11	9(18.8)	2(18.2)	1.000
Tigecycline	53	32(29.1)	21(15.7)	0.011	39	19(30.6)	20(16.3)	0.024	14	13(27.1)	1(9.1)	0.269
Doxycycline	30	10(9.1)	20(14.9)	0.167	23	6(9.7)	17(13.8)	0.420	7	4(8.3)	3(27.3)	0.112
Minocycline	22	10(9.1)	12(9.0)	0.971	15	4(6.5)	11(8.9)	0.558	7	6(12.5)	1(9.1)	1.000
Moxifloxacin[b]	53	28(25.5)	25(18.7)	0.200	34	13(21.0)	21(17.1)	0.519	19	15(31.2)	4(36.4)	0.734
Levofloxacin[b]	26	8(7.3)	18(13.4)	0.121	20	4(6.5)	16(13.0)	0.175	6	4(8.3)	2(18.2)	0.310
Ciprofloxacin	17	8(7.3)	9(6.7)	0.865	13	4(6.5)	9(7.3)	1.000	4	4(8.3)	0(0)	1.000
Number of patients administered:	–	–	–	0.810	–	–	–	0.148	–	–	–	0.367
One parenteral drug	15	6(5.5)	9(6.7)	–	9	1(1.6)	8(6.5)	–	6	5(10.4)	1(9.1)	–
Two parenteral drugs	161	70(63.6)	91(67.9)	–	124	38(61.3)	86(69.9)	–	37	32(66.7)	5(45.5)	–
Three parenteral drugs	62	31(28.2)	31(23.1)	–	47	21(33.9)	26(21.1)	–	15	10(20.8)	5(45.5)	–
More than three parenteral drugs	6	3(2.7)	3(2.2)	–	5	2(3.2)	3(2.4)	–	1	1(2.1)	0(0)	–
Months of treatment	25.6 (18.8, 37.8)	20.7 (16.2, 31.0)	30.0 (22.0, 43.3)	<0.001	27.7 (20.7, 40.8)	23.4 (18.1, 34.6)	30.0 (22.0, 44.0)	0.001	20.2 (15.9, 29.8)	18.0 (15.9, 26.8)	28.0 (16.0, 43.0)	0.179
Surgical resection	10	2	8	0.192	7	1	6	0.427	3	1	2	0.086

[a]*Data are the number (percentage; the number of patients who succeeded or failed treatment with the indicated drug divided by the total number of patients who succeeded or failed treatment) or median (interquartile range) of cases. Each antibiotic listed was included regardless of whether it was discontinued during the course of treatment.* [b]*Administered orally and/or intravenously.*

TABLE 3 | Treatment success with individual antibiotics.

Antibiotic	Total (*n* = 244)			*M. abscessus* subsp. *abscessus* pulmonary disease (*n* = 185)			*M. abscessus* subsp. *massiliense* pulmonary disease (*n* = 59)		
	Adjusted OR[a]	95% CI[a,b]	*P*-value	Adjusted OR	95% CI	*P*-value	Adjusted OR	95% CI	*P*-value
Clarithromycin	0.588	0.290–1.194	0.142	0.425	0.191–0.945	0.036	1.460	0.214–9.962	0.699
Azithromycin	1.558	0.844–2.877	0.156	2.339	1.141–4.794	0.020	0.295	0.061–1.418	0.128
Amikacin	3.275	1.221–8.788	0.018	5.911	1.247–28.012	0.025	15.023	1.294–174.400	0.030
Imipenem	2.078	1.151–3.753	0.015	2.050	1.018–4.126	0.044	1.357	0.280–6.575	0.705
Meropenem	1.218	0.390–3.806	0.735	1.787	0.486–6.574	0.382	0.341	0.026–4.487	0.413
Cefoxitin	1.121	0.659–1.908	0.672	1.253	0.656–2.394	0.495	0.610	0.133–2.795	0.524
Linezolid[c]	2.231	1.078–4.616	0.031	2.875	1.221–6.772	0.016	1.286	0.189–8.746	0.797
Tigecycline	2.040	1.079–3.857	0.028	1.971	0.931–4.173	0.076	2.614	0.291–23.514	0.391
Doxycycline	0.599	0.260–1.380	0.229	0.628	0.222–1.772	0.379	0.408	0.053–3.147	0.390
Minocycline	0.992	0.399–2.467	0.986	0.691	0.206–2.315	0.549	1.312	0.116–14.876	0.827
Moxifloxacin[c]	0.695	0.372–1.300	0.255	0.866	0.393–1.908	0.720	1.495	0.303–7.388	0.622
Levofloxacin[c]	0.474	0.193–1.162	0.103	0.453	0.142–1.445	0.181	0.242	0.032–1.857	0.172
Ciprofloxacin	1.026	0.372–2.831	0.960	1.155	0.330–4.039	0.822	0	0	0

[a]*OR, odds ratio; CI, confidence interval.* [b]*Adjusted for age, sex, body mass index, and radiographic findings.* [c]*Administered orally and/or intravenously.*

TABLE 4 | Adverse events*.

			Antibiotic-specific adverse events leading to treatment modification (*n* = 60)					
	Total patients (*n* = 192)	Total frequency of adverse events (*n* = 319)	Clarithromycin (*n* = 4) (199 patients)	Azithromycin (*n* = 3) (61 patients)	Amikacin (*n* = 26) (218 patients)	Imipenem (*n* = 3) (67 patients)	Linezolid (*n* = 9) (38 patients)	Tigecycline (*n* = 15) (53 patients)
Gastrointestinal distress	79(41.1)	143(44.8)	4	3	4	0	4	14
Diarrhea	15(7.8)	22(6.9)	0	0	0	0	0	0
Abdominal pain	13(6.8)	25(7.8)	1	1	0	0	1	0
Nausea	35(18.2)	66(20.7)	1	2	4	0	2	10
Vomiting	16(8.3)	30(9.4)	2	0	0	0	1	4
Dizziness	7(2.9)	15(4.7)	0	0	0	0	0	0
Ototoxicity	11(5.7)	15(4.7)	0	0	14	0	0	0
Nephrotoxicity	20(10.4)	34(10.7)	0	0	5	0	0	0
Hepatotoxicity	9(4.7)	15(4.7)	0	0	0	0	0	1
Hematologic toxicity	11(5.7)	26(8.2)	0	0	0	1	5	0
Leukopenia	5(2.6)	11(3.4)	0	0	0	1	2	0
Thrombocytopenia	2(1.0)	5(1.6)	0	0	0	0	2	0
Anemia	4(2.1)	10(3.13)	0	0	0	0	1	0
Insomnia	3(1.6)	6(1.9)	0	0	0	0	0	0
Fever	3(1.6)	5(1.6)	0	0	0	0	0	0
Headache	14(7.3)	22(6.9)	0	0	0	0	0	0
Myoclonus	3(1.6)	4(1.3)	0	0	0	0	0	0
Agitation	3(1.6)	3(0.9)	0	0	0	1	0	0
Taste alteration	10(5.2)	11(3.4)	0	0	0	0	0	0
Allergic reactions	19(9.9)	20(6.3)	0	0	3	1	0	0

**The patients affected by the adverse event listed are enumerated. Notably, a single patient is often affected by more than one event. Those antibiotics, which most frequently cause events that necessitates treatment modification, are listed.*

guidelines were analyzed including linezolid and tigecycline, two important drugs recently used more frequently. While the overall rate of treatment success remained very low, the incorporation of amikacin, imipenem, linezolid, and/or tigecycline into treatment regimens was associated with increased success. The overall safety of macrolide-based regimens was moderately satisfactory since no fatalities or disabilities resulted from treatment. However, the total incidence of adverse effects was high. Indeed, there were cases in which patients were unable to tolerate one or more potentially effective drugs, i.e.,

azithromycin, amikacin, imipenem, linezolid, and tigecycline, during the course of treatment.

Two recent meta-analyses reported disappointing treatment outcomes for *M. abscessus* pulmonary disease. The therapeutic efficiency rates were 54 and 45.6% for all patients, and 35 and 33.0% for patients diagnosed with pulmonary, *M. abscessus* subsp. *abscessus* infections (Pasipanodya et al., 2017; Kwak et al., 2019). Similar rates of treatment success are reported here, i.e., 45.1% for all cases of *M. abscessus* pulmonary disease and 33.5% for cases involving *M. abscessus* subsp. *abscessus*. As such, the therapeutic efficacy of *M. abscessus* pulmonary disease continues to be unsatisfactory, and is even worse for *M. abscessus* subsp. *abscessus* infections.

Amikacin exhibits a high level of antibacterial activity and a low rate of resistance *in vitro*; its successful use to treat pulmonary, *M. abscessus* infections has been reported (Olivier et al., 2014; Lee H. et al., 2017). Indeed, amikacin administered parenterally is regarded as one of the most active antibiotics available to treat *M. abscessus* pulmonary disease (Griffith et al., 2007). Consistent with this perception, amikacin administered in our study was strongly associated with the alleviation of symptoms and treatment success suggesting that amikacin remains an ideal, first choice for treating *M. abscessus* infections. Clinicians should be aware, however, that amikacin is ototoxic. As such, blood concentration of amikacin should be monitored continually to ensure safety.

The anti-*M. abscessus* activity of imipenem *in vitro* is variable; bacterial resistance was over 60% in some studies (Chua et al., 2015; Lee M.C. et al., 2017; Li B. et al., 2017). Imipenem was efficacious, however, in treating pulmonary *M. abscessus* disease in our study. Similar results were reported by Kwak et al. (2019). The elevated antimicrobial activity expressed by imipenem intracellularly provides one plausible explanation for the apparent difference in activity exhibited *in vitro* versus *in vivo* (Rominski et al., 2017). In this regard, the high *in vivo* killing activity of imipenem in an embryonic zebrafish test system was reported (Lefebvre et al., 2016). Moreover, it is likely that the combination of imipenem with other antibiotics has a synergistic or additive effect, which contributes to the treatment success associated with imipenem (Miyasaka et al., 2007; Le Run et al., 2019). Notably, imipenem caused the fewest severe, adverse side effects among the four dominant drugs (i.e., amikacin, imipenem, linezolid, and tigecycline) identified in this study suggesting that it should be included as a treatment option provided *in vitro* sensitivity testing demonstrates the susceptibility of the clinical *M. abscessus* isolate. Furthermore, a newly developed beta-lactamase inhibitor, relebactam, has been shown to significantly improve the anti-*M. abscessus* activity of imipenem *in vitro* and no additional consideration needed to be addressed when imipenem and relebactam are used together (Zhanel et al., 2018; Kaushik et al., 2019a).

Accumulated evidence suggests that linezolid possesses elevated anti-*M. abscessus* activity. Recently, we reported the high activity expressed by linezolid *in vitro* against clinical *M. abscessus* isolates collected from patients with lung diseases (Ye et al., 2019). A study conducted using a *Drosophila melanogaster*-infection model demonstrated the anti-*M. abscessus* activity of linezolid *in vivo* (Oh et al., 2014); the successful use of linezolid in treating clinical *M. abscessus* infections was also reported (Inoue et al., 2018). These results are supported by data presented here. Better outcomes occurred when linezolid was a component of multi-drug therapy used to treat *M. abscessus* pulmonary disease. Linezolid has the advantage that it can be administered orally. It penetrates well into both extracellular fluid and cells, making linezolid one of the more important options for treating *M. abscessus* infections (Honeybourne et al., 2003). Linezolid-induced myelosuppression, however, was the most severe event leading to treatment intervention in our study. Considering its high price and limited availability in some areas, linezolid may be a more appropriate secondary treatment choice, especially when antibiotic sensitivity testing demonstrates alternatives.

Tigecycline exhibits the potentially strongest antibacterial activity of any antibiotic against *M. abscessus in vitro*. One study conducted in Japan showed it exerts 100% bacteriostasis against *M. abscessus* at very low concentrations (MIC $\leq$ 0.5 μg/ml), which is far superior to the antibacterial effect of clarithromycin (62%) and linezolid (77%) at the CLSI recommended breakpoint (Hatakeyama et al., 2017). Similar results were found in both France (90%, MIC $\leq$ 1 μg/ml) and China (94.3%, MIC $\leq$ 2 μg/ml) (Mougari et al., 2016; Li G. et al., 2017). Moreover, the combination of tigecycline with clarithromycin *in vitro* produces synergistic antibacterial effects against *M. abscessus* (Zhang et al., 2017). Tigecycline also showed excellent therapeutic effects against *M. abscessus* infection in a clinical study. Wallace et al. (2014) reported that daily treatment of *M. abscessus* disease with 50–100 mg tigecycline for 1 month resulted in a clinical remission rate that exceeded 60%. Tigecycline also proved superior in treating *M. abscessus* infections in the study reported here, supporting the British Thoracic Society guidelines that list tigecycline as a first-line solution for treating *M. abscessus* infections (Haworth et al., 2017). It is pertinent to note that tigecycline-treated patients often suffered from severe nausea and vomiting. Notably, two newly developed tetracycline analogs, omadacycline and eravacycline, have been reported to show therapeutic potential in treatment of *M. abscessus* infection (Kaushik et al., 2019b; Shoen et al., 2019), with similar *in vitro* activity to tigecycline, but better tolerated.

The study described herein has several limitations. First, it is a retrospective analysis of data obtained at a single center, which could limit the generalization and accuracy of the results. Second, only a relatively small number of *M. abscessus* subsp. *massiliense* infected cases were included, consequently, their characteristics may not be well representative. Third, due to the simultaneous administration of multiple antibiotics, conclusions regarding the adverse effects of individual drugs may be inaccurate. Four, this study excluded subjects who failed to complete their follow-up visits. Conceivably, this failure occurs as a consequence of adverse drug side effects resulting in an underestimation of the adverse events that could otherwise lead to treatment modification. Finally, antibiotics are selected strictly according to guidelines or sputum culture results in our study, rather than at random, resulting in the occurrence of prescription bias. However, it is inevitable.

CONCLUSION

The success rate of *M. abscessus* pulmonary disease treatment is still unsatisfactory, albeit the use of amikacin, imipenem, linezolid, and tigecycline is associated with increased treatment success. Adverse effects are common due to the long-term combination anti-*M. abscessus* therapy. Ototoxicity caused by amikacin, gastrointestinal side effects caused primarily by tigecycline, and myelosuppression caused by linezolid were the most severe adverse effects observed.

DATA AVAILABILITY

The raw data supporting the conclusions of this manuscript will be made available by the authors, without undue reservation, to any qualified researcher.

AUTHOR CONTRIBUTIONS

All authors contributed to the preparation of the final manuscript. JC, LZ, YM, BL, and HC conceived and designed the study. MY, QG, YZ, LX, BL, and ZZ collected the clinical data and performed the clinical evaluations. BL and JC performed the statistical analyses. JC, LZ, and YM wrote the manuscript, which was reviewed, edited, and approved by all authors.

FUNDING

This work was supported by grants obtained from the National Natural Science Foundation of China (Nos. 81672063 and 81800003); the Natural Science Foundation of Shanghai Municipal Science and Technology Commission (No. 18ZR1431600); the Medical Guide Program of Shanghai Science and Technology Committee (Nos. 18411970600 and 19411969600); the New Frontier Technology Joint Project of Municipal Hospital, Shanghai Shenkang Hospital Development Center (No. SHDC12017113); and the Project of Top Clinical Medicine Centers and Key Disciplines Construction in Shanghai (No. 2017ZZ02012).

ACKNOWLEDGMENTS

We thank the patients who agreed to participate in this study. Dr. Stephen H. Gregory (Providence, RI, United States) helped write and edit this manuscript. This manuscript has been released as a preprint at BioRxiv (Chen et al., 2019).

SUPPLEMENTARY MATERIAL

The Supplementary Material for this article can be found online at: https://www.frontiersin.org/articles/10.3389/fmicb.2019.01977/full#supplementary-material

REFERENCES

Chen, J., Zhao, L., Mao, Y., Ye, M., Guo, Q., Zhang, Y., et al. (2019). Clinical efficacy and adverse effects of antibiotics used to treat *Mycobacterium abscessus* pulmonary disease. *BioRxiv*

Chua, K. Y., Bustamante, A., Jelfs, P., Chen, S. C., and Sintchenko, V. (2015). Antibiotic susceptibility of diverse *Mycobacterium abscessus* complex strains in new South Wales, Australia. *Pathology* 47, 678–682. doi: 10.1097/PAT.0000000000000327

Griffith, D. E. (2019). *Mycobacterium abscessus* and antibiotic resistance: same as it ever was. *Clin. Infect. Dis.* doi: 10.1093/cid/ciz071 [Epub ahead of print].

Griffith, D. E., Aksamit, T., Brown-Elliott, B. A., Catanzaro, A., Daley, C., Gordin, F., et al. (2007). An official ATS/IDSA statement: diagnosis, treatment, and prevention of nontuberculous mycobacterial diseases. *Am. J. Respir. Crit. Care Med.* 175, 367–416. doi: 10.1164/rccm.200604-571ST

Guo, Q., Chu, H., Ye, M., Zhang, Z., Li, B., Yang, S., et al. (2018). The Clarithromycin susceptibility genotype affects the treatment outcome of patients with *Mycobacterium abscessus* lung disease. *Antimicrob. Agents Chemother.* 62:e2360-17. doi: 10.1128/AAC.02360-2317

Hatakeyama, S., Ohama, Y., Okazaki, M., Nukui, Y., and Moriya, K. (2017). Antimicrobial susceptibility testing of rapidly growing mycobacteria isolated in Japan. *BMC Infect. Dis.* 17:197. doi: 10.1186/s12879-017-2298-98

Haworth, C. S., Banks, J., Capstick, T., Fisher, A. J., Gorsuch, T., Laurenson, I. F., et al. (2017). British thoracic society guidelines for the management of non-tuberculous mycobacterial pulmonary disease (NTM-PD). *Thorax* 72(Suppl. 2), ii1–ii64. doi: 10.1136/thoraxjnl-2017-210927

Hoefsloot, W., van Ingen, J., Andrejak, C., Angeby, K., Bauriaud, R., Bemer, P., et al. (2013). The geographic diversity of nontuberculous mycobacteria isolated from pulmonary samples: an NTM-NET collaborative study. *Eur. Respir. J.* 42, 1604–1613. doi: 10.1183/09031936.00149212

Honeybourne, D., Tobin, C., Jevons, G., Andrews, J., and Wise, R. (2003). Intrapulmonary penetration of linezolid. *J. Antimicrob. Chemother.* 51, 1431–1434. doi: 10.1093/jac/dkg262

Inoue, T., Tsunoda, A., Nishimoto, E., Nishida, K., Komatsubara, Y., Onoe, R., et al. (2018). Successful use of linezolid for refractory *Mycobacterium abcessus* infection: a case report. *Respir. Med. Case Rep.* 23, 43–45. doi: 10.1016/j.rmcr.2017.11.007

Kaushik, A., Ammerman, N. C., Lee, J., Martins, O., Kreiswirth, B. N., Lamichhane, G., et al. (2019a). In vitro activity of the new β-Lactamase inhibitors relebactam and vaborbactam in combination with β-Lactams against *Mycobacterium abscessus* complex clinical isolates. *Antimicrob. Agents Chemother.* 63:e2623-18. doi: 10.1128/AAC.02623-18

Kaushik, A., Ammerman, N. C., Martins, O., Parrish, N. M., and Nuermberger, E. L. (2019b). In vitro activity of new tetracycline analogs omadacycline and eravacycline against drug-resistant clinical isolates of *Mycobacterium abscessus*. *Antimicrob. Agents Chemother.* 63:e470-19. doi: 10.1128/AAC.00470-19

Kwak, N., Dalcolmo, M. P., Daley, C. L., Eather, G., Gayoso, R., Hasegawa, N., et al. (2019). *Mycobacterium abscessus* pulmonary disease: individual patient data meta-analysis. *Eur. Respir. J.* 54:1801991. doi: 10.1183/13993003.01991-2018

Le Run, E., Arthur, M., and Mainardi, J. L. (2019). In vitro and intracellular activity of imipenem combined with tedizolid, rifabutin, and avibactam against *Mycobacterium abscessus*. *Antimicrob. Agents Chemother.* 63:e1915-18. doi: 10.1128/AAC.01915-18

Lee, H., Myung, W., Koh, W. J., Moon, S. M., and Jhun, B. W. (2019). Epidemiology of nontuberculous mycobacterial infection, South Korea, -2016. *Emerg. Infect. Dis.* 25, 569–572. doi: 10.3201/eid2503.181597

Lee, H., Sohn, Y. M., Ko, J. Y., Lee, S. Y., Jhun, B. W., Park, H. Y., et al. (2017). Once-daily dosing of amikacin for treatment of *Mycobacterium abscessus* lung disease. *Int. J. Tuberc. Lung Dis.* 21, 818–824. doi: 10.5588/ijtld.16.0791

Lee, M. C., Sun, P. L., Wu, T. L., Wang, L. H., Yang, C. H., Chung, W. H., et al. (2017). Antimicrobial resistance in *Mycobacterium abscessus* complex isolated from patients with skin and soft tissue infections at a tertiary teaching hospital in Taiwan. *J. Antimicrob. Chemother.* 72, 2782–2786. doi: 10.1093/jac/dkx212

Lefebvre, A. L., Dubee, V., Cortes, M., Dorchene, D., Arthur, M., and Mainardi, J. L. (2016). Bactericidal and intracellular activity of beta-lactams against

Mycobacterium abscessus. *J. Antimicrob. Chemother.* 71, 1556–1563. doi: 10.1093/jac/dkw022

Li, B., Yang, S., Chu, H., Zhang, Z., Liu, W., Luo, L., et al. (2017). Relationship between antibiotic susceptibility and genotype in *Mycobacterium abscessus* clinical isolates. *Front. Microbiol.* 8:1739. doi: 10.3389/fmicb.2017.01739

Li, G., Pang, H., Guo, Q., Huang, M., Tan, Y., Li, C., et al. (2017). Antimicrobial susceptibility and MIC distribution of 41 drugs against clinical isolates from China and reference strains of nontuberculous mycobacteria. *Int. J. Antimicrob. Agents* 49, 364–374. doi: 10.1016/j.ijantimicag.2016.10.024

Li, B., Ye, M., Guo, Q., Zhang, Z., Yang, S., Ma, W., et al. (2018). Determination of MIC distribution and mechanisms of decreased susceptibility to bedaquiline among clinical isolates of *Mycobacterium abscessus*. *Antimicrob. Agents Chemother* 62:e175-18. doi: 10.1128/aac.00175-118

Lin, C., Russell, C., Soll, B., Chow, D., Bamrah, S., Brostrom, R., et al. (2018). increasing prevalence of nontuberculous mycobacteria in respiratory specimens from US-affiliated pacific island jurisdictions(1). *Emerg. Infect. Dis.* 24, 485–491. doi: 10.3201/eid2403.171301

Miyasaka, T., Kunishima, H., Komatsu, M., Tamai, K., Mitsutake, K., Kanemitsu, K., et al. (2007). In vitro efficacy of imipenem in combination with six antimicrobial agents against *Mycobacterium abscessus*. *Int. J. Antimicrob. Agents* 30, 255–258. doi: 10.1016/j.ijantimicag.2007.05.003

Mougari, F., Amarsy, R., Veziris, N., Bastian, S., Brossier, F., Bercot, B., et al. (2016). Standardized interpretation of antibiotic susceptibility testing and resistance genotyping for *Mycobacterium abscessus* with regard to subspecies and erm41 sequevar. *J. Antimicrob. Chemother.* 71, 2208–2212. doi: 10.1093/jac/dkw130

Nessar, R., Cambau, E., Reyrat, J. M., Murray, A., and Gicquel, B. (2012). *Mycobacterium abscessus*: a new antibiotic nightmare. *J. Antimicrob. Chemother.* 67, 810–818. doi: 10.1093/jac/dkr578

Oh, C. T., Moon, C., Park, O. K., Kwon, S. H., and Jang, J. (2014). Novel drug combination for *Mycobacterium abscessus* disease therapy identified in a drosophila infection model. *J. Antimicrob. Chemother.* 69, 1599–1607. doi: 10.1093/jac/dku024

Olivier, K. N., Shaw, P. A., Glaser, T. S., Bhattacharyya, D., Fleshner, M., Brewer, C. C., et al. (2014). Inhaled amikacin for treatment of refractory pulmonary nontuberculous mycobacterial disease. *Ann. Am. Thorac. Soc.* 11, 30–35. doi: 10.1513/AnnalsATS.201307-231OC

Pasipanodya, J. G., Ogbonna, D., Ferro, B. E., Magombedze, G., Srivastava, S., Deshpande, D., et al. (2017). Systematic review and meta-analyses of the effect of chemotherapy on pulmonary *Mycobacterium abscessus* outcomes and disease recurrence. *Antimicrob. Agents Chemother.* 61:e1206-17. doi: 10.1128/AAC.01206-1217

Rominski, A., Schulthess, B., Muller, D. M., Keller, P. M., and Sander, P. (2017). Effect of beta-lactamase production and beta-lactam instability on MIC testing results for *Mycobacterium abscessus*. *J. Antimicrob. Chemother.* 72, 3070–3078. doi: 10.1093/jac/dkx284

Shoen, C., Benaroch, D., Sklaney, M., and Cynamon, M. (2019). In vitro activities of omadacycline against rapidly growing mycobacteria. *Antimicrob. Agents Chemother.* 63:e2522-18. doi: 10.1128/AAC.02522-18

van Ingen, J., Aksamit, T., Andrejak, C., Bottger, E. C., Cambau, E., Daley, C. L., et al. (2018). Treatment outcome definitions in nontuberculous mycobacterial pulmonary disease: an NTM-NET consensus statement. *Eur. Respir. J.* 51:1800170. doi: 10.1183/13993003.00170-2018

Wallace, R. J. Jr, Dukart, G., Brown-Elliott, B. A., Griffith, D. E., Scerpella, E. G., and Marshall, B. (2014). Clinical experience in 52 patients with tigecycline-containing regimens for salvage treatment of *Mycobacterium abscessus* and *Mycobacterium chelonae* infections. *J. Antimicrob. Chemother.* 69, 1945–1953. doi: 10.1093/jac/dku062

Ye, M., Xu, L., Zou, Y., Li, B., Guo, Q., Zhang, Y., et al. (2019). Molecular analysis of linezolid-resistant clinical isolates of *Mycobacterium abscessus*. *Antimicrob. Agents Chemother.* 63:e1842-18. doi: 10.1128/AAC.01842-1818

Zhanel, G. G., Lawrence, C. K., Adam, H., Schweizer, F., Zelenitsky, S., Zhanel, M., et al. (2018). Imipenem–relebactam and meropenem–vaborbactam: two novel carbapenem-b-lactamase inhibitor combinations. *Drugs* 78, 65–98. doi: 10.1007/s40265-017-0851-859

Zhang, Z., Lu, J., Liu, M., Wang, Y., Zhao, Y., and Pang, Y. (2017). In vitro activity of clarithromycin in combination with other antimicrobial agents against *Mycobacterium abscessus* and *Mycobacterium massiliense*. *Int. J. Antimicrob. Agents* 49, 383–386. doi: 10.1016/j.ijantimicag.2016.12.003

Conflict of Interest Statement: The authors declare that the research was conducted in the absence of any commercial or financial relationships that could be construed as a potential conflict of interest.

frontiers in Medicine

ORIGINAL RESEARCH
published: 26 November 2019
doi: 10.3389/fmed.2019.00273

Specific Interventions for Implementing a Patient-Centered Approach to TB Care in Low-Incidence Cities

Adrià Pujol-Cruells[1] *and Cristina Vilaplana*[1,2]*

[1] Experimental Tuberculosis Unit, Fundació Institut Germans Trias i Pujol, Universitat Autònoma de Barcelona, Badalona, Spain, [2] Centro de Investigación Biomédica en Red de Enfermedades Respiratorias (CIBERES), Madrid, Spain

Background: According to the latest Guidelines from the World Health Organization, there is an increasing need for patient-centered tuberculosis disease management given the socio-economic factors influencing the tuberculosis epidemic. In the present study, we aimed to study TB in Barcelona city from an anthropological point of view and to devise a series of specific proposals to implement a patient-centered approach in our setting.

Methods: We carried out a qualitative study using an anthropological approach in Barcelona in the period between November 2017 and November 2018 and proposed specific interventions based on our observations.

Results: In practice, in our environment (a low-incidence European country where tuberculosis tends to present in patients with multiple social problems), and despite the goodwill of the care teams, there are no established and stable circuits, or specific tools to ensure that this is done routinely. Based on our observations, we have devised a series of specific proposals to implement a patient-centered approach. With these interventions we aim to (a) directly ameliorate TB patients well-being in any diagnostic/healthcare management center and (b) at more general level, to increase TB detection and treatment adherence.

Conclusions: The patient-centered TB management recommended by the WHO might be essential for patients' well-being, but there is a lack of circuits or working protocols that ensure its implementation in a regulated manner. In the present manuscript we explain the various concrete measures that we propose in our region and which could be put into practice in other cities or geographic regions with similar epidemiological characteristics.

Keywords: tuberculosis, patient-centered approach, care management, interventions, socio-economic factors, anthropology

OPEN ACCESS

Edited by:
Delia Goletti, Istituto Nazionale per le Malattie Infettive Lazzaro Spallanzani (IRCCS), Italy

Reviewed by:
Leonel Lagunes, Vall d'Hebron University Hospital, Spain
Frédéric Méchaï, Hôpital Avicenne, France

***Correspondence:**
Cristina Vilaplana
cvilaplana@igtp.cat;
cvilaplana@gmail.com

Specialty section:
This article was submitted to Infectious Diseases - Surveillance, Prevention and Treatment, a section of the journal Frontiers in Medicine

Received: *11 June 2019*
Accepted: *11 November 2019*
Published: *26 November 2019*

Citation:
Pujol-Cruells A and Vilaplana C (2019) Specific Interventions for Implementing a Patient-Centered Approach to TB Care in Low-Incidence Cities. Front. Med. 6:273. doi: 10.3389/fmed.2019.00273

INTRODUCTION

According to the latest global report on tuberculosis (TB) published by the World Health Organization (WHO), there were up to 10 million cases of TB and 1.3 million TB-related deaths in 2017 (1). Following the global trend, the incidence rate in Europe is decreasing. In Spain, after two epidemic peaks, coinciding first with the abundance of parenteral drug users among people

infected with HIV (in the late 1980s and 1990s), and then with the large-scale migration from countries with a high incidence of TB found in the early 2000s, TB is relatively well-controlled and is also decreasing in incidence (2). As such, the main problems in epidemiological terms are the high incidence in large cities and delays in diagnosis (an average of 60 days from the onset of symptoms according to the latest data available) (3). In the case of Barcelona, a model TB control program established by the city's Public Health Agency, which allows an interchange of information between clinical TB units, case managers and public health nurses, as well as healthcare agents (4), thereby facilitating the active monitoring, detection and follow-up of patients and access to the complete data for all cases, has been operating for more than 30 years. This has led Barcelona to be considered a laboratory in which the problems and challenges of TB control programs in Western Europe, especially in large cities, can be studied. In the latest report (with data from 2016), the incidence rate was 16.2/100,000 inhabitants, distributed unevenly in the various districts depending on their levels of income (up to 43.8/100,000 in the Ciutat Vella district, for example). About half of these patients were born outside Spain, the percentage of patients with socio-economic vulnerability was estimated at 7.3% and there was an increase in homelessness and alcoholism. The percentage of patients with completed treatment was lower in the elderly, the homeless, those addicted to parenteral drugs and those with a history of imprisonment, partly due to the high mortality in these groups (3).

One of the aspects that the latest WHO report highlighted is that, in order to achieve the reductions in incidence necessary to meet the milestones set for 2030, the socio-economic factors influencing the TB epidemic must be addressed (1). Unfortunately, this is not the only problem, as the latest WHO publication regarding TB treatment guidelines (5) clearly suggests that a patient-centered approach is required in the treatment of TB patients. Such an approach considers that it is insufficient to cure only the illness and that the patient must also be cured. For this: (1) the patient must participate actively in the process, (2) their preferences, needs and values must be taken into account, and (3) a complete approach, including both mental health and social aspects, must be used. There is sufficient evidence to support this more holistic-type approach in TB has been shown to have an important impact on both patient well-being and treatment outcomes (6).

In the present manuscript we aimed to study TB in Barcelona city from an anthropological point of view and to devise a series of specific proposals to implement a patient-centered approach; applicable to our setting but which could be extrapolated to other cities with similar epidemiological situations.

METHODS

We carried out a qualitative study using an anthropological approach in Barcelona in the period between November 2017 and November 2018. The field work was divided into three phases. First phase was floating observation of 40 patients and 8 health professionals: initial phase of prospecting, without intervention. The second phase was participatory observation: real follow-up including informal conversations and unstructured interviews with patients diagnosed with TB ($n = 22$), and health professionals including medical and nursing staff, social workers and health agents ($n = 29$). No data from the participants was recorded, only the anthropologist impressions. The third phase was collaborative observation: proposing strategies for intervention in the community.

The study was conducted within the STAGE-TB project (registered at ClinicalTrials.gov, identifier: NCT03691883), coordinated by the Experimental Tuberculosis Unit; and its protocol and procedures were reviewed and approved by the correspondent responsible institutional review committees.

RESULTS

Our qualitative study confirmed the high prevalence of social exclusion associated with this disease. In Barcelona, the paradigmatic patient is an immigrant with difficulties entering the social and working environment of the region and with language-related communication problems. The social exclusion associated with TB is determined by both the personal, family and legal status of the individual (whether native or migrant) as well as by the added problem of the disease itself, which given the resulting chronicity, associated disability and hospitalization (when required) acts as a barrier (not always symbolic) that hinders or prevents the patient from finding work, having a place to live and establishing social relationships. Healthcare workers recognize well-situations of poverty, malnutrition, social exclusion, and fragility at a mental health level; but there are no established circuits or protocols that allow addressing appropriately these situations.

Moreover, hospitalization or the termination of any activity considered normal for the individual causes the patient to feel trapped in limbo, which can hinder their reintegration into the environment, especially the working environment. In addition, there are two cultural perceptions around the disease: in stabilized environments, TB is associated with pathological social states and is therefore seen as an anomaly, whereas in less structured social environments, TB is perceived as a consequence of the pervading conditions. The social exclusion (and socio-economic factors in general) associated with the illness, as well as the duration of medical treatments, also has an impact on the institutions and health personnel that these patients attend, and they are often not aware of the quality of the service they receive.

Depending on the different geographical origins of the patients, there is also a cultural shock between the patients and their new social framework (which also includes the area of healthcare), since the disease brings individuals into contact with cultural realities to which they are not accustomed, mainly due to differences in customs and gender perspectives. This generates isolation in these patients and means that, although they tend to recognize the seriousness of the illness (and its associated medical problems), this perception does not always translate into healthy behaviors. In order to minimize this cultural shock and its impact on individuals, the design of

activities in which patients can participate is often necessary. However, the offer is limited and must take into account the cultural point of view.

Based on our observations, we have devised a series of specific proposals to implement a patient-centered approach, applicable to Barcelona and which could be extrapolated to other cities with similar epidemiological situations. With these interventions we aim to a) directly ameliorate TB patients well-being in any diagnostic/healthcare management center and b) at more general level, to increase TB detection and treatment adherence. These proposals are set out in **Table 1** and can be divided depending on the level at which they are to be applied: (a) at the diagnostic and/or treatment center, which can improve the conditions of the patients directly, and (b) at the population level in general, affecting neighborhoods with the highest risk of TB.

At the level of the diagnostic and/or treatment center (**Table 1** and **Figure 1**), it is essential to carry out activities that mitigate unemployment or the illegal behavior, stigma and uprooting of patients, especially if they are admitted. These activities must include leisure activities, health, training, and psychological support (programmed; compulsory or voluntary) and be adapted to the patients' cultural context (gender, age, religion, customs, etc.). Moreover, the centers must be equipped with suitable facilities and spaces to carry them out and there must be a network of agreements and collaborations between the centers and the facilities in the city, and particularly in the patients' neighborhood. At an internal level, we believe that both the presence of a regularly scheduled institutional therapy in the form of group sessions attended by both patients and healthcare staff and social mentoring program (in-house or outsourced through contracts or collaborations with mentoring associations) should be implemented.

With regard to the interventions of a more general nature proposed for application in neighborhoods with the highest incidence of TB (**Table 1**), it would be important to have information tools (i.e., leaflets, infographics, videos) in different languages (in Barcelona: in Catalan, Spanish, French, English, Arabic, Urdu, Chinese) and universal access, with the participation of patients during their design; to organize talks and conferences on the disease in which patients or ex-patients also participate, thereby taking full advantage of the figure of the "expert patient"; and to ensure the continuing specialized training of professionals. Given the profile of an individual potentially affected with TB (with the concomitant social pathology that affects detection, diagnosis and treatment adherence), we believe that the creation of interdisciplinary teams from professionals already working on the ground would be essential (**Figure 2**).

The holistic and multidisciplinary approach proposed requires substantial human and financial resources. Unfortunately, a concrete estimation of its cost is very difficult to be calculated, as it depends on the setting where to be implemented and the resources available (including the type of Healthcare System). However, we made the exercise of detailing the items which in our opinion should be considered when budgeting the different proposed interventions. We have included this information as **Table 2**, which could be used to calculate the amount of funding needed once applied to the cost of living, cost of salaries, and other cost measures of the specific country/region where to implement the intervention.

DISCUSSION

One of the limitations of the study is that we focused on the anthropological approach and didn't conduct an associated epidemiological study to perform a precise description of the studied population (including their geographical origin, spoken language and detailed social condition). However, our observations were in line with results of the quantitative studies carried out in this city (2, 3, 7) and similar to findings from other major European cities (8, 9). The treatment management options recommended by the WHO in its guidelines are currently applied well in Spain [in Barcelona, for example, the percentage of cured bacillary pulmonary cases or those who have completed treatment is as high as 92.5% (3)], except for the administration of DOTS (performed in 30.4% of patients, reaching 71% in users of injected drugs (UDI) and 90% in homeless people, although rarely via telematics) and the lack of uniformity in terms of supply.

The main problem arises, however, when it comes to treatment-adherence interventions. The WHO recommendations (5) regarding the provision of health education and advice to patients are met relatively well in Spain by all persons involved (patients and healthcare personnel). However, there are no guidelines or recommendations for activities to ensure the uniformity of actions and their fulfillment. This situation worsens when it comes to recognizing and addressing situations of poverty, malnutrition, social exclusion and fragility at a mental health level. Thus, although these problems are usually correctly identified at a healthcare level, it is often logistically difficult to resolve them and, if this is achieved, it is often solely due to the goodwill of all those involved (medical and nursing staff, health agents, social workers at the centers and associations). Moreover, there is currently little or no coordination or uniformity, and there are no established circuits or protocols that allow comprehensive care to be provided. Thus, although there are links to other public-health programs and sufficient resources to properly address patients with co-morbidities (such as HIV co-infection), other problems, such as those from the mental health sphere, are often under-diagnosed and, therefore, under-treated.

Another of the main problems of TB in our region is that, despite being aware of the precarious socio-economic factors present in some patients, it is difficult to include these patients, as requested by the WHO, in publicly offered services and community-based resources and support, mainly due to the lack of established protocols and circuits.

Given this situation at the local level of a large city (Barcelona), as seen from our anthropological work, and taking into account the recommendations of the WHO (5) and those of "The working group for TB control in big cities and urban risk groups in the

TABLE 1 | Specific interventions proposed to implement the patient-centered approach to TB care.

Level of intervention	Proposals	Expected impacts
In diagnostic or treatment centers	Scheduled activities (leisure, health, training, psychological support) available to TB patients, adapted from a cultural point of view (gender, age, religion, customs, etc.), performed in suitable spaces, in-house or in neighborhood, or city facilities (libraries, museums, swimming pools, gyms) thanks to collaboration agreements.	For patients: To increase patient well-being and mental balance, favor their integration into society, establish a bond with the city, minimize culture shock, decrease para/illegal behaviors. For society in general: increase awareness. For centers: to offer a more complete portfolio covering the patient-centered approach.
	Regularly scheduled institutional group sessions with both patients and staff attending.	Two-way flow of information; to reveal problems, doubts and fears; increase treatment adherence.
	Social mentoring activities, in-house or outsourced, thanks to collaboration agreements with other institutions or NGOs.	To accelerate and increase reinsertion, emancipation and adherence to treatment, while reducing isolation and unhealthy habits, in the framework of interventions to generate, reconnect or strengthen the bonds of the individual with society.
In high TB incidence neighborhoods	Information tools (i.e., leaflets, infographics, videos), in different languages, of universal access, patients coauthoring. Two versions: one for patients and their relatives, another one for the general population.	For patients: to increase treatment adherence, bond with healthcare staff and increase patient confidence. For relatives: to resolve doubts and give them tools to handle day-to-day problems. For the general population: to increase awareness, to promote early diagnosis.
	Conferences, seminars, informal talks on the disease, its management and its impact; patients involved; conducted using community infrastructures and spaces: schools, civic centers, libraries, museums, places of worship, leisure and health facilities (gymnasia, swimming pools, shopping centers).	To increase awareness of the presence of the disease in the environment; increase health literacy; reduce fears and resolve doubts.
	Continuing education for healthcare professionals on TB screening, diagnosis, management and treatment; carried out periodically; i.e., refresher courses, infographics, etc.	To increase awareness of the presence of the disease and reduce diagnostic delay; to refresh and update information on TB management.
	Creating interdisciplinary teams; at city, regional or national level; recommended to include healthcare workers, mental health therapists, social science workers, nutritionists, and patients (expert patient).	To generate documents, protocol circuits, and guidelines that ensure the implementation of a global approach to the management of TB patients.

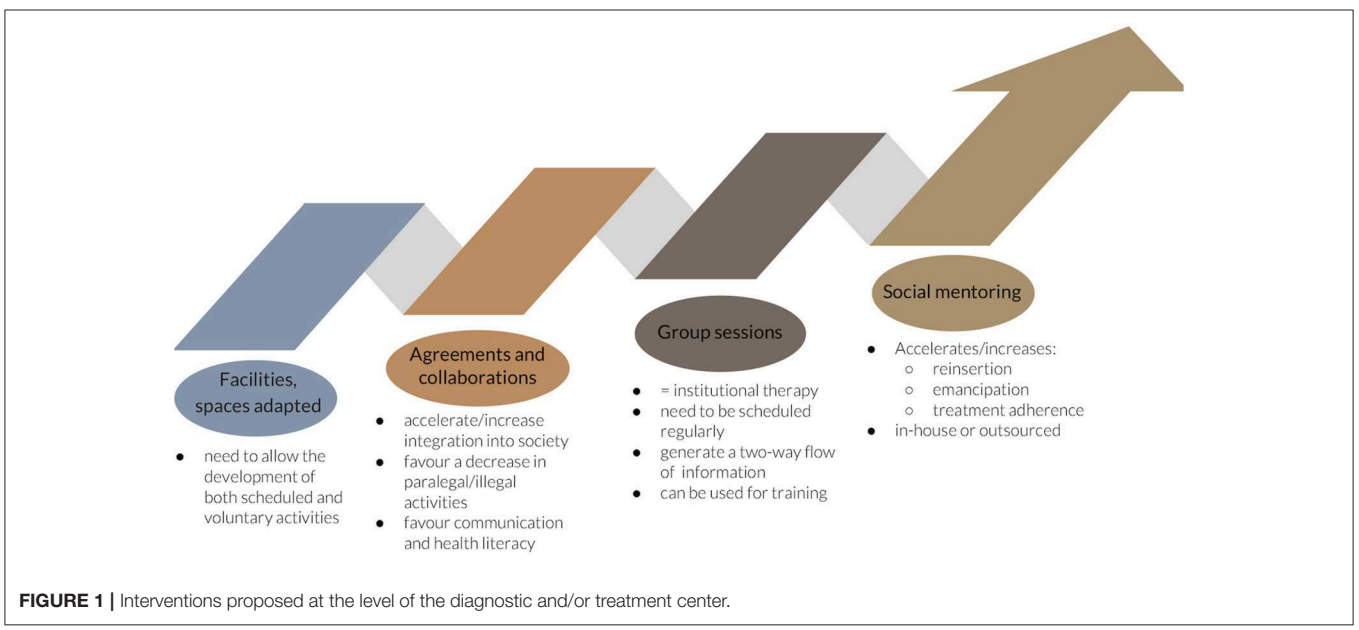

FIGURE 1 | Interventions proposed at the level of the diagnostic and/or treatment center.

EU" (9), we have devised a series of specific proposals applicable to Barcelona that could be extrapolated to other cities with similar epidemiological situations.

Interventions proposed at the level of the diagnostic and/or treatment center, apart from facilitating the leisure options and training available at the centers, and working on how to stop

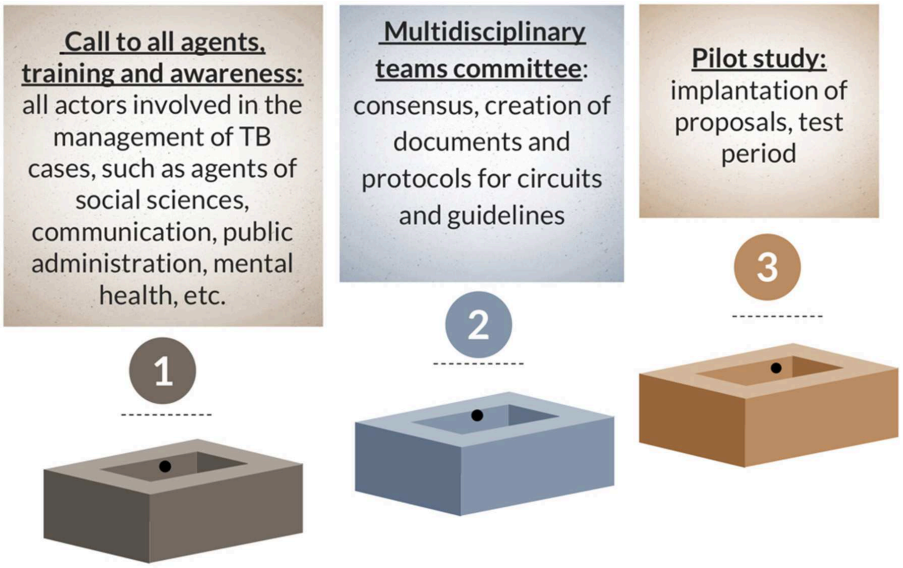

FIGURE 2 | Creation of interdisciplinary teams: phases.

transmission and spread of the disease, ensure that there is no discontinuity between the hospital/residential world and that of the general population outside this institutional context. It also adds value to those centers that offer it, since the quality of the services provided increases beyond strictly medical care (which is already covered nowadays). At an internal level, regularly scheduled institutional therapy help strengthen messages related to the disease, encourage a two-way flow of information and can be used to carry out training. They also have an important impact on the outcomes of the disease (10). This type of activity could form part of the group of interventions that favor treatment adherence and the psychological support defined by the WHO (5). Finally, we propose that a social mentoring program should be implemented, to accelerate and increase reintegration, emancipation and treatment adherence, while reducing both isolation and unhealthy habits, in the framework of interventions to generate, reconnect or strengthen the ties of individuals with society (11).

With regard to the interventions of a more general nature proposed for application in neighborhoods with the highest incidence of TB, we must make an effort to intensify the presence and implementation of tools that enhance visibility of the disease given the fact that poor population information and inadequate training of professionals result in a delay in diagnosis. In this sense, it would be important to ensure the participation of patients during their design. Similar experiences have shown that joint development (by professionals and patients working together) of the information (the story) plays a key role in the solution to the problem (12, 13).

All these communication tools and activities should applied twice: once for patients and their friends and families, and the second time for the general population (distributed in geographic regions at higher risk). In this regard, it should be noted that, in order to optimize resources, it would be advisable to use existing resources that have proven useful in other regions or countries with a similar TB incidence and characteristics. All these initiatives need to be carried out using community infrastructures and space in order to link them to society itself, especially schools, civic centers, libraries, places of worship, and leisure and health facilities (gymnasia, municipal swimming pools, shopping centers). The continuing specialized training of professionals is also indispensable (5), especially in low-impact countries (such as those in Western Europe), and can be done by way of refresher courses or much simpler tools to encourage professionals to take into account the illness in these environments, such as infographics and reminders in the clinic.

On the creation of interdisciplinary teams from professionals already working on the ground, we do believe it would represent a significant step toward tackling the illness and increasing patient wellbeing. These teams could be created at a city, regional or national level, and it may be advisable for them to be led by local Public Health Agencies. Although this approach has not been tested in tuberculosis in our setting, similar initiatives, such as the management of care for people with complex needs, which involves the coordination of health services (including mental health) at both the primary care and hospital levels, social services (both at a community and an individual level), and a specialized community support team (formed by geriatricians, pharmacists, occupational therapists, dieticians), have been implemented (14).

To accomplish this goal, the following sequence of steps would be required: (1) a call to all agents, including the main actors involved in TB care (professionals in the fields of social sciences, public administration, politics, and communication, from the legislative world, criminologists, teachers from all walks of life (especially adults), nutritionists, therapists and others). In this first session, all these agents would be summoned and

TABLE 2 | Suggested items to be considered when budgeting the specific interventions proposed.

Interventions proposed	Items to be considered when budgeting
Scheduled activities available to TB patients	If done in-house: • costs of adapting/transforming the in-house spaces to make them suitable for the purposes. • salary of professionals organizing and/or conducting the activities or effort cost. Costs can be diminished/suppressed by establishing collaboration agreements with neighborhood or city facilities (libraries, museums, swimming pools, gyms).
Regularly scheduled institutional group sessions with both patients and staff attending.	• Salary for a psychologist/therapist.
Social mentoring activities, in-house or outsourced, thanks to collaboration agreements with other institutions or NGOs.	• Salary for a program supervisor (administrative management of the team, formative supervision, monitoring performance). • Salary for mentors. • Mentors' travel expenses (including per diem). • Communication support (i.e., Mobile phones, internet connection). • Cost of training the mentors. These costs could be decreased/ suppressed by establishing collaboration agreements with local associations and NGO to partially cover the activity.
Information tools for patients and relatives and for the general population.	• Costs of designing the information material (payment-as-a-service or effort cost of professionals). • Costs of translations. • Costs of publishing the material. • Costs of distributing the material (salary or effort cost of distributor/s).
Communication activities	• Effort cost of professionals giving the communication activities. This cost can be diminished/suppressed if the professionals agree to voluntary work. • Cost of renting community infrastructures and spaces. This cost can be diminished/suppressed by establishing collaboration agreements with city council or similar local institutional bodies.
Continuing education for healthcare professionals on TB	• Costs of performing an educational course. It will depend on the format and channel: webinar, videos, tutorials, classroom course. Can include effort cost of professionals involved (including professors), internet domain, editing. Costs can be diminished by establishing collaboration agreements with universities, foundations and NGO which can contribute to the activity. • Costs of designing educational material (payment-as-a-service or effort cost of professionals) and publishing educational material.
Creating interdisciplinary teams	Minimal team: • Effort cost of 1 MD to coordinate the program and to act as the interlocutor with the physicians of hospitals and other institutions feeding the program with patients. • Effort cost for 1 nurse to act as the interlocutor with the MD in charge of the program and the nurse team at territorial level about the specific cases. • Salary of 1 healthcare manager/administrative to manage the team and to coordinate the collaboration agreements with the institutions and facilities. • Effort cost for 1 healthcare worker. • Effort cost for 1 social assistant. • Effort cost for 1 expert patient and/or costs of meetings with expert patients. Minimal team needs coordination with mental health therapists and nutritionists, that in case of being included in the team their effort cost or salary would need to be also included.

trained, and they would be invited to put forward their reflections and proposals at a second meeting. A Multidisciplinary Teams Committee, in other words a group of people from all the different levels that would lead the initiative and ensure its good performance, would also be created. The second step would be the pooling of new approaches and points of view from all these other disciplines in order to create a pilot team that can work on the search for improvements and solutions for patients, reaching a consensus and generating documents, along with protocol circuits and guidelines that ensure a global approach to the disease. Again, we emphasize that both the screening for mental disorders and counseling and psychological support for patients are very important for the entire duration of disease follow-up and treatment, especially in those most vulnerable at the social level [such as refugees or immigrants (15) or in cases of multi-drug resistance (16, 17)], and these need to be both offered and provided, then routinely scheduled in a regulated manner.

Finally, under the tutelage of the Multidisciplinary Teams Committee, and once all proposals have been analyzed, the interdisciplinary pilot team should be appointed, its ideal test performance and main lines of work (areas, agents) defined, and the proposals implemented in the territory during a trial period. Although initially there may be multiple solutions for financing these teams (including the association of this initiative with a research project), it is important that the local public administration assumes responsibility for the economic viability of these teams beyond the pilot stage.

From an economic point of view, we have envisaged several interventions with a potential wide range of feasibility depending on the available resources at local or governmental level. As the funds for the implementation of actions might be unassumable by the diagnostic/healthcare management centers and the National Health System (which can vary a lot between different countries sharing the same epidemiology in terms of TB), collaboration

agreements with local associations, NGO, city council or similar local institutional bodies need to be established, in order to partially cover or contribute to the activity, and thus to decrease or even suppress part of the costs. Further studies should be conducted in order to elucidate at which extent some of the actions proposed here could also be implemented in low-income countries, which due to their high-TB prevalence could benefit even more of their impact if proven successful.

CONCLUSION

The WHO recommendations in terms of tackling TB are very meaningful from the point of view of addressing the suffering of patients beyond the disease itself, and although care teams are usually aware of this, there are currently still no circuits or working protocols that define the necessary interventions or circuits that ensure their implementation in a regulated manner. With this publication, we hope to highlight this shortcoming while explaining the various concrete measures that we propose in our region and which could be put into practice in other cities or geographic regions with similar epidemiological characteristics, once adapted to the limitations of the new setting.

TAKE HOME MESSAGE

There is an increasing need for patient-centered tuberculosis disease management, but this is not done routinely. In this article we propose a series of specific interventions that could be easily implemented in low-incidence cities during care management.

DATA AVAILABILITY STATEMENT

All datasets generated for this study are included in the article/supplementary material.

ETHICS STATEMENT

The studies involving human participants were reviewed and approved by the correspondent responsible institutional review committees, both the Germans Trias i Pujol Hospital Ethics Committee (study approval code: PI-17-064) and the Vall d'Hebron Hospital Clinical Research Ethics Committee (code PR(AG)101/2017). Verbal informed consent was obtained from all participants because the study was based on informal conversations, no questionnaires, or structured interviews were conducted and no personal data from the participants were recorded. Written informed consent for participation was not required for this study in accordance with the national legislation and the institutional requirements.

AUTHOR'S NOTE

We would like to emphasize that all the reflections presented have been possible thanks to TB patients, all healthcare staff involved, Servicios Clínicos SLU, the Barcelona Public Health Agency, and the health agents of Barcelona. Preliminary results of the study were presented at the XXII International Workshop on TB conducted in Barcelona on the 26–27 November 2018, and published as a conference abstract in Rev Enf Emerg 2018;17:159–160.

AUTHOR CONTRIBUTIONS

AP-C conducted the floating and participatory observation phases of the field work. Both AP-C and CV contributed in the design of the study, worked in the analysis and interpretation together, and in the collaborative observation by proposing strategies for intervention in the community. The authors worked together to draft the manuscript and approved its final version.

FUNDING

This work was supported solely by the Experimental Tuberculosis Unit funds. CVM has a Miguel Servet II contract funded by the Instituto Carlos III (ISCIII, CPII18/00031). Funds were received from the Centro de Investigación Biomédica en Red de Enfermedades Respiratorias (CIBERES) to cover the open access publication fees. The funding bodies involved did not have any role in the design of the study and collection, analysis, interpretation of data or in writing the manuscript.

REFERENCES

1. The World Health Organization. *Global Tuberculosis Report 2018*. Geneva: World Health Organization (2018). Available online at: https://apps.who.int/iris/bitstream/handle/10665/255052/9789241550000-eng.pdfjsessionid=58A839DAF56776E5A12C760DF4EAD839?sequence=1
2. Cayla JA, Millet J-P, Garcia de Olalla P, Martin V, Nelson J, Orcau A. The current status of tuberculosis in the world: the influence of poverty, prisons, HIV, immigration, and control programmes. In: *Art & Science of Tuberculosis Vaccine Development, 2nd Edn*. Oxford University Press (2010). p. 17–29. Available online at: http://tbvaccines.usm.my/finlay/
3. Orcau À, Caylà JA, Rius C. *La tuberculosi a Barcelona*. Barcelona: Informe 2016 (2018). Available online at: http://www.aspb.cat/wp-content/uploads/2018/10/ASPB_Tuberculosi-Barcelona-Informe-2016-1.pdf
4. Ospina J. Agentes comunitarios de salud, una estrategia efectiva en tuberculosis con poblaciones inmigrantes. *Rev Enfermedades Emergentes*. (2018) 17:158–9.
5. World Health Organization. *Guidelines for Treatment of Drug-Susceptible Tuberculosis and Patient Care,* 1st edn. Geneva: WHO press, World Health Organization (2017). Available online at: http://apps.who.int/iris/bitstream/handle/10665/255052/9789241550000-eng.pdfjsessionid=58A839DAF56776E5A12C760DF4EAD839?sequence=1
6. O'Donnell MR, Daftary A, Frick M, Hirsch-Moverman Y, Amico KR, Senthilingam M, et al. Re-inventing adherence: toward a patient-centered model of care for drug-resistant tuberculosis and HIV. *Int J Tuberc Lung Dis*. (2016) 20:430–4. doi: 10.5588/ijtld.15.0360
7. Jové N, Masdeu E, Brugueras S, Millet J, Sánchez F, Ospina J, et al. Incidencias en el tratamiento de la tuberculosis. Acciones para mejorar la adherencia y el estudio de contactos. *Rev Enfermedades Emergentes*. (2018) 17:155–7.
8. Anderson C, Anderson SR, Maguire H, Hayward AC, Story A. Tuberculosis in London: the convergence of clinical and social complexity. *Eur Respir J*. (2016) 48:1233–6. doi: 10.1183/13993003.00749-2016

9. van Hest NA, Aldridge RW, de Vries G, Sandgren A, Hauer B, Hayward A, et al. Tuberculosis control in big cities and urban risk groups in the European Union: a consensus statement. *Eurosurveillance*. (2014) 19:20728. doi: 10.2807/1560-7917.ES2014.19.9.20728
10. Street RL, Makoul G, Arora NK, Epstein RM. How does communication heal? Pathways linking clinician-patient communication to health outcomes. *Patient Educ Couns*. (2009) 74:295–301. doi: 10.1016/j.pec.2008.11.015
11. Holt-Lunstad J. Why social relationships are important for physical health: a systems approach to understanding and modifying risk and protection. *Annu Rev Psychol.* (2018) 69:437–58. doi: 10.1146/annurev-psych-122216-011902
12. Chavan D. Fighting TB requires empowered patients. *BMJ*. (2017) 356:i6344. doi: 10.1136/bmj.i6344
13. Pulvirenti M, Mcmillan J, Lawn S. Empowerment, patient centred care and self-management. *Heal Expect.* (2014) 17:303–10. doi: 10.1111/j.1369-7625.2011.00757.x
14. Anglada A, Alfonso A. *Model d'atenció a les Persones amb Necessitats Complexes.* (2018). Available online at: http://www.consorci.org/coneixement/cataleg-de-publicacions/169/model-datencio-a-les-persones-amb-necessitats-complexes
15. Dhavan P, Dias HM, Creswell J, Weil D. An overview of tuberculosis and migration. *Int J Tuberc Lung Dis*. (2017) 21:610–23. doi: 10.5588/ijtld.16.0917
16. Baral SC, Aryal Y, Bhattrai R, King R, Newell JN. The importance of providing counselling and financial support to patients receiving treatment for multi-drug resistant TB: mixed method qualitative and pilot intervention studies. *BMC Public Health.* (2014) 14:46. doi: 10.1186/1471-2458-14-46
17. Walker IF, Baral SC, Wei X, Huque R, Khan A, Walley J, et al. Multidrug-resistant tuberculosis treatment programmes insufficiently consider comorbid mental disorders. *Int J Tuberc Lung Dis.* (2017) 21:603–9. doi: 10.5588/ijtld.17.0135

Conflict of Interest: The authors declare that the research was conducted in the absence of any commercial or financial relationships that could be construed as a potential conflict of interest.

frontiers in Microbiology

ORIGINAL RESEARCH
published: 15 January 2020
doi: 10.3389/fmicb.2019.03017

Digging Deeper to Save the Old Anti-tuberculosis Target: D-Alanine–D-Alanine Ligase With a Novel Inhibitor, IMB-0283

Jianzhou Meng[1†], Peng Gao[2†], Xiao Wang[1], Yan Guan[1], Yishuang Liu[1] and Chunling Xiao[1]*

[1] Institute of Medicinal Biotechnology, Chinese Academy of Medical Sciences and Peking Union Medical College, Beijing, China, [2] Department of Microbiology, Li Ka Shing Faculty of Medicine, The University of Hong Kong, Hong Kong, China

OPEN ACCESS

Edited by:
Miguel Viveiros,
New University of Lisbon, Portugal

Reviewed by:
Sukhendu Mandal,
University of Calcutta, India
Marco Pieroni,
University of Parma, Italy

***Correspondence:**
Chunling Xiao
xiaocl304@163.com

[†] These authors have contributed equally to this work

Specialty section:
This article was submitted to Antimicrobials, Resistance and Chemotherapy, a section of the journal Frontiers in Microbiology

Received: 14 June 2019
Accepted: 16 December 2019
Published: 15 January 2020

Citation:
Meng J, Gao P, Wang X, Guan Y, Liu Y and Xiao C (2020) Digging Deeper to Save the Old Anti-tuberculosis Target: D-Alanine–D-Alanine Ligase With a Novel Inhibitor, IMB-0283. Front. Microbiol. 10:3017. doi: 10.3389/fmicb.2019.03017

The emergence of drug-resistant *Mycobacterium tuberculosis* (Mtb) has hampered treatments for tuberculosis, which consequently now require novel agents to overcome such drug resistance. The genetically stable D-alanine–D-alanine ligase A (DdlA) has been deemed as an excellent therapeutic target for tuberculosis. In the present study, a competitive inhibitor (IMB-0283) of DdlA was obtained via high-throughput screening. The minimum inhibitory concentrations (MIC) of IMB-0283 for the standard and clinical drug-resistant Mtb strains ranged from 0.25 to 4.00 μg/mL, whereas the conventional inhibitor of DdlA, D-cycloserine (DCS), only inhibited the growth of the standard Mtb strain at 16 μg/mL. The lethal effect of IMB-0283 on Mtb was found to act intracellularly in a DdlA-dependent manner. Specifically, IMB-0283 prevented the synthesis of neonatal cell walls but did not damage mature cell walls. Compared with those of DCS, IMB-0283 exhibited lower cytotoxicity and a higher selective index (SI). At the same dosages of treatment, IMB-0283 reduced bacterial load (log CFU/mL) in an acute animal model from 5.58 to 4.40, while DCS did not yield any such treatment efficacy. Taken together, the lower cytotoxicity and more efficacious *in vivo* activity of IMB-0283 suggest that it is a promising lead compound for antituberculosis drug development.

Keywords: *Mycobacterium tuberculosis*, drug-resistance, D-alanine–D-alanine ligase, inhibitor, D-cycloserine

INTRODUCTION

Tuberculosis (TB) is remains as a high-burden disease and has claimed millions of lives all over the world due to infections of Mtb. Multidrug-resistant TB occurs in 3.5% of new cases and 18% of previously treated cases, and extensive drug-resistant TB has been on the rise in recent years (WHO, 2018). Hence, conventional chemotherapeutics have become inert in attempts to combat

Abbreviations: DCS, D-cycloserine; DdlA, D-alanine–D-alanine ligase A; INH, isoniazid; MIC, minimum inhibitory concentrations; Mtb, *Mycobacterium tuberculosis*; RMP, rifampin; SI, selective index; TB, tuberculosis.

drug-resistant Mtb infections, which consequently now require novel agents to overcome such drug resistance.

Validating whether a therapeutic target with a novel mechanism is worthy of further drug discovery and development is difficult, time-consuming, and requires tremendous resources. To efficiently utilize limited resources, we aimed to leverage a known druggable target since several old drug targets have been previously recognized as promising candidates. Our selection criteria for such old druggable targets were as follows: (1) genetic stability of the target, which may lessen the probability of drug resistance; and (2) the present inhibitor of the target is restricted due to severe side effects but not drug resistance. D-alanine–D-alanine ligase A (DdlA, EC 6.3.2.4, and Rv2981c), the target of DCS (Halouska et al., 2014), is an excellent drug target for treating TB since its mutation rate to generate resistant strains is much smaller than that of other targets (McGrath et al., 2014). However, the neurological and psychiatric side effects of DCS limit its clinical application (Kass and Shandera, 2010). Therefore, it is necessary to exploit novel anti-TB compounds that target Mtb DdlA. In the present study, a safe and low-toxicity inhibitor of DdlA was obtained with potent anti-TB activity both *in vitro* and *in vivo*.

MATERIALS AND METHODS

Bacteria and Plasmids

All chemicals used in this study were purchased from Sigma (Sigma-Aldrich, St. Louis, MO, United States) unless otherwise stated. Mtb H37Rv (ATCC27294) and other clinical drug-resistant strains conserved by the Chinese Center For Disease Control And Prevention were cultured in Middlebrook 7H9 broth (supplemented with glycerol and polysorbate 80) in combination with Middlebrook albumin-dextrose-catalase (ADC) enrichment or 7H10 agar solid media supplemented with oleic acid-albumin-dextrose-catalase (OADC) enrichment (ADC + 0.003% oleic acid) (Allen, 1998). *Escherichia coli* (*E. coli*) DH5α and *E. coli* BL21 (DE3) plyS (TransGen Biotech, Inc., Beijing, China) were cultured in Luria–Bertani (LB) broth or on LB agar plates. Plasmid pET28a (+) was conserved by our lab and plasmid pAZI9479 was kindly gifted by Professor Francesca Forti (Forti et al., 2009). Kanamycin was added at concentrations of 100 μg/mL for *E. coli*, while hygromycin was added at 200 μg/mL for *Escherichia coli* and at 100 μg/mL for Mtb. Isopropyl β-D-1-thiogalactopyranoside (IPTG) was used as an inducer to express DdlA in *E. coli* BL21 (DE3) plyS, and pristinamycin (Santa Cruz Biotech, Santa Cruz, CA, United States) was used to induce gene expression in Mtb.

Molecular Manipulations

The Mtb H37Rv genome was extracted from the log phase cells as previously described in Mtb protocols (Gordhan and Parish, 2001). All PCR reagents were purchased from TransGen Biotech. The primers for amplification *ddl*A were designed using software primer 5.0 based on the sequence in the NCBI database (GenBank accession number: 888415). The primers *ddl*A F (5'-AAAAGAATTCGTGAGTGCTAACGACCGGC-3′) and *ddl*A R (5′-AAAAAAGCTTCTAGTGCAGGCCCACGCCG-3′) were used to amplify the whole fragment of *ddl*A for protein expression, and primers *ddl*AM F (5′-AATTCCATGGGTGAGTGCTAACGACCGGC-3′) and *ddl*AM R (5′-CGCCCATATGGGGTTTGACGAACACCGGTA-3′) were used to synthesize the former fragment of *ddl*A for constructing a conditional mutant strain. The lineated parts of the sequences denote the limited digestion sites (*Eco*RI, *Hin*dIII, *Nco*I, and *Nde*I).

The purified PCR product of the *ddl*A gene was cloned into plasmid pET28a (+)*Eco*RI-*Hin*dIII sites to generate pET28a (+)-*ddl*A; the fragment of *ddl*AM was cloned into pAZI9479 *Nco*I-*Nde*I sites to obtain pAZI9479-DM. Sequencing was subsequently performed to ensure that there were no mutations.

Construction of the Conditional Mutant Bacteria

The bacteria and plasmids were treated as previously described (Meng et al., 2015). First, 1 μg of UV-illuminated plasmid pAZI9479-DM (no more than 5 μL) was mixed with 200 μL of competent cells in a 0.2-cm electroporation cuvette (Bio-rad, Hercules, CA, United States), and the cuvette was pulsed at a strength of 2.5 kV, 25 uF, and 1000 Ω resistance with a Gene Pulser Xcell (Bio-rad). These bacteria were resuscitated in 5 mL of 7H9 broth for 24 h at 37°C and were then spread on 7H10 plates containing 0.5 μg/mL of pristinamycin and 100 μg/mL of hygromycin that were incubated at 37°C for 4 weeks until colonies formed. Plasmid-positive bacteria were determined via sequencing, and the resultant mutant strain was designated as Mtb-KD.

Expression and Purification of DdlA

The log-phase *E. coli* BL21 (DE3) pLysS-bearing plasmid pET28a (+)-*ddl*A were induced by IPTG (final concentration of 0.3 mM) at 28°C for 8 h, and the recombinant protein carrying a hexahistidine tag at the N-terminal was purified by Ni^{2+} ion-affinity chromatography using a bouncing gradient of 40–100–200–400 mM imidazole in washing buffer (20 Mm of Tris–HCl, pH of 8.0, 500 mM of NaCl, 1 mM of dithiothreitol). The eluted fractions were analyzed by SDS-PAGE and were visualized with Coomassie Brilliant Blue R-250 gel staining. The purified DdlA was desalted on a PD-10 column (GE Healthcare, Piscataway, NJ, United States), concentrated through a 10-kDa cut-off Millipore Centricon device (Millipore, Billerica, MA, United States), and was stored at −80°C with 50% glycerol. The concentration of the enzyme was identified via the BCA protein assay kit (TransGen Biotech).

Kinetic Analysis of DdlA

The activity of DdlA was monitored by coupling with pyruvate kinase (PK) and lactate dehydrogenase (LDH; Sigma-Aldrich) to detect the release of ADP. Reactions were proceeded in 96-well plates (at 37°C) containing 50 mM of Tris–HCl (pH 8.0), 10 mM of $MgCl_2$, 10 mM of KCl, 1 mM of dithiothreitol, 250 μM of ATP, 1000 μM of D-alanine (D-Ala), 1 mM of phosphoenolpyruvic acid (PEP), 0.5 mM of NADH, 2 μg of DdlA, 1 U of pyruvate

kinase (PK) and 1 U of lactate dehydrogenase (LDH). The assay system was monitored via a Perkin Elmer EnSpire® 2300 Multimode Plate Reader (PerkinElmer, MA, United States) by detecting decreases in NADH.

The calibration curve of the ultraviolet absorption of NADH at 340 nm to its concentrations was fabricated before studying the enzymatic kinetics of DdlA. The kinetic parameters of DldA were determined using serial twofold dilutions of one substrate (from 1 mM to 31.25 μM), while the other substrate was held constant at 1 mM. Km and Vmax values were calculated using non-linear regression of the Michaelis-Menten model in GraphPad Prism 5.0 (GraphPad Software, Inc., San Diego, CA, United States). Kcat was calculated based on the molecular weight of DdlA (42 kDa).

Screening of Inhibitors

A high-throughput screening assay was designed according to kinetic parameters. Systems containing 1 μL of dimethyl sulfoxide (DMSO) were used as negative controls, while the positive control systems contained heat-inactivated DdlA. Specifically, 1 μL of samples diluted at 2 mg/mL were added to a 96-well plate with a final concentration of 20 μg/mL. Parameters signal window, Z′ factor, and an assay variability ratio were used to assess the reliability of the model (Iversen et al., 2006). Via this model, we screened through 150,000 synthetic compounds. The inhibition rate was calculated as follows:

$$\mathrm{IR} = \left(1 - \frac{\mathrm{A}p - \mathrm{A}s}{\mathrm{A}p - \mathrm{A}n}\right) \times 100\%$$

in which the IR, A*n*, A*s*, and A*p* denote the inhibition rate and the ultraviolet absorption of the negative control, sample, and positive control, respectively. The IR threshold was defined at 30%. The IRs of inhibitors in twofold serial dilutions to DdlA were detected to calculate their IC_{50} values using the non-linear regression module of GraphPad Prism 5.0. The reaction rates of systems containing various concentrations of substrate (100, 200, 300, 400, 500, and 600 μM) and inhibitors (10 or 40 μg/mL) were detected to determine their inhibitory modes. Lineweaver-Burk plots and Dixon plots were applied to analyze the results.

Antibacterial Activity *in vitro*

The minimal inhibitory concentration (MIC) of IMB-0283 (J&K Chemical Company, Beijing, China, synthesized by Enamine) to Mtb was determined as previously described (Darby and Nathan, 2010). Briefly, the mid-log phase H37Rv and the other clinical drug-resistant strains were ultrasonically suspended and adjusted to a final concentration of 1–2 × 10^5 CFU/mL in 7H9 broth. Then, 100 μL of suspension was exposed to the compound in serial twofold dilutions, from 128 μg/mL to 0.063 μg/mL, in 96-well plates in triplicate. INH and RMP were used as positive controls. After 2 weeks of incubation at 37°C, the viability of bacteria was detected using a resazurin microtiter assay (Montoro et al., 2005). The synergistic effects of IMB-0283 with INH and RMP were tested as previously described (Shen et al., 2010). INH and RMP were twofold diluted from 16 μg/mL to 0.008 μg/mL, and their MIC values to H37Rv were determined when the concentration of IMB-0283 was set at 0.25 × MIC.

The sensitivity of Mtb-KD cultured with higher or lower concentrations of pristinamycin (0.1 and 0.1 × 10^{-4} μg/mL) to IMB-0283 was tested to confirm if it interacted with DdlA in bacteria, and DCS was used as a positive control.

Morphology of Mtb Treated With IMB-0283

The log phase of Mtb H37Rv was treated with 0.35 μg/mL of IMB-0283 and was incubated for 12 h or 7 days, and Mtb morphological transformations were detected as previously described (Shen et al., 2010). The washed bacterial pellets were spotted on Si chips (Ted Pella, Inc., Redding, CA, United States) and were fixed with 2.5% glutaraldehyde. The chips were washed and dehydrated in a graded ethanol series. Samples were coated with Au/Pd (E-1045 ion sputter coater, Hitachi High Technologies Co., Tokyo, Japan) after being critical point-dried (Bal-Tec CPD 030 Critical Point Dryer, Bal-Tec AG, Liechtenstein, Germany). The bacteria morphologies were surveyed by a Quanta200 scanning electron microscope (FEI, Oregon, United States).

Cytotoxicity Assay

HepG2 cells (*ATCCHB-8065*) and Vero green-monkey kidney cells (*ATCCC1008*) were cultured in Dulbecco's modified eagle's medium (DMEM) supplemented with 10% fetal bovine serum (FBS) and 1% antibiotics (100 U/mL penicillin), and were incubated at 5% CO_2 in a humidified atmosphere at 37°C (Heracell 150, Thermo Electron Corp., Waltham, MA, United States). After 24 h of incubation, the adhered exponential cells (1 × 10^5 cells/100 μL) were washed three times with fresh medium. IMB-0283 was added at a triple dilution from 900 μg/mL to 1.23 μg/mL with the medium, while DCS was diluted from 3000 μg/mL to 4.11 μg/mL. DMSO (1%) was added to induce a solvent effect, and normal-growth cells were used as negative controls. 3-[4, 5-dimethylthiazol-2-yl]-2, 5-diphenyl tetrazolium bromide (MTT) were used to detect cell viability at 2 days later (Correia et al., 2014). TC_{50} values were calculated using non-linear regression (curve fit) of the log inhibitor vs. the normalized response-variable slope module of GraphPad Prism 5.0.

IMB-0283 Activity in a Mouse Model of TB

Specific pathogen-free (SPF) male Balb/c mice were purchased from the Institute of Laboratory Animal Sciences at the Chinese Academy of Medical Sciences and Peking Union Medical College. All animal experiments were supervised and approved by the Institutional Animal Care and Use Committee of the Institute of Medicinal Biotechnology. Twenty-six mice (6–8 weeks old, 18–20 g) were infected with Mtb H37Rv (about 100 CFU) via the 099C A4224 Inhalation Exposure System (Glas-col, Terre Haute, IN, United States). At 15 days after inoculum, two mice were anesthetized and decapitated to confirm the success of infection. DCS, INH, IMB-0283, and vehicle (0.5% CMC-Na) were administered through a gavage route (six mice per group). All chemicals were dosed at 25 mg/kg. Mice were sacrificed after

15 administrations (five times per week) to quantify pulmonary bacterial loads via counting CFUs.

RESULTS

Expression, Purification, and Kinetic Characterization of DdlA

The protein, DdlA, was purified from *E. coli* BL21 (DE3) pLysS-harboring pET28a (+)-ddlA via immobilized metal affinity chromatography with Ni^{2+}-NTA agarose. The purified protein was verified by SDS-PAGE (**Figure 1**), and DdlA (42 kDa) was visualized between 35 and 48 kDa.

The initial reaction rate of DdlA was determined by correlating the concentrations of ATP and D-Ala to the UV absorbances of NADH. The reaction rates of DdlA affected by concentrations of substrates were detected to calculate its enzymatic kinetic parameters (**Figure 2** and **Table 1**). The Kms for ATP and D-Ala were 450.6 μM and 1780 μM, respectively, and their Vmax values were 20.29 $\mu Mmin^{-1}$ and 36.61 $\mu Mmin^{-1}$, respectively. Kcat values, calculated by dividing Vmax with the enzyme concentration, for ATP and D-Ala were 405.8 min^{-1} and 732.19 min^{-1}, respectively. These results were consistent with those reported previously (Prosser and de Carvalho, 2013).

HTS Assay and Identification of DdlA Inhibitor

The A high-throughput screening assay was established according to the enzymatic parameters of DdlA. The signal window, Z′-factor and assay variability ratio of the screening model were 12.87, 0.76, and 0.24, respectively, indicating that it was a reliable screening model. Via this model, 48 compounds (inhibition ratio ≥ 30%) were obtained from our library (the positive rate was 0.032%). Among these inhibitors, IMB-0283 displayed the most potent inhibitory activity to DdlA, with an IC_{50} of 6.16 μM (**Figure 3**).

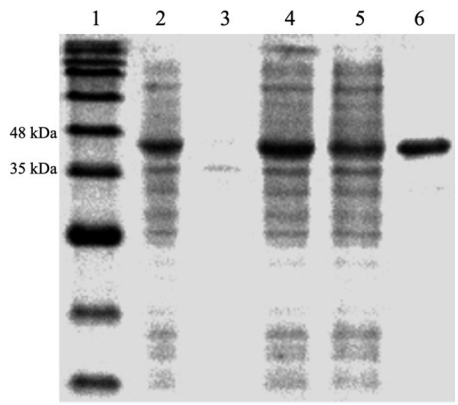

FIGURE 1 | SDS-PAGE analysis of the expression and purification of enzyme DdlA. Lane 1 represents the pre-sharp protein standard. Lane 2 shows the whole protein of the recombinant cell. Lane 3 shows the precipitate protein. Lane 4 shows the supernatant fluid. Lane 5 shows the effluent liquid. Lane 6 shows the purified DdlA.

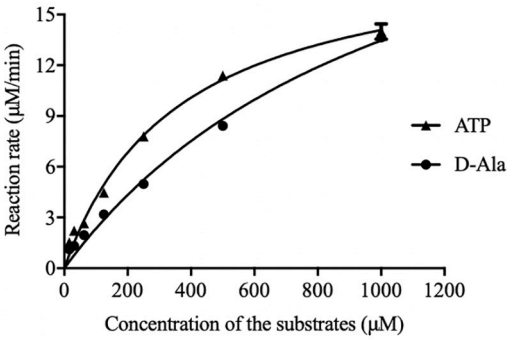

FIGURE 2 | Initial reaction rates of DdlA affected by concentration of ATP and D-Ala. The kinetics parameters of DdlA were calculated via the Michaelis-Menten model. The reaction rates affected by ATP and D-Ala (which were twofold diluted from 1 mM to 31.25 μM) were detected to calculate the kinetic parameters via non-linear regression of the Michaelis-Menten model in GraphPad Prism 5.0 (n = 3).

TABLE 1 | Kinetic parameters of DdlA.

Substrate	Km (μM)	Vmax ($\mu Mmin^{-1}$)	Kcat[a] (min^{-1})
ATP	359.90 ± 30.53	19.15 ± 0.705	383.00 ± 14.14
D-Ala	1113.00 ± 153.90	28.44 ± 2.444	568.79 ± 48.93

Kcat[a] was calculated via Vmax/[E].

The reaction rates of the assays affected by various concentrations of inhibitors and substrates were measured to analyze inhibitory modes and to calculate Ki values. IMB-0283 competed with both substrates of DdlA with Ki values of 4.444 μM (ATP) and 32.647 μM (D-Ala) (**Figure 4**). Ki values of DCS for these substrates were 106.599 μM and 182.108 μM, indicating that IMB-0283 had a better affinity to DdlA compared to that of DCS.

Anti-tuberculosis Activity of IMB-0283

IMB-0283 potently inhibited H37Rv at an MIC of 0.5 μg/mL, while the MIC of DCS was 16 μg/mL. IMB-0283 also displayed antibacterial activity to several clinical strains, with MICs ranging from 0.5 μg/mL to 4.0 μg/mL (**Table 2**), while DCS did not show any inhibitory effect. These results indicated that IMB-0283 had no cross-resistance with that of conventional anti-TB drugs.

The MIC of INH against H37Rv was reduced eightfold, from 0.125 μg/mL to 0.016 μg/mL, when combined with IMB-0283 at 0.125 μg/mL. For RMP, the MIC decreased from 0.063 μg/mL to 0.016 μg/mL. This finding suggests that there is a synergistic effect between IMB-0283 and either INH or RMP.

IMB-0283 Intracellularly Interacts With DdlA

A fragment (about 600 bp) of *ddl*A starting from ATG was cloned into pAZI9479 to generate pAZI9479KD. The mutant Mtb-KD was generated by inserting pAZI9479KD into the Mtb

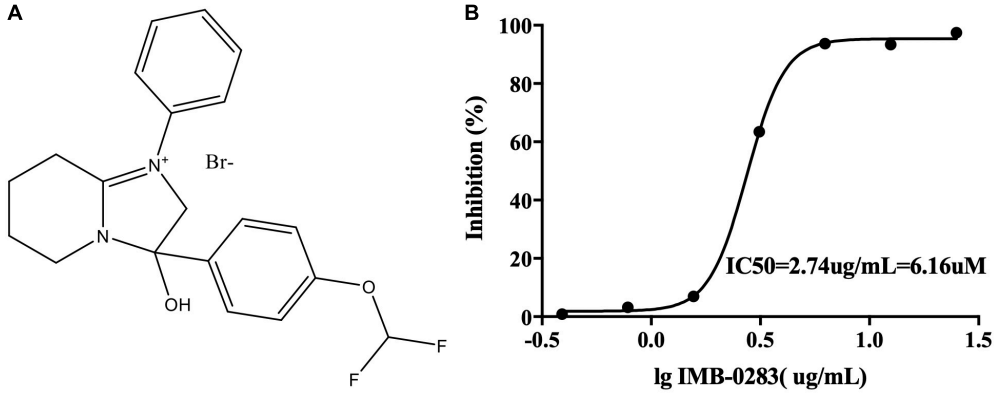

FIGURE 3 | The structure of IMB-0283 and its IC_{50} value for DdlA. **(A)** The structure of IMB-0283. **(B)** The IC_{50} value of IMB-0283 to DdlA. Results are presented as the mean ± SD (n = 3).

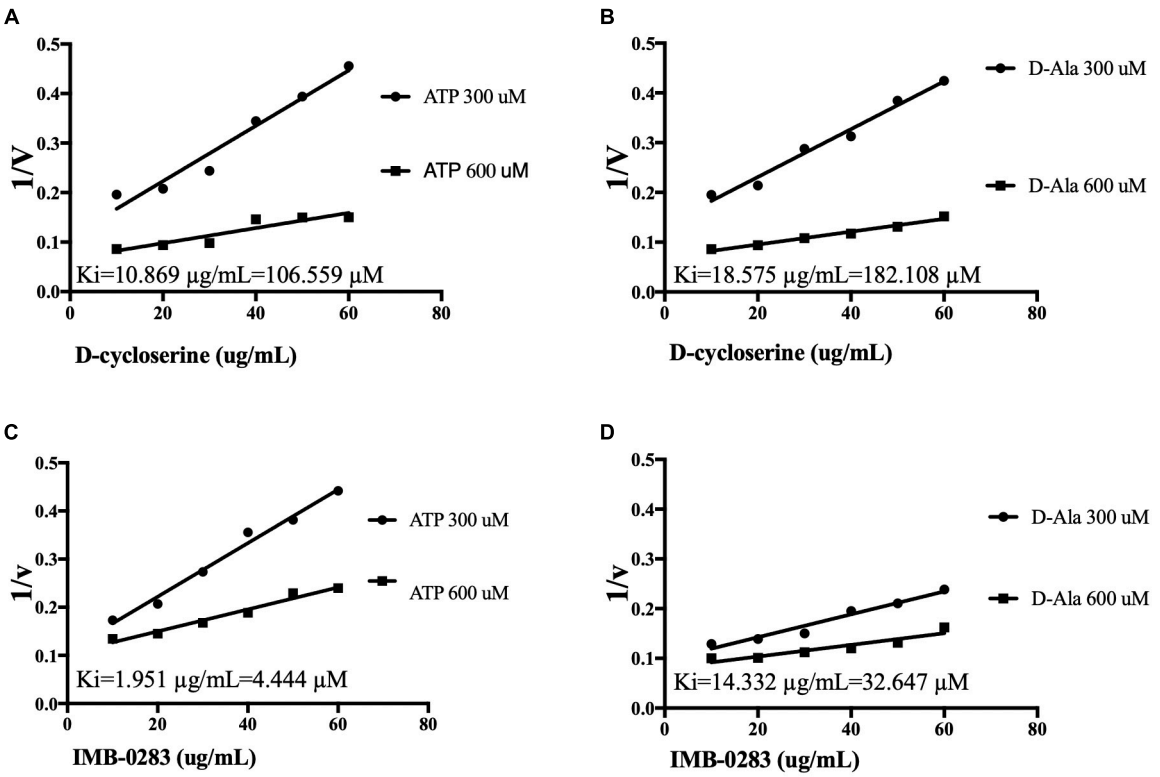

FIGURE 4 | Ki values of inhibitors calculated by Dixon-plots for DdlA. Reactions were monitored when inhibitors varied from 10 to 60 μg/mL, while one substrate was fixed at 1000 μM and the other substrate was either 300 or 600 μM (n = 3). Panels **(A,B)** show the Ki values of DCS to DdlA. Panels **(C,D)** show the Ki values of IMB-0283 to the enzyme.

chromosome. In this mutant strain, the expression of *ddl*A was under the control of pristinamycin. A higher concentration of pristinamycin (0.1 μg/mL) led to overexpression of *ddlA*, while a lower concentration of pristinamycin (0.1×10^{-4} μg/mL) corresponded to knock-down of *ddlA*. **Figure 5A** shows that the mutant bacteria were not able to grow on the 7H10 plates without pristinamycin, while the growth of wild-type Mtb was independent of pristinamycin. These results demonstrate that DalA was essential for Mtb. Susceptibilities of Mtb-KD cultured with different concentrations of inducer to IMB-0283 were detected to confirm whether the lethal effect was dependent on inhibiting DdlA intracellularly. When the *ddlA* gene was knocked-down, IMB-0283 and DCS inhibited the mutant at 0.25 μg/mL and 1 μg/mL, respectively. Their MIC values climbed to 2 μg/mL and 32 μg/mL, respectively, when the *ddlA* gene was overexpressed (**Figure 5B**). Consistent

TABLE 2 | Anti-tuberculous activity of IMB-0283.

Mtb strains	Drug sensitivity background*							MIC (μg/mL)
	INH	RMP	EMB	STR	CPM	KAN	OFX	
H37RV	S	S	S	S	S	S	S	0.5
FJ05349	S	S	S	S	S	S	S	0.5
FJ05060	S	S	S	S	S	S	S	0.5
FJ05195	R	R	R	R	S	R	R	4.0
FJ05120	R	R	S	S	S	S	S	2.0
FJ05189	R	R	S	S	S	S	S	1.0
xz	R	R	S	R	R	S	R	4.0

INH, isoniazid; RMP, rifampin; EMB, ethambutol; STR, streptomycin; CPM, cefpiramide; KAN, kanamycin; OFX, ofloxacin; MIC, minimum inhibitory concentrations; S, sensitive; R, resistant.

with the findings of DCS, the divergences of MIC values indicated that IMB-0283 inhibited Mtb bacteria in a DdlA-dependent manner.

Morphological Alterations of Mtb Treated With IMB-0283

Morphological changes of Mtb treated with IMB-0283 were monitored to determine whether the inhibitor of DdlA altered the shape of Mtb. Mtb bacteria had a typical long-rod morphology resembling the log phase of bacteria at 12 h after treatment (**Figures 6A,B**). Shapes of these bacteria changed dramatically by 7 days after exposure to IMB-0283, during which they became shrunken, shorter, and fragmented (**Figure 6C**). These results indicate that IMB-0283 inhibited and killed Mtb by inhibiting cell-wall synthesis but not destroying mature cell walls.

Cytotoxicity of IMB-0283

Next, the TC_{50} values of IMB-0283 to HepG2 and Vero cells were evaluated (**Table 3**). Although the TC_{50} values of DCS for these mammalian cells were larger than 1,000 μg/mL, the SI index of DCS was only about 80. While the TC_{50} values of IMB-0283 for HepG2 and Vero cells were 115.4 μg/mL and 249.8 μg/mL, respectively, the SI index of IMB-0283 was far greater than 200. These results indicated that IMB-0283 might be safer than DCS.

IMB-0283 Activity in a Mouse Model of TB

Finally, the antibacterial activity of IMB-0283 in a mouse model of TB was evaluated (**Figure 7**). After 15 administrations (five times per week) at a dosage of 25 mg/kg, INH reduced the Mtb load in mouse lungs from 5.58 to 3.29 (log CFU/mL), but DCS did not yield any antibacterial activity ($P > 0.5$). IMB-0283 significantly decreased the bacteria load to 4.40, exhibiting much more potent antibacterial capacity than that of DCS ($P < 0.0001$).

DISCUSSION

The selection of a specific therapeutic target for high-throughput screening determines the output of lead compounds; hence,

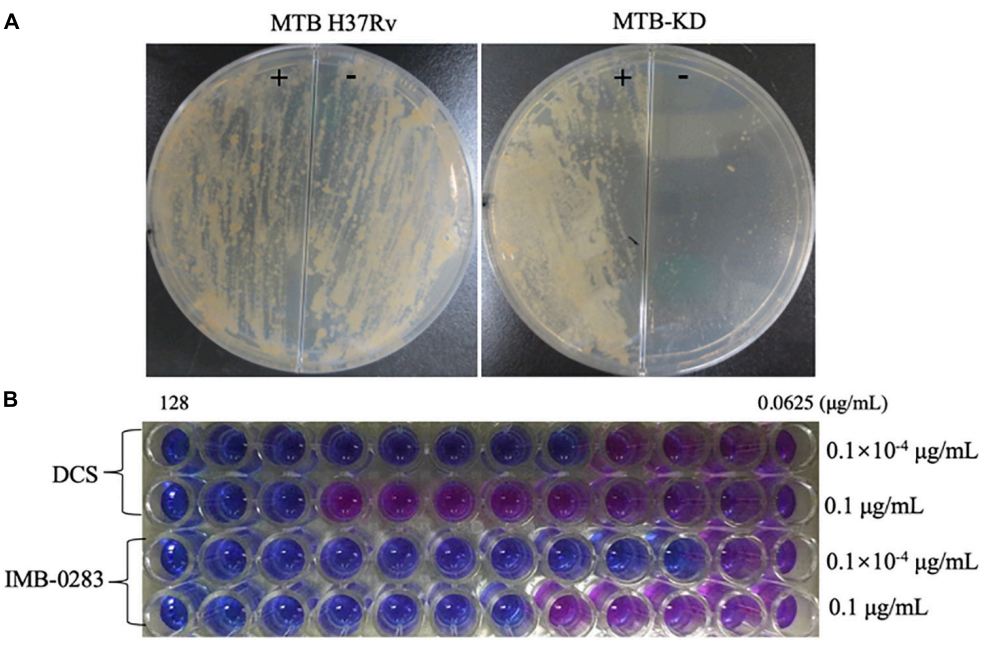

FIGURE 5 | DdlA is essential for Mtb growth and IMB-0283 inhibits Mtb growth in a DdlA-dependent manner. A conditional mutant strain, Mtb-KD, and its sensitivities to DCS and IMB-0283 were confirmed by culturing with different concentrations of pristinamycin. **(A)** Wild-type and mutant Mtb H37Rv were lineated on 7H10 solid medium in the presence (+) or absence (–) of 0.1 μg/mL of pristinamycin; the former formed lawns on the medium independent of the presence of the inducer, while the latter formed colonies only on the medium containing inducer. **(B)** DCS inhibited mutant Mtb at 1 μg/mL or 32 μg/mL when cultured with 0.1×10^{-4} μg/mL (repressed) or 0.1 μg/mL (induced) of inducer. At the same conditions, IMB-0283 inhibited the mutant strain at either 0.25 or 2 μg/mL.

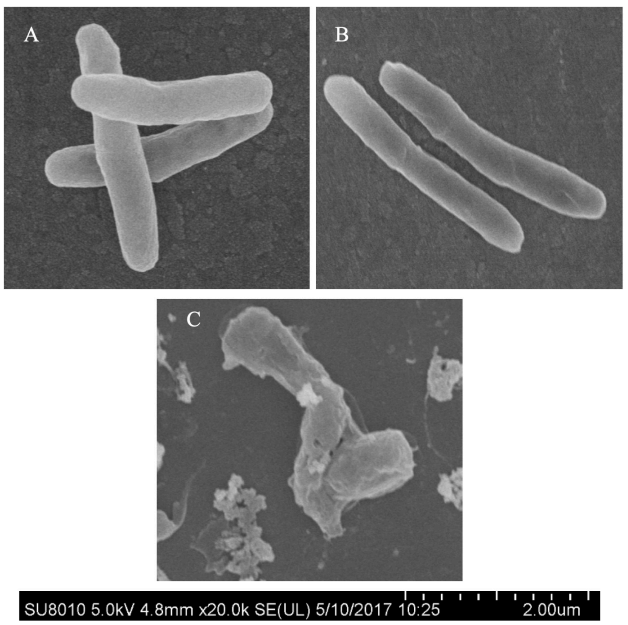

FIGURE 6 | Morphological transformations of Mtb treated with IMB-0283. **(A)** The log phase Mtb. **(B)** Mtb treated with IMB-0283 for 12 h. Bacteria in **(A,B)** were uniform and exhibited a typical long-rod morphology. **(C)** Morphologies of Mtb treated for 7 days became shrunken, shorter, and fragmented.

TABLE 3 | Cytotoxicity profiles of IMB-0283 compared with those of DCS.

Compound	MTBH37Rv	HepG2		Vero	
	MIC (μg/mL)	TC_{50} (μg/mL)	SI	TC_{50} (μg/mL)	SI
DCS	16	1380	86.25	2044	127.75
IMB-0283	0.5	115.4	230.8	249.8	499.6

DCS, D-cycloserine; MIC, minimum inhibitory concentrations; SI, selective index which was calculated via TC_{50}/MIC.

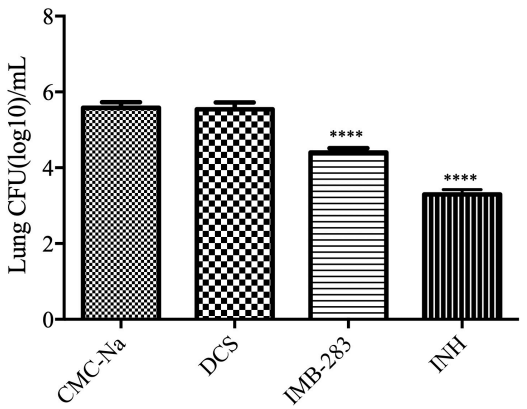

FIGURE 7 | Bacteriostatic activity of IMB-0283 in BALB/C mice. DCS, IMB-0283, and INH were each administered at 25 mg/kg 15 times, and the vehicle CMC-Na was used as a negative control. INH and IMB-0283 reduces the bacterial load in lungs from 5.58 to 3.29 or 4.40 (log CFU/mL), respectively, but DCS showed no antibacterial activity ($P > 0.5$). ****Statistically significant difference from the negative control ($P < 0.0001$; $n = 6$).

it is questionable to establish high-throughput screening models based on essential gene products to search for inhibitors, as there are often considerable discrepancies between the essentiality and drugability of the resultant proteins (Gashaw et al., 2011). Therefore, we aimed to identify and test novel anti-mycobacterial compounds based on previously confirmed drug targets. The integrity of the cell wall is vital in supporting cell growth and virulence, as well as in influencing antimicrobial resistance (Abrahams and Besra, 2018). The processes for synthesizing and assembling cell walls have been targeted by several chemotherapeutics (Bhat et al., 2017). The reticular peptidoglycan of Mtb not only withstands exoteric osmotic pressure, but also provides anchor sites for other cell-wall components (Kieser and Rubin, 2014). The generation of peptidoglycans starts from the synthesis of intracellular glycopeptide precursors that are matured by conjugating with d-alanyl-d-alanine. The synthesis of this dipeptide can be interrupted by DCS, and DdlA has been shown to be the primary target of DCS (Halouska et al., 2014). Although the severe side effects of DCS have limited its application in TB treatment, it has been demonstrated that DdlA is much more stable genetically than other anti-TB drug targets (McGrath et al., 2014). Therefore, researchers have attempted to exploit novel inhibitors that may supersede DCS (Wu et al., 2008; Triola et al., 2009; Vehar et al., 2011; Ameryckx et al., 2018). However, most screening assays have been carried out using DdlB of *E. coli*, the crystal structure of which is distinct from that of DdlA in Mtb (Bruning et al., 2011). Whether or not these inhibitors inhibit the growth of Mtb has not yet been reported. Consequently, there has been a continued need to search for novel inhibitors of Mtb DdlA specifically.

In the present study, a credible high-throughput screening model was established to search for specific inhibitors of Mtb DdlA from our chemical library. The cut-off value was set at 30% to obtain as many compounds as possible and to exclude ineffective inhibitors. Forty-eight compounds were obtained that had considerable inhibitory capacities to the Mtb enzyme. Among these chemicals, IMB-0283 competitively inhibited DdlA similar to that of DCS, and it nearly equally inhibited both standard and clinical drug-resistant Mtb strains. IMB-0283 also exhibited bacteriostatic effects of both INH and RMP *in vitro*. We consulted PubChem for analogs of IMB-0283 for further information. There were 238 similar analogs that were obtained via PubChem, but little information regarding their biological activities were reported. This suggested that IMB-0283 may represent the first of this category to be found to inhibit Mtb. Future studies should test the inhibitory capacities of a series of several derivatives to DdlA of Mtb to analyze the structure-activity relationships of IMB-0283, which may provide clues to further optimize IMB-0283. Through

measuring sensitivities of our conditional mutant strain, Mtb-KD, cultured with low or high inducers to IMB-0283, we found that IMB-0283 inhibited the catalytic activity of DdlA intracellularly. Although the larger divergences in enzyme-inhibitory and antibacterial activities suggested that DdlA may not be the primary target of IMB-0283, IMB-0283 can interfere with the formation of cell walls but do not damage mature cell walls. Compared with properties of DCS, IMB-0283 exhibited less cellular toxicity and more bacteriostatic activity in a mouse model of TB.

Although the present study elucidated that IMB-0283 may represent a promising drug for the TB treatment, further research is needed to better understand its underlying mechanisms and to further confirm its low toxicity. In future studies, we plan to investigate the interactions of IMB-0283 with DdlA through crystallization, by which we may be able to optimize IMB-0283 in order to develop more potent and specific inhibitors. Additionally, we plan to screen for resistant Mtb strains to evaluate the probability to generate IMB-0283-resistant mutations, as well as to expound upon mechanisms by which IMB-0283 inhibit Mtb. Lastly, comprehensive studies should be conducted to determine the adsorption, distribution, metabolism, excretion, and toxicity (ADMET) properties of these IMB-0283-modified compounds. Through these future studies, we expected to identify other promising anti-TB agents based on IMB-0283.

DATA AVAILABILITY STATEMENT

The raw data supporting the conclusions of this article will be made available by the authors, without undue reservation, to any qualified researcher.

ETHICS STATEMENT

The animal study was reviewed and approved by the Institutional Animal Care and Use Committee of the Institute of Medicinal Biotechnology.

AUTHOR CONTRIBUTIONS

JM and PG: experimental operation and manuscript preparation. XW and YG: data collection. YL: data analysis. CX: literature search and experimental design.

FUNDING

This study was supported by the National Major Scientific and Technological Special Project for "Significant New Drugs Development" (Grant No. 2015ZX09102007-009) and AMS Initiative for Innovative Medicine (Grant No. 2016-I2M-1-013), the National Natural Science Foundation of Chinese (81803412 and 81903678), and the Fundamental Research Funds for Central Public-interest Scientific Institution (Centre for Tuberculosis) (Grant No. 2017PT31010).

ACKNOWLEDGMENTS

We are very grateful to Prof. Chuanyou Li (Beijing Chest Hospital, Capital Medical University and Beijing Tuberculosis and Thoracic Tumor Research Institute, China) for his guidance and assistance in the manipulation of *Mycobacterium tuberculosis*.

REFERENCES

Abrahams, K. A., and Besra, G. S. (2018). Mycobacterial cell wall biosynthesis: a multifaceted antibiotic target. *Parasitology* 145, 116–133. doi: 10.1017/s0031182016002377

Allen, B. W. (1998). "Mycobacteria: general culture methodology and safety considerations," in *Mycobacteria Protocols*, eds T. Parish, and N. G. Stoker (Totowa, NJ: Humana Press), 15–30. doi: 10.1385/0-89603-471-2:15

Ameryckx, A., Thabault, L., Pochet, L., Leimanis, S., Poupaert, J. H., Wouters, J., et al. (2018). 1-(2-Hydroxybenzoyl)-thiosemicarbazides are promising antimicrobial agents targeting D-alanine-D-alanine ligase in bacterio. *Eur. J. Med. Chem.* 159, 324–338. doi: 10.1016/j.ejmech.2018.09.067

Bhat, Z. S., Rather, M. A., Maqbool, M., Lah, H. U. L., Yousuf, S. K., and Ahmad, Z. (2017). Cell wall: a versatile fountain of drug targets in Mycobacterium tuberculosis. *Biomed. Pharmacother.* 95, 1520–1534. doi: 10.1016/j.biopha.2017.09.036

Bruning, J. B., Murillo, A. C., Chacon, O., Barletta, R. G., and Sacchettini, J. C. (2011). Structure of the *Mycobacterium tuberculosis* D-alanine:D-alanine ligase, a target of the antituberculosis drug D-cycloserine. *Antimicrob. Agents Chemother.* 55, 291–301. doi: 10.1128/AAC.00558-10

Correia, I., Adão, P., Roy, S., Wahba, M., Matos, C., Maurya, M. R., et al. (2014). Hydroxyquinoline derived vanadium(IV and V) and copper(II) complexes as potential anti-tuberculosis and anti-tumor agents. *J. Inorg. Biochem.* 141, 83–93. doi: 10.1016/j.jinorgbio.2014.07.019

Darby, C. M., and Nathan, C. F. (2010). Killing of non-replicating *Mycobacterium tuberculosis* by 8-hydroxyquinoline. *J. Antimicrob. Chemother.* 65, 1424–1427. doi: 10.1093/jac/dkq145

Forti, F., Crosta, A., and Ghisotti, D. (2009). Pristinamycin-inducible gene regulation in mycobacteria. *J. Biotechnol.* 140, 270–277. doi: 10.1016/j.jbiotec.2009.02.001

Gashaw, I., Ellinghaus, P., Sommer, A., and Asadullah, K. (2011). What makes a good drug target? *Drug Discov. Today* 16, 1037–1043. doi: 10.1016/j.drudis.2011.09.007

Gordhan, B. G., and Parish, T. (2001). "Gene replacement using pretreated DNA," in *Mycobacterium Tuberculosis Protocols*, eds T. Parish, and N. G. Stoker, (Totowa, NJ: Humana Press), 77–92. doi: 10.1385/1-59259-147-7:077

Halouska, S., Fenton, R. J., Zinniel, D. K., Marshall, D. D., Barletta, R. G., and Powers, R. (2014). Metabolomics analysis identifies D-alanine-D-alanine ligase as the primary lethal target of D-cycloserine in Mycobacteria. *J. Proteome Res.* 13, 1065–1076. doi: 10.1021/pr4010579

Iversen, P. W., Eastwood, B. J., Sittampalam, G. S., and Cox, K. L. (2006). A comparison of assay performance measures in screening assays: signal window, Z′ factor, and assay variability ratio. *J. Biomol. Screen.* 11, 247–252. doi: 10.1177/1087057105285610

Kass, J. S., and Shandera, W. X. (2010). Nervous system effects of antituberculosis therapy. *CNS Drugs* 24, 655–667. doi: 10.2165/11534340-000000000-00000

Kieser, K. J., and Rubin, E. J. (2014). How sisters grow apart: mycobacterial growth and division. *Nat. Rev. Microbiol.* 12, 550–562. doi: 10.1038/nrmicro3299

McGrath, M., Gey van Pittius, N. C., van Helden, P. D., Warren, R. M., and Warner, D. F. (2014). Mutation rate and the emergence of drug resistance in *Mycobacterium tuberculosis*. *J. Antimicrob. Chemother.* 69, 292–302. doi: 10.1093/jac/dkt364

Meng, J. Z., Yang, Y. H., Xiao, C. L., Guan, Y., Hao, X. Q., Deng, Q., et al. (2015). Identification and validation of aspartic acid semialdehyde dehydrogenase as a new anti-mycobacterium tuberculosis target. *Int. J. Mol. Sci.* 16, 23572–23586. doi: 10.3390/ijms161023572

Montoro, E., Lemus, D., Echemendia, M., Martin, A., Portaels, F., and Palomino, J. C. (2005). Comparative evaluation of the nitrate reduction assay, the MTT test, and the resazurin microtitre assay for drug susceptibility testing of clinical isolates of *Mycobacterium tuberculosis*. *J. Antimicrob. Chemother.* 55, 500–505. doi: 10.1093/jac/dki023

Prosser, G. A., and de Carvalho, L. P. S. (2013). Kinetic mechanism and inhibition of *Mycobacterium tuberculosis* D-alanine:D-alanine ligase by the antibiotic D-cycloserine. *FEBS J.* 280, 1150–1166. doi: 10.1111/febs.12108

Shen, G. H., Wu, B. D., Hu, S. T., Lin, C. F., Wu, K. M., and Chen, J. H. (2010). High efficacy of clofazimine and its synergistic effect with amikacin against rapidly growing mycobacteria. *Int. J. Antimicrob. Agents* 35, 400–404. doi: 10.1016/j.ijantimicag.2009.12.008

Triola, G., Wetzel, S., Ellinger, B., Koch, M. A., Hübel, K., Rauh, D., et al. (2009). ATP competitive inhibitors of D-alanine–D-alanine ligase based on protein kinase inhibitor scaffolds. *Bioorg. Med. Chem.* 17, 1079–1087. doi: 10.1016/j.bmc.2008.02.046

Vehar, B., Hrast, M., Kovaè, A., Konc, J., Mariner, K., Chopra, I., et al. (2011). Ellipticines and 9-acridinylamines as inhibitors of D-alanine:D-alanine ligase. *Bioorg. Med. Chem.* 19, 5137–5146. doi: 10.1016/j.bmc.2011.07.020

WHO, (2018). *Global Tuberculosis Report 2018*. Geneva: World Health Organization.

Wu, D. L., Kong, Y. H., Han, C., Chen, J., Hu, L. H., Jiang, H. L., et al. (2008). D-alanine:D-alanine ligase as a new target for the flavonoids quercetin and apigenin. *Int. J. Antimicrob. Agents* 32, 421–426. doi: 10.1016/j.ijantimicag.2008.06.010

Conflict of Interest: The authors declare that the research was conducted in the absence of any commercial or financial relationships that could be construed as a potential conflict of interest.

frontiers in Microbiology

ORIGINAL RESEARCH
published: 15 January 2020
doi: 10.3389/fmicb.2019.02918

Genomic Insights Into the *Mycobacterium kansasii* Complex: An Update

Tomasz Jagielski[1†], Paulina Borówka[2,3], Zofia Bakuła[1], Jakub Lach[2,4], Błażej Marciniak[2,4], Anna Brzostek[5], Jarosław Dziadek[5], Mikołaj Dziurzyński[6], Lian Pennings[7], Jakko van Ingen[7], Manca Žolnir-Dovč[8] and Dominik Strapagiel[2,4*†]*

[1] Department of Applied Microbiology, Faculty of Biology, Institute of Microbiology, University of Warsaw, Warsaw, Poland, [2] Biobank Lab, Department of Molecular Biophysics, Faculty of Biology and Environmental Protection, University of Łódź, Łódź, Poland, [3] Department of Anthropology, Faculty of Biology and Environmental Protection, University of Łódź, Łódź, Poland, [4] BBMRI.pl Consortium, Wroclaw, Poland, [5] Institute of Medical Biology, Polish Academy of Sciences, Łódź, Poland, [6] Department of Bacterial Genetics, Faculty of Biology, Institute of Microbiology, University of Warsaw, Warsaw, Poland, [7] Department of Medical Microbiology, Radboud University Medical Center, Nijmegen, Netherlands, [8] Laboratory for Mycobacteria, University Clinic of Respiratory and Allergic Diseases, Golnik, Slovenia

OPEN ACCESS

Edited by:
Miguel Viveiros,
New University of Lisbon, Portugal

Reviewed by:
Igor Mokrousov,
Saint Petersburg Pasteur Institute, Russia
Vikram Saini,
All India Institute of Medical Sciences, India

***Correspondence:**
Tomasz Jagielski
t.jagielski@biol.uw.edu.pl
Dominik Strapagiel
dominik.strapagiel@biol.uni.lodz.pl

†These authors have contributed equally to this work

Specialty section:
This article was submitted to Antimicrobials, Resistance and Chemotherapy, a section of the journal Frontiers in Microbiology

Received: 24 August 2019
Accepted: 04 December 2019
Published: 15 January 2020

Citation:
Jagielski T, Borówka P, Bakuła Z, Lach J, Marciniak B, Brzostek A, Dziadek J, Dziurzyński M, Pennings L, van Ingen J, Žolnir-Dovč M and Strapagiel D (2020) Genomic Insights Into the Mycobacterium kansasii Complex: An Update. Front. Microbiol. 10:2918. doi: 10.3389/fmicb.2019.02918

Only very recently, has it been proposed that the hitherto existing *Mycobacterium kansasii* subtypes (I–VI) should be elevated, each, to a species rank. Consequently, the former *M. kansasii* subtypes have been denominated as *Mycobacterium kansasii* (former type I), *Mycobacterium persicum* (II), *Mycobacterium pseudokansasii* (III), *Mycobacterium innocens* (V), and *Mycobacterium attenuatum* (VI). The present work extends the recently published findings by using a three-pronged computational strategy, based on the alignment fraction-average nucleotide identity, genome-to-genome distance, and core-genome phylogeny, yet essentially independent and much larger sample, and thus delivers a more refined and complete picture of the *M. kansasii* complex. Furthermore, five canonical taxonomic markers were used, i.e., 16S rRNA, *hsp65*, *rpoB*, and *tuf* genes, as well as the 16S-23S rRNA intergenic spacer region (ITS). The three major methods produced highly concordant results, corroborating the view that each *M. kansasii* subtype does represent a distinct species. This work not only consolidates the position of five of the currently erected species, but also provides a description of the sixth one, i.e., *Mycobacterium ostraviense* sp. nov. to replace the former subtype IV. By showing a close genetic relatedness, a monophyletic origin, and overlapping phenotypes, our findings support the recognition of the *M. kansasii* complex (MKC), accommodating all *M. kansasii*-derived species and *Mycobacterium gastri*. None of the most commonly used taxonomic markers was shown to accurately distinguish all the MKC species. Likewise, no species-specific phenotypic characteristics were found allowing for species differentiation within the complex, except the non-photochromogenicity of *M. gastri*. To distinguish, most reliably, between the MKC species, and between *M. kansasii* and *M. persicum* in particular, whole-genome-based approaches should be applied. In the absence of clear differences in the distribution of the virulence-associated region of difference 1 genes among the *M. kansasii*-derived species, the pathogenic potential of each of these species can only be speculatively assessed based on their prevalence among the clinically relevant population. Large-scale molecular epidemiological studies

are needed to provide a better understanding of the clinical significance and pathobiology of the MKC species. The results of the *in vitro* drug susceptibility profiling emphasize the priority of rifampicin administration in the treatment of MKC-induced infections, while undermining the use of ethambutol, due to a high resistance to this drug.

Keywords: *Mycobacterium kansasii* complex, *Mycobacterium ostraviense* sp. nov., non-tuberculous mycobacteria (NTM), whole genome sequencing, taxonomy

INTRODUCTION

Non-tuberculous mycobacteria (NTM) comprise all species of the *Mycobacterium* genus, except those aetiologically implicated in tuberculosis (TB) and leprosy, that is members of the *M. tuberculosis* complex and *M. leprae* or *M. lepromatosis*, respectively. More than 180 NTM species have been recognized to date (LPSN database, 2019). This figure, however, will soon need to be revised, since several new species, on average, are continuously being added every year (Tortoli, 2014). With the increasing number of mycobacterial species descriptions, the number of reported infections, essentially due to NTM, is also growing on a global level. Not as much an enlarging spectrum of NTM species, but more a heightened clinical awareness, expanding population of vulnerable hosts, and advancement of diagnostic and surveillance services are responsible for this scenario (Sood and Parrish, 2017). Although many of the newly described NTM species are potentially pathogenic, having been isolated from clinically affected individuals, only less than a third has consistently been associated with significant health disorders in humans.

Mycobacterium kansasii is one of the most virulent and prevalent NTM pathogen in human medicine. It was first described by Buhler and Pollak in 1953 from a series of respiratory samples of patients with a TB-like pulmonary disease (Buhler and Pollak, 1953). The species was originally named a "yellow bacillus" to emphasize its brilliant yellow pigmentation on exposure to light, but amended thereupon to *M. tuberculosis luciflavum* by Middlebrook (Middlebrook, 1956) and *M. luciflavum* by Manten (Manten, 1957). The current species name (*M. kansasii*) was proposed by Hauduroy in 1955 and refers to where its first isolations were performed (Kansas City, USA) (Hauduroy, 1955). Since the early 1960s, *M. kansasii* infections have been among the very top of all NTM diseases reported worldwide. A remarkable upsurge in the incidence of *M. kansasii* infections was seen at the turn of 1980s and 1990s, with the burgeoning of the HIV/AIDS epidemic, and persisted until the first antiretroviral therapies became widely available (Horsburgh and Selik, 1989; Witzig et al., 1995; Santin and Alcaide, 2003). Currently, *M. kansasii* is one of the six most frequently isolated NTM species across the world. The prevalence of this pathogen is exceptionally high in Slovakia, Poland, and the UK, with the isolation rate of 36, 35, and 11%, respectively, compared to a mean isolation rate of 5% in Europe and 4% globally (Hoefsloot et al., 2013). Chronic, fibro-cavitary lung disease, with upper lobe predominance, and with an overall clinical picture mimicking classical TB, is the most common manifestation attributable to *M. kansasii* (Matveychuk et al., 2012; Moon et al., 2015; Bakuła et al., 2018b). Much rarer are extrapulmonary infections, such as lymphadenitis, skin and soft-tissue infections, and disseminated disease (Liao et al., 2007; Chen et al., 2008; Park et al., 2012; Shaaban et al., 2014). The exact epidemiology of *M. kansasii* disease is difficult to ascertain because case reporting is not mandatory in most countries and differentiation between isolation (colonization) and infection may be diagnostically challenging. Moreover, the incidence rates are influenced by a combination of demographic and clinical factors, including patient geographical origin and HIV status. Pulmonary *M. kansasii* infections tend to cluster in specific geographical areas, such as central Europe or metropolitan centers of London, Brasilia, and Johannesburg (Hoefsloot et al., 2013). Strong epidemiological disparities exist in terms of HIV reactivity. The annual rate of *M. kansasii* infection among HIV-seropositive patients has been reported to be as high as 532 per 100,000 population, whereas in non-HIV infected individuals it has been calculated at 0.06–2.2 per 100,000 population (Marras and Daley, 2004; Ricketts et al., 2014). Not only the incidence rates, but also the sources of *M. kansasii* infections and routes of transmission are poorly defined. Similar to other NTM, *M. kansasii* infections are believed to be acquired from environmental exposures rather than by person-to-person transmission, although a case of interfamilial clustering has been described (Ricketts et al., 2014). Contrary to other NTM, *M. kansasii* has only sporadically been isolated from soil, natural water systems or animals. Instead, the pathogen has often been recovered from municipal tap water, which is considered its major environmental reservoir (Falkinham, 1996; Thomson et al., 2013).

The genetic structure of *M. kansasii* was first investigated in the early 1990s. A pioneering work by Ross et al. showed the existence of a genetic subspecies of *M. kansasii* by sequencing of the 5′ end of the 16S rRNA gene (Ross et al., 1992). Subsequent studies involving the amplification of the 16S-23S rRNA spacer region (Abed et al., 1995), PCR-restriction analysis (PRA) of the highly-conserved *hsp65* gene (Plikaytis et al., 1992; Telenti et al., 1993) and Southern blot hybridization with the major polymorphic tandem repeat (MPTR) (Hermans et al., 1992) or insertion sequence-like element, IS*1652* (Yang et al., 1993) as a probe have confirmed *M. kansasii* as a genetically heterogeneous species. The genetic variability of *M. kansasii* was clearly demonstrated in a study of Picardeau et al. who divided the species into five subspecies or (sub-)types, based on the analysis of restriction fragment length polymorphisms (RFLPs) using the MPTR probe, pulsed-field gel electrophoresis (PFGE), amplified fragment length polymorphism (AFLP) analysis, and

PRA of the *hsp65* gene (Picardeau et al., 1997). The validity of the five *M. kansasii* subtypes was further corroborated by sequencing of the 16S-23S rRNA gene or internal transcribed spacer (ITS) region (Alcaide et al., 1997). Somewhat later, two novel types (VI and VII) have been described, according to their *hsp65* restriction profiles and sequencing results of the 16S rRNA gene and the 16S-23S rRNA spacer (Richter et al., 1999; Taillard et al., 2003). Moreover, *M. kansasii* isolates with an intermediate type I (I/II) and atypical type II (IIb) have been reported. Whereas, the former had type I-specific sequence of the *hsp65* gene and type II-specific sequence of the spacer region, the latter displayed type II-specific spacer sequence and a unique *hsp65* gene sequence (Iwamoto and Saito, 2005). The separateness of the *M. kansasii* subspecies was further supported by polymorphisms at other genetic loci, including the RNA polymerase gene (*rpoB*) and the translational elongation factor Tu (*tuf*), successfully applied for the differentiation between the subspecies I-VI (Kim et al., 2001; Bakuła et al., 2016). Noteworthy, the inter-subspecies differences have been detected at the protein level. For each of the six (I–VI) *M. kansasii* subspecies, specific matrix-assisted laser desorption-ionization time-of-flight (MALDI TOF) mass spectral profiles have recently been established (Murugaiyan et al., 2018).

Finally, the genetic diversity of *M. kansasii* exists not only between the subspecies but also between strains of the same subspecies. This has been repeatedly evidenced upon AFLP, PFGE, repetitive unit (rep-)PCR profiling (Alcaide et al., 1997; Iinuma et al., 1997; Picardeau et al., 1997; Gaafar et al., 2003; Zhang et al., 2004; Wu et al., 2009; Thomson et al., 2014; Kwenda et al., 2015; Bakuła et al., 2018a) and more recently, by a newly developed typing method, based on the analysis of variable number of tandem repeat (VNTR) loci (Bakuła et al., 2018a).

Across all genetic studies performed so far on *M. kansasii*, a controversy has been growing over the taxonomic rank of the genetic variants of the species, best reflected by their terminology, which includes subspecies, subtypes, and genotypes.

The purpose of this study was to resolve the phylogenetic and taxonomic structure of *M. kansasii* by combining whole genome sequencing with traditional polyphasic classification approaches. The use of a polyphasic strategy, incorporating phylogenetic, biochemical, and chemotaxonomic criteria for resolving the taxonomic identity of mycobacterial species, especially within the NTM group, has been heavily advocated (Saini et al., 2009).

The issue of molecular taxonomy of *M. kansasii* has been addressed in a very recent work by Tagini et al. (2019), which appeared shortly before the completion of our own draft. The present study extends the recently published findings by using a new independent sample and somewhat different methodology, and thus delivers a more refined and complete picture of the *M. kansasii* complex.

MATERIALS AND METHODS

Strains and Culture Conditions

A total of 27 *M. kansasii* strains were used in the study (**Table 1**). Included in this number were 21 single-patient, epidemiologically unrelated, clinical isolates and 6 environmental isolates. The strains were originally recovered before 2016 from 8 countries, i.e., the Netherlands ($n = 8$), Poland ($n = 5$), the Czech Republic ($n = 4$), Spain ($n = 2$), Belgium ($n = 1$), Germany ($n = 3$), South Korea ($n = 3$), and Italy ($n = 1$). Patients from whom the strains had been collected were classified as having, or not, a pulmonary NTM disease according to the criteria of the American Thoracic Society (ATS) (Griffith et al., 2007). The type strains of *M. kansasii* (ATCC 12478^T), *M. gastri* (DSM 43505^T), *M. marinum* (DSM 44344^T), *M. szulgai* (DSM 44166^T), *M. conspicuum* (DSM 44136^T), *M. riyadhense* (DSM 45176^T). and *M. tuberculosis* H37Rv were also included in the study.

All strains were maintained as frozen stocks and cultured on Löwenstein-Jensen or Middlebrook 7H10 agar (Becton-Dickinson, Franklin Lakes, USA) medium, supplemented with oleic acid, albumin, dextrose, and catalase, and incubated at either 30 or 37°C.

Species Identification and Genotyping

The strains were identified as *M. kansasii* by using high pressure liquid chromatography (HPLC) of cell wall mycolic acids, in accordance with the Centers for Disease Control and Prevention (CDC) guidelines (Butler et al., 1996) and by the GenoType Mycobacterium CM/AS assay (Hain Lifescience, Nehren, Germany), according to the manufacturer's instructions. For genotypic identification, total DNA was purified from solid bacterial cultures with a standard extraction method described previously (Santos et al., 1992). Genotyping of *M. kansasii* strains was performed by PCR-RFLP analysis of the *hsp65*, *rpoB*, and *tuf* genes, as reported elsewhere (Telenti et al., 1993; Kim et al., 2001; Bakuła et al., 2016).

Biochemical Profiling

The strains were evaluated for a panel of biochemical characteristics by conventional laboratory procedures (CLSI; Clinical and Laboratory Standards Institute, 2011). These comprised tests for niacin accumulation, nitrate and tellurite reduction, Tween 80 hydrolysis (10 days), catalase (thermostable and semi-quantitative), β-glucosidase, arylsulfatase (3 and 14 days), urease (5 days), and pyrazynamidase. Inhibition tests of tolerance to thiphene-2-carboxylic acid hydrazide (TCH), 5% sodium chloride, and acidic (pH 5.5) conditions were also carried out. In addition, cultural features, including colony morphology, photochromogenicity, the ability to grow on MacConkey agar without crystal violet, and at different temperatures (25, 35, and 45°C) were assessed. For each assay, each strain was tested in triplicate. Only if at least two replications produced identical results, the test was considered complete.

Drug Susceptibility Testing

To test antimicrobial susceptibility, minimal inhibitory concentrations (MICs) for 13 drugs, including isoniazid (INH), rifampicin (RMP), streptomycin (STR), ethambutol (EMB), clarithromycin (CLR), amikacin (AMK), rifabutin (RFB), moxifloxacin (MFX), ciprofloxacin (CFX), co-trimoxazole (SXT), linezolid (LZD), doxycycline (DOX), and ethionamide (ETO), were determined by the microdilution method, using the Sensititre® SLOMYCO plates (TREK Diagnostic Systems, Cleveland, USA), following the Clinical and Laboratory

TABLE 1 | Epidemiological, microbiological, and clinical characteristics of *M. kansasii* strains under the study.

No.	ID	Type[a]	Strain no.	Collected at[b]	Collection date	Geographic location	Host disease	Isolation source[c]	PCR-RFLP			PCR-sequencing[d]				GenBank no.
									hsp65	*rpoB*	*tuf*	*hsp65*	*rpoB*	*tuf*	ITS	
1	5MK	I*	NLA001000521	RUMC	2010	Nijmegen, Netherlands	NTM disease	BAL	I	I	I	ND	I	ND	95%	MWKY01
2	6MK	I	ATCC25221	FB	1968	Borstel, Germany	NTM disease	sputum	I	I	I	I	I	ND	I	CP019885
3	1MK	I	NLA001000927	RUMC	2010	Nijmegen, Netherlands	NTM disease	sputum	I	I	I	I	I	ND	I	CP019883
4	4MK	I	NLA001000449	RUMC	2010	Nijmegen, Netherlands	NTM disease	sputum	I	I	I	I	I	I	I	CP019884
5	10MK	I	6200	WMU	2008	Warsaw, Poland	NTM disease	sputum	I	I	I	I	I	ND	I	CP019886
6	9MK	I	7728	WMU	2009	Warsaw, Poland	NTM disease	BW	I	I	I	I	I	ND	I	CP019888
7	11MK	I	7744	WMU	2009	Warsaw, Poland	NTM disease	BW	I	I	I	I	I	ND	I	CP019887
8	5JD	I	1010001495	RUMC	ND	Czech Republic	NA	water	I	I	I	I	I	ND	I	LWCL01
9	K4	I	K4	SMC	2008	Ulsan, South Korea	NTM disease	sputum	HaeIII: I BstEII: II	I	I	96%	I	I	I	NKQW01
10	K14	I**	K14	SMC	2011	Seoul, South Korea	NTM disease	sputum	HaeIII: I BstEII: II	II	II	96%	95%	97%	95%	NKQY01
11	K19	I**	K19	SMC	2012	Seoul, South Korea	none	sputum	HaeIII: I BstEII: II	II	II	96%	95%	97%	95%	NKQX01
12	12MK	II	2193	WMU	2011	Warsaw, Poland	none	BW	II	II	II	97%	95%	ND	95%	MWQA01
13	3MK	II	NLA001001128	RUMC	2010	Nijmegen, the Netherlands	none	BAL	II	II	II	96%	95%	ND	96%	MWKX01
14	7MK	II	B11073207	RUMC	2011	Nijmegen, Netherlands	none	sputum	II	II	II	97%	95%	ND	95%	MWKZ01
15	8MK	II	B11063838	RUMC	2011	Nijmegen, Netherlands	none	BAL	II	II	II	96%	95%	97%	96%	MWKV01
16	3B/6JD	II	1010001469	RUMC	ND	Italy	NA	water	II	II	II	97%	95%	ND	95%	LWCM01
17	H47	II	H47	HB	1999	Bilbao, Spain	NTM disease	sputum	II	II	II	ND	ND	ND	ND	NKRA01
18	H48	II	H48	HB	1999	Bilbao, Spain	none	sputum	II	II	II	ND	ND	ND	ND	NKQZ01
19	14_15	III	14_15	IPH	2015	Šumperk, Czech Rep.	none	sputum	III	III	III	ND	ND	ND	ND	NKRB01
20	174_15	III	174_15	IPH	2015	Karviná, Czech Rep.	NTM disease	sputum	III	III	III	ND	ND	ND	ND	NKRD01
21	3JD	III	1010001468	RUMC	ND	Belgium	NA	soil	III	III	III	ND	96%	95%	91%	LWCJ01
22	2JD	IV	1010001458	RUMC	ND	Germany	NA	tap water	III	III	III	97%	93%	96%	93%	LWCI01
23	241/15	IV	241/15	IPH	2015	Karviná, Czech Rep.	none	sputum	IV	IV	IV	ND	ND	ND	ND	NKRE01
24	1JD	V	1010001454	RUMC	ND	Germany	NA	tap water	V	V	V	95%	96%	96%	92%	LWCH01
25	4JD	V	1010001493	RUMC	ND	The Netherlands	NA	water	V	V	V	95%	97%	96%	93%	LWCK01
26	49_15	V	49_11	HID	2011	Warsaw, Poland	none	BW	V	V	V	ND	ND	ND	ND	NKRC01
27	2MK	VI	NLA001001166	RUMC	2010	Nijmegen, Netherlands	none	sputum	VI	VI	VI	96%	92%	94%	91%	MWKW01

[a]According to the WGS-based (MiSI method) grouping; M. kansasii strains NLA001000521, K14, and K19 had originally been described as types I/II (*) and IIb (**), based on the PCR-RFLP/PCR-sequencing analysis of the hsp65, rpoB, and/or tuf genes.

[b]RUMC, Radboud University Medical Center, Nijmegen, the Netherlands; FB, Forschungszentrum Borstel, Germany; WMU, Department of Internal Medicine, Pulmonology, and Allergology, Warsaw Medical University, Warsaw, Poland; SMC, Department of Medicine, Samsung Medical Center, Sungkyunkwan University School of Medicine, Seoul, South Korea; HB, Hospital de Basurto, Bilbao, Spain; IPH, Institute of Public Health in Ostrava, Czech Republic; HID, Hospital of Infectious Diseases in Warsaw, Poland.

[c]BAL, bronchoalveolar lavage; BW, bronchial washing.

[d]M. kansasii type was established based on at least 99% similarity of a query sequence with the respective one of the M. kansasii ATCC12478 (type I) reference strain. For other than type I strains, similarity of the query sequence with the respective sequence of the M. kansasii ATCC12478 reference strain was indicated.

NA, not applicable; ND, no data.

TABLE 2 | Genome features of *M. kansasii* strains under the study.

No.	ID	Type[a]	Strain no.	Sequencing platform	Genome size (bp)	Coverage	GenBank no.
1	5MK	I*	NLA001000521	MiSeq	6 649 816	44.6	MWKY01
2	6MK	I	ATCC25221	MiSeq	6 462 452	36	CP019885
3	1MK	I	NLA001000927	MiSeq	6 421 275	35	CP019883
4	4MK	I	NLA001000449	MiSeq	6 440 784	39	CP019884
5	10MK	I	6200	MiSeq	6 421 364	39	CP019886
6	9MK	I	7728	MiSeq	6 463 923	33	CP019888
7	11MK	I	7744	MiSeq	6 434 062	45.8	CP019887
8	5JD	I	1010001495	NextSeq 500	6 358 240	28	LWCL01
9	K4	I	K4	NextSeq 500	6 503 804	58	NKQW01
10	K14	I**	K14	NextSeq 500	6 640 863	60	NKQY01
11	K19	I**	K19	NextSeq 500	6 652 978	60	NKQX01
12	12MK	II	2193	MiSeq	6 254 980	33	MWQA01
13	3MK	II	NLA001001128	MiSeq	6 251 123	46	MWKX01
14	7MK	II	B11073207	MiSeq	6 123 476	34.6	MWKZ01
15	8MK	II	B11063838	MiSeq	6 126 434	44	MWKV01
16	3B/6JD	II	1010001469	NextSeq 500	6 266 032	34	LWCM01
17	H47	II	H47	NextSeq 500	6 238 170	53	NKRA01
18	H48	II	H48	NextSeq 500	6 217 650	29	NKQZ01
19	14_15	III	14_15	HiSeq2500	6 363 138	293	NKRB01
20	174_15	III	174_15	HiSeq2500	6 342 319	173	NKRD01
21	3JD	III	1010001468	NextSeq 500	6 141 835	24	LWCJ01
22	2JD	IV	1010001458	NextSeq 500	6 027 332	37	LWCI01
23	241/15	IV	241/15	HiSeq2500	6 093 288	147	NKRE01
24	1JD	V	1010001454	NextSeq 500	6 171 688	25	LWCH01
25	4JD	V	1010001493	NextSeq 500	5 627 124	29	LWCK01
26	49_11	V	49_11	HiSeq2500	6 634 420	280	NKRC01
27	2MK	VI	NLA001001166	MiSeq	6 443 486	33	MWKW01

[a]*According to the WGS-based (MiSI method) grouping; M. kansasii strains NLA001000521, K14, and K19 had originally been described as types I/II (*) and IIb (**), based on the PCR-RFLP/PCR-sequencing analysis of the hsp65, rpoB, and/or tuf genes.*

Standards Institute (CLSI) recommendations (CLSI; Clinical and Laboratory Standards Institute, 2011).

Genome Sequencing and Assembly

For the whole-genome sequencing, chromosomal DNA from all 27 *M. kansasii* strains under the study was extracted by mechanical cell (100 mg pellet) disruption by using zirconia ceramic beads in a FastPrep-24 instrument (MP Biomedicals, Valiant Co., Yantai, China) and further extracted chemically followed with a DNAzol® reagent (Invitrogen, Carlsbad, USA).

DNA concentration, its purity and integrity was determined using a Qubit high-sensitivity (HS) assay kit (ThermoFisher, Waltham, USA).

Paired-end libraries were prepared from 1 ng of high-quality genomic DNA with the Nextera XT DNA sample preparation kit according to the manufacturer's instructions (Illumina Inc., San Diego, USA). The libraries were sequenced on a HiSeq 2500 or a NextSeq 500 instrument (Illumina, San Diego, USA) at a read length of 2 × 150 bp. The quality of reads before and after pre-processing was assessed using FastQC (v0.11.5) (Andrews, 2010). The raw reads were trimmed with TrimGalore ver. 0.43 (http://www.bioinformatics.babraham.ac.uk/projects/trim_galore/), and *de novo* assembled with the SPAdes Genome Assembler ver. 3.10.0 (Nurk et al., 2013). Scaffold-level assembly was tested using Quast (QUality ASsesment Tool) (Gurevich et al., 2013) to generate basic genome statistics.

In addition to genomes of 27 *M. kansasii* strains, sequenced in this study, genomes of other 53 *Mycobacterium* sp. strains were analyzed. The genomic sequences of these strains were retrieved from the GenBank database (http://www.ncbi.nlm.nih.gov/genbank/) and their appropriate accession numbers were provided in **Supplementary Table 6**.

Genomic Data Availability

The assembled genomes were deposited under NCBI BioProject accession numbers: PRJNA374853 and PRJNA317047. The genomes were deposited in the GenBank under accession numbers provided in **Table 1** and **Supplementary Table 6**.

Annotation and Comparative Genome- and Gene-Scale Analyses

Gene identification and annotation were achieved using the DFAST pipeline v1.0.5 with default settings (Tanizawa et al., 2017).

The genomic relatedness between the strains analyzed was assessed using the MiSI (Microbial Species Identifier) method, based on a combination of genome-wide average nucleotide identity (gANI) and alignment fraction (AF) of orthologous genes (Varghese et al., 2015). The gANI and AF values of 96.5 and 0.6, respectively, were assumed as cutoffs for species delimitation.

As a second method to evaluate the genomic relatedness, the Genome-to-Genome Distance Calculator (GGDC at http://ggdc.dsmz.de) was used. This algorithm was designed to replace standard DNA–DNA hybridization (DDH) by calculating DNA-DNA relatedness (Meier-Kolthoff et al., 2013a).The genome-to-genome distance (GGD) value of 0.0258 was identified as a maximum threshold to assign a genome pair to the same species.

The pairwise ANI and AF values were determined from using ANIcalculator (v1.0) (Yoon et al., 2017).

Full-length sequences of the 16S rRNA (1537 bp; MH794239.1), *hsp65* (664 bp; NC_000962.3:528608–530230), *rpoB* (3439 bp; C_000962.3:759807–763325), *tuf* (1191 bp; NC_000962.3:784821–786011) genes, and the 16S-23S rRNA intergenic spacer region (ITS) (358 bp; AL123456.3:1473359–1473716) were extracted from the whole-genome sequence of the *M. tuberculosis* reference strain H37Rv, using CLC Genomic Workbench 10 (Qiagen, Valencia, USA), and were used, each, as a reference for alignments with the respective sequences of other mycobacterial species. Sequences from the same loci of the draft genomes analyzed were identified using the blastn algorithm. Due to a significant variation of the sought sequences, whenever necessary, they were extracted manually or downloaded from the NCBI database (https://www.ncbi.nlm.nih.gov/).

Identification of RD1-14 Genes

To establish the presence of genes within 14 regions of deletions RD1-14, DIFFIND software with -c 0.7 (sequence identity threshold) and -s2 0.5 (length difference cut-off) parameters was used (Marciniak et al., 2017). Identification of RD1-14 genes was based on the alignment of amino acid sequences of predicted genes from the analyzed genomes to the reference database. As references were used amino acid sequences produced by RD1-14 genes from the *M. tuberculosis* reference strain H37Rv (Accession no.: NC_000962.3) and listed by Brosch et al. (2002).

Phylogenetic Analysis

Core-genome single-ortholog tree was built as described previously (Tagini et al., 2019). Briefly, OrthoFinder (ver. 2.3.4) and MAFFT (ver. 7.310) were used to create core-genome concatemers for the analyzed genomes (Katoh and Standley, 2013; Emms and Kelly, 2019), which were submitted to FastTree (version 2.1.11 Double precision) for maximum-likelihood core-genome phylogeny calculations (Price et al., 2010). The tree was midpoint rooted in FigTree version 1.4.4 (https://github.com/rambaut/figtree).

For single-gene phylogenies, the respective sequences of each genetic locus were subjected to multiple alignment in MEGA X software (ClustalW algorithm) (Kumar et al., 2018). The resulting fragments were further trimmed to remove unnecessary gaps or regions, to a final length of 1,537, 644, 3,439, 1,180, and 277 bp for 16S RNA *hsp65*, *rpoB*, *tuf*, and 16S-23S rRNA ITS region, respectively. The so prepared sequences were used for evolutionary distance calculation according to the Jukes-Cantor model (Jukes and Cantor, 1969). Phylogenetic trees for each target locus sequences were built using the neighbor-joining method and midpoint rooted with the MEGA X software (Saitou and Nei, 1987). Tree topologies were evaluated by bootstrap analysis based on 1,000 replications (Felsenstein, 1985).

Furthermore, a concatenated tree was constructed based on the 16sRNA, *rpoB*, and *hsp65* gene sequences combined. Sequence concatenation was performed with Sequence Matrix 1.8 software (Vaidya et al., 2011), further corrected in Geneious Prime (Kearse et al., 2012), and plotted in MEGA X. Sequence similarity matrices were generated using Bioedit ver. 7.0.5 (IDENTIFY matrice) (Hall, 1999).

RESULTS AND DISCUSSION

Sequencing of 27 *M kansasii* genomes yielded a mean coverage of 66.4x per genome. The average number of contigs per genome was 129 (±229) corresponding to an average N50 score of 4933 kb (±2,605 kb).

The genome sizes and GC contents ranged from 5.6 to 6.6 Mbp (avg. 6.2 Mbp ± 0.3 Mbp) and from 65.86 to 66.38 (avg. 66.14 ± 0.10), respectively. These values were consistent with the data reported for previously assembled *M. kansasii* genomes (**Table 2**).

The whole-genome-level relatedness among the 27 *M. kansasii* strains under the study was assessed with three species identification-relevant parameters, namely the alignment fraction (AF) of orthologous genes, the average nucleotide identity (ANI), and the genome-to-genome distance (GGD) (**Tables 3** and **4**). The AF/ANI metrics were also computed for genomic sequences of another 32 *M. kansasii* strains and 24 *Mycobacterium* sp. strains, representing 5 NTM species and 5 *M. tuberculosis* complex species, all extracted from NCBI databases (**Supplementary Table 6**). Whereas, the GGD analysis was performed on 69 genomes in total, including 59 *M. kansasii* genomes and 10 genomes representing single NTM (other than *M. kansasii*) and *M. tuberculosis* complex species (**Supplementary Table 6**).

The AF values for all *M. kansasii* strains ranged between 0.6 and 1.0. The lowest AF value recorded for two strains, members of the same *M. kansasii* genotype was 0.69 (type I, range 0.69–1.0). Within all other types, the AF values were 0.85 or higher.

All *M. kansasii* genotypes showed AF values equal to or below 0.75 with strains of other *Mycobacterium* species, except for *M. gastri* and *M. persicum*, which yielded AF values as high as 0.86 with *M. kansasii* type IV and V (range, 0.79–0.86) or 0.99 with *M. kansasii* type II (range, 0.89–0.99), respectively (**Table 3A**).

Pairwise ANI values for any *M. kansasii* strains affiliated with different types never exceeded the 95–96% threshold (range, 88.6–94.9%), commonly used as a boundary of species delineation (Richter and Rosselló-Móra, 2009; Varghese et al., 2015). Whereas, the ANI values for strains of the same *M. kansasii* genotype were always higher than 98.8%. The ANI values between *M. kansasii* and other *Mycobacterium*

TABLE 3 | Pairwise alignment fractions (**A**) and average nucleotide identities (**B**) for *M. kansasii* subtypes and outgroup species.

Subtype/group[a]	*M. kansasii* I	*M. kansasii* II+	*M. kansasii* II	*M. persicum*	*M. kansasii* III	*M. kansasii* IV	*M. kansasii* V	*M. kansasii* VI	MTBC	*M. tuberculosis*	*M. africanum*	*M. bovis*	*M. caprae*	*M. microti*	*M. conspicuum*	*M. gastri*	*M. marinum*	*M. riyadhense*	*M. szulgai*
A																			
M. kansasii I	**0.69–1.0**																		
M. kansasii II+	0.65–0.9	**0.89–0.99**																	
M. kansasii II	0.65–0.89	0.89–0.99	**0.91–0.99**																
M. persicum	0.65–0.9	0.89–0.99	0.89–0.99	**0.92–0.99**															
M. kansasii III	0.64–0.87	0.75–0.86	0.75–0.85	0.76–0.86	**0.85–0.99**														
M. kansasii IV	0.63–0.85	0.78–0.84	0.78–0.84	0.79–0.84	0.74–0.84	**0.97**													
M. kansasii V	0.61–0.89	0.75–0.88	0.75–0.88	0.77–0.87	0.73–0.89	0.81–0.88	**0.85–0.98**												
M. kansasii VI	0.64–0.87	0.8–0.86	0.8–0.85	0.8–0.86	0.74–0.84	0.76–0.82	0.75–0.86	**0.9–0.98**											
MTBC	0.4–0.75	0.48–0.75	0.48–0.75	0.49–0.74	0.47–0.74	0.52–0.75	0.51–0.74	0.49–0.74	**0.9–1.0**										
M. tuberculosis	0.41–0.73	0.5–0.73	0.5–0.73	0.51–0.72	0.48–0.73	0.54–0.73	0.53–0.72	0.5–0.72	0.91–0.99	**0.95–0.99**									
M. africanum	0.4–0.74	0.5–0.74	0.5–0.74	0.51–0.73	0.48–0.73	0.54–0.74	0.53–0.73	0.49–0.73	0.92–0.99	0.93–0.97	**0.96–0.99**								
M. bovis	0.4–0.75	0.49–0.75	0.49–0.75	0.5–0.74	0.47–0.74	0.53–0.75	0.52–0.74	0.49–0.74	0.9–1.0	0.91–0.97	0.93–0.98	**0.96–1.0**							
M. caprae	0.4–0.73	0.5–0.73	0.5–0.73	0.51–0.72	0.48–0.73	0.54–0.73	0.53–0.73	0.49–0.72	0.92–0.97	0.93–0.97	0.95–0.97	0.94–0.97	–*						
M. microti	0.4–0.7	0.48–0.7	0.48–0.7	0.49–0.7	0.47–0.7	0.52–0.7	0.51–0.7	0.49–0.69	0.9–0.94	0.91–0.93	0.92–0.93	0.9–0.94	0.92–0.92	–*					
M. conspicuum	0.45–0.6	0.55–0.59	0.55–0.58	0.55–0.59	0.53–0.59	0.56–0.6	0.54–0.62	0.56–0.59	0.43–0.65	0.45–0.64	0.44–0.64	0.44–0.65	0.44–0.63	0.43–0.62	–*				
M. gastri	0.6–0.84	0.74–0.83	0.74–0.83	0.75–0.82	0.72–0.84	0.82–0.86	0.79–0.86	0.73–0.81	0.54–0.75	0.57–0.73	0.56–0.74	0.56–0.75	0.56–0.73	0.54–0.7	0.54–0.6	–*			
M. marinum	0.5–0.68	0.63–0.68	0.64–0.67	0.63–0.68	0.6–0.68	0.63–0.68	0.62–0.72	0.63–0.66	0.48–0.74	0.5–0.73	0.5–0.73	0.49–0.74	0.5–0.73	0.48–0.7	0.55–0.55	0.62–0.7	–*		
M. riyadhense	0.5–0.66	0.61–0.65	0.61–0.65	0.62–0.65	0.58–0.66	0.64–0.65	0.63–0.7	0.61–0.64	0.53–0.77	0.55–0.75	0.55–0.76	0.54–0.77	0.55–0.75	0.53–0.72	0.55–0.59	0.65–0.68	0.59–0.63	–*	
M. szulgai	0.5–0.69	0.62–0.68	0.63–0.67	0.62–0.68	0.59–0.68	0.62–0.68	0.62–0.73	0.63–0.67	0.47–0.73	0.49–0.71	0.49–0.72	0.48–0.73	0.49–0.72	0.47–0.68	0.59–0.6	0.61–0.7	0.62–0.62	0.66–0.71	–*
B																			
M. kansasii I	**98.82–100.0**																		
M. kansasii II+	93.2–94.22	**99.66–99.99**																	
M. kansasii II	93.2–94.22	99.66–99.99	**99.66–99.98**																
M. persicum	93.25–94.16	99.68–99.99	99.68–99.99	**99.7–99.99**															
M. kansasii III	93.23–93.78	92.71–92.91	92.76–92.87	92.71–92.91	**99.61–100.0**														
M. kansasii IV	92.9–93.3	93.8–93.93	93.8–93.89	93.81–93.93	92.62–92.81	**99.87–99.9**													
M. kansasii V	93.96–94.22	94.72–94.91	94.72–94.91	94.73–94.91	93.61–93.77	94.38–94.51	**98.9–99.99**												
M. kansasii VI	90.48–90.88	88.55–88.73	88.55–88.71	88.58–88.73	90.4–90.53	88.82–88.96	89.18–89.34	**99.66–99.94**											
MTBC	81.52–81.79	81.6–81.79	81.6–81.79	81.64–81.78	81.57–81.81	81.85–81.98	81.88–82.04	81.04–81.22	**99.83–100.0**										
M. tuberculosis	81.52–81.72	81.6–81.71	81.6–81.7	81.64–81.71	81.57–81.74	81.85–81.97	81.88–82.0	81.04–81.15	99.83–99.96	**99.88–99.96**									
M. africanum	81.56–81.74	81.66–81.78	81.66–81.77	81.69–81.78	81.65–81.77	81.89–81.97	81.9–82.01	81.07–81.18	99.87–99.98	99.87–99.94	**99.92–99.98**								
M. bovis	81.56–81.76	81.66–81.79	81.66–81.79	81.69–81.78	81.66–81.81	81.91–81.98	81.93–82.04	81.07–81.22	99.87–100.0	99.87–99.94	99.9–99.95	**99.95–100.0**							
M. caprae	81.57–81.71	81.64–81.73	81.64–81.7	81.68–81.73	81.65–81.74	81.91–81.95	81.9–81.99	81.08–81.14	99.83–99.96	99.83–99.89	99.88–99.93	99.94–99.96	–*						
M. microti	81.65–81.79	81.65–81.74	81.65–81.71	81.7–81.74	81.68–81.8	81.94–81.97	81.9–82.01	81.06–81.18	99.89–99.94	99.89–99.91	99.92–99.94	99.9–99.93	99.9–99.9	–*					
M. conspicuum	80.79–80.97	80.88–81.09	80.91–81.06	80.88–81.09	80.81–81.0	81.05–81.12	81.06–81.19	80.39–80.47	81.23–81.33	81.26–81.33	81.23–81.29	81.26–81.32	81.3–81.32	81.27–81.28	–*				
M. gastri	92.13–92.39	92.89–93.04	92.94–93.03	92.89–93.04	92.1–92.27	95.15–95.18	93.64–93.76	88.73–88.79	81.85–81.95	81.88–81.91	81.85–81.89	81.86–81.91	81.9–81.91	81.93–81.95	81.12–81.14	–*			
M. marinum	81.37–81.53	81.29–81.48	81.29–81.46	81.32–81.48	81.33–81.57	81.64–81.67	81.71–81.79	80.96–81.01	80.34–80.47	80.34–80.43	80.35–80.43	80.39–80.47	80.39–80.41	80.41–80.43	79.81–79.84	81.61–81.62	–*		
M. riyadhense	81.63–81.83	81.63–81.78	81.63–81.72	81.66–81.78	81.66–81.86	81.99–82.04	82.03–82.12	81.19–81.25	82.5–82.61	82.54–82.59	82.5–82.56	82.55–82.61	82.54–82.55	82.55–82.56	81.2–81.23	82.06–82.07	80.39–80.41	–*	
M. szulgai	81.06–81.35	81.18–81.49	81.18–81.49	81.18–81.25	81.11–81.45	81.34–81.43	81.37–81.46	80.69–80.77	81.13–81.25	81.16–81.22	81.13–81.19	81.18–81.25	81.17–81.2	81.21–81.22	80.82–80.82	81.41–81.42	80.06–80.06	83.19–83.21	–*

[a]*Each M. kansasii subtype was represented by a group of 2–31 strains (genomes). The M. kansasii II group included 7 strains (2193, NLA001001128, B11073207, B11063838, 1010001469, H47, and H48); the M. persicum group included 4 strains [AFPC-000227 (T) (Shahraki et al., 2017), MK4, MK15, and MK42 (Tagini et al., 2019)]; the M. kansasii II+ group incorporated strains of both M. kansasii II and M. persicum groups (11 strains in total). The M. kansasii groups III, V, and VI included strains of respective genotypes collected for this study as well as strains which had elsewhere been designated as M. pseudokansasii (MK21, MK35, and MK142), M. innocens (MK13), and M. attenuatum (MK41, MK136, MK191), accordingly (Tagini et al., 2019). In addition, genomes of six M. tuberculosis, five M. africanum, five M. bovis, and single M. caprae, M. microti, M. conspicuum, M. gastri, M. marinum, M. riyadhense, and M. szulgai strains were analyzed. The MTBC contained genomes of all the aforesaid M. tuberculosis, M. africanum, M. bovis, M. caprae, and M. microti strains (18 strains in total). See* ***Supplementary Table 6****.*

**The values were not given, since only one genome sequence per species was analyzed; AF/ANI values calculated within the groups of strains (genomes) are indicated in bold. The AF and gANI values of 0.6 and 96.5, respectively, were identified as minimum thresholds to assign a genome pair to the same species.*

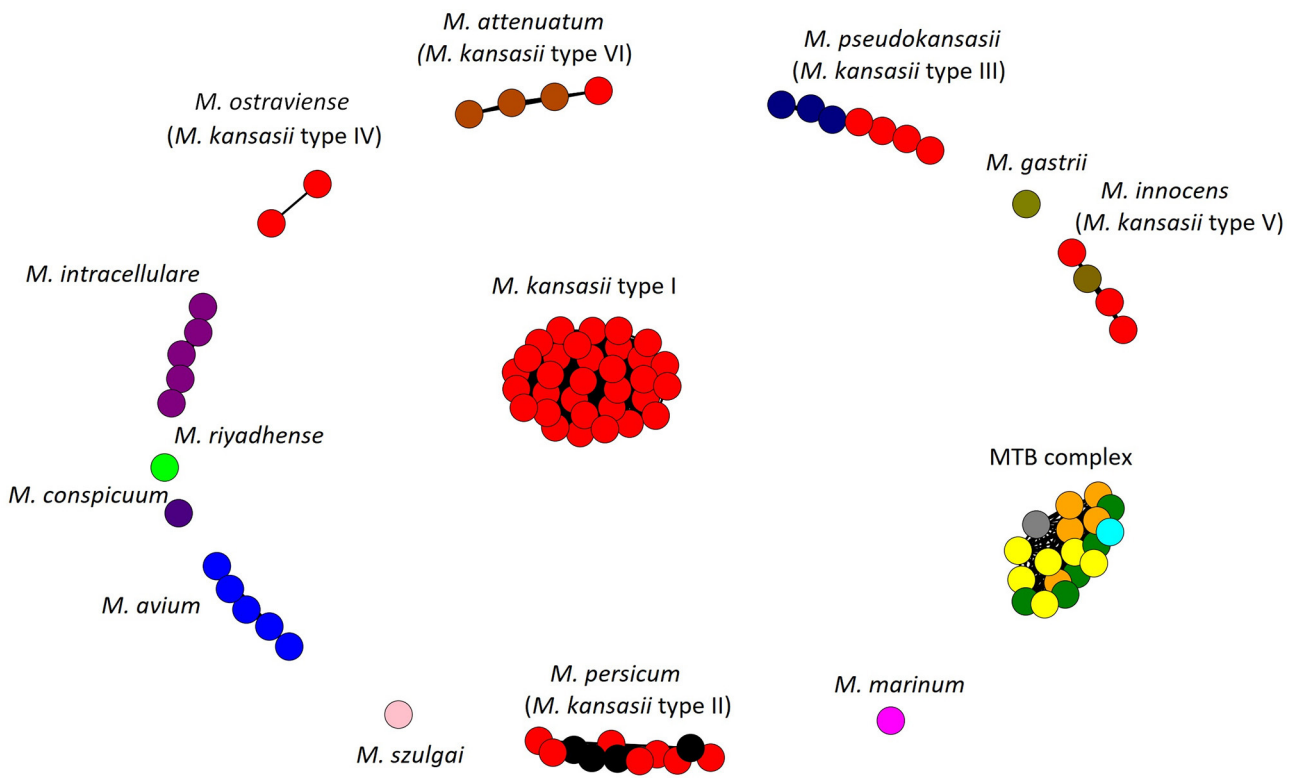

FIGURE 1 | Application of the Microbial Species Identifier (MiSI) method in classifying *Mycobacterium kansasii* subtype I-VI strains. Separation of different species into different cliques is depicted. Each color represents a species, while each circle—a genome of that species. Within cliques corresponding to *M. persicum* (formerly subtype II), *M. pseudokansasii* (III), *M. innocens* (V), and *M. attenuatum* (VI), genomes, which had been analyzed previously and first assigned to newly proposed species are shown in other than red color. Within the *M. tuberculosis* (MTB) complex clique, genomes of *M. tuberculosis*, *M. africanum*, *M. bovis*, *M. caprae*, and *M. microti* are depicted in yellow, orange, green, blue, and gray, respectively.

species were all below 95% (range, 80.4–94.9%) except between *M. kansasii* genotype II and *M. persicum* (range, 99.7–99.9%) and between *M. kansasii* genotype IV and *M. gastri* (95.2%) (**Table 3B**).

The AF and ANI metrics were also analyzed combinatorially, using the Microbial Species Identifier (MiSI) algorithm. The MiSI method sorts the analyzed genomes into species-like taxa or cliques, based on the AF and ANI species-level cut-off values set at 0.6 and 96.5%, respectively (Varghese et al., 2015). For a total of 83 mycobacterial genomes studied, 15 different cliques were configured. The results were pictorially summarized in **Figure 1**. The genomes of 59 *M. kansasii* strains were clearly divided into six cliques, each containing strains of a distinct *M. kansasii* subtype (I–VI) only. All the remaining NTM species had their genomes clustered within separate cliques, except that four genomes of strains classified as *M. persicum* were allocated in the *M. kansasii* genotype II clique. The genomes of 19 strains, representing five *M. tuberculosis* complex species were accommodated in a single cluster (clique).

The results of the AF/ANI calculations were fully corroborated by the GGD analysis, which serves as an *in silico* equivalent of the laboratory-based DNA-DNA hybridization (DDH) (Auch et al., 2010; Meier-Kolthoff et al., 2013b). Here, all strains contained within the *M. kansasii* genotypes shared enough sequence similarity to be considered as separate species (**Table 4**). The intra-genotype GGD values ranged from 0.0 to 0.0138, and thus fell under the recommended cut-off value of $\leq$0.0258, corresponding to a 70% DDH cut-off, for species demarcation (Meier-Kolthoff et al., 2013b). Much higher were the GGD values between strains representing different *M. kansasii* genotypes (range, 0.0601–0.124) or between any *M. kansasii* and any other *Mycobacterium* species (range, 0.0563–0.1971). The only exception was when comparing genomes of *M. kansasii* type II to any of *M. persicum*, for which the GGD values were between 0.0003 and 0.0044 (**Table 4**).

Another whole genome-level approach to clarify the taxonomic relationships between the six *M. kansasii* subtypes was the core-genome phylogenetic analysis. A dendrogram based on the concatenated 615,565-amino-acid sequences from 1,752 single-copy orthologous genes clearly separated all *M. kansasii* subtypes (**Figure 2**). All strains belonging to the same subtype formed distinct clades, supported by high bootstrap values (76.7–100%). Noteworthy, strains of *M. persicum* located in the same clade as the *M. kansasii* type II strains, whereas *M. gastri* branched sisterly to *M. kansasii* type IV. The topology of the tree supports the separation of *M. kansasii* subtypes, as

TABLE 4 | Genome-to-genome distance (GGD) of *M. kansasii* subtypes and other mycobacterial outgroup species.

Subtype/group[a]	*M. kansasii* I	*M. kansasii* II+	*M. kansasii* II	*M. persicum*	*M. kansasii* III	*M. kansasii* IV	*M. kansasii* V	*M. kansasii* VI	MTBC	*M. tuberculosis*	*M. africanum*	*M. bovis*	*M. caprae*	*M. microti*	*M. conspicuum*	*M. gastri*	*M. marinum*	*M. riyadhense*	*M. szulgai*
M. kansasii I	**0.0–0.0138**																		
M. kansasii II+	0.0657–0.077	**0.0002–0.0045**																	
M. kansasii II	0.0657–0.077	0.0003–0.0045	**0.0004–0.0045**																
M. persicum	0.0665–0.0766	0.0002–0.0044	0.0003–0.0044	**0.0002–0.004**															
M. kansasii III	0.0707–0.0755	0.0802–0.0818	0.0804–0.0818	0.0802–0.0817	**0.0001–0.006**														
M. kansasii IV	0.0751–0.0796	0.0699–0.0707	0.0701–0.0707	0.0699–0.0706	0.0826–0.0837	**0.0025**													
M. kansasii V	0.0656–0.0688	0.0601–0.0614	0.0601–0.0613	0.0602–0.0614	0.0715–0.0732	0.0647–0.0654	**0.0006–0.014**												
M. kansasii VI	0.1006–0.1038	0.123–0.124	0.123–0.124	0.123–0.1239	0.106–0.1068	0.1214–0.1221	0.1185–0.1197	**0.0011–0.0045**											
MTBC	0.1861–0.1889	0.1864–0.1879	0.1864–0.1879	0.1868–0.1875	0.1866–0.1878	0.1865–0.1872	0.1851–0.1865	0.1903–0.1914	**0.0016–0.0042**										
M. tuberculosis	0.1867–0.1886	0.1866–0.1876	0.1866–0.1876	0.187–0.1874	0.1868–0.1876	0.1869–0.187	0.1854–0.1864	0.1912–0.1914	0.0025–0.0042	**–***									
M. africanum	0.1861–0.1882	0.1864–0.1875	0.1864–0.1875	0.1868–0.1871	0.1866–0.1874	0.1865–0.1866	0.1851–0.1859	0.1903–0.1905	0.0022–0.0041	0.0041	**–***								
M. bovis	0.1867–0.1886	0.1866–0.1876	0.1866–0.1876	0.1869–0.1873	0.1868–0.1875	0.1868–0.1869	0.1854–0.1862	0.1909–0.1911	0.0016–0.0026	0.0025	0.0022	**–***							
M. caprae	0.1867–0.1884	0.1866–0.1877	0.1866–0.1877	0.187–0.1874	0.1867–0.1875	0.1869–0.1869	0.1852–0.1862	0.1912–0.1913	0.0016–0.0038	0.0038	0.0035	0.0016	**–***						
M. microti	0.1869–0.1889	0.1867–0.1879	0.1867–0.1879	0.187–0.1875	0.187–0.1878	0.1871–0.1872	0.1855–0.1865	0.1911–0.1911	0.0026–0.0042	0.0042	0.0029	0.0026	0.0038	**–***					
M. conspicuum	0.1925–0.1947	0.1915–0.1933	0.1915–0.1932	0.1916–0.1933	0.1925–0.1939	0.1921–0.1922	0.1909–0.192	0.1957–0.1971	0.1934–0.194	0.1937	0.1934	0.194	0.194	0.1939	**–***				
M. gastri	0.0842–0.0866	0.0788–0.0797	0.0791–0.0797	0.0788–0.0797	0.087–0.0883	0.0563–0.0567	0.0721–0.0728	0.1228–0.1231	0.1856–0.1863	0.1863	0.1856	0.1861	0.1862	0.1863	0.1928	**–***			
M. marinum	0.1876–0.1905	0.1886–0.1892	0.1886–0.1892	0.1886–0.1891	0.1893–0.1902	0.1891–0.1891	0.1872–0.1881	0.194–0.1942	0.1974–0.1982	0.1981	0.1974	0.198	0.1982	0.198	0.2027	0.1888	**–***		
M. riyadhense	0.185–0.1881	0.1872–0.1878	0.1872–0.1878	0.1872–0.1876	0.1865–0.1874	0.1849–0.1852	0.1843–0.1857	0.1904–0.1911	0.1822–0.1828	0.1828	0.1826	0.1822	0.1826	0.1828	0.1919	0.1851	0.1981	**–***	
M. szulgai	0.1886–0.1934	0.1887–0.1931	0.1887–0.1931	0.1924–0.1931	0.1871–0.1922	0.1914–0.1914	0.1904–0.1915	0.1939–0.1943	0.1929–0.1935	0.1932	0.1934	0.193	0.1935	0.1929	0.195	0.1909	0.2024	0.1726	**–***

[a]*Each M. kansasii subtype was represented by a group of 2–31 strains (genomes). The M. kansasii II group included 7 strains (2193, NLA001001128, B11073207, B11063838, 1010001469, H47, and H48); the M. persicum group included 4 strains [AFPC−000227 (T) (Shahraki et al., 2017), MK4, MK15, and MK42 (Tagini et al., 2019)]; the M. kansasii II+ group incorporated strains of both M. kansasii II and M. persicum groups (11 strains in total). The M. kansasii groups III, V, and VI included strains of respective genotypes collected for this study as well as strains which had elsewhere been designated as M. pseudokansasii (MK21, MK35, and MK142), M. innocens (MK13), and M. attenuatum (MK41, MK136, MK191), accordingly (Tagini et al., 2019). In addition, genomes of single M. tuberculosis, M. africanum, M. bovis, M. caprae, M. microti, M. conspicuum, M. gastri, M. marinum, M. riyadhense, and M. szulgai strains were analyzed. The MTBC contained genomes of all the aforesaid M. tuberculosis, M. africanum, M. bovis, M. caprae, and M. microti strains (5 strains in total). See* ***Supplementary Table 6****.*

**The values were not given, since only one genome sequence per species was analyzed. GGDs calculated within the groups of strains (genomes) are indicated in bold. The GGD values lower than 0.0258 were used to assign a genome pair to the same species.*

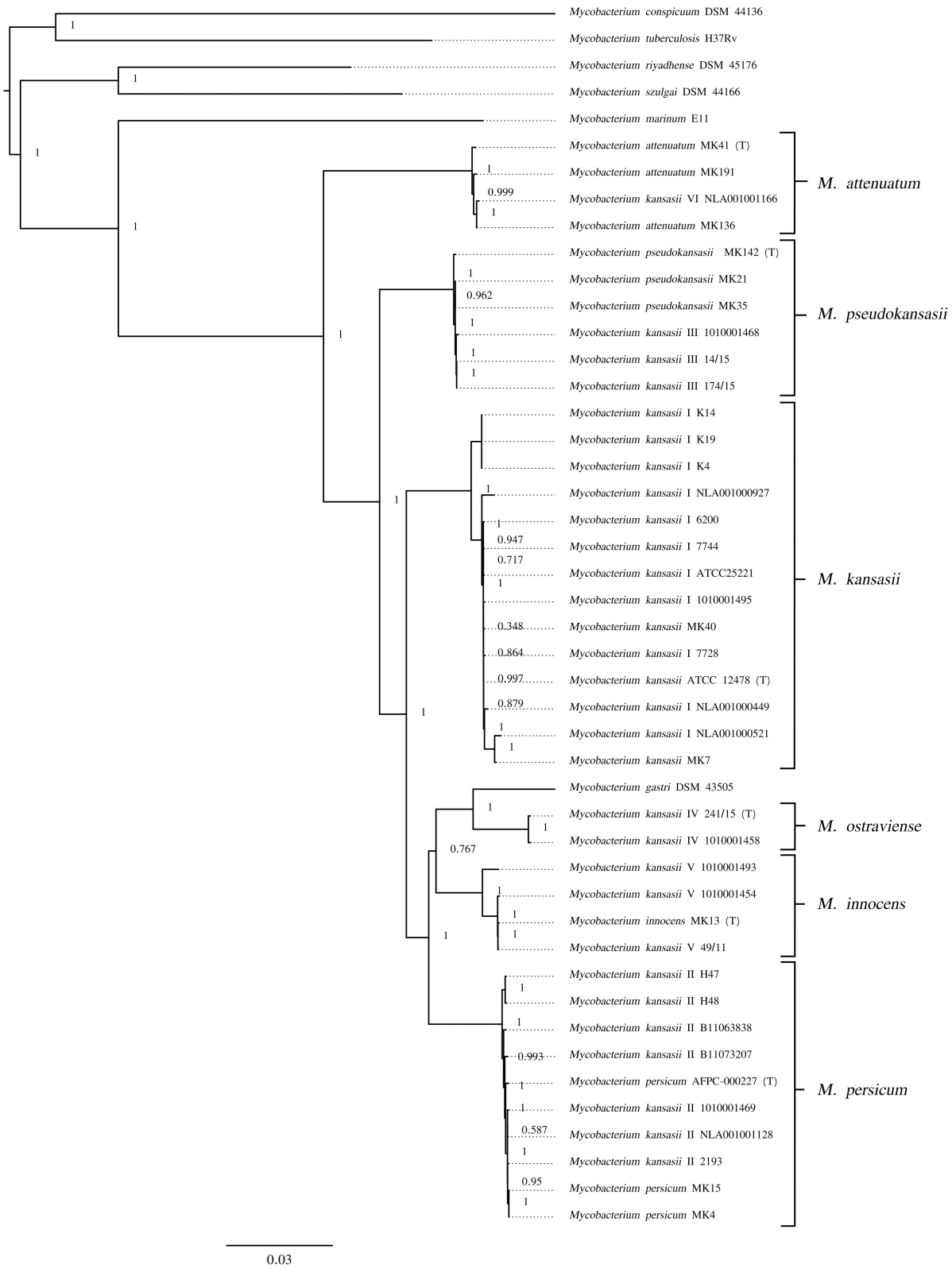

FIGURE 2 | Maximum-likelihood phylogenetic tree based on the amino acid alignment of concatenated single-copy orthologous genes. Bar, number of amino acid substitutions per amino acid site. Node supports were computed using the Shimodaira-Hasegawa test.

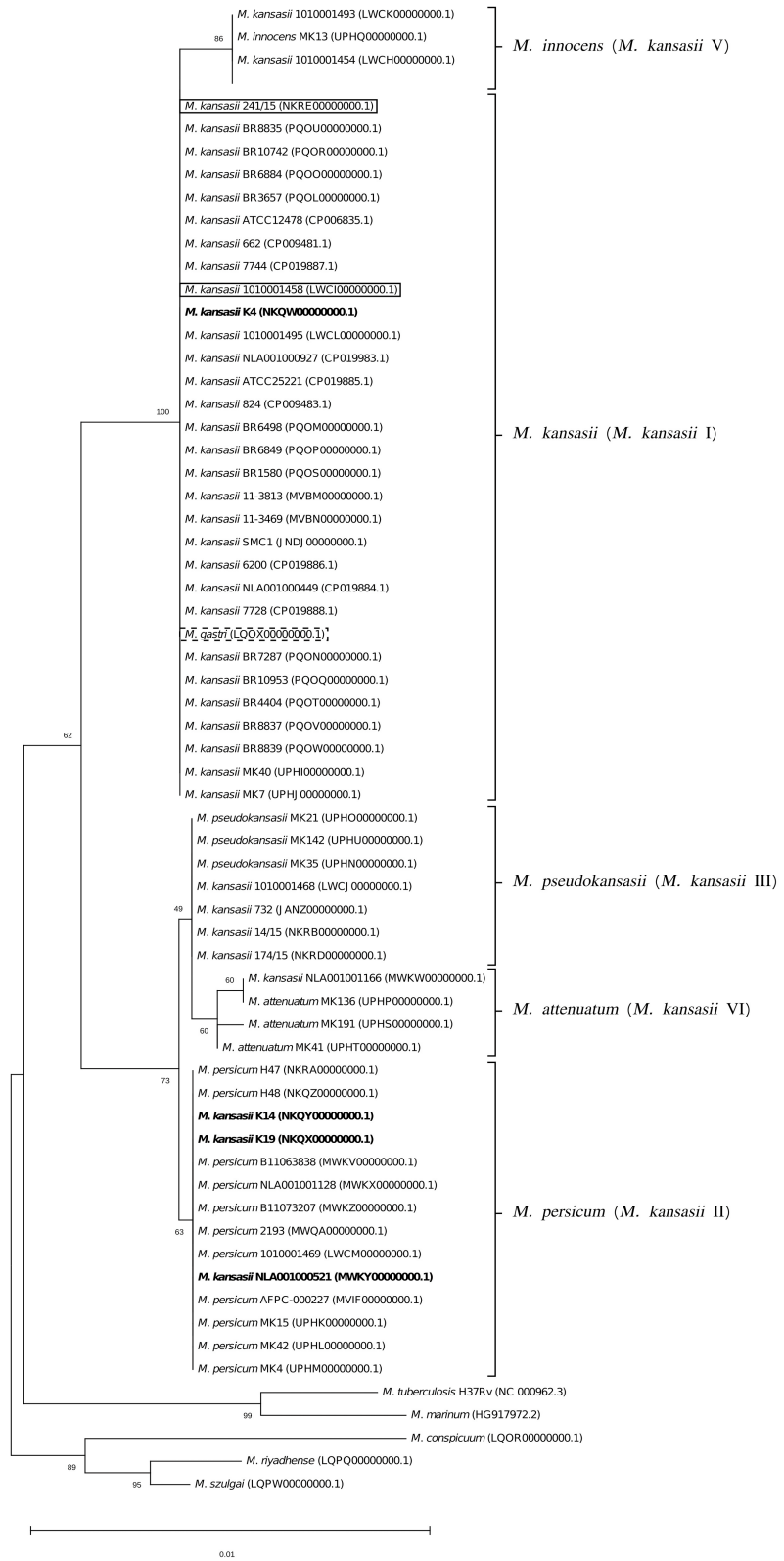

FIGURE 3 | Phylogenetic tree based on 16S rRNA gene sequences, constructed using the Neighbor-Joining method. The bootstrap values were calculated from 1,000 replications. Bootstrap values are given at nodes. Strains of *M. kansasii* type IV (241/15, 1010001458) and *M. gastri* are shown boxed in solid and dashed lines, respectively. Strains of *M. kansasii* type I, as per WGS-based analysis, that clustered either within type I or II, upon single-gene or concatenated gene phylogenies are shown in bold. GenBank accession numbers for the sequences are parenthesized. Bar, 0.01 substitutions per nucleotide position.

distinct species, with *M. kansasii* type II being conspecific with *M. persicum*.

The taxonomic position of *M. kansasii* genotypes was also examined using phylogenetic inferences from five genetically conserved loci, including the canonical 16S rRNA gene, the ITS region, and three protein-coding genes, namely *hsp65*, *tuf*, and *rpoB*, all being widely applied as molecular markers for the classification of mycobacteria (Tortoli, 2014). Multi-alignment and phylogenetic analyses for each of the five loci was conducted on the sequences of all 59 *M. kansasii* strains and single strains of *M. tuberculosis* and five other NTM species (**Supplementary Table 6**).

Pairwise alignments of the 1,537-bp sequences of 16S rRNA gene from *M. kansasii* strains showed that they were highly similar or identical (99–100% sequence similarity), both within and between the subtypes (**Supplementary Table 1**). At the same time, strains of *M. kansasii* shared 98–98.6% similarity with *M. tuberculosis* and more than 98% similarity with other NTM species. The 16S rRNA gene sequences were identical between *M. persicum* and *M. kansasii* type II, and between *M. gastri* and *M. kansasii* types I and IV.

Comparisons of the 277-bp ITS sequences from *M. kansasii* strains showed at most 85 and 98% similarities with the corresponding sequences from *M. tuberculosis* and other NTM species, respectively. Only sequences from *M. kansasii* type II and *M. persicum* were almost identical, sharing 99.2–100% similarity (**Supplementary Table 2**). The ITS sequence similarities within and between different *M. kansasii* subtypes fell under relatively wide ranges, i.e., 92.1–100% and 81.2–100%, respectively. The highest inter-subtype similarity values (>95%) were observed between three *M. kansasii* type I strains (K14, K19, and NLA00100521) and strains of *M. kansasii* type II. The type II-specific ITS sequences of those three type I strains accounted for the high intra-type heterogeneity (92.1–100% sequence similarity).

Sequence analysis of the 644-bp *hsp65* gene fragments showed similarities of 90.3–92.3% between *M. kansasii* and *M. tuberculosis*, and 90.9–97.9% between *M. kansasii* and other NTM species, except *M. persicum* which shared 99.5–100% similarity with *M. kansasii* type II (**Supplementary Table 3**). Alignments of the *hsp65* gene sequences from members of different *M. kansasii* subtypes yielded similarities of <98%. The only exception were three strains (K4, K14, and K19) of *M. kansasii* type I sharing up to 99.8% similarity with *M. kansasii* type II strains.

The results of the partial *tuf* (1,180 bp) gene analysis were similar to those obtained with the *hsp65* gene (**Supplementary Table 4**). The *tuf* gene sequence similarities between *M. kansasii* and *M. tuberculosis* were 93.4% at most, while those between *M. kansasii* and other NTM species were always below 98%, except that sequences of *M. kansasii* type II and *M. persicum* were identical. The similarity indexes calculated for *M. kansasii* of different subtypes did not exceed 98.3%, except that two strains of type I (K14 and K19) had the same *tuf* sequences as *M. kansasii* type II strains.

Finally, alignments of the partial *rpoB* (3,439 bp) gene sequences found all *M. kansasii* strains to share <89% sequence similarity with *M. tuberculosis* and <96% similarity with NTM species, but again not *M. persicum*, whose sequences were identical or nearly identical with those of *M. kansasii* type II (**Supplementary Table 5**). The level of the *rpoB* gene sequence similarity between members of different *M. kansasii* subtypes was consistently below 98%, excluding two type I strains (K14 and K19), which displayed high similarity or identity with type II strains.

To better illustrate the phylogenetic relatedness of *M. kansasii* subtypes, phylogenetic trees inferred from five individual loci were constructed (**Figures 3**–**7**). A separate tree was created using the concatenated 16S rRNA, *hsp65*, and *rpoB* genes (**Figure 8**), since such an approach is known to increase considerably discrimination and robustness of the dendrogram analysis (Devulder et al., 2005). In all but one dendrograms, all *M. kansasii* strains could be spread into six highly supported (bootstrap values $\geq$ 93%) clusters, according to their subtype affiliation (**Figures 4**–**8**). The 16S rRNA gene-based dendrogram was different in that it contained no cluster specific for *M. kansasii* type IV. Two type IV strains clustered together with *M. kansasii* type I strains (**Figure 3**). Noteworthy, in the same cluster the type strain of *M. gastri* was placed. A feature, which was apparent across all the trees was that strains of *M. kansasii* type II clustered along with *M. persicum*. Moreover, there were four *M. kansasii* type I strains that branched within that cluster. Two of these strains (K14 and K19) were always present in the *M. kansasii* type II-*M. persicum* cluster, whereas another two belonged to that cluster only in the trees based on the ITS region (strain no. NLA00100521), 16S rRNA gene (NLA00100521), and *hsp65* gene (strain no. K4). Having the type I-specific *hsp65* gene sequence (sequevar I) and type II-specific ITS sequence (sequevar II), strain no. NLA00100521 represents the so-called intermediate type I (I/II), considered a transitional form between environmental type II and human-adapted type I (Iwamoto and Saito, 2005). Whereas, strains K14 and K19 can be identified as atypical type II (IIb) due to their type II ITS sequence and unique, yet most similar to type II, *hsp65* sequences (Iwamoto and Saito, 2005). Captivatingly, strain K4 had the same unique *hsp65* gene sequence, with all the other sequences being characteristic of type I. Thus, the strain represents the so far unreported variant of *M. kansasii* type I, which can be tentatively designated as atypical type I (Ib).

Altogether, the results from the genome-wide comparisons demonstrated the six (I–VI) *M. kansasii* subtypes to represent distinct species. This was also the conclusion of the recent study by Tagini et al., who based their results upon ANI and GGD analysis of the genomes of 21 *M. kansasii* strains comprising all six subtypes (Tagini et al., 2019) (Twenty of these strains were used in the present work). Also, single- and multigene phylogenies, highly congruent between this and already published study, were indicative of species-level demarcations between *M. kansasii* subtypes. From these findings, Tagini et al. were first to propose new species designations, namely *M. pseudokansasii*, *M. innocens*, and *M. attenuatum*, replacing the former types III, V, and VI, respectively. The most prevalent type I was preserved under the '*M. kansasii*' designation. Whereas, *M. kansasii* type II was found, as in our

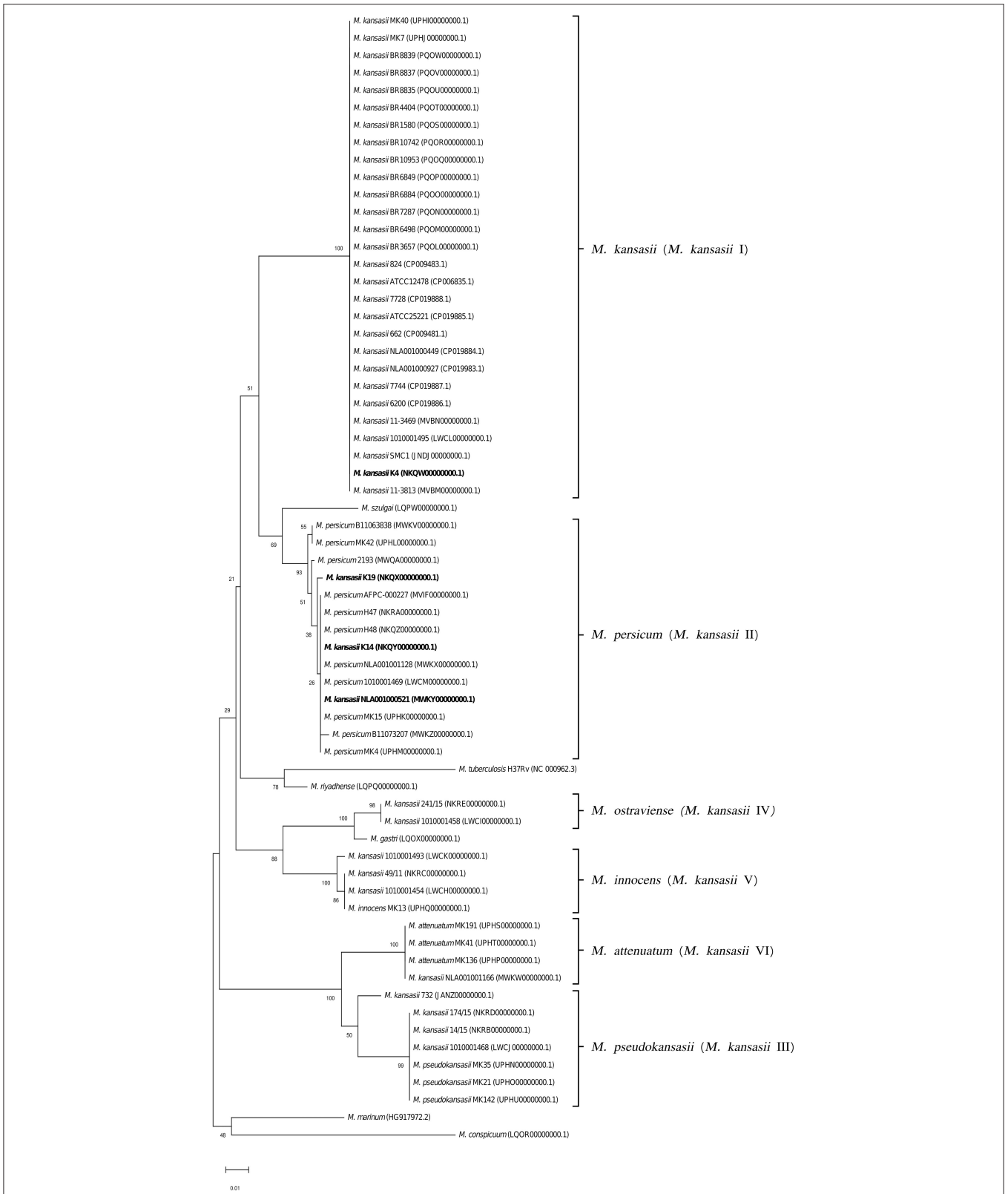

FIGURE 4 | Phylogenetic tree based on ITS sequences constructed using the Neighbor-Joining method. The bootstrap values were calculated from 1,000 replications. Bootstrap values are given at nodes. Strains of *M. kansasii* type I, as per WGS-based analysis, that clustered either within type I or II, upon single-gene or concatenated gene phylogenies are shown in bold. GenBank accession numbers for the sequences are parenthesized. Bar, 0.01 substitutions per nucleotide position.

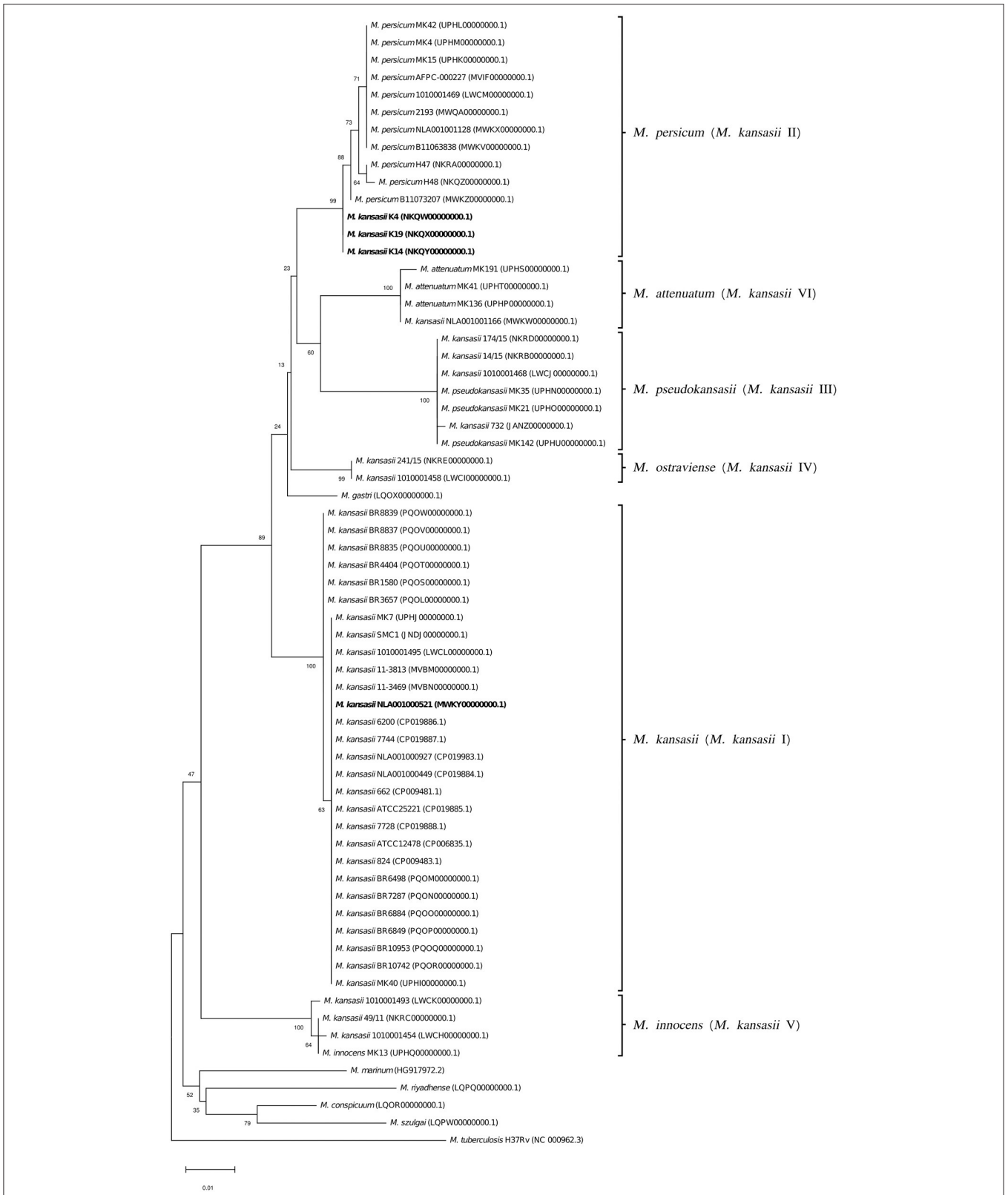

FIGURE 5 | Phylogenetic tree based on *hsp65* gene sequences constructed using the Neighbor-Joining method. The bootstrap values were calculated from 1,000 replications. Bootstrap values are given at nodes. Strains of *M. kansasii* type I, as per WGS-based analysis, that clustered either within type I or II, upon single-gene or concatenated gene phylogenies are shown in bold. GenBank accession numbers for the sequences are parenthesized. Bar, 0.01 substitutions per nucleotide position.

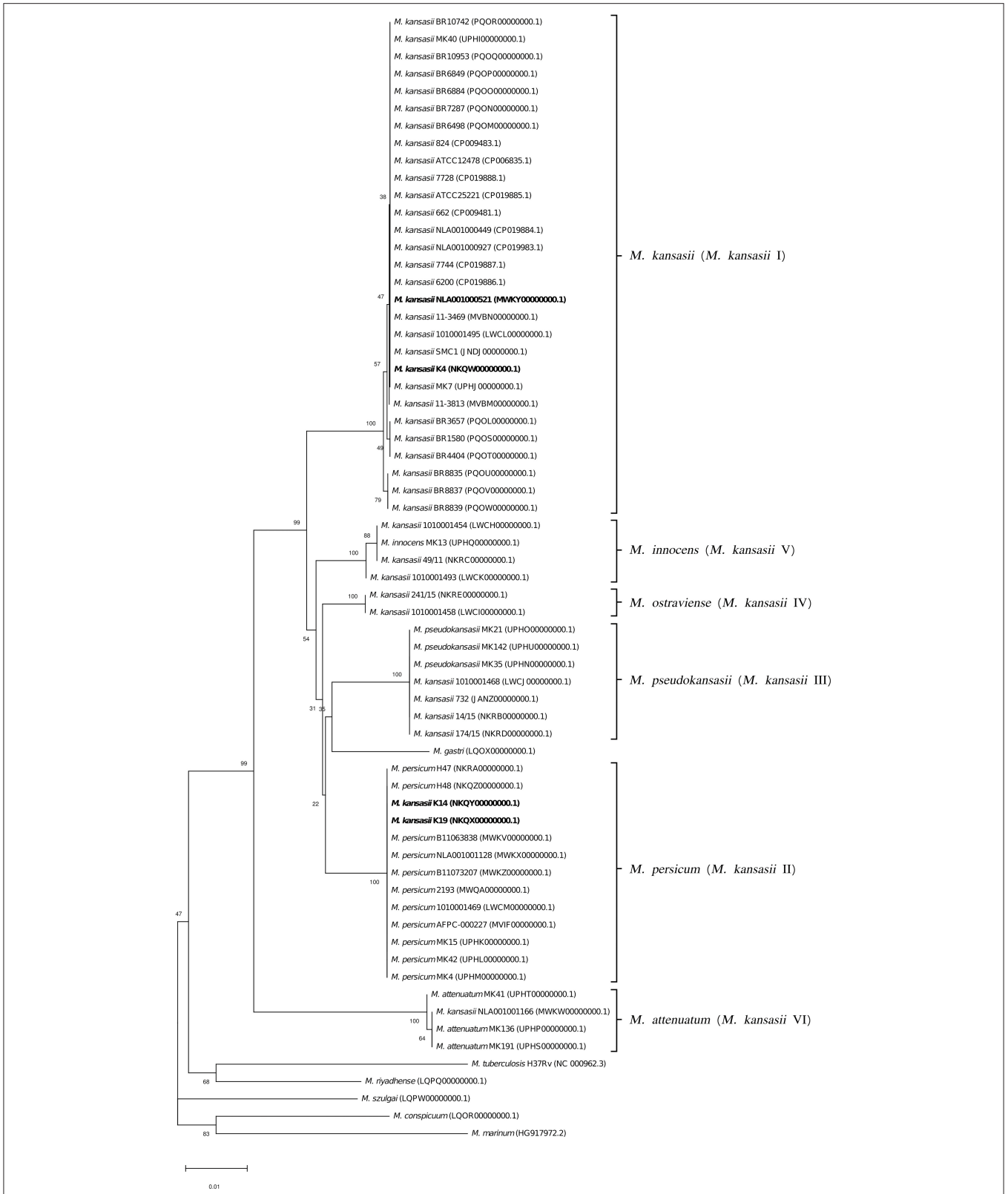

FIGURE 6 | Phylogenetic tree based on *tuf* gene sequences constructed using the Neighbor-Joining method. The bootstrap values were calculated from 1,000 replications. Bootstrap values are given at nodes. Strains of *M. kansasii* type I, as per WGS-based analysis, that clustered either within type I or II, upon single-gene or concatenated gene phylogenies are shown in bold. GenBank accession numbers for the sequences are parenthesized. Bar, 0.01 substitutions per nucleotide position.

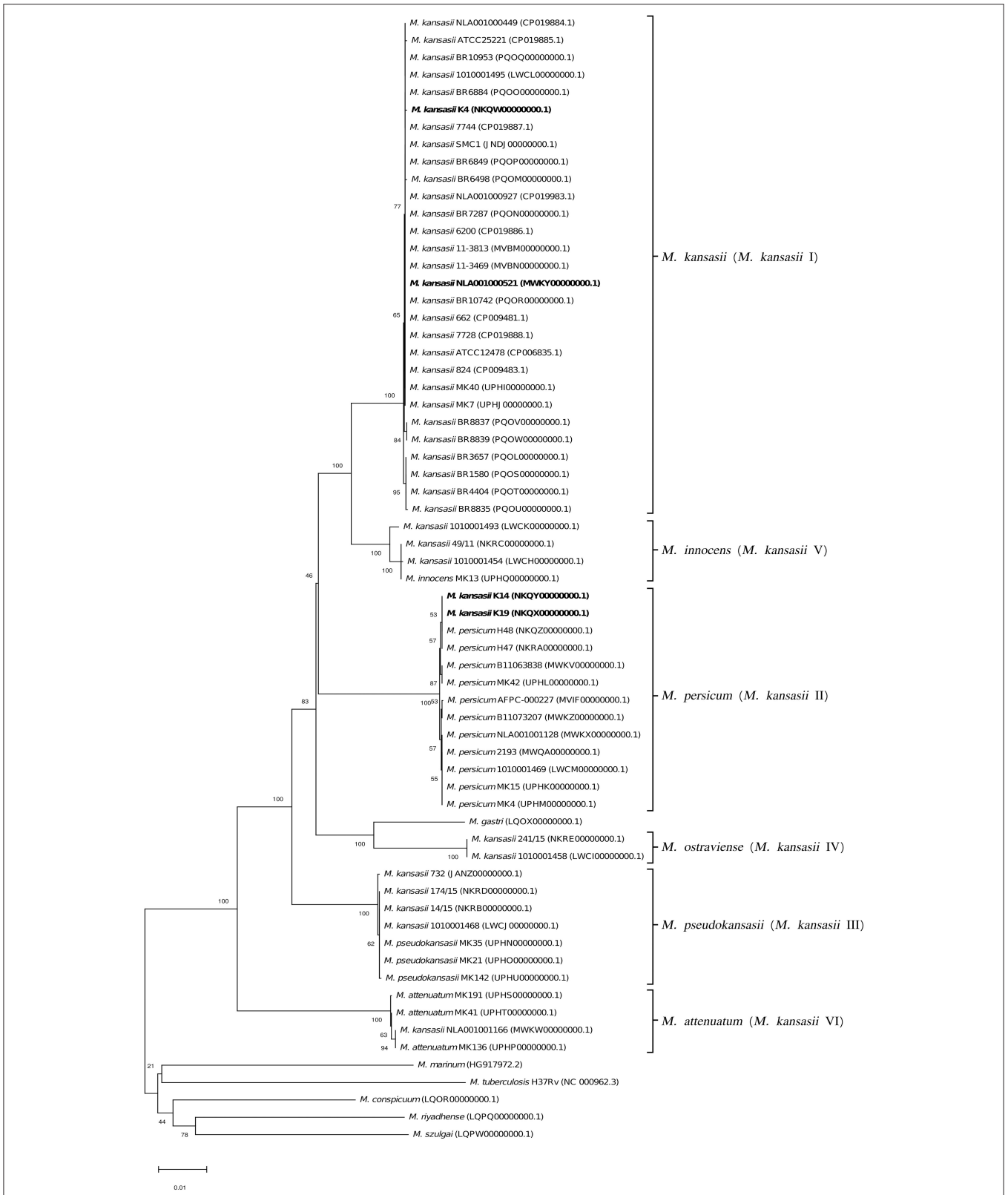

FIGURE 7 | Phylogenetic tree based on *rpoB* sequences constructed using the Neighbor-Joining method. The bootstrap values were calculated from 1,000 replications. Bootstrap values are given at nodes. Strains of *M. kansasii* type I, as per WGS-based analysis, that clustered either within type I or II, upon single-gene or concatenated gene phylogenies are shown in bold. GenBank accession numbers for the sequences are parenthesized. Bar, 0.01 substitutions per nucleotide position.

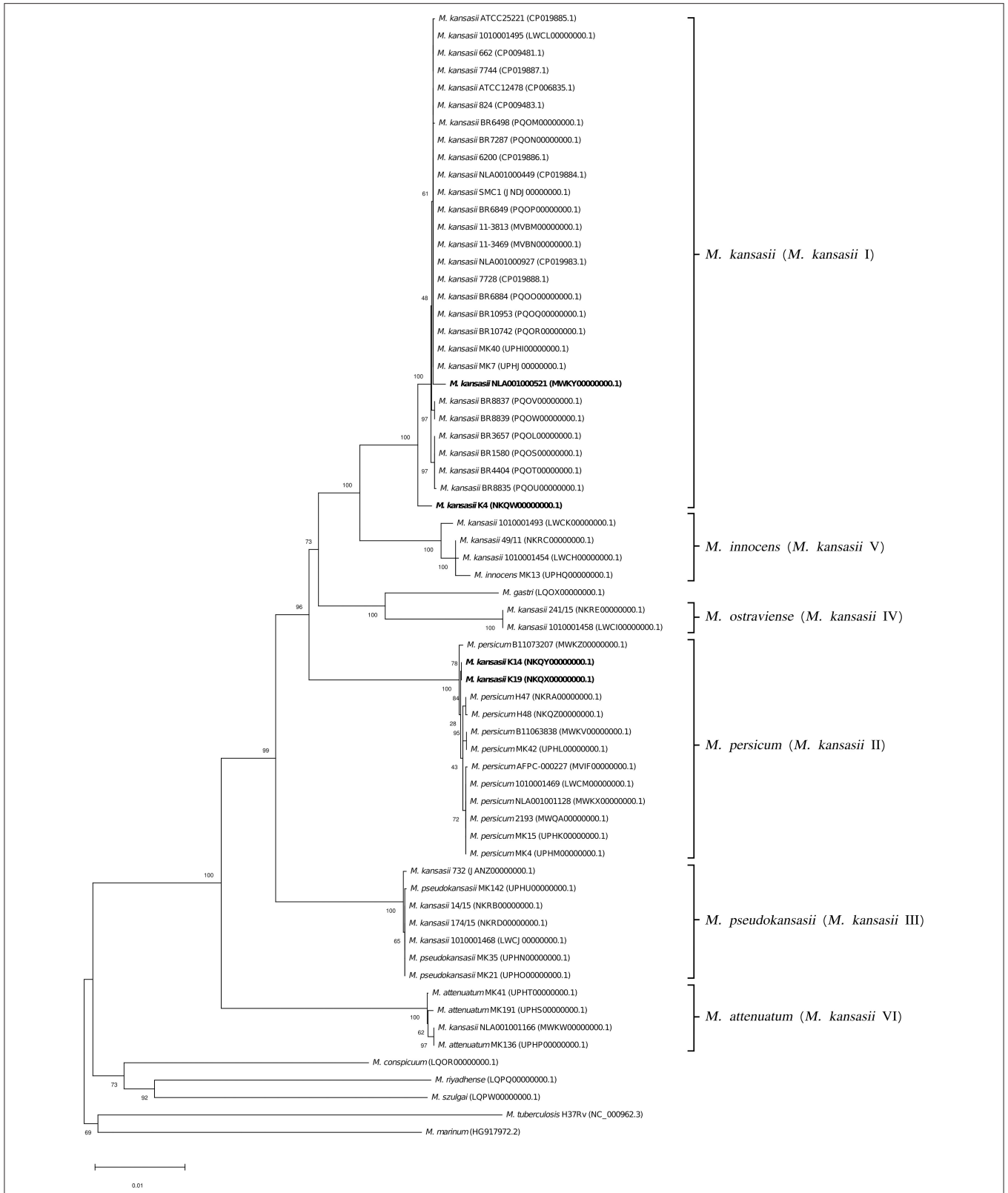

FIGURE 8 | Phylogenetic tree based on concatenated 16S rRNA, *hsp65*, and *rpoB* gene sequences constructed using the Neighbor-Joining method. The bootstrap values were calculated from 1,000 replications. Bootstrap values are given at nodes. Strains of *M. kansasii* type I, as per WGS-based analysis, that clustered either within type I or II, upon single-gene or concatenated gene phylogenies are shown in bold. GenBank accession numbers for the sequences are parenthesized. Bar, 0.01 substitutions per nucleotide position.

study, conspecific with *M. persicum*. Therefore, we share the view of assigning this name to all *M. kansasii* type II strains. In fact, the conspecificity of *M. persicum* and *M. kansasii* type II would have been disclosed upon the original description of the species (*M. persicum*), if the authors had included *M. kansasii* type II in the genome-based comparative analysis (Shahraki et al., 2017).

The two *M. kansasii* type IV strains, analyzed in our study, fully satisfied the genomic criteria for a separate species. This was also implied by our predecessors, but in the absence of any type strain, they could not formally establish the species. Here, we propose a new species name, *Mycobacterium ostraviense* sp. nov., to accommodate *M. kansasii* type IV strains, with a strain no. 241/15, as a type. The description of this new species is given at the end of the article.

The taxonomic status of *M. kansasii* type VII remains an enigma. Neither the strain nor its genomic sequence is available, precluding any relevant phylogenetic analyses. This type was reported only once (Taillard et al., 2003), and given the similarity of its *hsp65* RFLP banding patterns, which served as the only diagnostic means, to those of type III, it is plausible that type VII is a product of misidentification.

Since the mid-1990s, the PCR-RFLP analysis, based on single-copy, orthologous genes (*hsp65*, *rpoB*, and *tuf*) has been widely used for the identification of a plethora of NTM species, including *M. kansasii* and its subtypes (Alcaide et al., 1997; Devallois et al., 1997; Kim et al., 2001; da Silva Rocha et al., 2002; Santin and Alcaide, 2003; Zhang et al., 2004; Kwenda et al., 2015; Bakuła et al., 2016). However, PCR-RFLP typing may not seldom produce misleading results. Single nucleotide polymorphisms can alter the recognition sites of the restriction enzymes and thus generate either patterns unidentifiable or corresponding to those of other species. Also, sequence analysis, even conducted on a combination of genes, may not resolve the species identity adequately. This is best illustrated in the already discussed strains of atypical type IIb, which despite sharing nearly 99% average nucleotide identity with type I, had their 16S rRNA, *hsp65*, and *rpoB* gene sequences, either individually or concatenated, more closely associated with type II. The type IIb strains would have been considered type II (*M. persicum*), if they had not been inspected at the whole genome-level. Thus, neither PCR-RFLP profiling nor single or multilocus sequencing allows unequivocal identification of *M. persicum*. A definite diagnosis should be supported by the genome-wide analysis. Still, the two type IIb strains, under this study, displayed the type I-specific *hsp65* RFLP patterns, upon digestion with HaeIII (but not with BstEII, which was type II-specific). This feature can be exploited for differentiation between types I and II, if whole-genome sequencing is not affordable. Nevertheless, a new, robust genetic marker allowing for fast and accurate identification of all *M. kansasii*-derived species (former types I-VI), bypassing the need for whole-genome analysis, would be of great benefit. For this, a more in-depth, comparative analysis of the genomes of more strains representing the six *M. kansasii*-derived species, and other NTM species, will have to be undertaken.

There has been a continuing debate on how the differences between *M. kansasii* subtypes translate into pathogenicity. The prevailing view is that only types I and II are true human pathogens, with the latter having been associated with immunodeficiency, and HIV infection in particular, whereas all the remaining types are considered non-pathogenic, and their sporadic isolation from clinical samples has been interpreted as colonization or environmental contamination (Tortoli et al., 1994; Taillard et al., 2003). Indeed, *M. kansasii* type I is the most commonly detected among clinical isolates and the predominant cause of *M. kansasii* disease worldwide (Alcaide et al., 1997; Kim et al., 2001; Gaafar et al., 2003; Santin and Alcaide, 2003; Taillard et al., 2003; Zhang et al., 2004; da Silva Telles et al., 2005; Shitrit et al., 2006; Thomson et al., 2014; Kwenda et al., 2015; Bakuła et al., 2016). Infections attributable to *M. kansasii* type II are much rarer (Taillard et al., 2003; Zhang et al., 2004; Shitrit et al., 2006; Bakuła et al., 2016), and those caused by other types are almost unreported in the literature. Still, types III, IV, and VI have been recognized among clinical isolates (Alcaide et al., 1997; Picardeau et al., 1997; Santin and Alcaide, 2003; Thomson et al., 2014; Kwenda et al., 2015) with types IV and VI implicated in the disease (Santin and Alcaide, 2003; Thomson et al., 2014). Due to the paucity of isolations of *M. kansasii* other than type I, their clinical relevance remains obscure. Some new light on this problem may be shed by the findings of an international, multicenter investigation, currently in progress, on the global distribution of *M. kansasii* subtypes. So far, we have documented nine confirmed cases of *M. kansasii* disease, etiologically linked to either types III, IV, V or VI (Jagielski et al., data unpublished). In this context, the newly proposed species names for types V (*M. innocens*) and VI (*M. attenuatum*) may not reflect the true phenotype of those bacteria.

Searching for the genetic determinants of pathogenicity, a key genomic region associated with *M. tuberculosis* virulence, known as "region of difference 1" (RD1) was interrogated across the genomes of *M. kansasii* subtypes for its functional integrity (i.e., presence of RD1 genes). The RD1 encodes a secretory apparatus (ESX-1 type VII secretion system) responsible for exporting two highly potent antigens and virulence factors—the 6-kDa early secreted antigenic target (ESAT-6) and the 10-kDa culture filtrate protein (CFP-10) (Berthet et al., 1998). These proteins, encoded by the same operon, play a critical role in modulation of the host immune response through inhibition of phagosome maturation, cytosolic translocation of mycobacteria or granuloma formation (MacGurn and Cox, 2007; van der Wel et al., 2007; Volkman et al., 2010). The *esat-6* (*esxA*) and *cfp-10* (*esxB*) genes have also been demonstrated in some NTM species, including *M. kansasii* (types I-V), *M. szulgai*, *M. marinum*, and *M. riyadhense* (van Ingen et al., 2009). Furthermore, the ESAT-6/CFP-10-mediated translocation of bacilli into the cytosol has been proven to occur in *M. kansasii* type I, but not in *M. kansasii* type V (Houben et al., 2012).

Our analysis showed the presence of six RD1 genes (*rv3871*-5 and *rv3877*), including the ESAT-6 and CFP-10-coding genes and two other genes (*rv3871* and *rv3877*) coding for the essential components of the ESX-1 secretion system, in all types of *M. kansasii* and other NTM species (**Table 5**). Only single strains of *M. kansasii* type I, *M. marinum*, and *M. szulgai* were devoid of the *rv3872* gene coding for PE35, conjectured to play a role in the regulation of *esxB*/*A* expression (Brodin et al., 2006).

TABLE 5 | Distribution of region of difference 1 (RD1) genes among *M. kansasii* strains and other mycobacterial outgroup species.

No.	Species/genotype	ID	Strain no.[a]	Locus[b]									GenBank no.
				Rv3879c	Rv3876	Rv3878	Rv3877	Rv3873	Rv3871	Rv3874	Rv3875	Rv3872	
1	*M. kansasii* I	5MK	NLA001000521[D*]	–	+	–	+	+	+	+	+	+	MWKY01
2	*M. kansasii* I	6MK	ATCC25221[D*]	+	+	–	+	+	+	+	+	+	CP019885
3	*M. kansasii* I	1MK	NLA001000927[D*]	–	+	–	+	+	+	+	+	+	CP019883
4	*M. kansasii* I	4MK	NLA001000449[D*]	–	+	–	+	+	+	+	+	+	CP019884
5	*M. kansasii* I	10MK	6200[D*]	–	+	–	+	+	+	+	+	+	CP019886
6	*M. kansasii* I	9MK	7728[D*]	+	+	–	+	+	+	+	+	+	CP019888
7	*M. kansasii* I	11MK	7744[D*]	–	+	–	+	+	+	+	+	+	CP019887
8	*M. kansasii* I	5JD	1010001495[E*]	–	+	–	+	+	+	+	+	+	LWCL01
9	*M. kansasii* I	K4	K4[D*]	+	+	–	+	+	+	+	+	+	NKQW01
10	*M. kansasii* I	K14	K14[D*]	+	+	–	+	+	+	+	+	+	NKQY01
11	*M. kansasii* I	K19	K19[N*]	+	+	–	+	+	+	+	+	+	NKQX01
12	*M. kansasii* I	–	ATCC12478[D]	–	+	–	+	+	+	+	+	+	CP0006835
13	*M. kansasii* I	–	824[NI]	–	+	–	+	+	+	+	+	+	CP009483
14	*M. kansasii* I	–	BR3657[D]	–	+	–	+	+	+	+	+	+	PQOL01
15	*M. kansasii* I	–	BR6849[D]	–	+	–	+	+	+	+	+	+	PQOP01
16	*M. kansasii* I	–	SMC1[E]	–	+	–	+	+	+	+	+	+	JNDJ01
17	*M. kansasii* I	–	BR8837[D]	–	+	–	+	+	+	+	+	+	PQOV01
18	*M. kansasii* I	–	BR6498[D]	+	+	–	+	+	+	+	+	+	PQOM01
19	*M. kansasii* I	–	11_3813[R]	–	+	–	+	+	+	+	+	–	MVBM01
20	*M. kansasii* I	–	BR6884[D]	+	+	–	+	+	+	+	+	+	PQOO01
21	*M. kansasii* I	–	BR10742[D]	+	+	–	+	+	+	+	+	+	PQOR01
22	*M. kansasii* I	–	BR1580[D]	+	+	–	+	+	+	+	+	+	PQOS01
23	*M. kansasii* I	–	BR4404[D]	+	+	–	+	+	+	+	+	+	PQOT01
24	*M. kansasii* I	–	BR8839[D]	+	+	–	+	+	+	+	+	+	PQOW01
25	*M. kansasii* I	–	662[NI]	+	+	–	+	+	+	+	+	+	CP009481
26	*M. kansasii* I	–	BR7287[D]	+	+	–	+	+	+	+	+	+	PQON01
27	*M. kansasii* I	–	BR10953[D]	+	+	–	+	+	+	+	+	+	PQOQ01
28	*M. kansasii* I	–	BR8835[D]	+	+	–	+	+	+	+	+	+	PQOU01
29	*M. kansasii* I	–	11_3469[R]	+	+	–	+	+	+	+	+	+	MVBN01
30	*M. kansasii* I	–	MK40[U]	+	+	–	+	+	+	+	+	+	UPHI01
31	*M. kansasii* I	–	MK7[U]	+	+	–	+	+	+	+	+	+	UPHJ01
32	*M. kansasii* II	12MK	2193[N*]	–	–	–	+	+	+	+	+	+	MWQA01
33	*M. kansasii* II	3MK	NLA001001128[N*]	–	–	–	+	+	+	+	+	+	MWKX01
34	*M. kansasii* II	7MK	B11073207[N*]	–	–	–	+	+	+	+	+	+	MWKZ01
35	*M. kansasii* II	8MK	B11063838[N*]	+	–	–	+	+	+	+	+	+	MWKV01
36	*M. kansasii* II	3B/6JD	1010001469[E*]	–	–	–	+	+	+	+	+	+	LWCM01
37	*M. kansasii* II	H47	H47[D*]	–	–	–	+	+	+	+	+	+	NKRA01

(Continued)

TABLE 5 | Continued

No.	Species/genotype	ID	Strain no.[a]	Locus[b]									GenBank no.
				Rv3879c	Rv3876	Rv3878	Rv3877	Rv3873	Rv3871	Rv3874	Rv3875	Rv3872	
38	*M. kansasii* II	H48	H48^{N*}	–	–	–	+	+	+	+	+	+	NKQZ01
39	*M. persicum*	–	AFPC–000227^{D}	–	–	–	+	+	+	+	+	+	MVIF01
40	*M. persicum*	–	MK15^{U}	–	–	–	+	+	+	+	+	+	UPHK01
41	*M. persicum*	–	MK4^{U}	–	–	–	+	+	+	+	+	+	UPHM01
42	*M. persicum*	–	MK42^{U}	–	–	–	+	+	+	+	+	+	UPHL01
43	*M. kansasii* III	14_15	14_15^{N*}	+	+	–	+	+	+	+	+	+	NKRB01
44	*M. kansasii* III	174_15	174_15^{D*}	–	+	–	+	+	+	+	+	+	NKRD01
45	*M. kansasii* III	3JD	1010001468^{E*}	+	+	–	+	+	+	+	+	+	LWCJ01
46	*M. kansasii* III	–	732^{U}	+	+	–	+	+	+	+	+	+	JANZ01
47	*M. pseudokansasii*	–	MK142^{D}	–	+	–	+	+	+	+	+	+	UPHU01
48	*M. pseudokansasii*	–	MK21^{U}	–	+	–	+	+	+	+	+	+	UPHO01
49	*M. pseudokansasii*	–	MK35^{U}	+	+	–	+	+	+	+	+	+	UPHN01
50	*M. kansasii* IV	2JD	1010001458^{E*}	+	+	–	+	+	+	+	+	+	LWCI01
51	*M. kansasii* IV	241/15	241/15^{N*}	–	+	–	+	+	+	+	+	+	NKRE01
52	*M. kansasii* V	1JD	1010001454^{E*}	–	+	–	+	+	+	+	+	+	LWCH01
53	*M. kansasii* V	4JD	1010001493^{E*}	–	+	–	+	+	+	+	+	+	LWCK01
54	*M. kansasii* V	49_11	49_11^{N*}	–	+	–	+	+	+	+	+	+	NKRC01
55	*M. innocens*	–	MK13^{U}	–	+	–	+	+	+	+	+	+	UPHQ01
56	*M. kansasii* VI	2MK	NLA001001166^{N*}	–	–	–	+	+	+	+	+	+	MWKW01
57	*M. attenuatum*	–	MK41^{N}	–	–	–	+	+	+	+	+	+	UPHT01
58	*M. attenuatum*	–	MK136^{U}	–	–	–	+	+	+	+	+	+	UPHP01
59	*M. attenuatum*	–	MK191^{U}	+	–	–	+	+	+	+	+	+	UPHS01
60	*M. tuberculosis*	–	Beijing–like	+	+	–	+	+	+	+	+	+	CP017597
61	*M. africanum*	–	GM041182	+	+	+	+	+	+	+	+	+	NC_015758
62	*M. bovis*	–	09_1191	+	+	–	+	+	+	+	+	+	JPFP01
63	*M. caprae*	–	Allgaeu	+	+	+	+	+	+	+	+	+	CP016401
64	*M. microti*	–	12	+	+	+	+	–	–	–	–	–	CP010333
65	*M. conspicuum*	–	DSM44136	ND									LQOR01.1
66	*M. gastri*	–	DSM43505	–	+	–	+	+	+	+	+	+	LQOX01
67	*M. marinum*	–	E11	–	+	–	+	+	+	+	+	–	HG917972
68	*M. riyadhense*	–	DSM45176	–	–	–	+	+	+	+	+	+	LQPQ01
69	*M. szulgai*	–	DSM44166	+	–	–	+	+	+	+	+	–	LQPW01

[a] *The presence of a given gene was marked with a "+" and highlighted in gray; the superscript letters refer to isolation source:* ^{D}*–clinical strains implicated in NTM disease;* ^{N}*–clinical strains not implicated in NTM disease;* ^{R}*–clinical strain from the rhesus macaque (Macaca mulatta);* ^{U}*–clinical strains with unknown relation to NTM disease;* ^{E}*–environmental strains. Strains whose genomes were sequenced in this study are marked with an asterisk (*).*

The *rv3876* gene was demonstrated in all *M. kansasii* types except for types II (*M. persicum*) and VI (*M. attenuatum*). Neither it was present in *M. szulgai* and *M. riyadhense*. The protein encoded by this gene is an ESX-1 secretion-associated protein EspI. It was shown that inactivation of the *rv3876* gene did not impair secretion of ESAT-6 (Brodin et al., 2006). More recently, however, EspI was found to negatively regulate the ESX-1 secretion system in *M. tuberculosis*, in response to low cellular ATP levels. EspI was thus hypothesized to play a possible role during the latent phase of infection (Zhang et al., 2014).

The *rv3879c* gene, coding for another ESX-1 secretion-associated protein EspK, was variably distributed among *M. kansasii* strains. It was detected in half of the strains of types I and III, while being absent in all but one strains of types II and VI, and all type V strains. EspK seems not to be involved in virulence, since the *rv3879c* homolog deletion mutant of *M. bovis* was not attenuated in the guinea pig model (Inwald et al., 2003). Moreover, similar to *rv3876*, inactivation of the EspK-coding gene did not abolish ESAT-6 secretion (Brodin et al., 2006). Contrastingly, EspK of *M. marinum* was found crucial for the ESX-1-mediated secretion of EspB (Rv3881c), required for virulence and growth in macrophages (McLaughlin et al., 2007). It is thus conceivable that EspK may influence the pathogenicity also in *M. kansasii*.

Collectively, based on the distribution of RD1 genes, neither of the *M. kansasii* types could be categorized as being more or less pathogenic, given that all genes essential for the functioning of the ESX-1 secretion machinery were uniformly present in *M. kansasii* strains, and that the absence of certain genes was reported in both clinically relevant and neutral strains. To explore more in depth the genetic background of virulence in *M. kansasii*, more advanced, functional studies should be performed, with a focus not only on the RD1 genes but several other genes flanking that cluster, which together form the "extended RD1" region. Furthermore, we cannot exclude that the pathogenic and non-pathogenic *M. kansasii* strains differ in terms of expression of the RD1 genes or activity of their proteins. More RD1-targeted experimental investigations are required to validate such scenarios.

Analysis of other than RD1 regions of deletions (RD2-14) did not show any consistent (i.e., shared across all strains of a given species) species-specific pattern of RD genes (**Supplementary Data Sheet 2**). It was noteworthy, however, that the only two genes found in the RD3 locus were present in either of the two most pathogenic *M. kansasii* types I and II. The *rv1577* gene occurred in more than 90% of *M. kansasii* type I and almost 73% of *M. kansasii* type II. Whereas, the *rv1586* gene was demonstrated exclusively in *M. kansasii* type I, at a frequency of nearly 81%. Likewise, only *M. kansasii* types I and II harbored genes of the RD11 locus. The *rv2651* gene was present in 90 and 73% of *M. kansasii* type I and II, respectively. The *rv2646* was evidenced in slightly more than 60% of *M. kansasii* type I. Interestingly, both RD3 and RD11 represent phage inserts within the *M. tuberculosis* genome, and are thought to generate antigenic variation (Ahmed et al., 2007).

It has been canonically accepted, upon description of new species, to provide a detailed phenotypic characterization. However, in the era of genomic-based bacterial taxonomy, the significance of the phenotype has much eroded and the use of conventional biochemical testing has been increasingly abandoned. The algorithm for routine differential diagnostics of NTM species should obligatorily include only growth rate and pigment production (Tortoli et al., 2017).

For closely-related species, the diagnostic value of phenotyping is virtually negligible, as demonstrated also in this study (**Table 6**). All strains, irrespective of subtype (species), were almost invariably photochromogenic, niacin-negative, and grew at 25 and 37°C, but not at 45°C, in the presence of 5% (w/v) NaCl or on MacConkey agar without crystal violet. They were all resistant to thiophene-2-carboxylic acid hydrazide (TCH) and presented a strong catalase activity, but none exhibited pyrazynamidase activity or arylsulfatase at 3 days. Some variability was observed when testing for nitrate and tellurite reduction, Tween 80 hydrolysis, and urease activity. The only marked difference between the subtypes (species) was that strains of *M. ostraviense* (formerly *M. kansasii* type IV) were, unlike all other species, unable to reduce nitrate and that their catalase was heat-liable. Whether these features are stable within the species need to be verified on a larger set of strains. Interestingly, both these features are typical for *M. gastri* (Kent and Kubica, 1985), with which *M. ostraviense* shares the highest genetic similarity, as evidenced upon whole-genome analysis. *Mycobacterium gastri*, a casual resident of human stomach and only exceptionally pathogenic (Velayati et al., 2005), is easily distinguishable from all *M. kansasii*-derived species, as it is non-photochromogenic.

Finally, drug susceptibility profiles of 30 mycobacterial strains, including type strains of three newly established species, by Tagini et al. (2019), were compared within and between the species (former *M. kansasii* types) (**Table 7**). Shortly, all strains were susceptible to RIF, RFB, AMK, SXT, MFX, LZD, and CLR (except one CLR-resistant strain of *M. kansasii*). Of these drugs, only RIF and CLR showed interspecies differences in their activity, with the MICs for *M. kansasii* and *M. persicum* slightly higher than for other *M. kansasii*-derived species. More than 80% of strains were resistant to EMB. Among these, were all strains of *M. kansasii* (former type I), *M. persicum* (II), and *M. ostraviense* (IV). Single strains of *M. kansasii*, *M. pseudokansasii*, and *M. attenuatum* were resistant to CIP. The MICs of STR and DOX varied widely (<0.5–16 mg/L vs. 1–>16 mg/L), yet the highest values (16 vs. >16 mg/L) were observed only for strains of *M. kansasii*, *M. persicum*, and *M. attenuatum*. The INH and ETO MICs were low, and within relatively narrow ranges (<0.25–2 mg/L vs. <0.3–0.6 mg/L). These findings confirm the key observations from previous studies, on the susceptibility of *M. kansasii* strains to RIF and their high resistance to EMB (da Silva Telles et al., 2005; Wu et al., 2009; Shahraki et al., 2017; Bakuła et al., 2018c). This, confronted with the ATS recommendation of a three-drug (INH-RIF-EMB) regimen for the treatment of *M. kansasii* disease, speaks for exclusion of EMB and its replacement with other potent drug, such as moxifloxacin.

In conclusion, the present paper updates and extends the findings of earlier investigation on the taxonomy of *M. kansasii*.

TABLE 6 | Phenotypic characteristics of *M. kansasii* strains under the study.

Type/Strain no.[a]			Morphology[b]	Pigment[c]	Growth in/post 7 days at/on[d]:				Tolerance of[e]:		Niacin	Reduction of:		Arylsulfatase		Tween 80 hydrolysis[f]	Catalase[g]		Urease[h]	PZA[i]
					25°C	37°C	45°C	MCA	TCH	NaCl 5%		nitrate	tellurite	3–day	14–day		SQ	HS		
*Mycobacterium kansasii**			SR	P^{99}; $S^{<1}$; $N^{<1}$	+	+	−	$-^{99}$	$+^{99}$	$-^{99}$	$-^{99}$	$+^{99}$	$-^{84}$	$-^{99}$	$+^{55}$	$+^{99}$	$>45^{99}$	$+^{95}$	$+^{97}$	$-^{99}$
M. kansasii	I (11)	NLA001000521	RY	P	+	+	−	−	+	−	−	+	−	−	3+	+	17	−	−	−
		ATCC25221	RW	N	+	+	−	−	+	−	−	+	−	−	3+	+	74	+	+	−
		NLA001000927	RY	P	+	+	−	−	+	−	−	+	−	−	3+	+	54	+	+	−
		NLA001000449	RY	P	+	+	−	−	+	−	−	+	−	−	3+	+	50	+	−	−
		6200	RY	P	+	+	−	−	+	−	−	+	−	−	4+	+	52	+	−	−
		7728	RY	P	+	+	−	−	+	−	−	+	−	−	3+	+	70	+	−	−
		7744	RY	P	+	+	−	−	+	−	−	+	−	−	2+	+	59	+	−	−
		1010001495	RY	P	+	+	−/+	−	+	−	−	+	−	−	4+	+	65	+	−	−
		K4	RY	P	+	+	−/+	−	+	−	−	+	−	−	3+	+	54	+	−	−
		K14	RY	P	+	+	−	−	+	−	−	+	−	−	3+	+	41	+	+	−
		K19	RY	P	+	+	−	−	+	−	−	+	−	−	3+	+	51	+	+	−
			RY^{91}	P^{91}	$+^{100}$	$+^{100}$	$-^{82}$	$-^{100}$	$+^{100}$	$-^{100}$	$-^{100}$	$+^{100}$	$-^{100}$	$-^{100}$	$\geq 3+^{91}$	$+^{100}$	$>40^{91}$	$+^{91}$	$-^{64}$	$-^{100}$
M. persicum	II (8)	2193	RY	P	+	+	−	−	+	−	−	−	−	−	3+	−	44	+	−	−
		NLA001001128	RY	P	+	+	−	−	+	−	−	+	+	−	3+	−	40	+	+	−
		B11073207	RY	P	+	+	−	−	+	−	−	+	−	−	3+	−	44	+	+	−
		B11063838	RY	P	+	+	−	−	+	−	−	+	−	−	3+	−	43	+	+	−
		1010001469	RY	P	+	+	−	−	+	−	−	+	−	−	4+	+	18	−	−	−
		H47	RY	P	+	+	−	−	+	−	−	+	+	−	4+	+	45	+	+	−
		H48	RY	P	+	+	−	−	+	−	−	+	−	−	3+	+	47	+	+	−
		AFPC−000227 (T)**	RY	P	−	−	−	−	NT	NT	−	+	−	NT	NT	+	>45	+	−	NT
			RY^{100}	P^{100}	$+^{88}$	$+^{88}$	$-^{100}$	$-^{100}$	$+^{100}$	$-^{100}$	$-^{100}$	$+^{88}$	$-^{75}$	$-^{100}$	$\geq 3+^{100}$	$+^{50}$	$\geq 40^{88}$	$+^{88}$	$+^{63}$	$-^{100}$
M. pseudokansasii	III (4)	14_15	RY	P	+	+	−	−	+	−	−	+	−	−	3+	+	9	−	+	−
		174_15	RY	P	+	+	−	−	+	−	−	+	−	−	1+	+	8	−	+	−
		1010001468	RY	P	+	+	−	−	+	−	−	+	+	−	3+	+	30	+	−	−
		MK142	RY	P	+	+	−	−	+	−	−	+	−	−	2+	+	45	+	+	−
		MK142 (T)***	RY	NT	NT	NT	NT	NT	NT	NT	−	+	NT	NT	NT	+	NT	NT	v	NT
			RY^{100}	P^{100}	$+^{100}$	$+^{100}$	$-^{100}$	$-^{100}$	$+^{100}$	$-^{100}$	$-^{100}$	$+^{100}$	$-^{75}$	$-^{100}$	$\geq 2+^{75}$	$+^{100}$	$\geq 30^{50}$	$+^{50}$	$+^{60}$	$-^{100}$
M. ostraviense	IV (2)	1010001458	RY	P	+	+	−	−	+	−	−	−	−	−	1+	−	53	−	−	−
		241/15 (T)	RY	P	+	+	−	−	+	−	−	−	−	−	1+	+	48	−	−	−
			RY^{100}	P^{100}	$+^{100}$	$+^{100}$	$-^{100}$	$-^{100}$	$+^{100}$	$-^{100}$	$-^{100}$	$-^{100}$	$-^{100}$	$-^{100}$	$\geq 1+^{100}$	$+^{50}$	$>40^{100}$	$-^{100}$	$-^{100}$	$-^{100}$
M. innocens	V (4)	1010001454	RY	P	+	+	−	−	+	−	−	+	−	−	2+	+	78	+	+	−
		1010001493	RW	N	+	+	−	−	+	−	−	+	−	−	1+	+	3	−	−	−
		49_11	RY	P	+	+	−	−	+	−	−	+	−	−	3+	+	43	+	+	−
		MK13 (T)	RY	P	+	+	−	−	+	−	−	+	−	−	1+	−	39	+	+	−
		MK13 (T)***	Y	NT	NT	NT	NT	NT	NT	NT	−	v	NT	NT	NT	v	NT	NT	v	NT
			RY^{60}	P^{80}	$+^{100}$	$+^{100}$	$-^{100}$	$-^{100}$	$+^{100}$	$-^{100}$	$-^{100}$	$+^{80}$	$-^{100}$	$-^{100}$	$\geq 1+^{100}$	$+^{60}$	$>30^{75}$	$+^{75}$	$+^{60}$	$-^{100}$
M. attenuatum	VI (2)	NLA001001166	RY	P	+	+	−	−	+	−	−	+	−	−	3+	−	60	+	+	−
		MK41 (T)	RY	P	+	+	−	−	+	−	−	+	−	−	2+	+	45	+	+	−
		MK41 (T)***	Y	NT	NT	NT	NT	NT	NT	NT	v	v	NT	NT	NT	+	NT	NT	v	NT
			RY^{67}	P^{100}	$+^{100}$	$+^{100}$	$-^{100}$	$-^{100}$	$+^{100}$	$-^{100}$	$-^{67}$	$+^{67}$	$-^{100}$	$-^{100}$	$\geq 2+^{100}$	$+^{67}$	$>40^{100}$	$+^{100}$	$+^{67}$	$-^{100}$

All test reactions are given as "+" (positive), "–" (negative) or "v" (variable); NT, not tested. Numbers in superscripts represent percentage of strains reacting as indicated.

[a] *According to the WGS-based (MiSI method) grouping. Vertically are given the newly proposed names for each of the M. kansasii subtype; (T), type strain.*

* *Results according to Kent and Kubica (1985); prior to subtype delineation.*

** *Results according to Shahraki et al. (2017).*

*** *Results according to Tagini et al. (2019).*

[b] *Colony morphology: S, smooth; R, rough; Y, yellow/beige; W, white.*

[c] *Photochromogenicity: N, non-photochromogenic; P, photochromogenic; S, scotochromogenic.*

[d] *MCA, MacConkey agar without crystal violet.*

[e] *TCH, thiophene-2-carboxylic acid hydrazide.*

[f] *After 10 days.*

[g] *SQ, semi-quantitative catalase [mm]; HS, heat-stable catalase.*

[h] *after 5 days; v, variable.*

[i] *PZA, pyrazinamidase activity, after 4 days.*

TABLE 7 | Drug susceptibility profiles of *M. kansasii* strains under the study.

Type[a]		MIC [mg/L] of[b]												
	Strain no.	RIF	CLR	INH	EMB	STR	AMK	SXT	RFB	MXF	LZD	CIP	DOX	ETO
M. kansasii	I (11)	NLA001000521	0.25	0.25	2	>16	8	2	<0.12	<0.25	<0.12	2	2	4	<0.3
		ATCC25221	0.25	0.12	2	16	4	2	<0.12	<0.25	<0.12	2	1	4	0.6
		NLA001000927	0.25	0.12	2	16	4	1	<0.12	<0.25	<0.12	1	1	4	0.6
		NLA001000449	0.25	>64	2	>16	8	4	<0.12	<0.25	<0.12	2	2	8	<0.3
		6200	0.25	0.25	2	>16	8	2	0.12	<0.25	<0.12	2	2	16	<0.3
		7728	1	0.5	2	>16	16	8	0.12	<0.25	0.25	4	4	>16	<0.3
		7744	1	0.12	1	>16	4	2	<0.12	<0.25	<0.12	<1	1	4	<0.3
		1010001495	0.25	0.12	2	16	8	2	<0.12	<0.25	<0.12	<1	1	4	<0.3
		K4	0.5	0.25	2	>16	4	2	0.12	<0.25	<0.12	2	1	4	<0.3
		K14	1	0.5	2	>16	8	4	0.12	<0.25	<0.12	2	1	8	<0.3
		K19	0.5	0.25	1	>16	4	2	0.12	<0.25	<0.12	2	0.5	4	<0.3
		MIC50/90	0.25/1	0.25/0.5	2/2	>16/>16	8/8	2/4	<0.12/<0.12	<0.25/<0.25	<0.12/<0.12	2/2	1/2	4/16	<0.3/0.6
		MIC range	0.25-1	0.12->64	1-2	16->16	4-16	1-8	<0.12-0.12	<0.25	<0.12–0.25	<1–4	0.5–4	4–>16	<0.3–0.6
M. persicum	II (7)	2193	0.5	0.12	1	16	2	<1	<0.12	<0.25	<0.12	<1	0.25	2	<0.3
		NLA001001128	1	0.25	1	>16	16	8	<0.12	<0.25	<0.12	4	2	8	<0.3
		B11073207	0.25	0.12	1	16	4	2	<0.12	<0.25	<0.12	2	0.5	4	<0.3
		B11063838	1	0.5	1	>16	8	4	<0.12	<0.25	<0.12	2	1	16	<0.3
		1010001469	1	0.12	1	>16	16	2	<0.12	<0.25	<0.12	2	2	8	<0.3
		H47	1	0.5	2	>16	4	2	0.12	<0.25	0.25	2	1	8	0.6
		H48	0.25	1	1	>16	8	8	2	<0.25	<0.12	4	1	8	<0.3
		MIC50/90	1/1	0.25/1	1/2	>16/>16	8/16	2/8	<0.12/2	<0.25/<0.25	<0.12/0.25	2/4	1/2	8/16	<0.3/0.6
		MIC range	0.25–1	0.12–1	1–2	16/>16	2–16	<1–8	<0.12–2	<0.25	<0.12–0.25	<1–4	0.25–2	2–16	<0.3–0.6
M. pseudokansasii	III (4)	14_15	<0.12	0.12	1	>16	4	4	0.5	<0.25	<0.12	2	1	1	<0.3
		174_15	0.12	0.12	2	>16	8	2	<0.12	<0.25	<0.12	2	2	4	<0.3
		1010001468	0.5	<0.06	1	16	4	<1	<0.12	<0.25	<0.12	<1	0.5	2	<0.3
		MK142	0.25	0.25	0.5	1	2	<1	<0.12	<0.25	0.25	<1	4	4	<0.3
		MIC50/90	0.12/0.5	0.12/0.25	1/2	16/>16	4/8	<1/4	<0.12/0.5	<0.25/<0.25	<0.12/0.25	<1/2	1/2	2/4	<0.3/<0.3
		MIC range	<0.12–0.5	<0.06–0.25	0.5–2	1–>16	2–8	<1–4	<0.12–0.5	<0.25	<0.12–0.25	<1–2	0.5–4	1–4	<0.3
M. ostraviense	IV (2)	1010001458	<0.12	<0.06	1	16	4	2	0.12	<0.25	<0.12	<1	0.5	4	<0.3
		241/15	<0.12	0.06	2	>16	4	4	0.12	<0.25	<0.12	2	2	2	<0.3
		MIC50/90	<0.12/<0.12	<0.06/0.06	1/2	16/>16	4/4	2/4	0.12/0.12	<0.25/<0.25	<0.12/<0.12	<1/2	0.5/2	2/4	<0.3/<0.3
		MIC range	<0.12	<0.06–0.06	1–2	16–>16	4	2–4	0.12	<0.25	<0.12	<1–2	0.5–2	2–4	<0.3
M. innocens	V (4)	1010001454	0.5	<0.06	2	4	4	2	0.12	<0.25	<0.12	2	1	4	<0.3
		1010001493	<0.12	0.12	<0.25	4	4	2	0.12	<0.25	0.25	2	2	4	<0.3
		49_11	0.5	<0.06	1	>16	<0.5	<1	<0.12	<0.25	0.5	4	2	8	<0.3
		MK13	<0.12	0.12	<0.25	1	4	2	2	<0.25	0.25	<1	2	1	<0.3
		MIC50/90	<0.12/0.5	<0.06/0.12	<0.25/2	4/>16	4/4	2/2	0.12/2	<0.25/<0.25	0.25/0.5	2/4	2/2	4/8	<0.3/<0.3
		MIC range	<0.12–0.5	<0.06–0.12	<0.25–2	1–>16	<0.5–4	<1–2	<0.12–2	<0.25	<0.12–0.5	<1–4	1–2	1–8	<0.3
M. attenuatum	VI (2)	NLA001001166	0.25	0.12	2	16	8	1	<0.12	<0.25	<0.12	2	1	8	<0.3
		MK41	0.5	0.5	0.5	4	16	8	<0.12	<0.25	0.5	<1	4	>16	<0.3
		MIC50/90	0.25/0.5	0.12/0.5	0.5/2	4/16	8/16	1/8	<0.12/<0.12	<0.25/<0.25	<0.12/0.5	<1/2	1/4	8/>16	<0.3/<0.3
		MIC range	0.25–0.5	0.12–0.5	0.5–2	4–16	8–16	1–8	<0.12	<0.25	<0.12–0.5	<1–2	1–4	8–>16	<0.3
TOTAL	MIC50/90	0.25/1	0.12/0.5	1/2	>16/>16	4/16	2/8	<0.12/0.12	<0.25/<0.25	<0.12–0.25	2/4	1/2	4/16	<0.3/<0.3	
	MIC range	<0.12–1	<0.06–>64	<0.25–2	1–>16	<0.5–16	<1–8	<0.12–2	<0.25	<0.12–0.5	<1–4	0.25–4	1–>16	<0.3–0.6	

Please note, that for some isolates those data were reported elsewhere (Bakuła et al., 2018c).

[a] *According to the WGS-based (MiSI method) grouping. Vertically are given the newly proposed names for each of the M. kansasii subtypes.*

[b] *RIF, rifampicin; CLR, clarithromycin; INH, isoniazid; EMB, ethambutol; STR, streptomycin; AMK, amikacin; SXT, co-trimoxazole; RFB, rifabutin; MXF, moxifloxacin; LZD, linezolid; CIP, ciprofloxacin; DOX, doxycycline; ETO, ethionamide.*

Not only does it further substantiate the delineation of new species from the *M. kansasii* group to replace the former subtypes I–VI, but consolidates the position of five of the so erected species, and provides a description of the sixth one, *M. ostraviense*, a successor of the subtype IV. By showing a close genetic relatedness, a monophyletic origin, and overlapping phenotypes, our findings support the recognition of the *M. kansasii* complex (MKC), accommodating all *M. kansasii*-derived species and *M. gastri*. Neither of the most commonly used taxonomic markers can accurately distinguish all the MKC species. Likewise, no species-specific phenotypic characteristics exist that would allow identification of the species, except the non-photochromogenicity of *M. gastri*. In the context of the previously proposed polyphasic strategy in resolving species boundaries and their interrelatedness, FAME (fatty acid methyl ester) analysis, as an adjunct typing method, might be useful (Saini et al., 2009). However, preparatory techniques for FAME analysis are typically time-consuming, laborious, and material-intensive. Furthermore, chromatography-dedicated facilities require investment in instrumentation and training, and despite their services being offered by universities and other centres, they are often less accessible than sequencing facilities, even in the developing countries.

To distinguish, most reliably, between the MKC species, and between *M. kansasii* and *M. persicum* in particular, whole-genome-based approaches should be applied.

Since no clear differences in the repertoire of the virulence-associated RD1 genes have been observed among the *M. kansasii*-derived species, the pathogenic capacity of each of these species can only be speculated based on their prevalence among the clinically relevant population. Large-scale molecular epidemiological studies are needed to gain a better understanding of the clinical significance and pathobiology of the MKC species.

Description of *Mycobacterium ostraviense* sp. nov. Jagielski and Ulmann

Mycobacterium ostraviense [os.tra.vi.en'se. N.L. neut. adj. *ostraviense* pertaining to Ostravia, the Latin name of Ostrava, a city in the north-east of the Czech Republic where one of the strain was isolated].

The species name refers to the former *M. kansasii* subtype IV. Mature colonies, of rough surface and photochromogenic, are observed on Löwenstein-Jensen medium after more than 7 days of incubation at 37°C (**Supplementary Figure 1**). No growth occurs at 45°C and on the media containing TCH or 5% (w/v) NaCl. Similar to other MKC species, it tests positive for the semi-quantitative catalase (>45 mm) and 14-day arylsulfatase activity, while negative for niacin accumulation, tellurite reduction, and urease and pyrazynamidase activities. Unlike to other *M. kansasii*-derived species but similar to *M. gastri*, it does not reduce nitrates, nor it produces a heat-stable (68°C) catalase. Strongly resistant to ethambutol (>16 mg/L) but susceptible to amikacin, clarithromycin, co-trimoxazole, linezolid, fluoroquinolones, and rifamycins.

The species has the same 16S rRNA sequences as *M. kansasii* (former subtype I) and *M. gastri*, yet it displays unique sequences at the *hsp65*, *tuf*, and *rpoB* genes, and the ITS locus. At the genomic level, it is most closely related to *M. gastri*, with pairwise ANI and GGD values of 95.2 and 0.056, respectively.

The type strain, $241/15^{T}$ was isolated from a sputum of a patient with no NTM disease, based in Karviná, near Ostrava, in the Moravian-Silesian Region of the Czech Republic. The type strain has been deposited in the Leibniz Institute German Collection of Microorganisms and Cell Cultures (DSMZ; Braunschweig, Germany) under the accession number DSM 110538.

DATA AVAILABILITY STATEMENT

All datasets generated for this study are included in the article/**Supplementary Material**.

ETHICS STATEMENT

Analyses were based on data that did not contain any sensitive personal information. Therefore, informed consent and ethical approval were not required in like with local legislation.

AUTHOR CONTRIBUTIONS

TJ conceptualized and supervised the study, provided the funding, organized and integrated the data, and wrote the manuscript. PB, JL, and DS performed bioinformatic analyses including AF-ANI, GGD, and phylogenetic tree analysis. ZB performed culturing, subtyping, and phenotypic profiling of *M. kansasii* strains. BM carried out analysis on regions of difference 1-14 (RD1-14) with a homemade script Diffind. AB carried out DNA isolations for whole-genome sequencing. JD analyzed the results on the distribution of the RD1-14 genes in *M. kansasii* genomes. MD constructed the core-genome phylogenies. LP performed drug susceptibility testing. JI provided 13 *M. kansasii* strains of subtypes I-VI and critically reviewed the manuscript. MŽ-D co-performed phenotypic assays.

FUNDING

This work was supported by the National Centre for Research and Development grant (to: TJ) through the LIDER Programme under contract no. LIDER/044/457/L-4/12/NCBR/2013. DS, JL, and BM were supported by the Polish Ministry of Science and Higher Education grant under contract no. DIR/WK/2017/2018/01-1.

ACKNOWLEDGMENTS

The authors are indebted to Aleksandra Safianowska (Department of Internal Medicine, Pulmonology, and Allergology, Warsaw Medical University, Warsaw, Poland), Won-Jung Koh (Division of Pulmonary and Critical Care Medicine; Department of Medicine, Samsung Medical Center, Sungkyunkwan University School of Medicine, South Korea), Vit Ulmann (Institute of Public Health, Ostrava, Czech Republic), Miren J. Unzaga Barañano (Clinical Microbiology and Infection Control, Basurto Hospital, Bilbao, Spain), Joanna Humiecka (Hospital of Infectious Diseases in Warsaw, Poland),

and Katharina Kranzer (National Reference Laboratory for Mycobacteria, Research Center Borstel, Borstel, Germany) for their kind providing some of *M. kansasii* strains used in this study.

Special appreciation is extended to Fernando Alcaide and David Rodriguez-Temporal (Department of Pathology and Experimental Therapy, Universitat de Barcelona, Hospitalet de Llobregat, Spain) for their kind reviewing of the manuscript and valuable comments.

SUPPLEMENTARY MATERIAL

The Supplementary Material for this article can be found online at: https://www.frontiersin.org/articles/10.3389/fmicb.2019.02918/full#supplementary-material

Supplementary Tables 1–6 are published inside **Supplementary Data Sheet 1**.

Supplementary Table 1 | Pairwise similarities (%) between 16S rRNA sequences.

Supplementary Table 2 | Pairwise similarities (%) between ITS sequences.

Supplementary Table 3 | Pairwise similarities (%) between *hsp65* sequences.

Supplementary Table 4 | Pairwise similarities (%) between *tuf* sequences.

Supplementary Table 5 | Pairwise similarities (%) between *rpoB* sequences.

Supplementary Table 6 | Strains (genomes) used in different genetic analyses.

Supplementary Figure 1 | Macro- and micromorphology of colonies of four recently established species within the *M. kansasii* complex. Colonies photographed after 2 weeks of growth at 37°C on Löwenstein-Jensen medium, and additional 72 h post-light exposure (upper row of images). Cell morphological patterns upon Ziehl-Neelsen stain (magnification, x100), and scanning electron microscopy (magnification, x6,000). Scale bar 2 μM is applicable for *M. pseudokansasii*, *M. ostraviense*, and *M. innocens*, while scale bar 3 μM applies to *M. attenuatum*.

Supplementary Data Sheet 2 | Distribution of region of difference 2-14 (RD2-14) genes among *M. kansasii* strains and other mycobacterial outgroup species.

REFERENCES

Abed, Y., Bollet, C., and de Micco, P. (1995). Demonstration of *Mycobacterium kansasii* species heterogeneity by the amplification of the 16S-23S spacer region. *J. Med. Microbiol.* 42, 112–114. doi: 10.1099/00222615-43-2-156

Ahmed, N., Saini, V., Raghuvanshi, S., Khurana, J. P., Tyagi, A. K., Tyagi, A. K., et al. (2007). Molecular analysis of a leprosy immunotherapeutic bacillus provides insights into *Mycobacterium* evolution. *PLoS ONE* 2:e968. doi: 10.1371/journal.pone.0000968

Alcaide, F., Richter, I., Bernasconi, C., Springer, B., Hagenau, C., Schulze-Röbbecke, R., et al. (1997). Heterogeneity and clonality among isolates of *Mycobacterium kansasii*: implications for epidemiological and pathological studies. *J. Clin. Microbiol.* 35, 1959–1964.

Andrews, S. (2010). *FastQC: A Quality Control Tool for High Throughput Sequence Data*. Available online at: http://www.bioinformatics.babraham.ac.uk/projects/fastqc

Auch, A. F., Klenk, H. P., and Göker, M. (2010). Standard operating procedure for calculating genome-to-genome distances based on high-scoring segment pairs. *Stand. Genomic Sci.* 2, 142–148. doi: 10.4056/sigs.541628

Bakuła, Z., Brzostek, A., Borówka, P., Zaczek, A., Szulc-Kiełbik I, Podpora, A., Parniewski, P., et al. (2018a). Molecular typing of *Mycobacterium kansasii* using pulsed-field gel electrophoresis and a newly designed variable-number tandem repeat analysis. *Sci. Rep.* 8:e4462. doi: 10.1038/s41598-018-21562-z

Bakuła, Z., Kościuch, J., Safianowska, A., Proboszcz, M., Bielecki, J., van Ingen, J., et al. (2018b). Clinical, radiological and molecular features of *Mycobacterium kansasii* pulmonary disease. *Respir. Med.* 139, 91–100. doi: 10.1016/j.rmed.2018.05.007

Bakuła, Z., Modrzejewska, M., Pennings, L., Proboszcz, M., Safianowska, A., Bielecki, J., et al. (2018c). Drug susceptibility profiling and genetic determinants of drug resistance in *Mycobacterium kansasii*. *Antimicrob Agents Chemother. C* 62, e01788–e01717. doi: 10.1128/AAC.01788-17

Bakuła, Z., Modrzejewska, M., Safianowska, A., van Ingen, J., Proboszcz, M., Bielecki, J., et al. (2016). Proposal of a new method for subtyping of *Mycobacterium kansasii* based upon PCR restriction enzyme analysis of the *tuf* gene. *Diagn. Microbiol. Infect. Dis.* 84, 318–321. doi: 10.1016/j.diagmicrobio.2015.12.009

Berthet, F. X., Rasmussen, P. B., Rosenkrands, I., Andersen, P., and Gicquel, B. (1998). A *Mycobacterium tuberculosis* operon encoding ESAT-6 and a novel low-molecular-mass culture filtrate protein (CFP-10). *Microbiology* 144, 3195–3203. doi: 10.1099/00221287-144-11-3195

Brodin, P., Majlessi, L., Marsollier, L., de Jonge, M. I., Bottai, D., Demangel, C., et al. (2006). Dissection of ESAT-6 system 1 of *Mycobacterium tuberculosis* and impact on immunogenicity and virulence. *Infect. Immun.* 74, 88–98. doi: 10.1128/IAI.74.1.88-98.2006

Brosch, R., Gordon, S. V., Marmiesse, M., Brodin, P., Buchrieser, C., Eiglmeier, K., et al. (2002). A new evolutionary scenario for the *Mycobacterium tuberculosis* complex. *Proc. Natl. Acad. Sci. U.S.A.* 99, 3684–3689. doi: 10.1073/pnas.052548299

Buhler, V. B., and Pollak, A. (1953). Human infection with atypical acid-fast organisms; report of two cases with pathologic findings. *Am. J. Clin. Pathol.* 23, 363–374. doi: 10.1093/ajcp/23.4.363

Butler, W. R., Floyd, M. M., Silcox, V., Cage, G., Desmond, E., Duffey, P. S., et al. (1996). *Standardized Method for HPLC Identification of Mycobacteria*. HPLC users group in cooperation with Centers for Disease Control and Prevention. Atlanta, GA: U.S. Public Health Service, CDC.

Chen, Y. P., Yen, Y. S., Chen, T. Y., Yen, C. L., Shieh, C. C., and Chang, K. C. (2008). Systemic *Mycobacterium kansasii* infection mimicking peripheral T-cell lymphoma. *APMIS* 116, 850–858. doi: 10.1111/j.1600-0463.2008.00935.x

CLSI; Clinical and Laboratory Standards Institute (2011). *Susceptibility Testing of Mycobacteria, Nocardiae, and Other Aerobic Actinomycetes; Approved Standard*, 2nd Edn. CLSI document M24-A2. Clinical and Laboratory Standards Institute, Wayne, IL.

da Silva Rocha, A., Werneck Barreto, A. M., Dias Campos, C. E., Villas-Bôas da Silva, M., Fonseca, L., Saad, M. H., et al. (2002). Novel allelic variants of *Mycobacteria* isolated in Brazil as determined by PCR-restriction enzyme analysis of *hsp65*. *J. Clin. Microbiol.* 40, 4191–4196. doi: 10.1128/JCM.40.11.4191-4196.2002

da Silva Telles, M. A., Chimara, E., Ferrazoli, L., and Riley, L. W. (2005). *Mycobacterium kansasii*: antibiotic susceptibility and PCR-restriction analysis of clinical isolates. *J. Med. Microbiol.* 54, 975–979. doi: 10.1099/jmm.0.45965-0

Devallois, A., Goh, K. S., and Rastogi, N. (1997). Rapid identification of mycobacteria to species level by PCR-restriction fragment length polymorphism analysis of the hsp65 gene and proposition of an algorithm to differentiate 34 mycobacterial species. *J. Clin. Microbiol.* 35, 2969–2973.

Devulder, G., Pérouse de Montclos, M., and Flandrois, J. P. (2005). A multigene approach to phylogenetic analysis using the genus *Mycobacterium* as a model. *Int. J. Syst. Evol. Microbiol.* 55, 293–302. doi: 10.1099/ijs.0.63222-0

Emms, D. M., and Kelly, S. (2019). OrthoFinder: phylogenetic orthology inference for comparative genomics. *Genome Biol.* 20:238. doi: 10.1186/s13059-019-1832-y

Falkinham, J. O. (1996). Epidemiology of Infection by nontuberculous mycobacteria. *Clin. Microbiol. Rev.* 9, 177–215. doi: 10.1128/CMR.9.2.177

Felsenstein, J. (1985). Confidence limits on phylogenies: an approach using the bootstrap. *Evolution* 39, 783–791. doi: 10.1111/j.1558-5646.1985.tb00420.x

Gaafar, A., Unzaga, M. J., Cisterna, R., Clavo, F. E., Urra, E., Ayarza, R., et al. (2003). Evaluation of a modified single-enzyme amplified-fragment

length polymorphism technique for fingerprinting and differentiating of *Mycobacterium kansasii* type I isolates. *J. Clin. Microbiol.* 41, 3846–3850. doi: 10.1128/JCM.41.8.3846-3850.2003

Griffith, D. E., Aksamit, T., Brown-Elliott, B. A., Catanzaro, A., Daley, C., Gordin, F., et al. (2007). ATS Mycobacterial Diseases Subcommittee; American Thoracic Society; Infectious Disease Society of America. An official ATS/IDSA statement: diagnosis, treatment, and prevention of nontuberculous mycobacterial diseases. *Am. J. Respir. Crit. Care Med*. 175, 367–416. doi: 10.1164/rccm.200604-571ST

Gurevich, A., Saveliev, V., Vyahhi, N., and Tesler, G. (2013). QUAST: quality assessment tool for genome assemblies. *Bioinformatics* 29, 1072–1075. doi: 10.1093/bioinformatics/btt086

Hall, T. A. (1999). BioEdit: a user-friendly biological sequence alignment editor and analysis program for Windows 95/98/NT. *Nucleic Acids Symp. Ser.* 41, 95–98.

Hauduroy, P. (1955). *Derniers Aspects du monde des Mycobactéries*. Paris: Masson et Cie, 73.

Hermans, P. W., van Soolingen, D., and van Embden, J. D. (1992). Characterization of a major polymorphic tandem repeat in *Mycobacterium tuberculosis* and its potential use in the epidemiology of *Mycobacterium kansasii* and *Mycobacterium gordonae*. *J. Bacteriol.* 174, 4157–4165. doi: 10.1128/jb.174.12.4157-4165.1992

Hoefsloot, W., van Ingen, J., Andrejak, C., Angeby, K., Bauriaud, R., Bemer, P., et al. (2013). The geographic diversity of nontuberculous mycobacteria isolated from pulmonary samples: a NTM-NET collaborative study. *Eur. Respir. J.* 42, 1604–1613. doi: 10.1183/09031936.00149212

Horsburgh, C. R. Jr., and Selik, R. M. (1989). The epidemiology of disseminated nontuberculous mycobacterial infection in the acquired immunodeficiency syndrome (AIDS). *Am. Rev. Respir. Dis.* 139, 4–7. doi: 10.1164/ajrccm/139.1.4

Houben, D., Demangel, C., van Ingen, J., Perez, J., Baldeón, L., Abdallah, A. M., et al. (2012). ESX-1-mediated translocation to the cytosol controls virulence of mycobacteria. *Cell. Microbiol.* 14, 1287–1298. doi: 10.1111/j.1462-5822.2012.01799.x

Iinuma, Y., Ichiyama, S., Hasegawa, Y., Shimokata, K., Kawahara, S., and Matsushima, T. (1997). Large-restriction-fragment analysis of *Mycobacterium kansasii* genomic DNA and its application in molecular typing. *J. Clin. Microbiol.* 35, 596–599.

Inwald, J., Jahans, K., Hewinson, R. G., and Gordon, S. V. (2003). Inactivation of the *Mycobacterium bovis* homologue of the polymorphic RD1 gene Rv3879c (Mb3909c) does not affect virulence. *Tuberculosis* 83, 387–393. doi: 10.1016/j.tube.2003.08.018

Iwamoto, T., and Saito, H. (2005). Comparative study of two typing methods *hsp65* PRA and ITS sequencing revealed a possible evolutionary link between *Mycobacterium kansasii* type I and II isolates. *FEMS Microbiol. Lett*. 254, 129–133. doi: 10.1111/j.1574-6968.2005.00013.x

Jukes, T. H., and Cantor, C. R. (1969). "Evolution of protein molecules," in *Mammalian Protein Metabolism*, ed H. N. Munro (New York, NY: Academic Press), 21–132.

Katoh, K., and Standley, D. M. (2013). MAFFT multiple sequence alignment software version 7: improvements in performance and usability. *Mol. Biol. Evol.* 30, 772–780. doi: 10.1093/molbev/mst010

Kearse, M., Moir, R., Wilson, A., Stones-Havas, S., Cheung, M., Sturrock, S., et al. (2012). Geneious Basic: an integrated and extendable desktop software platform for the organization and analysis of sequence data. *Bioinformatics* 28, 1647–1649. doi: 10.1093/bioinformatics/bts199

Kent, P. T., and Kubica, G. P. (1985). *Public Health Mycobacteriology. A Guide for the Level III Laboratory*. Atlanta, GA: Centers for Disease Control.

Kim, B. J., Lee, K. H., Park, B. N., Kim, S. J., Bal, G. H., Kim, S. J., et al. (2001). Differentiation of mycobacterial species by PCR-restriction analysis of DNA (343 base pairs) of the RNA polymerase gene (*rpoB*). *J. Clin. Microbiol.* 39, 2102–2109. doi: 10.1128/JCM.39.6.2102-2109.2001

Kumar, S., Stecher, G., Li, M., Knyaz, C., and Tamura, K. (2018). MEGA X: Molecular Evolutionary Genetics Analysis across computing platforms. *Mol. Biol. Evol.* 35, 1547–1549. doi: 10.1093/molbev/msy096

Kwenda, G., Churchyard, G. J., Thorrold, C., Heron, I., Stevenson, S., Duse, A. G., et al. (2015). Molecular characterization of clinical and environmental isolates of *Mycobacterium kansasii* isolates from South African gold mines. *J. Water Health* 13, 190–202. doi: 10.2166/wh.2014.161

Liao, C. H., Lai, C. C., Ding, L. W., Hou, S. M., Chiu, H. C., Chang, S. C., et al. (2007). Skin and soft tissue infection caused by non-tuberculous mycobacteria. *Int. J. Tuberc. Lung Dis.* 11, 96–102.

LPSN database (2019). *List of Prokaryotic Names With Standing in Nomenclature*. Available online at: http://www.bacterio.net/ (accessed August 24, 2019).

MacGurn, J. A., and Cox, J. S. (2007). A genetic screen for *Mycobacterium tuberculosis* mutants defective for phagosome maturation arrest identifies components of the ESX-1 secretion system. *Infect. Immun.* 75, 2668–2678. doi: 10.1128/IAI.01872-06

Manten, A. (1957). Antimicrobial susceptibility and some other properties of photochromogenic mycobacteria associated with pulmonary disease. *Antonie van Leeuwenhoek. J. Microbiol. Serol.* 23, 357–363. doi: 10.1007/BF02545888

Marciniak, B., Borówka, P., and Strapagiel, D. (2017). *DIFFIND – The Sequence Difference Finder*. Available online at: https://github.com/BiobankLab/DIFFIND

Marras, T. K., and Daley, C. L. (2004). A systematic review of the clinical significance of pulmonary *Mycobacterium kansasii* isolates in HIV infection. *J. Acquir. Immune Defic. Syndr.* 36, 883–889. doi: 10.1097/00126334-200408010-00001

Matveychuk, A., Fuks, L., Priess, R., Hahim, I., and Shitrit, D. (2012). Clinical and radiological features of *Mycobacterium kansasii* and other NTM infections. *Respir. Med.* 106, 1472–1477. doi: 10.1016/j.rmed.2012.06.023

McLaughlin, B., Chon, J. S., MacGurn, J. A., Carlsson, F., Cheng, T. L., Cox, J. S., et al. (2007). A mycobacterium ESX-1-secreted virulence factor with unique requirements for export. *PLoS Pathog.* 3:e105. doi: 10.1371/journal.ppat.0030105

Meier-Kolthoff, J. P., Auch, A. F., Klenk, H. P., and Göker, M. (2013a). Genome sequence-based species delimitation with confidence intervals and improved distance functions. *BMC Bioinformatics* 14:60. doi: 10.1186/1471-2105-14-60

Meier-Kolthoff, J. P., Göker, M., Spröer, C., and Klenk, H. P. (2013b). When should a DDH experiment be mandatory in microbial taxonomy? *Arch. Microbiol.* 195, 413–418. doi: 10.1007/s00203-013-0888-4

Middlebrook, G. (1956). Diagnostic and biological problems of isoniazid-resistant tubercle bacilli. *Bull. Un. Int. Tuberc.* 26, 179–205.

Moon, S. M., Park, H. Y., Jeon, K., Kim, S. Y., Chung, M. J., Huh, H. J., et al. (2015). Clinical significance of *Mycobacterium kansasii* isolates from respiratory specimens. *PLoS ONE* 10:e0139621. doi: 10.1371/journal.pone.0139621

Murugaiyan, J., Lewin, A., Kamal, E., Bakuła, Z., van Ingen, J., Ulmann, V., et al. (2018). MALDI spectra database for rapid discrimination and subtyping of *Mycobacterium kansasii*. *Front. Microbiol.* 9:e587. doi: 10.3389/fmicb.2018.00587

Nurk, S., Bankevich, A., Antipov, D., Gurevich, A. A., Korobeynikov, A., Lapidus, A., et al. (2013). "Assembling genomes and mini-metagenomes from highly chimeric reads," in *Annual International Conference on Research in Computational Molecular Biology* (Berlin; Heidelberg Springer).

Park, S. Y., Lee, G. R., Min, J. W., Jung, J. Y., Jeon, Y. D., Shin, H. S., et al. (2012). A case of *Mycobacterium kansasii* lymphadenitis in HIV-infected patient. *Infect. Chemother.* 44, 526–529. doi: 10.3947/ic.2012.44.6.526

Picardeau, M., Prod'hom, G., Raskine, L., LePennec, M. P., and Vincent, V. (1997). Genotypic characterization of five subspecies of *Mycobacterium kansasii*. *J. Clin. Microbiol.* 35, 25–32.

Plikaytis, B. B., Plikaytis, B. D., Mitchell, A., Yakrus, W., Butler, R., Woodley, C. L., et al. (1992). Differentiation of slowly growing *Mycobacterium* species, including *Mycobacterium tuberculosis*, by gene amplification and restriction fragment length polymorphism analysis. *J. Clin. Microbiol.* 30, 1815–1822.

Price, M. N., Dehal, P. S., and Arkin, A. P. (2010). FastTree 2 – approximately maximum-likelihood trees for large alignments. *PLoS ONE*. 5:e9490. doi: 10.1371/journal.pone.0009490

Richter, E., Niemann, S., Rüsch-Gerdes, S., and Hoffner, S. (1999). Identification of *Mycobacterium kansasii* by using a DNA probe (AccuProbe) and molecular techniques. *J. Clin. Microbiol.* 37, 964–970.

Richter, M., and Rosselló-Móra, R. (2009). Shifting the genomic gold standard for the prokaryotic species definition. *Proc. Natl. Acad. Sci. U.S.A.* 106, 19126–19131. doi: 10.1073/pnas.0906412106

Ricketts, W. M., O'Shaughnessy, T. C., and van Ingen, J. (2014). Human-to-human transmission of *Mycobacterium kansasii* or victims of a shared source? *Eur. Respir. J.* 44, 1085–1087. doi: 10.1183/09031936.00066614

Ross, B. C., Jackson, K., Yang, M., Sievers, A., and Dwyer, B. (1992). Identification of a genetically distinct subspecies of *Mycobacterium kansasii*. *J. Clin. Microbiol.* 30, 2930–2933.

Saini, V., Raghuvanshi, S., Talwar, G. P., Ahmed, N., Khurana, J. P., Hasnain, S. E., et al. (2009). Polyphasic taxonomic analysis establishes *Mycobacterium indicus pranii* as a distinct species. *PLoS ONE* 4:e6263. doi: 10.1371/journal.pone.0006263

Saitou, N., and Nei, M. (1987). The neighbor-joining method: a new method for reconstructing phylogenetic trees. *Mol. Biol. Evol.* 4, 406–425.

Santin, M., and Alcaide, F. (2003). *Mycobacterium kansasii* disease among patients infected with human immunodeficiency virus type 1: improved prognosis in the era of highly active antiretroviral therapy. *Int. J. Tuberc. Lung Dis.* 7, 673–677.

Santos, A. R., De Miranda, A. B., Lima, L. M., Suffys, P. N., and Degrave, W. M. (1992). Method for high yield preparation in large and small scale of nucleic acids from mycobacteria. *J. Microbiol. Methods* 28, 1236–1243.

Shaaban, H., Layne, T., Sensakovic, J. W., and Boghossian, J. (2014). *Mycobacterium kansasii* septicaemia in an AIDS patient complicated by acute respiratory distress syndrome and acute liver failure. *Int. J. STD AIDS* 25, 152–154. doi: 10.1177/0956462413496080

Shahraki, A. H., Trovato, A., Mirsaeidi, M., Borroni, E., Heidarieh, P., Hashemzadeh, M., et al. (2017). *Mycobacterium persicum* sp. nov., a novel species closely related to *Mycobacterium kansasii* and *Mycobacterium gastri*. *Int. J. Syst. Evol. Microbiol.* 67, 1766–1770. doi: 10.1099/ijsem.0.001862

Shitrit, D., Baum, G. L., Priess, R., Lavy, A., Shitrit, A. B., Raz, M., et al. (2006). Pulmonary *Mycobacterium kansasii* infection in Israel, 1999-2004: clinical features, drug susceptibility, and outcome. *Chest* 129, 771–776. doi: 10.1378/chest.129.3.771

Sood, G., and Parrish, N. (2017). Outbreaks of nontuberculous mycobacteria. *Curr. Opin. Infect. Dis.* 30, 404–409. doi: 10.1097/QCO.0000000000000386

Tagini, F., Aeby, S., Bertelli, C., Droz, S., Casanova, C., Prod'hom, G., et al. (2019). Phylogenomics reveal that *Mycobacterium kansasii* subtypes are species-level lineages. Description of *Mycobacterium pseudokansasii* sp. nov., *Mycobacterium innocens* sp. nov. and *Mycobacterium attenuatum* sp. nov. *Int. J. Syst. Evol. Microbiol.* 69, 1696–1704. doi: 10.1099/ijsem.0.003378

Taillard, C., Greub, G., Weber, R., Pfyffer, G. E., Bodmer, T., Zimmerli, S., et al. (2003). Clinical implications of *Mycobacterium kansasii* species heterogeneity: Swiss National Survey. *J. Clin. Microbiol.* 41, 1240–1244. doi: 10.1128/JCM.41.3.1240-1244.2003

Tanizawa, Y., Fujisawa, T., and Nakamura, Y. (2017). DFAST: a flexible prokaryotic genome annotation pipeline for faster genome publication. *Bioinformatics* 34, 1037–1039. doi: 10.1093/bioinformatics/btx713

Telenti, A., Marchesi, F., Balz, M., Bally, F., Böttger, E. C., and Bodmer, T. (1993). Rapid identification of mycobacteria to the species level by polymerase chain reaction and restriction enzyme analysis. *J. Clin. Microbiol.* 31, 175–178.

Thomson, R., Tolson, C., Carter, R., Coulter, C., Huygens, F., and Hargreaves, M. (2013). Isolation of nontuberculous mycobacteria (NTM) from household water and shower aerosols in patients with pulmonary disease caused by NTM. *J. Clin. Microbiol.* 51, 3006–3011. doi: 10.1128/JCM.00899-13

Thomson, R., Tolson, C., Huygens, F., and Hargreaves, M. (2014). Strain variation amongst clinical and potable water isolates of *M. kansasii* using automated repetitive unit PCR. *Int. J. Med. Microbiol.* 304, 484–489. doi: 10.1016/j.ijmm.2014.02.004

Tortoli, E. (2014). Microbiological features and clinical relevance of new species of the genus *Mycobacterium*. *Clin. Microbiol. Rev.* 27, 727–752. doi: 10.1128/CMR.00035-14

Tortoli, E., Fedrizzi, T., Meehan, C. J., Trovato, A., Grottola, A., Giacobazzi, E., et al. (2017). The new phylogeny of the genus *Mycobacterium*: the old and the news. *Infect. Genet. Evol.* 56, 19–25. doi: 10.1016/j.meegid.2017.10.013

Tortoli, E., Simonetti, M. T., Lacchini, C., Penati, V., and Urbano, P. (1994). Tentative evidence of AIDS-associated biotype of *Mycobacterium kansasii*. *J. Clin. Microbiol.* 32, 1779–1782.

Vaidya, G., Lohman, D. J., and Meier, R. (2011). SequenceMatrix: concatenation software for the fast assembly of multi-gene datasets with character set and codon information. *Cladistics* 27, 171–180. doi: 10.1111/j.1096-0031.2010.00329.x

van der Wel, N., Hava, D., Houben, D., Fluitsma, D., van Zon, M., Pierson, J., et al. (2007). *M. tuberculosis* and *M. leprae* translocate from the phagolysosome to the cytosol in myeloid cells. *Cell* 129, 1287–1298. doi: 10.1016/j.cell.2007.05.059

van Ingen, J., de Zwaan, R., Dekhuijzen, R., Boeree, M., and van Soolingen, D. (2009). Region of difference 1 in nontuberculous *Mycobacterium* species adds a phylogenetic and taxonomical character. *J. Bacteriol.* 191, 5865–5867. doi: 10.1128/JB.00683-09

Varghese, N. J., Mukherjee, S., Ivanova, N., Konstantinidis, K. T., Mavrommatis, K., Kyrpides, N. C., et al. (2015). Microbial species delineation using whole genome sequences. *Nucleic Acids Res.* 43, 6761–7671. doi: 10.1093/nar/gkv657

Velayati, A. A., Boloorsaze, M. R., Farnia, P., Mohammadi, F., Karam, M. B., Masjedi, M. R., et al. (2005). *Mycobacterium gastri* causing disseminated infection in children of same family. *Pediatr. Pulmonol.* 39, 284–287. doi: 10.1002/ppul.20186

Volkman, H. E., Pozos, T. C., Zheng, J., Davis, J. M., Rawls, J. F., and Ramakrishnan, L. (2010). Tuberculous granuloma induction via interaction of a bacterial secreted protein with host epithelium. *Science* 327, 466–469. doi: 10.1126/science.1179663

Witzig, R. S., Fazal, B. A., Mera, R. M., Mushatt, D. M., Dejace, P. M., Greer, D. L., et al. (1995). Clinical manifestations and implications of coinfection with *Mycobacterium kansasii* and human immunodeficiency virus type 1. *Clin. Infect. Dis.* 21, 77–85. doi: 10.1093/clinids/21.1.77

Wu, T. S., Leu, H. S., Chiu, C. H., Lee, M. H., Chiang, P. C., Wu, T. L., et al. (2009). Clinical manifestations, antibiotic susceptibility and molecular analysis of *Mycobacterium kansasii* isolates from a university hospital in Taiwan. *J. Antimicrob. Chemother.* 64, 511–514. doi: 10.1093/jac/dkp238

Yang, M., Ross, B. C., and Dwyer, B. (1993). Identification of an insertion sequence-like element in a subspecies of *Mycobacterium kansasii*. *J. Clin. Microbiol.* 31, 2074–2079.

Yoon, S. H., Ha, S. M., Lim, J. M., Kwon, S. J., and Chun, J. (2017). A large-scale evaluation of algorithms to calculate average nucleotide identity. *Antonie van Leeuwenhoek*. 110, 1281–1286. doi: 10.1007/s10482-017-0844-4

Zhang, M., Chen, J. M., Sala, C., Rybniker, J., Dhar, N., and Cole, S. T. (2014). EspI regulates the ESX-1 secretion system in response to ATP levels in *Mycobacterium tuberculosis*. *Mol. Microbiol.* 93, 1057–1065. doi: 10.1111/mmi.12718

Zhang, Y., Mann, L. B., Wilson, R. W., Brwon-Elliott, B. A., Vincent, V., Iinuma, Y., et al. (2004). Molecular analysis of *Mycobacterium kansasii* isolates from the United States. *J. Clin. Microbiol.* 42, 119–125. doi: 10.1128/JCM.42.1.119-125.2004

Conflict of Interest: The authors declare that the research was conducted in the absence of any commercial or financial relationships that could be construed as a potential conflict of interest.

frontiers in Microbiology

ORIGINAL RESEARCH
published: 30 January 2020
doi: 10.3389/fmicb.2020.00053

Long-Term Effects of Multi-Drug-Resistant Tuberculosis Treatment on Gut Microbiota and Its Health Consequences

Jinyu Wang[1†], Ke Xiong[1†], Shanliang Zhao[2], Chao Zhang[1], Jianwen Zhang[1], Lei Xu[1] and Aiguo Ma[1]*

[1] *Institute of Nutrition and Health, School of Public Health, Qingdao University, Qingdao, China,* [2] *Linyi People's Hospital, Linyi, China*

OPEN ACCESS

Edited by:
Onya Opota, Université de Lausanne, Switzerland

Reviewed by:
Alinne Castro, Universidade Católica Dom Bosco (UCDB), Brazil
Henning Seedorf, Temasek Life Sciences Laboratory, Singapore

****Correspondence:***
Aiguo Ma
magfood@qdu.edu.cn

† These authors have contributed equally to this work

Specialty section:
This article was submitted to Antimicrobials, Resistance and Chemotherapy, a section of the journal Frontiers in Microbiology

Received: *24 September 2019*
Accepted: *13 January 2020*
Published: *30 January 2020*

Citation:
Wang J, Xiong K, Zhao S, Zhang C, Zhang J, Xu L and Ma A (2020) Long-Term Effects of Multi-Drug-Resistant Tuberculosis Treatment on Gut Microbiota and Its Health Consequences. Front. Microbiol. 11:53. doi: 10.3389/fmicb.2020.00053

Gut microbiota dysbiosis has adverse health effects on human body. Multi-drug-resistant tuberculosis (MDR-TB) treatment uses a variety of antibiotics typically for more than 20 months, which may induce gut microbiota dysbiosis. The aim of this study is to investigate the long-term effects of MDR-TB treatment on human gut microbiota and its related health consequences. A total of 76 participants were recruited at a hospital in Linyi, China. The study included one active MDR-TB treatment group, one recovered group from MDR-TB and two treatment-naive tuberculosis groups as control. The two treatment-naïve tuberculosis groups were constructed to match the sex and the age of the active MDR-TB treatment and the recovered group, respectively. The fecal and blood samples were collected and analyzed for gut microbiota and metabolic parameters. An altered gut microbiota community and a loss of richness were observed during the MDR-TB treatment. Strikingly, 3–8 years after recovery and discontinuing the treatment, the gut microbiota still exhibited an altered taxonomic composition ($p = 0.001$) and a 16% decrease in richness ($p = 0.018$) compared to the gut microbiota before the treatment. The abundance of fifty-eight bacterial genera was significantly changed in the MDR-TB recovered group versus the untreated control group. Although there were persistent and pervasive gut microbiota alterations, no gastrointestinal symptom such as abdominal pain, diarrhea, nausea, flatulence, and constipation was observed in the recovered group. However, chronic disorders may be indicated by the elevated level of low-density lipoprotein cholesterol (LDLC) ($p = 0.034$) and total cholesterol (TC) ($p = 0.017$). These adverse lipid changes were associated with the altered gut bacterial taxa, including phylum Firmicutes and Verrucomicrobia and genera *Adlercreutzia*, *Akkermansia, Butyricicoccus*, *Coprococcus*, *Clostridioides*, *Eubacterium*, *Erysipelatoclostridium*, *Fusicatenibacter*, *Klebsiella*, *Psychrobacter,* and *Streptococcus*. Collectively, MDR-TB treatment induced a lasting gut microbiota dysbiosis, which was associated with unfavorable changes in lipid profile.

Keywords: antibiotics, gut microbiota, metabolic markers, multi-drug-resistant tuberculosis, long-term effects

INTRODUCTION

Tuberculosis (TB) is a communicable disease caused by *Mycobacterium tuberculosis*. TB is characterized by necrotizing granulomatous inflammation, which mainly happens in the lung (about 85% of the cases) (Dheda et al., 2016). Over the past decades, multi-drug-resistant tuberculosis (MDR-TB), which is resistant to both isoniazid and rifampicin, is emerging. In 2016, 490,000 new cases of MDR-TB occurred (World Health Organization, 2017). MDR-TB treatment consists of a variety of narrow-spectrum and broad-spectrum antibiotics and lasts for at least 20 months. A course of treatment consists of an 8-month intensive treatment with one injection drug from kanamycin, amikacin or capreomycin, and four oral drugs from first-line drugs (isoniazid, rifampicin, ethambutol, pyrazinamide, rifabutin, and rifapentine), fluoroquinolones (levofloxacin, moxifloxacin, and gatifloxacin) and second-line oral bacteriostatic drugs (ethionamide, prothionamide, cycloserine, terizidone, para-aminosalicylic acid, and para-aminosalicylate sodium). Then the administration of the four oral antibiotic drugs continues for another 12 months (World Health Organization, 2014).

Gut microbiota plays an important role in human health, involving in the development of immune system, the regulation of metabolism, the protection from pathogen overgrowth, the regulation of intestinal endocrine hormone, the biosynthesis of vitamins and the provision of energy (Sommer and Backhed, 2013). There is growing concern about the negative effects of antibiotics on gut microbiota and human health.

Antibiotic administration has a catastrophic disturbance on intestinal microbiota (Francino, 2016). Altered abundance of 30% gut bacteria and decreased richness, diversity and evenness of the whole gut bacteria can be induced by the use of broad-spectrum antibiotics (Dethlefsen et al., 2008). After discontinuing the antibiotics, gut microbiota can either return to the composition before the treatment or achieve a new equilibrium (Sommer et al., 2017). This process is driven by both external (e.g., host-controlled environmental and physiochemical properties of the gastrointestinal tract) and internal selections (e.g., cooperation or competition among microorganisms for limited resources) (Sommer et al., 2017). The extent to which the disturbed gut microbiota recovers to its initial state depends on the degree of the disturbance. Changes of only specific taxa and genes (e.g., an augmented expression of resistant genes) of the gut microbiota were observed after short-course administration of ciprofloxacin (Dethlefsen et al., 2008; Dethlefsen and Relman, 2011). However, after prolonged exposure to multiple antibiotics in the case of TB treatment, the composition of the gut microbiota exhibited a dramatic shift even after a long period of recovering (Namasivayam et al., 2017; Wipperman et al., 2017).

The antibiotic-induced gut microbiota dysbiosis has adverse health consequences, including metabolic disorder, allergy, inflammatory bowel disease, and infectious disease (Vangay et al., 2015). Epidemiological studies suggested an association between antibiotic exposure and an increased risk of obesity and diabetes (Bailey et al., 2014; Boursi et al., 2015). Rodent research also found that antibiotic exposure led to increased adiposity with up-regulated lipogenesis and triglyceride (TG) synthesis (Cho et al., 2012; Cox et al., 2014). The fecal transplantation from antibiotic-treated mice into germ-free mice led to higher fat mass compared with the fecal transplantation from mice without antibiotic treatment, suggesting the role of gut microbiota in the antibiotic-induced adiposity (Cox et al., 2014). In addition, gut microbiota interacts with the immune system to ensure proper differentiation and complete development of immunity (Maynard et al., 2012). Infancy is a critical window for immunity development. Antibiotic exposure during infancy caused an impaired immunity system and was associated with a higher risk of allergy and autoimmune disease (Droste et al., 2000; Johnson et al., 2005; Hviid et al., 2011). Finally, a loss of gut microbiota diversity after antibiotic exposure led to increased vulnerability of host to infections. For example, recurrent *Clostridium difficile* infection was associated with decreased gut microbiota diversity, which was commonly observed during antibiotic exposure (Chang et al., 2008). Increased susceptibility to the infections of *Salmonella enterica* and *Escherichia coli* was also reported after using antibiotics (Lawley et al., 2008; Croswell et al., 2009; Deshmukh et al., 2014).

None of the previously studied antibiotic therapy has a comparable disturbance on gut microbiota as MDR-TB treatment. Little is known about the effects of MDR-TB treatment on human gut microbiota and its consequences on human health. The aim of this study is to investigate the effects of MDR-TB treatment on gut microbiota and human health, especially the long-term effects.

MATERIALS AND METHODS

Ethics Statement

This study was approved by the Ethics Committee of Qingdao Center of Disease Control and Prevention (No. 201703). The study was conducted in accordance with the Declaration of Helsinki, as well as national and institutional standards. Informed written consent was obtained from all participants.

Study Design and Population

The study was conducted at a hospital in Linyi City, Shandong, China from November 2017 to February 2018. The study included four groups: a MDR-TB treated group (n = 6), a MDR-TB recovered group (n = 18), and two untreated groups (n = 24 for untreated group 1 and n = 28 for untreated group 2). The MDR-TB treated group included participants, who were diagnosed as having pulmonary MDR-TB and under MDR-TB treatment. The MDR-TB recovered group included participants, who were previously treated and recovered from pulmonary MDR-TB. The untreated group included participants, who were diagnosed as having pulmonary TB and had not received any treatment. Untreated group 1 and untreated group 2 were constructed as controls to match the sex and the age of the MDR-TB treated group and the MDR-TB recovered group, respectively.

Pulmonary TB was diagnosed according to the WHO guidelines by clinical symptoms, computed tomography scan and sputum smear tests (World Health Organization, 2013).

The patient information including sex, age, drug sensitivity, and disease history was extracted from the hospital database. Drug sensitivity to isoniazid and rifampicin was determined by a phenotypic drug susceptibility test using a Lowenstein–Jensen medium (World Health Organization, 2014). Population characteristics for each group were described in **Table 1**. All participants were HIV-negative and had no history of liver and kidney disease.

Procedures

Upon the visit to the hospital, blood samples and fecal samples were collected from the patients after overnight fasting. The incidence of adverse gastrointestinal events (abdominal pain, diarrhea, nausea, flatulence, and constipation) in the past month was collected from the patients by a standard questionnaire. The blood samples were analyzed for fasting plasma glucose (FPG), lipid profile [total cholesterol (TC), low-density lipoprotein cholesterol (LDLC), high-density lipoprotein cholesterol (HDLC) and TG] and liver function (alanine aminotransferase (ALT), aspartate transaminase (AST) and AST/ALT) by UniCel DxC 800 Synchron Clinical Systems (Beckman Coulter, CA, United States). The fecal samples were stored in 4°C for no more than 24 h and then transferred to −80°C for storage. During the contact with the patients, researchers followed the safety procedure of the hospital by wearing protective lab clothing, gloves and masks. No infectious material was taken out of the hospital.

16S rRNA Sequencing

DNA was extracted from the fecal samples using a Power Soil DNA isolation kit (MO BIO Laboratories, CA, United States). The 16S rRNA V3-V4 region was amplified using primers 338F (5′- ACTCCTACGGGAGGCAGCA-3′) and 806R (5′-GGACTACHVGGGTWTCTAAT-3′) as described by Castrillo et al. (2017). PCR reaction was carried out in a 50 μL system with 10 μL buffer, 0.2 μL Q5 high-fidelity DNA polymerase, 10 μL high GC enhancer, 1 μL dNTP, 10 μM of each primer and 60 ng extracted DNA. The PCR products were purified using DNA clean beads. A second round of PCR reaction was then carried out in a 40 μL system with 20 μL 2 × high-fidelity PCR master mix, 8 μL ddH_2O, 10 μM of each primer and 10 μL PCR products from the first step. PCR products were detected on 1.8% agarose gels and purified using a MinElute PCR purification kit (QIAGEN, Hilden, Germany). The paired end reads were merged using FLASH version 1.2.11 (Magoč and Salzberg, 2011). Chimeric reads were filtered out using UCHIME version 8.1 and the filtered reads were clustered to operational taxonomic unit (OTU) based on 97% similarity using USEARCH version 10.0 (Edgar et al., 2011). The taxonomic assignment of OTU was performed by RDP classifier version 2.2 with confidence threshold at 0.8 (Qiong et al., 2007).

Statistical Analysis

The alpha diversity indices (ACE, Shannon index, and Shannon evenness) were calculated using Mothur (Schloss et al., 2009). The ACE was calculated using the following formula (Chao and Lee, 1992):

$$S_{ACE} = S_{abund} + \frac{S_{rare}}{C_{ACE}} + \frac{F_1}{C_{ACE}} r^2_{ACE}$$

$$r^2_{ACE} = \max\left[\frac{S_{rare}\sum_{i=1}^{10} i\,(i-1)\,F_i}{C_{ACE}\,(N_{rare})\,(N_{rare}-1)} - 1, 0\right]$$

S_{rare} is the number of rare species in a sample (species abundance ≤10) and S_{abund} is the number of abundant species (species abundance >10). C_{ACE} = 1-F_1/N_{rare} estimates the proportion of all individuals in rare species that are not singletons, whereas F_i is the number of species with i individuals and $N_rare = \sum_{i=1}^{10} iF_i$.

The Shannon index and Shannon evenness were calculated using the following formula (Shannon and Weaver, 1949):

$$\text{Shannon index (H)} = -\sum_{i=1}^{s} p_i \ln p_i$$

$$\text{Shannon evenness (E)} = H/H_{max}$$

p_i is the number of individuals in species i divided by the total number of individuals. S is the number of species. H_{max} is the maximum diversity possible.

The principal coordinate analyses (PCoA) and PERMANOVA based on unweighted UniFrac distance and Bray-Curtis dissimilarity were performed to compare microbiota community at OTU level using R version 3.4 (Bray and Curtis, 1957; Lozupone et al., 2006). Linear discriminant analysis (LDA) effect size (LEfSe) was adopted to identify biomarkers between clinical groups at the phylum and genus level with a LDA score >2 (Segata et al., 2011). The functional profile of microbial communities was predicted by phylogenetic investigation of communities by reconstruction of unobserved states (PICRUSt) (Langille et al., 2013). The network of microbiota was constructed at the genus level by sparse correlation by compositional data (SparCC) and filtered by $p > 0.05$ and $r > 0.1$ (Friedman and Alm, 2012). Statistically significant difference between groups was evaluated using a Mann–Whitney U test due to the non-normal distribution of the data (Mann and Whitney, 1947). Correlations between metabolic parameters and microbiota taxa were analyzed by a Spearman rank correlation test (Spearman, 1904). The Mann–Whitney U test and Spearman rank correlation test were performed in SPSS version 25.

RESULTS

The patients in the MDR-TB treated group had a mean age of 41 and a female percentage of 17%. These patients were under MDR-TB treatment for 2–14 months (**Table 1**). The participants in the MDR-TB recovered group had a mean age of 52 and a female percentage of 55%. The recovered group had been under MDR-TB treatment for 2–5 years and discontinued the treatment for 3–8 years. Due to the significant difference of the

TABLE 1 | Demographic characteristics of the participants (n = 76).

Group	Number of subjects	Age (years)	Female percentage (%)	Time on MDR-TB treatment	Time after MDR-TB treatment	Drug resistance to isoniazid and rifampicin
Untreated 1	24	40 ± 18	17	N/A [a]	N/A	Sensitive
Treated	6	41 ± 22	17	2–14 months	N/A	Resistant
Untreated 2	28	48 ± 12	48	N/A	N/A	Sensitive
Recovered	18	52 ± 12	55	2–5 years	3–8 years	Resistant

The age data are represented as mean ± SD. Untreated group 1 and untreated group 2 are the age and sex matched controls for the multi-drug-resistant tuberculosis (MDR-TB) treated group and the MDR-TB recovered group, respectively. [a]N/A, not applicable.

age and sex between the MDR-TB treated group and the MDR-TB recovered group, two untreated groups were constructed as controls to match the sex and the age of the MDR-TB treated group and the MDR-TB recovered group, respectively. The MDR-TB treatment for the patients was individualized and generally included one injection drug of kanamycin, amikacin or capreomycin, and four oral drugs (pyrazinamide, one fluoroquinolone drug of levofloxacin or moxifloxacin, and two second-line oral bacteriostatic drugs of prothionamide, cyloserine or para-aminosalicylic acid). A detailed description of the individualized MDR-TB treatment used in our participants was provided in **Supplementary Table S1**.

The microbiota richness, diversity and evenness were calculated at the OTU level. The microbiota richness was measured by ACE, which was based on the presence of the OTU. The results showed a decreased ACE in the treated group (p = 0.025) and in the recovered group (p = 0.018) compared to their corresponding control groups (**Figure 1A**). The microbiota diversity was measured by a Shannon index, which was based on both the number and the evenness of the observed OTUs. The results indicated a significant increase of the Shannon index in the recovered group compared to its control group (p = 0.004), while no significant change of the Shannon index was observed in the treated group compared to its control group (**Figure 1B**). The Shannon evenness (measuring the distribution of OTU) showed a significantly higher value in the recovered group than its control group ($p < 0.001$), while no difference was observed between the treated group and its control group (**Figure 1C**).

The similarities and differences of gut microbiota communities among these four groups were portrayed by the PCoA of unweighted UniFrac, which was based on the presence of the OTU and their phylogenetic distance (**Figure 2A**). The results showed an obvious separation between the recovered group and untreated group 2, and a slight shift to the top of the treated group compared to untreated group 1. The p-value for PERMANOVA based on unweighted UniFrac between the MDR-TB treated group and untreated group 1 was 0.003; while the p-value between the MDR-TB recovered group and untreated group 2 was 0.001. No separation was observed between the two untreated groups (p = 0.520). Principal component 1 accounted for 18.95% of the inter-sample variation. The variation was primarily driven by the recovered group, which was clustered into the left and separated from the other three groups. Principal component 2 accounted for 10.71% of the inter-sample variation. And the variation was driven by the treated and the recovered groups, which were clustered onto the top and separated from the untreated groups on the bottom.

The alteration of the gut microbiota composition was also assessed by the PCoA of Bray-Curtis dissimilarity, which was based on the abundance of the observed OTU (**Figure 2B**). The p-value for PERMANOVA based on Bray-Curtis dissimilarity between the MDR-TB recovered group and untreated group 2 was 0.001. No separation was observed between the treated group and untreated group 1 (p = 0.141) and between the two untreated groups (p = 0.826). Principal component 1 and principal component 2 accounted for 11.92% and 8.78% of the inter-sample variation, respectively. Both principal component 1 and principal component 2 were driven by the recovered group, which was clustered onto the top and left corner and separated from the other groups.

To further illustrate the alteration of the gut microbiota, a LEfSe analysis was performed at the phylum level. Three phyla were identified as the biomarkers (LDA > 2) that differentiated the treated group from its control group, including Actinobacteria, Bacteroidetes and Firmicutes (**Supplementary Figure S1A**). Three phyla were identified as the biomarkers (LDA > 2) that differentiated the recovered group from its control group, including Bacteroidetes, Cyanobacteria, and Patescibacteria (**Supplementary Figure S1B**). The relative abundance of Actinobacteria and Firmicutes declined (p = 0.009 for Actinobacteria and p = 0.029 for Firmicutes) under the MDR-TB treatment and rebounded to the pretreated level after discontinuing the MDR-TB treatment (**Figure 3**). Bacteroidetes showed an increase in response to MDR-TB treatment (p = 0.038) and did not return to the pretreated level after discontinuing the treatment (p = 0.029). For Cyanobacteria and Patescibacteria, no response was observed to the MDR-TB treatment, but they significantly decreased after recovery ($p < 0.001$ for Cyanobacteria and Patescibacteria).

Closer examinations identified 17 bacterial genera as the biomarkers (LDA > 2) in response to the MDR-TB treatment, most of which (n = 16) decreased (**Supplementary Figure S2**). Fifty-eight biomarkers (LDA > 2) were identified between the MDR-TB recovered group and untreated group 2, in which 28 decreased and 30 increased (**Supplementary Figure S3**). Network analysis indicated close correlations among the bacterial genera (**Supplementary Figure S4**). The functional profile of the gut community was predicted by PICRUSt. No significant difference was observed between the MDR-TB treated group and

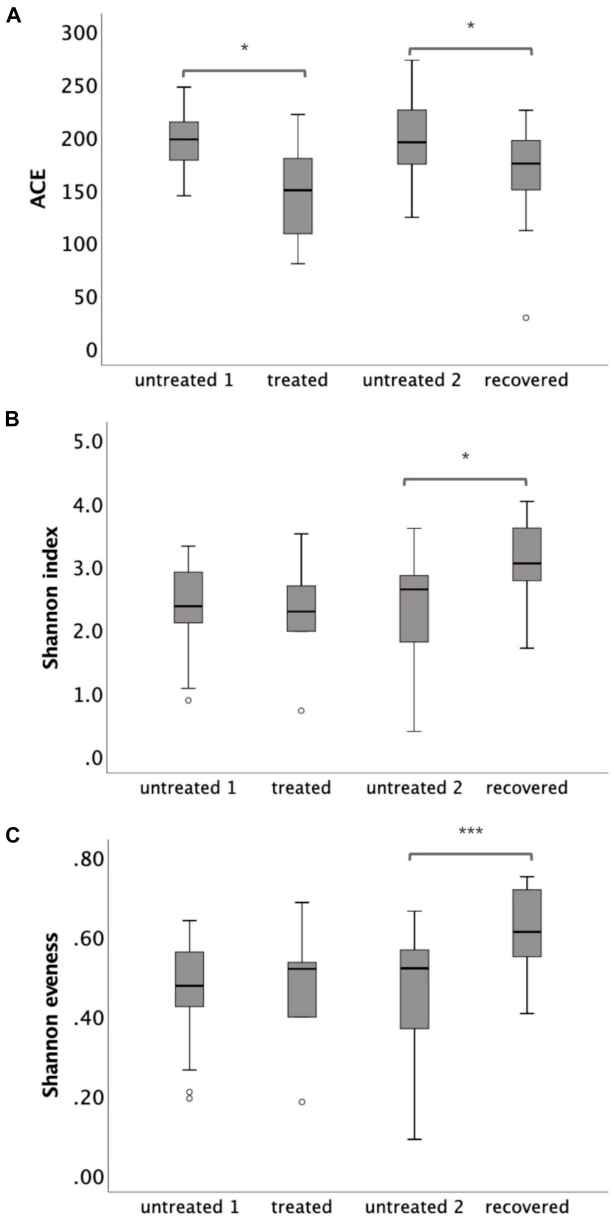

FIGURE 1 | The α-diversity of gut microbiota at the operational taxonomic unit (OTU) level, which was measured by **(A)** ACE, **(B)** Shannon index, and **(C)** Shannon evenness. Statistical significance was calculated between the multi-drug-resistant tuberculosis (MDR-TB) treated group and untreated group 1 and between the MDR-TB recovered group and untreated group 2 (Mann–Whitney *U* test). $*p < 0.05$, $***p < 0.001$.

untreated group 1 or between the MDR-TB recovered group and untreated group 2 (**Supplementary Figure S5**).

Although there were dramatic alterations in gut microbiota, no gastrointestinal symptom was observed in the recovered group. Metabolic parameters were measured to investigate the potential effects of the gut microbiota dysbiosis on the host metabolism (**Table 2**). The recovered group exhibited a higher LDLC ($p = 0.034$) and TC ($p = 0.017$) level compared to those of the untreated group, while no significant difference was observed for HDLC, TG, and FPG. In addition, ALT, AST, and AST/ALT (evaluating liver function) were within the normal range and showed no significant difference between the recovered group and the untreated group, indicating that the altered lipid profile was not caused by liver damage.

The increased level of LDLC and TC was associated with the altered gut bacteria as shown in **Figure 4**. The LDLC level was negatively associated with Verrucomicrobia ($r = -0.437$, $p = 0.006$), *Akkermansia* ($r = -0.437$, $p = 0.006$) and *Streptococcus* ($r = -0.341$, $p = 0.036$), and it was positively associated with *Adlercreutzia* ($r = 0.342$, $p = 0.036$), *Clostridioides* ($r = 0.392$, $p = 0.015$), *Fusicatenibacter* ($r = 0.389$, $p = 0.016$), Lachnospiraceae ND3007 group ($r = 0.406$, $p = 0.012$), Prevotellaceae NK3B31 group ($r = 0.358$, $p = 0.027$), *Eubacterium xylanophilum* group ($r = 0.361$, $p = 0.026$) and *Eubacterium ruminantium* group ($r = 0.405$, $p = 0.012$). The serum TC content was negatively associated with Firmicutes ($r = -0.35$, $p = 0.032$), *Butyricicoccus* ($r = -0.369$, $p = 0.023$), *Coprococcus* 1 ($r = -0.409$, $p = 0.011$), *Erysipelatoclostridium* ($r = -0.403$, $p = 0.012$), *Psychrobacter* ($r = -0.332$, $p = 0.042$), and *Streptococcus* ($r = -0.420$, $p = 0.009$), while it was positively associated with *Fusicatenibacter* ($r = 0.381$, $p = 0.018$), *Klebsiella* ($r = 0.339$, $p = 0.038$), Lachnospiraceae FCS020 group ($r = 0.364$, $p = 0.025$), Lachnospiraceae ND3007 group ($r = 0.371$, $p = 0.022$), and Lachnospiraceae UCG001 group ($r = 0.327$, $p = 0.045$).

DISCUSSION

Multi-drug-resistant tuberculosis treatment uses a variety of antibiotics and often lasts for at least 20 months. Such high antibiotic exposure may have a large impact on gut microbiota and human health, which is currently unknown. We report a pervasive and persistent effect of MDR-TB treatment on the community structure and the richness of human gut microbiota. These changes were not reversed 3–8 years after recovery and discontinuing the MDR-TB treatment. In addition, the altered gut microbiota was correlated with the metabolic changes including an increased LDLC and TC level.

An altered gut microbiota composition and a 26% drop in gut microbiota richness (measured by ACE) were observed in the MDR-TB treated group compared to the untreated group. However, due to the limited number of participants included in the MDT-TB treated group, the results need to be interpreted with caution.

The gut microbiota community in the recovered group was significantly different from that of the untreated group, and had a 16% decreased richness. According to the resilience theory, gut microbiota as an ecosystem can return to its original equilibrium or achieve a new equilibrium after disturbance cessation, depending on the strength of the disturbance and the stability of the microbiota (Sommer et al., 2017). Different degrees of gut microbiota recovery after discontinuing antibiotic treatment have been previously reported. For a short-course single antibiotic treatment with a 5-day ciprofloxacin administration, the taxonomic composition

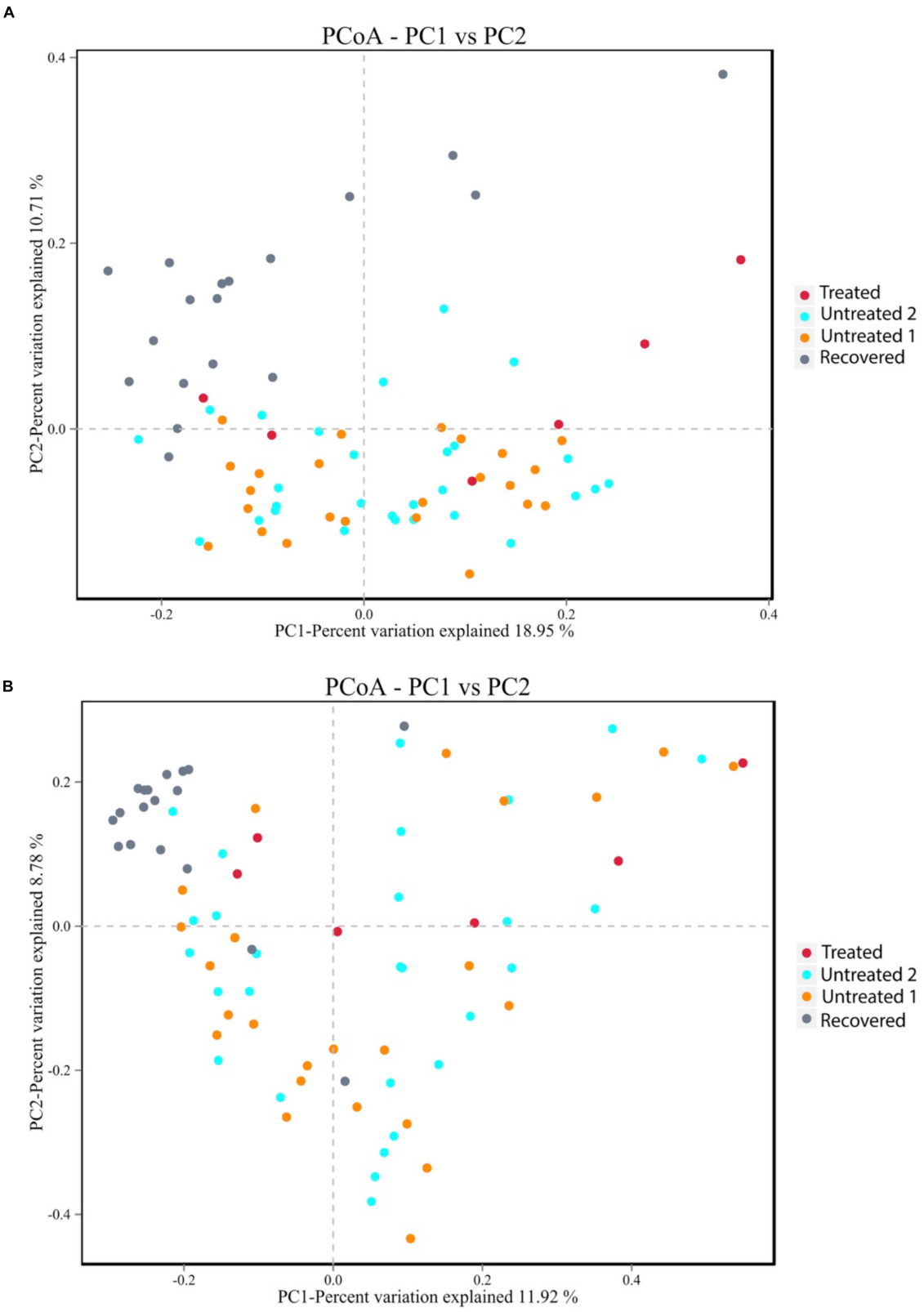

FIGURE 2 | Principal coordinate analysis plot based on **(A)** the unweighted UniFrac distance at the operational taxonomic unit (OTU) level and **(B)** the Bray-Curtis dissimilarity at the OTU level. Untreated group 1 and untreated group 2 are the sex and age matched controls for the multi-drug-resistant tuberculosis (MDR-TB) treated group and the MDR-TB recovered group, respectively.

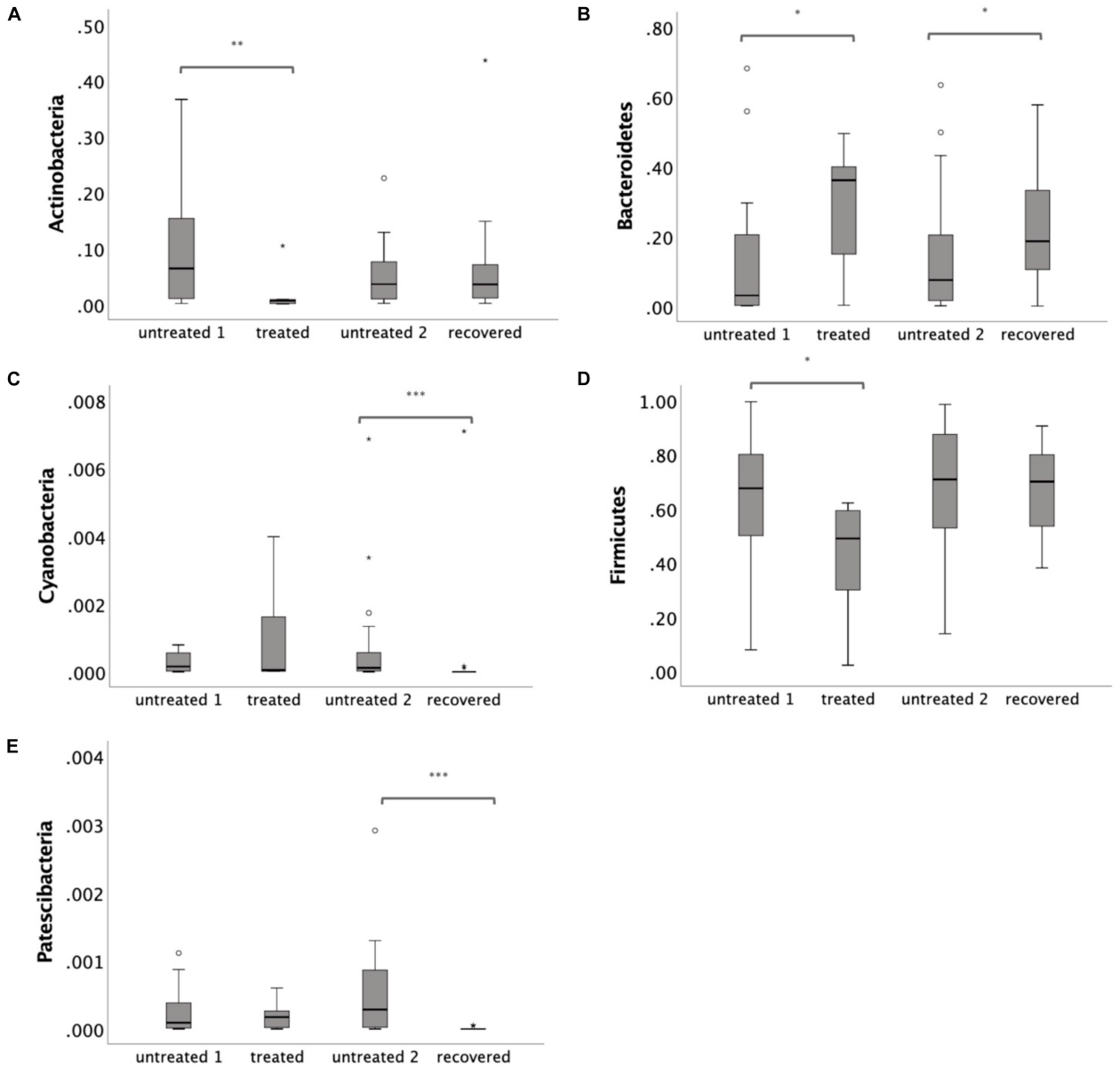

FIGURE 3 | Relative abundance of individual phylum: **(A)** Actinobacteria **(B)** Bacteroidetes **(C)** Cyanobacteria **(D)** Firmicutes and **(E)** Patescibacteria. Statistical significance was calculated between the multi-drug-resistant tuberculosis (MDR-TB) treated group and untreated group 1, and between the MDR-TB recovered group and untreated group 2 (Mann–Whitney *U* test). $^{*}p < 0.05$, $^{**}p < 0.01$, $^{***}p < 0.001$.

of the gut microbiota was not distinguishable from that of the untreated group after a 4-week recovery (Dethlefsen et al., 2008). For a high antibiotic exposure, a 6-month TB treatment using a combination of isoniazid, pyrazinamide, ethambutol, and rifampin, led to altered microbiota community 1.2 years after treatment cessation (Wipperman et al., 2017). In both the ciprofloxacin treatment and the TB treatment, the gut microbiota richness rebounded to the level before the treatment (Dethlefsen et al., 2008; Wipperman et al., 2017). None of the previously studied antibiotic treatment has comparable disturbance on gut microbiota as the MDR-TB treatment. This may explain the irreversible decrease in microbiota richness and alteration in gut microbiota community structure by the MDR-TB treatment as observed in our study. The new equilibrium after the MDR-TB treatment could be due to direct effects like the elimination of certain bacterial species by the use of antibiotics, as well as indirect effects such as autotrophic bacteria that rely on the fermentation products of the eliminated bacteria or competitive bacteria that compete with the eliminated bacteria (Sommer et al., 2017). The correlations among the gut bacteria were also suggested by our network analysis.

TABLE 2 | Metabolic changes in the MDR-TB recovered group compared to its sex and age matched control group.

Metabolic factors	Untreated TB group 2 (n = 22)	MDR-TB recovered group (n = 17)	p-value[a]
LDLC (mmol/L)	2.2 (0.6)	2.7 (0.8)	0.034
HDLC (mmol/L)	1.1 (0.4)	1.3 (0.4)	0.714
TC (mmol/L)	4.2 (1.3)	4.7 (0.9)	0.017
TG (mmol/L)	0.8 (0.4)	1.0 (0.8)	0.509
FPG (mmol/L)	4.9 (1.0)	5.2 (1.5)	0.388
ALT (IU/L)	14.7 (8.0)	16.0 (11.0)	0.269
AST (IU/L)	18.8 (13.6)	20.0 (6.5)	0.681
AST/ALT	1.4 (0.8)	1.2 (0.7)	0.357

Data are presented as median (IQR) due to the non-normal distribution of the data. MDR-TB, multi-drug resistant tuberculosis; TB, tuberculosis; LDLC, low-density lipoprotein cholesterol; HDLC, high-density lipoprotein cholesterol; TC, total cholesterol; TG, triglyceride; FPG, fasting plasma glucose; ALT, alanine aminotransferase; AST, aspartate transaminase. [a]Statistical significance was calculated using the Mann–Whitney U test.

Although the recovered patients harbored a very different gut microbiota community, no participant in the recovered group presented gastrointestinal symptoms such as diarrhea, abdominal pain, nausea, flatulence or constipation. Gut microbiota contributes to a substantial proportion (about 6%) of the variation in blood lipids, independent of age, gender and host genetics (Fu et al., 2015). The dysbiosis of gut microbiota is closely associated with metabolic disorders, such as diabetes, obesity, and dyslipidemia (Boursi et al., 2015; Vangay et al., 2015). Consistently, our study found an elevated level of LDLC and TC in the recovered group, which was correlated with the altered gut microbiota taxa.

Several mechanisms could explain the correlation between the elevated LDLC, TC and the altered gut microbiota taxa. First, certain bacteria in the large intestine could convert bile acids to secondary bile acids such as deoxycholic acid and lithocholic acid (Allayee and Hazen, 2015). These secondary bile acids could be reabsorbed into the blood stream, function as signaling molecules and improve liver function and metabolic homeostasis (Thomas et al., 2009; Ryan et al., 2014). The Firmicutes was known to be involved in bile acid metabolism and its abundance was positively associated with the content of secondary bile acids (Jones et al., 2008; Vrieze et al., 2014). We found that the reduced Firmicutes in the MDR-TB recovered group was correlated with the increased serum TC level. Second, short chain fatty acids including acetate, propionate and butyrate were claimed to modulate lipid metabolism in peripheral tissues (Kimura et al., 2013). The genus *Coprococcus* is a major producer of butyrate (Rioscovian et al., 2016). In our work, the decreased *Coprococcus* was correlated with the increased TC level in the recovered group. Third, certain bacteria could produce trimethylamine (TMA) through the metabolism of dietary choline and L-carnitine. The generated TMA could be further metabolized to trimethylamine N-oxide, which inhibits reverse cholesterol transportation and increases LDLC (Wang et al., 2011; Koeth et al., 2013). The gut bacterium responsible for TMA production is unclear. However, a strong correlation was previously reported between the blood TMA level and several gut taxa, including Prevotellaceae (Koeth et al., 2013). We observed a positive correlation between Prevotellaceae and the LDLC level.

In conclusion, the patients' gut microbiota was irreversibly changed with a 16% drop in richness and a dramatically altered taxonomic composition 3–8 years after recovery and discontinuing the MDR-TB treatment. The lasting gut microbiota dysbiosis was associated with an adverse lipid profile including increased LDLC and TC. Our results pointed to a gut-microbiota-mediated adverse health effect of MDR-TB treatment

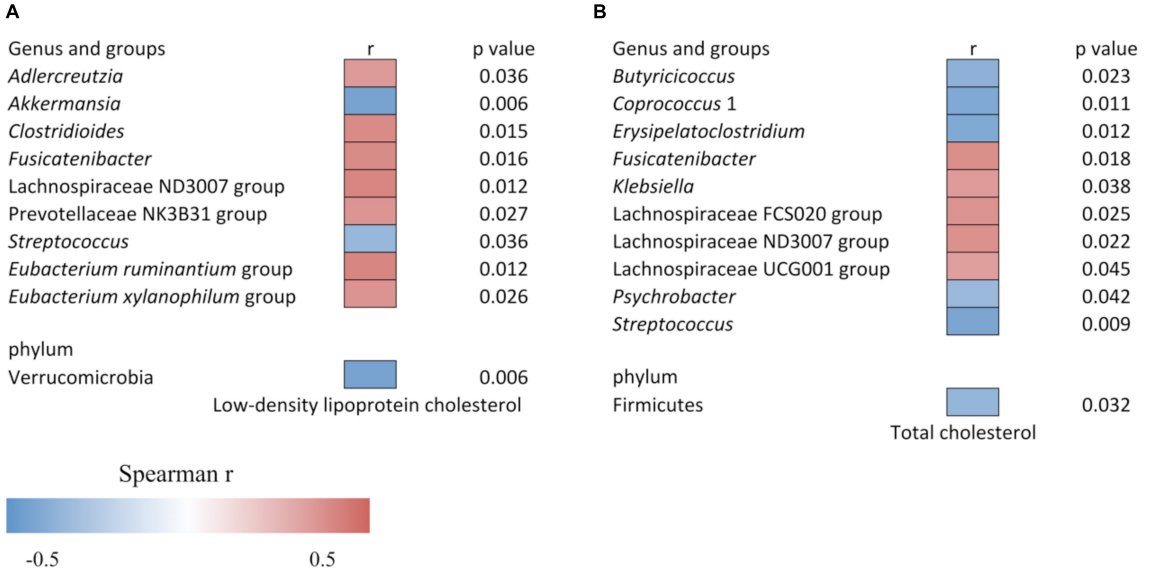

FIGURE 4 | Heat map of the Spearman correlation **(A)** between relative abundance of gut bacteria and low-density lipoprotein cholesterol level, and **(B)** between relative abundance of gut bacteria and total cholesterol level. The heat map color represents the Spearman correlation coefficient (r). Data is filtered for $p < 0.05$.

and a potential need for gut microbiota reconstruction. Fecal microbiome transplantation or probiotics supplementation may be a potential solution. Further study is warranted to confirm the necessity and the safety of gut microbiota reconstruction after MDR-TB treatment.

DATA AVAILABILITY STATEMENT

The sequencing was performed by Hiseq 2500 platform (Illumina, CA, United States). The sequencing data has been uploaded onto the National Center for Biotechnology Information Sequence Read Archive database with an accession number of PRJNA553646.

ETHICS STATEMENT

The studies involving human participants were reviewed and approved by the Ethics Committee of Qingdao Center of Disease Control and Prevention. The patients/participants provided their written informed consent to participate in this study.

AUTHOR CONTRIBUTIONS

AM designed the study and revised the manuscript. SZ, CZ, JZ, and LX collected the samples. JW and KX analyzed the data and prepared the manuscript. All authors read and approved the final version of the manuscript.

FUNDING

This study was funded by the National Natural Science Foundation of China (No. 81673160) and by Qingdao University (Nos. DC1900009730 and DC1900009731). The funders had no role in the study design, data collection, result interpretation, and the decision to submit work for publication.

SUPPLEMENTARY MATERIAL

The Supplementary Material for this article can be found online at: https://www.frontiersin.org/articles/10.3389/fmicb.2020.00053/full#supplementary-material

REFERENCES

Allayee, H., and Hazen, S. L. (2015). Contribution of gut bacteria to lipid levels: another metabolic role for microbes? *Circ. Res.* 117, 750–754. doi: 10.1161/CIRCRESAHA.115.307409

Bailey, L. C., Forrest, C. B., Zhang, P., Richards, T. M., Livshits, A., and Derusso, P. A. (2014). Association of antibiotics in infancy with early childhood obesity. *JAMA Pediatr.* 168, 1063–1069. doi: 10.1001/jamapediatrics.2014.1539

Boursi, B., Mamtani, R., Haynes, K., and Yang, Y. (2015). The effect of past antibiotic exposure on diabetes risk. *Eur. J. Endocrinol.* 172, 639–648. doi: 10.1530/EJE-14-1163

Bray, J. R., and Curtis, J. T. (1957). An ordination of the upland forest communities of southern wisconsin. *Ecol. Monogr.* 27, 326–349. doi: 10.2307/1942268

Castrillo, G., Teixeira, P. J., Paredes, S. H., Law, T. F., de Lorenzo, L., Feltcher, M. E., et al. (2017). Root microbiota drive direct integration of phosphate stress and immunity. *Nature* 543, 513–518. doi: 10.1038/nature21417

Chang, J. Y., Antonopoulos, D. A., Kalra, A., Tonelli, A. R., Khalife, W. T., Schmidt, T. M., et al. (2008). Decreased diversity of the fecal microbiome in recurrent *Clostridium difficile*-associated diarrhea. *J. Infect. Dis.* 197, 435–438. doi: 10.1086/525047

Chao, A., and Lee, S. M. (1992). Estimating the number of classes via sample coverage. *J. Am. Stat. Assoc.* 87, 210–217. doi: 10.1080/01621459.1992.10475194

Cho, I., Yamanishi, S., Cox, L. M., Methe, B. A., Zavadil, J., Li, K., et al. (2012). Antibiotics in early life alter the murine colonic microbiome and adiposity. *Nature* 488, 621–626. doi: 10.1038/nature11400

Cox, L. M., Yamanishi, S., Sohn, J., Alekseyenko, A. V., Leung, J. M., Cho, I., et al. (2014). Altering the intestinal microbiota during a critical developmental window has lasting metabolic consequences. *Cell* 158, 705–721. doi: 10.1016/j.cell.2014.05.052

Croswell, A., Amir, E., Teggatz, P., Barman, M., and Salzman, N. H. (2009). Prolonged impact of antibiotics on intestinal microbial ecology and susceptibility to enteric *Salmonella* infection. *Infect. Immun.* 77, 2741–2753. doi: 10.1128/IAI.00006-09

Deshmukh, H., Liu, Y., Menkiti, O. R., Mei, J., Dai, N., Oleary, C. E., et al. (2014). The microbiota regulates neutrophil homeostasis and host resistance to *Escherichia coli* K1 sepsis in neonatal mice. *Nat. Med.* 20, 524–530. doi: 10.1038/nm.3542

Dethlefsen, L., Huse, S. M., Sogin, M. L., and Relman, D. A. (2008). The pervasive effects of an antibiotic on the human gut microbiota, as revealed by deep 16s rRNA sequencing. *PLoS Biol.* 6:e280. doi: 10.1371/journal.pbio.0060280

Dethlefsen, L., and Relman, D. A. (2011). Incomplete recovery and individualized responses of the human distal gut microbiota to repeated antibiotic perturbation. *Proc. Natl. Acad. Sci. U.S.A.* 108, 4554–4561. doi: 10.1073/pnas.1000087107

Dheda, K., Barry, C. E. III, and Maartens, G. (2016). Tuberculosis. *Lancet* 387, 1211–1226. doi: 10.1016/s0140-6736(15)00151-8

Droste, J., Wieringa, M., Weyler, J., Nelen, V. J., Vermeire, P. A., and Van Bever, H. P. (2000). Does the use of antibiotics in early childhood increase the risk of asthma and allergic disease. *Clin. Exp. Allergy* 30, 1547–1553.

Edgar, R. C., Haas, B. J., Clemente, J. C., Quince, C., and Knight, R. (2011). UCHIME improves sensitivity and speed of chimera detection. *Bioinformatics* 27, 2194–2200. doi: 10.1093/bioinformatics/btr381

Francino, M. P. (2016). Antibiotics and the human gut microbiome: dysbioses and accumulation of resistances. *Front. Microbiol.* 6:1543. doi: 10.3389/fmicb.2015.01543

Friedman, J., and Alm, E. J. (2012). Inferring correlation networks from genomic survey data. *PLoS Comput. Biol.* 8:e1002687. doi: 10.1371/journal.pcbi.1002687

Fu, J., Bonder, M. J., Cenit, M. C., Tigchelaar, E. F., Maatman, A., Dekens, J. A. M., et al. (2015). The gut microbiome contributes to a substantial proportion of the variation in blood lipids. *Circ. Res.* 117, 817–824. doi: 10.1161/CIRCRESAHA.115.306807

Hviid, A., Svanstrom, H., and Frisch, M. (2011). Antibiotic use and inflammatory bowel diseases in childhood. *Gut* 60, 49–54. doi: 10.1136/gut.2010.219683

Johnson, C. C., Ownby, D. R., Alford, S. H., Havstad, S., Williams, L. K., Zoratti, E. M., et al. (2005). Antibiotic exposure in early infancy and risk for childhood atopy. *J. Allergy Clin. Immunol.* 115, 1218–1224. doi: 10.1016/j.jaci.2005.04.020

Jones, B. V., Begley, M., Hill, C., Gahan, C. G. M., and Marchesi, J. R. (2008). Functional and comparative metagenomic analysis of bile salt hydrolase activity in the human gut microbiome. *Proc. Natl. Acad. Sci. U.S.A.* 105, 13580–13585. doi: 10.1073/pnas.0804437105

Kimura, I., Ozawa, K., Inoue, D., Imamura, T., Kimura, K., Maeda, T., et al. (2013). The gut microbiota suppresses insulin-mediated fat accumulation via the short-chain fatty acid receptor GPR43. *Nat. Commun.* 4, 1829–1829. doi: 10.1038/ncomms2852

Koeth, R. A., Wang, Z., Levison, B. S., Buffa, J. A., Org, E., Sheehy, B., et al. (2013). Intestinal microbiota metabolism of *L*-carnitine, a nutrient in red meat, promotes atherosclerosis. *Nat. Med.* 19, 576–585. doi: 10.1038/nm.3145

Langille, M. G. I., Zaneveld, J., Caporaso, J. G., McDonald, D., Knights, D., Reyes, J. A., et al. (2013). Predictive functional profiling of microbial communities

using 16s rRNA marker gene sequences. *Nat. Biotechnol.* 31, 814–821. doi: 10.1038/nbt.2676

Lawley, T. D., Bouley, D. M., Hoy, Y. E., Gerke, C., Relman, D. A., and Monack, D. M. (2008). Host transmission of *Salmonella enterica* serovar typhimurium is controlled by virulence factors and indigenous intestinal microbiota. *Infect. Immun.* 76, 403–416. doi: 10.1128/IAI.01189-07

Lozupone, C., Hamady, M., and Knight, R. (2006). UniFrac-an online tool for comparing microbial community diversity in a phylogenetic context. *BMC Bioinformatics* 7:371. doi: 10.1186/1471-2105-7-371

Magoč, T., and Salzberg, S. L. (2011). FLASH: fast length adjustment of short reads to improve genome assemblies. *Bioinformatics* 27, 2957–2963. doi: 10.1093/bioinformatics/btr507

Mann, H. B., and Whitney, D. R. (1947). On a test of whether one of two random variables is stochastically larger than the other. *Ann. Mathematical Statist.* 18, 50–60. doi: 10.1214/aoms/1177730491

Maynard, C. L., Elson, C. O., Hatton, R. D., and Weaver, C. T. (2012). Reciprocal interactions of the intestinal microbiota and immune system. *Nature* 489, 231–241. doi: 10.1038/nature11551

Namasivayam, S., Maiga, M., Yuan, W., Thovarai, V., Costa, D. L., Mittereder, L., et al. (2017). Longitudinal profiling reveals a persistent intestinal dysbiosis triggered by conventional anti-tuberculosis therapy. *Microbiome* 5, 71–88. doi: 10.1186/s40168-017-0286-2

Qiong, W., Garrity, G. M., Tiedje, J. M., and Cole, J. R. (2007). Naive bayesian classifier for rapid assignment of rRNA sequences into the new bacterial taxonomy. *Appl. Environ. Microbiol.* 73, 5261–5267. doi: 10.1128/AEM.00062-07

Rioscovian, D., Ruasmadiedo, P., Margolles, A., Gueimonde, M., Reyesgavilan, C. G. D. L., and Salazar, N. (2016). Intestinal short chain fatty acids and their link with diet and human health. *Front. Microbiol.* 7:185. doi: 10.3389/fmicb.2016.00185

Ryan, K. K., Tremaroli, V., Clemmensen, C., Kovatchevadatchary, P., Myronovych, A., Karns, R., et al. (2014). FXR is a molecular target for the effects of vertical sleeve gastrectomy. *Nature* 509, 183–188. doi: 10.1038/nature13135

Schloss, P. D., Westcott, S. L., Ryabin, T., Hall, J. R., Hartmann, M., Hollister, E. B., et al. (2009). Introducing mothur: open-source, platform-independent, community-supported software for describing and comparing microbial communities. *Appl. Environ. Microbiol.* 75, 7537–7541. doi: 10.1128/AEM.01541-09

Segata, N., Izard, J., Waldron, L., Gevers, D., Miropolsky, L., Garrett, W. S., et al. (2011). Metagenomic biomarker discovery and explanation. *Genome Biol.* 12, 60–78. doi: 10.1186/gb-2011-12-6-r60

Shannon, C. E., and Weaver, W. (1949). *The Mathematical Theory of Communication*. Urbana: University of Illinois Press.

Sommer, F., Anderson, J. M., Bharti, R., Raes, J., and Rosenstiel, P. (2017). The resilience of the intestinal microbiota influences health and disease. *Nat. Rev. Microbiol.* 15, 630–638. doi: 10.1038/nrmicro.2017.58

Sommer, F., and Backhed, F. (2013). The gut microbiota-masters of host development and physiology. *Nat. Rev. Microbiol.* 11, 227–238. doi: 10.1038/nrmicro2974

Spearman, C. (1904). The proof and measurement of correlation between two things. *Am. J. Psychol.* 15, 72–101.

Thomas, C., Gioiello, A., Noriega, L. G., Strehle, A., Oury, J., Rizzo, G., et al. (2009). TGR5-mediated bile acid sensing controls glucose homeostasis. *Cell Metab.* 10, 167–177. doi: 10.1016/j.cmet.2009.08.001

Vangay, P., Ward, T., Gerber, J. S., and Knights, D. (2015). Antibiotics, pediatric dysbiosis, and disease. *Cell Host Microbe* 17, 553–564. doi: 10.1016/j.chom.2015.04.006

Vrieze, A., Out, C., Fuentes, S., Jonker, L., Reuling, I., Kootte, R. S., et al. (2014). Impact of oral vancomycin on gut microbiota, bile acid metabolism, and insulin sensitivity. *J. Hepatol.* 60, 824–831. doi: 10.1016/j.jhep.2013.11.034

Wang, Z., Klipfell, E., Bennett, B. J., Koeth, R. A., Levison, B. S., Dugar, B., et al. (2011). Gut flora metabolism of phosphatidylcholine promotes cardiovascular disease. *Nature* 472, 57–63. doi: 10.1038/nature09922

Wipperman, M. F., Fitzgerald, D. W., Juste, M. A. J., Taur, Y., Namasivayam, S., Sher, A., et al. (2017). Antibiotic treatment for tuberculosis induces a profound dysbiosis of the microbiome that persists long after therapy is completed. *Sci. Rep.* 7:10767. doi: 10.1038/s41598-017-10346-6

World Health Organization (2013). *Systematic Screening for Active Tuberculosis: Principles and Recommendations*. Geneva: World Health Organization.

World Health Organization (2014). *Companion Handbook to the WHO Guidelines for the Programmatic Management of Drug-Resistant Tuberculosis*. Geneva: World Health Organization.

World Health Organization (2017). *Global Tuberculosis Report*. Geneva: World Health Organization.

Conflict of Interest: The authors declare that the research was conducted in the absence of any commercial or financial relationships that could be construed as a potential conflict of interest.

frontiers in Microbiology

ORIGINAL RESEARCH
published: 19 February 2020
doi: 10.3389/fmicb.2020.00081

Rational Choice of Antibiotics and Media for *Mycobacterium avium* Complex Drug Susceptibility Testing

Jérémy Jaffré[1,2], Alexandra Aubry[1,2], Thomas Maitre[1], Florence Morel[1,2], Florence Brossier[1,2†], Jérôme Robert[1,2], Wladimir Sougakoff[1,2], Nicolas Veziris[1,2,3] and the CNR-MyRMA (Centre National de Référence des Mycobactéries et de la Résistance des Mycobactéries aux Antituberculeux)*

[1] AP-HP (Assistance Publique Hôpitaux de Paris), Centre National de Référence des Mycobactéries et de la Résistance des Mycobactéries aux Antituberculeux, Groupe Hospitalier Universitaire Sorbonne Université, Hôpital Pitié Salpêtrière, Paris, France, [2] INSERM, U1135, Centre d'Immunologie et des Maladies Infectieuses, Sorbonne Université, Cimi-Paris, Paris, France, [3] AP-HP (Assistance Publique Hôpitaux de Paris), Groupe Hospitalier Universitaire, Sorbonne Université, Hôpital Saint-Antoine, Paris, France

OPEN ACCESS

Edited by:
Miguel Viveiros, New University of Lisbon, Portugal

Reviewed by:
Divakar Sharma, Indian Institute of Technology Delhi, India
Amit Kaushik, Johns Hopkins University, United States

***Correspondence:**
Nicolas Veziris
nicolas.veziris@sorbonne-universite.fr

†*Deceased*

Specialty section:
This article was submitted to Antimicrobials, Resistance and Chemotherapy, a section of the journal Frontiers in Microbiology

Received: *18 September 2019*
Accepted: *15 January 2020*
Published: *19 February 2020*

Citation:
Jaffré J, Aubry A, Maitre T, Morel F, Brossier F, Robert J, Sougakoff W, Veziris N and the CNR-MyRMA (Centre National de Référence des Mycobactéries et de la Résistance des Mycobactéries aux Antituberculeux) (2020) Rational Choice of Antibiotics and Media for Mycobacterium avium Complex Drug Susceptibility Testing. Front. Microbiol. 11:81. doi: 10.3389/fmicb.2020.00081

The Clinical and Laboratory Standards Institute recommends the use of Mueller Hinton (MH) medium to perform drug susceptibility testing (DST) of *Mycobacterium avium* complex (MAC) using the microdilution method. For MAC, there has been no study on the impact of media on the determination of minimum inhibitory concentrations (MICs) of antibiotics other than clarithromycin. This study aimed at determining the impact of two media used for DST of MAC and at augmenting the number of pertinent MICs for MAC species encountered in clinical practice. MICs of antibiotics used for the treatment of MAC infections were determined for 158 clinical MAC isolates (80 *M. avium*, 40 *M. intracellulare*, 35 *M. chimaera,* two *M. yongonense* and one *M. timonense*) in MH and 7H9 broths using the SLOMYCO Sensititre™ system (TREK Diagnostic Systems, East Grinstead, United Kingdom). The modal MICs determined in both media were the same for linezolid, moxifloxacin, rifabutin and amikacin but not for clarithromycin, rifampin and ethambutol. The kappa test for MICs converted to susceptibility categories showed an excellent agreement for clarithromycin, a moderate agreement for linezolid and a weak agreement for moxifloxacin and amikacin. For amikacin, 7H9 allowed a better distinction (fewer intermediate strains) of wild-type populations than MH. Existing breakpoints for linezolid and moxifloxacin are spread through the distribution of MICs for wild-type populations. The only breakpoints that can be used rationally are those for amikacin and clarithromycin. For amikacin, 7H9 performs better than MH, whereas both media perform equally for clarithromycin. Given that testing in 7H9, as opposed to MH, allows easier MIC measurements and yields greater reproducibility, we propose the use of 7H9 medium for DST of MAC.

Keywords: drug susceptibility testing, *Mycobacterium avium* complex, SLOMYCO Sensititre™, 7H9, Mueller Hinton, clarithromycin, amikacin

Abbreviations: BTS, British Thoracic Society; CLSI, Clinical and Laboratory Standards Institute; DST, drug susceptibility testing; I, intermediate susceptibility; MAC, *Mycobacterium avium* complex; ME, major error; mE, minor error; MH, Mueller Hinton; MIC, minimum inhibitory concentration; NTM, nontuberculous mycobacteria; R, resistance; S, susceptibility; SGM, slowly growing mycobacteria; VME, very major error.

INTRODUCTION

Nontuberculous mycobacteria (NTM) are ubiquitous microorganisms isolated mainly from water and soil. In 1959, Runyon proposed the first classification of NTM into four groups, the first three comprising "Slowly Growing Mycobacteria" (SGM) and the fourth of "Rapidly Growing Mycobacteria."

The most common SGM are the species belonging to the *Mycobacterium avium* complex (MAC), comprising especially *Mycobacterium avium*, *Mycobacterium intracellulare* and *Mycobacterium chimaera*. MAC organisms can cause different conditions in humans such as pulmonary disease, lymphadenitis and disseminated infection (Griffith et al., 2007). The incidence of MAC infections is increasing in most industrialized countries, possibly because of the increase in immunocompromised and/or older patients (Griffith et al., 2007; Prevots et al., 2010). These infections require antibiotic therapy based on macrolides (azithromycin or clarithromycin) combined with a rifamycin (rifampin or rifabutin) and ethambutol. Parenteral or inhaled amikacin may be added to this regimen for severe cases (Griffith et al., 2007, 2018; Olivier et al., 2017). Clofazimine, moxifloxacin, linezolid and bedaquiline are alternative drugs proposed mainly for the treatment of infections caused by macrolide-resistant MAC, but clinical evidence of their efficacy is lacking (Griffith et al., 2007; Koh et al., 2013; Jo et al., 2014; Philley et al., 2015).

The Clinical and Laboratory Standards Institute (CLSI) published guidelines for drug susceptibility testing (DST) of NTM in 2011, mainly reproduced by the British Thoracic Society (BTS) in 2017, and updated in 2018 (Clinical and Laboratory Standards Institute [CLSI], 2011, 2018; Haworth et al., 2017). As for MAC, both CLSI and BTS agree that, for clarithromycin susceptibility, the isolate be tested prior to the initiation of treatment in patients who satisfy the diagnostic criteria of nontuberculous mycobacterial lung disease of the American Thoracic Society/Infectious Disease Society of America. Indeed, a strong relationship between *in vitro* activity and *in vivo* efficacy of clarithromycin has been well established in clinical trials (Dautzenberg et al., 1995; Wallace et al., 1996, 2014; Tanaka et al., 1999; Kobashi et al., 2012). When testing macrolides, the pH of the medium is critical for the interpretation of the minimal inhibitory concentration (MIC) (Truffot-Pernot et al., 1991). Cation-adjusted Mueller Hinton (MH) medium has a pH of 7.4 whereas 7H9 medium has a pH of 6.8. Consequently, CLSI guidelines propose different breakpoints according to the medium employed only for clarithromycin (Clinical and Laboratory Standards Institute [CLSI], 2011, 2018).

The BTS also recommends amikacin susceptibility testing of isolates collected prior to initiation of treatment (Haworth et al., 2017). New CLSI guidelines published in 2018 likewise propose amikacin testing and give two breakpoints, depending on the route of administration (intravenous or inhaled) (Clinical and Laboratory Standards Institute [CLSI], 2018).

In case of resistance to clarithromycin, CLSI recommends DST of moxifloxacin and linezolid, whereas BTS recommends testing a wider panel of antibiotics to guide treatment regimens (Clinical and Laboratory Standards Institute [CLSI], 2011, 2018; Haworth et al., 2017).

Although used for the treatment of MAC infections, no clinical breakpoints have been defined for ethambutol and rifamycins.

Therefore, our goals were to determine the impact of the media used for MAC DST and to augment MIC data for clinically relevant MAC species.

MATERIALS AND METHODS

Bacterial Strains and Growth Conditions

The study involved 158 clinically relevant MAC isolates sent to the French National Reference Centre for Mycobacteria from 2015 to 2017. The isolates were grown on Löwenstein-Jensen medium and incubated at 37°C in ambient air. Before April 2016, isolates were identified with the GenoType Mycobacterium CM line probe assay (Hain Lifescience, Nerhen, Germany) associated with the sequencing of the internal transcribed spacer (ITS) region and, after this date, with the GenoType NTM-DR assay (Hain Lifescience). Mixed NTM infections were ruled out from the study.

The reference strain *M. avium* ATCC 700898 was used for the quality control of MIC determinations and for reproducibility testing of the technique.

MIC Determination

For each strain, DST was performed in parallel once in MH and once in 7H9 broth by microdilution using the SLOMYCO Sensititre™ system (TREK Diagnostic Systems, East Grinstead, United Kingdom) and MICs were determined according to the instructions of the CLSI and manufacturer. In practice, a suspension (0.5 McFarland standard) of each isolate was transferred into the two assessed media: cation-adjusted MH broth and Middlebrook 7H9 broth, both supplemented with 5% oleic albumin dextrose catalase (OADC). The final suspension was inoculated into the tray that was subsequently incubated at 37°C in ambient air. The tray was examined after 7 days of incubation and MICs were determined visually using an inverted mirror. In case of insufficient growth, trays were reincubated and read again after 10 to 14 days. The lowest concentration of antimicrobial that inhibited visible growth was taken as the MIC. Results were considered to be invalid if no growth was detected in the control well.

For each strain, 13 antimicrobial agents were tested but only results concerning the MICs of those recommended for treatment of MAC infections (clarithromycin, moxifloxacin, linezolid, amikacin, ethambutol, rifampin, rifabutin) are presented in this work.

The range of tested concentrations for each antibiotic of interest is given in **Supplementary Table S1**.

SIR (Susceptibility, Intermediate Susceptibility, Resistance) Categorization

For clarithromycin, two breakpoints were used to categorize MICs according to the medium inoculated: with MH broth

TABLE 1 | Antimicrobial agents and interpretive criteria for *Mycobacterium avium* complex used in the study.

Antimicrobial agent	Medium	MIC (mg/L) for category		
		S	I	R
Amikacin (IV)	MH and 7H9	≤16	32	≥64
Amikacin (liposomal or inhaled)	MH and 7H9	≤64	–	≥128
Clarithromycin	MH (pH 7.3–7.4)	≤8	16	≥32
	7H9 (pH 6.8)	≤16	32	≥64
Linezolid	MH and 7H9	≤8	16	≥32
Moxifloxacin	MH and 7H9	≤1	2	≥4

S, susceptible; I: intermediate; R: resistant.

(pH 7.4), clarithromycin susceptibility was assumed at an MIC of ≤8 mg/L as opposed to ≤16 mg/L when 7H9 broth (pH 6.8) was used. No breakpoint is proposed in the recent CLSI guidelines (Clinical and Laboratory Standards Institute [CLSI], 2018) to interpret the clarithromycin MIC measured in 7H9. We therefore used the breakpoint proposed in 2011 for the radiometric instrument method (Clinical and Laboratory Standards Institute [CLSI], 2011) since the pH is the same in both cases. To interpret moxifloxacin and linezolid MICs obtained in both media, we used the breakpoints defined by the CLSI for broth microdilution at pH 7.4 (susceptible strain if moxifloxacin MIC ≤ 1 mg/L and linezolid MIC ≤ 8 mg/L) (Clinical and Laboratory Standards Institute [CLSI], 2018). For amikacin, we applied the breakpoint defined by the CLSI in 2018 for the intravenous route (susceptible strain if MIC ≤ 16 mg/L) (Brown-Elliott et al., 2013; Clinical and Laboratory Standards Institute [CLSI], 2018). These breakpoints are summarized in **Table 1**.

Statistical Analysis

Reproducibility was evaluated by measuring MICs of the reference strain *M. avium* ATCC 700898 six times in both media. The results are expressed as a percentage of agreement compared to reference values given by the CLSI.

MIC_{50} and MIC_{90} values were determined from MIC distributions and were defined as the MICs required to inhibit the growth of 50% and 90% of the studied strains.

ECOFF and modal MIC (defined by the most frequent MIC value for each distribution of aggregated MICs for each species and drug), were calculated using the EUCAST excel tool ECOFF Finder (European Committee on Antimicrobial Susceptibility Testing [EUCAST], 2019, http://www.eucast.org/mic_distributions_and_ecoffs/). We chose to present ECOFF 95% values since the MICs showed a non-wild-type distribution, some reflecting acquired resistance.

MIC and susceptibility results obtained with both media were compared. Confirmed discordant results were classified as either very major errors [VME, defined as resistance (R) in MH but susceptibility (S) in 7H9], major errors (ME, S in MH and R in 7H9), or minor errors [mE, intermediate (I) in one medium but S or R in the other]. MICs determined in MH broth were considered the reference values.

The agreement between both methods was expressed as percent concordance and the strength of the agreement was determined using kappa scores which are considered to be excellent, strong, moderate, weak, very weak or null when they are 1–0.8, 0.8–0.6, 0.6–0.4, 0.4–0.2, 0.2–0 or ≤0, respectively.

RESULTS

Strains Included in the Study

A total of 158 MAC isolates were included in the study. These strains were collected from 141 patients. 14 patients had between two and four strains included in the study (total of 31 strains), with a mean interval between two strains of 6.5 months. These strains belonged to different species: 80 *M. avium* (51%), 40 *M. intracellulare* (25%), 35 *M. chimaera* (22%), 2 *Mycobacterium yongonense* (1%) and 1 *Mycobacterium timonense* (1%). These strains were isolated from various pulmonary specimens (90%) and extrapulmonary samples (10%) such as blood cultures and lymph node biopsies. They were isolated from 141 patients, 96 (68%) who had a history of long-term macrolide treatment, 20 (14%) who had no history of treatment, and 25 (18%) whose history of treatment was unknown.

Reproducibility

Reproducibility results are shown in **Supplementary Table S2**.

The concordance percentages obtained for the three antibiotics for which the CLSI proposes breakpoints were 100% with both media tested, except for clarithromycin in MH (67%).

MICs

The distribution of MIC values determined in MH and 7H9 for MAC species is shown in **Figure 1** and in **Supplementary Figures S1, S2**. MIC_{50}, MIC_{90}, Modal MIC, percentage of concordance, kappa and ECOFF values are shown in **Table 2**.

Amikacin modal MICs were identical for the three species (*M. avium, M. intracellulare* and *M. chimaera*) in MH and 7H9 (16 mg/L) except for *M. intracellulare* in 7H9 (8 mg/L). Ethambutol, linezolid, moxifloxacin and rifabutin modal MICs were within one or two titer steps of each other for the three species in both media. Clarithromycin and rifampin modal MICs were higher for *M. avium* than for *M. intracellulare* and *M. chimaera*.

Three strains were unusual MAC members: one *M. timonense* and two *M. yongonense* for which it was not possible to draw any conclusion concerning the distribution of MIC values because of the limited sample size (**Supplementary Table S3**).

Impact of the pH of the Medium on the MICs of Antibiotics Recommended for Treatment of MAC Infections

For MAC, modal MICs were the same in both media for amikacin (16 mg/L), linezolid (32 mg/L) moxifloxacin (2 mg/L) and rifabutin (≤0.25 mg/L), but not for rifampin (2 mg/L in MH vs. > 8 mg/L in 7H9), clarithromycin (2 mg/L in MH vs.

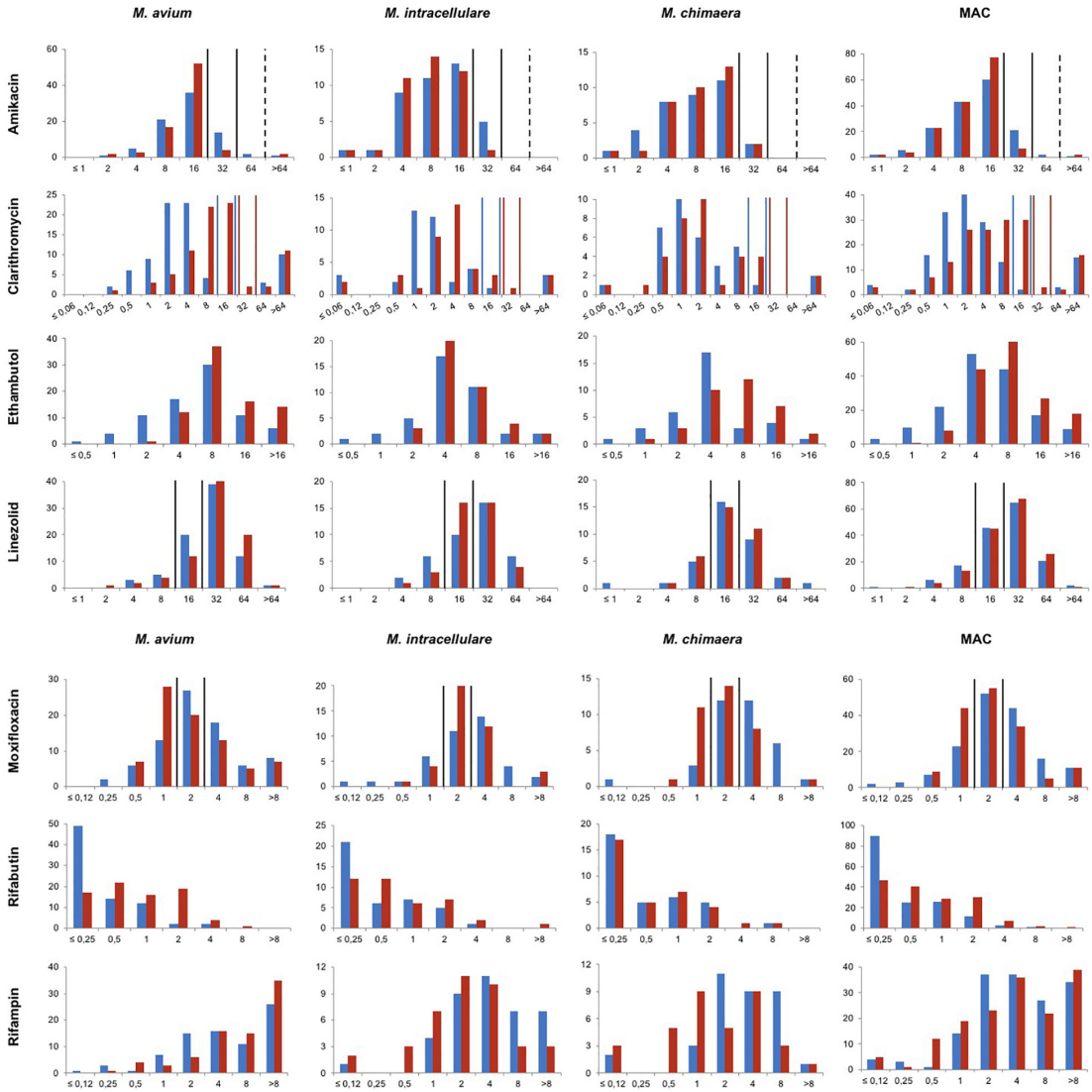

FIGURE 1 | Distribution of MICs for *M. avium*, *M. intracellulare*, *M. chimaera* and *M. avium* complex clinical isolates determined in MH and 7H9 broths. *x*-axis represents the MICs in mg/L. *y*-axis represents the number of strains. Blue and red bars represent values obtained in MH and 7H9 broth, respectively. Vertical lines represent the CLSI susceptibility breakpoints. For amikacin, breakpoints for the intravenous route are represented in full lines and for the liposomal or inhalation route in dotted lines. For clarithromycin, breakpoints for MICs determined in MH and 7H9 are represented in blue and red lines, respectively.

8 mg/L in 7H9) and ethambutol (4 mg/L in MH vs. 8 mg/L in 7H9) (**Table 2**).

The concordance percentages for MIC values determined in both media are low to moderate: from 27% for clarithromycin to 60% for linezolid. These results are confirmed by the kappa test revealing a very weak agreement for clarithromycin, ethambutol, rifabutin and rifampin ($0 < k \leq 0.2$), a weak agreement for amikacin and moxifloxacin ($0.2 < k \leq 0.4$) and a moderate agreement for linezolid ($0.4 < k \leq 0.6$) (**Table 2**).

When MICs of the four drugs whose breakpoints were available (**Table 1**) were converted into interpretive categories, the kappa test showed a weak agreement for amikacin and moxifloxacin, a moderate agreement for linezolid and an excellent agreement for clarithromycin ($k \geq 0.8$). The concordance percentage was between 59% (moxifloxacin) and 98% (clarithromycin) (**Table 3**). VME and ME were observed for moxifloxacin (respectively, 3 and 2%) and linezolid (2% for both), and mE were observed for all drugs, up to 36% for moxifloxacin (**Table 3**).

Among strains resistant to clarithromycin or amikacin in the two media for which search for resistance mutations was performed, the results of the genotypic drug susceptibility testing were the following:

- among the 18 strains categorized resistant to clarithromycin in both media, 12 strains (67%) harbored an *rrl* mutation in at position 2058 or 2059,
- among the 2 strains categorized resistant to amikacin in both media, 1 harbored a mutation in *rrs* at the 1408 position.

TABLE 2 | MICs (mg/L) determined in MH and 7H9 for *M. avium* complex overall and for the species *M. avium, M. intracellulare*, and *M. chimaera*.

						MIC values	
	N	Modal MIC MH/7H9	MIC_{50} MH/7H9	MIC_{90} MH/7H9	Tentative ECOFF 95% MH/7H9	% Concordance	Kappa coefficient
Amikacin							
M. avium complex	158	16/16	16/16	32/16	32/32	57	0.39
M. avium	80	16/16	16/16	32/16	32/32	56	0.3
M. intracellulare	40	16/8	8/8	32/16	NA/32	55	0.39
M. chimaera	35	16/16	8/8	16/16	32/32	57	0.43
Clarithromycin							
M. avium complex	158	2/8	2/8	64/>64	8/32	27	0.18
M. avium	80	2/16	3/8	>64/>64	8/32	19	0.12
M. intracellulare	40	1/4	2/4	8/16	8/16	20	0.13
M. chimaera	35	1/2	1/2	8/16	4/16	46	0.37
Ethambutol							
M. avium complex	158	4/8	4/8	16/>16	16/32	37	0.18
M. avium	80	8/8	8/8	16/>16	32/16	35	0.13
M. intracellulare	40	4/4	4/4	8/16	16/8	43	0.17
M. chimaera	35	4/8	4/8	16/16	8/32	34	0.17
Linezolid							
M. avium complex	158	32/32	32/32	64/64	64/64	60	0.43
M. avium	80	32/32	32/32	64/64	64/64	49	0.25
M. intracellulare	40	32/16	32/24	64/32	>64/64	70	0.58
M. chimaera	35	16/16	16/16	32/32	64/64	74	0.61
Moxifloxacin							
M. avium complex	158	2/2	2/2	8/8	8/4	46	0.24
M. avium	80	2/1	2/2	8/8	8/4	55	0.35
M. intracellulare	40	4/2	3/2	8/4	8/4	48	0.26
M. chimaera	35	2/2	4/2	8/4	8/4	20	−0.08
Rifabutin							
M. avium complex	158	≤0.25/≤0.25	≤0.25/0.5	2/2	1/0.5	39	0.17
M. avium	80	≤0.25/0.5	≤0.25/1	1/2	0.5/4	27	0.06
M. intracellulare	40	≤0.25/≤0.25	≤0.25/0,5	2/2	0.5/0.5	48	0.3
M. chimaera	35	≤0.25/≤0.25	≤0.25/0.5	2/2	0.5/0.5	57	0.37
Rifampin							
M. avium complex	158	2/>8	4/4	>8/>8	>8/NA	35	0.09
M. avium	80	>8/>8	4/8	>8/>8	NA/NA	40	0.04
M. intracellulare	40	4/2	4/2	>8/8	>8/>8	31	0.1
M. chimaera	35	2/1	4/2	8/8	>8/>8	29	0.15

NA, not available, ECOFF above the test concentration range.

Interestingly, among the strains categorized intermediate to clarithromycin or amikacin whatever the medium, no resistance mutation was found.

DISCUSSION

There are several issues concerning DST of NTM, from the lack of data regarding breakpoint availability to the scarcity of data establishing a correlation between *in vitro* assays and patient outcomes.

Recent studies have shown the impact of the media used on the determination of MICs for mycobacteria (Lavollay et al., 2014; Aziz et al., 2017). The goal of this study was to compare those measured in MH and 7H9 broths.

Regarding the reproducibility of results obtained with the reference strain *M. avium* ATCC 700898, we identified a major issue linked to the low percentage of agreement obtained with clarithromycin tested in MH broth (67%) whereas it was 100% in 7H9 broth. It could be related to antibiotic instability, a problem possibly influencing MIC measurements, as pointed out recently (Schoutrop et al., 2018). Indeed, this latter study revealed an important decrease of ≥75% in clarithromycin concentration in cation-adjusted MH broth medium over 14 days of incubation at 37°C while amikacin levels remain stable. In consequence, current MIC determinations could lead to false high MICs thus underestimating drug susceptibility.

CLSI and BTS recommend the performance of clarithromycin susceptibility testing of isolates taken prior to the initiation of

TABLE 3 | Comparison of amikacin, clarithromycin, linezolid and moxifloxacin susceptibility results determined using SLOMYCO Sensititre™ panels (TREK Diagnostic Systems) according to the medium employed (very major errors are given in bold and underlined, major errors in bold, and minor errors are underlined).

			7H9			% Agreement (kappa)
			S	I	R	
Amikacin	**MH**	**S**	132	2	0	87 (0.35)
		I	17	4	0	
		R	0	1	2	
Clarithromycin	**MH**	**S**	136	2	0	98 (0.92)
		I	1	1	0	
		R	0	0	18	
Linezolid	**MH**	**S**	14	7	**3**	73 (0.52)
		I	1	27	18	
		R	**3**	11	74	
Moxifloxacin	**MH**	**S**	27	5	**3**	59 (0.38)
		I	21	25	6	
		R	**5**	25	41	

treatment. As expected, the main difference between the MICs determined in the two media was observed for clarithromycin due to the difference in their pH (6.8 in 7H9 vs. 7.4 in MH) (**Table 2** and **Supplementary Figure S1**; Truffot-Pernot et al., 1991). However, using previous CLSI breakpoints given for testing in 7H9 medium with radiometric testing (Clinical and Laboratory Standards Institute [CLSI], 2011), only rare minor errors were observed when MICs were converted into the SIR categories (2%) (**Table 3**).

Both guidelines also recommend the performance of amikacin susceptibility testing of isolates taken prior to initiation of treatment (Haworth et al., 2017; Clinical and Laboratory Standards Institute [CLSI], 2018). In both media, the MICs of amikacin were better correlated than those of clarithromycin (57 vs. 27%), but SIR concordance was lower (87 vs. 98%) (**Tables 2**, **3**). In particular, when MICs were converted into SIR categories, 17 strains (11%) were categorized as I in MH and S in 7H9. Among these 17 strains, none was identified in patients who had been treated previously with amikacin. Moreover, of these, 12 were screened for mutation in *rrl*, none was mutated. Finally, the MIC distribution was Gaussian in MH and 7H9 media (**Figure 1** and **Supplementary Figures S1, S2**). Thus, we believe that these 17 strains belong to the wild-type MAC strain population and should not be categorized as I. We propose to either modify the breakpoint in MH from 16 to 32 mg/L, or to measure the amikacin MIC in 7H9.

Susceptibility testing of moxifloxacin and linezolid may be considered for macrolide-resistant strains, although no *in vitro-in vivo* correlation has yet been established (Koh et al., 2013; Haworth et al., 2017; Clinical and Laboratory Standards Institute [CLSI], 2018). For linezolid and moxifloxacin, agreement was weak to moderate between both methods (**Table 3**), and in up to 5% of MICs that were converted into SIR categories there were VME and ME. Several reasons can explain this lack of agreement between the results obtained using the two media. The first is that the proposed breakpoints are spread through the distribution of the MICs of the wild-type strains (**Figure 1** and **Supplementary Figures S1, S2**). Therefore, small MIC variations that are not clinically relevant may modify the categorization. The second reason is linked to the TREK microplate system. Reading is difficult, requires trained staff and is easier when the test is performed in 7H9 rather than in MH broth (personal observation). Overall, as MICs are high and there is no clear demonstration of activity of these drugs in humans (Schön and Chryssanthou, 2017), we propose not to perform *in vitro* susceptibility testing for moxifloxacin and linezolid.

Finally, although ethambutol and rifamycins are used for the treatment of MAC infections, no clinical breakpoints have been defined for these drugs (Clinical and Laboratory Standards Institute [CLSI], 2018). In their absence, agreement was measured based on MICs. It must be mentioned that for rifabutin and rifampin, the concentration range tested in broth does not cover the entire MIC distribution, either because concentrations are too high (rifabutin) or too low (rifampin) (**Figure 1**). However, despite overall high *in vitro* MICs, it has been shown that rifamycins and ethambutol do prevent selection of clarithromycin resistance (May et al., 1997; Gordin et al., 1999; Benson et al., 2003), and a recent study reported a better clinical response when rifampin and/or ethambutol MICs were below 8 mg/L (Kwon et al., 2018). If these results are confirmed, this concentration could be used as a clinical breakpoint.

Regarding MIC profiles among MAC members, our data confirm previous studies showing that MICs for *M. avium* are rather equivalent to or higher than those for other members of the MAC (Renvoisé et al., 2014; Litvinov et al., 2018). Also, rifampin MICs for *M. chimaera* isolates were lower than for *M. avium*, in line with a recent study (Maurer et al., 2018). Regarding the rarely described *M. timonense* and *M. yongonense*, our data are in favor of lower amikacin MICs for these species than for other members of MAC. Given the small number of strains in our study and in the literature, more data are needed to know the wild-type susceptibility profiles of these two species.

ECOFF values were close to those described in 2018 by Maurer et al., for clarithromycin, amikacin and rifabutin (a difference of no more than one dilution, except for rifabutin, in *M. chimaera*) and added data for ethambutol, rifampin and moxifloxacin (Maurer et al., 2018).

In conclusion, there is no major difference between MICs measured in 7H9 and MH broth for most antibiotics with the exception of clarithromycin and amikacin. For clarithromycin, the MIC values obtained with the two media evaluated are significantly different. Nevertheless, there is no clinical impact on SIR categorization when using breakpoints adapted to the media employed. However, for amikacin, 7H9 broth allows a better distinction between wild and resistant populations by limiting the number of strains categorized "intermediate." Moreover, the 7H9 broth seems to offer a better growth of mycobacteria than the MH medium which makes it possible to render the results of the DST faster (from the first reading on day seven) without

requiring a second reading on D10 or D14 as it can happen with the MH broth.

In addition, better growth of mycobacteria facilitates the reading of MICs, thus reducing inter-operator variability and improving the reproducibility of the technique. Since the only difference we've shown between the two media are in favor of the 7H9 medium, we recommend using the 7H9 broth supplemented with 5% OADC instead of CAMH broth supplemented with 5% OADC for DST of MAC.

MEMBERS OF THE CNR-MyRMA

Members of the CNR-MyRMA are Emmanuelle Cambau, Faïza Mougari, Emmanuel Lécorché, Vincent Jarlier, and Isabelle Bonnet.

DATA AVAILABILITY STATEMENT

All datasets generated for this study are included in the article/**Supplementary Material**.

ETHICS STATEMENT

According to French law at the time of start of the study and in accordance with the ethical standards of our hospitals' institutional review boards (Committee for the Protection of Human Subjects), informed consent was not obtained because this observational study did not modify existing diagnostic or therapeutic strategies.

AUTHOR CONTRIBUTIONS

NV and AA conceived and designed the study. JJ, AA, FM, FB, WS, TM, and NV performed the experiments and collected the data. JJ wrote the manuscript which was reviewed and approved by AA, FM, FB, JR, WS, TM, and NV.

FUNDING

Part of SLOMYCO plates, MH and 7H9 media used in this study was generously provided by Thermo Fischer Scientific. CNR-MyRMA is supported by an annual grant from Santé Publique France.

ACKNOWLEDGMENTS

We thank the laboratory technicians for their expert assistance. We also thank all bacteriologists and clinicians who sent isolates to the French National Reference Centre for Mycobacteria. Part of this work was presented, in part, at the 49th Union World Conference on Lung Health in 2018 at the Hague, Netherlands, and at the Mycobactéries meeting in 2018 in Saint-Quentin en Yvelines, France.

SUPPLEMENTARY MATERIAL

The Supplementary Material for this article can be found online at: https://www.frontiersin.org/articles/10.3389/fmicb.2020.00081/full#supplementary-material

REFERENCES

Aziz, D. B., Low, J. L., Wu, M. L., Gengenbacher, M., Teo, J. W. P., Dartois, V., et al. (2017). Rifabutin is active against *Mycobacterium abscessus* complex. *Antimicrob. Agents Chemother.* 61:AAC.00155-17. doi: 10.1128/AAC.00155-17

Benson, C. A., Williams, P. L., Currier, J. S., Holland, F., Mahon, L. F., MacGregor, R. R., et al. (2003). A prospective, randomized trial examining the efficacy and safety of clarithromycin in combination with ethambutol, rifabutin, or both for the treatment of disseminated *Mycobacterium avium* complex disease in persons with acquired immunodeficiency syndrome. *Clin. Infect. Dis.* 37, 1234–1243. doi: 10.1086/378807

Brown-Elliott, B. A., Iakhiaeva, E., Griffith, D. E., Woods, G. L., Stout, J. E., Wolfe, C. R., et al. (2013). In vitro activity of amikacin against isolates of *Mycobacterium avium* complex with proposed MIC breakpoints and finding of a 16S RRNA gene mutation in treated isolates. *J. Clin. Microbiol.* 51, 3389-3394. doi: 10.1128/JCM.01612-13

Clinical and Laboratory Standards Institute [CLSI] (2011). *Susceptibility Testing of Mycobacteria, Nocardiae, and Other Aerobic Actinomycetes*, 2nd Edn. Wayne, PA: CLSI.

Clinical and Laboratory Standards Institute [CLSI] (2018). *Susceptibility Testing of Mycobacteria, Nocardiae, and Other Aerobic Actinomycetes*, 3rd Edn. Wayne, PA: CLSI.

Dautzenberg, B., Piperno, D., Diot, P., Truffot-Pernot, C., and Chauvin, J. P. (1995). Clarithromycin in the treatment of *Mycobacterium avium* lung infections in patients without AIDS. Clarithromycin study group of france. *Chest* 107, 1035–1040. doi: 10.1378/chest.107.4.1035

European Committee on Antimicrobial Susceptibility Testing [EUCAST] (2019). *s. d. MIC Distributions and Epidemiological Cut-Off Value (ECOFF) Setting. Consulté le 29 janvier 2019*. Sweden: EUCAST. doi: 10.1378/chest.107.4.1035

Gordin, F. M., Sullam, P. M., Shafran, S. D., Cohn, D. L., Wynne, B., Paxton, L., et al. (1999). A randomized, placebo-controlled study of rifabutin added to a regimen of clarithromycin and ethambutol for treatment of disseminated infection with *Mycobacterium avium* complex. *Clin. Infect. Dis.* 28, 1080-1085. doi: 10.1086/514748

Griffith, D. E., Aksamit, T., Brown-Elliott, B. A., Catanzaro, A., Daley, C., Gordin, F., et al. (2007). An official ATS/IDSA statement: diagnosis, treatment, and prevention of nontuberculous *Mycobacterial* diseases. *Am. J. Respir. Crit. Care Med.* 175, 367-416. doi: 10.1164/rccm.200604-571ST

Griffith, D. E., Eagle, G., Thomson, R., Aksamit, T. R., Hasegawa, N., Morimoto, K., et al. (2018). Amikacin liposome inhalation suspension for treatment-refractory lung disease caused by *Mycobacterium avium* complex (CONVERT): a prospective, open-label, randomized study. *Am. J. Respir. Crit. Care Med.* 198, 1559–1569. doi: 10.1164/rccm.201807-1318OC

Haworth, C. S., Banks, J., Capstick, T., Fisher, A. J., Gorsuch, T., Laurenson, I. F., et al. (2017). British thoracic society guideline for the management of non-tuberculous Mycobacterial pulmonary disease (NTM-PD). *BMJ Open Respir. Res* 4:e000242. doi: 10.1136/bmjresp-2017-2242

Jo, K. W., Kim, S., Lee, J. Y., Lee, S. D., Kim, W. S., Kim, D. S., et al. (2014). Treatment outcomes of refractory MAC pulmonary disease treated with drugs with unclear efficacy. *J. Infect. Chemother.* 20, 602-606. doi: 10.1016/j.jiac.2014.05.010

Kobashi, Y., Abe, M., Mouri, K., Obase, Y., Kato, S., and Oka, M. (2012). Relationship between clinical efficacy for pulmonary MAC and drug-sensitivity

test for isolated MAC in a recent 6-Year period. *J. Infect. Chemother.* 18, 436-443. doi: 10.1007/s10156-011-0351-x

Koh, W. J., Hong, G., Kim, S. Y., Jeong, B. H., Park, H. Y., Jeon, K., et al. (2013). Treatment of refractory *Mycobacterium avium* complex lung disease with a moxifloxacin-containing regimen. *Antimicrob. Agents Chemother.* 57, 2281-2285. doi: 10.1128/AAC.02281-2212

Kwon, B. S., Kim, M. N., Sung, H., Koh, Y., Kim, W. S., Song, J. W., et al. (2018). In vitro MIC values of rifampin and ethambutol and treatment outcome in *Mycobacterium avium* complex lung disease. *Antimicrob. Agents Chemother.* 62:AAC.0491-18. doi: 10.1128/AAC.00491-18

Lavollay, M., Dubée, V., Heym, B., Herrmann, J. L., Gaillard, J. L., Gutmann, L., et al. (2014). In vitro activity of cefoxitin and imipenem against *Mycobacterium abscessus* complex. *Clin. Microbiol. Infect.* 20, O297–O300. doi: 10.1111/1469-0691.12405

Litvinov, V., Makarova, M., Galkina, K., Khachaturiants, E., Krasnova, M., Guntupova, L., et al. (2018). Drug susceptibility testing of slowly growing non-tuberculous mycobacteria using slomyco test-system. *PLoS One* 13:e0203108. doi: 10.1371/journal.pone.0203108

Maurer, F. P., Pohle, P., Kernbach, M., Sievert, D., Hillemann, D., Rupp, J., et al. (2018). Differential drug susceptibility patterns of *Mycobacterium chimaera* and other members of the *Mycobacterium avium*-intracellulare complex. *Clin. Microbiol. Infect.* 25, 379.e1–379.e7. doi: 10.1016/j.cmi.2018.06.010

May, T., Brel, F., Beuscart, C., Vincent, V., Perronne, C., Doco-Lecompte, T., et al. (1997). Comparison of combination therapy regimens for treatment of human immunodeficiency virus-infected patients with disseminated bacteremia due to *Mycobacterium avium*. ANRS Trial 033 curavium group. Agence Nationale de Recherche Sur Le Sida. *Clin. Infect. Dis.* 25, 621–629. doi: 10.1086/513753

Olivier, K. N., Griffith, D. E., Eagle, G., McGinnis, J. P., Micioni, L., Liu, K., et al. (2017). Randomized trial of liposomal amikacin for inhalation in nontuberculous mycobacterial lung disease. *Am. J. Respir. Crit. Care Med.* 195, 814-823. doi: 10.1164/rccm.201604-0700OC

Philley, J. V., Wallace, R. J., Benwill, J. L., Taskar, V., Brown-Elliott, B. A., Thakkar, F., et al. (2015). Preliminary results of bedaquiline as salvage therapy for patients with nontuberculous mycobacterial lung disease. *Chest* 148, 499-506. doi: 10.1378/chest.14-2764

Prevots, D. R., Shaw, P. A., Strickland, D., Jackson, L. A., Raebel, M. A., Blosky, M. A., et al. (2010). Nontuberculous mycobacterial lung disease prevalence at four integrated health care delivery systems. *Am. J. Respir. Crit. Care Med.* 182, 970-976. doi: 10.1164/rccm.201002-0310OC

Renvoisé, A., Bernard, C., Veziris, N., Galati, E., Jarlier, V., and Robert, J. (2014). Significant difference in drug susceptibility distribution between *Mycobacterium avium* and *Mycobacterium intracellulare*. *J. Clin. Microbiol.* 52, 4439-4440. doi: 10.1128/JCM.02127-2114

Schön, T., and Chryssanthou, E. (2017). Minimum inhibitory concentration distributions for *Mycobacterium avium* complex-towards evidence-based susceptibility breakpoints. *Int. J. Infect. Dis.* 55, 122-124. doi: 10.1016/j.ijid.2016.12.027

Schoutrop, E. L. M., Brouwer, M. A. E., Jenniskens, J. C. A., Ferro, B. E., Mouton, J. W., Aarnoutse, R. E., et al. (2018). The stability of antimycobacterial drugs in media used for drug susceptibility testing. *Diagn. Microbiol. Infect. Dis* 92, 305-308. doi: 10.1016/j.diagmicrobio.2018.06.015

Tanaka, E., Kimoto, T., Tsuyuguchi, K., Watanabe, I., Matsumoto, H., Niimi, A., et al. (1999). Effect of clarithromycin regimen for *Mycobacterium avium* complex pulmonary disease. *Am. J. Respir. Crit. Care Med.* 160, 866-872. doi: 10.1164/ajrccm.160.3.9811086

Truffot-Pernot, C., Ji, B., and Grosset, J. (1991). Effect of PH on the in vitro potency of clarithromycin against *Mycobacterium avium* complex. *Antimicrob. Agents Chemother.* 35, 1677–1678. doi: 10.1128/aac.35.8.1677

Wallace, R. J., Brown, B. A., Griffith, D. E., Girard, W. M., and Murphy, D. T. (1996). Clarithromycin regimens for pulmonary *Mycobacterium avium* complex. the first 50 patients. *Am. J. Respir. Crit. Care Med.* 153(6 Pt 1), 1766-1772. doi: 10.1164/ajrccm.153.6.8665032

Wallace, R. J., Brown-Elliott, B. A., McNulty, S., Philley, J. V., Killingley, J., Wilson, R. W., et al. (2014). Macrolide/Azalide therapy for nodular/bronchiectatic *Mycobacterium avium* complex lung disease. *Chest* 146, 276-282. doi: 10.1378/chest.13-2538

Conflict of Interest: The authors declare that the research was conducted in the absence of any commercial or financial relationships that could be construed as a potential conflict of interest.

frontiers in Microbiology

ORIGINAL RESEARCH
published: 22 April 2020
doi: 10.3389/fmicb.2020.00667

Multi-Label Random Forest Model for Tuberculosis Drug Resistance Classification and Mutation Ranking

Samaneh Kouchaki[1]*, *Yang Yang*[1,2], *Alexander Lachapelle*[1], *Timothy M. Walker*[3,4,5], *A. Sarah Walker*[3,4,6], *CRyPTIC Consortium*, *Timothy E. A. Peto*[3,4,6], *Derrick W. Crook*[3,4,6] *and David A. Clifton*[1]

[1] Department of Engineering Science, Institute of Biomedical Engineering, University of Oxford, Oxford, United Kingdom, [2] Oxford-Suzhou Centre for Advanced Research, Suzhou, China, [3] Nuffield Department of Medicine, University of Oxford, Oxford, United Kingdom, [4] National Institute of Health Research Oxford Biomedical Research Centre, John Radcliffe Hospital, Oxford, United Kingdom, [5] Oxford University Clinical Research Unit, Ho Chi Minh City, Vietnam, [6] NIHR Biomedical Research Centre, Oxford, United Kingdom

Resistance prediction and mutation ranking are important tasks in the analysis of Tuberculosis sequence data. Due to standard regimens for the use of first-line antibiotics, resistance co-occurrence, in which samples are resistant to multiple drugs, is common. Analysing all drugs simultaneously should therefore enable patterns reflecting resistance co-occurrence to be exploited for resistance prediction. Here, multi-label random forest (MLRF) models are compared with single-label random forest (SLRF) for both predicting phenotypic resistance from whole genome sequences and identifying important mutations for better prediction of four first-line drugs in a dataset of 13402 *Mycobacterium tuberculosis* isolates. Results confirmed that MLRFs can improve performance compared to conventional clinical methods (by 18.10%) and SLRFs (by 0.91%). In addition, we identified a list of candidate mutations that are important for resistance prediction or that are related to resistance co-occurrence. Moreover, we found that retraining our analysis to a subset of top-ranked mutations was sufficient to achieve satisfactory performance. The source code can be found at http://www.robots.ox.ac.uk/∼ davidc/code.php.

Keywords: drug resistance, mutation ranking, MLRF, SLRF, tuberculosis

OPEN ACCESS

Edited by:
Miguel Viveiros,
New University of Lisbon, Portugal

Reviewed by:
Francesc Coll,
University of London, United Kingdom
Wouter Deelder,
University of London, United Kingdom

***Correspondence:**
Samaneh Kouchaki
samaneh.kouchaki@eng.ox.ac.uk

Specialty section:
This article was submitted to Antimicrobials, Resistance and Chemotherapy, a section of the journal Frontiers in Microbiology

Received: *02 January 2020*
Accepted: *24 March 2020*
Published: *22 April 2020*

Citation:
Kouchaki S, Yang Y, Lachapelle A, Walker TM, Walker AS, CRyPTIC Consortium, Peto TEA, Crook DW and Clifton DA (2020) Multi-Label Random Forest Model for Tuberculosis Drug Resistance Classification and Mutation Ranking. Front. Microbiol. 11:667. doi: 10.3389/fmicb.2020.00667

1. INTRODUCTION

As reported by the World Health Organization, resistance co-occurrence is very common, and is especially so between first-line drugs for treating tuberculosis (TB): isoniazid (INH), ethambutol (EMB), rifampicin (RIF), and pyrazinamide (PZA) (World Health Organization, 2017). Two types of resistance co-occurrence are especially important: (i) multi-drug resistant TB (MDR-TB) defined as cases that are resistant to at least INH and RIF; and (ii) extensively drug-resistant TB (XDR-TB), defined as isolates that are resistant to INH and RIF plus any of the fluoroquinolones such as levofloxacin or moxifloxacin and at least one of the three injectable second-line drugs, including amikacin, capreomycin, or kanamycin. Hence, resistance co-occurrence to anti-TB drugs has become an urgent public health concern (World Health Organization, 2017).

Conventional methods for resistance prediction from whole genome sequences are usually based on identifying specific known resistance-conferring variants (i.e., single nucleotide polymorphisms; insertions or deletions) and interpreting (i) the presence of any of them as indicating resistance;

and (ii) the absence of all of them as indicating susceptibility to an individual drug (Schleusener et al., 2017). Most techniques are based on a library of resistance-conferring variants for each individual drug (Georghiou et al., 2012; Coll et al., 2015; Walker et al., 2015). However, due to high dimensionality of the sequencing data and unknown resistance mechanisms, these techniques do not necessarily result in high classification performance especially for less-studied drugs. Moreover, such methods predict resistance drug-by-drug based on known mutations for each drug, rather than by jointly predicting MDR- or XDR-TB.

Some mutations are commonly seen in strains that are resistant to multiple drugs (e.g., MDR-TB and XDR-TB isolates). This is likely to be because they have no, or very limited, fitness cost (Eldholm et al., 2015). This suggests that predicting the global phenotype (e.g., MDR-TB), rather than individually predicted phenotypes (e.g., resistance to INH), could be a promising approach. *katG*_315 was the most common MDR-TB mutation in a dataset of 608 susceptible and 403 MDR-TB isolates in Hazbón et al. (2006) and also a recent study of 5310 isolates (Manson et al., 2017). Moreover, the proportion of isolates with *katG*_315 mutations was higher in MDR-TB isolates than mono-resistant isolates, supporting the hypothesis that these strains have a lower fitness cost and are better able to acquire and tolerate additional mutations. Similarly, *katG*_315, *rpoB*_445, and *rpoB*_450 mutations were found to be associated with MDR-TB isolates in another study (Van Rie et al., 2001) which identified 90% of all MDR-TB in their 5-year dataset. Borrell et al. (2013) observed that the *gyrA*_D94G mutation was associated with greater fitness than the *gyrA*_G88C mutation when co-existing with *rpoB* mutations in strains that are resistant to both RIF and quinolones. The later points to a likely epistatic interaction between *gyrA*_D94G and *rpoB*.

Multi-label learning provides a potential solution to such challenges. Multi-label learning is an important classification technique if each sample in a dataset is associated with multiple labels (e.g., resistance/susceptibility to multiple drugs) and if there are correlations between labels (e.g., for resistance co-occurrence, there are around 2,000 isolates that are resistant to both INH and RIF). In this case, learning each label independently, ignoring correlations between labels, results in lower performance. Instead of considering resistance to each drug individually, the multi-label technique learns a single model for all drugs, and makes a prediction at the sample level. This method is closer to the clinical reality, where drug resistance phenotypes are not typically independent of one another due to using regimens made up of a combination of drugs. Resistance co-occurrence is especially common in first-line drugs, since standard regimens require them to be used together. Existing machine learning methods for TB prediction in the literature have focused on single-drug prediction (Periwal et al., 2011; Zhang et al., 2013; Farhat et al., 2016; Yang et al., 2018; Deelder et al., 2019), and ignored epistasis and correlation of resistance between drugs. Building a multi-label model to account for both of the latter may improve predictive performance and be useful for extracting important MDR- or XDR-TB resistance-associated mutations. In the context of this study, we compared multi-label random forests (MLRFs) with single-label random forests (SLRFs) for the prediction of phenotypic TB resistance. Analysing drugs with high resistance co-occurrence (e.g., RIF and INH) simultaneously should enable patterns reflecting resistance co-occurrence to be exploited for resistance prediction. MLRF and SLRF models, on the other hand, would perform closely for drugs that the resistance co-occurrence is less common. We also conduct feature analysis for mutation ranking. We trained our models on a database of 13402 isolates with resistance phenotypes for up to 11 first- and second-line anti-TB drugs (INH, EMB, PZA, RIF, streptomycin, amikacin, moxifloxacin, fluoroquinolones-ofloxacin, kanamycin, capreomycin, ciprofloxacin). Resistance/susceptibility to all first-line drugs individually, MDR-TB, and cases with resistance to the four first-line drugs (denoted FDR-TB) were considered as labels (i.e., classification "ground truth") for the analysis. There were few XDR-TB cases (245 isolates) in our dataset due to the high percentage of missing labels, hence XDR-TB was not considered in our study. MLRF predicts labels for all considered drugs simultaneously and also can rank all associated mutations that are important in drug resistance prediction. Such analysis can also help to find mutations associated with resistance co-occurrence. In a substudy, the models were retrained (and the classification performance was recalculated) on a subset of ranked features instead of using all available features; this substudy allows us to evaluate the influence of selected highly-ranked features on the classification performance (as might be useful in creating a lightweight system for use in real-time, in practice).

In summary, to date, RF-based studies for drug resistance prediction have only considered each drug individually (Farhat et al., 2016; Kouchaki et al., 2019). However, greater power may be obtained with RFs through multi-label analysis incorporating information from all drugs to include the co-occurrence of drug resistance and epistasis. Being an ensemble method, the MLRF also has advantages considering that there are fewer resistant examples available than susceptible isolates (i.e., datasets are highly imbalanced) that are common in the study of TB genomics. We focus on comparing MLRFs and SLRFs in terms of classification performance, mutation ranking, and the effect of feature selection on the performance.

2. MATERIALS AND METHODS

We studied a diverse and large dataset collected from 16 countries across six continents.

2.1. Whole Genome Sequencing

Details of DNA sequencing and our data source (including the European Nucleotide Archive/Sequence Read Archive accession numbers) are presented in Walker et al. (2015) and CRyPTIC Consortium and the 100,000 Genomes Project (2018) and **Supplementary I**. Sequenced reads were aligned to the reference MTB strain, and nucleotide bases were filtered based on the sequencing and alignment quality, and per-base coverage. Low confidence nucleotide bases were denoted as null calls. There are several ways to treat a null call in an isolate: (i) removing the sample completely from the analysis, which greatly reduces

the sample size (since 34% of isolates have one or more null calls in the genetic regions of interest) and generalisability; (ii) considering the null calls as no variants (i.e., mutation presence = 0), which is a conservative option and means that performance will be an underestimate of true performance if all variants were known; (iii) considering null values as missing and impute their values, on either a single or multiple basis. We chose the second option (assuming absence of variant) because the total number of variant positions across the genetic regions of interest (5919 positions) and across all isolates (13402) with null calls was very small (0.19%); and because of the complexity of multiple imputation models that would be needed for (iii), based on the 5919 positions. This approach is effectively a "single" hard (i.e., conservative) imputation.

2.2. Data Description

The dataset used in this paper contains 13402 isolates collected from across the world. In this study, we followed previous work in which 23 genes (**Table S1**) were targeted containing known resistance-associated mutations (Walker et al., 2015). For each isolate, the presence/absence of a variant was represented by a binary variable, with 1 indicating presence and 0 indicating absence. Across the 23 candidate genes, in total, 5919 variants were found across isolates, including multiple variants at the same position. The mean number of variants per isolate was 14, ranging between 1 and 132. Hence, a binary vector of length 5919 was formed for each isolate, and considered to be our feature space (i.e., set of input variables). For each drug and isolate, a binary label of resistance/susceptible was considered. The "ground truth" phenotypic information was available for up to 11 anti-TB drugs using culture and confirmed selective culturing on Lowenstein-Jensen media. Not all samples were tested against all drugs with missing values, especially for second-line drugs where missingness of the phenotypical label was substantial. There were only a few XDR-TB cases (245 isolates) in our dataset due to the high percentage of missing labels and hence XDR-TB was not considered in our study.

For the four first-line drugs, more isolates were susceptible than were resistant. For example, more than 88% of isolates tested for EMB and PZA and 75% for INH and RIF were susceptible. Moreover, there were several isolates with multiple drug resistance considering the four first-line drugs (**Figure 1**).

2.3. Predicting TB Drug Resistance From Sequence

Existing methods predominantly classify drug resistance as present or absent based on a library of predetermined variants from the literature. These methods, here denoted direct association (DA), use a logical "OR" rule to classify an isolate against a given drug: the isolate is labeled as resistant if any of its mutations is a previously-known resistant variant. Otherwise, it is classified as susceptible (i.e., if only susceptible variants exist in the isolate). The library described by Walker et al. (2015) was used throughout the classification comparison here.

2.4. MLRF for TB Classification

The RF is an ensemble method that is based on building several independent decision tree classifiers on different subsets of the dataset. It considers the combination (often the average) of the output of each independent classifier to improve performance in producing overall predictions.

Multi-label learning is a supervised problem in which several labels are learned simultaneously. In the TB data, there are many cases of MDR-TB, as shown in **Figure 1** (World Health Organization, 2017). Using multi-labels (i.e., all phenotypes simultaneously, rather than considering each independently) can reduce the training time as only one model is learned, and predictive performance can be increased (Evgeniou and Pontil, 2004) due to learning correlation between inputs and the multiple outputs. The RF model can be extended to learn and predict multiple drugs simultaneously considering a joint score (Gini index) across all considered drugs (Faddoul et al., 2012). Specifically in each decision tree, for each pair (f, x) of a feature f (mutation) and a value x (isolate) with a label y (resistance phenotype) at node (t):

$$\text{Gini index,} \quad \mathrm{GI}_J(t,f,x) = \sum_{y \in Y} \mathrm{GI}_y(t,f,x) \tag{1}$$

where Y is the number of labels (two for MDR-TB and four for FDR-TB) and GI_J and GI_y are the joint and per-label Gini indices, respectively. The objective is to minimize Equation (1) and hence (f, x) is selected to best separate (defined by a lower joint Gini index) the data at each node in the tree. Hence, during training, it can compute the importance of each feature by averaging the impurity decrease associated with each mutation.

Figure S1 shows a sample decision tree from a forest learned by MLRF for the four first-line drugs (EMB, INH, RIF, and PZA). In comparison, a tree learned by SLRF for EMB is shown in **Figure S2**. The tree grows in the best-node-first fashion (defined by impurity reduction[1]).

*katG*_S315T, *rpoB*_S450L, *embB*_M306V, *embB*_Q497R, and *embB*_M306I are common mutations in both trees. *katG*_S315T was the most highly-ranked feature in both trees, but other rankings of features vary between models. A feature (mutation) that results in the lowest Gini index is selected to best split the data at each node. The MLRF learns a joint Gini index (Equation 1), and hence finds that feature that best splits the data considering all drugs. In contrast, the SLRF only considers the Gini index based on one drug at each node (e.g., EMB). After the node split, another feature is selected that further reduces the Gini index. Building various trees on different subsets of the data can then automatically pick important features. Consequently, MLRF ranks mutations to best classify resistance to *all* drugs. Hence, it also helps the model learn mutations associated with resistance co-occurrence. Conversely, SLRF ranks mutations to best classify an *individual* drug ignoring any co-occurrence. The SLRF also ranks some mutations from *other* drugs as being important as seen in **Supplementary B**, which effectively reflects underlying interaction between phenotypes. After building the

[1] A node split decreases the gini impurity criterion for the two descendent nodes.

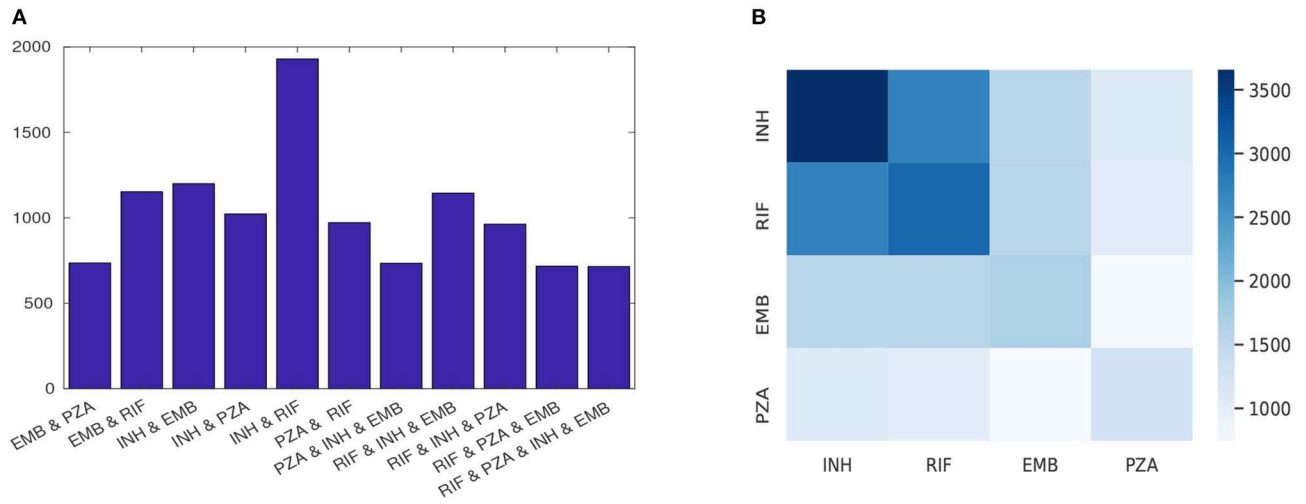

FIGURE 1 | The phenotypic profile of first-line drugs; **(A)** each row shows the number of isolates that are resistant to at least the indicated drugs combination and **(B)** heatmap quantifying the number of instances of resistance co-occurrence between drugs. Off-diagonal elements show resistance co-occurrence between different drugs and diagonal elements show resistant to a single drug.

models, samples traverse each tree by starting at the root node, reaching a leaf node. The classification is calculated at the leaf node by majority vote and the final classification is obtained by averaging results across trees.

2.5. Multi-Label Stratification

Stratified sampling (i.e., taking an equal proportion from each class) is especially important in TB analysis due to the imbalanced nature of the data and the co-occurrence of drug resistance for different drugs, with some resistance patterns being much rarer than others (**Table S4**). Hence, an iterative algorithm termed multi-label stratified cross-validation (Sechidis et al., 2011) was considered here to avoid the use of subsets without any examples of rare labels. Multi-label stratified cross-validation starts with a label combination that has the fewest samples. Considering rare label combinations before more frequent combinations increases the chance of distributing these rare examples evenly among prediction of the data between training and test sets. In each iteration, one sample from the most rare combination is selected and added to a partition depending on the number of samples with that label already in each partition. Then, the partitioning continues with another sample with the same label if any remain; otherwise, a sample from the second-most rare label combination is considered. This process continues until all samples are assigned to a subset.

2.6. Feature Spaces

To evaluate the performance of our model and to obtain feature rankings, five feature sets were considered: [F1] the baseline feature space of all variants found within 23 candidate genes (N = 5,918); [F2] as a subset of feature set F1 includes only drug-associated genes for a particular drug (N = 3,366 that obtained by only considering the variants within the genes that are known to be associated with the first line drugs, **Supplementary A**); [F3] known variants from (Walker et al., 2015) for all first-line drugs (N = 1874); [F4] and [F5] are obtained by dropping isolates with any known resistance-associated mutations from feature sets F1 and F2, respectively — that is, feature sets F4 and F5 allow us to investigate whether phenotypically resistant isolates without well-known resistance mutations can be identified from other sequence variations (N = 4,755 and 2,417, respectively). Feature set F1 includes all variants spaces, which is preferable for less-studied drugs. For well-studied drugs, using the known catalog of resistance-associated mutations has been shown to perform well.

2.7. Training and Testing

For all experiments, model construction and evaluation was performed over 10 iterations of five-fold multi-label stratified cross-validation. In each iteration, 20% of the dataset was used as the test set and the remaining 80% of the data as the training set. Here, the "internal" cross-validation on the 80% training dataset was used to select a decision threshold that maximizes the accuracy; this threshold was then used for prediction in the test set. Moreover, we considered fixed RF hyper-parameters for both techniques (50 estimators with maximum depth of two and maximum features as the square root of input variants). The performance in terms of accuracy, sensitivity, specificity, and area-under-the-ROC-curve (AUC) was calculated for the test set (for reporting final "hold-out" results).

$$\begin{aligned} \text{Accuracy} &= \frac{\text{TP} + \text{TN}}{\text{TP} + \text{TN} + \text{FP} + \text{FN}} \\ \text{Sensitivity} &= \frac{\text{TP}}{\text{TP} + \text{FN}}, \ \text{Specificity} = \frac{\text{TN}}{\text{TN} + \text{FP}}. \end{aligned} \tag{2}$$

where TP, TN, FP, and FN are true positive, true negative, false positive, and false negative, respectively, and where P and N are resistance and susceptible samples, respectively. The output of

the models is a probability estimate $P(C_1|\underline{\mathbf{X}})$ of the posterior probability of input feature vector $\underline{\mathbf{X}}$ belonging to class C_1 (resistant). We then define a threshold k on $P(C_1|\underline{\mathbf{X}})$, such that a classification of $\underline{\mathbf{X}} \mapsto C_1$ (i.e., resistant) is made if $P > k$, and a classification of $\underline{\mathbf{X}} \mapsto C_0$ (i.e., susceptible) if $P \leq k$. Varying threshold k results in different TP, FP, FN, and TN rates and thus sensitivity and specificity vary according to the value of $k \in [0, 1]$. However, AUC is calculated over all value of k, and is therefore insensitive to any particular choice of decision threshold k. The workflow of examined classifiers can be seen in **Supplementary C**.

3. RESULTS

3.1. Comparison of Top Performing Classifier and DA

Table 1 compares the performance of DA and the best performing model considering feature sets F1-F5 for INH, EMB, RIF, PZA, MDR-TB, and FDR-TB. Our results show that the MLRF is the best performing model for all drugs except for PZA. feature set F3 was the best feature set for INH, RIF, and MDR-TB, while feature F1 was the best feature set for EMB, PZA, and FDR-TB all in terms of AUC. DA showed higher specificity in comparison with the best performing model, but had lower sensitivity and AUC in all cases.

3.2. Detailed Comparison of MLRF, SLRF, and DA

Supplementary D provides further details of the classification results. In terms of classification performance, both SLRF and MLRF perform fairly similarly with slight improvements in AUC and sensitivity considering MLRF especially for INH and RIF ($p < 0.01$). Compared to DA, sensitivity increased for all drugs (considering feature sets F1 and F3) and for all drugs except RIF when considering feature set F2. Both MLRF and SLRF had higher AUC than DA considering feature sets F1-F3 for EMB, considering feature set F3 for INH and RIF, considering feature sets F1 and F3 for MDR-TB and considering all feature sets for PZA and FDR-TB.

3.3. Mutation Ranking

The 10 most important mutations based on MLRF and SLRF and feature sets F1-F5 is shown in **Supplementary E**. In summary:

- There were several known mutations that were commonly ranked as being important for the purpose of prediction, regardless of model (MLRF and SLRF) and drug: (i) *katG*_S315T, *rpoB*_S450L and *embB*_M306V for feature set F1; and (ii) the latter three mutations along with *embB*_M306I for feature sets F2-F3. These are the most common known resistance mutations associated with INH, RIF, and EMB, respectively (Walker et al., 2015). However, each of these highly-related mutations had different importance values and resulted in different classification performance across various MLRFs and SLRFs trained on different feature sets.
- Analysis using feature set F4 identified several important mutations from other genes related to second-line drugs (e.g., *rrs*_G349A and *eis*_C-12T).
- There was considerable overlap between mutations ranked for all first-line drugs and FDR-TB. In other words, SLRF ranking for a given drug indicated multiple mutations that are associated with *other* drugs.
- Several mutations selected as being important were not in the DA library and were not lineage defining. Some of these mutations occurred within genes associated with a given first-line drug. Detailed information of their occurrence in isolates is shown in **Supplementary F**.
- Considering (i) feature set F1, (ii) all variants in drug-associated genes for a given drug from feature set F2, and (iii) known drug-resistant variants for a given drug extracted from feature set F3, resulted in identifying a list of candidate mutations that are important for resistance prediction or are related to resistance co-occurrence (**Supplementary G**).

3.4. MLRF and SLRF Performance on a Subset of Important Features

As described earlier, a substudy introduced retraining models on a subset of ranked features (instead of using feature sets F1-F5). **Table 2** and **Figures 2**, **3** summarize the performance of the different classifiers when the feature set is restricted to that subset of mutations in feature sets F1-F3 ranked above importance thresholds of {0.05, 0.01, 0.005, and 0.001} (details in **Supplementary E**). In summary:

- The best model for each drug (**Table 2**) still performs better than DA even when using a subset of important mutations (16–37 mutations) for INH, EMB, PZA, MDR-TB, and FDR-TB in terms of AUC and sensitivity ($p < 0.01$).
- Considering only 16–37 features rather than the larger feature sets F1-F5 resulted in better performance for EMB and FDR-TB and very similar performance for others (**Table 2**).
- The SLRF performed better for EMB, PZA, and FDR-TB when restricted to using highly-related mutations in this way.
- Increasing the number of features (i.e., decreasing the threshold on feature importance used to select features in this substudy) did not always improve the performance (e.g., FDR-TB).
- Increasing the number of features usually increased sensitivity while reducing specificity.

4. DISCUSSION

Our analysis demonstrates that machine learning methods, specifically MLRF (considering feature sets F1-F3), had higher sensitivity but lower specificity compared with DA (at their points of higher accuracy). Sensitivity and AUC increased substantially for PZA and FDR-TB when using MLRFs. There may be several reasons for this finding, including (i) the existence of additional resistance-associated mutations to those reported in the literature; (ii) the existence of certain combinational patterns of resistance-related and epistasis and lineage-related mutations; and (iii) co-occurrence of resistance

TABLE 1 | Performance of the best machine learning classifier and DA considering INH, EMB, RIF, PZA, MDR-TB, and FDR-TB.

	DA			Best method			
Drugs	**Sensitivity**	**Specificity**	**AUC**	**Feature set + Classifier**	**Sensitivity**	**Specificity**	**AUC**
INH	91.15 ± 1.19	98.96 ± 0.25	95.05 ± 0.60	F3 + MLRF	93.76* ± 0.80	97.79 ± 0.35	96.01* ± 0.47
EMB	85.10 ± 1.79	94.91 ± 0.38	90.00 ± 0.97	F1 + MLRF	91.75* ± 1.81	91.58* ± 0.77	91.70* ± 0.75
RIF	91.52 ± 1.34	98.68 ± 0.21	95.10 ± 0.65	F3 + MLRF	93.16* ± 0.80	98.02 ± 0.32	96.00* ± 0.40
PZA	43.21 ± 2.72	98.58 ± 0.23	70.89 ± 1.35	F1 + SLRF	87.27* ± 1.74	90.71* ± 0.72	88.99* ± 0.84
FDR-TB	37.34 ± 3.97	98.59 ± 0.22	67.96 ± 1.99	F1 + MLRF	87.58* ± 2.79	92.98* ± 0.45	90.28* ± 1.23
MDR-TB	89.84 ± 1.34	99.12 ± 0.178	94.48 ± 0.69	F3 + MLRF	93.70* ± 0.76	97.45 ± 0.36	95.58* ± 0.41

*Sensitivity, specificity and AUC (mean ± standard error) were reported. The Wilcoxon signed-rank test was used to calculate the p-value of each method compared with the DA and *$p < 0.01$ vs. DA.*

TABLE 2 | Performance of best models restricting to only important mutations for classification.

Drug	**INH**	**EMB**	**RIF**	**PZA**	**FDR-TB**	**MDR-TB**
Best model	IF3 (0.001) + MLRF	IF3 (0.005) + SLRF	IF3 (0.001) + MLRF	IF1 (0.001) + SLRF	IF3 (0.01) + SLRF	IF3 (0.001) + MLRF
Number of mutations	37	17	37	32	16	37
Sensitivity	92.88 (↓ 0.28) ± 0.93	91.10 (↓ 0.65) ± 1.76	92.19 (↓ 0.07) ± 1.10	84.73 (↓ 2.54) ± 2.49	91.74 (↑ 4.16) ± 3.37	93.76 (↑ 0.06) ± 1.33
Specificity	97.88 (↑ 0.09) ± 0.31	92.70 (↑ 1.12) ± 0.51	97.77 (↓ 0.22) ± 0.52	92.83 (↓ 2.12) ± 0.52	90.06 (↓ 2.92) ± 0.61	97.38 (↓ 0.07) ± 0.49
AUC	95.48 (↓ 0.53) ± 0.40	91.90 (↑ 0.20) ± 0.82	94.98 (↓ 1.02) ± 0.53	88.78 (↓ 0.21) ± 1.17	90.90 (↑ 0.62) ± 1.56	95.47 (↓ 0.11) ± 0.62

*The number of mutations used for the classification, best model and performance for INH, EMB, RIF, PZA, MDR-TB, and FDR-TB are shown. Increase/decrease in performance in comparison with the best model in **Table 1** are indicated with up/down arrows, respectively. "I" prefix refers to our substudy.*

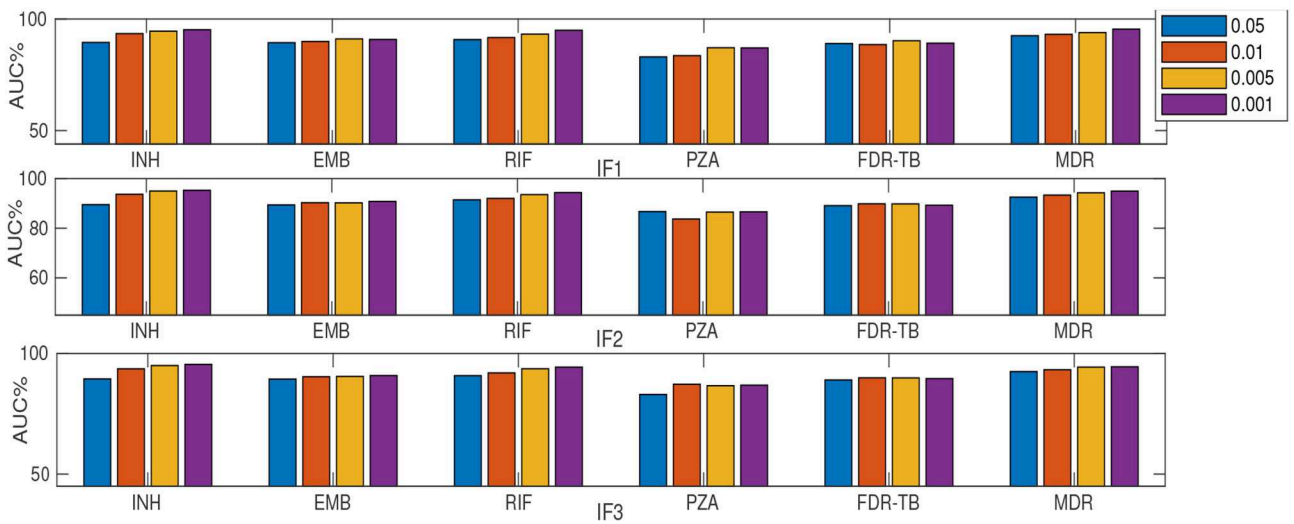

FIGURE 2 | AUC (%) comparison considering MLRF and four thresholds {0.05, 0.01, 0.005, and 0.001} for feature selection. "I" prefix refers to our substudy.

(for the 23 genes considered in this paper). **Supplementary G** provides a list of possible candidates for (i) and (iii). Lower specificity could be due to the existence of several isolates with resistance-associated mutations that were incorrectly labeled as susceptible. It could be because of limitations in the routine phenotyping relating to dichotomous thresholds of "resistant" vs. "susceptible" applied to a continuous measure of the minimum inhibitory concentration, as is well-known for M306V for example (Khan et al., 2019). This could also have some additional negative effects on prediction of co-occurring resistance. Another reason could be the threshold setting for obtaining sensitivity and specificity. There is a trade-off between sensitivity and specificity in which increasing one can result in decreasing the other. The use of feature sets F4 and F5 resulted in lower prediction performance then other feature sets mainly because of very low numbers of resistant isolates left after dropping those with known resistant-associated mutations (**Supplementary H**).

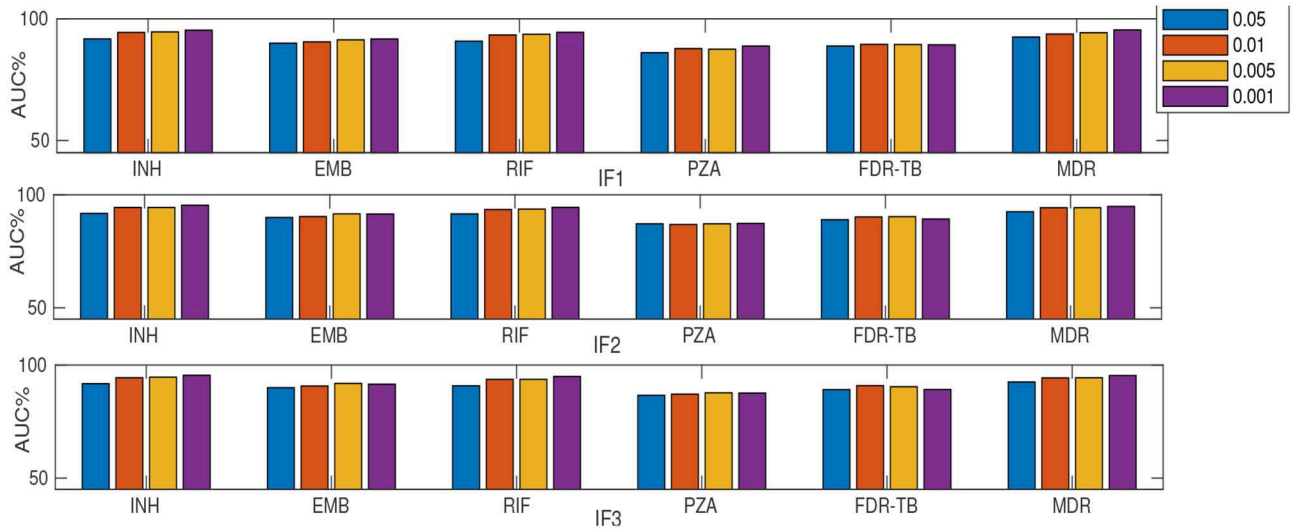

FIGURE 3 | AUC (%) comparison considering SLRF and four thresholds {0.05, 0.01, 0.005, and 0.001} for feature selection. "I" prefix refers to our substudy.

The best method based on MLRF had only slightly higher sensitivity and AUC compared to SLRF for most drugs (**Supplementary D**), possibly because of several common MDR-TB mutations, i.e. *katG*_315 being a strong resistance-conferring variant, as in Hazbón et al. (2006). As the feature space is the same for MLRF and SLRF models, both techniques can take advantage of using the occurrence of mutations that is more likely to occur in multi-drug resistant samples. However, learning one model for all labels as in MLRF makes better use of such mutations as it learns all drugs simultaneously. Consequently, MLRF also enhances performance for single drugs by using existing resistance co-occurrence. PZA was a notable exception, potentially due to the existence of many less strong variants related to PZA resistance. Another reason for the very close AUC between MLRF and SLRF could be that we fixed the RF hyper-parameters (number of decision trees, maximum number of variant for each decision tree,...) for both techniques. Future work introducing a separate parameter optimization could possibly increase the difference in performance.

Our results confirmed the importance of several known mutations with resistance co-occurrence (e.g., *katG*_S315T, *rpoB*_S450L, and *embB*_M306V). Feature set F3 was the best feature set for well-studied drugs (INH, RIF, and MDR-TB) but feature F1 was better for others. This shows that there are additional mutations that are *not* within the current library of known mutations (used for DA) but which are important in classifying resistance; additional co-occurrence patterns of mutations may exist, as might weak interactions between mutations that may have joint effects. Classification based on MLRF and feature sets F1 and F2 mainly identified known resistance-associated mutations as being important. This builds confidence in our approach. However, after removing isolates with any known variants, several mutations were ranked as being important (i) from other genes (e.g., related to second-line drugs); (ii) from known lineage-defining variants; and (iii) that were not in the library and were not lineage-defining (by checking if they occurred in more than one lineage, **Supplementary F, G**). Our results thereby confirm the possibility of additional important mutations (for prediction) to those already known to be important for TB resistance classification. We note that the tree depth was not limited for the learning procedure. Consequently, as we go deeper in the trees learned based on feature set F1, all other features can be seen. However, in TB there are a few strong mutations with high importance values (e.g., *katG*_S350L) which result in very low importance values for other mutations. Removing the impact of such highly important mutations as in feature sets F4 and F5 would allow investigation of whether or not phenotypically resistant isolates without well-known resistance mutations can be identified from other sequence variations. In other words, although a deeper tree can see wider spectrum of mutations, feature sets F4 and F5 can zoom in other sequence variations by avoiding the impact of highly important mutations.

Considering only the top-ranked mutations (as in our substudy) resulted in higher AUC compared to DA for all drugs except RIF (**Table 2**). Thus a small number (16-37) of important features are generally sufficient for RF-based classification. Similar to considering the whole feature set, IF1 and IF3 outperformed IF2, IF4 and IF5 (where "I" prefix refers to our substudy). However, the MLRF only performed better then the SLRF for INH, RIF, and MDR-TB. Considering IF1-IF5, the SLRF was trained on important mutations for each drug and not on the highest-ranking mutations based on MLRF. Hence, different feature sets were used for SLRF and MLRF training. SLRF based on only important features for PZA, FDR-TB, and EMB had better performance compared with the common features based on MLRF. The MLRF was better for INH, RIF, and MDR-TB, possibly because the variants related to these drugs were stronger predictors, while those of PZA and FDR-TB reflect a potential combination effect between variants that are individually weak prediction of resistance. That is, the pattern of resistance for INH, RIF, and MDR-TB dominates the multi label learning,

while the other can be captured by the SLRF. Moreover, errors in routine phenotypes of individual drugs impact MLRF more than SLRF. One limitation of the SLRF model is that it ranked highly many weak variants that are lineage-related mutations (**Supplementary D**). We need to note that lineage defining mutations might be helpful where resistance is over-represented in one lineage (e.g., MDR-TB in lineage 2). **Figure 2** demonstrates that increasing the number of features by reducing the feature selection threshold usually increases AUC, but this is not always the case; e.g., IF1 and IF2 for FDR-TB (**Figure 2**). Consequently, our results indicate the importance of feature ranking to reduce the effect of unrelated mutations in the learning process. Another important conclusion of our work is that by increasing the number of features used, sensitivity improved at the expense of related specificity, confirming that a smaller feature set better predicts susceptible samples while there is a need to have more features to better predict resistant samples (**Supplementary E**). A trade-off typically exists between sensitivity and specificity.

We note there are several limitations regarding our analysis. An assumption of feature ranking should be that the input features are independent; if there are some highly correlated features, any of them could be selected as an important feature. In other words, machine learning techniques, including RF, aim to identify patterns in the data that contribute to predictions. After selecting one such feature, the importance of other correlated features is decreased considering the classification performance. From a classification point of view, it is actually useful to do this as it removes the features whose effect is already described by other closely-related features. Hence, SLRF and MLRF are typically based on correlation and not causation, which means that lineage associate mutations, in addition to mutations conferring resistance to other drugs, can be used in the learning. However, ranking such mutations as important is a limitation of existing machine learning techniques in general. This mainly impacts performance in local settings, where the level of resistance co-occurrence between first- and second-line drugs is different, or where such mutations are completely absent or very abundant. Considering population level structure and cluster effect in the learning will be considered as a future work. For feature selection, an additional step might be helpful to indicate the correlated variants. Such effects can be decreased by random selection of features but they cannot be removed completely.

Random selection may also affect the selection of rare but important mutations. We note that the dataset in our application, which reflects the imbalance encountered in clinical practice, with (for example) a high percentage of samples resistant to INH + RIF that can bias feature ranking in favor of those more common labels. Finally, other limitations include any errors in phenotypes that may exist; considering equal importance for all mutations; and ignoring data with missing labels.

5. CONCLUSION

MLRF and SLRF classifiers were investigated for TB resistance classification and mutation ranking considering different subsets of extracted variants. Several common mutations were identified as important which could confirm the existence of several MDR- and FDR-TB associated patterns. Furthermore, restricting analysis to the 16–37 top-ranked mutations might be useful in creating a lightweight system for use in practice. The main advantage of machine learning methods, especially in our application with a large number of features, is hence capturing any association between the feature space and the prediction of resistance, in addition to learning potentially new mutations associated with MDR-TB and FDR-TB (rather than simply predicting resistance to independent drugs).

DATA AVAILABILITY STATEMENT

The datasets analyzed for this study can be found in the Walker et al. (2015) and CRyPTIC Consortium and the 100,000 Genomes Project (2018).

AUTHOR CONTRIBUTIONS

DWC, SK, TP, AW, TW, YY, and DAC contributed toward study design. SK, YY, and DAC contributed toward data analysis. SK wrote the manuscript with comments from YY, AW, TW, and DAC. All authors contributed feedback on the manuscript.

FUNDING

This research was funded by the CRyPTIC consortium which is funded by a Wellcome Trust/Newton Fund-MRC Collaborative Award [200205/Z/15/Z] and the Bill & Melinda Gates Foundation Trust [OPP1133541], and was supported by the National Institute for Health Research (NIHR) Oxford Biomedical Research Centre. TP and AW are NIHR Senior Investigators. YY was supported by the Oxford Suzhou Centre for Advanced Research (OSCAR).

MEMBERS OF THE CRYPTIC CONSORTIUM

Derrick W. Crook, Timothy E. A. Peto, A. Sarah Walker, Sarah J. Hoosdally, Ana L. Gibertoni Cruz, Joshua Carter, Clara Grazian, Sarah G. Earle, Samaneh Kouchaki, Alexander Lachapelle, Yang Yang, David A. Clifton and Philip W. Fowler, University of Oxford; Zamin Iqbal, Martin Hunt and Jeffrey Knaggs, European Bioinformatics Institute; E. Grace Smith, Priti Rathod, Lisa Jarrett and Daniela Matias, Public Health England, Birmingham; Daniela M. Cirillo, Emanuele Borroni, Simone Battaglia, Arash Ghodousi, Andrea Spitaleri and Andrea Cabibbe, Emerging Bacterial Pathogens Unit, IRCCS San Raffaele Scientific Institute, Milan; Sabira Tahseen, National Tuberculosis Control Program Pakistan, Islamabad; Kayzad Nilgiriwala and Sanchi Shah, The Foundation for Medical Research, Mumbai; Camilla Rodrigues, Priti Kambli, Utkarsha Surve and Rukhsar Khot, P. D. Hinduja National Hospital and Medical Research Centre, Mumbai; Stefan Niemann, Thomas A. Kohl and Matthias Merker, Research Center Borstel; Harald Hoffmann, Katharina Todt and Sara Plesnik, Institute of Microbiology & Laboratory

Medicine, IML red, Gauting; Nazir Ismail, Shaheed Vally Omar and Lavania Joseph, National Institute for Communicable Diseases, Johannesburg; Guy Thwaites, Thuong Nguyen Thuy Thuong, Nhung Hoang Ngoc, Vijay Srinivasan, and Timothy M. Walker, Oxford University Clinical Research Unit, Ho Chi Minh City; David Moore, Jorge Coronel, and Walter Solano, London School of Hygiene and Tropical Medicine and Universidad Peruana Cayetano Heredia, Lima; George F. Gao, Guangxue He, Yanlin Zhao and Chunfa Liu, China CDC, Beijing; Aijing Ma, Shenzhen Third People's Hospital, Shenzhen; Baoli Zhu, Institute of Microbiology, CAS, Beijing; Ian Laurenson and Pauline Claxton, Scottish Mycobacteria Reference Laboratory, Edinburgh; Anastasia Koch, Robert Wilkinson, University of Cape Town; Ajit Lalvani, Imperial College London; James Posey, CDC Atlanta; Jennifer Gardy, University of British Columbia; Jim Werngren, Public Health Agency of Sweden; Nicholas Paton, National University of Singapore; Ruwen Jou, Mei-Hua Wu, Wan-Hsuan Lin, CDC Taiwan; Lucilaine Ferrazoli, Rosangela Siqueira de Oliveira, Institute Adolfo Lutz, São Paulo.

Authors contributing to the CRyPTIC consortium are (in alphabetical order): Irena Arandjelovic, Faculty of Medicine, Institute of Microbiology and Immunology, University of Belgrade, Belgrade, Serbia; Angkana Chaiprasert, Faculty of Medicine Siriraj Hospital, Mahidol University, Thailand; Iñaki Comas, Instituto de Biomedicina de Valencia (IBV-CSIC). Calle Jaime Roig, Valencia, Spain; FISABIO Public Health, Valencia, Spain; CIBER in Epidemiology and Public Health, Madrid, Spain; Francis A. Drobniewski, Imperial College, London, United Kingdom; Maha R. Farhat, Harvard Medical School, Boston, MA, United States; Qian Gao, Shanghai Medical College, Fudan University, Shanghai, China; Rick Ong Twee Hee, Saw Swee Hock School of Public Health, National University of Singapore, Singapore; Vitali Sintchenko, Centre for Infectious Diseases and Microbiology–Public Health, University of Sydney, Sydney, NSW, Australia; Philip Supply, Univ. Lille, CNRS, Inserm, CHU Lille, Institut Pasteur de Lille, U1019 - UMR 8204 - CIIL - Centre d'Infection et d'immunité de Lille, Lille, France; and Dick van Soolingen, National Institute for Public Health and the Environment (RIVM), Bilthoven, Netherlands.

SUPPLEMENTARY MATERIAL

The Supplementary Material for this article can be found online at: https://www.frontiersin.org/articles/10.3389/fmicb.2020.00667/full#supplementary-material

Data Sheet 1 | SRA/ENA accession numbers and phenotypes to four first-line drugs.

REFERENCES

Borrell, S., Teo, Y., Giardina, F., Streicher, E. M., Klopper, M., Feldmann, J., et al. (2013). Epistasis between antibiotic resistance mutations drives the evolution of extensively drug-resistant tuberculosis. *Evol. Med. Public Health* 2013, 65–74. doi: 10.1093/emph/eot003

Coll, F., McNerney, R., Preston, M. D., Guerra-Assuncao, J. A., Warry, A., Hill-Cawthorne, G., et al. (2015). Rapid determination of anti-tuberculosis drug resistance from whole-genome sequences. *Genome Med.* 7:51. doi: 10.1186/s13073-015-0164-0

CRyPTIC Consortium and the 100,000 Genomes Project (2018). Prediction of susceptibility to first-line tuberculosis drugs by DNA sequencing. *N. Engl. J. Med*. 379, 1403–1415. doi: 10.1056/NEJMoa1800474

Deelder, W., Christakoudi, S., Phelan, J., Diez Benavente, E., Campino, S., McNerney, R., et al. (2019). Machine learning predicts accurately *Mycobacterium tuberculosis* drug resistance from whole genome sequencing data. *Front. Genet*. 10:922. doi: 10.3389/fgene.2019.00922

Eldholm, V., Monteserin, J., Rieux, A., Lopez, B., Sobkowiak, B., Ritacco, V., et al. (2015). Four decades of transmission of a multidrug-resistant mycobacterium tuberculosis outbreak strain. *Nat. Commun*. 6:7119. doi: 10.1038/ncomms8119

Evgeniou, T., and Pontil, M. (2004). Regularized multi-task learning," in *Proceedings of the Tenth ACM SIGKDD International Conference on Knowledge Discovery and Data Mining* (Seattle, WA: ACM), 109–117. doi: 10.1145/1014052.1014067

Faddoul, J. B., Chidlovskii, B., Gilleron, R., and Torre, F. (2012). "Learning multiple tasks with boosted decision trees," in *Joint European Conference on Machine Learning and Knowledge Discovery in Databases* (Berlin; Heidelberg: Springer), 681–696. doi: 10.1007/978-3-642-33460-3_49

Farhat, M. R., Sultana, R., Iartchouk, O., Bozeman, S., Galagan, J., Sisk, P., et al. (2016). Genetic determinants of drug resistance in *Mycobacterium tuberculosis* and their diagnostic value. *Am. J. Respir. Critical Care Med.* 194, 621–630. doi: 10.1164/rccm.201510-2091OC

Georghiou, S. B., Magana, M., Garfein, R. S., Catanzaro, D. G., Catanzaro, A., and Rodwell, T. C. (2012). Evaluation of genetic mutations associated with *Mycobacterium tuberculosis* resistance to amikacin, kanamycin and capreomycin: a systematic review. *PLoS ONE* 7:e33275. doi: 10.1371/journal.pone.0033275

Hazbón, M. H., Brimacombe, M., del Valle, M. B., Cavatore, M., Guerrero, M. I., Varma-Basil, M., et al. (2006). Population genetics study of isoniazid resistance mutations and evolution of multidrug-resistant *Mycobacterium tuberculosis*. *Antimicrob. Agents Chemother*. 50, 2640–2649. doi: 10.1128/AAC.00112-06

Khan, Z. A., Siddiqui, M. F., and Park, S. (2019). Current and emerging methods of antibiotic susceptibility testing. *Diagnostics* 9:49. doi: 10.3390/diagnostics9020049

Kouchaki, S., Yang, Y., Walker, T. M., Walker, A. S., Wilson, D. J., Peto, T. E., et al. (2019). Application of machine learning techniques to tuberculosis drug resistance analysis. *Bioinformatics* 35, 2276–2282. doi: 10.1093/bioinformatics/bty949

Manson, A. L., Cohen, K. A., Abeel, T., Desjardins, C. A., Armstrong, D. T., Barry, C. E. III, et al. (2017). Genomic analysis of globally diverse *Mycobacterium tuberculosis* strains provides insights into the emergence and spread of multidrug resistance. *Nat. Genet*. 49:395. doi: 10.1038/ng.3767

Periwal, V., Rajappan, J. K., Jaleel, A. U., and Scaria, V. (2011). Predictive models for anti-tubercular molecules using machine learning on high-throughput biological screening datasets. *BMC Res. Notes* 4:504. doi: 10.1186/1756-0500-4-504

Schleusener, V., Köser, C. U., Beckert, P., Niemann, S., and Feuerriegel, S. (2017). *Mycobacterium tuberculosis* resistance prediction and lineage classification from genome sequencing: comparison of automated analysis tools. *Sci. Rep*. 7:46327. doi: 10.1038/srep46327

Sechidis, K., Tsoumakas, G., and Vlahavas, I. (2011). "On the stratification of multi-label data," in *Joint European Conference on Machine Learning and Knowledge Discovery in Databases* (Berlin; Heidelberg: Springer), 145–158. doi: 10.1007/978-3-642-23808-6_10

Van Rie, A., Warren, R., Mshanga, I., Jordaan, A. M., van der Spuy, G. D., et al. (2001). Analysis for a limited number of gene codons can predict drug resistance of *Mycobacterium tuberculosis* in a high-incidence community. *J. Clin. Microbiol*. 39, 636–641. doi: 10.1128/JCM.39.2.636-641.2001

Walker, T. M., Kohl, T. A., Omar, S. V., Hedge, J., Elias, C. D. O., Bradley, P., et al. (2015). Whole-genome sequencing for prediction of *Mycobacterium*

tuberculosis drug susceptibility and resistance: a retrospective cohort study. *Lancet Infect. Dis*. 15, 1193–1202. doi: 10.1016/S1473-3099(15)00062-6

World Health Organization (2017). *Who Meeting Report of a Technical Expert Consultation: Non-Inferiority Analysis of Xpert MTB/RIF*.

Yang, Y., Niehaus, K. E., Walker, T. M., Iqbal, Z., Walker, A. S., Wilson, D. J., et al. (2018). Machine learning for classifying tuberculosis drug-resistance from dna sequencing data. *Bioinformatics* 34, 1666–1671. doi: 10.1093/bioinformatics/btx801

Zhang, H., Li, D., Zhao, L., Fleming, J., Lin, N., Wang, T., et al. (2013). Genome sequencing of 161 *Mycobacterium tuberculosis* isolates from china identifies genes and intergenic regions associated with drug resistance. *Nat. Genet*. 45, 1255–1260. doi: 10.1038/ng.2735

Conflict of Interest: The authors declare that the research was conducted in the absence of any commercial or financial relationships that could be construed as a potential conflict of interest.

frontiers in Microbiology

ORIGINAL RESEARCH
published: 08 May 2020
doi: 10.3389/fmicb.2020.00781

Detecting Ethambutol Resistance in *Mycobacterium tuberculosis* Isolates in China: A Comparison Between Phenotypic Drug Susceptibility Testing Methods and DNA Sequencing of *embAB*

Ma-chao Li[1†], Rong Chen[1,2†], Shi-qiang Lin[3†], Yao Lu[1,4], Hai-can Liu[1], Gui-lian Li[1], Zhi-guang Liu[1], Xiu-qin Zhao[1], Li-li Zhao[1] and Kang-Lin Wan[1]**

[1] State Key Laboratory for Infectious Disease Prevention and Control, Collaborative Innovation Center for Diagnosis and Treatment of Infectious Diseases, National Institute for Communicable Disease Control and Prevention, Chinese Center for Disease Control and Prevention, Beijing, China, [2] Pathogenic Biology Institute, University of South China, Hengyang, China, [3] Department of Bioinformatics, College of Life Sciences, Fujian Agriculture and Forestry University, Fuzhou, China, [4] School of Laboratory Medicine and Life Sciences, Wenzhou Medical University, Wenzhou, China

With the increasing incidence of drug-resistant tuberculosis (DR-TB), determining a rapid and accurate drug susceptibility testing (DST) method to identify ethambutol (EMB) resistance in *Mycobacterium tuberculosis* has become essential for patient management in China. Herein, we evaluated the correlation between three phenotypic DST methods, namely, proportion method (PM), MGIT 960 system, and microplate alamar Blue assay (MABA), and DNA sequencing of *embAB* in 118 *M. tuberculosis* isolates from China. When the results of the phenotypic DST methods were compared with those of DNA sequencing, the overall agreement and kappa values of the PM, MGIT 960 system, and MABA were 81.4% and 0.61, 77.1% and 0.55, and 84.7% and 0.67, respectively. The agreement for EMB resistance between MABA and PM was significantly higher than that between the MGIT 960 system and PM (P = 0.02). Moreover, among the isolates with detectable *embAB* mutations, 97.2% (70/72 isolates) harbored mutations in *embB*. The analysis of *embB* mutations predicted EMB resistance with 81.3% sensitivity, 86.8% specificity, and 83.1% accuracy. Thus, MABA may be a better phenotypic DST method for detecting EMB resistance. DNA sequencing of *embB* may be useful for the early identification of EMB resistance and the consequent optimization of the treatment regimen.

Keywords: *Mycobacterium tuberculosis*, ethambutol resistance, phenotypic drug susceptibility testing, DNA sequencing, microplate alamarBlue assay

OPEN ACCESS

Edited by:
Jesica Mazza-Stalder, CHU de Lausanne (CHUV), Switzerland

Reviewed by:
Divakar Sharma, Indian Institute of Technology Delhi, India
Shibali Das, Washington University School of Medicine in St. Louis, United States

***Correspondence:**
Li-li Zhao
zhaolili@icdc.cn
Kang-Lin Wan
wankanglin@icdc.cn

[†] These authors have contributed equally to this work

Specialty section:
This article was submitted to Antimicrobials, Resistance and Chemotherapy, a section of the journal Frontiers in Microbiology

Received: *12 December 2019*
Accepted: *01 April 2020*
Published: *08 May 2020*

Citation:
Li M, Chen R, Lin S, Lu Y, Liu H, Li G, Liu Z, Zhao X, Zhao L and Wan K-L (2020) Detecting Ethambutol Resistance in Mycobacterium tuberculosis Isolates in China: A Comparison Between Phenotypic Drug Susceptibility Testing Methods and DNA Sequencing of embAB. Front. Microbiol. 11:781. doi: 10.3389/fmicb.2020.00781

INTRODUCTION

Despite a decreasing trend in the incidence of tuberculosis (TB) in recent years, TB remains a major public health threat in China; in 2018, the World Health Organization (WHO) estimated 900,000 new cases and 37,000 deaths (World Health Organization [WHO], 2018). According to the latest national baseline survey, 5.7% of new cases and 26.5% of previously treated cases are drug-resistant TB (DR-TB) (Zhao et al., 2012). DR-TB, particularly multidrug-resistant TB (MDR-TB), generally requires lengthy, more costly, and more toxic treatment regimens, which are associated with higher risks of treatment failure and disease relapse. Rapid and accurate detection of drug resistance is thus crucial for timely optimizing treatment regimens and reducing treatment failure to prevent the transmission of DR-TB and the development of MDR-TB.

Ethambutol (EMB) is an essential first-line anti-TB drug that is routinely recommended in combination with other drugs for treating TB and DR-TB. It also serves as a key drug in second-line regimens for MDR-TB when drug susceptibility testing (DST) results are available. EMB acts against bacterium through inhibiting membrane-associated arabinosyl transferases, encoded by the *embCAB* operon (*embC*, *embA*, and *embB*) (Telenti et al., 1997; Safi et al., 2013), which are necessary for biosynthesis of arabinogalactan in the cell wall. Previous studies showed that the majority of EMB-resistant isolates carry mutations within *embB*, primarily at codon 306 (*embB*306) (Zhang et al., 2013; Brossier et al., 2015), suggesting that the mutations might be used as promising diagnostic markers for the rapid detection of EMB resistance. Furthermore, certain mutations within the upstream region (UR) of *embA* are associated with EMB resistance (Cui et al., 2014; Brossier et al., 2015; Zhao et al., 2015). However, the presence of these mutations in *embAB* was also observed in EMB-susceptible isolates (Shi et al., 2011; Zhao et al., 2015; Li et al., 2016; Sun et al., 2018). Besides, there are no mutations within the particular genes responsible for EMB resistance in some EMB-resistant isolates, implying the involvement of other resistance mechanisms (Sharma and Bisht, 2017; Sharma et al., 2018). As per the literature, significant discordance exists between the phenotypic and genotypic methods for EMB susceptibility testing (Kim, 2005; Garrigo et al., 2007; Cheng et al., 2014; Zhang et al., 2014). Hence, it is necessary to evaluate concordance across phenotypic and genotypic methods for EMB resistance testing. In the present study, we compared the correlation between three phenotypic EMB susceptibility testing methods and DNA sequencing of *embAB* mutations in 118 *Mycobacterium tuberculosis* (*M. tuberculosis*) isolates from China.

MATERIALS AND METHODS

M. tuberculosis Isolates and DST

In total, 118 *M. tuberculosis* isolates collected from 118 unrelated patients with pulmonary TB were contained in this study. DST of TB isolates to antitubercular drugs isoniazid (INH), rifampin (RIF), streptomycin (SM), and EMB was performed on Lowenstein–Jensen (L-J) proportion method (PM) according to the WHO guideline, with the critical concentrations being 0.2 μg/ml for INH, 40 μg/ml for RIF, 4.0 μg/ml for SM, and 2.0 μg/ml for EMB (World Health Organization [WHO], 2009). EMB susceptibility testing was also performed with all isolates using the MGIT 960 system and microplate alamarBlue assay (MABA). The MGIT 960 system was carried out according to the manufacturer's instructions, with the critical concentration of 5.0 μg/ml (Garrigo et al., 2007). MABA was performed as previously described (Leonard et al., 2008). Briefly, the isolate in the log phase was adjusted with saline to McFarland standard 1 and diluted 1:25 in 7H9 broth containing 10% OADC (BD, Franklin Lakes, NJ, United States). Then, 100 μl bacterial suspension was used to inoculate each well of the 96-well plate. EMB was serially diluted twofold in 100 μl 7H9 broth, and the final concentrations were 32, 16, 8, 4, 2, 1, and 0.5 μg/ml. The final volume of each well was 200 μl, containing 100 μl of EMB solution and 100 μl of bacterial suspension. Furthermore, EMB-free (inoculum-only) controls were used to determine the addition time for alamarBlue. Plates were sealed and incubated at 37°C for 1 week. The indicator (25 μl alamarBlue mixed with 25 μl 10% Tween-80) was added to the EMB-containing group when the drug-free control showed a color change (blue to pink). The minimum inhibitory concentration (MIC) value was defined as the lowest EMB concentration that inhibited bacterial growth and prevented a color change. The breakpoint MIC for EMB was taken as 4 μg/ml (Leonard et al., 2008).

DNA Amplification and Sequencing

The hot regions conferring EMB resistance, including *embA* UR (145 bp upstream to codon 164) and *embB* (codons 159–518), of all isolates were amplified using the following primers: *emb*-S1, AACCTAGGAACGGTGACT, and *emb*-A1, CAACCTGTGGCTTCTTCT; *emb*-S2, AACT TCGTCGGGCTCAAG, and *emb*-A2, TAACGCAGGTTC TCGGTATA (Sun et al., 2018). The PCR program included an initial denaturation at 94°C for 5 min, followed by 30 cycles of denaturation at 94°C for 40 s, annealing at 58°C for 40 s, and extension at 72°C for 1 min and a final extension at 72°C for 5 min. All amplified products were then sequenced. The sequence data were aligned to the H37Rv reference genome (GenBank accession number NC_000962) using BioEdit 7.05.3.

Data Analysis

Data were analyzed with SPSS 16.0 statistical software (SPSS Inc., Chicago, IL, United States). Statistical analysis was performed using the chi-square test or Fisher's exact test as appropriate, and probability levels < 0.05 were considered as statistically significant. Agreement between different testing results was evaluated with the kappa statistic. The kappa values of < 0.2, 0.2–0.4, 0.41–0.6, 0.61–0.8, and 0.81–1.0 indicated poor agreement, fair agreement, moderate agreement, good agreement, and excellent agreement, respectively (Altman, 1999).

RESULTS

Based on DST by PM, 105, 99, 69, and 72 isolates were resistant to INH, RIF, SM, and EMB, respectively. Overall, 92 isolates were MDR, and 47 isolates were resistant to all four first-line drugs. Eight isolates were poly-drug resistant while five isolates were sensitive to all four drugs.

Of the 118 isolates, 72, 55, and 80 were identified to be EMB resistant by the PM, MGIT 960 system, and MABA, respectively (**Table 1**). For the 72 isolates determined as being EMB resistant by the PM, 61 (84.7%, 61/72 isolates) harbored at least one mutation within *embAB*. By contrast, 11 (23.9%) of 46 phenotypically susceptible isolates harbored *embAB* mutations. Further, 50 (90.1%) of the 55 isolates identified to be EMB resistant by the MGIT 960 system showed *embAB* mutations, with the mutations also occurring in 22 of 63 (34.9%) EMB-susceptible isolates. Finally, 67 (83.8%) of the 80 isolates determined to be EMB resistant by MABA carried *embAB* mutations; five (13.2%) of 38 EMB-susceptible isolates also showed *embAB* mutations. When results of the three phenotypic DST methods were compared with those of DNA sequencing results, the overall agreement and kappa values were 81.4% and 0.61, 77.1% and 0.55, and 84.7% and 0.67 for the PM, MGIT 960 system, and MABA, respectively. **Table 1** summarizes the results of MABA in comparison with those of the PM and MGIT 960 system. The concordance rate for EMB resistance between MABA and PM was significantly higher than that between MGIT 960 and PM (P = 0.02), with overall agreement/kappa values of 89.8%/0.78 and 78.8%/0.59, respectively.

All isolates displaying discordant results between the MGIT 960 system/PM and MABA were further analyzed (**Table 2**). Twenty-five isolates were determined to be susceptible by the MGIT 960 system but resistant by MABA, including 17 isolates (68.0%, 17/25 isolates) with *embAB* mutations. Of them, 18 (72.0%, 18/25 isolates) had MICs of 4 μg/ml, four (16.0%, 4/25 isolates) had MICs of 8 μg/ml, and three (12.0%, 3/25 isolates) had MICs of 16 μg/ml. In addition, two isolates without *embAB* mutations were determined to be resistant by PM but susceptible by MABA, and they had MICs of 1 μg/ml. In contrast, 10 isolates, including six isolates (60.0%, 6/10 isolates) harboring *embAB* mutations, were identified to be susceptible by PM but resistant by MABA; of them, seven isolates (70.0%, 7/10 isolates) had MICs of 4 μg/ml, and three isolates (30.0%, 3/10 isolates) had MICs of 16 μ g/ml.

Of the isolates with detectable *embAB* mutations, 97.2% (70/72 isolates) had mutations within *embB* (**Table 3**). All *embB* mutations existed within codons 306–497. An amino acid replacement at codon 306 was the most frequent and occurred in 58 isolates (82.9%, 58/70 isolates). Met306 was noted to be replaced by Val (38 isolates), Ile (15 isolates), and Leu (five isolates). Of all the isolates with the *embB*306 mutation, three showed MICs of < 4 μg/ml (0.5, 1.0, and 2.0 μg/ml). The next most prevalent mutated codon was 406. Mutations at this codon were observed in seven isolates, two of which had MICs lower than 4 μg/ml (2 μg/ml). Other mutations were detected at codons 319 (three isolates), 328 (two isolates), 497 (two isolates), and 412 (one isolate). In addition, 14 EMB-resistant isolates displayed nucleotide changes within *embA* UR, including at −43 (two isolates), −16 (five isolates), −12 (three isolates), −11 (three isolates), and −5 bp sites (one isolate). Notably, most mutations within *embA* UR were accompanied by other mutations in *embB*. Only two isolates carried single *embA* UR mutations at −43 and −11 bp, with MICs of 8 μg/ml.

With reference to the results of MABA, the sensitivities, specificities, and accuracies for detection of the EMB resistance via DNA sequencing analysis of the different regions and codons in *embAB* are summarized in **Table 4**. Screening *embB* achieved satisfactory accuracy (83.1%). Inclusion of *embA* increased the assay accuracy to 84.7%. In addition, analyzing the *embB*306 mutations predicted EMB resistance with 68.8% sensitivity, 92.1% specificity, and 76.3% accuracy.

DISCUSSION

In China, phenotypic DST based on L-J solid media and the liquid culture system MGIT 960 is routinely performed with all *M. tuberculosis* isolates. The presence of *embAB* mutations, particularly *embB*306, which are believed to be the major cause of EMB resistance in *M. tuberculosis*, has also been reported in EMB-susceptible isolates (Plinke et al., 2009; Zhao et al., 2015; Li et al., 2016; Sun et al., 2018). Because these routine phenotypic DST methods are notoriously problematic (Garrigo et al., 2007; Cheng et al., 2014; Zhang et al., 2014), presumably inaccurate results may be the major cause for the detection of "EMB-susceptible" isolates harboring *embAB* mutations (Plinke et al., 2009; Campbell et al., 2011). Identifying false susceptibility to EMB is of considerable importance for the successful treatment of DR-TB, especially MDR-TB, as treatment regimens for these patients should include any active first-line drug for improved outcomes. Thus, there is increasing emphasis on developing a reliable method to detect EMB resistance.

In this study, we found that in comparison with DNA sequencing, the overall agreement values for the PM, MGIT 960 system, and MABA were 81.4, 77.1, and 84.7%, respectively. The kappa values were 0.61 (good agreement), 0.55 (moderate agreement), and 0.67 (good agreement) for these three phenotypic DST methods. As evident, EMB resistance determined by MABA showed the best correlation with DNA sequencing results. We also examined concordance across all three phenotype DST methods by calculating the kappa coefficients. There was a good agreement for EMB between PM and MABA (κ, 0.78). Although PM is the gold standard recommended by the WHO and the current standard method used in China for EMB susceptibility testing of *M. tuberculosis* isolates, it requires at least 28 days before results can be obtained. As a rapid phenotypic DST based on liquid media, MABA can reduce the turnaround time to less than 14 days, which makes it a better choice for identifying EMB resistance.

Twenty-seven isolates exhibited discordant results between the PM/MGIT 960 system and MABA. Of them, 18 isolates

TABLE 1 | Agreement between phenotype DST and DNA sequencing.

DST method results	No. of isolates with sequencing results				No. of isolates with MABA results			
	M	NM	Agreement (%)	Kappa value	R	S	Agreement (%)	Kappa value
PM								
R	61	11	81.4	0.61	70	2	89.8	0.78
S	11	35			10	36		
MGIT 960 system								
R	50	5	77.1	0.55	55	0	78.8	0.59
S	22	41			25	38		
MABA								
R	67	13	84.7	0.67	/	/	/	/
S	5	33			/	/		

Abbreviations: M, mutation; NM, no mutation; R, resistant; S, susceptible.

TABLE 2 | Analysis of isolates with discordant results between the PM/MGIT 960 system and MABA.

Resistance patterns obtained during DST with			Sequencing results	No. of isolates
PM	**MGIT 960 system**	**MABA (MICs μg/ml)**		
R	S	S (1.0)	NM	2
S	S	R (4.0)	NM	2
S	S	R (4.0)	M	5
R	S	R (4.0)	M	10
R	S	R (4.0)	NM	1
R	S	R (8.0)	NM	3
R	S	R (8.0)	M	1
S	S	R (16.0)	NM	2
S	S	R (16.0)	M	1

Abbreviations: R, resistant; S, susceptible; M, mutation; NM, no mutation.

(66.7%) had MICs of 4.0 μg/ml, which was the breakpoint MIC definition of EMB resistance. Furthermore, there were four (14.8%) isolates with MICs of 8.0 μg/ml, which is close to the breakpoint MIC. EMB is a slow-acting anti-TB drug, and culture-based methods can be problematic because of the bacteriostatic nature of EMB. The storage conditions of the drug and the type of medium used also influence the drug activity (Piersimoni et al., 2006). The MIC range of EMB-susceptible and EMB-resistant strains was relatively narrow (Madison et al., 2002; Cheng et al., 2014), and the critical breakpoints of different phenotypic DST methods were different (Madison et al., 2002; Banu et al., 2014; Cheng et al., 2014). Additionally, the presence of microcolonies on solid media and the proximity of EMB MICs of clinical isolates near the critical concentration could make determination of resistance difficult (Parsons et al., 2004; Plinke et al., 2009). Significant discrepancies were encountered when comparing the results obtained in different phenotypic DST methods (Plinke et al., 2009; Cheng et al., 2014; Ahmad et al., 2016). Hence, there were reports suggesting that molecular tests for detecting EMB resistance warranted accurate EMB susceptibility results (Lacoma et al., 2015; Ahmad et al., 2016).

With reference to results of MABA, 67 (83.8%) of 80 EMB-resistant isolates contained at least one mutation in *embAB*. This result validated that *embAB* mutations are associated with EMB resistance (Brossier et al., 2015; Zhao et al., 2015). The majority of *embAB* mutations were concentrated in *embB*. Of them, *embB*306 was the most frequent and was detected in 68.8% (55/80 isolates) isolates. The *embB*306 mutation was also detected in EMB-susceptible isolates. However, the mutation frequency in EMB-resistant isolates 68.8% (55/80 isolates) was significantly higher than that in EMB-susceptible isolates (7.9%, 3/38 isolates). A previous study indicated these mutations were likely to be important, in that they represent the first step toward acquiring EMB resistance (Safi et al., 2013), indicating the need to gain insight into the molecular basis of EMB resistance. It is also desirable to have a better understanding of treatment outcomes and treatment failure in patients infected with strains carrying *embB* mutations. Despite the fact that 14 EMB-resistant isolates harbored *embA* mutations in this study, 12 had additional mutations in *embB*. These multiple mutations were shown to be correlated with high-level EMB resistance (Sun et al., 2018).

Although 83.8% EMB-resistant isolates were identified with DNA sequencing of *embAB*, the inclusion of *embA* in molecular diagnoses only marginally increased the testing sensitivity by 2.5%. The best strategy at present for molecular diagnostics is selective targeting of *embB* (81.3% sensitivity, 86.8% specificity, and 83.1% accuracy). Analyzing the *embB*306 mutation could predict EMB resistance with 68.8% sensitivity, 92.1% specificity, and 76.3% accuracy. Thus, the effects of this mutation on detecting EMB resistance were relatively limited.

There were still some EMB-resistant isolates determined by phenotypic DST methods (PM, MGIT, and MABA), which lacked *embAB* mutations. This implied that these strains probably harbored mutations outside *embAB* (Safi et al., 2013; He et al., 2015; Tulyaprawat et al., 2019) or that the resistance may have been caused by other mechanisms, such as overexpressed efflux pumps and loss of porins (Sharma and Bisht, 2017; Sharma et al., 2018). Careful interpretation of a negative DNA sequencing result (no mutation) is thus necessary in the accurate management of suspected DR-TB.

TABLE 3 | Mutations in *embCAB* among 118 *M. tuberculosis* isolates.

Mutations		No. of isolates						
embA UR	***embB***	MICs (μ g/ml)						
		≤0.5	**1.0**	**2.0**	**4.0**	**8.0**	**16.0**	**≥32.0**
G(-43)C		0	0	0	0	1	0	0
C(-11)T		0	0	0	0	1	0	0
C(-16)G	Met306Ile	0	0	0	0	0	1	0
C(-16)T	Met306Ile	0	0	0	0	1	0	1
C(-16)A	Met306Ile	0	0	0	0	1	0	0
	Met306Ile/Gly406Asp	0	0	0	0	0	1	0
	Met306Ile/Gly406Ser	0	0	0	0	1	0	0
	Met306Ile	1	0	0	4	2	2	0
G(-5)A	Met306Leu	0	0	0	0	1	0	0
	Met306Leu	0	1	0	0	1	2	0
G(-43)C	Met306Val	0	0	0	0	0	0	1
C(-16)G	Met306Val	0	0	0	0	0	1	0
C(-12)T	Met306Val	0	0	0	0	1	0	1
C(-11)A	Met306Val	0	0	0	0	0	0	2
	Met306Val/Gln497His	0	0	0	0	0	0	1
	Met306Val	0	0	1	6	18	3	3
	Tyr319Cys	0	0	0	0	2	1	0
	Asp328Tyr	0	0	0	1	0	1	0
C(-12)T	Gly406Ala	0	0	0	0	0	0	1
	Gly406Ala	0	0	0	0	1	1	0
	Gly406Asp	0	0	2	0	0	0	0
	Ser412Pro	0	0	0	0	0	0	1
	Gln497Arg	0	0	0	0	0	1	0
NM	NM	20	8	5	8	3	1	1

Abbreviation: NM, no mutation.

TABLE 4 | Summary of DNA sequencing of *embAB* and MABA.

Locus or codon	No. of isolates				*P*-value	Sensitivity (%)	Specificity (%)	Accuracy (%)
	Resistant		Susceptible					
	M	**NM**	**M**	**NM**				
embA	14	66	0	38	0.02*	17.5	100.0	44.1
embA(-16)	5	75	0	38	0.28	6.3	100.0	36.4
embB	65	15	5	33	0.00**	81.3	86.8	83.1
emb306	55	25	3	35	0.00**	68.8	92.1	76.3
embAB	67	13	5	33	0.00**	83.8	86.8	84.7

*Abbreviations: M, mutation; NM, no mutation. *P < 0.05 (significant); **P < 0.01 (highly significant).*

This study also contained several limitations. (i) The number of isolates included was relatively limited. Additional research containing more isolates will be required to evaluate the effectiveness of the MABA and DNA sequencing. (ii) DNA sequencing is unable to identify EMB-resistant isolates that do not carry mutations in *embAB*. (iii) The association between *embB*306 mutation and other drug resistance was not evaluated.

CONCLUSION

Our results indicated that MABA is suitable for detecting EMB resistance, showing good concordance with traditional PM methods and *embAB* mutations. DNA sequencing to screen *embB* may be useful for the rapid identification of EMB resistance. However, we do not suggest phenotypic DST methods to be replaced with DNA sequencing in China. It may be used as an

initial diagnosis tool for the early identification of EMB resistance and consequently optimizing the treatment regimens.

DATA AVAILABILITY STATEMENT

The raw data supporting the conclusions of this article will be made available by the authors, without undue reservation, to any qualified researcher.

ETHICS STATEMENT

The studies involving human participants were reviewed and approved by the Ethics Committee of National Institute for Communicable Disease Control and Prevention, Chinese Center for Disease Control and Prevention. The patients/participants provided their written informed consent to participate in this study.

AUTHOR CONTRIBUTIONS

LZ and K-LW conceived and designed the study. LZ, ML, HL, and SL analyzed the data. ML, RC, YL, GL, ZL, and XZ performed the laboratory experiments. ML, RC, YL, and HL contributed to the data collection and analysis. LZ, K-LW, and SL wrote the manuscript. All authors read and approved the final manuscript.

FUNDING

This study was supported by the projects from National Key Program of Mega Infectious Diseases (Grant No. 2018ZX10302302) and National Basic Research Program of China (973 Program, Grant No. 2015CB554202). The funder had no role in the study design, data collection and analysis, decision to publish, or manuscript preparation.

REFERENCES

Ahmad, S., Mokaddas, E., Al-Mutairi, N., Eldeen, H. S., and Mohammadi, S. (2016). Discordance across phenotypic and molecular methods for drug susceptibility testing of drug-resistant *Mycobacterium tuberculosis* isolates in a low TB incidence country. *PLoS One* 11:e0153563. doi: 10.1371/journal.pone.0153563

Altman, D. G. (1999). "Inter-rater agreement," in *Practical Statistics for Medical Research*, ed. D. G. Altman (London: Chapman & Hall), 403–409.

Banu, S., Rahman, S. M., Khan, M. S., Ferdous, S. S., Ahmed, S., Gratz, J., et al. (2014). Discordance across several methods for drug susceptibility testing of drug-resistant *Mycobacterium tuberculosis* isolates in a single laboratory. *J. Clin. Microbiol.* 52, 156–163. doi: 10.1128/JCM.02378-13

Brossier, F., Sougakoff, W., Bernard, C., Petrou, M., Adeyema, K., Pham, A., et al. (2015). Molecular analysis of the embCAB locus and embR gene involved in ethambutol resistance in clinical isolates of *Mycobacterium tuberculosis* in France. *Antimicrob. Agents Chemother.* 59, 4800–4808. doi: 10.1128/AAC.00150-15

Campbell, P. J., Morlock, G. P., Sikes, R. D., Dalton, T. L., Metchock, B., Starks, A. M., et al. (2011). Molecular detection of mutations associated with first- and second-line drug resistance compared with conventional drug susceptibility testing of *Mycobacterium tuberculosis*. *Antimicrob. Agents Chemother.* 55, 2032–2041. doi: 10.1128/AAC.01550-10

Cheng, S., Cui, Z., Li, Y., and Hu, Z. (2014). Diagnostic accuracy of a molecular drug susceptibility testing method for the antituberculosis drug ethambutol: a systematic review and meta-analysis. *J. Clin. Microbiol.* 52, 2913–2924.

Cui, Z., Li, Y., Cheng, S., Yang, H., Lu, J., Hu, Z., et al. (2014). Mutations in the embC-embA intergenic region contribute to *Mycobacterium tuberculosis* resistance to ethambutol. *Antimicrob. Agents Chemother.* 58, 6837–6843. doi: 10.1128/AAC.03285-14

Garrigo, M., Aragon, L. M., Alcaide, F., Borrell, S., Cardeñosa, E., Galán, J. J., et al. (2007). Multicenter laboratory evaluation of the MB/BacT Mycobacterium detection system and the BACTEC MGIT 960 system in comparison with the BACTEC 460TB system for susceptibility testing of *Mycobacterium tuberculosis*. *J. Clin. Microbiol.* 45, 1766–1770.

He, L., Wang, X., Cui, P., Jin, J., Chen, J., Zhang, W., et al. (2015). ubiA (Rv3806c) encoding DPPR synthase involved in cell wall synthesis is associated with ethambutol resistance in *Mycobacterium tuberculosis*. *Tuberculosis* 95, 149–154. doi: 10.1016/j.tube.2014.12.002

Kim, S. J. (2005). Drug-susceptibility testing in tuberculosis: methods and reliability of results. *Eur. Respir. J.* 25, 564–569.

Lacoma, A., Molina-Moya, B., Prat, C., Pimkina, E., Diaz, J., Dudnyk, A., et al. (2015). Pyrosequencing for rapid detection of *Mycobacterium tuberculosis* second-line drugs and ethambutol resistance. *Diagn. Microbiol. Infect. Dis.* 83, 263–269. doi: 10.1016/j.diagmicrobio.2015.07.004

Leonard, B., Coronel, J., Siedner, M., Grandjean, L., Caviedes, L., Navarro, P., et al. (2008). Inter- and intra-assay reproducibility of microplate Alamar blue assay results for isoniazid, rifampicin, ethambutol, streptomycin, ciprofloxacin, and capreomycin drug susceptibility testing of *Mycobacterium tuberculosis*. *J. Clin. Microbiol.* 46, 3526–3529. doi: 10.1128/JCM.02083-07

Li, Y., Wang, Y., Zhang, Z., Gao, H., Wang, H., Cao, J., et al. (2016). Association between embB Codon 306 mutations, phenotypic resistance profiles, and genotypic characterization in clinical *Mycobacterium tuberculosis* Isolates from Hebei, China. *Antimicrob. Agents Chemother.* 60, 7295–7302.

Madison, B., Robinson-Dunn, B., George, I., Gross, W., Lipman, H., Metchock, B., et al. (2002). Multicenter evaluation of ethambutol susceptibility testing of *Mycobacterium tuberculosis* by agar proportion and radiometric methods. *J. Clin. Microbiol.* 40, 3976–3979.

Parsons, L. M., Somoskovi, A., Urbanczik, R., and Salfinger, M. (2004). Laboratory diagnostic aspects of drug resistant tuberculosis. *Front. Biosci.* 9:2086–2105. doi: 10.2741/1290

Piersimoni, C., Olivieri, A., Benacchio, L., and Scarparo, C. (2006). Current perspectives on drug susceptibility testing of *Mycobacterium tuberculosis* complex: the automated nonradiometric systems. *J. Clin. Microbiol.* 44, 20–28.

Plinke, C., Cox, H. S., Kalon, S., Doshetov, D., Rüsch-Gerdes, S., Niemann, S., et al. (2009). Tuberculosis ethambutol resistance: concordance between phenotypic and genotypic test results. *Tuberculosis* 89, 448–452.

Safi, H., Lingaraju, S., Amin, A., Kim, S., Jones, M., Holmes, M., et al. (2013). Evolution of high-level ethambutol-resistant tuberculosis through interacting mutations in decaprenylphosphoryl-beta-D-arabinose biosynthetic and utilization pathway genes. *Nat. Genet.* 45, 1190–1197. doi: 10.1038/ng.2743

Sharma, D., and Bisht, D. (2017). *M. tuberculosis* hypothetical proteins and proteins of unknown function: hope for exploring novel resistance mechanisms as well as future target of drug resistance. *Front. Microbiol.* 8:465. doi: 10.3389/fmicb.2017.00465

Sharma, D., Bisht, D., and Khan, A. U. (2018). Potential alternative strategy against drug resistant tuberculosis: a proteomics prospect. *Proteomes* 6:26. doi: 10.3390/proteomes6020026

Shi, D., Li, L., Zhao, Y., Jia, Q., Li, H., Coulter, C., et al. (2011). Characteristics of embB mutations in multidrug-resistant *Mycobacterium tuberculosis* isolates in Henan. China. *J. Antimicrob. Chemother.* 66, 2240–2247. doi: 10.1093/jac/dkr284

Sun, Q., Xiao, T. Y., Liu, H. C., Zhao, X. Q., Liu, Z. G., Li, Y. N., et al. (2018). Mutations within embCAB are associated with variable level of ethambutol

resistance in *Mycobacterium tuberculosis* Isolates from China. *Antimicrob. Agents Chemother.* 62, e1279-17. doi: 10.1128/AAC.01279-17

Telenti, A., Philipp, W. J., Sreevatsan, S., Bernasconi, C., Stockbauer, K. E., Wieles, B., et al. (1997). The emb operon, a gene cluster of *Mycobacterium tuberculosis* involved in resistance to ethambutol. *Nat. Med.* 3, 567–570.

Tulyaprawat, O., Chaiprasert, A., Chongtrakool, P., Suwannakarn, K., and Ngamskulrungroj, P. (2019). Association of ubiA mutations and high-level of ethambutol resistance among *Mycobacterium tuberculosis* Thai clinical isolates. *Tuberculosis* 114, 42–46. doi: 10.1016/j.tube.2018.11.006

World Health Organization [WHO] (2009). *Guidelines for Surveillance of Drug Resistance in Tuberculosis*, 4th Edn. Geneva: World Health Organization.

World Health Organization [WHO] (2018). *Global Tuberculosis Report 2018*. Geneva: WHO.

Zhang, H., Li, D., Zhao, L., Fleming, J., Lin, N., Wang, T., et al. (2013). Genome sequencing of 161 *Mycobacterium tuberculosis* isolates from China identifies genes and intergenic regions associated with drug resistance. *Nat. Genet.* 45, 1255–1260. doi: 10.1038/ng.2735

Zhang, Z., Wang, Y., Pang, Y., and Kam, K. M. (2014). Ethambutol resistance as determined by broth dilution method correlates better than sequencing results with embB mutations in multidrug-resistant *Mycobacterium tuberculosis* isolates. *J. Clin. Microbiol,*. 52, 638–641. doi: 10.1128/JCM.02713-13

Zhao, L. L., Sun, Q., Liu, H. C., Wu, X. C., Xiao, T. Y., Zhao, X. Q., et al. (2015). Analysis of embCAB mutations associated with ethambutol resistance in multidrug-resistant *Mycobacterium tuberculosis* isolates from China. *Antimicrob. Agents Chemother.* 59, 2045–2050. doi: 10.1128/AAC.04933-14

Zhao, Y., Xu, S., Wang, L., Chin, D. P., Wang, S., Jiang, G., et al. (2012). National survey of drug-resistant tuberculosis in China. *N. Engl. J. Med.* 366, 2161–2170. doi: 10.1056/NEJMoa1108789

Conflict of Interest: The authors declare that the research was conducted in the absence of any commercial or financial relationships that could be construed as a potential conflict of interest.

frontiers in Medicine

ORIGINAL RESEARCH
published: 19 May 2020
doi: 10.3389/fmed.2020.00161

Whole Genome Sequencing and Spatial Analysis Identifies Recent Tuberculosis Transmission Hotspots in Ghana

Prince Asare[1,2,3]*, *Isaac Darko Otchere*[1], *Edmund Bedeley*[1], *Daniela Brites*[4,5], *Chloé Loiseau*[4,5], *Nyonuku Akosua Baddoo*[6], *Adwoa Asante-Poku*[1], *Stephen Osei-Wusu*[1], *Diana Ahu Prah*[1], *Sonia Borrell*[4,5], *Miriam Reinhard*[4,5], *Audrey Forson*[6], *Kwadwo Ansah Koram*[1], *Sebastien Gagneux*[4,5] and *Dorothy Yeboah-Manu*[1,2]*

[1] Noguchi Memorial Institute for Medical Research, College of Health Sciences, University of Ghana, Accra, Ghana, [2] West African Centre for Cell Biology of Infectious Pathogens, University of Ghana, Accra, Ghana, [3] Department of Biochemistry, Cell and Molecular Biology, University of Ghana, Accra, Ghana, [4] Department of Medical Parasitology and Infection Biology, Swiss Tropical and Public Health Institute, Basel, Switzerland, [5] University of Basel, Basel, Switzerland, [6] Department of Chest Diseases, Korle-Bu Teaching Hospital, Korle-Bu, Accra, Ghana

OPEN ACCESS

Edited by:
Jesica Mazza-Stalder, CHU de Lausanne (CHUV), Switzerland

Reviewed by:
Nitya Singh, University of Florida, United States
Loïc Deblais, The Ohio State University, United States

***Correspondence:**
Prince Asare
pasare@noguchi.ug.edu.gh
Dorothy Yeboah-Manu
dyeboah-manu@noguchi.ug.edu.gh

Specialty section:
This article was submitted to Infectious Diseases – Surveillance, Prevention and Treatment, a section of the journal Frontiers in Medicine

Received: 10 January 2020
Accepted: 09 April 2020
Published: 19 May 2020

Citation:
Asare P, Otchere ID, Bedeley E, Brites D, Loiseau C, Baddoo NA, Asante-Poku A, Osei-Wusu S, Prah DA, Borrell S, Reinhard M, Forson A, Koram KA, Gagneux S and Yeboah-Manu D (2020) Whole Genome Sequencing and Spatial Analysis Identifies Recent Tuberculosis Transmission Hotspots in Ghana. Front. Med. 7:161. doi: 10.3389/fmed.2020.00161

Whole genome sequencing (WGS) is progressively being used to investigate the transmission dynamics of *Mycobacterium tuberculosis* complex (MTBC). We used WGS analysis to resolve traditional genotype clusters and explored the spatial distribution of confirmed recent transmission clusters. Bacterial genomes from a total of 452 MTBC isolates belonging to large traditional clusters from a population-based study spanning July 2012 and December 2015 were obtained through short read next-generation sequencing using the illumina HiSeq2500 platform. We performed clustering and spatial analysis using specified R packages and ArcGIS. Of the 452 traditional genotype clustered genomes, 314 (69.5%) were confirmed clusters with a median cluster size of 7.5 genomes and an interquartile range of 4–12. Recent tuberculosis (TB) transmission was estimated as 24.7%. We confirmed the wide spread of a Cameroon sub-lineage clone with a cluster size of 78 genomes predominantly from the Ablekuma sub-district of Accra metropolis. More importantly, we identified a recent transmission cluster associated with isoniazid resistance belonging to the Ghana sub-lineage of lineage 4. WGS was useful in detecting unsuspected outbreaks; hence, we recommend its use not only as a research tool but as a surveillance tool to aid in providing the necessary guided steps to track, monitor, and control TB.

Keywords: ***Mycobacterium tuberculosis*, *Mycobacterium africanum*, molecular epidemiology, whole genome sequence, recent transmission, cluster**

INTRODUCTION

Tuberculosis (TB), a contagious disease of antiquity, affects millions of people annually (1). In 1993, the World Health Organization (WHO) declared it a global health emergency, hence calling for more resources and studies for effective control of the disease. In 2017 alone, an estimated 10 million new TB cases with 1.6 million deaths were reported globally, making TB the number one infectious disease killer and one of the top 10 killer diseases (1). TB is caused by a group of

closely related acid-fast bacilli called *Mycobacterium tuberculosis* complex (MTBC). TB in humans is caused mainly by *M. tuberculosis sensu stricto* (MTBss) and *M. africanum* (MAF), which are further divided into seven lineages (L): MTBss subdivided into L1–L4 and L7, and MAF L5 and L6 (2, 3).

The global TB control strategy aims at having a TB-free world by attaining zero deaths, disease, and suffering due to TB (4). One of the activities to achieve this is to investigate the transmission dynamics of the disease to understand risk factors leading to occurrence of the disease within distinct population for design of appropriate preventive interventions. The study of the spread of these TB lineages has been made possible through molecular epidemiology (molepi) studies (5). The traditional molepi tools including IS*6110* DNA fingerprinting, spacer oligonucleotide typing (spoligotyping), and mycobacteria interspersed repetitive-unit–variable-number tandem repeat (MIRU-VNTR) typing have been used extensively in previous studies and found to have varying discriminatory power (6, 7). However, whole genome sequencing (WGS) analysis is considered the ultimate for strain typing and confirmation of strain clusters (7–9).

In a previous population-based study, we used the combined resolution power of MIRU-VNTR typing and spoligotyping (MIRU/Spoligo) for strain differentiation followed with clustering analysis to estimate the extent of recent transmission in Ghana (10). We estimated a high recent transmission rate of 41.2% and found 53.1% of all isolates belonging to one of 276 clusters. Yet, it has been indicated that the combined resolution of spoligotyping and MIRU-VNTR may not be enough to distinguish between very closely related strains resulting from recent transmission (7). Consequently, in this current study, we used a WGS approach to further resolve large MIRU/Spoligo defined TB clusters (referred to as traditional clusters) and explore epidemiological factors including their spatial distribution.

MATERIALS AND METHODS

Study Design and Population

This study involved a retrospective analysis of selected isolates obtained from a population-based study conducted from July 2012 to December 2015 and sampled within two administrative districts in Ghana: Accra Metropolitan Assembly (AMA) and East Mamprusi District (MamE). All isolates were obtained from pulmonary TB cases with informed consent from all participants. Within the population-based prospective study, sputum samples were collected from consecutive clinically diagnosed pulmonary TB patients reporting to 12 selected health facilities within an urban setting (AMA) and a rural setting (MamE). The methods that were used for sputum sampling during the population-based study conformed to WHO guidelines (two sputa per patient). We defined a pulmonary TB case as any individual with a suspected case of TB that was confirmed both clinically and bacteriologically. Detailed demographic and epidemiological data were obtained from consented participants.

Further description of the study locale and participant data are provided elsewhere (5, 10).

Isolate Selection, DNA Extraction, and WGS

The isolate collection for the analysis was a convenient sample of all cases belonging to 40 large clusters (cluster size > 5) comprising 473 isolates from our previous study (10). Every manipulation of live MTBC bacilli was done in the biosafety level 3 facility of the NMIMR. As a recap, a cluster was defined as two or more isolates (same strain) that share an indistinguishable spoligotype and 15 locus MIRU-VNTR allelic pattern, but allowing for one missing allelic data at any one of the *difficult-to-amplify* MIRU loci (VNTR 2,163, 3,690, and 4,156), following which we categorized the size of a cluster using the total number of isolates into categories of small (2 isolates), medium (3–5 isolates), large (6–20 isolates), and very large (>20 isolates). For this current study, only large and very large clusters belonging to the three most dominant MTBC lineages (L4, L5, and L6) in Ghana were considered for analysis. All isolates have been previously characterized including drug susceptibility to isoniazid and rifampicin using standard phenotypic and genotypic techniques (5, 10). DNA extraction was performed using a modified cetyl trimethyl ammonium bromide (CTAB) protocol as previously described (11). The only amendment to our previous extraction protocol was that, to obtain enough intact (non-fragmented) genomic DNA (gDNA), bacteria cells were heat inactivated at 80°C (instead of 95°C) for 30 min in cell lysis buffer. Heat inactivating the bacterial cells at 95°C rather produces a lot of fragmented gDNA, which is not ideal for obtaining a quality sequencing output. Illumina sequencing libraries were prepared using NEBNEXT ULTRA II FS DNA library preparation kit (New England Biolabs) and multiplex paired-end (or in special cases single-end) sequenced at the Genomics Facility of the University of Basel using the illumina HiSeq2500 NGS platform (Illumina, San Diego, CA, United States) with raw read sequence lengths of either 101, 125, or 126 nucleotides (nt). Information on raw sequence data (BioProject ID: PRJNA616081) are provided in **Supplementary Table 1**.

Whole Genome Sequence Analysis and Variance Calling

The raw fastq illumina reads were trimmed of illumina adaptor and low-quality reads using Trimmomatic v 0.33 with a sliding window of 5:20 (12). We dropped all reads with read length <20 nt and employed the mem algorithm in BWA v0.7.13 (13) to align the filtered reads to a reconstructed MTBC ancestral sequence obtained from a previous report (14). The chromosome coordinates and the annotation used was based on the genome of the laboratory reference strain *M. tuberculosis* H37Rv (NC_000962.3). We excluded also duplicated reads after marking with the Mark Duplicate module of Picard v2.9.1 (https://github.com/broadinstitute/picard). Single-nucleotide polymorphisms (SNPs) were called with mpileup implemented in Samtools v1.2 (15) and VarScan v2.4.1 (16). We used a quality threshold score of 20 for both minimum mapping quality and minimum base quality. Sample SNPs were called using the majority allele (SNPs were considered to have reached fixation within an isolate

with a minimum frequency of 90%) in positions supported by at least seven fold coverage; on the other hand, the ancestor state was called when the SNP within-isolate frequency was ≤10%; otherwise, we classified them as indeterminate. We classified a genome as a possible mixed infection or contaminated if it had more than 120 heterogeneous base calls. All SNPs were annotated using snpEff v4.11 (17) with H37Rv reference annotation (NC_000962.3). We excluded genome positions in highly repetitive and variable regions (PE/PPE genes), phages, insertion sequences, and regions with at least 50-bp identities to other regions in the genome (18). After all the filtering steps, we also additionally excluded genomes with average coverage lower than 15×, leaving 452 genomes for subsequent analysis. The mean coverage for all the 452 genomes was 77× with a standard deviation of 27× (**Supplementary Table 1**).

Phylogenetic Analysis

All 452 genomes that passed the filtering steps were used to generate a multifasta alignment file containing only polymorphic sites using customized python scripts. A position was considered polymorphic if at least one genome had an SNP at that position. We excluded genome positions with >10% missing calls. Both the GTR-GAMMA and GTR-CAT models with 1,000 rapid bootstrap inferences followed by a thorough maximum-likelihood search performed in CIPRES (19) were used to infer a maximum likelihood phylogenetic tree using the MPI parallel version of RaxML v8.2.3 (20) on the multi-fasta alignment file. Phylogenetic trees constructed using the GTR-GAMMA model did not produce any substantially different topologies and did not affect clustering analysis compared to the GTR-CAT model; consequently, we resorted to using GTR-CAT since results are produced faster. The best-scoring maximum likelihood topology trees generated were rooted on *M. canettii* as outgroup. Phylogenetic trees were plotted and annotated using the ggtree package (21, 22) and graphics enhanced using ggplot2 (23) all implemented in R version 3.6.0 (24) (http://cran.r-project.org/). We calculated pairwise SNP distances between genomes using the ape package (25) implemented in R version 3.6.0 (24).

Cluster Definition and Analysis

Clustering analysis was based on the assumption that strains with the same DNA fingerprint may be epidemiologically linked and associated with recent TB transmission (26). Only one genome per participant was included in the analysis. Based on proposed SNP thresholds from various studies, three genomic cluster definitions were explored; a cutoff at 5 SNPs (9), 10 SNPs (27), and 12 SNPs (28, 29). Using the multi-fasta file and the cluster package (30) implemented in R version 3.6.0 (24), we set the three thresholds of 5, 10, and 12 and generated separate datasets containing a list of clusters per SNP threshold specified. We performed further downstream analysis on selected clustered cases after sticking to a threshold of 10 SNPs. The size of a cluster was defined using the total number of genomes in the cluster classified into categories of small (2 genomes), medium (3–5 genomes), and large (>5 genomes). The recent TB transmission rate and population size used for clustering analysis was estimated using the $n - 1$ formula described by Glynn et al. (31) (see **Supplementary Data**) (31).

Within-Host Micro-Evolution of Longitudinal Isolates

To help set a threshold for defining genomic cluster, we performed a within-host microevolution analysis using genomes from cases with multiple TB episodes (longitudinal isolates). In addition to the clustered cases, WGS of three randomly selected MTBC isolate pairs obtained from three longitudinal cases were carried out using the protocols described above. Isolates from these three cases were chosen because they belong to the three most dominant lineage/sub-lineages found in Ghana being Cameroon, Ghana, and MAF West African 1. These isolates were investigated for within-host micro-evolution by calculating pairwise SNP distances between each pair of sequence from the same case using MEGA v10.0.5 (32).

Data Management and Analysis

We included in our analysis both genomic and epidemiological data. Analysis that involved statistical inferences was carried out using the Stata statistical package version 14.2 (Stata Corp., College Station, TX, USA). The GIS coordinates of the participants' self-reported district of residence were used to construct a spatial representation of the MTBC isolates using R version 3.6.0 (24) and the ArcMap employed in ArcGIS (Economic and Social Research Institute, version 10.1) (33). The GIS coordinate information was combined with the genomic, epidemiological, and other demographic data to analyze risk factors for clustering.

RESULTS

Characteristics of the Study Population

Out of the 473 isolates, each from a single case, 452 (95.6%) were passed for downstream analysis (**Figure 1**). Of the passed genomes, 71.4% (319/447) and 28.6% (128/447) of the infected participants were from males and females, respectively, with a median age of 35 years (range, 27 to 45 years). Five participants had no record of gender. A large proportion of the participants (73.6%, 315/428) had a sputum-smear microscopy grade of at least 2+.

SNP Threshold Selection and Clustering Analysis

Three longitudinal TB cases were randomly chosen for within-host micro-evolution analysis. The three cases had two isolates each, belonging to the Cameroon (FU080), Ghana (FU049), and MAF West African 1 (FU031) genotypes. All three cases received the same set of anti-TB drugs (isoniazid, rifampicin, ethambutol, and pyrazinamide). Case FU080 was male, 39 years of age, diagnosed with a sputum-smear microscopy grade of 2+, and the follow-up sample was taken at month 5 (153 days) of treatment (**Figure 2**). Case FU049 was female, 33 years of age and diagnosed with a smear grade of 3+ but sputum-smear microscopy grade of scanty 3 at 49 days of follow-up. Case FU031 was male, 51 years of age, and diagnosed with a smear grade of 3+ and had a smear

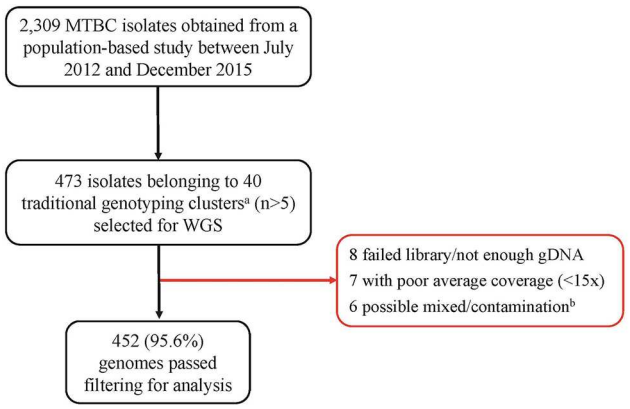

FIGURE 1 | Pipeline for sample selection and whole genome sequencing. MTBC, *Mycobacterium tuberculosis* complex; WGS, Whole genome sequencing. [a]We defined traditional genotyping clusters as previously described clusters identified using mycobacterial interspersed repetitive-unit–variable-number tandem-repeat analysis and spoligotyping tools. [b]Genomes with heterozygous SNPs >120 were classified as possible mixed infection or contamination and hence removed from further analysis.

grade of 1+ at 175 days of follow-up. The SNP distances between each genome pair is shown in **Figure 2**. On average, there were 1.3 (4/3) SNPs accrued in 126 days [(153+49+175)/3]. This implies that, within 3 years, it is possible to accrue approximately 11 SNPs, all things being equal. Consequently, our analysis and inferences were based on a 10 SNP cutoff.

All 452 genomes were broadly grouped into the three main phylogenetic lineages found in Ghana (lineages 4, 5, and 6) (**Figure 3**, **Supplementary Figures 1–3**). The traditional genotype clusters were found to form close to distinct monophyletic clades upon reconstructing the phylogenetic tree using WGS data (**Supplementary Figure 1**). Some monophyletic clades, however, contained more than one large traditional genotype cluster. Whereas, no cluster of L5 was observed (as per genetic distances), we identified three small clusters of L6 and several clusters for L4. We identified 67 clusters with a median cluster size of 7.5 genomes (range, 4 to 12) and total number of clustered genomes being 314 (**Figures 4A,B**). Eight large clusters were observed with the largest cluster consisting of 78 genomes (**Figure 3**, **Figure 4A**). The estimated clustering rate (recent transmission rate) was 24.7% (**Figure 4B**). In addition to the SNP threshold at 10, we explored also SNP thresholds at 5 and 12 (**Supplementary Figures 2**, **3**).

Recent Transmission Hotspots and Characteristics of Large Clusters

A total of 146 genomes constituting eight large clusters (defined as cluster size > 5 in *Materials and methods*) (**Table 1** and **Figures 2**, **5**) were observed from the clustering analysis with 10 SNP threshold. The smallest of these large clusters had a cluster size of seven genomes (whole genome sequence cluster 25; WGSC-25), whereas the largest had 78 genomes (WGSC-5), which formed a quarter of all clustered cases (78/314, 25%). All the large clusters belonged to lineage 4 with Cameroon sub-lineage predominating (WGSC-5, WGSC-13, WGSC-25, and WGSC-42) followed by the Ghana sub-lineage (WGSC-11 and WGSC-28). The two remaining large clusters belonged to the Haarlem (WGSC-6) and LAM (WGSC-49) sub-lineages. Not more than 138 variable SNPs were observed within these large clusters. The median pairwise SNP distance within these large clusters was seven SNPs. Apart from 7 isolates, all remaining 139/146 isolates were sensitive to both isoniazid and rifampicin. Interestingly, 5/7 INH-resistant isolates belonged to the same cluster (WGSC-11) and were from individuals residing in the same sub-district (Ayawaso) (**Figures 5**, **6**). Only two isolates belonging to WGSC-5 were resistant to INH. The ratio of male to female cases infected with the clustered genomes was confirmed to be significantly higher (3:1, 231/81) compared to the general population (2:1) and twice as much among large clusters (4:1, 115/29) ($p < 0.05$). Two participants had no record of gender. Two large clusters (WGSC-25 and WGSC-42) were made up of only males.

All cases belonging to large clusters spanned the entire 3.5-year sampling period and were distributed among 20 districts/sub-districts but generally clustered within Accra metropolis (**Figures 5**, **6**), which is made up of six sub-districts. Most of the large clusters exhibited a geographically clustered distribution even though not exclusive. For example, whereas hotspot for WGSC-11 and WGSC-42 was the Ayawaso sub-district, WGSC-13 and WGSC-5 were found mostly in the Ablekuma sub-district, the main identified hotspot of recent transmission (**Supplementary Figure 4** and **Supplementary Table 2**).

Socio-Demographic Characteristics of Individuals Infected With a Strain From the Largest Cluster (WGSC-5)

This largest transmitting cluster made up of 78 cases exhibited an interesting geographical distribution. Except for two cases from Northern Ghana, all 76/78 cases in this cluster were from Southern Ghana of which 19 were found in Ablekuma (**Figures 5**, **6B** and **Supplementary Figure 4**). The two cases from Northern Ghana shared no SNP difference between them. One case had no record of residential location. There were 59 males and 17 females with a median age of 34 (IQR, 24–43). Two participants had no record of gender. A greater proportion (77.8%, 42/54) of individuals responded living in compound houses at city suburb (66.1%, 37/56) with an average monthly income of not more than 300 Ghanaian cedis (92.8%, 52/56) or 60 USD in its equivalence. The median number of individuals living in a giving household was 12 (IQR, 5–20). On average, there were more unskilled laborers (60.7%, 34/56) than skilled laborers (16.1%, 9/56) with the remaining 23.2% (13/56) being unemployed including students.

DISCUSSION

In this study, our main goal was to use a WGS approach to resolve large traditional genotype clusters (MIRU/Spoligo defined

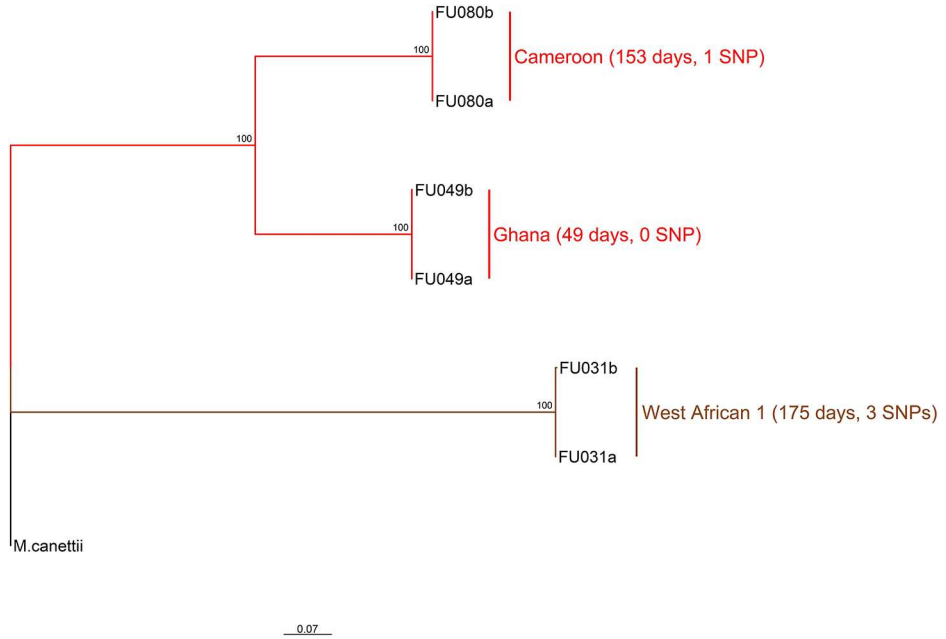

FIGURE 2 | Phylogenetic relationship of six *M. tuberculosis* complex longitudinal isolates obtained from three participants. The two major branches constitute the top two MTBC lineages found in Ghana and color coded as red for lineage 4 and brown for lineage 5. Lineage 4 is further split into the dominant Cameroon and Ghana sub-lineage. The sub-lineages, days between sampling for each participant as well as the number of SNPs observed between sample pairs are annotated on the tree rooted on *M. canettii*. This analysis involved seven nucleotide sequences. All ambiguous positions were removed for each sequence pair (pairwise deletion option). There was a total of 2104 positions in the final dataset. Evolutionary analyses were conducted in MEGA v10.0.5 (32).

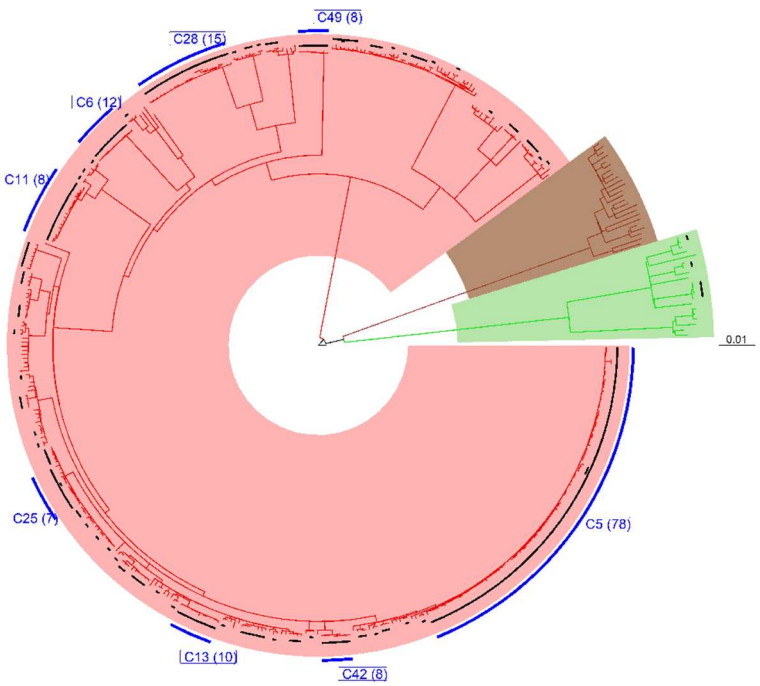

FIGURE 3 | Phylogenetic reconstruction of 452 *M. tuberculosis* complex isolates showing clustering at a threshold of 10 SNPs. The tree was built with an alignment file containing 11,041 variable positions and rooted on *M. canettii*. Black bars plotted on the tips of the branches indicate the clustered cases at the defined threshold of 10 SNPs. Blue bars represent large clusters (cluster size >5) with the number of clustered cases indicated in brackets. The three major branches constitute the three main MTBC lineages found in Ghana and color coded as red for lineage 4, brown for lineage 5, and green for lineage 6.

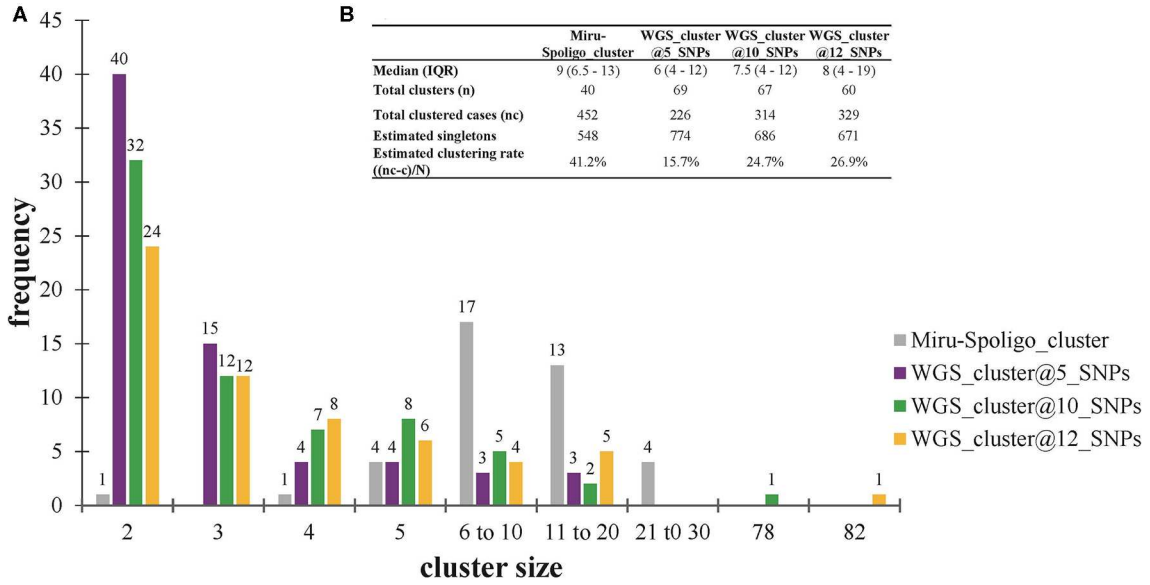

	Miru-Spoligo_cluster	WGS_cluster @5_SNPs	WGS_cluster @10_SNPs	WGS_cluster @12_SNPs
Median (IQR)	9 (6.5 - 13)	6 (4 - 12)	7.5 (4 - 12)	8 (4 - 19)
Total clusters (n)	40	69	67	60
Total clustered cases (nc)	452	226	314	329
Estimated singletons	548	774	686	671
Estimated clustering rate ((nc-c)/N)	41.2%	15.7%	24.7%	26.9%

FIGURE 4 | Clustering analysis stratified by cluster definition. **(A)** Frequency of clusters per cluster definition. **(B)** Estimated clustering rate per cluster definition. The estimated population size ($N = 1000$) used for estimating the clustering rate are explained in *Materials and methods* (see **Supplementary Data**). Singletons were calculated from the estimated population size of 1,000 individuals. IQR, interquartile range.

TABLE 1 | Characteristics and risk factor analysis of large genomic clusters resulting from a threshold of 10 SNPs.

Number	WGS cluster code	Number of cases in cluster	Number of variable fixed SNPs	Median pairwise SNP (IQR)	Lineage (sub-lineage[a])	Lineage classification by Stucki/Coll	Any drug resistance[b]	Gender, male:female	Median age (IQR)
1	WGSC-5	78	138	7 (6–9)	L4 (Cameroon)	L4.6.2/L4.6.2.2	2	59:17	34 (24–43)
2	WGSC-28	15	39	7 (5–7)	L4 (Ghana)	L4.10/L4.8	ND	11:4	39 (32–51)
3	WGSC-6	12	18	5 (3–6)	L4 (Haarlem)	NA/L4.6	ND	11:1	38 (28–48)
4	WGSC-13	10	23	5 (5–6)	L4 (Cameroon)	L4.6.2/L4.6.2.2	ND	8:2	42.5 (32–49)
5	WGSC-11	8	22	8 (6.5–8.5)	L4 (Ghana)	NA/L4.6.2	5	5:3	32.5 (28–41.5)
6	WGSC-42	8	6	3 (1–3.5)	L4 (Cameroon)	L4.6.2/L4.6.2.2	ND	8:0	25.5 (22.5–28.5)
7	WGSC-49	8	13	4 (1–7.5)	L4 (LAM)	L4.3/L4.3.1	ND	6:2	42 (32–54)
8	WGSC-25	7	16	4 (3–9)	L4 (Cameroon)	L4.6.2/L4.6.2.2	ND	7:0	39 (28–50)

WGS, Whole genome sequencing; L4, lineage 4; ND, none determined; IQR, interquartile range.

[a] *Sub-lineage defined using spoligotyping.*

[b] *Number of participants carrying strains with drug resistance to either isoniazid or rifampicin.*

clusters) and explore some epidemiological characteristics including spatial distribution of confirmed large clusters. Major findings from our analysis indicate that (1) estimated recent TB transmission rate using WGS at a SNP threshold of 10 remains high at 24.7%, and (2) there is wide spread of a clone of the Cameroon sub-lineage of lineage 4 with an ongoing transmission at hotspots mostly found within the Ablekuma sub-district of the Accra metropolis.

WGS was first used in 2011 to delineate two unrelated transmission events among a cohort of drug users with identical MIRU-VNTR profiles from Vancouver and ever since it has been used in some large studies to understand TB transmission dynamics (34–36). Despite the continuous progress and decreasing costs of WGS-based typing, there are some important pertaining challenges such as the lack of standardization of WGS analysis pipelines and genomic distances (SNP distance) for defining clusters (37). A first step in analyzing WGS data for transmission studies is usually to define SNP threshold to identify cluster, and the assumption is that, isolates from cases separated by SNPs less than or equal to the specified threshold are epidemiologically linked (38). The mutation rate established from our within-host microevolution analysis using

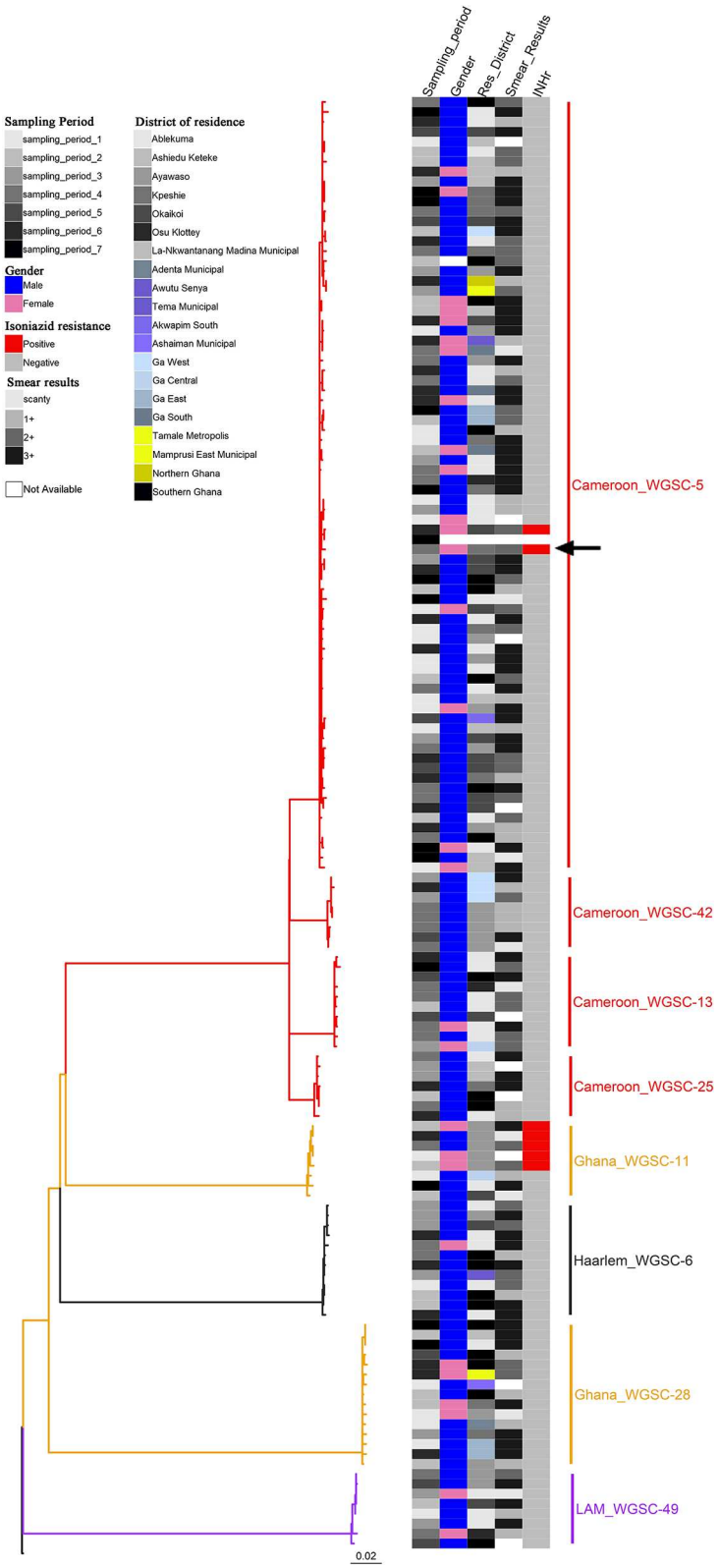

FIGURE 5 | Phylogenetic reconstruction of 146 *M. tuberculosis* complex isolates rooted on *M. canettii* showing characteristics of the eight identified large clusters as defined by a threshold of 10 SNPs. The heat map shows some characteristics of the clustered cases including sampling period (column 1), gender (column 2), residential district (column 3), smear results (column 4), and drug resistance status to isoniazid (column 5). There was only one rifampicin resistant isolate (black arrow). The color codes are defined in the key. All cases belong to lineage 4.

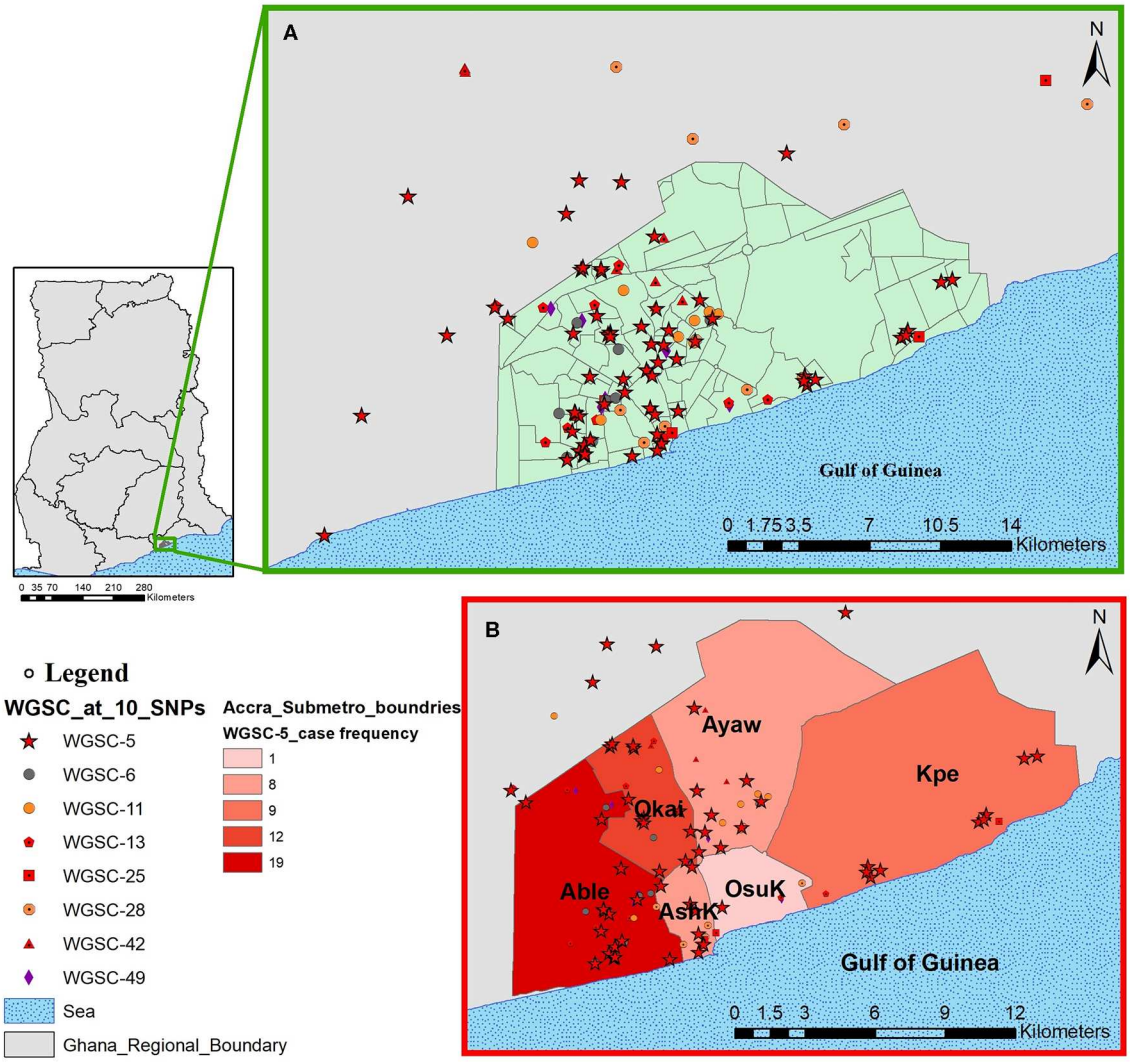

FIGURE 6 | Spatial distribution of pulmonary tuberculosis cases belonging to large clusters in and around Accra metropolis. The geographical distribution of cases from all eight large clusters is shown in **(A)** and the relative distribution of cases from the largest cluster highlighted in **(B)** stratified by Accra metropolis sub-district. Abbreviations: Able, Ablekuma sub-district; Okai, Okaikoi sub-district; AshK, AShiedu Keteke sub-district; OsuK, Osu Klottey sub-district; Ayaw, Ayawaso sub-district; Kpe, Kpeshie sub-district.

the main lineage/sub-lineage population, suggested a cut-off at 11 SNPs will be adequate to define a cluster. Consequently, we chose a SNP threshold of 10 for our analysis. This chosen threshold is ideal as other similarly high TB transmission settings like Malawi, have used the same threshold to infer recent transmission (27). Though our genome coverage cut-off was 15x, we had an overall mean genome coverage of 77x (± 27x) for all 452 genomes. Our cut-off is similar to that used in comparable studies which based their analysis on genome coverage cut-off of 10x, 15x, or 20x (27, 39–42).

We previously estimated the recent transmission index to be 41.2%, using MIRU/Spoligo which is higher than the current estimate of 24.7% using WGS analysis. This reduced rate was anticipated as the discriminatory power of WGS analysis is higher (43). Nevertheless, the 24.7% estimated recent transmission rate is still high comparable to 30% from a similarly high transmission setting like Malawi (27, 44) and predicts the occurrence of undetected recent transmission of large clusters. With the exception of three clusters of lineage 6, all the remaining 64 clusters were lineage 4 and no cluster from lineage 5. This finding confirms our previous report of reduced recent transmission of MAF lineages (L5 and L6) compared to MTBs and has stressed the need for further studies to investigate the continuous prevalence of MAF in West Africa. The observation of nearly distinct monophyletic clades from the reconstructed phylogenetic tree implies that traditional genotyping may still be useful as initial screening tools to help reduce the huge cost of WGS of all isolates especially in large-size population-based studies.

Within our study population, we did not identify any cluster consisting of multidrug-resistant strains, confirming our previous report of the unlikeliness of a drug-resistant TB strain to be involved in a recent transmission event (10). This observation may be due to the low proportion (2–4%) of MDR among MTBC isolates in Ghana (10, 11) or probably due to the reduced fitness cost associated to resistance conferring mutations (45, 46). Moreover, only 7/146 cases belonging to large genomic clusters were resistant to INH. Interestingly, 5/7 INH-resistant isolates belonged to the same Ghana sub-lineage cluster (WGSC-11). The Ghana sub-lineage has previously been associated with drug resistance (5, 11). Though the size of the cluster is not very large (cluster size of 8), this is nonetheless worrying since recent transmission of such drug-resistant clone may pose a great challenge to TB control in the sub-region. Until recently, drug-resistant clones were thought to be less fit and less likely to transmit from person to person; however, recent studies have documented evidence of transmission even though not involving large clusters (42, 47, 48). There is therefore the need to identify and control such difficult-to-treat drug-resistant clones to stop their spread.

Our population-based study included two distant regions in Ghana; the Northern region (in Northern Ghana) and the Greater Accra region (in Southern Ghana). Except for three cases from Northern Ghana (**Supplementary Figure 4** and **Supplementary Table 2**), all 146 cases belonging to large genomic clusters were found in Southern Ghana. Two of the only three large genomic clustered cases from Northern Ghana were found within the largest cluster (WGSC-5, **Figure 5**). These cases were, however, very closely related, sharing the same most recent common ancestral node and in fact no SNP difference between them, suggesting direct person-to-person transmission. A careful examination of their demographic data also showed that, indeed, these two individuals have the same family name and most probably comes from the same family. We show that the clustering of TB cases in Ablekuma observed in our previous study (5) was most probably due to recent TB transmission. This is not surprising as Ablekuma is the most densely populated of the six sub-districts of Accra metropolis (49). Our analysis suggests that there may be super-spreaders in Ablekuma and probably Okaikoi, which recorded the second highest numbers (19 and 12, respectively; **Figure 6** and **Supplementary Figure 4**) that belonged to the largest cluster (WGSC-5). Majority of the individuals in this high transmitting cluster were found to inhabit the city suburbs in densely populated compound houses. Their low-income status combined with over-crowding may be driving factors for the ongoing transmission in this hotspot. A high smear grade of over 70% of cases being at least 2+ signifies that these individuals are likely to have been actively transmitting the pathogen prior to diagnosis in their homes and neighboring communities, indicating that other individuals may have been infected.

The goal of universal screening is what most TB control programs are geared toward especially detecting MDR cases. Our study has identified hotspots not only for recent TB transmission of drug-sensitive strains but also spread of INH-resistant strain. We encourage more similar studies as it can identify geographical zones of highest need to support the national TB control program (NTP) with a targeted and guided approach to controlling TB. Case search approaches targeted at high-risk areas may be more effective in TB control (50). We have shown that application of WGS in a molepi study has aided the recognition of specific *M. tuberculosis* strains (e.g., cluster WGSC-11 associated with drug resistance), which can be predictive of INH drug-resistant TB in the Ghanaian contexts that could and can help provide indications of the TB case source similar to TB strains elsewhere (51). Also, we have been able to identify hotspots of recent TB transmission within the Accra Metropolis; hence, we recommend an urgent action to curtail the continual spread of the pathogen.

DATA AVAILABILITY STATEMENT

The raw sequence data are available under the BioProject ID: PRJNA616081 with the various accession numbers specified in **Supplementary Table 1**.

ETHICS STATEMENT

The studies involving human participants were reviewed and approved by Scientific and Technical Committee and the Institutional Review Board of Noguchi Memorial Institute for Medical Research, University of Ghana (FWA00001824). Written informed consent to participate in this study was provided by the participants' legal guardian/next of kin.

AUTHOR CONTRIBUTIONS

DY-M designed the study, provided supervision and support, provided intellectual input, and wrote the manuscript. PA performed most of the laboratory procedures, collated the epidemiological and laboratory data, did all statistical and cluster analysis on the data, and wrote the manuscript. SO-W performed some laboratory procedures and provided all associated data and provided useful comments to writing the manuscript. NB and AF supported the enrollment and collection of clinical and demographic data from the health facilities. EB, MR, and DP performed some laboratory procedures and provided all associated data and helped with preliminary analysis. IO performed some laboratory procedures and provided all associated data, performed some analysis, and provided useful comments to writing the manuscript. DB, CL, and SB provided supervision, support, and intellectual input, and critically reviewed the manuscript. AA-P contributed to the study design, performed some laboratory procedures, and provided all associated data and provided useful comments to writing the manuscript. KK provided supervision and support, intellectual input, and useful comments to writing the manuscript. SG designed the study, provided supervision and support, provided intellectual input, and critically reviewed the manuscript.

All coauthors reviewed and approved the final manuscript before submission.

FUNDING

This work was supported by a Wellcome Trust Intermediate Fellowship Grant (097134/Z/11/Z) to DY-M. Funders had no role in the study design; collection, analysis, and interpretation of data; in the writing of the report; and in the decision to submit the paper for publication. DY-M, PA, and IO had full access to all the data used in the study. PA, DY-M had the final responsibility for the decision to submit for publication.

ACKNOWLEDGMENTS

The authors are grateful for the administrative support of Dr. Frank Bonsu, NTP, Ghana, and to all laboratory heads, nurses, and study participants who made the study a success. We thank all national service personnel who provided great help in completing the questionnaires and making sputum samples available for laboratory investigations. Calculations requiring high computing power were performed at sciCORE (http://scicore.unibas.ch/) scientific computing core facility at University of Basel. Prince Asare was supported by a West African Center for Cell Biology of Infectious Pathogens (WACCBIP)–World Bank ACE Ph.D. Studentship. IO was supported by the Swiss-African Research Cooperation–SARECO Fellowship grant (SA_IO110).

SUPPLEMENTARY MATERIAL

The Supplementary Material for this article can be found online at: https://www.frontiersin.org/articles/10.3389/fmed.2020.00161/full#supplementary-material

REFERENCES

1. WHO. Global Tuberculosis Report. World Health Organization (2018). Available online at: http://www.who.int/tb/publications/global_report/en/ (retrieved September 26, 2018).
2. Blouin Y, Hauck Y, Soler C, Fabre M, Vong R, Dehan C, et al. Significance of the identification in the horn of Africa of an exceptionally deep branching *Mycobacterium Tuberculosis* clade. *PLoS ONE*. (2012) 7:e52841. doi: 10.1371/journal.pone.0052841
3. de Jong BC, Antonio M, Gagneux S. *Mycobacterium africanum*–review of an important cause of human tuberculosis in West Africa. *PLoS Negl Trop Dis*. (2010) 4:e744. doi: 10.1371/journal.pntd.0000744
4. WHO. Gear up to end TB: Introducing the end TB strategy. (2015) Available online at: World Health Organization https://www.who.int/tb/End_TB_brochure.pdf (retrieved February 2, 2019).
5. Yeboah-Manu D, Asare P, Asante-Poku A, Otchere ID, Osei-Wusu S, Danso E, et al. Spatio-temporal distribution of *Mycobacterium Tuberculosis* complex strains in ghana. *PLoS ONE*. (2016) 11:e0161892. doi: 10.1371/journal.pone.0161892
6. Jagielski T, van Ingen J, Rastogi N, Dziadek J, Mazur PK, Bielecki J. Current methods in the molecular typing of *Mycobacterium Tuberculosis* and other mycobacteria. *Biomed Res Int*. (2014) 2014:645802. doi: 10.1155/2014/645802
7. Jamieson FB, Teatero S, Guthrie JL, Neemuchwala A, Fittipaldi N, Mehaffy C. Whole-genome sequencing of the *Mycobacterium Tuberculosis* manila sublineage results in less clustering and better resolution than mycobacterial interspersed repetitive-unit-variable-number tandem-repeat (MIRU-VNTR) typing and spoligotyping. *J Clin Microbiol*. (2014) 52:3795–8. doi: 10.1128/JCM.01726-14
8. Senghore M, Otu J, Witney A, Gehre F, Doughty EL, Kay GL, et al. Whole-genome sequencing illuminates the evolution and spread of multidrug-resistant tuberculosis in Southwest Nigeria. *PLoS ONE*. (2017) 12:e0184510. doi: 10.1371/journal.pone.0184510
9. Walker TM, Ip CL, Harrell RH, Evans JT, Kapatai G, Dedicoat MJ, et al. Whole-genome sequencing to delineate *Mycobacterium Tuberculosis* outbreaks: a retrospective observational study. *Lancet Infect Dis*. (2013) 13:137–46. doi: 10.1016/S1473-3099(12)70277-3
10. Asare P, Asante-Poku A, Prah DA, Borrell S, Osei-Wusu S, Otchere ID, et al. Reduced transmission of *Mycobacterium africanum* compared to *Mycobacterium Tuberculosis* in urban West Africa. *Int J Infect Dis*. (2018) 73:30–42. doi: 10.1016/j.ijid.2018.05.014
11. Otchere ID, Asante-Poku A, Osei-Wusu S, Baddoo A, Sarpong E, Ganiyu AH, et al. Detection and characterization of drug-resistant conferring genes in *Mycobacterium Tuberculosis* complex strains: a prospective study in two distant regions of ghana. *Tuberculosis*. (2016) 99:147–54. doi: 10.1016/j.tube.2016.05.014
12. Bolger AM, Lohse M, Usadel B. Trimmomatic: a flexible trimmer for Illumina sequence data. *Bioinformatics*. (2014) 30:2114–20. doi: 10.1093/bioinformatics/btu170
13. Li H, Durbin R. Fast and accurate long-read alignment with burrows-wheeler transform. *Bioinformatics*. (2010) 26:589–95. doi: 10.1093/bioinformatics/btp698
14. Comas I, Chakravartti J, Small PM, Galagan J, Niemann S, Kremer K, et al. Human T cell epitopes of *Mycobacterium Tuberculosis* are evolutionarily hyperconserved. *Nat Genet*. (2010) 42:498–503. doi: 10.1038/ng.590
15. Li H. A statistical framework for SNP calling, mutation discovery, association mapping and population genetical parameter estimation from sequencing data. *Bioinformatics*. (2011) 27:2987–93. doi: 10.1093/bioinformatics/btr509
16. Koboldt DC, Zhang Q, Larson DE, Shen D, McLellan MD, Lin L, et al. VarScan 2: somatic mutation and copy number alteration discovery in cancer by exome sequencing. *Genome Res*. (2012) 22:568–76. doi: 10.1101/gr.129684.111
17. Cingolani P, Platts A, Wang le L, Coon M, Nguyen T, Wang L, et al. A program for annotating and predicting the effects of single nucleotide polymorphisms, SnpEff: SNPs in the genome of *Drosophila melanogaster* strain w1118; iso-2; iso-3. *Fly*. (2012) 6:80–92. doi: 10.4161/fly.19695
18. Stucki D, Brites D, Jeljeli L, Coscolla M, Liu Q, Trauner A, et al. *Mycobacterium Tuberculosis* lineage 4 comprises globally distributed and geographically restricted sublineages. *Nat Genet*. (2016) 48:1535–43. doi: 10.1038/ng.3704
19. Miller MA, Pfeiffer W, Schwartz T. Creating the CIPRES Science Gateway for inference of large phylogenetic trees. In: *Paper presented at the 2010 Gateway Computing Environments Workshop (GCE)*. (2010). doi: 10.1109/GCE.2010.5676129
20. Stamatakis A. RAxML version 8: a tool for phylogenetic analysis and post-analysis of large phylogenies. *Bioinformatics*. (2014) 30:1312–3. doi: 10.1093/bioinformatics/btu033
21. Yu G, Lam TTY, Zhu H, Guan Y. Two methods for mapping and visualizing associated data on phylogeny using ggtree. *Mol Biol Evol*. (2018) 35:3041–3. doi: 10.1093/molbev/msy194
22. Yu G, Smith DK, Zhu H, Guan Y, Lam TT-Y. ggtree: an r package for visualization and annotation of phylogenetic trees with their covariates and other associated data. *Methods Ecol Evol*. (2017) 8:28–36. doi: 10.1111/2041-210X.12628
23. Wickham H. *Ggplot2: Elegant Graphics for Data Analysis*. New York, NY: Springer-Verlag (2016). doi: 10.1007/978-3-319-24277-4
24. Team RC. *R: A Language and Environment for Statistical Computing*. R Foundation for Statistical Computing. (2019).

25. Paradis E, Schliep K. ape 5.0: an environment for modern phylogenetics and evolutionary analyses in R. *Bioinformatics*. (2019) 35:526–8. doi: 10.1093/bioinformatics/bty,633
26. Hall A. What is molecular epidemiology?. *Trop Med Int Health*. (1996) 1:407–8. doi: 10.1046/j.1365-3156.1996.d01-96.x
27. Guerra-Assunção JA, Crampin AC, Houben R, Mzembe T, Mallard K, Coll F, et al. Large-scale whole genome sequencing of *M*. tuberculosis provides insights into transmission in a high prevalence area. *eLife*. (2015) 4:e05166. doi: 10.7554/eLife.05166
28. Walker TM, Lalor MK, Broda A, Saldana Ortega L, Morgan M, Parker L, et al. Assessment of *Mycobacterium Tuberculosis* transmission in Oxfordshire, UK, 2007-12, with whole pathogen genome sequences: an observational study. *Lancet Respir Med*. (2014) 2:285–92. doi: 10.1016/S2213-2600(14)70027-X
29. Yang C, Luo T, Shen X, Wu J, Gan M, Xu P, et al. Transmission of multidrug-resistant *Mycobacterium Tuberculosis* in Shanghai, China: a retrospective observational study using whole-genome sequencing and epidemiological investigation. *Lancet Infect Dis*. (2017) 17:275–84. doi: 10.1016/S1473-3099(16)30418-2
30. Maechler M, Rousseeuw P, Struyf A, Hubert M, Hornik K. Cluster: Cluster Analysis Basics and Extensions. R package version 2.0.9. (2019).
31. Glynn JR, Vynnycky E, Fine PE. Influence of sampling on estimates of clustering and recent transmission of *Mycobacterium Tuberculosis* derived from DNA fingerprinting techniques. *Am J Epidemiol*. (1999) 149:366–71. doi: 10.1093/oxfordjournals.aje.a009822
32. Kumar S, Stecher G, Li M, Knyaz C, Tamura K. MEGA X: Molecular evolutionary genetics analysis across computing platforms. *Mol Biol Evol*. (2018) 35:1547–9. doi: 10.1093/molbev/msy096
33. ESRI. *Environmental Systems Resource Institute*. Redlands, CA: ESRI. (2010).
34. Gardy JL, Johnston JC, Ho Sui SJ, Cook VJ, Shah L, Brodkin E, et al. Whole-genome sequencing and social-network analysis of a tuberculosis outbreak. *New Eng J Med*. (2011) 364:730–9. doi: 10.1056/NEJMoa1003176
35. Lalor MK, Casali N, Walker TM, Anderson LF, Davidson JA, Ratna N, et al. The use of whole-genome sequencing in cluster investigation of a multidrug-resistant tuberculosis outbreak. *Eur Respir J*. (2018) 51:1702313. doi: 10.1183/13993003.02313-2017
36. Walker TM, Monk P, Smith EG, Peto TEA. Contact investigations for outbreaks of Mycobacterium tuberculosis advances through whole genome sequencing. *Clin Microbiol and Infect*. (2013) 19:796–802. doi: 10.1111/1469-0691.12183
37. Merker M, Kohl TA, Niemann S, Supply P. The evolution of strain typing in the *Mycobacterium Tuberculosis* complex. *Adv Exp Med Biol*. (2017) 1019:43–78. doi: 10.1007/978-3-319-64371-7_3
38. Stimson J, Gardy J, Mathema B, Crudu V, Cohen T, Colijn, C. Beyond the SNP threshold: identifying outbreak clusters using inferred transmissions. *Mol Biol Evol*. (2019) 36:587–603. doi: 10.1093/molbev/msy242
39. Brites D, Loiseau C, Menardo F, Borrell S, Boniotti MB, Warren R, et al. a new phylogenetic framework for the animal-adapted *Mycobacterium Tuberculosis* complex. *Front Microbiol*. (2018) 9:2820. doi: 10.3389/fmicb.2018.02820
40. Guerra-Assuncao JA, Houben RM, Crampin AC, Mzembe T, Mallard K, Coll F, et al. Recurrence due to relapse or reinfection with *Mycobacterium Tuberculosis*: a whole-genome sequencing approach in a large, population-based cohort with a high HIV infection prevalence and active follow-up. *J Infect Dis*. (2015) 211:1154–63. doi: 10.1093/infdis/jiu574
41. Votintseva AA, Pankhurst LJ, Anson LW, Morgan MR, Gascoyne-Binzi D, Walker TM, et al. Mycobacterial DNA extraction for whole-genome sequencing from early positive liquid (MGIT) cultures. *J Clin Microbiol*. (2015) 53:1137–43. doi: 10.1128/JCM.03073-14
42. Walker TM, Merker M, Knoblauch AM, Helbling P, Schoch OD, van der Werf MJ, et al. A cluster of multidrug-resistant *Mycobacterium Tuberculosis* among patients arriving in Europe from the horn of Africa: a molecular epidemiological study. *Lancet Infect Dis*. (2018) 18:431–40. doi: 10.1016/S1473-3099(18)30004-5
43. Stucki D, Ballif M, Bodmer T, Coscolla M, Maurer AM, Droz S, et al. Tracking a tuberculosis outbreak over 21 years: strain-specific single-nucleotide polymorphism typing combined with targeted whole-genome sequencing. *J Infect Dis*. (2015) 211:1306–16. doi: 10.1093/infdis/jiu601
44. Yates TA, Khan PY, Knight GM, Taylor JG, McHugh TD, Lipman M, et al. The transmission of *Mycobacterium Tuberculosis* in high burden settings. *Lancet Infect Dis*. (2016) 16:227–38. doi: 10.1016/S1473-3099(15)00499-5
45. Gagneux S. Fitness cost of drug resistance in *Mycobacterium Tuberculosis*. *Clin Microbiol Infect*. (2009) 15:66–8. doi: 10.1111/j.1469-0691.2008.02685.x
46. Melnyk AH, Wong A, Kassen R. The fitness costs of antibiotic resistance mutations. *Evol Appl*. (2015) 8:273–83. doi: 10.1111/eva.12196
47. Arandjelovic I, Merker M, Richter E, Kohl TA, Savic B, Soldatovic I, et al. Longitudinal outbreak of multidrug-resistant tuberculosis in a hospital setting, Serbia. *Emerg Infect Dis*. (2019) 25:555–8. doi: 10.3201/eid2503.181220
48. Coscolla M, Barry PM, Oeltmann JE, Koshinsky H, Shaw T, Cilnis M, et al. Genomic epidemiology of multidrug-resistant *Mycobacterium Tuberculosis* during transcontinental spread. *J Infect Dis*. (2015) 212:302–10. doi: 10.1093/infdis/jiv025
49. GSS. Ghana Statistical Service, District Analytical Report. 2010 Population and Housing Census. Accra Metropolitan. (2014).
50. Zelner JL, Murray MB, Becerra MC, Galea J, Lecca L, Calderon R, et al. Identifying hotspots of multidrug-resistant tuberculosis transmission using spatial and molecular genetic data. *J Infect Dis*. (2016) 213:287–94. doi: 10.1093/infdis/jiv387
51. Varghese B, al-Omari R, Grimshaw C, Al-Hajoj S. Endogenous reactivation followed by exogenous re-infection with drug resistant strains, a new challenge for tuberculosis control in Saudi Arabia. *Tuberculosis*. (2013) 93:246–9. doi: 10.1016/j.tube.2012.12.001

Conflict of Interest: The authors declare that the research was conducted in the absence of any commercial or financial relationships that could be construed as a potential conflict of interest.

frontiers in Public Health

ORIGINAL RESEARCH
published: 12 June 2020
doi: 10.3389/fpubh.2020.00190

Physical Measures to Reduce Exposure to Tap Water–Associated Nontuberculous Mycobacteria

Grant J. Norton[1], *Myra Williams*[2], *Joseph O. Falkinham III*[2] *and Jennifer R. Honda*[1]*

[1] Department of Biomedical Research, Center for Genes, Environment and Health, National Jewish Health, Denver, CO, United States, [2] Department of Biological Sciences, Virginia Tech, Blacksburg, VA, United States

Nontuberculous mycobacteria (NTM) that cause human disease can be isolated from household tap water. Easy-to-use physical methods to reduce NTM from this potential source of exposure are needed. Filters and UV disinfection have been evaluated for their ability to reduce numbers of waterborne non-NTM organisms from drinking water, but their efficacy in reducing NTM counts are not well-established. Thus, five commercially available disinfection methods were evaluated for their potential as practical, efficient, and low-cost methods to reduce NTM from tap water. First, suspensions of tap water–adapted *Mycobacterium smegmatis* were passed through either a point-of-use, disposable, 7-day or 14-day Pall-Aquasafe filter. The 7-day filter prevented passage of *M. smegmatis* in effluent water for 13 days, and the 14-day filter prevented the passage of *M. smegmatis* for 25 days. Second, a granular activated carbon filter system failed to significantly reduce *Mycobacterium abscessus* and *Mycobacterium avium* numbers. Third, suspensions of tap water–adapted *M. abscessus*, *M. avium*, and *M. chimaera* ("MycoCocktail") were passed through the "LifeStraw GO" hollow-fiber, two-stage membrane filtration system. LifeStraw GO prevented passage of the MycoCocktail suspension for the entire 68-day evaluation period. Finally, two different water bottle UV sterilization systems, "Mountop" and "SteriPEN," were evaluated for their capacity to reduce NTM numbers from tap water. Specifically, MycoCocktail suspensions were dispensed into Mountop and SteriPEN water bottles and UV treated as per the manufacturer instructions once daily for 7 days, followed by a once weekly treatment for up to 56 days. After 4 days of daily UV treatment, both systems achieved a >4 log reduction in MycoCocktail CFU. After the 56-day evaluation period, suspension and biofilm-associated CFU were measured, and a >4 log reduction in CFU was maintained in both systems. Taken together, physical disinfection methods significantly reduced NTM numbers from tap water and may be easy-to-use, accessible applications to reduce environmental NTM exposures from drinking water.

Keywords: ***Mycobacterium smegmatis*, *Mycobacterium abscessus*, *Mycobacterium avium*, *Mycobacterium chimaera*, tap water, point of use filters, UV disinfection, biofilm**

OPEN ACCESS

Edited by:
Onya Opota,
Université de Lausanne, Switzerland

Reviewed by:
Loïc Deblais,
The Ohio State University, United States
Stephen Cose,
University of London, United Kingdom

***Correspondence:**
Jennifer R. Honda
HondaJ@njhealth.org

Specialty section:
This article was submitted to Infectious Diseases – Surveillance, Prevention and Treatment, a section of the journal Frontiers in Public Health

Received: *21 February 2020*
Accepted: *27 April 2020*
Published: *12 June 2020*

Citation:
Norton GJ, Williams M, Falkinham JO III and Honda JR (2020) Physical Measures to Reduce Exposure to Tap Water–Associated Nontuberculous Mycobacteria. Front. Public Health 8:190. doi: 10.3389/fpubh.2020.00190

INTRODUCTION

There are an estimated 180,000 individuals living in the United States with nontuberculous mycobacterial (NTM) pulmonary disease (1). A proportion of individuals are at heightened risk for NTM infection and development of pulmonary disease. These include individuals with prior occupational lung damage (e.g., black lung, smoking, and COPD), bronchiectasis, prior infection with *Mycobacterium tuberculosis*, immunodeficiency due to HIV infection, and immunodeficiency due to cancer or chemotherapies (2, 3). In addition, otherwise healthy elderly, slender, and taller women and men are at increased risk for NTM infection (4–6). Individuals in each of these risk groups are also at risk for repeated NTM infections due to their ubiquity in the environment even following the resolution of symptoms after successful antibiotic therapy (7).

NTM are intimately associated with natural and built freshwater systems (8, 9) and linked to exposure from household showerhead water and biofilms by DNA fingerprint comparisons (10). Moreover, NTM and other opportunistic premise plumbing pathogens (OPPPs), including *Pseudomonas aeruginosa*, *Acinetobacter baumannii*, *Stenotrophomonas maltophilia*, and *Legionella pneumophila*, surround humans as colonists of drinking water systems (11). As relapse due to NTM reinfection or reactivation of latent infection occurs at frequencies between 25 and 50%, it is of value to identify methods to reduce environmental exposure to NTM in the built household environment.

Reduction of exposure to waterborne NTM could be potentially accomplished by the removal of NTM from household water using a variety of methods, including filtration. To be effective, filtration must prevent the passage of NTM cells, demanding a filter with a pore size of 0.22 μm. These particular filters have been found to reduce the frequency of false-positive acid-fast stains in a tuberculosis laboratory (12) and healthcare-associated infections in bone marrow transplant recipients (13). The replacement of showerheads with 0.22 μm pore size filters also reduced total bacterial counts in shower water and aerosols compared to unfiltered water (14).

In contrast to the 0.22-μm filters, granular activated charcoal (carbon, GAC) filters do not prevent the passage of NTM as their pores are larger than 0.45 μm in diameter (15). In fact, NTM have been shown to colonize GAC filters (15). Specifically, filters loaded with a total of 2.9×10^5 CFU of *Mycobacterium avium* yielded a total of 4.4×10^7 after 3 weeks and 9.4×10^7 CFU after 5 weeks. Although the number of *M. avium* declined after the fifth week, the data showed that the CFU of *M. avium* in the filtrates were far in excess of the number added to the filter, suggesting that the *M. avium* cells can also grow on the filter. Other studies have also demonstrated that passage of rural groundwater through powdered activated carbon filters led to increased numbers of heterotrophic-plate-count bacteria (16).

Although filtration can be used to remove NTM from drinking water, NTM are staggeringly resistant to chlorine and other disinfectants used in drinking water treatment systems. In fact, NTM are substantially more resistant to common methods of water disinfection, such as chlorine, monochloramine, and ozone, than *Escherichia coli* (17). Due to their innate resistance to disinfectants, propensity to form biofilms within piping systems, and ability to survive in low-carbon environments, eradication of NTM from premise plumbing is a nearly impossible task. However, similar to other bacteria, NTM are susceptible to ultraviolet (UV) light (18, 19). Short-wave UV-C radiation (253.7 nm) has been demonstrated to cause lethal damage to microbial biomolecules, most notably by inducing cross-linking of thymine residues in DNA, and is considered an effective germicidal (20). Because of this, a number of large-scale and point-of-use UV water disinfection systems have been developed and are available to consumers (21). However, it has been demonstrated that clinically relevant NTM isolates, such as *M. avium hominissuis*, are more resistant to UV radiation than the coliforms commonly used in water purification system testing (22). Therefore, it is unknown if these commercially available UV-C water disinfection systems could be an effective means of reducing NTM in drinking water.

Herein, we describe the evaluation of the efficacy of filter removal or UV-C–mediated killing of tap water–associated NTM by devices that can be commercially purchased and used by individuals.

MATERIALS AND METHODS

NTM Isolates

Mycobacterium smegmatis VT307; *Mycobacterium avium* A5; *Mycobacterium chimaera* MA3820; *Mycobacterium abscessus* P-1-Ay-1; and clinical respiratory isolates *M. abscessus* P2A, *M. avium* P1A, and *M. chimaera* AH16 (23) were used in this study.

Growth of NTM in Culture

NTM isolates were grown in 50 mL of Middlebrook 7H9 broth (BD, Sparks, MD) containing 0.5% (vol/vol) glycerol and 10% (vol/vol) oleic acid-albumin with aeration (120 rpm) for 4 days at 37°C for *M. smegmatis* and *M. abscessus* or 7 days at 37°C for *M. avium* and *M. chimaera*. In some cases, 500-mL nephelometry flasks were used to measure and record turbidity as absorbance (540 nm) daily and/or cultures were diluted and plated on Middlebrook 7H10 agar plates (BD, Sparks, MD) containing 0.5% (vol/vol) glycerol and 10% (vol/vol) oleic acid-albumin to determine colony forming units (CFU).

NTM Acclimation to Tap Water

Following growth in microbiological culture media, isolates were acclimated in sterile tap water. Water acclimation was performed in order to replicate the environment within household plumbing based on previously reported differences in disinfectant susceptibility between water- and media-grown NTM isolates (17). Cultures were transferred to sterile 50-mL centrifuge tubes, centrifuged at 5,000 × g for 20 min, supernatants removed, and the cell pellets resuspended in 50 mL of sterile Blacksburg, VA, or Denver, CO, tap water. Centrifugation was repeated, and the cells were again resuspended in 50 mL of sterile Blacksburg or Denver tap water. For water acclimation, suspensions were transferred into sterile

250-mL baffled flasks and incubated at room temperature (filter experiments) or 37°C (UV experiments) with aeration (120 rpm) for 7 days.

Measurement of Filtration Efficacy of Pall Medical In-line Filters

Suspensions of sterile tap water and *M. smegmatis* were prepared as described above section. Pall-Aqua safe water filters AQ14F1SA and AQ7F1SA 0.2 μm pore size intended for 7- and 14-day use, respectively, were tested (**Supplementary Figure 1**). Both had void volumes of 33.5 mL, defined as the volume of sterile, disinfectant-free Blacksburg tap water held by the filter before the appearance of any eluate. Pall filters were inoculated by vacuum/pressure-free passage of water-acclimated suspensions of *M. smegmatis* VT307. The number of NTM passing through the filter (i.e., eluate) was measured as CFU on Middlebrook 7H10 agar medium over time. Over the course of the 30-day test period, filters were incubated in an upright position at ambient room temperature (25°C). Samples of filter material were also obtained following the 30-day test period and suspended in sterile tap water, and after vortexing, NTM numbers were measured as CFU on 7H10 agar.

Passage and Growth of NTM in Granular Activated Carbon (GAC) Filters

A GAC filter system was tested (GE, Smart Water™ Shower Filter, Model GXSM01HWW, GE, Louisville, KY) as depicted in **Supplementary Figure 1**. The density of each water-acclimated suspension of *M. avium* A5 or *M. abscessus* P-1-Ay-1 in sterile, disinfectant-free Blacksburg tap water was 3 log cells/mL. Two identical filters were inoculated with the volume of cell suspension equal to the void volume and incubated overnight at room temperature. For one of the filters, 1 L of sterile, disinfectant-free Blacksburg tap water was passed through the filter and the eluate collected in a sterile 2-L flask. For the second filter, 1 L of non-sterile, disinfectant-free Blacksburg tap water was passed through the filter and the eluate collected in a second sterile 2-L flask. The bacterial cells in a 50-mL aliquot of each eluate were pelleted by centrifugation (5,000 x g for 20 min), suspended 10 mL sterile disinfectant-free tap water, and the CFU/mL of the concentrated suspension measured by spreading 0.1 mL of each suspension on 7H10 agar. The effect of passage of 1 L of sterile, disinfectant-free tap water (Filter 1) or non-sterile, disinfectant-free tap water (Filter 2) through the filters on NTM colony counts was measured weekly for up to 8 weeks.

Next, to measure the CFU on GAC filters, the filter was removed from the filter holder and cut into 1-cm sections using a saw that was sterilized by alcohol flaming. Each section was broken up using a sterilized mortar and pestle, and 1 gm of the material was suspended in 10 mL of sterile 0.01 M Tris buffer (pH 7), 10^6 M Zwittergent 3–12, 10^3 M EGTA, and 0.01% peptone (24) to disrupt hydrophilic and hydrophobic associations between NTM and GAC particles, and shaken (one reciprocation per second) for 60 min at room temperature. The GAC particles were allowed to settle by gravity, and the CFU/mL in the supernatant was determined by spreading 0.1 mL of each suspension on 7H10 agar. Colonies were counted after 10–14 days incubation at 37°C. The bacterial density of the GAC particulate suspension and the total NTM CFU that were bound to the 1-cm section of the GAC filter were calculated. The total NTM CFU in the GAC filter was calculated by summing the values for each section. As a control, a GAC filter was inoculated as described above and immediately removed and processed to measure the total NTM per filter to provide counts actually added and recovered from each filter.

Sterile tap water was continuously passed through filters and samples of the eluate were collected immediately after passing the suspension through the filter every 3 days to 4 weeks. At each time point, the number of CFU passing through the filter was measured. After the 30-day use period, filter samples were collected and suspended and CFU per gm of filter measured.

"MycoCocktail" Preparation

A schematic detailing the preparation of the "MycoCocktail" is shown in **Supplementary Figure 2**. In brief, after water acclimation, suspensions were transferred to 50-mL conical vials and vortexed thoroughly. Suspensions were then diluted 1:1,000 in sterile tap water and mixed together in order to achieve a MycoCocktail containing a mixture of *M. abscessus*, *M. avium*, and *M. chimaera* with a total CFU between 1 x 10^4 and 1 x 10^5/mL. MycoCocktail was subsequently used in inoculation of LifeStraw GO, Mountop, and SteriPEN systems and prepared fresh for each independent experiment.

Measurement of Filtration Efficacy of LifeStraw Go Bottle

The LifeStraw Go (LIFESTRAW S.A., Lausanne, Switzerland) bottle contained two filters: an activated carbon capsule and a hollow fiber membrane (**Supplementary Figure 3**). On first use, LifeStraw Go bottles were rinsed twice with 650-mL volumes of sterile Blacksburg tap water in order to remove any materials remaining from bottle manufacturing or assembly. After two-fold washing, the bottles were filled with 650 mL of sterile Blacksburg tap water and incubated overnight to thoroughly wet the filters. A 650-mL aliquot of MycoCocktail was dispensed into the LifeStraw Go bottle and allowed to equilibrate for 1 day to simulate the typical consumer filling, but not immediately using, the bottle. Using sterile tubing and a sterile suction flask, 100 mL of the liquid was withdrawn into the suction flask (**Supplementary Figure 4D**). The number of NTM on 7H10 agar was measured. The lid of the LifeStraw Go bottle was unscrewed, and 100 mL of MycoCocktail was added and incubated overnight. Every day after inoculation, sample collection and MycoCocktail enumeration was repeated for an additional 10 days.

Testing Two UV-C Disinfection Systems Against NTM

Two different types of UV-C disinfection water bottle systems were tested: Mountop Water Purifier Bottle (201330464721.4; GE) and SteriPEN Aqua UV Water Purifier Kit (Article #60110075; Brita LP, Oakland, CA). Both bottle systems utilize a 90-s treatment cycle of 254-nm UV-C radiation to disinfect 750 mL (Mountop) or 1 L (SteriPEN) of drinking water.

Differences in UV irradiation between both water bottle systems are depicted in **Supplementary Figure 3**. Mountop is equipped with a UV bulb on the bottom surface of the cap that emits UV-C radiation directly above the air–liquid interface. SteriPEN Aqua utilizes a cylindrical UV bulb that is completely submerged and is gently stirred during the treatment cycle. For all testing of Mountop and SteriPEN Aqua, three different bottle systems were screened in order to capture potential inconsistencies in the performance of each unit. Prior to evaluation of killing by UV-C radiation, systems were sterilized using Prolystica® enzymatic cleaner (STERIS, Mentor OH) and household bleach diluted in sterile Denver tap water. Water bottles were filled with 4:1,000 Prolystica®:sterile tap water and agitated vigorously on a rocking platform for 5 min. 1:1,000 bleach:sterile tap water was then added, and bottles were returned to shake for 5 min. Solutions were then discarded, and the bottles were filled with sterile tap water and shaken for 5 min to rinse. Rinsing steps were repeated two additional times, and after the final rinse, bottles were allowed to dry overnight at room temperature in a biosafety cabinet.

Measurement of the Efficacy of Mountop and SteriPEN Systems

In order to determine the effect of a single UV treatment (**Supplementary Figure 4A**), each bottle was inoculated with 750 mL (Mountop) or 1 L (SteriPEN) of freshly prepared MycoCocktail; 1 mL of the inoculum was removed immediately after inoculation, serially diluted, and plated for CFU on 7H10 agar to measure the initial CFU in the inoculum. Bottles were immediately sterilized with UV-C radiation according to the manufacturer's instructions (90-s treatment with 254 nm light), and 1 mL of the treated suspension was removed to determine the post-treatment NTM burden. For all UV-treated bottles, untreated bottles were included as controls. Suspensions were spread plated and also independently serially diluted and plated in duplicate for CFU on 7H10 agar. Images were taken of spread plates and, in regions where NTM growth was difficult to visualize, a region of representative growth was chosen and magnified approximately six-fold.

For 7-day evaluation of the efficacy of Mountop and SteriPEN with no water replacement (**Supplementary Figure 4B**), bottles were inoculated with MycoCocktail as described and incubated overnight at room temperature. The following day, bottles were UV-C irradiated per the manufacturer's instructions. After disinfection, 1 mL of the suspension from each bottle was removed and plated for CFU. These steps were repeated daily for 7 days.

For 56- or 21-day evaluation with water replacement (**Supplementary Figure 4C**), bottles were incubated overnight at room temperature after MycoCocktail inoculation. The following day, bottles were removed and UV-C irradiated to disinfect the cocktail (25, 26). The suspension in each bottle was then transferred to 1-L, 0.22-μm pore filters (Foxx Life Sciences LLC, Salem NH) and vacuum filtered. Filter membranes were excised using sterile razor blades and forceps and added to 10 mL of sterile Denver tap water in a 50-mL conical vial. Excised filters were vortexed thoroughly for 1 min in order to remove filter-associated NTM and 1 mL of the suspension was serially diluted and plated for CFU as previously described. Bottles were then refilled with sterile tap water and returned to incubate at room temperature. UV treatment, suspension plating, and water replacement were performed daily for 7 days after inoculation and then weekly until 21 or 56 days post-inoculation. All methods used with UV-treated bottles were replicated with untreated bottles with the exception of UV disinfection.

Biofilm Sampling of Mountop and SteriPEN Systems

In order to evaluate the contribution of biofilm formation on the inner surface of the water bottles, biofilms in Mountop and SteriPEN bottles were sampled. Four regions of each bottle were sampled: (1) the bottle cap, (2) a 4-cm^2 region of the air–liquid interface, (3) a 4-cm^2 region of the middle of the bottle, and (4) a 4-cm^2 region of the bottom of the bottle using a sterile synthetic swab (see schema detailed in **Figure 4A**). Swabs were collected, vortexed for 1 min in 1 mL sterile Denver tap water, and the suspension plated for CFU.

Comparing UV-C Susceptibility of NTM Isolates

After completion of 56 days of UV-disinfection and water replacement, representative colonies of *M. abscessus* P2A, *M. avium* P1A, and *M. chimaera* AH16 were picked from CFU plates. These isolates are referred to as "UV-adapted" and were inoculated into 8 mL Middlebrook 7H9 broth with ADC enrichment to establish stocks. Colonies of water-acclimated *M. abscessus*, *M. avium*, and *M. chimaera* were also picked, inoculated into 7H9 broth and prepared into stocks. Stocks were stored at −80°C until use. To compare differences in UV susceptibility between the water-acclimated and UV-adapted NTM isolates, 100 μl of each isolate was spread onto 7H10 agar. Spread plates were then exposed to 90 s of 254-nm UV-C radiation. During exposure, one half of the agar plate was covered with a notecard, and the other half remained directly exposed to UV-C. Plates were incubated at 37°C until growth appeared, and UV-C susceptibility of each isolate was determined qualitatively by the difference in growth between the covered and uncovered portion of the agar plate.

Statistics

Graphpad Prism 8 was used to perform unpaired *t*-tests as a measure of statistical significance. For all data shown, $p < 0.05$ was considered statistically significant. For multiple *t*-tests, *P*-values were adjusted using the Holm–Sidak method. Data shown are mean ± *SEM* for two or more independent experiments.

RESULTS

Efficient Removal of NTM by Pall Medical In-line Filters

Immediately and daily for 13 (7-day filter) or 25 days (14-day filter), 100 mL of the *M. smegmatis* tap water suspension was added through the input line of the filter, and the liquid flowing out (∼100 mL) was collected in a sterile flask. As triplicate samples were spread from the 100 mL effluent, the limit of

detection was <3.3 CFU/mL. Although *M. smegmatis* was recovered from the swabbed surface samples of the input side of the 7- and 14-day filters (77 and 57 CFU/cm^2, respectively), all effluent water passing through either the 7- or 14-day Pall filters over the 13- or 25-day test period were completely devoid of *M. smegmatis* (data not shown).

Inefficient Removal of NTM by GAC Filters

Although water filtered through a GAC filter modestly reduced *M. abscessus* and *M. avium* numbers in effluent water (**Tables 1A**, **2A**, respectively), removal was inconsistent and varied in count from below the limit of detection to over 4 log *M. abscessus* and *M. avium* per milliliter of effluent water. NTM were not only recovered from filter effluents across the 30-day sampling period, but viable NTM were also recovered from the GAC filters (**Tables 1B**, **2B**). Filter-associated burden of *M. abscessus* was much less than *M. avium* with, on average, ∼53 CFU/gm (*M. abscessus*) and ∼482 CFU/gm (*M. avium*) recovered from filter sections.

Total Removal of NTM by LifeStraw Go Bottle

MycoCocktail contained, on average, 5.7652 log *M. avium* A5, *M. chimaera* MA3820, and *M. abscessus* P-1-Ay-1 cells/mL at inoculation, a 1 x 10^4- to 1 x 10^5-fold higher concentration than typical culturable NTM burden in drinking water (27, 28). Over the course of 68 days, 100 mL of water was periodically removed aseptically through the drinking tube by suction and the number of NTM counted. Assuming that the bottle would be refilled due to consumption, the 100 mL sampled was replaced by 100 mL of MycoCocktail. At every sampling point (1, 4, 5, 6, 7, 11, 18, 25, 32, 40, 46, 53, and 68 days post-inoculation), no NTM (<3.3 CFU/mL) were recovered (data not shown).

Efficient Removal of NTM by Both Mountop and SteriPEN Systems After a Single UV Treatment

The efficiency of the manufacturer's standard protocol for the use of Mountop and SteriPEN systems in the reduction of MycoCocktail CFU in drinking water was evaluated (see schema, **Supplementary Figure 4A**). For both Mountop and SteriPEN systems, a single UV treatment significantly reduced the initial bacterial burden within each bottle (**Figure 1**). A stark reduction in inoculum CFU was observed on 7H10 agar plates spread with MycoCocktail pre- and post-treatment with UV-C in both systems (**Figures 1A,B**). However, as illustrated by the agar plate images, the reduction in bacterial burden achieved with the Mountop system was less than with SteriPEN. In the Mountop system, the reduction in NTM burden was, on average, 0.8850 log

TABLE 1A | *M. abscessus* in effluent water from GAC filter.

Time (days)	*M. abscessus* CFU/mL	
	Unfiltered	Filtered
0	8.3×10^5	$<3.3 \times 10^2$
1	3.2×10^5	7.0×10^3
2	4.0×10^5	$<3.3 \times 10^2$
3	1.6×10^6	$<3.3 \times 10^2$
4	6.6×10^4	3.0×10^4
5	2.4×10^4	3.3×10^3
6	5.1×10^6	$<3.3 \times 10^2$
7	1.1×10^5	$<3.3 \times 10^2$
8	3.1×10^5	6.7×10^3

Inoculum = 1.5 × 10^5 CFU.

TABLE 1B | *M. abscessus* in GAC filter.

Filter sample	CFU/gm GAC
FC-1 (Top)	48/gm
FC-2	54/gm
FC-3	<8/gm
FC-4	48/gm
FC-5	18/gm
FC-6 (Bottom)	145/gm

Inoculum = 1.5 × 10^5 CFU.
FC, "fractions cut" (6 – 1cm fractions total).

TABLE 2A | *M. avium* in effluent water from GAC filter.

Time (days)	*M. avium* CFU/mL effluent water	
	Unfiltered	Filtered
0	1.0×10^6	1.0×10^4
1	3.0×10^5	$<3.3 \times 10^3$
2	6.5×10^4	$<3.3 \times 10^3$
3	1.1×10^6	$<3.3 \times 10^3$
4	1.8×10^5	$<3.3 \times 10^3$
5	4.0×10^5	1.0×10^4
6	6.0×10^5	$<3.3 \times 10^3$
7	6.9×10^6	$<3.3 \times 10^3$
8	1.5×10^6	4.7×10^4

Inoculum = 2.0 × 10^5 CFU.

TABLE 2B | *M. avium* in GAC filter.

Filter sample	CFU/gm GAC
FC-1 (TOP)	1,100/g
FC-2	300/g
FC-3	500/g
FC-4	330/g
FC-5	430/g
FC-6 (Bottom)	230/g

Inoculum = 2.0 × 10^5 CFU.
FC, "fractions cut" (6 – 1cm fractions total).

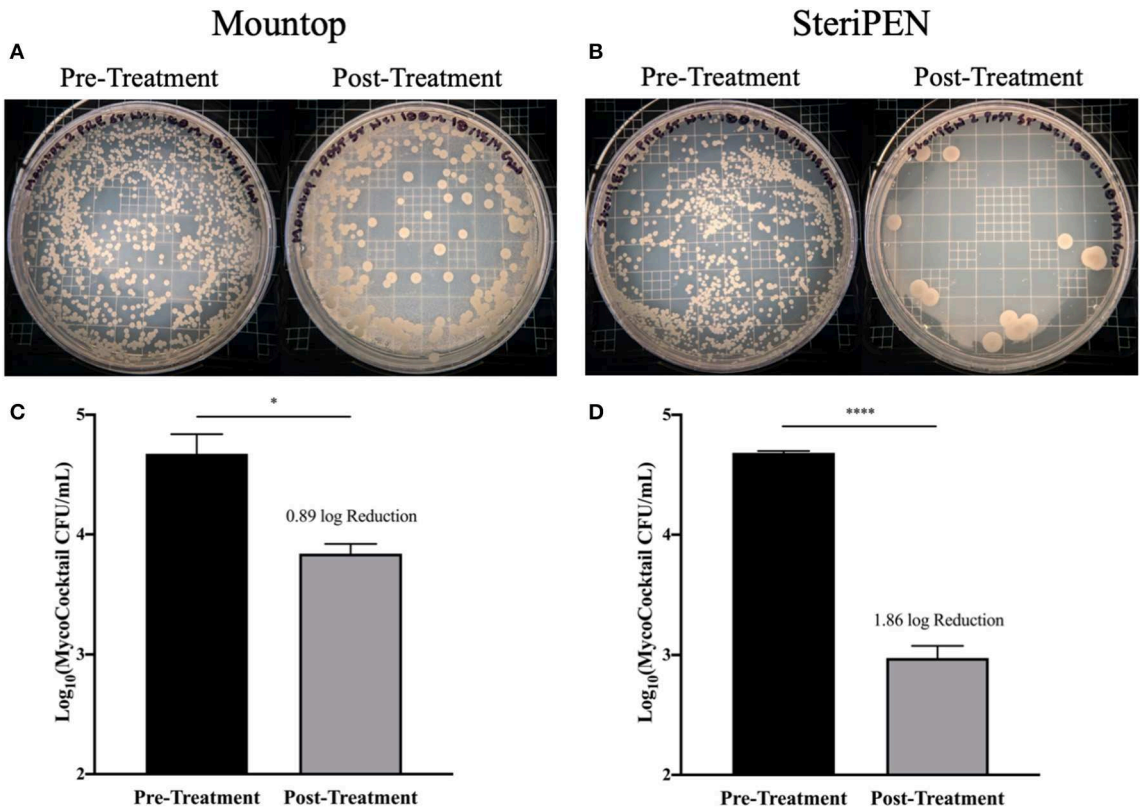

FIGURE 1 | NTM CFU is significantly reduced after single UV treatment in both and Mountop and SteriPEN systems. Mountop **(A,C)** and SteriPEN **(B,D)** systems were inoculated with MycoCocktail and immediately UV-C disinfected per the manufacturer's protocol. **(A,B)** Representative images of MycoCocktail CFU in Mountop and SteriPEN before and after UV treatment. **(C,D)** Log(MycoCocktail CFU) before (pretreatment) and after (post-treatment) UV disinfection. $n = 3$ independent CFU measurements per time point. ns, not significant; significant at $^{*}p < 0.05$, $^{****}p < 0.0001$.

(4.7404 log to 3.8553 log; $p < 0.05$; **Figure 1C**), and the SteriPEN system achieved an average reduction of 1.8603 log (4.6842 log to 2.8240 log; $p < 0.0001$; **Figure 1D**) after a single UV treatment.

Mountop Is Less Effective Than SteriPEN in Disinfecting NTM From Tap Water When Used Consistently for 7 Days

Next, the change in CFU after a single, initial inoculation of MycoCocktail in the presence or absence of UV-C treatment across a 7-day period (see schema, **Supplementary Figure 4B**) was evaluated. For the Mountop and SteriPEN bottles that were not UV-C treated, CFU remained consistent across 7 days (**Figures 2A,B** bottom row). However, with daily UV-C treatment, MycoCocktail CFU was progressively reduced across the sampling period as deduced by visual observation of viable colonies on 7H10 agar plates (**Figures 2A,B** top row). For the untreated MycoCocktail, NTM burden from inoculation to the end of the 7-day interval was 5.0544 log to 5.0669 log for SteriPEN and 5.0072 log to 5.0000 log for Mountop (**Figures 2C,D**). In comparing these values to UV-C treated MycoCocktail, the differences between treated and untreated bottles was not statistically significant for the Mountop system (4.5662 log to 2.3680 log across 7 days; **Figure 2C**). However, a significant decline in CFU was observed for the SteriPEN water bottle system compared to the untreated control (∼4.5441 log reduction across 7 days; **Figure 2D**).

Simply Replacing the Water in Mountop and SteriPEN Systems Reduced NTM Similar to UV-C Treatment

To determine the effect of water replacement on NTM CFU, both water bottle systems were initially inoculated with 4.8–4.9 log MycoCocktail CFU, UV-C irradiated, and water was replaced with sterile tap water daily for 7 days and weekly up until 21 days post-inoculation (see schema, **Supplementary Figure 4C**). Across all time points, CFU decreased for both Mountop and SteriPEN. This observation is illustrated by the similar appearance of NTM colony growth on 7H10 agar plates regardless of UV treatment (**Figures 3A,C**). Although the comparable decline in inoculum CFU in the absence of UV-C treatment was unexpected, unlike the UV-C treated inocula, the NTM burden in the untreated Mountop and SteriPEN bottles increased to ∼1 log/L at 14 and 21 days post-inoculation. For the UV-treated Mountop system, the average decline in CFU after the first UV treatment was 1.5950 log, and although this decline continued over time, it failed to consistently reach 0 CFU/mL

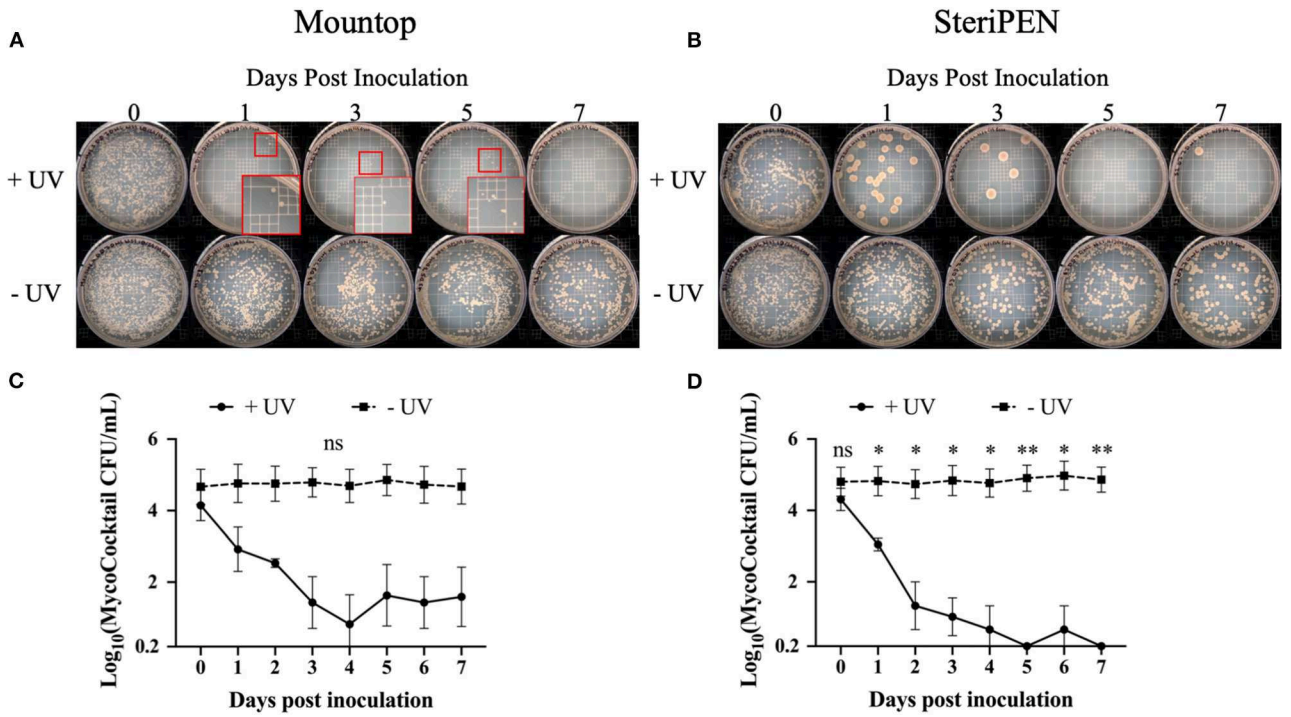

FIGURE 2 | NTM CFU is reduced by UV-C treatment. Mountop **(A,C)** and SteriPEN **(B,D)** systems were inoculated with MycoCocktail and allowed to incubate at room temperature overnight. After incubation, the MycoCocktail was UV-C disinfected per the manufacturer's protocol. "+UV" = water that was UV treated. "-UV" = water that was not exposed to UV. One milliliter of suspension was removed and plated for CFU and the systems were returned to incubate at room temperature. CFU plating was repeated daily for 7 days post-inoculation. **(A,B)** Representative images of MycoCocktail CFU in Mountop and SteriPEN across 7 days of daily UV-C disinfection. Smaller red boxes indicate regions where growth was difficult to visualize. Larger red boxes show colonies magnified ∼6-fold. **(C,D)** Log(MycoCocktail CFU) in SteriPEN and Mountop systems. $n = 3$ independent CFU measurements per timepoint. ns, not significant; significant at $^{*}p < 0.05$, $^{**}p < 0.01$.

across the 21-day observation interval (**Figure 3B**). The UV-treated SteriPEN achieved, on average, a 2.8744 log reduction in NTM counts after a single UV-C treatment and continued to decline to 0.3920 log CFU/mL by 4 days post-inoculation (**Figure 3D**).

Biofilm CFU Within Mountop and SteriPEN Bottles Is Negligible

Due to the hydrophobicity of NTM, the inner sections of each bottle were evaluated for the formation of NTM biofilms. Specifically, after 7 days of incubation with MycoCocktail, the bottles were emptied and the NTM CFU remaining in suspension enumerated. Next, four different areas of the emptied bottles were sampled for biofilms in the cap, air–liquid interface, side, and bottom wall (**Figure 4A**). In both Mountop and SteriPEN bottle systems, the cap contained the lowest number of detectable CFU and the side of the Mountop bottle and the bottom surface of the SteriPEN bottle showed the highest biofilm-associated CFU (**Figures 4B,D**). Although the CFU in suspension did not significantly differ between Day 0 and Day 7, biofilm associated CFU in both Mountop and SteriPEN accounted for <1% of the total CFU (**Figures 4C,E**).

UV-C Exposed NTM Do Not Show Increased Resistance to UV

Finally, we tested the possibility that the NTM that survived UV-C treatment after 56 days of incubation were innately resistant to UV-C irradiation. However, no significant difference in the growth of water-acclimated NTM and UV-C adapted isolates were observed (**Figure 5**). In comparing the UV-susceptibility between isolates of different species, it was observed that *M. abscessus* was most susceptible to UV-C treatment (100% killed in UV treatment), whereas *M. avium* and *M. chimaera* were less affected by UV-C treatment (**Figure 5**).

DISCUSSION

Methods to reduce environmental NTM exposures are critically needed. Because there is potential for NTM in tap water to be ingested and refluxed to cause lung infections (29, 30), suggestions to reduce bacterial numbers in drinking water are particularly important and timely. In this study, we tested a variety of physical methodologies to reduce NTM and demonstrate that both water filtration using Pall filters (section Efficient Removal of NTM by Pall Medical In-Line Filters) and UV-C irradiation (**Figures 1–4**) are effective in reducing the

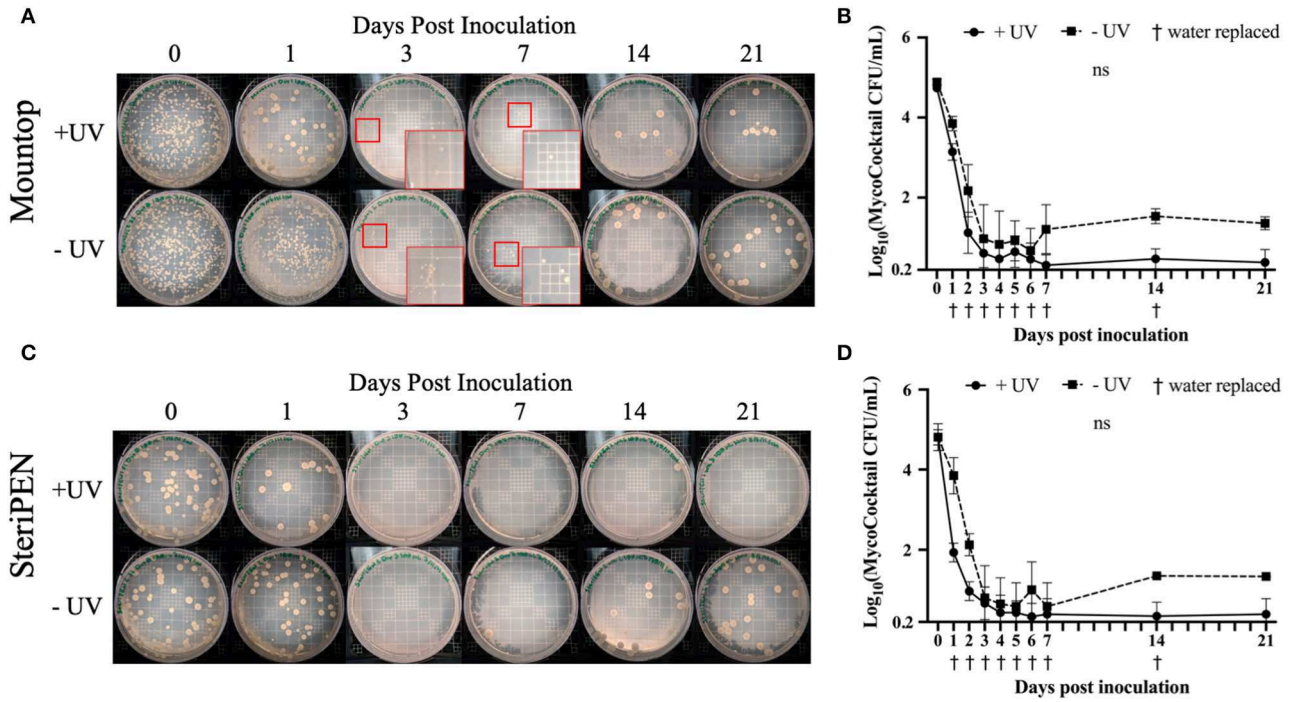

FIGURE 3 | The simple action of water replacement reduces NTM counts. Mountop **(A,B)** and SteriPEN **(C,D)** systems were inoculated with MycoCocktail and allowed to incubate at room temperature overnight. After incubation, the MycoCocktail was UV-C disinfected as per the manufacturer's protocol (+UV) or not exposed to UV (–UV). The suspensions within each system were filtered, plated for CFU, and the suspension replaced with sterile tap H_2O. CFU plating and water replacement was performed daily for 7 days and weekly up to 21 days post-inoculation. **(A,C)** Representative images of MycoCocktail CFU in Mountop and SteriPEN across 21 days of UV-disinfection. Smaller red boxes indicate regions where growth was difficult to visualize. Larger red boxes show colonies magnified ∼6-fold. **(B,D)** Log(MycoCocktail CFU) across 21 days with and without UV treatment by Mountop or SteriPEN. $n = 3$ (+UV) or $n = 2$ (–UV) independent CFU measurements per timepoint. ns, not significant.

number of *M. smegmatis* (Pall filter) as well as *M. abscessus*, *M. avium*, and *M. chimaera* (UV-C) from tap water.

In this work, we show that GAC filters do not prevent the passage of NTM and actually support the growth of NTM within the filter (**Tables 1**, **2**), results similar to other studies (15). However, in the case of point-of-use Pall filters and LifeStraw Go systems with ≤0.2 μm pore size, the reduction in CFU were at the limit of detection of NTM colonies, yet we refrain from making any wide-sweeping recommendations on whether whole residence or point-of-use filtration is more effective. Because it is likely that the majority of NTM in premise plumbing are resident in biofilms, whole-house filtration at the entry point for water would not theoretically be of use as the filtered water would be inoculated from the biofilm. However, we believe that point-of-use filtration at taps and showerheads would prove more effective in reducing exposure. It must be acknowledged that point-of-use filters are expensive and have a defined, manufacturer-indicated use life, after which they can break down or clog. To prevent clogging and extend its useful life, a 1- to 5-μm pore size prefilter can be employed to intercept larger particulates before they clog smaller pore size filters.

In assessments of Mountop and SteriPEN personal UV-C disinfection water bottle systems, we found that both systems were effective in eliminating *M. abscessus*, *M. avium*, and *M. chimaera* in a MycoCocktail (**Figure 1**) when the manufacturer's recommendations are followed. We also found that SteriPEN was more effective than Mountop in reducing NTM counts in water held in the bottle for 7 days (**Figure 2**). In the 21-day evaluation of suspension CFU with water replacement, a >3 log reduction in NTM CFU is observed both with and without UV treatment in either system (**Figure 3**). Because biofilm formation was found to contribute <1% of the total CFU contained within each bottle (**Figure 4**), it can be concluded that water replacement was responsible for the elimination of inoculum CFU in the absence of UV treatment. In contrast, when the water is not replaced regularly, the CFU remains rather stable across 7 days in the absence of UV and UV-C treatment reduces NTM counts (**Figure 2**) across a 7-day interval. This finding is corroborated by the observed decline in inoculum CFU after just a single UV treatment, in which the Mountop system eliminated 0.8850 log NTM CFU and SteriPEN eliminated 1.8603 log NTM CFU (**Figure 1**). The reduced disinfection efficacy of the Mountop bottle may be due to the innate architecture of the water bottle systems. In the Mountop system, UV is emitted from the bottle cap, whereas in the SteriPEN, the UV lamp is submerged in the water from the top to almost the bottom of the bottle. Therefore, as UV dose is a function of distance, cells are likely exposed to a

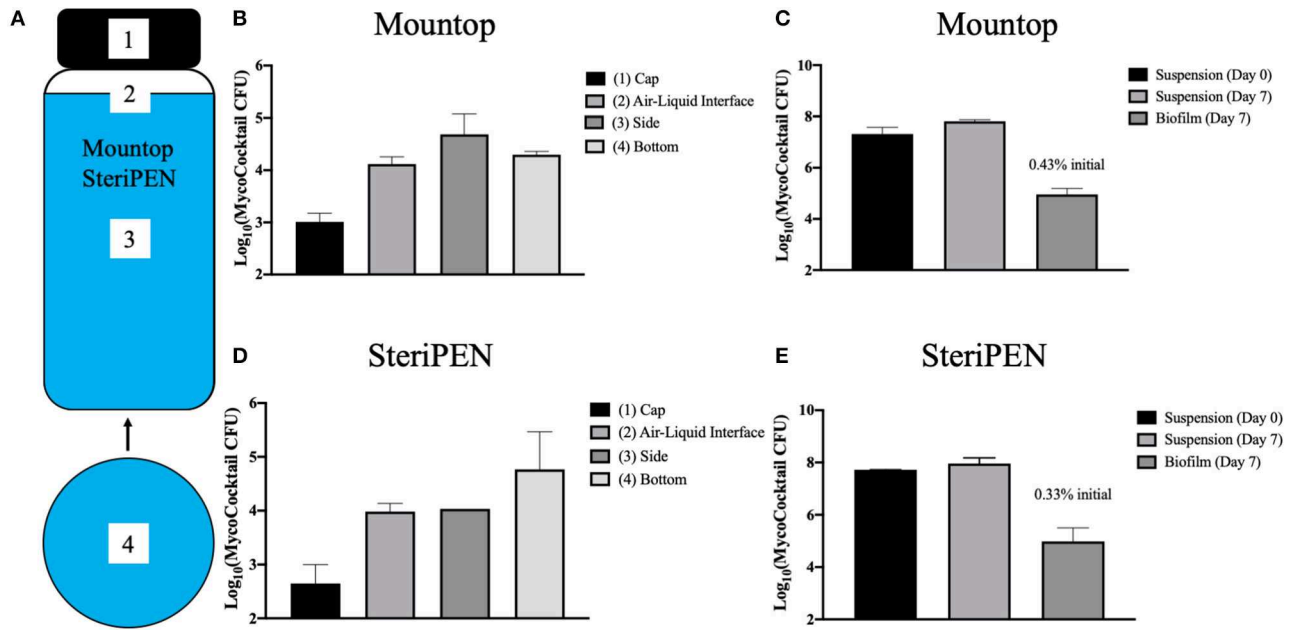

FIGURE 4 | Biofilm formation within Mountop and SteriPEN water bottles contribute little to total CFU. **(A)** Four regions of each water bottle system were sampled with sterile synthetic swabs to quantify biofilm-associated CFU: the interior surface of the bottle cap (1), a 4-cm^2 region at the air–liquid interface (2), a 4-cm^2 region completely submerged in inoculum (3), and a 4-cm^2 region of the interior bottom surface of the bottle (4). Mountop **(B,C)** and SteriPEN **(D,E)** systems were inoculated with MycoCocktail and an aliquot of the Day 0 suspension was plated for CFU. Bottles were then allowed to incubate undisturbed at room temperature for 7 days. At Day 7, an aliquot of the suspension was plated for CFU and biofilms within each system were sampled. Biofilm swabs were then plated for CFU and the CFU/cm^2 in each area was applied to each bottle's total surface area. Biofilm CFU was calculated as a percentage of the initial Day 0 suspension. **(B,D)** CFU of each region sampled for biofilm-associated CFU. **(C,E)** CFU of suspensions at Day 0 and Day 7 are compared to that of the biofilm at day 7. $n = 2$ independent experiments.

higher UV dose in the SteriPEN. Further, as UV must cross the air–liquid interface in the Mountop, it could be refracted, thus reducing dose (schema, **Supplementary Figure 3**). Although further analyses are needed to definitively determine why these two methods of UV treatment differ in their capacity to kill NTM, these findings suggest that the differences in the design of point-of-use UV-disinfection systems are important factors in their bactericidal activity. Thus, factors such as frequency of regular water replacement and the method of UV-C irradiation used likely contribute to NTM survival in these systems.

For UV-C irradiation to be effective, particulates should be removed by installation of a 1- to 5-μm pore size filter upstream of the irradiation unit and the clarity of the UV-irradiation chamber maintained by regular cleaning. Although the advantages of UV-disinfection for large- and small-scale applications is well-established, there is no information available to judge whether the dosages of UV are high enough in the bottles to increase the frequency of viable mutants; an unlikely but possible contraindication for its use. For example, would a consequence of UV disinfection in the bottles lead to the selection of UV-resistant mutants? Our data suggest that UV-C exposure does not lead to increased selection or production of UV-resistant NTM (**Figure 5**); however, more robust, large-scale analyses of the mutagenic consequences of repeated UV exposure on waterborne NTM are needed in future studies. In addition, although we found minimal biofilm formation on the inner surfaces of the water bottles after 7 days of incubation with MycoCocktail (**Figure 4**), the possibility of NTM-biofilm formation on unclean surfaces or in inadequately cleaned water bottles is likely to increase the resistance of tap water–associated NTM to disinfection by, potentially, a 100-fold (31).

A limitation of these studies is that NTM dose experiments were not performed, and conclusions are based on the change in CFU over time compared to the number of the initial inoculum and physical disinfection method used. However, as different species and isolates of NTM were tested, we predict that the results would be similar for other NTM species when testing these particular disinfection methods. In addition, although UV-C irradiation and filtration were independently assessed for their ability to reduce waterborne NTM burden, the compounding effect of both methods was not investigated in this study. Because both methods of water disinfection produced significant reductions in NTM CFU, we predict that the combination of methods would produce even more effective removal of NTM from drinking water. Furthermore, in order to be directly applicable to consumers, water treatment was only performed as designated by the manufacturers' protocols or typical use, and alternative treatment strategies that could have more significant impacts on NTM CFU were not investigated. Similarly, variables affecting typical consumer usage of these systems (i.e., water agitation, detergent-based cleaning, water storage container)

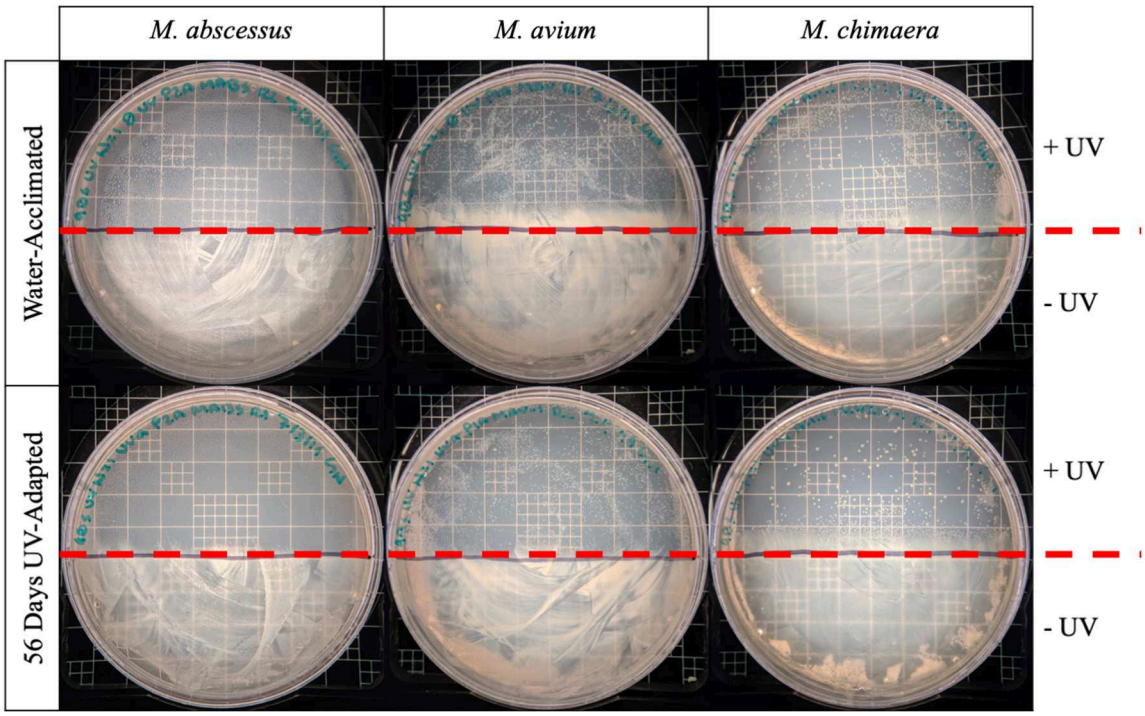

FIGURE 5 | Repeated UV exposure does not affect the susceptibility of NTM to UV-C. The sensitivity to UV-C treatment between unexposed (water acclimated, top row) *M. abscessus*, *M. avium*, and *M. chimaera* and 56-day UV-adapted *M. abscessus*, *M. avium*, and *M. chimaera* (56-days UV-adapted, bottom row) were compared for their ability to survive 90 s of UV-C irradiation. One hundred microliter of bacterial stock was spread onto 7H10 agar plates. Half of the plate was covered with by notecard to protect against UV-exposure and the other half was exposed directly to 254-nm UV-C light for 90 s. Plates were incubated at 37°C and the growth of the UV-C treated (above red line) and untreated (below red line) regions were visually compared.

were not manipulated in production of these data. The effect of UV and filter-based methods of water disinfection were performed using sterile tap water from Blacksburg, VA, or Denver, CO. Although the methods of disinfection assayed in this study worked equally well regardless of the tap water source, it is possible that variation in the chemistries of the tap water used in this study (i.e., pH, salinity, hardness) could have impacted the performance of the disinfection systems. Although beyond the scope of this study, it would be prudent to also test these methods of disinfection on the removal of NTM from natural waters, such as freshwater streams, where turbidity and leaf-litter likely impact the effectiveness of filtration or UV-disinfection (32).

Our results implicate the usefulness of filtration and UV-disinfection methodologies on the removal of NTM from U.S. municipal drinking water systems. However, in developing nations where access to municipal water may be limited, natural surface, and groundwater utilized for human consumption may also serve as important sources of NTM exposure. In rural West African communities and the Western Pacific, natural sources of drinking water, often of low quality, have been associated with *Mycobacterium ulcerans*, the causative agent of Buruli skin ulcers (33–36). However, the prevalence of pulmonary-associated NTM, such as MAC and *M. abscessus*, have not yet been extensively studied in respiratory specimens or in drinking water, which may be complicated by the high prevalence rates of *Mycobacterium tuberculosis* infection in certain low-income countries. Nonetheless, it would be useful to test the disinfection methods examined in this study for their effectiveness in removing NTM in drinking water from low-income countries globally and compare these results to drinking water from other developed countries where NTM pulmonary disease has been extensively studied (37–40).

Among the physical methods of water disinfection screened, both filtration and UV-C disinfection proved effective in significantly reducing the viable NTM population in spiked tap water. Based on these findings, we propose that commercially available water purification systems could provide a simple way for individuals at risk for NTM infection to reduce their exposure to waterborne NTM. Although further study is needed, these data are the first to address and suggest promise for point-of-use water purification devices against clinically relevant NTM species that reside in municipal drinking water systems of man-made built environments.

DATA AVAILABILITY STATEMENT

All datasets generated for this study are included in the article/**Supplementary Material**.

ETHICS STATEMENT

Clinical NTM isolates were from de-identified patients and ethical approval was reviewed by the National Jewish Health, Kaiser Permanente Hawai'i, and University of Colorado Institutional Review Boards (IRB) under protocols #HS-2903, FWA #00002344, and #15-0511, respectively, and determined the requirement for informed consent were waived.

AUTHOR CONTRIBUTIONS

JF and JH conceived and supervised the project. GN and MW performed the experiments. GN and JF performed statistical analyses. GN, JF, and JH wrote and edited all versions and the final manuscript.

ACKNOWLEDGMENTS

The Falkinham lab would like to acknowledge Pall Medical for their donation of the Pall in-line filters employed in the study and thank Karina Platt a 2010 Virginia Tech summer undergraduate research assistant for her contributions. The Honda lab recognizes the Holst Family for their inspiration, Dr. Edward Chan for thoughtful discussions, and support from the Padosi Foundation.

SUPPLEMENTARY MATERIAL

The Supplementary Material for this article can be found online at: https://www.frontiersin.org/articles/10.3389/fpubh.2020.00190/full#supplementary-material

REFERENCES

1. Strollo SE, Adjemian J, Adjemian MK, Prevots DR. The burden of pulmonary nontuberculous mycobacterial disease in the United States. *Ann Am Thorac Soc*. (2015) 12:1458–64. doi: 10.1513/AnnalsATS.201503-173OC
2. Al-Anazi KA, Al-Jasser AM, Al-Anazi WK. Infections caused by non-tuberculous *Mycobacteria* in recipients of hematopoietic stem cell transplantation. *Front Oncol*. (2014) 4:311. doi: 10.3389/fonc.2014.00311
3. Henkle E, Winthrop KL. Nontuberculous mycobacteria infections in immunosuppressed hosts. *Clin Chest Med*. (2015) 36:91–9. doi: 10.1016/j.ccm.2014.11.002
4. Yu JA, Pomerantz M, Bishop A, Weyant MJ, Mitchell JD. Lady Windermere revisited: treatment with thoracoscopic lobectomy/segmentectomy for right middle lobe and lingular bronchiectasis associated with non-tuberculous mycobacterial disease. *Eur J Cardiothorac Surg*. (2011) 40:671–5. doi: 10.1016/j.ejcts.2010.12.028
5. Kartalija M, Ovrutsky AR, Bryan CL, Pott GB, Fantuzzi G, Thomas J, et al. Patients with nontuberculous mycobacterial lung disease exhibit unique body and immune phenotypes. *Am J Respir Crit Care Med*. (2013) 187:197–205. doi: 10.1164/rccm.201206-1035OC
6. Olivier KN. Lady Windermere Dissected: More Form Than Fastidious. *Ann Am Thorac Soc*. (2016) 13:1674–6. doi: 10.1513/AnnalsATS.201607-521ED
7. Nishiuchi Y, Iwamoto T, Maruyama F. Infection sources of a common non-tuberculous *Mycobacterial pathogen*, *Mycobacterium avium* complex. *Front Med*. (2017) 4:27. doi: 10.3389/fmed.2017.00027
8. George KL, Parker BC, Gruft H, Falkinham JO 3rd. Epidemiology of infection by nontuberculous mycobacteria. II. Growth and survival in natural waters. *Am Rev Respir Dis*. (1980) 122:89–94.
9. Honda JR, Virdi R, Chan ED. Global environmental nontuberculous mycobacteria and their contemporaneous man-made and natural niches. *Front Microbiol*. (2018) 9:2029. doi: 10.3389/fmicb.2018.02029
10. Falkinham JO 3rd, Iseman MD, De Haas P, Van Soolingen D. *Mycobacterium avium* in a shower linked to pulmonary disease. *J Water Health*. (2008) 6:209–13. doi: 10.2166/wh.2008.232
11. Falkinham JO, Pruden A, Edwards M. Opportunistic premise plumbing *pathogens*: increasingly important pathogens in drinking water. *Pathogens*. (2015) 4:373–86. doi: 10.3390/pathogens4020373
12. Tu HZ, Chen CS, Huang TS, Huang WK, Chen YS, Liu YC, et al. Use of a disposable water filter for prevention of false-positive results due to nontuberculosis *Mycobacteria* in a clinical laboratory performing routine acid-fast staining for tuberculosis. *Appl Environ Microbiol*. (2007) 73:6296–8. doi: 10.1128/AEM.00325-07
13. Cervia JS, Farber B, Armellino D, Klocke J, Bayer RL, Mcalister M, et al. Point-of-use water filtration reduces healthcare-associated infections in bone marrow transplant recipients. *Transpl Infect Dis*. (2010) 12:238–41. doi: 10.1111/j.1399-3062.2009.00459.x
14. Perkins SD, Mayfield J, Fraser V, Angenent LT. Potentially pathogenic bacteria in shower water and air of a stem cell transplant unit. *Appl Environ Microbiol*. (2009) 75:5363–72. doi: 10.1128/AEM.00658-09
15. Rodgers MR, Blackstone BJ, Reyes AL, Covert TC. Colonisation of point of use water filters by silver resistant non-tuberculous *Mycobacteria*. *J Clin Pathol*. (1999) 52:629. doi: 10.1136/jcp.52.8.629a
16. Synder JWJr, Mains CN, Anderson RE, Bissonnette GK. Effect of point-of-use, activated carbon filters on the bacteriological quality of rural groundwater supplies. *Appl Environ Microbiol*. (1995) 61:4291–5. doi: 10.1128/AEM.61.12.4291-4295.1995
17. Taylor RH, Falkinham JO 3rd, Norton CD, Lechevallier MW. Chlorine, chloramine, chlorine dioxide, and ozone susceptibility of *Mycobacterium avium*. *Appl Environ Microbiol*. (2000) 66:1702–5. doi: 10.1128/AEM.66.4.1702-1705.2000
18. Bohrerova Z, Linden KG. Ultraviolet and chlorine disinfection of *Mycobacterium* in wastewater: effect of aggregation. *Water Environ Res*. (2006) 78:565–71. doi: 10.2175/106143006X99795
19. Yang JH, Wu UI, Tai HM, Sheng WH. Effectiveness of an ultraviolet-C disinfection system for reduction of healthcare-associated pathogens. *J Microbiol Immunol Infect*. (2019) 52:487–93. doi: 10.1016/j.jmii.2017.08.017
20. Santos AL, Oliveira V, Baptista I, Henriques I, Gomes NC, Almeida A, et al. Wavelength dependence of biological damage induced by UV radiation on bacteria. *Arch Microbiol*. (2013) 195:63–74. doi: 10.1007/s00203-012-0847-5
21. Nelson KY, Mcmartin DW, Yost CK, Runtz KJ, Ono T. Point-of-use water disinfection using UV light-emitting diodes to reduce bacterial contamination. *Environ Sci Pollut Res Int*. (2013) 20:5441–8. doi: 10.1007/s11356-013-1564-6
22. Shin GA, Lee JK, Freeman R, Cangelosi GA. Inactivation of Mycobacterium avium complex by UV irradiation. *Appl Environ Microbiol*. (2008) 74:7067–9. doi: 10.1128/AEM.00457-08
23. Hasan NA, Honda JR, Davidson RM, Epperson LE, Bankowski MJ, Chan ED, et al. Complete genome sequence of *Mycobacterium chimaera* strain AH16. *Genome Announc*. (2016) 4:16. doi: 10.1128/genomeA.01276-16
24. Camper AK, Lechevallier MW, Broadaway SC, Mcfeters GA. Evaluation of procedures to desorb bacteria from granular activated carbon. *J Microbiol Meth*. (1985) 3:187–98. doi: 10.1016/0167-7012(85)90046-6
25. Hydro-Photon, Inc. *SteriPEN Aqua User Guide*. (2014).
26. Shenzhen Mountop Outdoor Products Co., Ltd. *Mountop UV Water Purifier LED Lantern*. (2017).
27. Vaerewijck MJ, Huys G, Palomino JC, Swings J, Portaels F. Mycobacteria in drinking water distribution systems: ecology and significance for human health. *FEMS Microbiol Rev*. (2005) 29:911–34. doi: 10.1016/j.femsre.2005.02.001
28. Falkinham JO 3rd. Nontuberculous *Mycobacteria* from household plumbing of patients with nontuberculous mycobacteria disease. *Emerg Infect Dis*. (2011) 17:419–24. doi: 10.3201/eid1703.101510

29. Koh WJ, Lee JH, Kwon YS, Lee KS, Suh GY, Chung MP, et al. Prevalence of gastroesophageal reflux disease in patients with nontuberculous mycobacterial lung disease. *Chest*. (2007) 131:1825–30. doi: 10.1378/chest.06-2280
30. Thomson RM, Armstrong JG, Looke DF. Gastroesophageal reflux disease, acid suppression, and *Mycobacterium avium* complex pulmonary disease. *Chest*. (2007) 131:1166–72. doi: 10.1378/chest.06-1906
31. Steed KA, Falkinham JO 3rd. Effect of growth in biofilms on chlorine susceptibility of *Mycobacterium avium* and *Mycobacterium intracellulare*. *Appl Environ Microbiol*. (2006) 72:4007–11. doi: 10.1128/AEM.02573-05
32. WHO. *Results of Round II of the WHO International Scheme to Evaluate Household Water Treatment Technologies*. Geneva: World Health Organization (2019).
33. Dufour A, Cotruvo JA. *Pathogenic Mycobacteria in Water*. Cornwall: TJ International (lLtd) (2001).
34. Eddyani M, De Jonckheere JF, Durnez L, Suykerbuyk P, Leirs H, Portaels F. Occurrence of free-living amoebae in communities of low and high endemicity for Buruli ulcer in southern Benin. *Appl Environ Microbiol*. (2008) 74:6547–53. doi: 10.1128/AEM.01066-08
35. Lopez-Varela E, Garcia-Basteiro AL, Santiago B, Wagner D, Van Ingen J, Kampmann B. Non-tuberculous mycobacteria in children: muddying the waters of tuberculosis diagnosis. *Lancet Respir Med*. (2015) 3:244–56. doi: 10.1016/S2213-2600(15)00062-4
36. Yotsu RR, Suzuki K, Simmonds RE, Bedimo R, Ablordey A, Yeboah-Manu D, et al. Buruli ulcer: a review of the current knowledge. *Curr Trop Med Rep*. (2018) 5:247–56. doi: 10.1007/s40475-018-0166-2
37. Simons S, Van Ingen J, Hsueh PR, Van Hung N, Dekhuijzen PN, Boeree MJ, et al. Nontuberculous mycobacteria in respiratory tract infections, eastern Asia. *Emerg Infect Dis*. (2011) 17:343–9. doi: 10.3201/eid170310060
38. Chou MP, Clements AC, Thomson RM. A spatial epidemiological analysis of nontuberculous mycobacterial infections in Queensland, Australia. *BMC Infect Dis*. (2014) 14:279. doi: 10.1186/1471-2334-14-279
39. Marras TK, Campitelli MA, Lu H, Chung H, Brode SK, Marchand-Austin A, et al. Pulmonary Nontuberculous mycobacteria-associated deaths, Ontario, Canada, 2001-2013. *Emerg Infect Dis*. (2017) 23:468–76. doi: 10.3201/eid2303.161927
40. Axson EL, Bloom CI, Quint JK. Nontuberculous mycobacterial disease managed within UK primary care, 2006-2016. *Eur J Clin Microbiol Infect Dis*. (2018) 37:1795–803. doi: 10.1007/s10096-018-3315-6

Disclaimer: Tests were conducted without the knowledge or support of the manufacturers of Mountop or SteriPEN.

Conflict of Interest: The authors declare that the research was conducted in the absence of any commercial or financial relationships that could be construed as a potential conflict of interest.

frontiers in Medicine

CASE REPORT
published: 16 June 2020
doi: 10.3389/fmed.2020.00243

Disseminated *Mycobacterium chimaera* Following Open-Heart Surgery, the Heater–Cooler Unit Worldwide Outbreak: Case Report and Minireview

Emmanuel Lecorche[1,2,3]*, *Gauthier Pean de Ponfilly*[3], *Faiza Mougari*[1,2,3], *Hanaa Benmansour*[1,2,3], *Elodie Poisnel*[4], *Frederic Janvier*[5,6] and *Emmanuelle Cambau*[1,2,3] *on behalf of CNR-MyRMA*

[1] Université de Paris, IAME, INSERM, UMR1137, UFR de Médecine, Paris, France, [2] CNR-MyRMA, Centre National de Reference pour les Mycobactéries et les Antituberculeux, APHP, Paris, France, [3] APHP, Hôpital Lariboisière, Service de Microbiologie, Paris, France, [4] Service de Medecine Interne, Hôpital d'Instruction des Armées Sainte Anne, Toulon, France, [5] Service de microbiologie, Hôpital d'Instruction des Armées Sainte Anne, Toulon, France, [6] Ecole du Val-de-Grâce, Paris, France

OPEN ACCESS

Edited by:
Nicola Petrosillo,
Istituto Nazionale per le Malattie Infettive Lazzaro Spallanzani (IRCCS), Italy

Reviewed by:
Thomas Rogers,
Trinity College Dublin, Ireland
Emanuele Durante Mangoni,
University of Campania Luigi Vanvitelli, Italy

***Correspondence:**
Emmanuel Lecorche
emmanuel.lecorche@aphp.fr

Specialty section:
This article was submitted to Infectious Diseases – Surveillance, Prevention and Treatment, a section of the journal Frontiers in Medicine

Received: 07 October 2019
Accepted: 07 May 2020
Published: 16 June 2020

Citation:
Lecorche E, Pean de Ponfilly G, Mougari F, Benmansour H, Poisnel E, Janvier F and Cambau E (2020) Disseminated Mycobacterium chimaera Following Open-Heart Surgery, the Heater–Cooler Unit Worldwide Outbreak: Case Report and Minireview. Front. Med. 7:243. doi: 10.3389/fmed.2020.00243

Invasive cardiovascular infections by *Mycobacterium chimaera* associated with open-heart surgery have been reported worldwide since 2013. Here, we report a case of a 61 year old man, without any other particular medical background, who underwent cardiac surgery for replacing part of the ascending aorta by a bio-prosthetic graft. Eighteen months later, the patient was painful at the lower back with fever. A pyogenic vertebral osteomyelitis due to *M. chimaera* associated to graft infection was diagnosed after 6 months of sub-acute infection. The patient presented a disseminated disease with cerebral lesions, chorioretinitis, and chronic renal failure. Despite adequate antimicrobial treatment and graft explantation, the patient died after 6 years. We reviewed the literature on *M. chimaera* infections associated with open-heart surgery. The worldwide outbreak has been explained by airborne bioaerosol generated by the 3T heater–cooler unit (HCU) used during cardiac by-pass surgical procedures. These infections are difficult to diagnose because of a long latency period (up to several years), with no specific symptoms and a highly specialized microbiological diagnosis. The treatment is based on antibiotics and surgery. These infections are also difficult to treat, since the mortality rate is high around 50%. Prevention is necessary by modifying the use of HCUs in operating rooms.

Keywords: HCU, cardiac surgery, non-tuberculous mycobacteria, NTM, spondylodiscitis

BACKGROUND

Invasive cardiovascular infections due to *M. chimaera* secondary to open-heart surgery were first described in 2015 in Switzerland (1). These infections are difficult to diagnose because of non-specific symptoms, a difficult microbiological diagnostic, and a poor prognostic. They were attributed to contamination from the heater-cooler units (HCU) present in the operating rooms since similar strains of *M. chimaera* were found in their water tanks. In addition, since the strains from several patients, who underwent surgery at different periods, were also similar, a

common reservoir was sought. Since 2015, cases were reported worldwide not only in Europe (Switzerland, Germany, Netherlands, England, France, Italia, Spain, and Ireland) (1–6), but also in North America (United-States, Canada) (7, 8), Hong-Kong (9), New-Zeeland, and Australia (10). Most of the cases were due to the same epidemic strain similar to those found also in the HCUs (11). The epidemic strain has also been found in HCUs in China (12). In 2015, the European Center for Disease Prevention and Control issued a Rapid Risk Assessment (13) and the Food and Drug Administration published as well a safety communication about infections associated with heater-cooler devices and recommendations to deal with the risk (14).

Here, we report the case of a patient diagnosed in France for a *M. chimaera* infection following cardiac surgery, and subsequently reviewed the literature about this outbreak and discussed the patient case.

CASE PRESENTATION

A 61 year old man, without any particular medical background, underwent cardiac surgery in 2012 for replacing part of the ascending aorta by a bio-prosthetic graft and repairing the aortic arch due to a type I aortic dissection. During immediate follow up, a local infection was diagnosed at the coronary angiography insertion site. Since it was show to be caused by *Proteus mirabilis* and *Pseudomonas aeruginosa*, the patient was treated with 10 days of ceftazidime.

Eighteen months after the surgery (M18, see **Figure 1**), the patient presented fewer with a lower back pain that was intensified for 1 month. A positron emission tomography/computed tomography (PET-CT) suspected a graft infection with a pseudoaneurysm para-aortic. A transthoracic echocardiography did not show any signs of endocarditis and blood cultures remained negative. An empirical treatment was initiated with piperacillin-tazobactam, teicoplanin, and rifampicin.

At M24, vertebral magnetic resonance imaging (MRI) revealed lesions of the vertebral bodies at T8-T9-L4-L5-S1 and intervertebral disks between T8-T9 and L4-L5-S1, with an epidural abscess of 5 cm at the L3 and L4 levels, consistent with a pyogenic vertebral osteomyelitis (**Figure 2**). That was consistent with the PET-CT results showing metabolic activity around the peri-aortic graft in favor of infection. Transcutaneous vertebral biopsies, made at M27, were culture-positive for acid fast bacilli (AFB) after 21 days incubation on 7H9 liquid medium (BACT/ALERT® MP, Biomerieux) and subsequently on Lowenstein Jensen solid medium (Bio-Rad). The AFB isolate was identified first as *M. intracellulare* by GenoType® Mycobacterium CM (Hain Lifescience), and subsequently confirmed as *M. chimaera* by GenoType® NTM-DR (Hain Lifescience), ITS and *hsp65* sequencing. Susceptibility testing of the isolate was performed using a commercial microdilution method, SLOMYCO Myco Sensititre™ (Thermo Scientific™) and showed a wild type susceptibility pattern with a minimal inhibitory concentration (MIC) of clarithromycin at 2 mg/L, MIC of amikacin at 8 mg/L, MIC of linezolid at 32 mg/L and MIC of moxifloxacin at 4 mg/L. Three mycobacterial blood cultures performed at the same period were also positive for *M. chimaera*. The patient was treated with a 4-antibiotic regimen combining azithromycin, ethambutol, rifampicin, and moxifloxacin. The risk associated with graft explantation was felt to be prohibitively high, and the decision was therefore made to proceed with conservative management.

At M 29, 2 months after antimicrobial therapy has started, an ocular examination showed a bilateral chorioretinitis associated with uveitis of the left eye. At M30, a MRI of the brain, performed because of confusion, revealed diffuse hypersignals of both hemispheres consistent with cerebral miliary lesions. The patient showed then a worsening of the vertebral lesions and of the renal function. Because of the disseminated infection, it was decided to replace the aortic graft at M39. *M. chimaera* was isolated from explanted prosthetic tissues.

At M44, the patient underwent arthrodesis of thoracic spine. Due to the chronic renal failure, an arteriovenous fistula was created at M53. The patient showed pancytopenia at M72. At M73, the patient suffered from hepatic and neurologic decompensation. Unfortunately, the patient died at M78.

THE WORLDWIDE OUTBREAK OF DISSEMINATED *M. CHIMAERA* INFECTION ASSOCIATED TO OPEN-HEART SURGERY

The Causative Agent

M. chimaera is a slow growing non-tuberculous mycobacterium (NTM) belonging to the *Mycobacterium avium* complex (MAC) (15) and was first described in 2004 (16). Like *M. avium* and *M. intracellulare*, *M. chimaera* is predominantly seen in immunocompromised patients and in pulmonary infections in patients with chronic lung diseases. Among patients with sputum culture-positive with MAC, the patients with *M. chimaera* were less likely to meet criteria for infection than *M. avium* and *M. intracellulare*, suggesting a lower virulence or a different reservoir (17, 18). The natural reservoir of *M. chimaera* is not well-known and is supposed to be similar to other species of MAC. MAC can be found in distribution water systems (19) and *M. chimaera* was found frequently in household water (20). Drug susceptibility patterns of *M. chimaera* are comparable to those of the MAC with modal MIC of 2 mg/L for clarithromycin, 0.5 mg/L for rifabutin, 4–8 mg/L for rifampicin and ethambutol, 8 mg/L for amikacin, 4 mg/L for moxifloxacine, and 32 mg/L for linezolid (21).

Burden and Impact of the Disease

Over 120 cases of post-cardiac surgery *M. chimaera* infections have been reported worldwide. More cases are to be expected since many countries did not register any cases. Using data from Switzerland, the incidence of *M. chimaera* disseminated disease associated with open heart surgery was estimated to 156–282 cases per year in the 10 major cardiac valve replacement market countries (22). Using data from the national British investigation, the risk of *M. chimaera* infection for person who underwent cardiothoracic surgery significantly increased since 2012. Out of 10,000 patients undergoing open heart surgery, 300–400 were estimated to experience endocarditis by 5 years post-surgery and one to develop *M. chimaera* infection (2). A long latency period (median of 21 months) was observed between cardiac

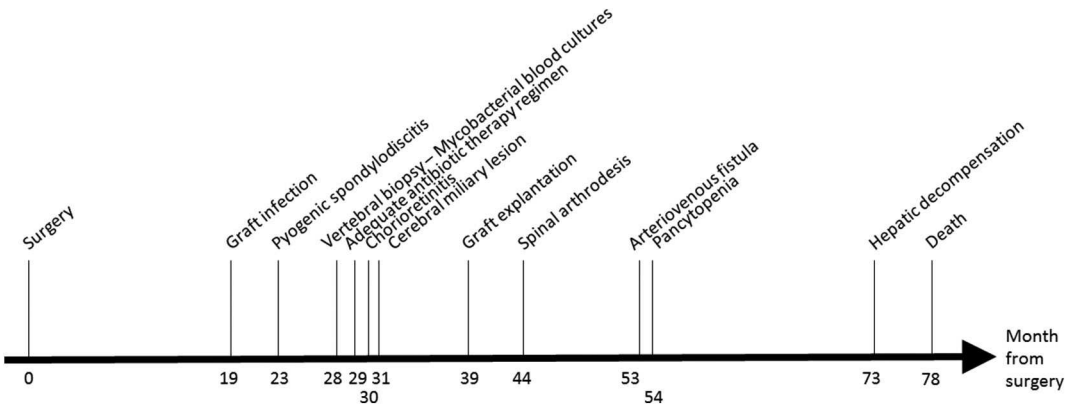

FIGURE 1 | Timeline of the patient's clinical course after cardiac surgery.

FIGURE 2 | Vertebral magnetic resonance imaging of the vertebral lesions. Vertebral magnetic resonance imaging revealed lesions of the vertebral bodies at T8-T9-L4-L5-S1 and invertebral disks between T8-T9 **(A)** and L4-L5-S1 **(B)**, with an epidural abscess of 5 cm at the L3 and L4 levels, consistent with a pyogenic vertebral osteomyelitis.

surgery and symptoms (23). The reported mortality rate for these infections was remarkably high, around 50% (24, 25). No cases were reported in healthcare workers related to the HCU epidemic. However, one case of *M. chimaera* pulmonary infection has been described in a healthcare worker previously exposed to HCU (26). Other devices such as thermoregulatory devices used for extracorporeal membrane oxygenation (ECMO) may be also at risk of transmission, but no cases were reported (27).

Transmission Routes

The first report described two cases, caused by closely related *M. chimaera* strains, as assessed by randomly amplified polymorphic DNA (RAPD)-PCR. The two patients had heart surgery 2 years apart from each other (28). Due to identical RAPD-PCR patterns, a deeper investigation was retrospectively conducted and six cases were finally detected in the institution (1). The prospective on-site observations and microbiological sampling in the hospital environment showed that *M. chimaera* was present in water circuits of the LivaNova HCU (25). HCU are essential components of cardiopulmonary bypass operation used during open-chest heart surgery. They are connected to the extracorporeal circuit enabling the warming of the patient's blood and the cooling of the cardioplegia solution, since tanks are filled with water. Water in the circuits does not come into direct contact with the patient. Interestingly, air sampling cultures in the operating room were also positive with *M. chimaera* when a HCU was running, but not when it was turned off. Laser particle measurement and microbial air cultures confirmed that during operation, mycobacterial particles were dispersed from the contaminated HCU into the air of the operating room via aerosolization, despite ultraclean air ventilation (27). The aerosol

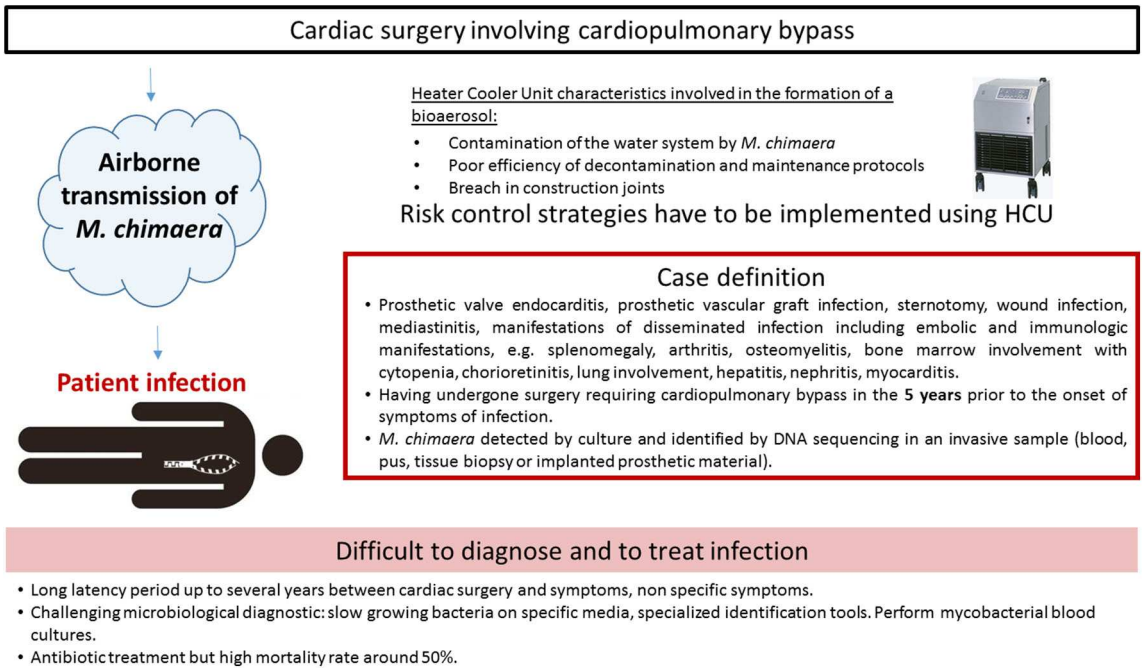

FIGURE 3 | *Mycobacterium chimaera* infections associated with open heart surgery characteristics.

was generated through a breach in construction joints on the tank cover and released into the operating environment via the rear cooling fan, thereby causing infection (10). Phylogenetic analysis by whole genome sequencing (WGS) showed a strong clustering of all *M. chimaera* epidemic isolates. They were indeed clonal isolates around the world in Europe, North America, or Australia (2, 29). Moreover, this cluster comprised isolates from patients, HCUs and water at the HCU industry production site (30). The most plausible hypothesis of such genetic similarity is that the devices were contaminated by a point source when manufactured before being sent to the cardiac surgery wards. Contamination and infections characteristics are presented in **Figure 3**.

Risk Factors

In the majority of cases, patients had undergone cardiac valve or aortic vascular graft surgery prior to diagnosis. However, patients who have undergone other operations that involve cardiopulmonary bypass, including heart or lung transplantation and introduction of ventricular assist devices are also at risk (23). To our knowledge, no cases have been described with other devices than LivaNova, formerly Sorin. It has been shown that the odds of NTM infection increase with the duration time a patient is exposed to a running HCU. The risk reached statistical significance for surgery time longer than 5 h (29). Survival analysis measured for a cohort of 30 cases identified several factors associated with better survival: younger age, mitral valve surgery, mechanical valve replacement, higher serum sodium concentration (30).

DIAGNOSIS AND TREATMENT

Clinical Manifestations

Patients exhibited a wide spectrum of disease including surgical site infection, e.g., prosthetic valve endocarditis (PVE), aortic graft infection or localized thoracic infection, as well as disseminated infection with diverse presentations, such as bacteraemia, osteomyelitis or other bone lesions, cholestatic hepatitis, granulomatous nephritis. Disseminated disease with encephalitis have also been described (31). Patients most commonly complained of non-specific symptoms such as fever, malaise, weight loss, cough, or dyspnea. Laboratory findings included cytopenia and elevated inflammatory markers, transaminase and creatinine blood levels (24). Eye involvement was correlated with the course of the systemic disease. Patients with few choroidal lesions had a favorable outcome, whereas all patients with widespread chorioretinitis died of systemic complications (32). Complications of *M. chimaera* infection are listed in **Table 1**.

Diagnosis

The European Center for Disease Prevention (33) and the American Center for Disease Control and Prevention (34) have formulated a case definition for *M. chimaera* infections associated with open heart surgery based on three criteria: (i) any of the clinical criteria, including prosthetic valve or vascular infection, localized infection, and disseminated infection, (ii) an exposure criteria, e.g., having undergone surgery requiring cardiopulmonary bypass in the 5 years prior to the onset of symptoms of infection, (iii) microbiological criteria, e.g., *M.*

TABLE 1 | Complications of *M. chimaera* infection.

Constitutional symptoms	Fever, fatigue, weight loss, night sweats, joint pain, shortness of breath
Cardiac	Prosthetic valve endocarditis and/or prosthetic vascular graft infection, pseudoaneurysm, aortic root abscess, aortic dissection, myocarditis
Localized infections	Surgical site infection, sternotomy wound infection mediastinitis
Embolic and immunologic manifestations	Splenomegaly, hepatitis, nephritis, disseminated granulomatous disease
Ocular infection	Chorioretinitis, panuveitis
Bone infection and bone marrow involvement	Cytopenia, osteomyelitis, spondylodiscitis arthritis

chimaera detected by culture or identified by DNA sequencing in an invasive sample. A 5 years period from surgery to presentation of symptoms has been mentioned, but the delay before diagnosis can be longer, the longest reported time being more than 6 years (35).

Mycobacterial cultures remain the essential investigation for all sample types: blood, tissue and bone biopsy, pus, and urine. Culture of *M. chimaera* from peripheral blood is the most common method of microbiological diagnosis (30). Its sensitivity increases by performing multiple samples: 3 sets of mycobacterial blood cultures on different days are recommended by the English guidance (36). It is essential to inform the laboratory of the possibility of *M. chimaera* infection, in order to ensure samples are taken into the correct containers, such as blood culture bottle specific for mycobacterial growth (e.g., BACTEC^{TM} Myco/F Lytic). Molecular technologies based on acid nucleic amplification can be used, especially on sterile samples (tissue biopsies, vascular graft) positive for acid fast bacilli at microscopic examination.

M. chimaera identification is challenging. It is slow growing in liquid and solid media, so growth detection may take between 2 and 8 weeks. Most laboratories can identify a *M. chimaera* isolate as a species of the *M. avium* complex (MAC), but precise speciation needs specialized tests (15), such as PCR sequencing of the internal transcribed spacer (ITS) sequence between 16S and 23S ribosomal DNA. *M. chimaera* is closely related to *M. intracellulare,* for instance they show only a single nucleotide difference in 16S ribosomal DNA sequences. *M. chimaera* can be misidentified as *M. intracellulare* by mass spectrometry (MALDI-TOF MS) or some commercial DNA hybridization probe assays (37). In fact, *M. chimaera* has been extensively classified as *M. intracellulare* before 2004 (18). Analysis of WGS is necessary to assess whether a clinical strain is related to the HCU outbreak strain (11). Microbiologic results should be considered alongside histopathology findings, e.g., detection of non-caseating granuloma and foamy macrophages with acid fast bacilli in cardiac or vascular tissues, prosthetic material, or in specimen from the sternotomy wound.

Transesophageal echocardiography (TOE) was shown to be more sensitive than transthoracic echocardiography in diagnosing *M. chimaera* PVE (3). TOE can be normal at presentation, while the patient later went on be diagnosed with PVE (30). Normal echocardiogram alone cannot be used to exclude infection and serial assessment should be considered. Computed tomography (CT) can assess aortic graft infection. Moreover PET-CT provides additional evidence in which standard CT has been equivocal and has also proved useful in the diagnosis of *M. chimaera* spondylodiscitis and PVE.

Differential Diagnosis

The presentation and laboratory features of the disease can be very similar to sarcoidosis (29). *M. chimaera* investigations should be undertaken in all patients for whom a diagnosis of sarcoidosis is being considered and who has an appropriate history of cardiothoracic surgery.

Treatment

The optimal treatment for *M. chimaera* HCU-related infections is not known. The combination of clarithromycin or azithromycin, rifampin, or rifabutin and ethambutol is the treatment regimen designed on the basis of that recommended for MAC lung disease (38). Antimicrobial susceptibility of *M. chimaera* strains isolated during the outbreak were fortunately all susceptible to clarithromycin and amikacin (3, 39). Given the disseminated nature of HCU-related infections and the poor outcome, parenteral amikacin, and fluoroquinolones were added (24, 40). According to guidelines, a minimum of 12 months therapy is indicated for non-HIV patients with disseminated MAC disease (38). The optimal duration of therapy in HCU-related infections is unknown and some patients required treatment for more than 24 months. Blood drug concentrations have to be monitored, a study reporting that half of the patients did not reached optimal drug levels (3). The removal of prosthetic materials was associated with a lower risk of mortality for classical PVE (41). Given technical difficulties and the risk of surgery, such decision has to be discussed with the cardiovascular surgeon in case of invasive infection with *M. chimaera* (30).

Preventive Measures

Several measures were proposed to minimize the risks of *M. chimaera* infections. The manufacturer updated its disinfection recommendations in 2015 with more frequent cleaning and disinfections of the water system (42). In addition, the manufacturer proposed complete refurbishment and replacement of the internal tubing of devices. Despite intensified cleaning and disinfection, surveillance samples from factory-new units still grew *M. chimaera* (43). Environmental testing and microbiological screening of HCUs could be performed. However, there is no standardization with regard to the collection of samples and the laboratory methods used (44).

Due to the difficulties to maintain water with good microbiological quality, different strategies were implemented in hospitals (45). The most definitive option was to remove HCUs from the operating room, though this may not be feasible for all facilities. A custom-made airtight housing for the HCU was also used in order to contain the bioaerosol. If a definitive mitigation strategy cannot be implemented, HCU should be oriented so that the aerosol from the exhaust is directed in the opposite way from the patient. However, the utility of this strategy is unproven and may continue to place the patient at risk (12).

DISCUSSION

M. chimaera was initially described in respiratory samples (16). Only one case of vertebral osteomyelitis was reported in a patient with prednisolone treatment, without history of cardiac surgery (46). Cases of disseminated *M. chimaera* infections were rare until 2015 (25). The involvement of this species in disseminated disease was quite unusual and led to the description of this outbreak associated with cardiac surgery. In the case of our patient, the surgery was performed in 2012 when the risk due to contaminated HCU was not known yet. The microbial diagnosis was rapidly done when the spondylodiscitis diagnosis was made, and isolation and identification of *M. chimaera* was done in a laboratory with expertise. The strain was genomically sequenced and was shown to cluster with the epidemic isolates. No sample was obtained from the HCU in this hospital at the time of the contamination and later. Although an adequate antimicrobial treatment was immediately given, the patient died 78 months later. We may think that an earlier replacement of aortic graft could have helped in the cure of the infection, but surgery could have been also lethal (40).

This case was the only one registered in this area of France, a second case being registered in the Paris area in 2010 were detailed elsewhere (47).

DATA AVAILABILITY STATEMENT

The data sequencing are now available on the NCBI platform (PRJNA576780, SAMN13008644, SRR10256732).

ETHICS STATEMENT

Written informed consent was obtained from the individual's next of kin for the publication of any potentially identifiable images or data included in this article.

AUTHOR CONTRIBUTIONS

EL, GP, and EC contributed to the manuscript. GP review the clinical case and EL reviewed the literature. EP took care of the patient. FM, HB, and FJ provide clinical and microbiological data. EC supervised this work.

FUNDING

CNR-MyRMA receives an annual grant from Santé Publique France and DGOS.

ACKNOWLEDGMENTS

We thank the technicians of Lariboisière Bacteriology laboratory for their expert technical assistance: Christine Bisilliat-Gardet, Véronique Charlier, Marie-Emmanuelle Hemet, Marilyne Lemaire, Isabelle Lacrampe, Patricia Lawson-Body, Marie Monjean, Fabienne Meunier, Sylvie Tenza, Odile Vissouarn, and all the others members of the laboratory. Collaborators: Alexandra Aubry, Isabelle Bonnet, Jeremy Jaffre, Vincent Jarlier, Hervé Jacquier, Florence Morel, Jerome Robert, Sabrina Temim, and Wladimir Sougakoff.

REFERENCES

1. Sax H, Bloemberg G, Hasse B, Sommerstein R, Kohler P, Achermann Y, et al. Prolonged outbreak of *Mycobacterium chimaera* infection after open-chest heart surgery. *Clin Infect Dis.* (2015) 61:67–75. doi: 10.1093/cid/civ198
2. Chand M, Lamagni T, Kranzer K, Hedge J, Moore G, Parks S, et al. Insidious risk of severe *Mycobacterium chimaera* infection in cardiac surgery patients. *Clin Infect Dis.* (2017) 64:335–42. doi: 10.1093/cid/ciw754
3. Kohler P, Kuster SP, Bloemberg G, Schulthess B, Frank M, Tanner FC, et al. Healthcare-associated prosthetic heart valve, aortic vascular graft, and disseminated *Mycobacterium chimaera* infections subsequent to open heart surgery. *Eur Heart J.* (2015) 36:2745–53. doi: 10.1093/eurheartj/ehv342
4. Cappabianca G, Paparella D, D'Onofrio A, Caprili L, Minniti G, Lanzafame M, et al. *Mycobacterium chimaera* infections following cardiac surgery in Italy: results from a National Survey Endorsed by the Italian Society of Cardiac Surgery. *J Cardiovasc Med.* (2018) 19:748–55. doi: 10.2459/JCM.0000000000000717
5. Zegri-Reiriz I, Cobo-Marcos M, Rodriguez-Alfonso B, Millán R, Dominguez F, Forteza A, et al. Successful treatment of healthcare-associated *Mycobacterium chimaera* prosthetic infective endocarditis: the first Spanish case report. *Eur Heart J Case Rep.* (2018) 2:yty142. doi: 10.1093/ehjcr/yty142
6. Health Protection Surveillance Centre (HPSC). *Report of Case Finding Investigation to Identify Mycobacterium chimaera Infections Potentially Associated with Heater-Cooler Units Used During cardiothoracic Surgery in Ireland* (2016).
7. Tan N, Sampath R, Abu Saleh OM, Tweet MS, Jevremovic D, Alniemi S, et al. Disseminated *Mycobacterium chimaera* infection after cardiothoracic surgery. *Open Forum Infect Dis.* (2016) 3:ofw131. doi: 10.1093/ofid/ofw131
8. Hamad R, Noly P-E, Perrault LP, Pellerin M, Demers P. *Mycobacterium chimaera* infection after cardiac surgery: first Canadian outbreak. *Ann Thorac Surg.* (2017) 104:e43–e5. doi: 10.1016/j.athoracsur.2017.01.115
9. Cheng VCC, Wong SC, Chen JHK, Wong SCY, Yuen KY. *Mycobacterium chimaera*-contaminated heater-cooler devices: the inner surface as the missing link? *J Hosp Infect.* (2018) 100:e157–e8. doi: 10.1016/j.jhin.2018.07.010
10. Robertson J, McLellan S, Donnan E, Sketcher-Baker K, Wakefield J, Coulter C. Responding to *Mycobacterium chimaera* heater-cooler unit contamination: international and national intersectoral collaboration coordinated in the state of Queensland, Australia. *J Hosp Infect.* (2018) 100:e77–e84. doi: 10.1016/j.jhin.2018.07.024
11. van Ingen J, Kohl TA, Kranzer K, Hasse B, Keller PM, Katarzyna Szafranska A, et al. Global outbreak of severe *Mycobacterium chimaera* disease after cardiac surgery: a molecular epidemiological study. *Lancet Infect Dis.* (2017) 17:1033–41. doi: 10.1016/S1473-3099(17)30324-9
12. Zhang X, Lin J, Feng Y, Wang X, McNally A, Zong Z. Identification of *Mycobacterium chimaera* in heater-cooler units in China. *Sci Rep.* (2018) 8:7843. doi: 10.1038/s41598-018-26289-5
13. European Centre for Disease Prevention and Control. *Invasive Cardiovascular Infection by Mycobacterium chimaera - 30 April 2015.* © European Centre for Disease Prevention and Control, Stockholm (2015).
14. Safety Communications. *Nontuberculous Mycobacterium Infections Associated with Heater-Cooler Devices*. FDA Safety Communication. Available online at: http://wayback.archive-it.org/7993/20170722215713/https:/www.fda.gov/MedicalDevices/Safety/AlertsandNotices/ucm466963.htm (Accessed April 12, 2019).
15. van Ingen J, Turenne CY, Tortoli E, Wallace RJ, Brown-Elliott BA. A definition of the *Mycobacterium avium* complex for taxonomical and clinical purposes, a review. *Int J Syst Evol Microbiol.* (2018) 68:3666–77. doi: 10.1099/ijsem.0.003026
16. Tortoli E, Rindi L, Garcia MJ, Chiaradonna P, Dei R, Garzelli C, et al. Proposal to elevate the genetic variant MAC-A, included in the *Mycobacterium avium* complex, to species rank as *Mycobacterium chimaera* sp. nov. *Int J Syst Evol Microbiol.* (2004) 54:1277–85. doi: 10.1099/ijs.0.02777-0

17. Boyle DP, Zembower TR, Reddy S, Qi C. Comparison of clinical features, virulence, and relapse among *Mycobacterium avium* complex species. *Am J Respir Crit Care Med.* (2015) 191:1310–7. doi: 10.1164/rccm.201501-0067OC
18. Schweickert B, Goldenberg O, Richter E, Göbel UB, Petrich A, Buchholz P, et al. Occurrence and clinical relevance of *Mycobacterium chimaera* sp. nov., Germany. *Emerging Infect Dis.* (2008) 14:1443–6. doi: 10.3201/eid1409.071032
19. Falkinham JO, Norton CD, LeChevallier MW. Factors influencing numbers of *Mycobacterium avium*, *Mycobacterium intracellulare*, and other Mycobacteria in drinking water distribution systems. *Appl Environ Microbiol.* (2001) 67:1225–31. doi: 10.1128/AEM.67.3.1225-1231.2001
20. Wallace RJ, Iakhiaeva E, Williams MD, Brown-Elliott BA, Vasireddy S, Vasireddy R, et al. Absence of *Mycobacterium intracellulare* and presence of *Mycobacterium chimaera* in household water and biofilm samples of patients in the United States with *Mycobacterium avium* complex respiratory disease. *J Clin Microbiol.* (2013) 51:1747–52. doi: 10.1128/JCM.00186-13
21. Maurer FP, Pohle P, Kernbach M, Sievert D, Hillemann D, Rupp J, et al. Differential drug susceptibility patterns of *Mycobacterium chimaera* and other members of the *Mycobacterium avium-intracellulare* complex. *Clin Microbiol Infect.* (2019) 25:379.e1–e7. doi: 10.1016/j.cmi.2018.06.010
22. Sommerstein R, Hasse B, Marschall J, Sax H, Genoni M, Schlegel M, Widmer AF. Swiss Chimaera taskforce. Global health estimate of invasive *Mycobacterium chimaera* infections associated with heater-cooler devices in cardiac surgery. *Emerging Infect Dis.* (2018) 24:576–8. doi: 10.3201/eid2403.171554
23. Sommerstein R, Schreiber PW, Diekema DJ, Edmond MB, Hasse B, Marschall J, et al. *Mycobacterium chimaera* outbreak associated with heater-cooler devices: piecing the puzzle together. *Infect Control Hosp Epidemiol.* (2017) 38:103–8. doi: 10.1017/ice.2016.283
24. Kasperbauer SH, Daley CL. *Mycobacterium chimaera* infections related to the heater-cooler unit outbreak: a guide to diagnosis and management. *Clin Infect Dis.* (2019) 68:1244–50. doi: 10.1093/cid/ciy789
25. Schreiber PW, Sax H. *Mycobacterium chimaera* infections associated with heater-cooler units in cardiac surgery. *Curr Opin Infect Dis.* (2017) 30:388–94. doi: 10.1097/QCO.0000000000000385
26. Rosero CI, Shams WE. *Mycobacterium chimaera* infection masquerading as a lung mass in a healthcare worker. *IDCases.* (2019) 15:e00526. doi: 10.1016/j.idcr.2019.e00526
27. Trudzinski FC, Schlotthauer U, Kamp A, Hennemann K, Muellenbach RM, Reischl U, et al. Clinical implications of *Mycobacterium chimaera* detection in thermoregulatory devices used for extracorporeal membrane oxygenation (ECMO), Germany, 2015 to 2016. *Euro Surveill.* (2016) 21:30398. doi: 10.2807/1560-7917.ES.2016.21.46.30398
28. Achermann Y, Rössle M, Hoffmann M, Deggim V, Kuster S, Zimmermann DR, et al. Prosthetic valve endocarditis and bloodstream infection due to *Mycobacterium chimaera*. *J Clin Microbiol.* (2013) 51:1769–73. doi: 10.1128/JCM.00435-13
29. Lyman MM, Grigg C, Kinsey CB, Keckler MS, Moulton-Meissner H, Cooper E, et al. Invasive nontuberculous mycobacterial infections among cardiothoracic surgical patients exposed to heater-cooler devices[1]. *Emerg Infect Dis.* (2017) 23:796–805. doi: 10.3201/eid2305.161899
30. Scriven JE, Scobie A, Verlander NQ, Houston A, Collyns T, Cajic V, et al. *Mycobacterium chimaera* infection following cardiac surgery in the United Kingdom: clinical features and outcome of the first 30 cases. *Clin Microbiol Infect.* (2018) 24:1164–70. doi: 10.1016/j.cmi.2018.04.027
31. Lau D, Cooper R, Chen J, Sim VL, McCombe JA, Tyrrell GJ, et al. *Mycobacterium chimaera* encephalitis post-cardiac surgery: a new syndrome. *Clin Infect Dis.* (2020) 70:692–5. doi: 10.1093/cid/ciz497
32. Zweifel SA, Mihic-Probst D, Curcio CA, Barthelmes D, Thielken A, Keller PM, et al. Clinical and histopathologic ocular findings in disseminated *Mycobacterium chimaera* infection after cardiothoracic surgery. *Ophthalmology.* (2017) 124:178–88. doi: 10.1016/j.ophtha.2016.09.032
33. EU Protocol for Case Detection, Laboratory Diagnosis and Environmental Testing of Mycobacterium chimaera Infections Potentially Associated with Heater-Cooler Units: Case Definition and Environmental Testing Methodology. European Centre for Disease Prevention and Control (2015) Available online at: http://ecdc.europa.eu/en/publications-data/eu-protocol-case-detection-laboratory-diagnosis-and-environmental-testing (Accessed May 25, 2019).
34. Interim Guide for the Identification of Possible Cases of Nontuberculous Mycobacterium Infections Associated with Exposure to Heater-Cooler Units. Centre for Disease Prevention and Control (2016) Available online at: https://www.cdc.gov/hai/outbreaks/heater-cooler.html (Accessed May 25, 2019).
35. Ben Appenheimer A, Diekema DJ, Berriel-Cass D, Crook T, Daley CL, Dobbie D, et al. *Mycobacterium chimaera* Outbreak Response: experience from four United States healthcare systems. *Open Forum Infect Dis.* (2016) 3:2392. doi: 10.1093/ofid/ofw195.10
36. Mycobacterium chimaera Infections: Guidance for Secondary Care. GOVUK. Available online at: https://www.gov.uk/government/publications/mycobacterium-chimaera-infections-guidance-for-secondary-care (Accessed May 26, 2019).
37. Lecorche E, Haenn S, Mougari F, Kumanski S, Veziris N, Benmansour H, et al. Comparison of methods available for identification of *Mycobacterium chimaera*. *Clin Microbiol Infect.* (2018) 24:409–13. doi: 10.1016/j.cmi.2017.07.031
38. Griffith DE, Aksamit T, Brown-Elliott BA, Catanzaro A, Daley C, Gordin F, et al. An official ATS/IDSA statement: diagnosis, treatment, and prevention of nontuberculous mycobacterial diseases. *Am J Respir Crit Care Med.* (2007) 175:367–416. doi: 10.1164/rccm.200604-571ST
39. Overton K, Mennon V, Mothobi N, Neild B, Martinez E, Masters J, et al. Cluster of invasive *Mycobacteria chimaera* infections following cardiac surgery demonstrating novel clinical features and risks of aortic valve replacement. *Intern Med J.* (2018) 48:1514–20. doi: 10.1111/imj.14093
40. Schreiber PW, Hasse B, Sax H. *Mycobacterium chimaera* infections after cardiac surgery-lessons learned. *Clin Microbiol Infect.* (2018) 24:1117–8. doi: 10.1016/j.cmi.2018.06.031
41. Mihos CG, Capoulade R, Yucel E, Picard MH, Santana O. Surgical versus medical therapy for prosthetic valve endocarditis: a meta-analysis of 32 studies. *Ann Thorac Surg.* (2017) 103:991–1004. doi: 10.1016/j.athoracsur.2016.09.083
42. Walker J, Moore G, Collins S, Parks S, Garvey MI, Lamagni T, et al. Microbiological problems and biofilms associated with *Mycobacterium chimaera* in heater-cooler units used for cardiopulmonary bypass. *J Hosp Infect.* (2017) 96:209–20. doi: 10.1016/j.jhin.2017.04.014
43. Schreiber PW, Kuster SP, Hasse B, Bayard C, Rüegg C, Kohler P, et al. Reemergence of *Mycobacterium chimaera* in heater-cooler units despite intensified cleaning and disinfection protocol. *Emerging Infect Dis.* (2016) 22:1830–3. doi: 10.3201/eid2210.160925
44. Hasse B, Hannan MM, Keller PM, Maurer FP, Sommerstein R, Mertz D, et al. International society of cardiovascular infectious diseases guidelines for the diagnosis, treatment and prevention of disseminated *Mycobacterium chimaera* infection following cardiac surgery with cardiopulmonary bypass. *J Hosp Infect*. (2020) 104:214–35. doi: 10.1016/j.jhin.2019.10.009
45. Marra AR, Diekema DJ, Edmond MB. *Mycobacterium chimaera* infections associated with contaminated heater-cooler devices for cardiac surgery: outbreak management. *Clin Infect Dis.* (2017) 65:669–74. doi: 10.1093/cid/cix368
46. Moutsoglou DM, Merritt F, Cumbler E. Disseminated *Mycobacterium chimaera* presenting as vertebral osteomyelitis. *Case Rep Infect Dis.* (2017) 2017:9893743. doi: 10.1155/2017/9893743
47. Daniau C, Lecorche E, Mougari F, Fournier S, Richomme X, Bernet C, et al. Invasive *Mycobacterium chimaera* infection in cardiac surgery; assessment of practices surrounding cardiopulmonary bypass equipment. *Hygiènes.* (2019) 27:351–9. doi: 10.25329/hy_xxvii_6-1

Conflict of Interest: The authors declare that the research was conducted in the absence of any commercial or financial relationships that could be construed as a potential conflict of interest.

frontiers in Microbiology

ORIGINAL RESEARCH
published: 23 June 2020
doi: 10.3389/fmicb.2020.01248

Activity-Based Protein Profiling Reveals That Cephalosporins Selectively Active on Non-replicating *Mycobacterium tuberculosis* Bind Multiple Protein Families and Spare Peptidoglycan Transpeptidases

Landys Lopez Quezada[1], Robert Smith[2], Tania J. Lupoli[1†], Zainab Edoo[3], Xiaojun Li[4], Ben Gold[1], Julia Roberts[1], Yan Ling[1], Sae Woong Park[1], Quyen Nguyen[5], Frank J. Schoenen[2], Kelin Li[5], Jean-Emmanuel Hugonnet[3], Michel Arthur[3], James C. Sacchettini[4], Carl Nathan[1‡] and Jeffrey Aubé[2,5*‡]*

[1] Department of Microbiology & Immunology, Weill Cornell Medical College, New York, NY, United States, [2] Chemical Methodologies & Library Development Center, The University of Kansas, Lawrence, KS, United States, [3] Sorbonne Université, Sorbonne Paris Cité, Université de Paris, INSERM, Centre de Recherche des Cordeliers, CRC, Paris, France, [4] Departments of Biochemistry and Biophysics, Texas A&M University, College Station, TX, United States, [5] Division of Chemical Biology and Medicinal Chemistry, UNC Eshelman School of Pharmacy, The University of North Carolina at Chapel Hill, Chapel Hill, NC, United States

As β-lactams are reconsidered for the treatment of tuberculosis (TB), their targets are assumed to be peptidoglycan transpeptidases, as verified by adduct formation and kinetic inhibition of *Mycobacterium tuberculosis* (Mtb) transpeptidases by carbapenems active against replicating Mtb. Here, we investigated the targets of recently described cephalosporins that are selectively active against non-replicating (NR) Mtb. NR-active cephalosporins failed to inhibit recombinant Mtb transpeptidases. Accordingly, we used alkyne analogs of NR-active cephalosporins to pull down potential targets through unbiased activity-based protein profiling and identified over 30 protein binders. None was a transpeptidase. Several of the target candidates are plausibly related to Mtb's survival in an NR state. However, biochemical tests and studies of loss of function mutants did not identify a unique target that accounts for the bactericidal activity of these beta-lactams against NR Mtb. Instead, NR-active cephalosporins appear to kill Mtb by collective action on multiple targets. These results highlight the ability of these β-lactams to target diverse classes of proteins.

Keywords: *M. tuberculosis*, cephalosporin, non-replicating, β-lactams, ABPP, click chemistry

OPEN ACCESS

Edited by:
Miguel Viveiros,
New University of Lisbon, Portugal

Reviewed by:
Arshad Khan,
The University of Texas Health Science Center at Houston, United States
Rita Berisio,
National Research Council (CNR), Italy

****Correspondence:***
Carl Nathan
cnathan@med.cornell.edu
Jeffrey Aubé
jaube@email.unc.edu

†Present address:
Tania J. Lupoli,
Department of Chemistry, New York University, New York, NY, United States

‡These authors share senior authorship

Specialty section:
This article was submitted to Antimicrobials, Resistance and Chemotherapy, a section of the journal Frontiers in Microbiology

Received: *16 October 2019*
Accepted: *15 May 2020*
Published: *23 June 2020*

Citation:
Lopez Quezada L, Smith R, Lupoli TJ, Edoo Z, Li X, Gold B, Roberts J, Ling Y, Park SW, Nguyen Q, Schoenen FJ, Li K, Hugonnet J-E, Arthur M, Sacchettini JC, Nathan C and Aubé J (2020) Activity-Based Protein Profiling Reveals That Cephalosporins Selectively Active on Non-replicating Mycobacterium tuberculosis Bind Multiple Protein Families and Spare Peptidoglycan Transpeptidases. Front. Microbiol. 11:1248. doi: 10.3389/fmicb.2020.01248

INTRODUCTION

The chemotherapy of tuberculosis (TB) remains challenging, with an urgent need for shorter, safer treatment whose effectiveness extends to TB resistant to current regimens (Murray et al., 2016). Cure of a high proportion of patients with drug-sensitive TB depends on use of multiple antibiotics for at least 6 months. In part, this is thought to reflect the phenotypic antimicrobial

resistance that is characteristic of non-replicating (NR) bacterial populations (Nathan, 2012). To this end, several strategies have been proposed to improve the treatment course against NR bacteria (Murray et al., 2016; Gold and Nathan, 2017). One strategy involved a search for drugs that can kill Mtb *in vitro* when it has been made NR by conditions that mimic those found in the host (Bryk et al., 2008; Mak et al., 2012; Grant et al., 2013; Gold and Nathan, 2017).

The bacterial cell wall is the target of many antibiotics, β-lactams among them. However, the cell wall of mycobacteria was considered refractory to inhibition by β-lactams for decades following the demonstration that penicillin was inactive against Mtb (Abraham et al., 1941). β-Lactams are the most highly prescribed antibiotics in modern medicine (Bush and Macielag, 2010) and have utility in diverse infections (Wivagg et al., 2014). Mtb's resistance to β-lactams was attributed to the natural resistance of its peptidoglycan transpeptidases, the robust production of a class A β-lactamase (BlaC), and the limited permeability of its thick, waxy outer cell wall. Peptidoglycan peptide crosslinking in mycobacteria relies largely but not completely on L,D-transpeptidases (Ldts) that catalyze transpeptidation via an active site cysteine rather than the serine of D,D-transpeptidases (Mainardi et al., 2005). D, D-transpeptidases along with D,D-carboxypeptidases and D,D-endopeptidases are the classical targets of β-lactams and are collectively called penicillin binding proteins (PBPs). In Mtb, as much as 80% of peptidoglycan crosslinks are mediated by Ldts (Lavollay et al., 2008) when cells are in stationary phase compared to 30–40% of the crosslinks in replicating cells (Wietzerbin et al., 1974).

Over the years, interest in β-lactams for the treatment of TB has undergone a renaissance, spurred in part by the discovery that the carbapenem, meropenem, combined with the β-lactamase inhibitor clavulanic acid, sterilized replicating cultures of Mtb within 2 weeks of incubation (Hugonnet et al., 2009), along with the demonstration of the vulnerability of Ldts to β-lactam inhibition. A long-term case study of 18 patients with extensively drug-resistant TB concluded that including meropenem/clavulanate in the treatment regimen was beneficial to outcomes (Payen et al., 2018). While various carbapenems, including faropenem, are the most effective β-lactams at inhibiting Mtb Ldts (Kumar et al., 2017), cephalosporins also bind the Ldts of Mtb (Dubee et al., 2012b; Kumar et al., 2017) and *Enterococcus faecium* (Dubee et al., 2012a). Also, a previous study observed that the activity of rifampicin, a first-line antimycobacterial, is enhanced when co-administered with several cephalosporins *in vitro* (Ramón-García et al., 2016). The underlying basis of this synergy remains unknown.

We recently screened a β-lactam library against Mtb under both replicating and NR conditions that mimic the host environment, the latter set of conditions consisted of hypoxia, low pH, a flux of nitric oxide generated from nitrite, and butyrate as a carbon source (Gold et al., 2015b). We found two cephalosporins, compounds **1** and **5**, that were exclusively active against NR Mtb and were cidal to Mtb in mouse bone marrow-derived macrophages (Gold et al., 2016b). Restriction of activity to NR Mtb raised the question whether these cephalosporins might have non-canonical targets (Baranowski and Rubin, 2016) beyond transpeptidation enzymes.

Further suggesting the likelihood of non-canonical targets, the NR-active cephalosporins bear an ester or an oxadiazole (an ester isostere) at the C2′ position of the cephalosporin core, rather than the free carboxylic acid characteristic of inhibitory cephalosporins (Chauvette and Flynn, 1966; Jen et al., 1972). The importance of the free carboxylic acid is highlighted in the crystal structure of the acyl-enzyme tetrahedral intermediate between PBP2x from *Streptococcus pneumoniae* and cefuroxime, which showed tight hydrogen bonding between Thr550 in the active site and the carboxylic acid of cefuroxime (Gordon et al., 2000). Loss of this interaction with Thr550 reduced affinity for 2nd- and 3rd-generation cephalosporins and increased resistance to cephalosporins in clinical isolates (Mouz et al., 1999). Furthermore, the crystal structures of the Mtb Ldt_{Mt1} (Correale et al., 2013) and Ldt_{Mt2} (Bianchet et al., 2017) showed tight hydrogen bonding interactions between three active site side chains and the carboxylate of several carbapenems bound to the active site cysteine.

Alternative targets of β-lactams, with no obvious relationship to enzymes involved in peptidoglycan metabolism, have been reported in other organisms. A monobactam inhibited the *Escherichia coli* signal peptidase SPase (Kuo et al., 1994). Crystallization of *E. coli* SPase with a β-lactam was achieved using a penem with an ester at the carboxylate position (Paetzel et al., 1998). Certain cephalosporins esterified at the C2″ carboxylate inhibit human leukocyte elastase (HLE) (Doherty et al., 1986).

In the NR state, peptidoglycan biosynthesis is anticipated to slow or completely arrest as the bacilli halt replication. Ldts, obvious candidate targets of β-lactams, play an essential role for replicating Mtb and their role in maintaining peptidoglycan synthesis in NR Mtb is not as well understood. Thus, we first tested if NR-active cephalosporins inhibited recombinant Mtb Ldts. To explore the possibility of non-canonical targets, we then turned to activity-based protein profiling (ABPP) to seek other potential target(s).

ABPP has been adopted to find binding partners for ligands that target cysteine, serine, and metallohydrolases, ATP-binding proteins, phosphatases, and other enzyme classes (Cravatt et al., 2008). ABPP makes use of alkyne or azide analogs of the ligand of interest, which can then be conjugated via a Cu(I)-mediated azide alkyne cycloaddition reaction to create a handle for enrichment and purification or labeling (Speers and Cravatt, 2009), followed by peptide mass fingerprinting to identify binding proteins. In Mtb, ABPP has been used to elucidate the serine hydrolase landscape of replicating and hypoxic NR cells (Ortega et al., 2016) and to identify a protein that binds agrimophol, a cidal natural product that disrupts Mtb's intrabacterial pH homeostasis (Zhao et al., 2015).

In this study, by using ABPP, we identified candidate target proteins for NR-active cephalosporins that belonged to diverse protein families. Conspicuously absent were Ldts and PBP transpeptidases and carboxypeptidases.

RESULTS

NR-Active Cephalosporins Do Not Inhibit Mtb Ldts and Are Not Susceptible to BlaC Cleavage

Given the importance of Ldts in Mtb's adaptation to stress conditions, we first queried if there was any notable interaction between Mtb Ldts and compounds **1**, **5**, and the carboxylic acid analog, **9c** (**Figure 1A**). Ldt_{Mt1} and Ldt_{Mt2} were selected for their critical role in mycobacterial biology (Schoonmaker et al., 2014). No inhibitory activity was detected (**Figure 1B**) with or without prior incubation with the compounds. The molar extinction coefficient ($\Delta\varepsilon$) of the hydrolyzed compounds was determined by incubating **1**, **5**, and **9c** with *Klebsiella pneumoniae* carbapenemase, KPC-2. Partial hydrolysis of **1** and **5** was achieved after 1,000 min while **9c** was rapidly hydrolyzed. Neither compound **1** nor **5** could be hydrolyzed by the Ldts. Furthermore, stopped-flow kinetics were performed using *E. faecium*. Ldt_{fm} failed to detect an interaction with **1** or **5**. Considering that **9c** interacted with Ldt_{Mt1}, Ldt_{Mt2}, and Ldt_{fm} as expected, it seemed likely that the lack of a charged carboxylate alters the binding of the compounds and, most likely, **1** and **5** do not have canonical cephalosporin targets. Next, we tested the susceptibility of the three compounds to hydrolysis by Mtb BlaC. Mtb BlaC was unable to hydrolyze **1** or **5**; however, as with KPC-2, **9c** was readily degraded with a turnover rate of 40 min^{-1} (**Figure 1B**). Neither **1** nor **5** inhibited BlaC hydrolysis of nitrocefin, even after a 2-h pre-incubation. These findings led us to opt for an unbiased approach to finding potential targets of **1** and **5**.

Chemo-Proteomic Approach to Target Identification

We synthesized alkyne analogs of **1** and **5** that retained NR activity comparable to that of the parent compounds (**Figures 1A,C**). The alkyne tag was coupled to either the C2′ carboxyl (C) or C7′ amino (N) group of each cephalosporin, yielding compounds **C1a**, **N1**, **C5**, and **N5**. All four tagged compounds retained NR activity and none gained activity against replicating Mtb (replicating MIC90 $\geq$ 100 μM; data not shown). Thus, we were able to apply the probe compounds to intact, live NR Mtb rather than having to treat lysates prepared from NR Mtb. Achieving reproducible and compound-specific labeling of both membrane-associated and cytoplasmic proteins required overcoming several technical challenges. In our preliminary experiments, we found that use of a biotin azide or a desbiotin azide linker led to problems with the elution of non-specific proteins bound to the agarose-streptavidin resin and the contamination of samples with streptavidin, which could

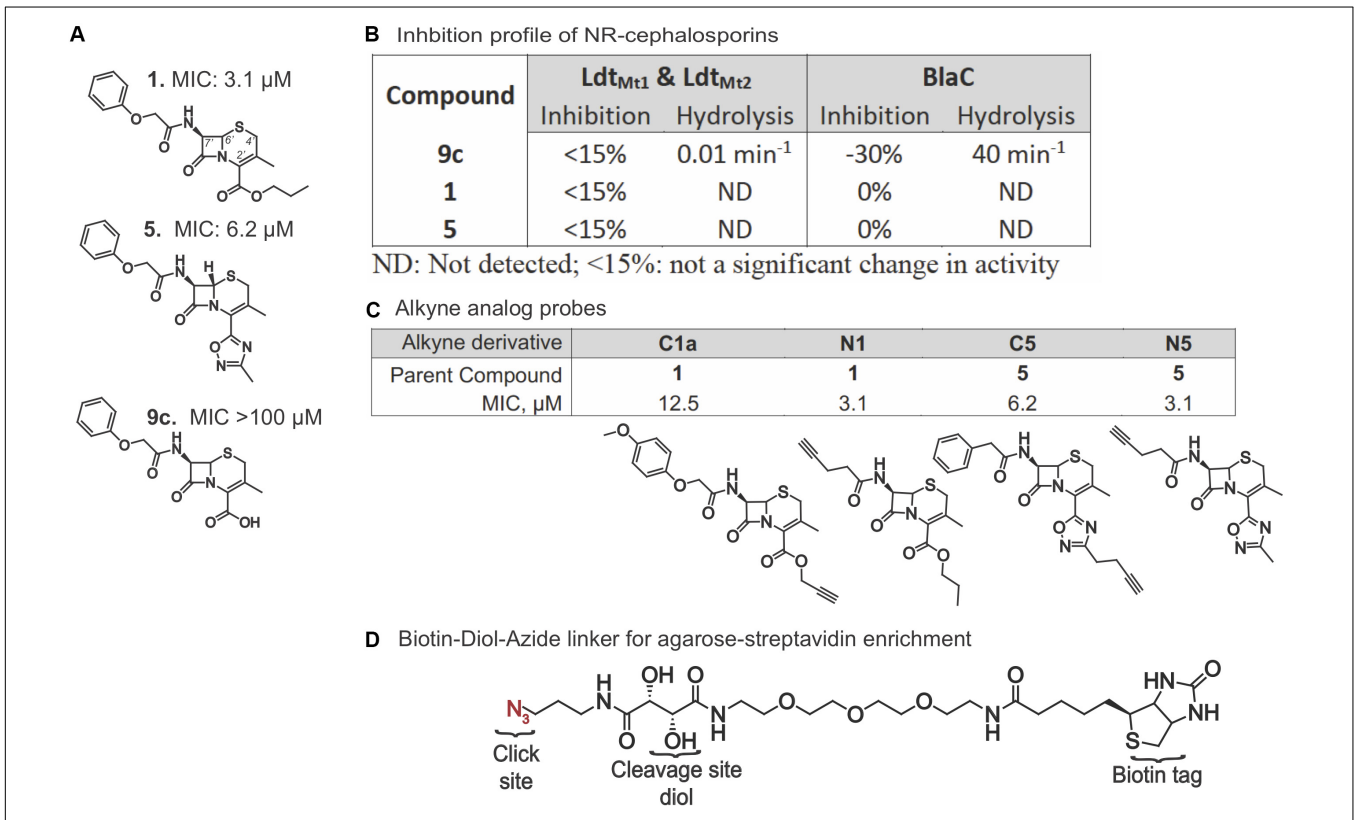

FIGURE 1 | Activity and design of alkyne probes for ABPP. **(A)** Structures and non-replicating (NR) MICs of compounds **1**, **5**, and **9c**. **(B)** Percent inhibition of nitrocefin hydrolysis and compound hydrolytic activity of Ldt_{Mt1}, Ldt_{Mt2}, and BlaC when incubated with compounds **1**, **5**, and **9c**. **(C)** Structure and NR MICs of alkyne derivatives. **(D)** Structure of the biotin-diol linker used for purification and identification of proteins bound to the cephalosporin probes.

mask target proteins of low abundance. We remedied this with a biotin linker containing a 1,2-diol near the azide (**Figure 1D**) that allowed periodate-mediated oxidative cleavage of the linker. We used a high biomass of Mtb to increase the likelihood of capturing low abundance protein(s). This required setting up experiments using a high bacterial inoculum and adjusting the compound concentrations to account for the inoculum effect observed in **1**, **5**, and many other β-lactams (Gold et al., 2016b), in which the compounds became less potent as the starting inoculum was raised from 0.01 OD_{580} to 0.1. Not only did the antimycobacterial activity of the alkynes mirror the activity of the parent compounds in standard MIC and charcoal agar resazurin assays (CARA) (**Figures 1C**, **2A**) where the OD_{580} is adjusted to 0.01, but they remained cidal despite the high inoculum of 5×10^8 CFU/ml (an approximate OD_{580} of 1.0) after 7 days of incubation (**Figure 2B**). Similar to the parent compounds (Gold et al., 2016b), activity of their alkyne analogs was largely dependent on the inclusion of nitrite in the NR conditions (**Figure 2C**). The standard MIC of the alkyne analogs and the parent compounds was comparable to that of oxyphenbutazone (OPB, **Supplementary Table S1**), which is active in the non-replicating 4-stress model (Gold et al., 2012).

The methods used to label, enrich, purify, and elute bound target proteins are shown schematically in **Figure 3**. **C1a**, which contained the alkyne handle at the C2′ carboxylic acid group, labeled the proteome more robustly than the **N1** probe, which carried the alkyne at C7′ amino moiety (**Figure 4A**). The same pattern was observed between **C5** and **N5** probes (**Figure 4B**), suggesting preferential orientation of these cephalosporins with binding partners to which they could most readily undergo the azide alkyne cycloaddition reaction and subsequent detection. Boiling the beads after the oxidation reaction did not release any additional biotinylated proteins (**Figure 4B**), suggesting that the periodate chemical cleavage was complete. Furthermore, no proteins were detected in the flow-through (**Figure 4C**), which indicated that binding of the tagged proteins to the streptavidin-agarose was comprehensive. Having removed the biotin tag, we visualized the proteins in the concentrated eluates by silver staining the SDS-PAGE gels (**Figure 4D**).

C5 and C1a Binding Proteins Are Not Involved in Peptidoglycan Synthesis

After optimizing assay conditions and purification steps (**Figure 3**), we conducted ABPP on two independent experiments using **C1a**, **C5**, and a vehicle control (1% DMSO). No probe-specific proteins were identified with the **N1** or **N5** probes and, therefore, analytical efforts were focused on results with **C1a** and **C5**. The **C5** probe pulled down a much smaller set of protein binders (39 proteins) than the **C1a** probe (426 proteins) (**Table 1**). The majority were not detected in the vehicle-treated control cells. Of the proteins identified using **C5**, 93% were also identified using **C1a**. In order to assess the specificity of binding, ABPP with **C1a** was conducted in the presence of **1** or **5** as competitors. Recovery of 185 of the 205 reproducible candidate binders was reduced by at least 100-fold when **C1a** was co-incubated with **1** and unaffected by co-incubation with **5** (**Table 1** and **Supplementary Table S2**). The set of 185 proteins included 28 of the 30 proteins that were pulled down with **C5**. Thus, the 30 proteins identified with **C5** were considered to be the most reproducible and specifically targeted by the NR-active cephalosporins. These were chosen for further study.

Genetic and Biochemical Studies of Non-essential Binding Protein

The proteins isolated with the **C5** probe belonged to several protein families, 16 of which are essential under replicating conditions (**Table 2**). Notably, known targets of β-lactams were not among them. Given that the compounds are specifically cidal to NR Mtb, we initially reasoned that these essential proteins may not be the targets whose inhibition would account for cidality only under NR conditions. Several of the proteins are predicted or have been verified to be involved in the following functions: fatty acid biosynthesis: DesA2, DesA1, HtdY, and

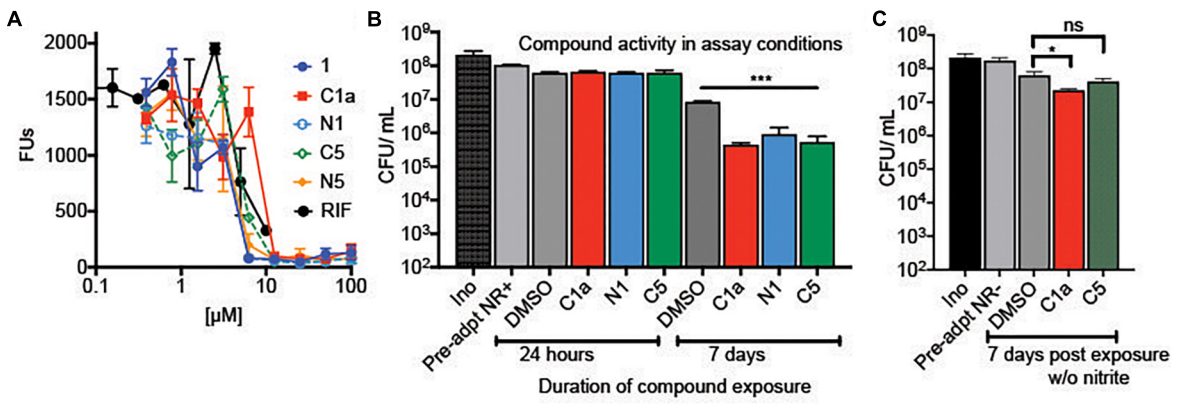

FIGURE 2 | Activity of alkyne analogs against Mtb at a high inoculum. **(A)** Activity of compound **1** and alkyne derivatives against NR Mtb in standard NR conditions at an initial OD_{580} of 0.1. **(B)** Cidality of alkyne analogs in the non-replicating pull-down assay conditions that included a 24-h pre-exposure to NR conditions and a high inoculum (OD_{580} of 1.0). Cells were exposed to alkyne analogs for 24 h or 7 days. After 7 days of exposure, **C1a**, **N1**, and **C5** significantly reduced viability (***$p < 0.005$). **(C)** Activity of alkyne analogs after 7 days under NR conditions without the flux of nitric oxide, *$p = 0.045$.

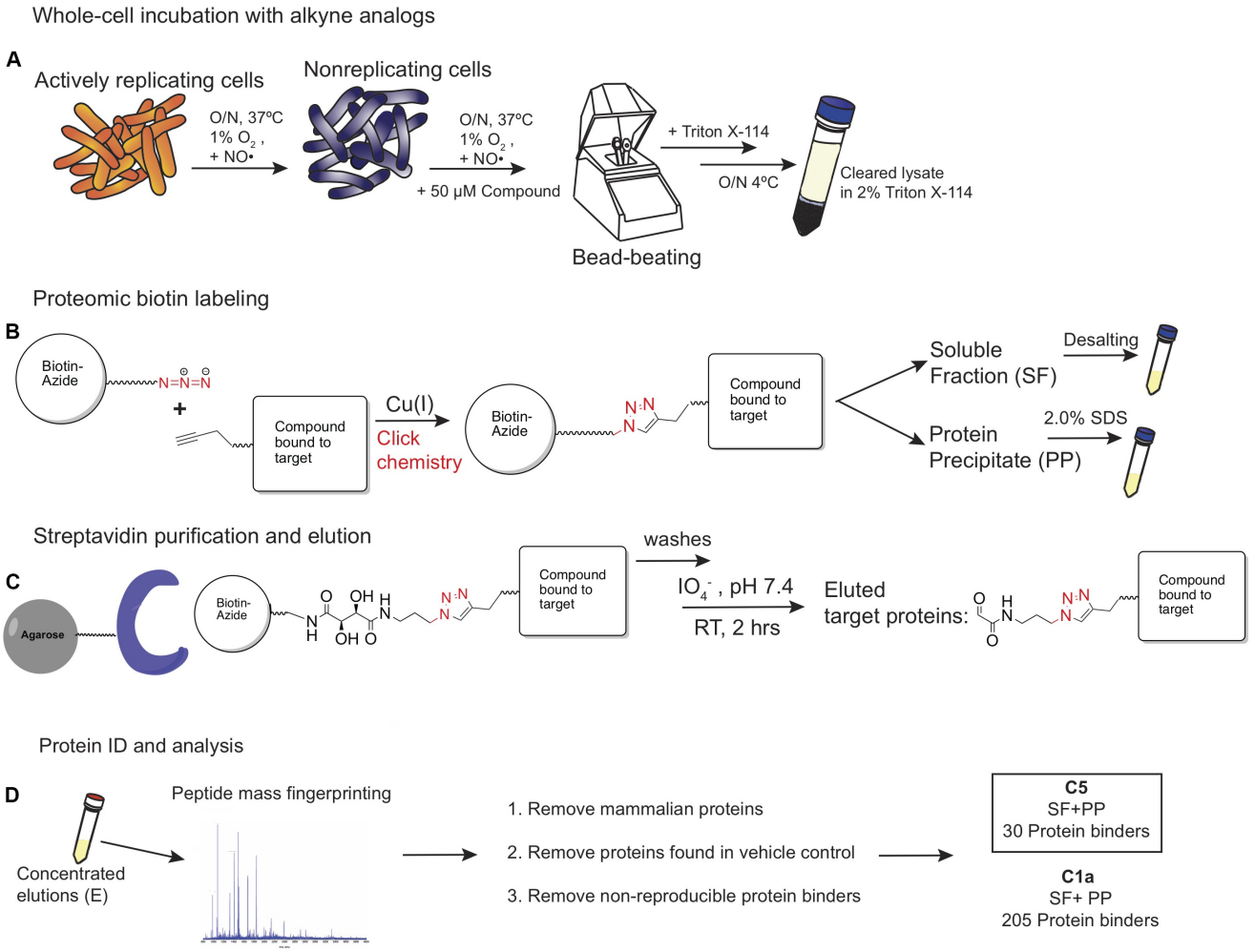

FIGURE 3 | The ABPP strategy used for labeling potential protein binders to **C1a**, **N1**, **C1**, and **N5**. **(A)** The strategy involved 24-h exposure of NR pre-conditioned Mtb cells to test compounds, lysis, and solubilization of cellular and membrane proteins in Triton X-114. **(B)** Conjugation of the probe–protein complex to the diol-biotin linker via a Cu(I)-catalyzed Huisgen's azide-alkyne cycloaddition reaction. **(C)** Streptavidin purification followed by periodate/diol linker cleavage. **(D)** Mass spectrometry analysis of eluents and removal of non-specific protein binders.

AcpM; β-oxidation: EchA1, FadD31, and Rv3224; ribosome function: Tsf, Tuf, RplJ, and Rv1738; universal stress proteins: Rv2005, Rv2623, and Rv1996 (**Table 2**). Of the proteins with non-essential roles under replicating conditions, 13 of the 14 NR-cephalosporin-binding proteins that are not essential under replicating conditions (DeJesus et al., 2017) were assessed for their potential essentiality under NR conditions.

We focused first on shortlisted proteins (**Table 2**) that are unannotated: Rv0250, Rv1738, and Rv0786. Of these, only Rv1738 has a published crystal structure (Bunker et al., 2015). The dimer of Rv1738 bears a striking similarity to the structure of *E. coli's* hibernation promoting factor, which plays a role in imposing an NR state. Accordingly, we purified recombinant Rv1738 protein (**Supplementary Figure S1**), which eluted in dimeric form (**Figure 5A**). When incubated with purified Mtb ribosomes, Rv1738 inhibited up to 80% of translation of luciferase mRNA in a concentration-dependent manner. Thus, Rv1738 appears to be an Mtb ortholog of hibernation factor. However, the addition of **1**, **5**, or **C5** did not alter this interaction (**Figure 5B**).

Rv0786 is an uncharacterized conserved protein. Although the percent sequence identity was below 25%, 66% of Rv0786's structure was predicted with 100% confidence by Phyre2 3D software (Kelley et al., 2015) to share similarities with class B3 metallo-β-lactamases (**Supplementary Figure S2A**). Rv0786 contained the metal binding site common to Class 3 β-lactamases such as FEZ-1 and AIM-1 (**Supplementary Figure S2B**) (Sun et al., 2018). To test the role of Rv0786 in the survival of the bacteria under NR conditions, a transposon mutant of *rv0786* from a predicted loss-of-function library was prepared in the Hung laboratory at the Broad Institute. The *rv0786* mutant showed neither decreased survival nor a change in response to **5** compared to the WT strain (**Supplementary Figures S2C,D**).

Loss-of-function transposon mutants from the Hung library for the following binding partners showed no change

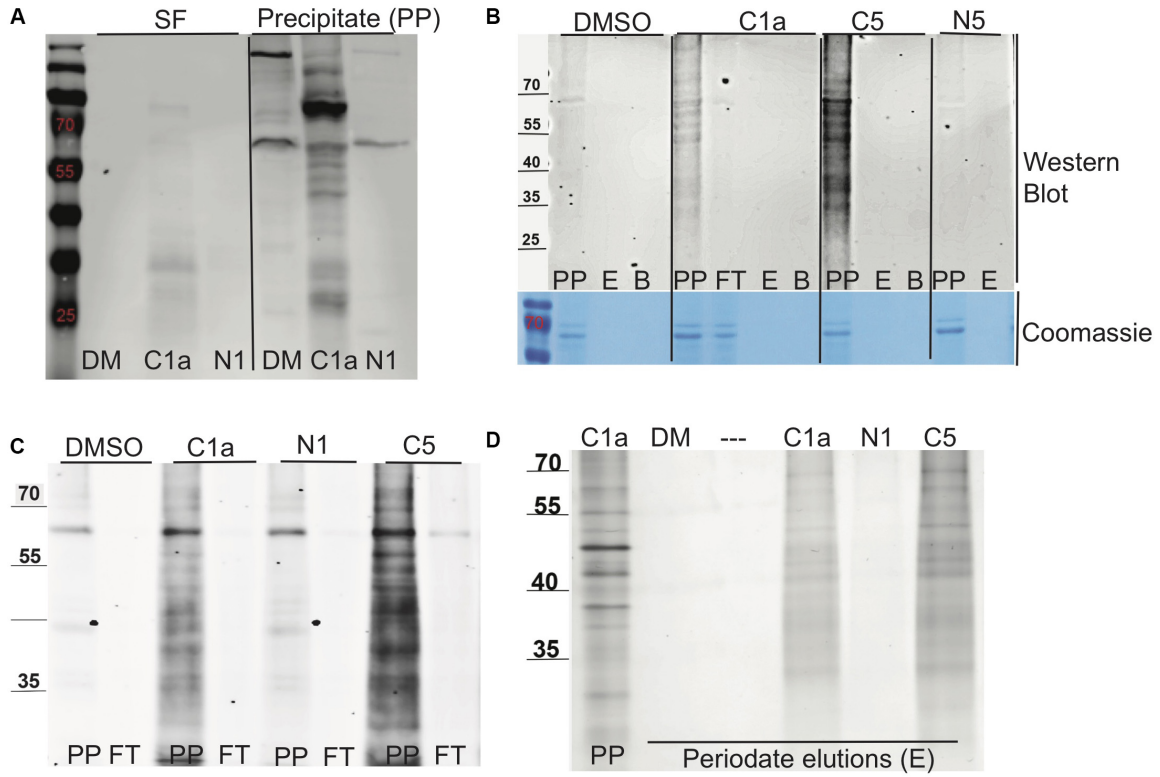

FIGURE 4 | Biotin labeling, streptavidin purification, and elution of proteins bound to NR-active cephalosporins. **(A)** The labeling of lysate proteins with click chemistry reaction was visualized by Western blot using Alexa Fluor streptavidin conjugate (Thermo Fisher Scientific, United States). The soluble fraction (SF) or precipitated (PP) protein samples treated for 24 h with DMSO (DM), **C1a**, or **N1**. **(B)** Western blot of the PP fraction following streptavidin purification of samples treated with DMSO, **C1a**, **C5**, or **N5**; precipitate (PP), periodate elution (E), boiled bead elution (B), streptavidin flow through (FT). Directly underneath is a loading control protein gel stained with Coomassie. **(C)** Western blot of PP fraction binding to streptavidin beads of samples treated with DMSO, **C1a**; **N1**; **C5**; precipitate (PP), streptavidin flow through (FT). **(D)** Silver staining of periodate elution (E) and **C1a** precipitate for comparison.

in the survival of the bacteria to the NR assay conditions. The mutants that we tested included those disrupted in the genes encoding the universal stress proteins Rv1996, Rv2005c, and Rv2326c (**Supplementary Figures S2C,D**, and data not shown), known or potential fatty acid metabolism enzymes Rv3224 (possible short chain dehydrogenase), Rv0222 (EchA1), and Rv3389 (putative HtdY) (**Figure 6A** and **Supplementary Figures S3A,B**), LldD (possible L-lactate dehydrogenase), and PdxH, pyridoxine 5′-oxidase (**Supplementary Figures S3A,B**).

TABLE 1 | Selection criterion and total number of final proteins identified.

Parent compound	**1**	**5**
Alkyne derivative (bait)	**C1a**	**C5**
Bacterial proteins with >2 unique peptides	426	39
Not found in DMSO	97%	82%
Competed with parent compound	45%	Not determined
Reproducible binders	48%	**77%**
	% of total number of proteins ID'd	
Precipitate fraction		
Bacterial proteins with >2 unique peptides	413	29
Not found in DMSO	406	24
Reproducible binders	**197**	**22**
Soluble Fraction		
Bacterial proteins with >2 unique peptides	13	10
Not found in DMSO	**8**	**8**

Numbers used to tabulate pull down totals and are bolded for emphasis.

The 4-stress NR model provides butyrate as the carbon source. Because there is a high degree of redundancy among enzymes involved in β-oxidation (Williams et al., 2011), we explored the pathway as a whole by altering the carbon source in the NR model. The carbon source markedly affected the susceptibility of Mtb to the NR-active cephalosporins (**Figures 6B,C**). Compared to standard NR conditions, in which the carbon source was butyrate, NR conditions lacking any carbon source reduced the susceptibility of Mtb both to the NR-active cephalosporins and to rifampicin (**Supplementary Figure S4B**). Compared to the control in which no carbon source was added, butyrate, propionate, and, to a lesser extent, hexanoate increased Mtb's susceptibility to **5**. In contrast, acetate increased Mtb's resistance to **5** and **1** without altering susceptibility to rifampicin (**Figure 6C**) compared to the no-carbon control. The non-fatty acid

carbon sources glutamate and glucose reduced the cidality of both **5** and rifampicin. These complex responses did not allow us to conclusively identify fatty acid oxidation as a pathway target.

Finally, we generated a knockout of *htpG*, which encodes a predicted protein chaperone (**Supplementary Figures S5A,B**) and obtained the knockout strain of *fecB*, a putative iron(III) dicitrate-binding protein (Xu et al., 2017). The strain deficient in FecB was slower than WT to recover after 3 days under NR conditions (**Supplementary Figure S5C**). Also striking, the Δ*htpG* strain had a fourfold decrease in $CARA_{MBC}$ when exposed to **1** and **5** (**Supplementary Figure S5D**) compared to the wild type. We purified recombinant HtpG and used differential scanning fluorimetry to determine if **5** binds HtpG. In contrast to HtpG's natural ligand, ADP, **5** did not alter the melting temperature of HtpG (**Supplementary Figure S5E**). This may indicate that conditions leading to binding in the intact cell were not recapitulated *in vitro* or that, indeed, there is no ligand-protein interaction.

DISCUSSION

The NR-active cephalosporins studied here were inactive on isolated Ldts and pulled down no Ldts or PBPs by ABPP. In contrast, ABPP identified at least 30 other cephalosporin binding proteins reproducibly and selectively. While one putative protein partner is predicted to be a metallo-β-lactamase, no other β-lactam-associated proteins were among the 30 candidate targets. Enzymes of fatty acid metabolism, universal stress

TABLE 2 | Potential cephalosporin binding proteins from NR cells.

Accession	Rv number	Gene	Essentiality?	Description
Fatty acid metabolism				
L7N5P2	Rv3224		No	PP: oxidoreductase, short-chain dehydrogenase/reductase family
O53442	Rv1094	desA2	Yes	PP: putative acyl-[acyl-carrier-protein] desaturase
Q7D7S1	Rv1925	fadD31	No	PP: acyl-CoA synthase
Q50824	Rv0685	desA1	Yes	PP: putative acyl-[acyl-carrier-protein] desaturase
L7N5S5	Rv0222	echA1	No	SF: probable enoyl-CoA hydratase; crotonase
P0A4W6	Rv2244	AcpM	Yes	SF: meromycolate extension acyl carrier protein
Q11198	Rv3389c	htdY	No	SF: 3-hydroxy acyl thioester dehydratase
Ribosomal/transcriptional function				
P66044	Rv0651	rplJ	Yes	PP: 50S ribosomal protein L10
Q10788	Rv2889c	tsf	Yes	PP/SF: elongation factor Ts
P0A558	Rv0685	tuf	Yes	PP: elongation factor Tu
P66701	Rv3457c	rpoA	Yes	PP: DNA-directed RNA polymerase subunit alpha
P64887	Rv1738	–	No	SF: uncharacterized protein Rv1738; potential hibernation factor
Universal stress proteins and chaperones				
P0A5F7	Rv1996	Usp	No	PP: universal stress protein; appears redundant
P64411	Rv2299c	htpG	No	PP: chaperone protein
P64921	Rv2005c	Usp	No	PP: universal stress protein; appears redundant
O06189	Rv2623	Usp	No	PP: universal stress protein
ATP synthesis				
P63671	Rv1309	atpG	Yes	PP: ATP synthase gamma chain
P63673	Rv1308	atpA	Yes	PP: ATP synthase subunit alpha
P63677	Rv1310	atpD	Yes	PP: ATP synthase subunit beta
Intermediary metabolism enzymes				
P0A544	Rv2996c	serA	Yes	PP: D-3-phosphoglycerate dehydrogenase
P60176	Rv3248c	sahH	Yes	PP: adenosylhomocysteinase; thioester hydrolase
P64178	Rv1436	gap	Yes	PP: glyceraldehyde-3-phosphate dehydrogenase
P65149	Rv3001c	ilvC	Yes	PP: ketol-acid reductoisomerase
Q10530	Rv0896	gltA2	Yes	PP: citrate synthase 1
P0A590	Rv2220	glnA1	Yes	PP: glutamine synthetase 1
P95143	Rv0694	lldD	No	PP: putative L-lactate dehydrogenase
P65682	Rv2607	pdxH	No	SF: pyridoxine/pyridoxamine 5′-phosphate oxidase
Unknown function				
O53291	Rv3044	fecB	No	SF: probable Fe(III)-dicitrate binding lipoprotein
O53672	Rv0250c	–	No	SF: uncharacterized protein
P71839	Rv0786c	–	No	SF: conserved protein

C5 pulldown proteins: PP, precipitate fraction; SF, soluble fraction.

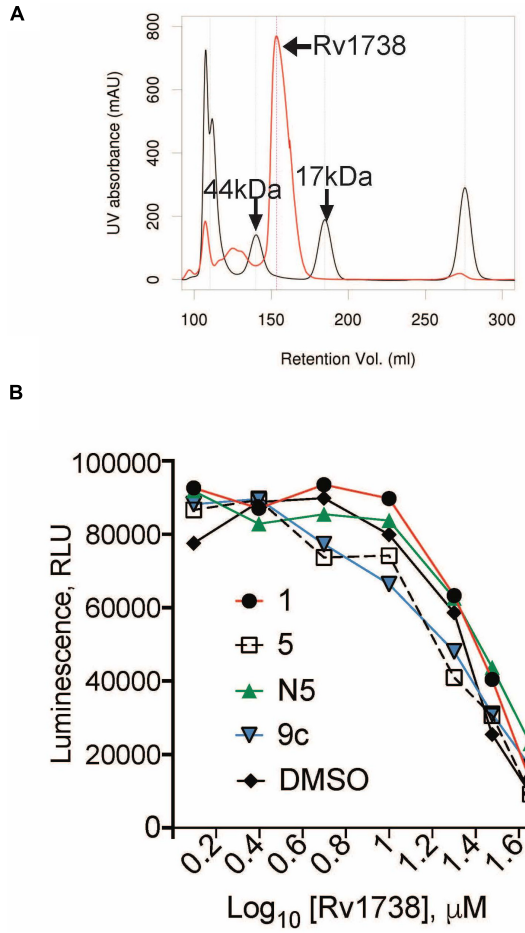

FIGURE 5 | Characterization of Rv1738 as a potential hibernation factor. **(A)** Size exclusion chromatography of purified Rv1738 (red), size standards (44 and 17 kDa) are in black. **(B)** Cell-free ribosome activity with increasing concentrations of Rv1738 incubated with 240 μM of **1**, **5**, **C5**, or **9c**. Luminescence (RLU) from the activity of the luciferase protein translated from the nano-luciferase mRNA, served as a surrogate measure of ribosomal activity.

proteins, and ribosome-associated proteins stood out as clusters, and several other enzymatic pathways were represented.

The isolation of seemingly unrelated chemical classes is not uncommon in the ABPP approach. A chemical proteomic strategy was used to isolate the targets of 10 alkyne β-lactone analogs in the proteomes of several Gram-negative and Gram-positive bacteria (Bottcher and Sieber, 2008), leading to isolation of acetyl-CoA hydrolases, several β-ketoacyl carrier protein synthases, ligases, and oxidoreductases, among other enzymes. Another study used several alkyne β-lactam probes including two penems containing an alkyne moiety either at the amino group (AmpN) or the carboxyl group (AmpC) and one cephalosporin with the alkyne at the amino group (CephN) (Staub and Sieber, 2008). Using *Pseudomonas putida* and two Gram-positive soil bacteria (*Listeria welshimeri* and *Bacillus licheniformis*) for their ABPP experiments, Staub and Sieber obtained similar results to ours in that AmpC, unlike AmpN, more readily bound non-PBPs. Even though the CephN contained a free carboxylic acid, in *B. licheniformis*, it bound a non-PBP protein called DltD, a membrane-bound thioesterase involved in lipoteichoic acid synthesis (Debabov et al., 2000; Staub and Sieber, 2008). Along with the high-molecular-weight and low-molecular-weight members of the PBP superfamily, Staub and Sieber also isolated β-ketoacyl-acyl carrier protein synthase III from multiple species with alkyne β-lactam probes. Thus, ABPP with β-lactam probes can identify non-canonical targets.

Several potential protein binders of **1** and **5** have roles in the Mtb stress response. Mutations in *fecB* rendered Mtb hypersusceptible to diverse classes of antibiotics, including vancomycin, isoniazid, ethambutol, and meropenem (Xu et al., 2017). Despite its annotation as an iron (III) dicitrate-binding periplasmic lipoprotein, knockout of *fecB* did not alter the mutant's ability to grow in iron-limiting or iron-replete conditions; however, the Δ*fecB* mutant was more permeable to ethidium bromide and fluorescently tagged vancomycin (Xu et al., 2017). The *fecB* mutant's weakened cell wall barrier could explain the increase in susceptibility to a wide range of antibiotics and perhaps also to nitroxidative stress. HtpG, the bacterial homolog of the eukaryotic chaperone Hsp90, has an important role in the adaptation of *E. coli* to environmental stresses, including incubation at high temperature (Grudniak et al., 2013) and host cell infection (Garcie et al., 2016); however, in Mtb, much remains to be learned about the nature and function of this chaperone (Lupoli et al., 2018). Using DSF, we did not detect interaction of compounds **1** and **5** with HtpG. In intact cells, the disruption in proteostasis caused by the loss of *htpG*, along with additional stresses after addition of β-lactam and nitric oxide, might lead to the increased sensitivity seen in the *htpG* knockout versus wild-type Mtb in the presence of compound.

Rv1738, encoding a 94-amino-acid protein considered non-essential for growth (DeJesus et al., 2017), is the most abundantly upregulated gene under hypoxic conditions (Sherman et al., 2001). *Rv1738* is also upregulated during NO stress (Voskuil et al., 2003). The crystal structure indicates that the dimer bears a close structural similarity to theβαββββα motif of hibernation promoting factor (Bunker et al., 2015). Purified Rv1738 appeared dimeric when eluted from a size exclusion column. When bacteria approach a dormant state, protein synthesis is retarded by the inactivation of their ribosomes. Ribosome modulation factor and hibernation factor promote and stabilize dimerization of the ribosomal subunits. The binding of these small proteins to the head domain of the 30S ribosomal subunit impedes the interaction of tRNAs and mRNAs with the 16S ribosomal RNA and induces a conformational change of the 30S subunit (Polikanov et al., 2012). Cryo-EM structures of ribosomes isolated from stationary phase *Mycobacterium smegmatis* showed 100S dimers but did show 70S ribosomes bound to a hibernation factor at the t-RNA binding site (Mishra et al., 2018). Our findings indicate that Rv1738 can behave like a hibernation promoting factor *in vitro* but how it does so remains to be determined. We did not find evidence that NR-active cephalosporins inhibit the action of Rv1738 *in vitro*, but we cannot exclude that they might do so in the intact cell.

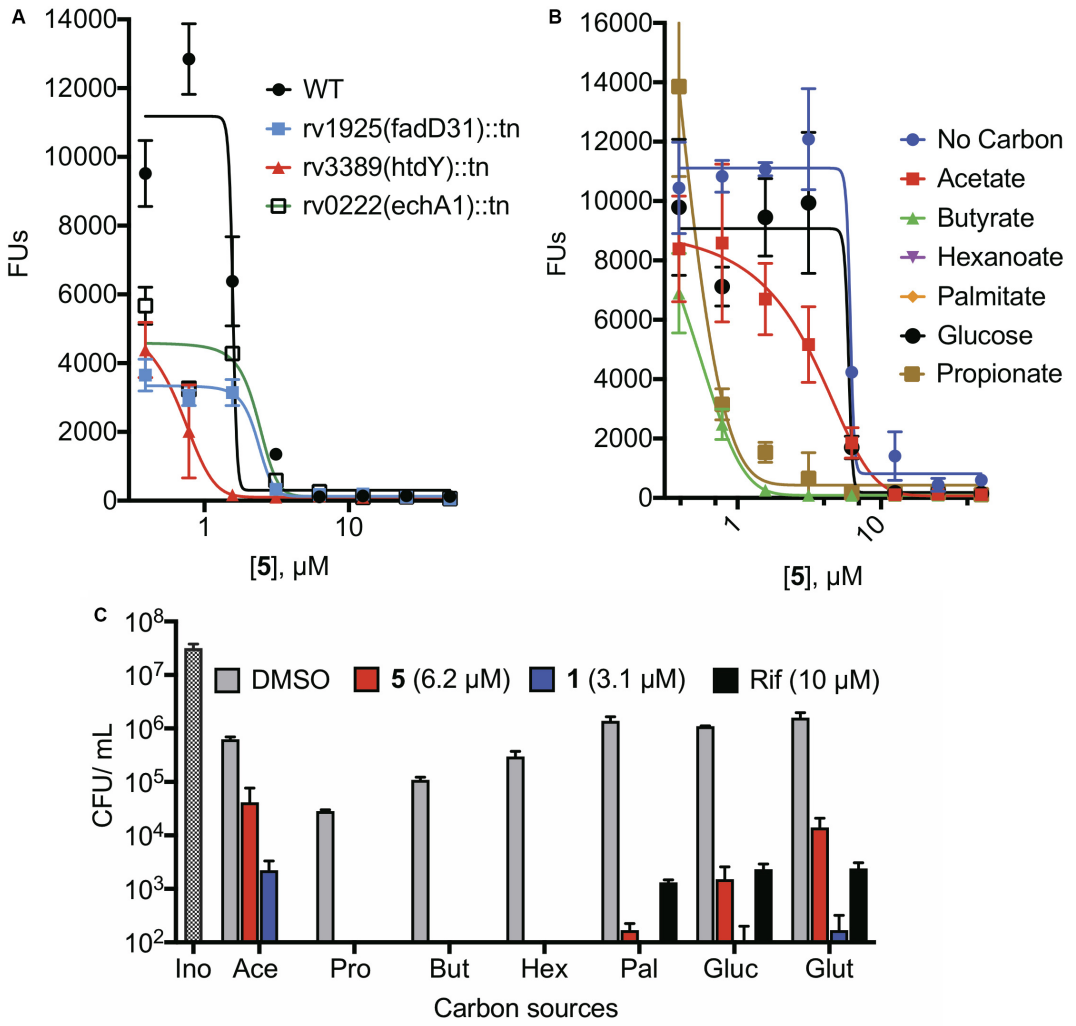

FIGURE 6 | Effects of fatty acid carbon sources on the activity of NR-active cephalosporins under NR conditions. **(A)** NR activity of 5 against transposon mutants in genes encoding enzymes involved in fatty acid metabolism. **(B)** NR activity of 5 using 0.05% acetate, 0.05% propionate, 0.05% butyrate, 0.015% hexanoate, 0.00025% palmitate, 0.2% glucose, or 0.2% glutamate as the sole carbon source in NR media. **(C)** When exposed to a concentration of compound equivalent to its $CARA_{MBC}$, reduction in viability after 7 days of treatment using various carbon sources in the NR media.

A meta-analysis of the *M. tuberculosis* transcriptomic landscape revealed that several genes encoding candidate binding proteins, including *rv2005c*, *rv199c*, and *rv2623* are upregulated when the bacilli are under stress conditions. *Rv2005c* encodes a universal stress protein and is upregulated under hypoxic conditions (Parvati Sai Arun et al., 2018). Rv2005c and Rv1996c belong to the same family of proteins as Rv2623, another universal stress protein. *Rv2623* is upregulated during NO exposure or hypoxic stress (Glass et al., 2017). Rv2623 has a role in the establishment of chronic infection in mice and overexpression slowed the growth of the cells (Drumm et al., 2009). However, the transposon mutants of *rv2623*, *rv1996*, or *rv2005* had no discernable phenotype in our NR 4-stress model. This does not exclude their possible collective relevance, given that the biological roles of Rv2005c and Rv1996c appear to be functionally redundant (Hingley-Wilson et al., 2010).

There is likely redundancy among the binding partners involved in fatty acid metabolism. Exposure to NO reportedly increased the expression of AcpM and other enzymes involved in fatty acid biosynthesis, and β-oxidation enzymes were induced by host intracellular environments (Parvati Sai Arun et al., 2018). This is consistent with the importance of host-derived fatty acids as carbon sources for Mtb during infection (McKinney et al., 2000; Schnappinger et al., 2003). Several studies have highlighted a link between central-carbon metabolism and antibiotic susceptibility and tolerance (Hicks et al., 2018; Lee et al., 2019) in which the bacterium altered its carbon flux to increase its survival during antibiotic stress. Because carbon metabolism in Mtb is distinctive and the metabolic fate of different carbon sources can differ (de Carvalho et al., 2010), further studies are needed to understand how these non-traditional cephalosporins affect the compartmentalization of

these carbon sources, particularly fatty acids. At an individual level, the functional loss of *fadD31* and *echA1* did not appear to affect the efficacy of **5** or **1** (data not shown), but there appears to be redundancy among genes in these classes (Williams et al., 2011); indeed, Mtb has over 100 genes annotated to be involved in the five reactions that convert fatty acids into acetyl-CoA.

In sum, the isolation of several protein families that are important in Mtb stress responses or adaptation to the host environment and that have mutually redundant members suggests that cephalosporins **1** and **5** may kill NR Mtb through collective inhibition of more than one target. However, it remains possible that there is a single, functionally relevant target we did not identify by ABPP due its low abundance or tight association with insoluble components, and it remains possible that the high abundance of several of the protein binders could explain their presence as pulldown clients. Moreover, one or more of the binding proteins that are essential under replicating conditions could represent the functionally relevant target or targets under NR conditions if the NR-active cephalosporins inhibit such target(s) partially and NR conditions disable the same target(s) as well, the combined effect being necessary to kill Mtb.

MATERIALS AND METHODS

Materials

Compounds **1**, **5**, and **9c** were synthesized as described below. The biotin-diol-azide linker was obtained from Click Chemistry Tools (Scottsdale, United States). Activated charcoal, sodium resazurin, sodium periodate, Triton X-114, isoniazid, rifampicin (Rif), and dimethyl sulfoxide (DMSO) were from Sigma-Aldrich, United States. The tris-(2-carboxyethyl)phosphine HCl (TCEP) and streptavidin-agarose beads used for enrichment and purification were from Thermo Fisher Scientific, United States.

Synthesis of Alkyne Probes

All starting β-lactams were prepared as described (Gold et al., 2016b).

n-Prop-2-yn-1-yl (6*R*,7*R*)-7-(2-(4-methoxyphenoxy) acetamido)-3-methyl-8-oxo-5-thia-1-azabicyclo [4.2.0]oct-2-ene-2-carboxylate (C1a)

To a solution of (6*R*,7*R*)-7-(2-(4-methoxyphenoxy)acetamido)-3-methyl-8-oxo-5-thia-1-azabicyclo[4.2.0]oct-2-ene-2-carboxylic acid (2.33 g, 6.17 mmol) in methyl isobutyl ketone (195 ml), a solution of potassium 2-ethylhexanoate hydrate (1.69 g, 9.25 mmol) in 1-butanol (37.5 ml) was added. The reaction became clouded. Hexanes were added until an off-white solid crashed out of solution. The precipitate (2.57 g, 6.17 mmol) was collected via filtration and used without further purification. To a suspension of this precipitate (2.57 g, 6.17 mmol) in DMF (30.9 ml, 0.20 M), 3-iodoprop-1-yne (4.79 ml, 30.9 mmol) was added. The mixture was allowed to stir at RT for 16 h. Solvent was removed and the residue was purified via silica gel MPLC to give **C1a** (1.78 g, 69%) as a white solid. Purity: 92%. ^{1}H NMR (400 MHz, DMSO-d_6) δ 9.00 (d, J = 8.3 Hz, 1H), 6.90–6.81 (m, 4H), 5.67 (dd, J = 8.3, 4.7 Hz, 1H), 5.12 (d, J = 4.7 Hz, 1H), 4.94–4.77 (m, 2H), 4.60–4.49 (m, 2H), 3.69 (s, 3H), 3.63–3.55 (m, 2H), 3.32 (s, 1H), 2.05 (s, 3H). ^{13}C NMR (101 MHz, DMSO-d_6) δ 168.7, 164.2, 161.3, 153.8, 151.8, 133.4, 121.3, 115.5, 114.5, 78.1, 77.9, 66.9, 58.8, 57.3, 55.4, 52.6, 29.2, 19.4. HR-MS (ESI): calculated for $C_{20}H_{21}N_2O_6S$ $[M + H]^+$ 417.1115; found, 417.1088.

Pent-4-ynoyl chloride

To a solution of pent-4-ynoic acid (1.55 g, 15 mmol) in DCM (15 ml) was added three drops of DMF at 0°C, followed by slow addition of oxalyl chloride (3.86 ml, 45 mmol). The reaction mixture was stirred at RT for 2 h, and then the solvent was removed under reduced pressure to afford the product (1.66 g, 95%) as an oil and used without purification.

(6*R*,7*R*)-3-Methyl-8-oxo-7-(pent-4-ynamido)-5-thia-1-azabicyclo[4.2.0]oct-2-ene-2-carboxylic acid

To a suspension of 7-ADCA (3.21 g, 15.0 mmol) in water (100 ml), $NaHCO_3$ (1.26 g, 15.0 mmol) and acetone (12.0 ml) were added, followed by the addition of pent-4-ynoyl chloride (1.75 g, 15.0 mmol). The reaction was stirred at RT for 16 h. DCM (100 ml) was added and the reaction mixture was acidified using 6N HCl to pH 2. The organic layer was removed and the aqueous portion was extracted again with DCM (100 ml). The organic extracts were combined, washed with brine, and dried over $MgSO_4$. Solvent was removed after filtration and the solid was suspended in ether and stirred for 8 h. The product was isolated through vacuum filtration as an off-white solid (3.43 g, 78%) and used without further purification.

n-Propyl (6*R*,7*R*)-3-methyl-8-oxo-7-(pent-4-ynamido) -5-thia-1-azabicyclo[4.2.0]oct-2-ene-2-carboxylate (N1)

0.13 g, 64% yield. Purity: 92%. A similar procedure to C1a was used for the synthesis with corresponding acid and 1-iodopopane. ^{1}H NMR (400 MHz, $CDCl_3$) δ 6.74 (d, J = 8.8 Hz, 1H), 5.79 (dd, J = 8.8, 4.7 Hz, 1H), 4.96 (d, J = 4.7 Hz, 1H), 4.27–4.09 (m, 2H), 3.49 (d, J = 18.3 Hz, 1H), 3.21 (d, J = 18.3 Hz, 1H), 2.57–2.46 (m, 4H), 2.13 (d, J = 0.9 Hz, 3H), 2.04–2.00 (m, 1H), 1.75–1.66 (m, 2H), 0.96 (t, J = 7.4 Hz, 3H). ^{13}C NMR (101 MHz, $CDCl_3$) δ 171.4, 164.5, 162.2, 131.2, 122.7, 82.5, 69.6, 67.3, 58.9, 57.1, 34.8, 30.2, 21.8, 20.0, 14.6, 10.4. HR-MS (ESI): calculated for $C_{16}H_{21}N_2O_4S$ $[M + H]^+$ 337.1217; found, 337.1228.

N-Hydroxypent-4-ynimidamide

To a solution of hydroxylamine hydrochloride (1.05 g, 15.0 mmol) in water (5 ml), sodium hydroxide (0.60 g, 15.0 mmol) was added. The resulting solution was added to pent-4-ynenitrile (1.19 g, 15.0 mmol) in about 2 min. The mixture was stirred at RT for 2 days. Solvent was removed and residue was treated with EtOH and the resulting suspension was filtered. The filtrate was concentrated *in vacuo* to afford product (0.84 g, 50%) as a white solid, which was used without further purification.

N-((6*R*,7*R*)-2-(3-But-3-yn-1-yl)-1,2,4-Oxadiazol-5-yl)-3-methyl-8-oxo-5-thia-1-azabicyclo[4.2.0]oct-2-en-7-yl)-2-phenylacetamide (C5)

To a solution of 2,4-dinitrophenol (0.92 g, 5.00 mmol) in DCM (20 ml), (6*R*,7*R*)-3-methyl-8-oxo-7-(2-phenylacetamido)-5-thia-1-azabicyclo[4.2.0]oct-2-ene-2-carboxylic acid in a minimal amount of 1,4-dioxane was added, followed by the addition of 1,3-diphenylcarbodiimide (0.97 g, 5.00 mmol) in DCM (10 ml). The mixture was stirred at RT for 30 min. After the filtration, *N*-hydroxypent-4-ynimidamide was added to the filtrate and the mixture was stirred at RT overnight. The mixture was then washed twice with sat. aq. $NaHCO_3$, filtered, and concentrated in vacuum to afford the residue, which was purified via silica gel MPLC (100% EtOAc) to give the intermediate (0.18 g) as a white solid, which was heated at 120°C in a vacuum oven overnight. Purification via silica gel MPLC afforded the desired product (68 mg, 39%, two steps) as a white solid. Purity: 98%. ^{1}H NMR (400 MHz, DMSO-d_6) δ 9.12 (d, J = 8.2 Hz, 1H), 7.33–7.19 (m, 5H), 5.72 (dd, J = 8.2, 4.7 Hz, 1H), 5.20 (d, J = 4.7 Hz, 1H), 3.75–3.47 (m, 4H), 2.97 (t, J = 7.1 Hz, 2H), 2.82 (t, J = 2.7 Hz, 1H), 2.63 (td, J = 7.2, 2.7 Hz, 2H), 2.15 (s, 3H). ^{13}C NMR (101 MHz, DMSO-d_6) δ 171.0, 170.2, 169.1, 165.2, 135.8, 132.7, 129.0, 128.2, 126.5, 115.7, 82.5, 72.2, 59.2, 57.6, 41.6, 29.0, 24.9, 19.8, 15.7. HR-MS (ESI): calculated for $C_{21}H_{21}N_4O_3S$ $[M + H]^+$ 409.1329; found, 409.1364.

N-((6*R*,7*R*)-3-Methyl-2-(3-Methyl-1,2,4-oxadiazol-5-yl)-8-oxo-5-thia-1-azabicyclo[4.2.0]oct-2-en-7-yl) pent-4-ynamide (N5)

A similar procedure to that described for **C5** was used starting with (6*R*,7*R*)-3-methyl-8-oxo-7-(pent-4-ynamido)-5-thia-1-azabicyclo[4.2.0]oct-2-ene-2-carboxylic acid and acetonitrile. Obtained 0.137 g (15% yield for the last two steps). Purity: 100%. ^{1}H NMR (400 MHz, $CDCl_3$) δ 6.62 (d, J = 8.6 Hz, 1H), 5.86 (dd, J = 8.6, 4.7 Hz, 1H), 5.08 (d, J = 4.7 Hz, 1H), 3.58 (d, J = 18.4 Hz, 1H), 3.33 (d, J = 18.4 Hz, 1H), 2.58–2.46 (m, 4H), 2.45 (s, 3H), 2.22 (s, 3H), 2.02 (t, J = 1.7 Hz, 1H). ^{13}C NMR (101 MHz, DMSO-d_6) δ 171.4, 170.2, 167.3, 165.3, 132.4, 115.5, 83.5, 71.5, 59.1, 57.5, 33.7, 29.0, 19.8, 14.1, 11.4. HR-MS (ESI): calculated for $C_{15}H_{17}N_4O_3S$ $[M + H]^+$ 333.1021; found, 333.0981.

Bacterial Strains and Growth Conditions

Actively growing WT *Mycobacterium tuberculosis* strain H37Rv (*Mtb*, ATCC 25618) was grown in Middlebrook 7H9 broth supplemented with 10% oleic acid, dextrose and catalase (OADC) (BD Difco, United States), 0.5% glycerol, and 0.02% Tyloxapol (Sigma) and incubated at 5% CO_2 and 20% O_2 at 37°C. H37Rv transposon mutants of Mtb *rv1925*, *lldD*, *rv3389*, *rv1996*, *rv2005*, *rv0786*, *rv3224*, *pdxH*, *fadD31*, *rv2623*, and *rv0222* H37Rv [a generous gift from Deborah Hung (Barczak et al., 2017)] were grown in Middlebrook 7H9 containing 25 μg/ml kanamycin. Non-replicating assays were done using a reported 4-stress model (Warrier et al., 2015; Gold et al., 2016b). In brief, replicating cells were washed twice and diluted to an OD_{580} of 0.1 in non-replicating (NR) medium: modified Sauton's base (0.05% KH_2PO_4, 0.05% $MgSO_4$, and 0.005% ferric ammonium citrate at pH 5.0) with 0.02% tyloxapol, 0.5% bovine serum albumin (BSA), 0.0001% $ZnSO_4$, and 0.05% $(NH_4)_2SO_4$ 0.085% NaCl; butyrate (0.05%) was used as the carbon source and a flux of nitric oxide was generated by adding 0.5 mM $NaNO_2$ to the acidified medium. For conditions involving different carbon sources, the butyrate was replaced with 0.05% acetate, 0.05% propionate, 0.015% hexanoate, 0.00025% palmitate, 0.2% glucose, or 0.2% glutamate, and the pH was adjusted to 5.0. The cells were incubated with 5% CO_2 and 1.0% O_2 at 37°C. Unless otherwise stated, cells were exposed to compounds for 7 days for the following assays: minimum inhibitory concentration (MIC), charcoal agar resazurin assay (CARA), or colony-forming unit (CFU).

Compound Activity (CFU/ml, MIC, and CARA)

Bacilli were enumerated by plating serially diluted bacterial cultures on 7H11 agar (BD Difco, Franklin Lakes, NJ, United States) plates supplemented with 0.5% glycerol and 10% OADC. MICs were determined by serially diluting compounds in DMSO and dispensing into 96-well plate with 200 μl of cells. The final DMSO concentrations did not exceed 1%. Compound dilutions were prepared the same day of experiments. For the replicating MIC assays, bacterial suspensions were diluted to an OD_{580} of 0.01 and added to the 96-well plate containing the compound. The MIC of a compound was the lowest concentration leading to ≥90% inhibition of the cell growth compared to cells treated with vehicle (DMSO). Growth was determined by OD_{580}. For non-replicating cells, the NR MIC was determined as described (Warrier et al., 2015) by resuspending cells from the NR plates and using 1/20 of the volume to inoculate a second plate containing replication-supporting, supplemented 7H9 broth. The latter plates were incubated under replicating conditions for 10–12 days before recording the OD_{580}. CARA plates were prepared and assayed as described (Gold et al., 2015a, 2016a). In brief, after 7 days of compound exposure, cells in the assay plate were resuspended and 10 μl were used to inoculate CARA plates containing agar with 4 g/L activated charcoal. After incubating the CARA plates for 7 days (replicating assay) or 12–14 days (NR assay), growth was estimated by adding 50 μl of 0.01% resazurin in PBS with 0.02% Tyl to each well of the CARA plates. The $CARA_{MBC}$ was defined as the lowest concentration of compound that reduced fluorescence to ≤1% of that in DMSO control wells for each strain, which corresponds to a difference in viable cell number of ≥2–3 $\log_{10}$ CFU (Gold et al., 2016a).

Ldts and BlaC Kinetics

Production, purification, and activity of Mtb Ldt_{Mt1} and Ldt_{Mt2} and *E. faecium* Ldt_{fm} were carried out as previously described (Cordillot et al., 2013; Edoo et al., 2017). Briefly, BlaC hydrolysis of **1**, **5**, and **9c** was determined by incubating 100 μM of each compound with 50 and 500 nM of the enzyme in 100 mM MES buffer at pH 6.4. Inhibition of BlaC-mediated hydrolysis of nitrocefin was tested by incubating 2 nM of BlaC in the presence of increasing concentration of **1**, **5**, and **9c** and 50 μM of nitrocefin. To account for time-dependent inhibition, 1 nM of BlaC was incubated for 2 h with the compounds prior to the

addition of nitrocefin. In the case of Ldt_{Mt1} and Ldt_{Mt2}, all kinetic tests were conducted in 100 mM sodium phosphate at pH 6.0 at 20°C. To asses Ldt hydrolysis of the compounds, 50 μM of **1**, **5**, or **9c** was incubated with increasing concentration of Ldt (0, 1, 5, and 10 μM). Inhibition of enzyme activity was determined by incubating 5 μM of the Ldt enzymes in the presence of test compounds (0, 25, 50, and 100 μM) and 50 μM of nitrocefin. Assays were performed using enzymes incubated for 30 min with the compounds prior to the addition of nitrocefin. Stopped flow kinetics were conducted using Ldt_{fm} in 100 mM sodium phosphate at pH 6.0 at 10°C. Ldt_{fm} (15 μM) and 20 μM of 1, 5, or imipenem were mixed, and the acylated form of Ldt_{fm} was monitored by mass spectrometry.

Bacterial Proteome Ligand Binding

Mtb cells were washed with PBS containing 0.02% Tyloxapol, diluted to an OD_{580} of 0.8–1.0 in 30-ml cultures, and pre-adapted to non-replicating conditions for 24 h. Following the pre-adaptation to NR conditions, 50–70 μM of compounds or vehicle control (DMSO) was added to the cultures and placed back in the 37°C incubator. After a 24-h exposure to compounds, cells were washed 2× with PBS containing 0.02% Tyloxapol, harvested, and stored at −80°C until ready for lysis. The protocol as shown in **Figure 3** was conducted twice.

Extraction buffers consisted of PBS containing Roche Protease Inhibitor Cocktail and 2% Triton X-114 in PBS (kept at 4°C) as previously described (Malen et al., 2010) with modifications. Samples were resuspended in ∼720 μl of PBS and transferred to bead beating tubes containing 500 μl of zirconium beads. Samples were maintained ice cold. Bacteria were lysed by bead beating and centrifuged for 5 min at 1400 × *g* to remove beads and unlysed cells. There was approximately 800 μl of lysate. Eighty microliters of PBS-20% Triton X-114 solution was added to each sample. Samples rotated gently at 4°C overnight. To remove insoluble material, samples were centrifuged at 4°C at 8600 × *g* for 10 min. In contrast to published protocols, samples were maintained chilled such that the detergent (membrane) fraction and aqueous phase were maintained in solution. In our experience, phase separation reduced the final yield of proteins.

Probe Conjugation, Purification and Enrichment of Target Proteins

Based on published general click chemistry protocols (Speers and Cravatt, 2009; Yang et al., 2013), samples were diluted with PBS to halve the detergent concentration (<1%) prior to incubating them overnight at 4°C with streptavidin beads. Once biotinylated proteins were removed, protein concentrations were determined using the Pierce BCA Protein Assay Kit (Thermo Fisher Scientific, United States) and samples were diluted to the same protein concentration (∼1 mg/ml). The samples were divided into 500-μl aliquots. For Cu(I) catalyzed Huisgen's azide alkyne cycloaddition reactions, the following was added to each sample: 5.0 μl of 5 mM diol-biotin-azide (50 μM final), 11.3 μl 50 mM TCEP (1 mM final), 7.0 μl 1.7 mM TBTA (tris[(1-benzyl-1H-1,2,3-triazol-4-yl)methyl]amine) (50 μM final), and 11.3 μl of 50 mM $CuSO_4$ (1 mM final). Samples were vortexed between each step and kept in the dark. The reaction proceeded for 1 h at RT with vortexing after 30 min of incubation. Some proteins precipitated out of solution. Accordingly, samples were centrifuged for 15 min at 10,000 × *g* and the pellet was set aside as the "precipitate." The pellet was washed with 500 μl of cold methanol and resuspended in 2.5% SDS to solubilize the proteins. The precipitate fractions were diluted to <0.2% SDS prior to the addition of the streptavidin beads. To stop the reaction in the supernatant or "soluble fraction" and remove excess reagents, samples were run through a PD-10 column (Bio-Rad). One hundred microliters of streptavidin-agarose bead slurry was added to each sample and incubated overnight at 4°C. The beads were washed 2× with 1 volume of PBS containing 0.1% Triton X-100 including one O/N wash. This was followed by three washes with PBS. Proteins were eluted from the beads by resuspending the slurry in 10 mM sodium periodate in 100 mM sodium phosphate buffer, pH 7.4. The samples were incubated for 30 min in the dark with rotation. Glucose (20 mM final) was added to quench the reactions. Samples were desalted using Zeba spin columns (Thermo Fisher Scientific). Samples were concentrated by TCA precipitation and analyzed by silver staining, Western blot, and mass spectrometry.

Rv1738 Purification and Ribosomal Inhibition

Rv1738 and ribosome functional assays were performed as previously described (Li et al., 2015) in which Rv1738 was cloned into p1602-dest (Life Technologies) with a C-terminal His6x tag on Rv1738. Rv1738 was purified with Ni^{2+} chromatography column (GE Healthcare), followed by size exclusion chromatography. A superdex 75 column (GE Healthcare) was used for size exclusion chromatography in a buffer containing 20 mM Tris–Cl (pH 7.5) and 150 mM NaCl, and the protein profile was compared with protein molecular size standards.

In order to purify *Mtb* ribosome, *Mtb* strain MC^27000 was grown in 7H9 medium supplemented with 10% OADC supplement (BD), 0.5% glycerol, 0.05% Tween-80, and 50 μg/ml pantothenic acid at 37°C until an OD_{600} of 1.0. Harvested cells were lysed in a bead beater (BioSpec) in lysis buffer [20 mM Tris–HCl (pH 7.5), 100 mM NH_4Cl, 10 mM $MgCl_2$, 0.5 mM EDTA, and 6 mM 2-mercaptoethanol]. The cell lysate was clarified by centrifugation at 30,000 × *g* for 1 h. The supernatant was pelleted in a sucrose cushion buffer [20 mM HEPES (pH 7.5), 1.1 M sucrose, 10 mM $MgCl_2$, 0.5 M KCl, and 0.5 mM EDTA] at 40,000 rpm in a Beckman Type 45Ti rotor for 20 h. The pellet was resuspended in a buffer of 20 mM Tris–HCl (pH 7.5), 1.5 M $(NH_4)_2SO_4$, 0.4 M KCl, and 10 mM $MgCl_2$. The suspension was then applied to a hydrophobic interaction column (Toyopearl Butyl-650S) and eluted with a reverse ionic strength gradient from 1.5 to 0 M $(NH_4)_2SO_4$ in a buffer containing 20 mM Tris–HCl (pH 7.5), 0.4 M KCl, and 10 mM $MgCl_2$. The eluted ribosome peak was changed to re-association buffer [5 mM HEPES-NaOH (pH 7.5), 10 mM NH_4Cl, 50 mM KCl, 10 mM $MgCl_2$, and 6 mM 2-mercaptoethanol] and concentrated before loading on top of a 10–40% linear sucrose gradient and centrifuged in a Beckman

SW28 rotor at 19,000 rpm for 19 h. The 70S fractions were concentrated to about A_{260} = 300 after removal of the sucrose. *Mtb* S30 cell-free extract was prepared according to methods (Swartz et al., 2004) and S100 extract was prepared by removing endogenous ribosomes from the S30 extract. The 15 μl of the S100 extract that includes translation factors such as initiation, elongation, termination, recycling factors, and aminoacyl tRNA synthetase was mixed with 5 μl 10 × salt buffer (2 M potassium glutamate, 0.8 M ammonium acetate, and 0.16 M magnesium acetate), 1 mM each of the 20 amino acids, 33 mM PEP, and 2% poly(ethylene glycol) 8000. Rv1738 or the compounds or their mixtures with ribosomes were added to the reactions prior to the master mix and mRNA. The reaction was started by the addition of nano-luciferase mRNA (200 ng in 2 μl) and 5 μl of 5× master mix (286 mM HEPES-KOH, pH 7.5, 6 mM ATP, 4.3 mM GTP, 333 μM folinic acid, and 853 μg/ml tRNA) to reach a final volume of 50 μl. The reaction was allowed to proceed for 40 min at 37°C and the luminescent signal was detected by the addition of 20 μl of the nano-luciferase substrate furimazine. **1**, **5**, **9c**, and **C5** were first tested in the cell-free translation assay to ensure that the compounds alone did not inhibit ribosomal activity. To test the impact that the compounds had on Rv1738-mediated inhibition of translation, we tested several combinations: ribosomes and 10 μM Rv1738 were incubated for 10 min followed by the addition of 240 μM of the compounds; ribosomes and 240 μM compounds were incubated for 10 min followed by the addition of 10 μM of Rv1738; 10 μM of Rv1738 was incubated with 240 μM compounds before mixing with ribosomes; and finally, the reaction was carried out in which 240 μM compounds and ribosome were co-incubated first, followed by the titration of Rv1738.

HtpG Characterization and Differential Scanning Fluorimetry (DSF)

Mycobacterium tuberculosis Δ*htpG* was generated using a suicide plasmid approach, which enlists Gateway cloning techniques and vectors. Briefly, ∼1100 bp fragments, including regions upstream and downstream of *htpG* (*rv2299c*), were amplified from chromosomal *M. tuberculosis* H37RvN DNA using primers 1–4 (**Supplementary Table S3**). The fragments were cloned into pDE43-XSTS (a temperature-sensitive plasmid) containing a zeocin resistance cassette, which was amplified from pGMCZ-PrpoB using primers 9 and 10 to produce pKO-XSTS-htpG-tb (Pelicic et al., 1997; Kim et al., 2011; Ganapathy et al., 2015). *M. tuberculosis* H37RvN was transformed with pKO-XSTS-htpG-tb and plated on 7H10 agar containing zeocin (50 μg/ml), followed by incubation at the permissive temperature of 37°C. Resulting transformants were then inoculated into 7H9 complete (with Tween-80) containing zeocin (25 μg/ml) at 37°C and grown to stationary phase. Cells were periodically plated on 7H10 agar with zeocin (50 μg/ml) containing 10% sucrose and incubated at the restrictive temperature of 40°C. Pyrocatechol (0.5 M) was added to plates that contained colonies and white colonies were inoculated into 7H9 complete (with Tween-80) containing zeocin (25 μg/ml) and grown at 37°C prior to purification of DNA and confirmation of allelic exchange by Southern blot. Southern blot of selected clones was performed using a DNA probe (∼400 bp) generated with primers 5–6 (**Supplementary Table S3**) in order to analyze genomic DNA from *M. tuberculosis* wild type and candidate Δ*htpG* clones digested with *Pvu*II (**Supplementary Figure S5**). Deletion of *htpG* and insertion of zeocin resistant cassette were confirmed by whole genome sequencing. For overexpression of HtpG in Mtb Δ*htpG*, we generated pMCH_pH60_SD_htpG using primers 11 and 12 (**Supplementary Table S3**), an episomal vector that expresses *htpG* under the control of the *hsp60* promoter, as has been previously described (Kim et al., 2011; White et al., 2018).

Recombinant *M. tuberculosis* HtpG was cloned and purified using previously described methods (Lupoli et al., 2016). The overexpression plasmid was constructed by overlap extension PCR cloning techniques (Bryksin and Matsumura, 2010) with pET-His-SUMO plasmid (Addgene #29711) and primer pair 7–8 (**Supplementary Table S3**). DNA samples were purified using a PCR purification kit (Qiagen) and transformed into Mach1 competent cells (Invitrogen). After confirmation of gene insertion by DNA sequencing, the selected plasmid was transformed into Rosetta2 competent cells (Novagen) for overexpression and purification using similar techniques to those previously described for other mycobacterial chaperones (Lupoli et al., 2016). For expression, *E. coli* Rosetta2 cultures containing His_6-SUMO-HtpG overexpression plasmid were grown in LB medium supplemented with 50 μg/ml carbenicillin, 30 μg/ml chloramphenicol, and 0.1% glucose, and then used to inoculate 0.5 L of LB medium (1:100) supplemented with 50 μg/ml carbenicillin and 30 μg/ml chloramphenicol at 37°C and grown to OD_{600} = 0.3–0.4 with shaking. Cells were cooled to 16°C and grown to OD_{600} ∼ 0.5 before induction with 0.01 mM isopropyl-β-D-thiogalactoside (IPTG) for 18 h with shaking. Cells were harvested by centrifugation (3100 × *g*, 10 min, 4°C) and pellet was resuspended on ice with 15 ml of Buffer A [25 mM tris(hydroxymethyl)aminomethane (Tris) (pH 8.0), 400 mM NaCl, 10% glycerol] containing 100 μg/ml lysozyme and 3 μg/ml DNaseI. The suspension was rocked for 30 min at 4°C prior to lysis by sonication on ice using a 30-s interval program at an amplitude of 5 for a total of 5 min. Samples were then ultracentrifuged at 39,191 × *g* for 30 min at 4°C. The resulting supernatant was added to 1.5 ml of washed Ni-NTA agarose resin (Qiagen) with 2 mM added imidazole and rocked at 4°C for 30 min. The resin was then washed with 30 ml of wash buffer (30 mM imidazole in Buffer A) and His_6-SUMO-HtpG was eluted with 10 ml of elution buffer (200 mM imidazole in Buffer A). The eluate fractions were dialyzed against 2 L of Buffer A overnight using a 10-kDa MWCO Slide-A-Lyzer dialysis cassette (Pierce). His_6-SUMO protease (0.04 mg/ml; His-Ulp1, purified from Addgene #31122) was added to the dialysis sample to cleave the His_6-SUMO tag from each protein as has been previously described (Uehara et al., 2010). To separate His-tagged and non-tagged proteins, the dialysis samples were then incubated with 1.5 ml of washed Ni-NTA resin for 1 h at 4°C. The flow-through and 3 ml of Buffer A were passed over the column, collected, and contained the desired untagged protein without non-native residues. The protein sample was concentrated to <1 ml using a 30-kDa MWCO Amicon Ultra Centrifugal Filter

Device (Millipore) at 4°C followed by flash freezing with $N_{2(l)}$ and storage at −80°C.

Differential scanning fluorimetry was carried out as previously described (Niesen et al., 2007). Briefly, assays were conducted in 25 mM Tris at pH 8.0, 400 mM NaCl, and 5% glycerol. After selecting the optimal protein concentration to be used, HtpG was mixed with test compounds and Sypro dye. The binding of the Sypro dye to HtpG as the temperature increased (25–90°C) was monitored using the Bio-Rad CFX qRT-PCR detection system and melting curves were derived using the CFX Maestro Analysis Software (Bio-Rad Laboratories, United States).

Statistical Analysis

Comparisons were analyzed by a two-tailed Student's *t*-test with GraphPad Prism 8. Values of $p < 0.05$ were considered significant. CARA assays and CFU data were presented as means ± standard deviation. Unless otherwise specified, experiments were carried out in triplicate.

DATA AVAILABILITY STATEMENT

The raw data supporting the conclusions of this article will be made available by the authors, without undue reservation, to any qualified researcher.

AUTHOR CONTRIBUTIONS

LL, RS, BG, CN, and JA conceived and designed the study. LL, TL, JR, YL, ZE, XL, and SP performed the experiments. RS, QN, and FS contributed to chemical synthesis. LL, ZE, XL, BG, J-EH, MA, JS, CN, and JA analyzed the data. LL wrote the manuscript. LL, CN, JA, BG, KL, TL, SP, XL, and ZE edited the manuscript. All authors contributed to the article and approved the submitted version.

FUNDING

This work was supported by the NIH Tri-Institutional TB Research Unit grant U19AI111143 and the Milstein Program in Chemical Biology and Translational Medicine. The Department of Microbiology and Immunology is supported by the William Randolph Hearst Trust. Work from the Department of Biochemistry and Biophysics at Texas Agricultural and Mechanical University was supported by the generosity of the Welch Foundation (A-0015).

ACKNOWLEDGMENTS

We thank Kristin Burns-Huang (Weill Cornell Medicine) for advice and editorial comments. We are indebted to Sabine Ehrt and Weizhen Xu (Weill Cornell Medicine) for the Δ*fecB* mutant and complemented strain, Milica Tesic Mark and Henrik Molina (Proteomics Resource Center, Rockefeller University) for assistance, Carolina Adura from the Rockefeller University High Throughput Screening Core for her guidance on DSF, Jamie Bean for his assistance in with sequencing the Δ*htpG* Mtb strain, Scott Gradia (University of California, Berkeley) for his gift of pETHis6 Sumo TIV LIC cloning vector, and Deborah Hung (Broad Institute) for generously sharing a transposon mutant library of Mtb. Creation of the transposon library was supported by the Broad Institute Tuberculosis donor group and the Pershing Square Foundation.

SUPPLEMENTARY MATERIAL

The Supplementary Material for this article can be found online at: https://www.frontiersin.org/articles/10.3389/fmicb.2020.01248/full#supplementary-material

REFERENCES

Abraham, E. P., Gardner, A. D., Chain, E., Heatley, N. G., Fletcher, C. M., and Jennings, M. A. (1941). Further observations on penicillin. *Lancet* 2, 177–189. doi: 10.1016/s0140-6736(00)72122-2

Baranowski, C., and Rubin, E. J. (2016). Could killing bacterial subpopulations hit tuberculosis out of the park? *J. Med. Chem.* 59, 6025–6026. doi: 10.1021/acs.jmedchem.6b00875

Barczak, A. K., Avraham, R., Singh, S., Luo, S. S., Zhang, W. R., Bray, M. A., et al. (2017). Systematic, multiparametric analysis of *Mycobacterium tuberculosis* intracellular infection offers insight into coordinated virulence. *PLoS Pathog.* 13:e1006363. doi: 10.1371/journal.ppat.1006363

Bianchet, M. A., Pan, Y. H., Basta, L. A. B., Saavedra, H., Lloyd, E. P., Kumar, P., et al. (2017). Structural insight into the inactivation of *Mycobacterium tuberculosis* non-classical transpeptidase LdtMt2 by biapenem and tebipenem. *BMC Biochem.* 18:8. doi: 10.1186/s12858-017-0082-4

Bottcher, T., and Sieber, S. A. (2008). Beta-lactones as privileged structures for the active-site labeling of versatile bacterial enzyme classes. *Angew. Chem. Int. Ed. Engl.* 47, 4600–4603. doi: 10.1002/anie.200705768

Bryk, R., Gold, B., Venugopal, A., Singh, J., Samy, R., Pupek, K., et al. (2008). Selective killing of nonreplicating mycobacteria. *Cell Host Microbe* 3, 137–145. doi: 10.1016/j.chom.2008.02.003

Bryksin, A. V., and Matsumura, I. (2010). Overlap extension PCR cloning: a simple and reliable way to create recombinant plasmids. *Biotechniques* 48, 463–465. doi: 10.2144/000113418

Bunker, R. D., Mandal, K., Bashiri, G., Chaston, J. J., Pentelute, B. L., Lott, J. S., et al. (2015). A functional role of Rv1738 in *Mycobacterium tuberculosis* persistence suggested by racemic protein crystallography. *Proc. Natl. Acad. Sci. U.S.A.* 112, 4310–4315. doi: 10.1073/pnas.1422387112

Bush, K., and Macielag, M. J. (2010). New beta-lactam antibiotics and beta-lactamase inhibitors. *Expert Opin. Ther. Pat.* 20, 1277–1293.

Chauvette, R. R., and Flynn, E. H. (1966). Chemistry of cephalosporin antibiotics. V. Amides and esters of cephalothin. *J. Med. Chem.* 9, 741–745. doi: 10.1021/jm00323a023

Cordillot, M., Dubee, V., Triboulet, S., Dubost, L., Marie, A., Hugonnet, J. E., et al. (2013). In vitro cross-linking of *Mycobacterium tuberculosis* peptidoglycan by L,D-transpeptidases and inactivation of these enzymes by carbapenems. *Antimicrob. Agents Chemother.* 57, 5940–5945. doi: 10.1128/aac.01663-13

Correale, S., Ruggiero, A., Capparelli, R., Pedone, E., and Berisio, R. (2013). Structures of free and inhibited forms of the L,D-transpeptidase LdtMt1 from *Mycobacterium tuberculosis*. *Acta Crystallogr. D Biol. Crystallogr.* 69, 1697–1706.

Cravatt, B. F., Wright, A. T., and Kozarich, J. W. (2008). Activity-based protein profiling: from enzyme chemistry to proteomic chemistry. *Annu. Rev. Biochem.* 77, 383–414. doi: 10.1146/annurev.biochem.75.101304.124125

de Carvalho, L. P., Fischer, S. M., Marrero, J., Nathan, C., Ehrt, S., and Rhee, K. Y. (2010). Metabolomics of *Mycobacterium tuberculosis* reveals compartmentalized co-catabolism of carbon substrates. *Chem. Biol.* 17, 1122–1131. doi: 10.1016/j.chembiol.2010.08.009

Debabov, D. V., Kiriukhin, M. Y., and Neuhaus, F. C. (2000). Biosynthesis of lipoteichoic acid in *Lactobacillus rhamnosus*: role of DltD in D-alanylation. *J. Bacteriol.* 182, 2855–2864. doi: 10.1128/jb.182.10.2855-2864.2000

DeJesus, M. A., Gerrick, E. R., Xu, W., Park, S. W., Long, J. E., Boutte, C. C., et al. (2017). Comprehensive essentiality analysis of the *Mycobacterium tuberculosis* genome via saturating transposon mutagenesis. *mBio* 8:e02133-16.

Doherty, J. B., Ashe, B. M., Argenbright, L. W., Barker, P. L., Bonney, R. J., Chandler, G. O., et al. (1986). Cephalosporin antibiotics can be modified to inhibit human leukocyte elastase. *Nature* 322, 192–194. doi: 10.1038/322192a0

Drumm, J. E., Mi, K., Bilder, P., Sun, M., Lim, J., Bielefeldt-Ohmann, H., et al. (2009). *Mycobacterium tuberculosis* universal stress protein Rv2623 regulates bacillary growth by ATP-Binding: requirement for establishing chronic persistent infection. *PLoS Pathog.* 5:e1000460. doi: 10.1371/journal.ppat.1000460

Dubee, V., Arthur, M., Fief, H., Triboulet, S., Mainardi, J. L., Gutmann, L., et al. (2012a). Kinetic analysis of *Enterococcus faecium* L,D-transpeptidase inactivation by carbapenems. *Antimicrob. Agents Chemother.* 56, 3409–3412. doi: 10.1128/aac.06398-11

Dubee, V., Triboulet, S., Mainardi, J. L., Etheve-Quelquejeu, M., Gutmann, L., Marie, A., et al. (2012b). Inactivation of *Mycobacterium tuberculosis* l,d-transpeptidase LdtMt(1) by carbapenems and cephalosporins. *Antimicrob. Agents Chemother.* 56, 4189–4195. doi: 10.1128/aac.00665-12

Edoo, Z., Arthur, M., and Hugonnet, J. E. (2017). Reversible inactivation of a peptidoglycan transpeptidase by a beta-lactam antibiotic mediated by beta-lactam-ring recyclization in the enzyme active site. *Sci. Rep.* 7:9136.

Ganapathy, U., Marrero, J., Calhoun, S., Eoh, H., De Carvalho, L. P. S., Rhee, K., et al. (2015). Two enzymes with redundant fructose bisphosphatase activity sustain gluconeogenesis and virulence in *Mycobacterium tuberculosis*. *Nat. Commun.* 6:7912.

Garcie, C., Tronnet, S., Garenaux, A., Mccarthy, A. J., Brachmann, A. O., Penary, M., et al. (2016). The bacterial stress-responsive Hsp90 Chaperone (HtpG) is required for the production of the genotoxin colibactin and the siderophore yersiniabactin in *Escherichia coli*. *J. Infect. Dis.* 214, 916–924. doi: 10.1093/infdis/jiw294

Glass, L. N., Swapna, G., Chavadi, S. S., Tufariello, J. M., Mi, K., Drumm, J. E., et al. (2017). *Mycobacterium tuberculosis* universal stress protein Rv2623 interacts with the putative ATP binding cassette (ABC) transporter Rv1747 to regulate mycobacterial growth. *PLoS Pathog.* 13:e1006515. doi: 10.1371/journal.ppat.1006515

Gold, B., and Nathan, C. (2017). Targeting phenotypically tolerant *Mycobacterium tuberculosis*. *Microbiol. Spectr.* 5:TBTB2-0031-2016.

Gold, B., Pingle, M., Brickner, S. J., Shah, N., Roberts, J., Rundell, M., et al. (2012). Nonsteroidal anti-inflammatory drug sensitizes *Mycobacterium tuberculosis* to endogenous and exogenous antimicrobials. *Proc. Natl. Acad. Sci. U.S.A.* 109, 16004–16011. doi: 10.1073/pnas.1214188109

Gold, B., Roberts, J., Ling, Y., Lopez Quezada, L., Glasheen, J., Ballinger, E., et al. (2016a). Visualization of the charcoal agar resazurin assay for semi-quantitative, medium-throughput enumeration of mycobacteria. *J. Vis. Exp.* 118:54690.

Gold, B., Roberts, J., Ling, Y., Quezada, L. L., Glasheen, J., Ballinger, E., et al. (2015a). Rapid, semiquantitative assay to discriminate among compounds with activity against replicating or nonreplicating *Mycobacterium tuberculosis*. *Antimicrob. Agents Chemother.* 59, 6521–6538. doi: 10.1128/aac.00803-15

Gold, B., Smith, R., Nguyen, Q., Roberts, J., Ling, Y., Lopez Quezada, L., et al. (2016b). Novel cephalosporins selectively active on nonreplicating *Mycobacterium tuberculosis*. *J. Med. Chem.* 59, 6027–6044. doi: 10.1021/acs.jmedchem.5b01833

Gold, B., Warrier, T., and Nathan, C. (2015b). A multi-stress model for high throughput screening against non-replicating *Mycobacterium tuberculosis*. *Methods Mol. Biol.* 1285, 293–315. doi: 10.1007/978-1-4939-2450-9_18

Gordon, E., Mouz, N., Duee, E., and Dideberg, O. (2000). The crystal structure of the penicillin-binding protein 2x from Streptococcus pneumoniae and its acyl-enzyme form: implication in drug resistance. *J. Mol. Biol.* 299, 477–485. doi: 10.1006/jmbi.2000.3740

Grant, S. S., Kawate, T., Nag, P. P., Silvis, M. R., Gordon, K., Stanley, S. A., et al. (2013). Identification of novel inhibitors of nonreplicating *Mycobacterium tuberculosis* using a carbon starvation model. *ACS Chem. Biol.* 8, 2224–2234. doi: 10.1021/cb4004817

Grudniak, A. M., Pawlak, K., Bartosik, K., and Wolska, K. I. (2013). Physiological consequences of mutations in the htpG heat shock gene of *Escherichia coli*. *Mutat. Res.* 745-746, 1–5. doi: 10.1016/j.mrfmmm.2013.04.003

Hicks, N. D., Yang, J., Zhang, X., Zhao, B., Grad, Y. H., Liu, L., et al. (2018). Clinically prevalent mutations in *Mycobacterium tuberculosis* alter propionate metabolism and mediate multidrug tolerance. *Nat. Microbiol.* 3, 1032–1042. doi: 10.1038/s41564-018-0218-3

Hingley-Wilson, S. M., Lougheed, K. E., Ferguson, K., Leiva, S., and Williams, H. D. (2010). Individual *Mycobacterium tuberculosis* universal stress protein homologues are dispensable in vitro. *Tuberculosis* 90, 236–244. doi: 10.1016/j.tube.2010.03.013

Hugonnet, J. E., Tremblay, L. W., Boshoff, H. I., Barry, C. E. III, and Blanchard, J. S. (2009). Meropenem-clavulanate is effective against extensively drug-resistant *Mycobacterium tuberculosis*. *Science* 323, 1215–1218. doi: 10.1126/science.1167498

Jen, T., Dienel, B., Frazee, J., and Weisbach, J. (1972). Novel cephalosporins. Modification of the C-4 carboxyl group. *J. Med. Chem.* 15, 1172–1174. doi: 10.1021/jm00281a020

Kelley, L. A., Mezulis, S., Yates, C. M., Wass, M. N., and Sternberg, M. J. (2015). The Phyre2 web portal for protein modeling, prediction and analysis. *Nat. Protoc.* 10, 845–858. doi: 10.1038/nprot.2015.053

Kim, J. H., Wei, J. R., Wallach, J. B., Robbins, R. S., Rubin, E. J., and Schnappinger, D. (2011). Protein inactivation in mycobacteria by controlled proteolysis and its application to deplete the beta subunit of RNA polymerase. *Nucleic Acids Res.* 39, 2210–2220. doi: 10.1093/nar/gkq1149

Kumar, P., Kaushik, A., Lloyd, E. P., Li, S. G., Mattoo, R., Ammerman, N. C., et al. (2017). Non-classical transpeptidases yield insight into new antibacterials. *Nat. Chem. Biol.* 13, 54–61. doi: 10.1038/nchembio.2237

Kuo, D., Weidner, J., Griffin, P., Shah, S. K., and Knight, W. B. (1994). Determination of the kinetic parameters of *Escherichia coli* leader peptidase activity using a continuous assay: the pH dependence and time-dependent inhibition by beta-lactams are consistent with a novel serine protease mechanism. *Biochemistry* 33, 8347–8354. doi: 10.1021/bi00193a023

Lavollay, M., Arthur, M., Fourgeaud, M., Dubost, L., Marie, A., Veziris, N., et al. (2008). The peptidoglycan of stationary-phase *Mycobacterium tuberculosis* predominantly contains cross-links generated by L,D-transpeptidation. *J. Bacteriol.* 190, 4360–4366. doi: 10.1128/jb.00239-08

Lee, J. J., Lee, S. K., Song, N., Nathan, T. O., Swarts, B. M., Eum, S. Y., et al. (2019). Transient drug-tolerance and permanent drug-resistance rely on the trehalose-catalytic shift in *Mycobacterium tuberculosis*. *Nat. Commun.* 10:2928.

Li, X., Sun, Q., Jiang, C., Yang, K., Hung, L. W., Zhang, J., et al. (2015). Structure of ribosomal silencing factor bound to *Mycobacterium tuberculosis* ribosome. *Structure* 23, 1858–1865. doi: 10.1016/j.str.2015.07.014

Lupoli, T. J., Fay, A., Adura, C., Glickman, M. S., and Nathan, C. F. (2016). Reconstitution of a *Mycobacterium tuberculosis* proteostasis network highlights essential cofactor interactions with chaperone DnaK. *Proc. Natl. Acad. Sci. U.S.A.* 113, E7947–E7956.

Lupoli, T. J., Vaubourgeix, J., Burns-Huang, K., and Gold, B. (2018). Targeting the proteostasis network for mycobacterial drug discovery. *ACS Infect. Dis.* 4, 478–498. doi: 10.1021/acsinfecdis.7b00231

Mainardi, J. L., Fourgeaud, M., Hugonnet, J. E., Dubost, L., Brouard, J. P., Ouazzani, J., et al. (2005). A novel peptidoglycan cross-linking enzyme for a beta-lactam-resistant transpeptidation pathway. *J. Biol. Chem.* 280, 38146–38152. doi: 10.1074/jbc.m507384200

Mak, P. A., Rao, S. P., Ping Tan, M., Lin, X., Chyba, J., Tay, J., et al. (2012). A high-throughput screen to identify inhibitors of ATP homeostasis in non-replicating *Mycobacterium tuberculosis*. *ACS Chem. Biol.* 7, 1190–1197. doi: 10.1021/cb2004884

Malen, H., Pathak, S., Softeland, T., De Souza, G. A., and Wiker, H. G. (2010). Definition of novel cell envelope associated proteins in Triton X-114 extracts of

Mycobacterium tuberculosis H37Rv. *BMC Microbiol.* 10:132. doi: 10.1186/1471-2180-10-132

McKinney, J. D., Honer Zu Bentrup, K., Munoz-Elias, E. J., Miczak, A., Chen, B., Chan, W. T., et al. (2000). Persistence of *Mycobacterium tuberculosis* in macrophages and mice requires the glyoxylate shunt enzyme isocitrate lyase. *Nature* 406, 735–738. doi: 10.1038/35021074

Mishra, S., Ahmed, T., Tyagi, A., Shi, J., and Bhushan, S. (2018). Structures of *Mycobacterium smegmatis* 70S ribosomes in complex with HPF, tmRNA, and P-tRNA. *Sci. Rep.* 8:13587.

Mouz, N., Di Guilmi, A. M., Gordon, E., Hakenbeck, R., Dideberg, O., and Vernet, T. (1999). Mutations in the active site of penicillin-binding protein PBP2x from *Streptococcus pneumoniae*. Role in the specificity for beta-lactam antibiotics. *J. Biol. Chem.* 274, 19175–19180. doi: 10.1074/jbc.274.27.19175

Murray, S., Mendel, C., and Spigelman, M. (2016). TB Alliance regimen development for multidrug-resistant tuberculosis. *Int. J. Tuberc. Lung Dis.* 20, 38–41. doi: 10.5588/ijtld.16.0069

Nathan, C. (2012). Fresh approaches to anti-infective therapies. *Sci. Transl. Med.* 4:140sr142.

Niesen, F. H., Berglund, H., and Vedadi, M. (2007). The use of differential scanning fluorimetry to detect ligand interactions that promote protein stability. *Nat. Protoc.* 2, 2212–2221. doi: 10.1038/nprot.2007.321

Ortega, C., Anderson, L. N., Frando, A., Sadler, N. C., Brown, R. W., Smith, R. D., et al. (2016). Systematic survey of serine hydrolase activity in *Mycobacterium tuberculosis* defines changes associated with persistence. *Cell Chem. Biol.* 23, 290–298. doi: 10.1016/j.chembiol.2016.01.003

Paetzel, M., Dalbey, R. E., and Strynadka, N. C. (1998). Crystal structure of a bacterial signal peptidase in complex with a beta-lactam inhibitor. *Nature* 396, 186–190. doi: 10.1038/24196

Parvati Sai Arun, P. V., Miryala, S. K., Rana, A., Kurukuti, S., Akhter, Y., and Yellaboina, S. (2018). System-wide coordinates of higher order functions in host-pathogen environment upon *Mycobacterium tuberculosis* infection. *Sci. Rep.* 8:5079.

Payen, M. C., Muylle, I., Vandenberg, O., Mathys, V., Delforge, M., Van Den Wijngaert, S., et al. (2018). Meropenem-clavulanate for drug-resistant tuberculosis: a follow-up of relapse-free cases. *Int. J. Tuberc. Lung Dis.* 22, 34–39. doi: 10.5588/ijtld.17.0352

Pelicic, V., Jackson, M., Reyrat, J. M., Jacobs, W. R. Jr., and Gicquel, B. (1997). Efficient allelic exchange and transposon mutagenesis in *Mycobacterium tuberculosis*. *Proc. Natl. Acad. Sci. U.S.A.* 94, 10955–10960. doi: 10.1073/pnas.94.20.10955

Polikanov, Y. S., Blaha, G. M., and Steitz, T. A. (2012). How hibernation factors RMF, HPF, and YfiA turn off protein synthesis. *Science* 336, 915–918. doi: 10.1126/science.1218538

Ramón-García, S., González del Río, R., Villarejo, A. S., Sweet, G. D., Cunningham, F., Barros, D., et al. (2016). Repurposing clinically approved cephalosporins for tuberculosis therapy. *Sci. Rep.* 6:34293. doi: 10.1038/srep34293

Schnappinger, D., Ehrt, S., Voskuil, M. I., Liu, Y., Mangan, J. A., Monahan, I. M., et al. (2003). Transcriptional adaptation of *Mycobacterium tuberculosis* within macrophages: insights into the phagosomal environment. *J. Exp. Med.* 198, 693–704. doi: 10.1084/jem.20030846

Schoonmaker, M. K., Bishai, W. R., and Lamichhane, G. (2014). Nonclassical transpeptidases of *Mycobacterium tuberculosis* alter cell size, morphology, the cytosolic matrix, protein localization, virulence, and resistance to beta-lactams. *J. Bacteriol.* 196, 1394–1402. doi: 10.1128/jb.01396-13

Sherman, D. R., Voskuil, M., Schnappinger, D., Liao, R., Harrell, M. I., and Schoolnik, G. K. (2001). Regulation of the *Mycobacterium tuberculosis* hypoxic response gene encoding alpha -crystallin. *Proc. Natl. Acad. Sci. U.S.A.* 98, 7534–7539. doi: 10.1073/pnas.121172498

Speers, A. E., and Cravatt, B. F. (2009). Activity-based protein profiling (ABPP) and click chemistry (CC)-ABPP by MudPIT mass spectrometry. *Curr. Protoc. Chem. Biol.* 1, 29–41. doi: 10.1002/9780470559277.ch090138

Staub, I., and Sieber, S. A. (2008). Beta-lactams as selective chemical probes for the in vivo labeling of bacterial enzymes involved in cell wall biosynthesis, antibiotic resistance, and virulence. *J. Am. Chem. Soc.* 130, 13400–13409. doi: 10.1021/ja803349j

Sun, Z., Hu, L., Sankaran, B., Prasad, B. V. V., and Palzkill, T. (2018). Differential active site requirements for NDM-1 beta-lactamase hydrolysis of carbapenem versus penicillin and cephalosporin antibiotics. *Nat. Commun.* 9:4524.

Swartz, J. R., Jewett, M. C., and Woodrow, K. A. (2004). Cell-free protein synthesis with prokaryotic combined transcription-translation. *Methods Mol. Biol.* 267, 169–182. doi: 10.1385/1-59259-774-2:169

Uehara, T., Parzych, K. R., Dinh, T., and Bernhardt, T. G. (2010). Daughter cell separation is controlled by cytokinetic ring-activated cell wall hydrolysis. *EMBO J.* 29, 1412–1422. doi: 10.1038/emboj.2010.36

Voskuil, M. I., Schnappinger, D., Visconti, K. C., Harrell, M. I., Dolganov, G. M., Sherman, D. R., et al. (2003). Inhibition of respiration by nitric oxide induces a *Mycobacterium tuberculosis* dormancy program. *J. Exp. Med.* 198, 705–713. doi: 10.1084/jem.20030205

Warrier, T., Martinez-Hoyos, M., Marin-Amieva, M., Colmenarejo, G., Porras-De Francisco, E., Alvarez-Pedraglio, A. I., et al. (2015). Identification of novel anti-mycobacterial compounds by screening a pharmaceutical small-molecule library against nonreplicating *Mycobacterium tuberculosis*. *ACS Infect. Dis.* 1, 580–585. doi: 10.1021/acsinfecdis.5b00025

White, D. W., Elliott, S. R., Odean, E., Bemis, L. T., and Tischler, A. D. (2018). *Mycobacterium tuberculosis* Pst/SenX3-RegX3 regulates membrane vesicle production independently of ESX-5 activity. *mBio* 9:e00778-18.

Wietzerbin, J., Das, B. C., Petit, J. F., Lederer, E., Leyh-Bouille, M., and Ghuysen, J. M. (1974). Occurrence of D-alanyl-(D)-meso-diaminopimelic acid and meso-diaminopimelyl-meso-diaminopimelic acid interpeptide linkages in the peptidoglycan of Mycobacteria. *Biochemistry* 13, 3471–3476. doi: 10.1021/bi00714a008

Williams, K. J., Boshoff, H. I., Krishnan, N., Gonzales, J., Schnappinger, D., and Robertson, B. D. (2011). The *Mycobacterium tuberculosis* beta-oxidation genes echA5 and fadB3 are dispensable for growth in vitro and in vivo. *Tuberculosis* 91, 549–555. doi: 10.1016/j.tube.2011.06.006

Wivagg, C. N., Bhattacharyya, R. P., and Hung, D. T. (2014). Mechanisms of beta-lactam killing and resistance in the context of *Mycobacterium tuberculosis*. *J. Antibiot.* 67, 645–654. doi: 10.1038/ja.2014.94

Xu, W., Dejesus, M. A., Rucker, N., Engelhart, C. A., Wright, M. G., Healy, C., et al. (2017). Chemical genetic nteraction profiling reveals determinants of intrinsic antibiotic resistance in *Mycobacterium tuberculosis*. *Antimicrob. Agents Chemother.* 61:e01334-17.

Yang, Y., Hahne, H., Kuster, B., and Verhelst, S. H. (2013). A simple and effective cleavable linker for chemical proteomics applications. *Mol. Cell Proteomics* 12, 237–244. doi: 10.1074/mcp.m112.021014

Zhao, N., Sun, M., Burns-Huang, K., Jiang, X., Ling, Y., Darby, C., et al. (2015). Identification of Rv3852 as an agrimophol-binding protein in *Mycobacterium tuberculosis*. *PLoS One* 10:e0126211. doi: 10.1371/journal.pone.0126211

Conflict of Interest: The authors declare that the research was conducted in the absence of any commercial or financial relationships that could be construed as a potential conflict of interest.

frontiers in Microbiology

ORIGINAL RESEARCH
published: 30 June 2020
doi: 10.3389/fmicb.2020.01182

Wild-Type MIC Distribution for Re-evaluating the Critical Concentration of Anti-TB Drugs and Pharmacodynamics Among Tuberculosis Patients From South India

Azger Dusthackeer[1†], Shainaba A. Saadhali[1†], Manonanthini Thangam[2], Sameer Hassan[3], Mahizhaveni Balasubramanian[1], Angayarkani Balasubramanian[1], Geetha Ramachandran[4], A. K. Hemanth Kumar[4], Kannan Thiruvenkadam[5], Govindarajan Shanmugam[1], Christy Rosaline Nirmal[1], Sam Ebenezer Rajadas[1], Sucharitha Kannappan Mohanvel[6] and Rajesh Mondal[1]*

[1] Department of Bacteriology, National Institute for Research in Tuberculosis, Chennai, India, [2] AU-KBC Research Centre, Anna University, Chennai, India, [3] Division of Neurogeriatrics, Karolinska Institutet, Solna, Sweden, [4] Department of Biochemistry, National Institute for Research in Tuberculosis, Chennai, India, [5] Department of Epidemiology, National Institute for Research in Tuberculosis, Chennai, India, [6] CAS in Botany, University of Madras, Chennai, India

OPEN ACCESS

Edited by:
Onya Opota,
University of Lausanne, Switzerland

Reviewed by:
Shashank Gupta,
Brown University, United States
Mihai Mares,
Ion Ionescu de la Brad University of Agricultural Sciences and Veterinary Medicine of Iaşi, Romania

***Correspondence:**
Azger Dusthackeer
azger@nirt.res.in

[†] These authors have contributed equally to this work

Specialty section:
This article was submitted to Antimicrobials, Resistance and Chemotherapy, a section of the journal Frontiers in Microbiology

Received: 10 January 2020
Accepted: 08 May 2020
Published: 30 June 2020

Citation:
Dusthackeer A, Saadhali SA, Thangam M, Hassan S, Balasubramanian M, Balasubramanian A, Ramachandran G, Kumar AKH, Thiruvenkadam K, Shanmugam G, Nirmal CR, Rajadas SE, Mohanvel SK and Mondal R (2020) Wild-Type MIC Distribution for Re-evaluating the Critical Concentration of Anti-TB Drugs and Pharmacodynamics Among Tuberculosis Patients From South India. Front. Microbiol. 11:1182. doi: 10.3389/fmicb.2020.01182

The World Health Organization (WHO) has developed specific guidelines for critical concentrations (CCs) of antibiotics used for tuberculosis (TB) treatment, which is universally followed for drug susceptibility testing (DST) of clinical specimens. However, the CC of drugs can differ significantly among the mycobacterial species based on the population, geographic location, and the prevalence of the infecting strain in a particular area. The association between CC and the minimal inhibitory concentration (MIC) of anti-TB drugs is poorly understood. In this study, we assessed the MICs of anti-TB drugs, including isoniazid (INH), rifampicin (RMP), moxifloxacin (MXF), ethambutol (ETH), and *p*-aminosalicylic acid (PAS) on drug-sensitive Mtb isolates from pulmonary TB patients in South India. The MIC assays performed using solid- and liquid-growth media showed changes in the CC of a few of the tested antibiotics compared with the WHO-recommended levels. Our observation suggests that the WHO guidelines could potentially lead to overdiagnosis of drug-resistant cases, which can result in inappropriate therapeutic decisions. To evaluate the correlation between drug-resistance and CC, we performed the whole-genome sequencing for 16 mycobacterial isolates, including two wild-type and 14 resistant isolates. Our results showed that two of the isolates belonged to the W-Beijing lineage, while the rest were of the East-African–Indian type. We identified a total of 74 mutations, including five novel mutations, which are known to be associated with resistance to anti-TB drugs in these isolates. In our previous study, we determined the serum levels of INH and RMP among the same patients recruited in the current study and estimated the MICs of the corresponding infected isolates in these cases. Using these data and the CCs for INH and RMP from the present

study, we performed pharmacodynamics (PD) evaluation. The results show that the PD of RMP was subtherapeutic. Together, these observations emphasize the need for optimizing the drug dosage based on the PD of large-scale studies conducted in different geographical settings.

Keywords: tuberculosis, minimum inhibitory concentration (MIC), critical concentration, drug resistance, pharmacodynamics (PD)

INTRODUCTION

Tuberculosis (TB) is an infectious disease caused by *Mycobacterium tuberculosis*. Globally, it is the leading cause of mortality from a single infectious disease agent (World Health Organization Technical Report, 2018). The World Health Organization has developed an "End TB" strategy to strengthen global TB control and to improve the treatment outcome (World Health Organization, 2018). It is anticipated that the TB epidemic will be significantly curtailed in the next 20 years, in countries imposing the End TB Strategy (World Health Organization, 2018). The current strategy of the TB treatment relies on drug susceptibility testing (DST) to identify patients with drug-resistant tuberculosis (Kim, 2005). Traditionally, the DST for *M. tuberculosis* complex (MTBC) organisms involves analyzing a single critical concentration (CC) of the drug, which provides information on the drug-susceptibility of MTBC to each of the anti-TB agent (Coeck et al., 2016; Ruesen et al., 2018). The CC is defined as the lowest concentration of an anti-TB drug that can inhibit the growth of at least 95% of wild-type *M. tuberculosis in vitro*, in solid media (Lowenstein–Jensen; LJ, slopes) or liquid medium (mycobacteria growth indicator tubes; MGIT) (Werngren et al., 2012). According to the WHO guidelines, the CCs for the first-line anti-TB drugs in LJ media and MGIT, respectively, are as follows: isoniazid (INH; 0.2 and 1.0 mg), rifampicin (RMP; 40 and 1.0 mg), ethambutol (EMB; 2.0 and 5.0 mg), and pyrazinamide (100 mg/L only in MGIT) (Canetti et al., 1963; World Health Organization, 2012). The WHO-recommended CCs of anti-TB drugs are universally followed to determine the susceptibility pattern of MTBC in DST.

However, growing evidence suggests that there are differences in CCs among various populations depending on the geographical location and the type of MTBC isolates prevalent in the community (Pasipanodya et al., 2012). Furthermore, the genotype and the polymorphism of the infecting MTBC can also affect the CC of anti-TB drugs (Leandro et al., 2013). Thus, while the WHO-recommended CCs have been followed uniformly for some anti-TB agents, other drugs have been modified from this international standard to accommodate the diversity in anti-TB drugs (Somasundaram and Paramasivan, 2006). Besides, the relevance of the WHO-recommended CC of drugs on the susceptibility of divergent MTBCs prevalent in a particular geographical location, as well as the clinical outcome of patients with TB, remains uncertain. The global pandemic of TB not only affects people of different genetic backgrounds but is also highly inconsistent and shows variable pharmacokinetics (PK) of anti-TB drugs among the population (Gumbo, 2010).

Because India is a densely populated country with significant diversity in cultural background, food habits, and socioeconomic status, the outcome of anti-TB treatment at the population level is expected to be heterogeneous (Naidoo et al., 2017). Hence, variability in the MICs of MTBC isolates and the prevalence of different isolates within communities are inevitable. This variability can also contribute to the variable rates of PK/PD and the area under the curve (AUC) concentration in patient samples treated with anti-TB drugs (Naidoo et al., 2017).

In this study, we assessed the CC of anti-TB drugs in wild-type MTBC isolates that are prevalent among pulmonary TB patients of South India. We used both solid and liquid media to determine the CC of MTBC isolates and correlated it with the serum PD values. Finally, we performed whole-genome sequencing of the selected drug-sensitive and drug-resistant MTBC isolates and correlated the data with the MIC/CC results. Our findings show a significant variation in the CC of MTBC isolates in clinical specimens, which may contribute to the overestimation of drug-resistant cases compared with the WHO standards. The practical outcome of this study may provide new insight into the WHO criteria for the CC of first-line anti-TB drugs.

MATERIALS AND METHODS

Bacterial Isolates

Wild-type clinical isolates of *M. tuberculosis* were isolated from the sputum samples of patients admitted for the PK study [A study to determine factors that influence plasma concentrations of first-line anti-TB drugs in adult TB patients receiving treatment according to Revised National Tuberculosis Control Program (RNTCP, India) guidelines]. The isolates were grown in Lowenstein–Jenson (LJ) medium. A set of six well-characterized, drug-resistant isolates was used as controls. Ethical approval for the study was obtained from the Institutional Ethics Committee, National Institute for Research in Tuberculosis.

Inclusion and exclusion criteria were as follows: MTBC cultures isolated from patients' specimen before the initiation of anti-TB treatment were used for the study. Those isolates from the patient who had received the treatment were not used for the study.

Statistical Analysis and Sample Size Calculation

All data in the questionnaire were entered into a Microsoft Excel sheet and analyzed using the STATA version 15.1 (StataCorp, Texas, USA). The data were cross-tabulated using frequency and percentage. The principal component analysis was performed

to identify the relatedness between the drugs MIC values and DST patterns.

The comparative study design was adopted to perform a more efficient investigation assuming 5% marginal error, 95% confidence interval, and a 5% chance of contamination, and the other possibility of missing in the 900 possible specimens collected for the PK study (Ramachandran et al., 2017). The proportion of wild-type isolates was kept as half (50%); with this, the study sample size was 284.

MIC Determination

The required antibiotics were procured from Sigma-Aldrich (St. Louis, MO, USA). The MIC determination was carried out by performing three methods parallelly following the methods described elsewhere (Schon et al., 2009; Jureen et al., 2010). The INH stock solution was prepared with double-distilled water. RMP was dissolved with dimethylformamide, and further dilutions were made using double-distilled water. Middlebrook 7H11 (7H11) agar containing oleic acid albumin dextrose catalase (OADC) plates with different concentrations of drugs were prepared individually by mixing the required concentration of the drug with 7H11 just before the pouring the plate. The isolates were subcultured in the LJ medium for 3 weeks before the start of the experiment. For the experiment, a smooth suspension of *M. tuberculosis* colony was prepared in Middlebrook 7H9 (7H9) broth containing OADC and left undisturbed for 5 min. The cell supernatant was matched to 0.5 McFarland Standard with 7H9. Of the resulting suspension, 5 μl was spotted on the drug-containing 7H11 plates in triplicate. A 1:100 dilution of the cells was further made and spotted on the drug-free 7H11 plate, which served as a control. The estimation of MIC for the drugs INH and RMP was performed at 0.008, 0.04, 0.2, 1, and 5 μg/ml and 4, 8, 16, 32, 64, and 128 μg/ml concentration, respectively, in 7H11 agar plates. The plates were incubated at 37°C until growth appears. The growth in 1:100 dilutions was assured in drug-free 7H11 while reading the results for each isolate. The lowest concentration of the drug with no growth or more than 99% inhibition in 7H11 was considered as MIC (Schon et al., 2009). Similarly, the assay was done in MGIT 960 (liquid culture) following the manufacturer's protocol. The concentrations of both the drugs ranged between 0.015 and 512 μg/ml. MYCOTBI (Thermo Fischer Scientific, Massachusetts, USA) was used to determine the DST according to the manufacturer's protocol. In this method, the following are the concentration ranges for each of the drugs: INH (0.03, 0.06, 0.125, 0.25, 0.5, 1, 2, 4 μg/ml), RMP (0.125, 0.25, 0.5, 1, 2, 4, 8, 16 μg/ml), ofloxacin (OFX) (0.125, 0.25, 0.5, 1, 2, 4, 8, 16 μg/ml), moxifloxacin (MXF) (0.06, 0.125, 0.25, 0.5, 1, 2, 4, 8 μg/ml), amikacin (AMI) (0.125, 0.25, 0.5, 1, 2, 4, 8, 16 μg/ml), streptomycin (STR) (0.25, 0.5, 1, 2, 4, 8, 16, 32 μg/ml), rifabutin (RFB) (0.125, 0.25, 0.5, 1, 2, 4, 8, 16 μg/ml), para-aminosalicylic acid (PAS) (0.5, 1, 2, 4, 8, 16, 32, 64 μg/ml), ethionamide (ETM) (0.3, 0.6, 1.2, 2.5, 5, 10, 20, 40 μg/ml), cycloserine (CYC) (2, 4, 8, 16, 32, 64, 128, 256 μg/ml), kanamycin (KAN) (0.6, 1.2, 2.5, 5, 10, 20, 40 μg/ml), and ethambutol (ETH) (0.5, 1, 2, 4, 8, 16, 32 μg/ml). At least five of the isolates were repeated and *M. tuberculosis* H37Rv was used multiple times in each method, and six isolates from the panel of cultures for proficiency testing were used in all three types of methods.

PK/PD Indices

The PK variability, including maximum peak concentration (C_{max}), exposure, or area under the time–concentration curve (AUC), was obtained using the plasma drug levels, measured at 2, 4, 6, and 8 h time points, from TB patients in Chennai, South India. Data for 100 patients are available in our institute (Hemanth Kumar et al., 2016). Pharmacodynamic (PD) indices such as 24-h AUC/MIC ratio and the peak/MIC ratio were calculated with the CC determined in this study using the MGIT 960 method.

In silico Analysis of the Whole-Genome Sequence Data

Sixteen isolates (2 sensitive and 14 resistant) were sequenced using paired-end Illumina MiSeq (NCBI Submission ID: SUB6703345). The quality of the sequence reads was analyzed using the FASTQC tool (McKenna et al., 2010). The sequence length of all the sequence reads was uniformly 150 bp. The reads with the quality Phred score, <28, were treated as lower quality and were trimmed off using a Trimmomatic tool (Bolger et al., 2014). Subsequently, the filtered sequence reads with better quality were aligned to the reference genome H37Rv using the short-read aligner Bowtie2 (Langmead and Salzberg, 2012). The aligned files were indexed and sorted using the SAMtools (an alignment file manipulating tools) (Li et al., 2009). The PCR duplicate in SAM files was removed and converted to BAM files using SAM tools to reduce the computational complexity of the analysis. The BAM files were analyzed for variants using mpileup in SAMtools followed by VarScan2, and in another way, the same BAM files were analyzed using Free Bayes and Genome Analysis Tool Kit (GATK) to generate VCF files (McKenna et al., 2010; Garrison and Marth, 2012; Koboldt et al., 2013). The single-nucleotide polymorphisms (SNPs) predicted from the variant analysis tools were compared, and only common SNPs with depth (DP) more significant than 10 and minimum mapping quality as 30 were filtered using VCF tools. Furthermore, the SNPs were annotated using SnpEff (Cingolani et al., 2012) to obtain the effect and location of variants. Using SNP Relate, an R/Bioconductor package (Zheng et al., 2012), principal component analysis (PCA) was made from a multisample variant file to study the variance among the samples. A small set of 12 PCA-correlated SNPs were identified, which are associated with the variation among samples. SNPs present in the wild-type samples NIRT_2 and NIRT_3 were compared with other drug-resistant samples NIRT_1 and NIRT_4 to NIRT_16. The variants in the multisample file were further clustered using the standard algorithm K-means clustering, and a dendrogram was made to study the phylogenetic relationship among samples. Each sample was also analyzed to find the strain type and the associated genotypes of *M. tuberculosis*. The most common genotypes among the genotypes of the same strain type were removed using customized Python script, and the resulting most significant variants were further analyzed and annotated to study the variant effects using tbvar, KVarQ, TBProfiler, and PhyResSE

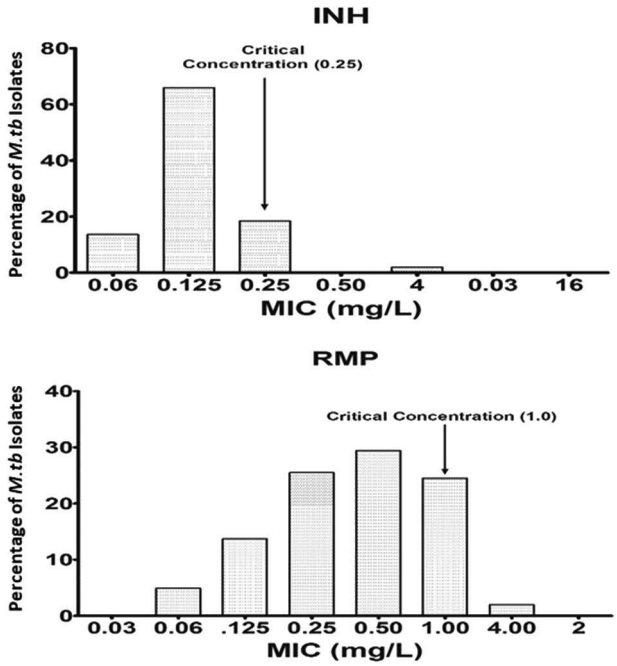

FIGURE 1 | Wild-type minimal inhibitory concentration (MIC) distribution of isoniazid (INH), and rifampicin (RMP) in 276 isolates of *M. tuberculosis* performed in 7H11 agar plates (solid media). The critical concentration determined in this study is indicated by the arrow and is the same as recommended by WHO using 7H10 agar plates. *Y*-axis represents the percentage of *M. tuberculosis* isolates, and the *X*-axis represents the MIC of the corresponding drugs.

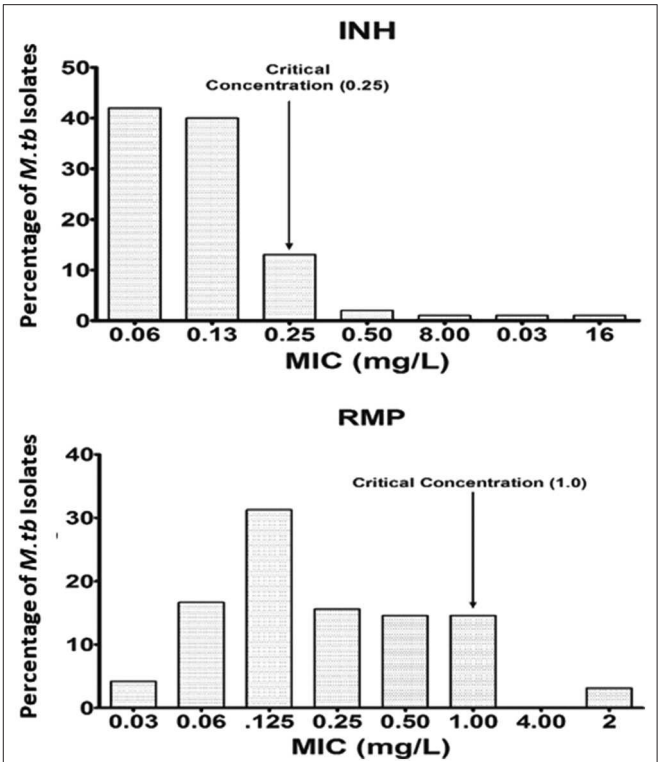

FIGURE 2 | Wild-type minimal inhibitory concentration (MIC) distribution of isoniazid (INH) and rifampicin (RMP) in 96 isolates of *M. tuberculosis* performed in MGIT 960 (liquid media). The critical concentration determined in this study is indicated by the arrow and is the same as recommended by WHO for RMP, whereas for INH, it is 0.25 mg/L as against 0.1 mg/L as recommended by WHO. *Y*-axis represents the percentage of *M. tuberculosis* isolates, and the *X*-axis represents the MIC of the corresponding drugs.

(Joshi et al., 2014; Steiner et al., 2014; Coll et al., 2015; Feuerriegel et al., 2015).

RESULTS

Wild-type MIC distribution of INH and RMP was determined using 276 isolates of *M. tuberculosis*, from the sputum specimens of TB patients before the start of the treatment, in the Middlebrook 7H11 agar plate. The required sample size was not achieved due to the contamination, and it was <4%; hence, there is a slight decrease in the number of tested isolates for the 7H11 agar method. Similarly, it was carried for the same drugs in 96 isolates out of 276 using the MGIT 960 system (liquid medium). The results are shown in **Figures 1**, **2**. The CC was determined using the maximum MIC level of 95% percentage, i.e., 95% percentile of wild type in this study as per the definition is indicated in the respective figures, and this clearly distinguished the susceptible isolates from the resistant ones in the MIC distribution. It was 0.25 and 1.0 mg/L using the 7H11 agar method and the same for MGIT 960 for INH and RMP, respectively. The values of CC recommended by WHO for INH and RMP were 0.2 and 1.0 mg/L for 7H11 agar, and 0.1 and 1.0 mg/L, respectively, for MGIT 960.

Using the observed C_{max} and AUC levels in the same population of patients (Hemanth Kumar et al., 2016), the PD was calculated using the CC determined for INH and RMP (**Table 1**). The optimal level of the PD indices is expected to be between 10 and 100 for the ratios C_{max}/MIC and AUC/MIC, respectively (Hemanth Kumar et al., 2016). The observed PD level for RMP is found to be below the expected level (5.0 and 27.9; **Table 1**), but for INH, it is well above the required ratios (45.2 and 164.4; **Table 1**) for C_{max}/MIC and AUC/MIC, respectively. Moreover, for eight of the patients, the individualized PD indices were determined with the MICs of the infecting *M. tuberculosis* isolate and their serum levels (C_{max} and AUC) in **Table 2**.

TABLE 1 | Results of pharmacokinetics (PK) and pharmacodynamics (PD) for isoniazid (INH) and rifampicin (RMP) obtained in this study.

Indices	RMP	INH
C_{max} *	5.0 (3.8–6.9)	11.3 (8.2–13.2)
AUC*	27.9 (20.1–33.9)	41.1 (33–59.9)
MIC	1.0	0.25
C_{max}/MIC	5.0	45.2
AUC/MIC	27.9	164.4

C_{max} and AUC values were obtained from Hemanth Kumar et al. (2016).

TABLE 2 | Individualized minimal inhibitory concentration (MIC), pharmacokinetics (PK) (Hemanth Kumar et al., 2016), and pharmacodynamics (PD) results for isoniazid (INH) and rifampicin (RMP) of eight patients in the study.

Patients	MICs in MGIT 960		PK (Hemanth Kumar et al., 2016)				PD			
			RMP		INH		RMP		INH	
	RMP	INH	C_{max}	AUC	C_{max}	AUC	C_{max}/MIC	AUC/MIC	C_{max}/MIC	AUC/MIC
1	0.5	0.5	4.02	29.94	8.49	48.2	**8.04**	**43.88**	16.98	96.4
2	0.5	0.25	3.26	18.56	10.30	37.76	**6.52**	**37.12**	41.2	151.04
3	0.06	0.06	6.20	36.74	13.49	62.78	103.33	612.33	224.8	1046.3
4	0.125	NA	6.29	28.67	NA	NA	50.32	229.36	NA	NA
5	1.0	0.125	6.9	79.53	11.59	39.79	**6.9**	**29.53**	92.72	318.32
6	0.5	0.06	4.82	26.73	8.01	27.21	**9.64**	**53.46**	133.5	453.5
7	0.06	0.06	7.16	46.94	8.75	33.58	119.3	782.3	139.16	559.6
8	0.5	0.125	0.5	2.91	7.71	33.98	**1**	**5.82**	61.68	271.84

Significant values were highlighted for PD-RMP alone.

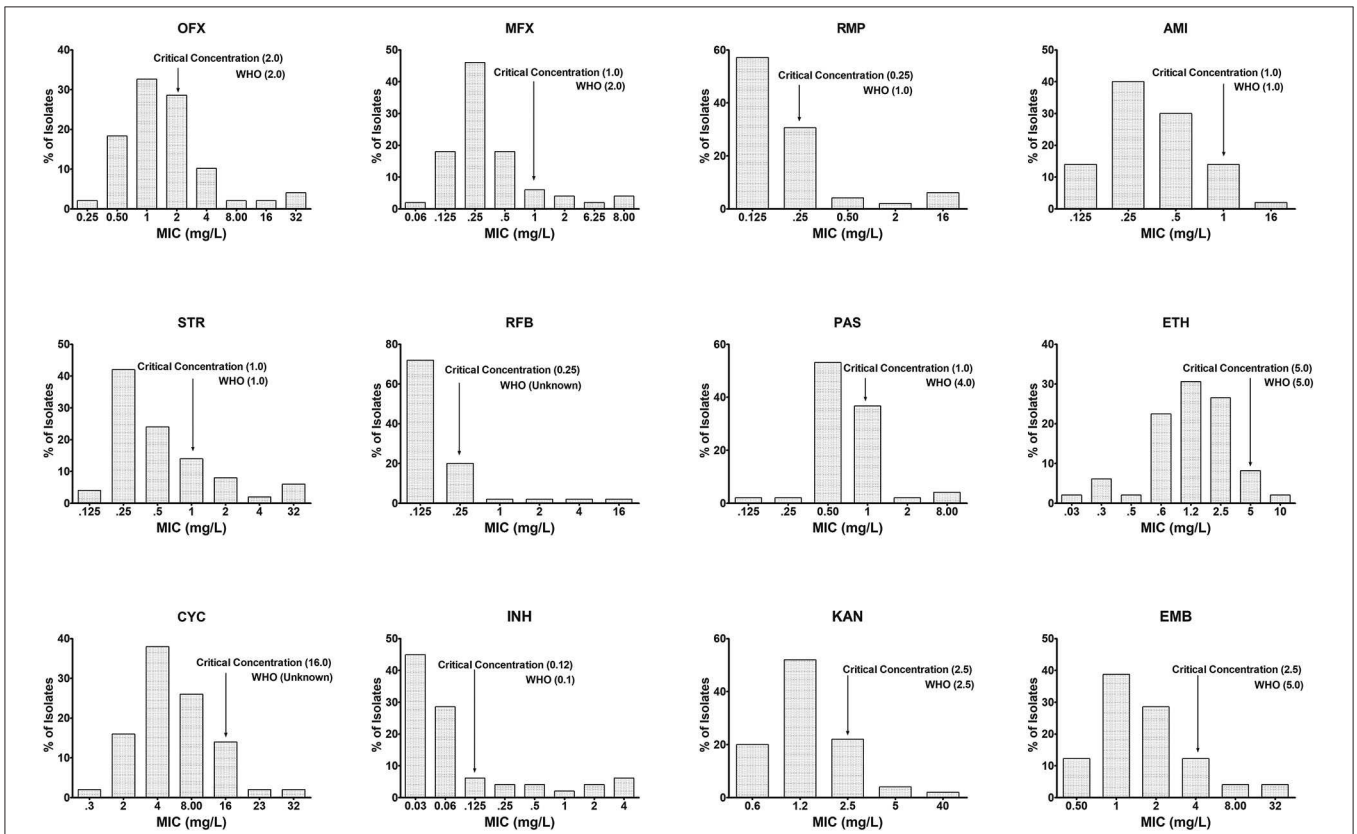

FIGURE 3 | Wild-type minimal inhibitory concentration (MIC) distribution using MYCOTBI plates for first- and second-line anti-TB drugs. The critical concentration determined in this study is indicated by the arrow, and the recommended concentration by WHO for each of the drug could be seen against each of the graph. Deviation from the WHO recommended MIC concentration was observed for RMP, *p*-aminosalicylic acid (PAS), moxifloxacin (MXF), and ethambutol (EMB). *Y*-axis represents the percentage of *M. tuberculosis* isolates, and the *X*-axis represents the MIC of the corresponding drugs.

Similarly, in 50 out of 276 isolates, the MICs of INH, RMP, OFX, MXF, AMI, STR, RFB, PAS, ETM, CYC, KAN, and ETH were determined using the Sensititre MYCOTBI plate. The data are shown in **Figure 3**. Using this method, we observed that the CC of INH [WHO−0.1 μg/ml; National Institute for Research in Tuberculosis (NIRT)−0.12 μg/ml], RMP (WHO−1 μg/ml; NIRT−0.25 μg/ml), MXF (WHO−2 μg/ml; NIRT−1 μg/ml), para-aminosalicylic acid (WHO−4 μg/ml; NIRT−1 μg/ml), and

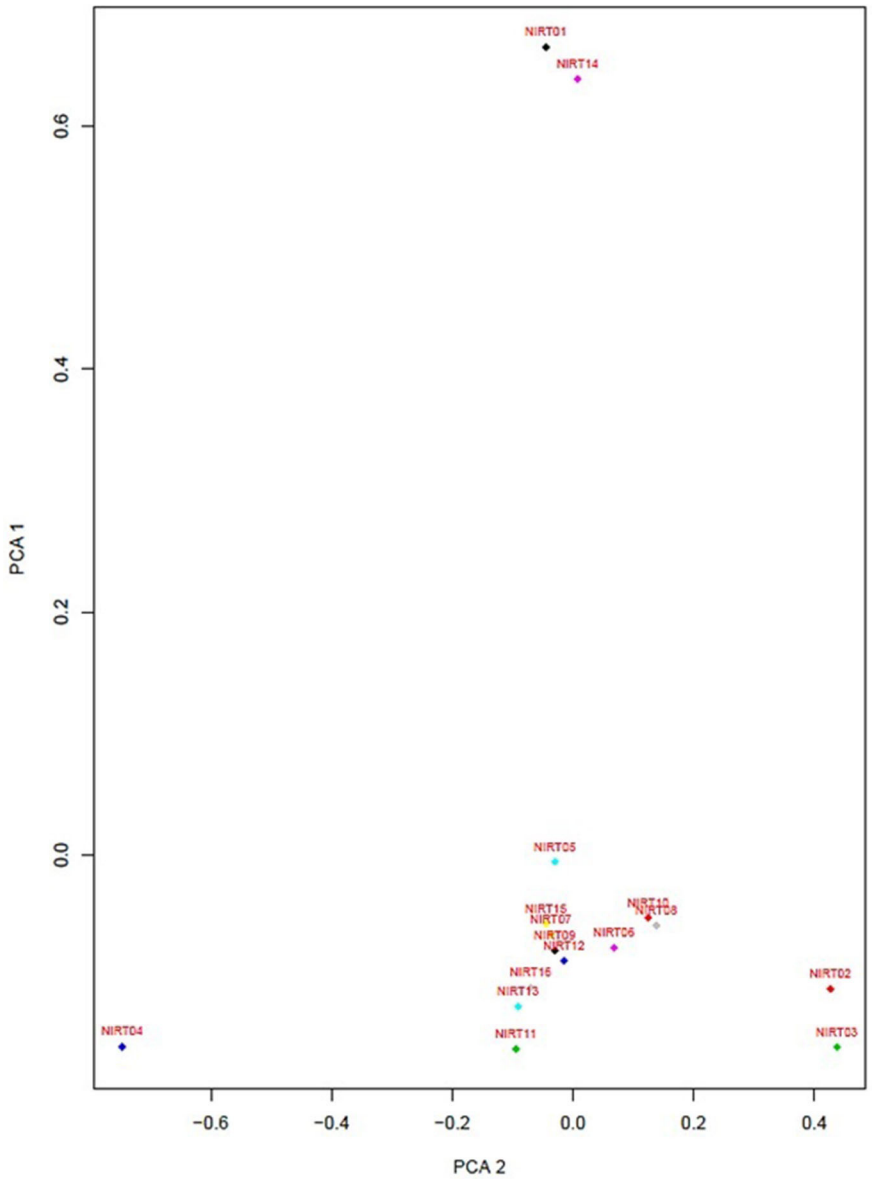

FIGURE 4 | Principle component factor analysis based on the single-nucleotide polymorphisms (SNPs) in the 16 isolates.

ETH (WHO−5 μg/ml; NIRT−4 μg/ml) varies from WHO recommendation (**Figure 3**).

Although both MGIT 960 and MYCOTBI involve the use of 7H9 liquid media, the critical concentration varies depending on the technique used, as seen in RMP and INH. The agreement between the susceptibility results in the 7H11 agar method vs. MGIT and 7H11 vs. MYCOTBI revealed more than 100% agreement with the latter but had 98 and 82.5% for RMP and INH, respectively for the earlier group (**Table S1**). Concordance and reproducibility were within the acceptable limits when repeatedly tested by each method (**Table S2**). The difference between the MICs was not more than two dilution steps in all instances, and the susceptibility pattern between 7H11 and MYCOTBI was 100% in comparison with the minimal MIC method using LJ medium and WHO-recommended CC levels for *M. tuberculosis* H37Rv as control. It was repeated thrice for 7H11 and twice for MGIT 960 and MYCOTBI, giving identical results (**Table S2**). There was a 100% concordance between DST results of 7H11 agar and LJ (minimal MIC method) for interpretation using WHO-recommended CCs for INH and RMP (data not shown). However, there was discordance between MGIT 960 vs. 7H11 agar and LJ among 12 isolates for the RMP susceptibility following WHO recommended CCs. When these 12 isolates were tested using line probe assay (LPA) (GenoType MTBDRplus Version 2.0), they were found to be susceptible to RMP (**Table S3**).

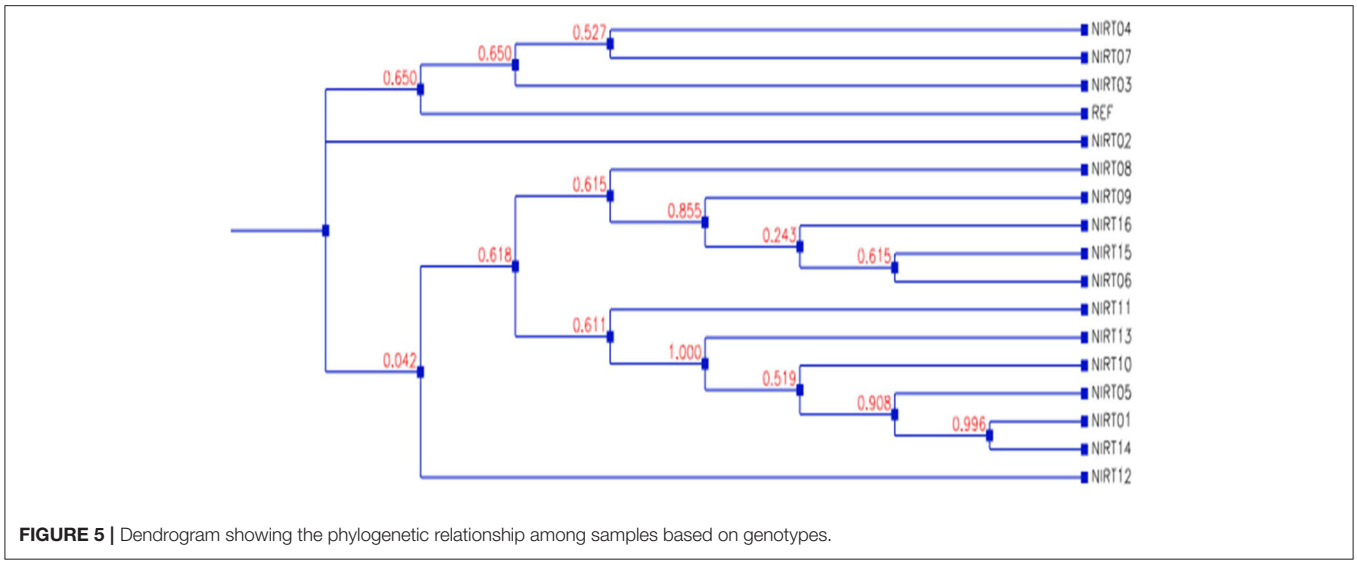

FIGURE 5 | Dendrogram showing the phylogenetic relationship among samples based on genotypes.

TABLE 3 | VCF summary statistics on output VCF files after variant calling and filtering.

Sequence	Seq. type	Total variants	Transition (Ts)	Transversion (Tv)
NIRT_01	Resistance	13,938	4,506	9,432
NIRT_02	Sensitive	12,396	5,466	6,726
NIRT_03	Sensitive	16,996	6,329	10,667
NIRT_04	Sensitive	12,185	5,173	7,012
NIRT_05	Resistance	9,102	3,488	5,614
NIRT_06	Resistance	10,989	4,521	6,468
NIRT_07	Resistance	14,029	6,251	7,778
NIRT_08	Resistance	13,579	5,364	8,215
NIRT_09	Resistance	6,997	3,440	3,557
NIRT_10	Resistance	7,274	3,291	3,983
NIRT_11	Resistance	5,705	2,818	2,887
NIRT_12	Resistance	6,687	3,186	3,501
NIRT_13	Resistance	5,597	2,797	2,800
NIRT_14	Resistance	4,062	2,025	2,037
NIRT_15	Resistance	5,666	2,453	3,213
NIRT_16	Resistance	5,808	2,250	3,558

In silico Analysis of the Whole-Genome Sequence Data

From the clinical isolates used in this study, whole-genome sequencing was done for 16 isolates and named as NIRT_01 to NIRT_16. The overall quality of the sequence reads assessed by the FastQC tool was good with a Phred score higher than 30, and there was no adapter content. The primary analysis of the sequences was done (**Table S4**). In all the sequences, the GC content was ≥65%, thus further establishing the quality of sequencing. The highest number of reads was found in NIRT_14 (47 million reads), and the least was found in NIRT_16 (14 million reads). Using Bowtie2, the filtered quality reads ($Q >$ 20) of the 16 clinical samples were mapped against the genome of *M. tuberculosis* H37Rv (accession number: NC_000962.3) considered a reference genome for this study. The overall alignment of these samples resulted in reads, aligned between 95 and 98% against the reference genome with more than 85% of the reads uniquely mapped against the reference. The BAM file after the alignment was subjected to removing PCR duplicate using SAM tools (**Table S5**). All the samples achieved an overall alignment rate higher than 95% except for two samples. We carried out a phylogenetic analysis to identify the lineage distribution of the 16 samples. The phylogenetic analysis seems to report 13 samples to belong to lineage 1, 2 belong to lineage 2, and 1 sample belongs to lineage 4 (**Figure 4**, **5** and **Table 3**). Furthermore, to study the sequence variation among these samples, GATK, Varscan2, and Freebayes2 were used for variant calling. The identified variants that were annotated using SnpEff and SNP Relate (R package) were used for association studies (**Tables 4**, **5**). A total number of 151,010 variants were identified, with the maximum number of variants seen in NIRT_03 and the least were identified in NIRT_14. We removed the common variants present in all isolates that did not account for any phenotype and removed the corresponding genotypes. The resultant SNPs were further annotated for any reported drug resistance activity using drug resistance databases and the literature. Out of the 74 variations found in 16 samples, which could account for the drug resistance activity, 5 of them were identified as novel mutations (**Table 6**). These five mutations were identified on four different genes such as arabinosyl transferase A (*embA*—Ala217Thr), DNA-directed RNA polymerase subunit beta (*rpoC*—Phe1175Leu), HTH-type transcriptional regulator (*ethR*—Thr130Ile and Ala161Val), and *rrs* (T17G and C517T) genes. Apart from these novel mutations, 24 other known mutations conferring the resistance were also observed (**Table 7**).

DISCUSSION

The wild-type MIC distribution of *M. tuberculosis* is necessary for determining the CCs, which in turn are essential for defining its

TABLE 4 | Phenotypic resistance pattern, its corresponding MICs determined by MYCOTBI in parentheses, and genotypic mutated genes.

Lab No.	Phenotypical resistance (MIC)	Corresponding genotypical mutated genes
NIRT_1	INH (0.5)	fabG1, katG
NIRT_4	OFX (16), ETH (20)	gyrA, gyrB
NIRT_5	RMP (2), INH (0.5), EMB (8)	rpoB, rpoC, katG, kasA, embC
NIRT_6	RMP (16), STR (8), PAS (5), RFB (16), CYC (128), INH (4), KAN (5), EMB (8)	rpoB, rpoC, katG, kasA, embC, embA, embB, embR
NIRT_7	OFX (16), INH (4)	gyrA, gyrB, katG, kasA
NIRT_8	INH (0.5)	katG, kasA
NIRT_9	RMP (2), CYC (32), INH (0.25)	rpoB, rpoC, katG, kasA
NIRT_11	OFX (4), INH (4), EMB (8)	gyrA, gyrB, katG, kasA, embC, embA, embB, embR
NIRT_13	INH (0.5)	katG, kasA
NIRT_14	OFX (8), MXF (4), RMP (>16), STR (>32), RFB (4), ETH (10), CYC (32), INH (>4), KAN (16)	gyrA, gyrB, rpoB, rpoC, rpsL, fabG1, KatG
NIRT_15	INH (4, 2)	katG, kasA

TABLE 5 | Lineage and strain type identified from the observed genotypes in samples.

Sample	Lineage	Name
NIRT10	Lineage 1	Indo-Oceanic EAI
NIRT06	Lineage 1	Indo-Oceanic EAI
NIRT09	Lineage 1	Indo-Oceanic EAI
NIRT02	Lineage 1	Indo-Oceanic EAI
NIRT03	Lineage 1	Indo-Oceanic EAI
NIRT04	Lineage 1	Indo-Oceanic EAI
NIRT07	Lineage 1	Indo-Oceanic EAI
NIRT08	Lineage 1	Indo-Oceanic EAI
NIRT01	Lineage 2/Beijing sublineage	East-Asian Beijing
NIRT05	Lineage 4/LAM	Euro-American LAM
NIRT14	Lineage 2/Beijing sublineage	East-Asian Beijing
NIRT15	Lineage 1	Indo-Oceanic EAI
NIRT12	Lineage 1	Indo-Oceanic EAI
NIRT11	Lineage 1	Indo-Oceanic EAI
NIRT16	Lineage 1	Indo-Oceanic EAI
NIRT13	Lineage 1	Indo-Oceanic EAI

TABLE 6 | Novel potential drug-resistant variants observed in the study.

S. No	Gene name	Mutation
1	*embA*	Ala217Thr
2	*rpoC*	Phe1175Leu
3	*ethR*	Thr130Ile
4	*ethR*	Ala161Val
5	*rrs*	T17G

TABLE 7 | Known and previously reported drug-resistant variants observed in the study.

S. No	Gene name	Mutation
1	gyr A	Gly247Ser
2	gyr A	Ala90Val
3	gyr A	Asp94Asn
4	rpoB	His445Arg
5	rpoB	Leu430Pro
6	embC	Ala774Ser
7	embC	Ala387Val
8	embB	Asp354Ala
9	embB	Gln497Lys
10	embB	Val135Met
11	embB	Gly836Arg
12	embB	Met306Ile
13	embB	Phe285Leu
14	embB	Gln497Arg
15	rpoC	Glu750Asp
16	rpoC	Phe831Leu
17	rpoC	Ile491Val
18	rpoC	Ala621Thr
19	kasA	Gly269Ser
20	kasA	Gly312Ser
21	kasA	Phe413Leu
22	ethA	Arg469Trp
23	ethA	Asn345Lys
24	pncA	Gly132Ala

susceptibility as suggested by numerous authors. It necessitates re-evaluation based on the evidence provided regarding the change in the level of certain anti-TB drugs (Schon et al., 2009; Jureen et al., 2010; Werngren et al., 2012). In the current work, as shown in **Figures 1**, **2**, the CC was determined to be identical for RMP in both 7H11 agar and MGIT 960 (1.0 mg/L). However, CC for INH in MGIT 960 was higher than that recommended by WHO. In this study, in a sample size of 96, it was found to be 0.25 mg/L in contrast to 0.1 mg/L as recommended by WHO (Canetti et al., 1963). Since the CCs determined in this study were similar to that prescribed by WHO for RMP using both 7H11 agar and MGIT 960 and in case of solid media alone for INH, the susceptibility pattern was very much similar to that observed using LJ medium by the minimal MIC method for all the isolates used. However, the MICs of 12 isolates were 0.25 mg/L for INH using MGIT 960. They were declared as resistant for INH based on WHO-recommended cutoff, but all these isolates were found to be susceptible to INH using LJ based resistant ratio method and 7H11 agar plates as well.

The lack of clarity in predicting clinical failure in the CC accuracy has led to the establishment of PK and antimicrobial PK/PD developed to detect susceptibility breakpoints for many antibiotics (Dalhoff et al., 2009). However, the outset of Gumbo Monte Carlo simulations defines the new susceptibility breakpoints considering microbiological and clinical consequence and states further that the CCs of first-line drugs could be factually incorrect (Gumbo, 2010). Based on the reason mentioned above and

findings, it is necessary to assess the CC of first-line drugs for variability prevailing genotype and polymorphism in a specific area.

Moreover, there were no detectable mutations in the reported genes responsible for drug resistance in INH using LPA (GenoType MTBDRplus Version 2.0) in these 12 isolates. Based on the intention laid by the WHO to reduce the time-consuming culture identification methods and drug resistance findings, the LPA was formulated (World Health Organization, 2007). In the established CC definition, the observed CC would be 0.25 mg/L using wild-type distribution for INH using MGIT 960 witnessed in this study as against WHO's recommended CC. Using this as a baseline value, these 12 isolates can be declared as susceptible, which are similar to the observed DST results based on LJ.

The principles of Canetti et al. (1963), recognized 50 years ago, state to implement a sensitivity test for the capability of organisms growing on a medium containing a wide range of known drugs. Our evaluation of the pivot predominant population was done by MYCOTBI; likewise, the most extensive collection of *M. tuberculosis* isolates from Uganda and the Republic of Korea, at DST level, were assessed by MYCOTBI plate (Lee et al., 2014). Considering the MYCOTBI results in a sample size of 50, changes in the CC were seen in RMP, MXF, ETH, and PAS.

PCA was performed to identify the conformational differences between the resistance patterns (Jamshidi et al., 2018). It classifies the drugs into three groups with data source MIC values of 16 isolates determined by MYCOTBI method, where the EMB, RFB, CYC, and PAS are having a higher variation, while the pattern is followed by other two group drugs as well (**Figure S1**). PCA, with the data source DST of these 16 isolates, classifies the drugs into two groups; where RMP, MXF, STR, KAN, AMI, OFX, and RFB have a higher variation with the pattern followed by the other two groups of drugs (**Figure S2**).

Whole-genome sequencing has emerged as a new diagnostic tool that assists in clinical decision making in infectious diseases (Jabbar et al., 2019). The whole-genome sequencing of tuberculosis isolates provides genomic information that is responsible for causing resistance (Cohen et al., 2019). To determine if any correlation exists between high-level resistance and the number of mutations present in the genome of isolates, whole-genome sequencing was done for 16 isolates whose MICs are known (Joshi et al., 2014; Steiner et al., 2014; Coll et al., 2015; Feuerriegel et al., 2015). The mutations related to resistant genes were analyzed, and no correlation between the amount of mutation and the level of resistance was observed. Out of the 74 variants associated with resistance, five were predicted to be new mutations and thus not reported earlier. The novelty and the potential of these five mutations to confer resistance should be evaluated further. Out of the 16 isolates sequenced, NIRT_2, and NIRT_3 were phenotypically sensitive, but had mutations corresponding to fluoroquinolones and ETH. Similarly, discrepancies between genotypic and phenotypic resistance have been reported in ETH, MXF (Chen et al., 2019), and STR (Chaidir et al., 2019). The drug resistance mechanisms are not well-studied (Gygli et al., 2019) especially for second-line anti-TB drugs, and thus, the specificity of the reported genetic mutations to confer phenotypic resistance is low. Apart from genetic mutations, there are also other mechanisms like efflux pumps that confer phenotypic resistance (Satta et al., 2017). Although whole-genome sequencing techniques and its interpretation have become highly advanced, it cannot be used as a standalone tool for predicting the clinical outcome of drug resistance in the current scenario.

Furthermore, innovative approaches need to be adapted to eliminate TB. By implying multidisciplinary, multisectoral approaches, the new Global Tuberculosis Network (GTN) intends to research the much needed therapeutic and diagnostic requirements in the surge to eliminate TB upon applying PK. GTN indeed perceives and studies the existing knowledge slits and renders potential solutions as well (Alffenaar et al., 2019). Thus, our study will be the first to examine the PD implication toward the primary drug line CC of wild-type MIC on *M. tuberculosis* clinical isolates from South India.

Upon analysis based on PD levels in eight patients, the RMP levels were subtherapeutic in five out of eight patients. In 2017, Ramachandran et al. reported suboptimal concentrations of RMP, INH, and pyrazinamide among 91, 16, and 17% of the patients tested. The current study was conducted using the isolates from patients included in the study by Ramachandran et al. (2017).

Using the average serum levels of RMP and INH from this study and the observed MICs of these drugs in the current study using MGIT, PD indices such as C_{max}/MIC and AUC/MIC ratios were suboptimal for RMP (5.0 and 27.9) and were above the expected limit for INH (45.2 and 164.4). This indicates that these patients received a dose of RMP, which was subtherapeutic in eliminating the pathogen with the prescribed dose for their body weight or else that their physiological system is not capable of maintaining the optimal level of RMP in the serum. In other words, in the majority of these patients, the expected level of action for RMP is suboptimal, and if it had been at the optimal levels, the rate of bacillary eradication and the sputum conversion would be much more rapid.

Although the smaller sample size might be the limitation of the study and a foregone conclusion cannot be arrived based on this sample size, the unexpected result of the subtherapeutic levels found in the majority of these patients to RMP should be noticed and taken care. RMP is one of the essential anti-TB drugs in the regimen to treat tuberculosis, and it implicates the prominence of such a study in a larger sample size, while this well-worn finding will pave the way for an amicable target proposed in terms of End TB Strategy by World Health Organization (2018).

CONCLUSION

MICs of anti-TB drugs for the wild-type isolates of *M. tuberculosis* were determined. We were able to predict the CC in both solid and liquid media. The WHO recommended concentration was used to compare the observed CC among the isolates for INH and RMP and was found to be similar in the case of solid media (7H11 agar). Changes in the CCs were noted

for INH in MGIT 960, and similar changes were found for MXF, ETH, and PAS in liquid media using MYCOTBI as against the WHO recommended. CC for RMP was found to be identical to that recommended by WHO in both 7H11 and MGIT 960 but differ in MYCOTBI. The therapeutic levels for RMP noted in eight patients were suboptimal for five out of eight patients, and these findings necessitate carrying out a similar exercise in a more significant number of isolates and patients to ascertain the results in this study. The genomes of 16 mycobacterial isolates (including 2 wild types and 14 resistant isolates) were subjected to whole-genome sequencing to identify mutations that can be associated with drug resistance. Two of them were in Beijing, one was Euro-American, and the rests were East African–Indian (EAI) strain types. A total of 74 mutations were identified that are known to be associated with drug resistance in these isolates, while five mutations were identified that appeared to be novel and required further analysis to confer their role in resistance. These findings highlight the need for optimizing the drug dosage based on PD from large-scale studies in different geographical settings.

DATA AVAILABILITY STATEMENT

The gene sequence from the 16 isolates has been submitted to the NCBI repository with SRA accession: PRJNA596377 (https://www.ncbi.nlm.nih.gov/bioproject/PRJNA596377).

ETHICS STATEMENT

The studies involving human participants were reviewed and approved by Institutional Ethics Committee of National Institute for Research in Tuberculosis, Chennai, India. The patients/participants provided their written informed consent to participate in this study.

AUTHOR CONTRIBUTIONS

AD conceptualized the study. AD, SS, MB, and AB performed the bacteriological part of the study. SH and MT performed the analysis of the whole-genome sequence. KT did the statistical analysis for this study. GR and AK were involved in the PK part of the study. The first draft of the manuscript was written by AD and SS. AZ, CN, SR, SM, and RM oversaw the final analysis and writing of this manuscript. All authors contributed to the article and approved the submitted version.

FUNDING

This study was supported by funding from the LDCE committee of the Indian Council of Medical Research, New Delhi.

ACKNOWLEDGMENTS

The authors would like to profusely thank the director of NIRT for permitting us to carry out the study.

SUPPLEMENTARY MATERIAL

The Supplementary Material for this article can be found online at: https://www.frontiersin.org/articles/10.3389/fmicb.2020.01182/full#supplementary-material

REFERENCES

Alffenaar, J. C., Gumbo, T., Dooley, K. E., Peloquin, C. A., McIlleron, H., Zagorski, A., et al. (2019). Integrating pharmacokinetics and pharmacodynamics in operational research to End TB. *Clin. Infect. Dis.* 70, 1774 –1780. doi: 10.1093/cid/ciz942

Bolger, A. M., Lohse, M., and Usadel, B. (2014). Trimmomatic: a flexible trimmer for Illumina sequence data. *Bioinformatics* 30, 2114–2120. doi: 10.1093/bioinformatics/btu170

Canetti, G., Froman, S., Grosset, J., Hauduroy, P., Langerova, M., Mahler, H. T., et al. (1963). Mycobacteria: laboratory methods for testing drug sensitivity and resistance. *Bull. World Health Organ.* 29, 565–578.

Chaidir, L., Ruesen, C., Dutilh, B. E., Ganiem, A. R., Andryani, A., Apriani, L., et al. (2019). Use of whole-genome sequencing to predict *Mycobacterium tuberculosis* drug resistance in Indonesia. *J. Glob. Antimicrob. Resist.* 16, 170–177. doi: 10.1016/j.jgar.2018.08.018

Chen, X., He, G., Wang, S., Lin, S., Chen, J., and Zhang, W. (2019). Evaluation of whole-genome sequence method to diagnose resistance of 13 anti-tuberculosis drugs and characterize resistance genes in clinical multi-drug resistance *Mycobacterium tuberculosis* isolates from China. *Front. Microbiol.* 10:1741. doi: 10.3389/fmicb.2019.01741

Cingolani, P., Platts, A., Wang le, L., Coon, M., Nguyen, T., Wang, L., et al. (2012). A program for annotating and predicting the effects of single nucleotide polymorphisms, SnpEff: SNPs in the genome of *Drosophila melanogaster* strain w1118; iso-2; iso-3. *Fly* 6, 80–92. doi: 10.4161/fly.19695

Coeck, N., de Jong, B. C., Diels, M., De Rijk, P., Ardizzoni, E., Van Deun, A., et al. (2016). Correlation of different phenotypic drug susceptibility testing methods for four fluoroquinolones in *Mycobacterium tuberculosis*. *J. Antimicrob. Chemother.* 71, 1233–1240. doi: 10.1093/jac/dkv499

Cohen, K. A., Manson, A. L., Desjardins, C. A., Abeel, T., and Earl, A. M. (2019). Deciphering drug resistance in *Mycobacterium tuberculosis* using whole-genome sequencing: progress, promise, and challenges. *Genome Med.* 11:45. doi: 10.1186/s13073-019-0660-8

Coll, F., McNerney, R., Preston, M. D., Guerra-Assuncao, J. A., Warry, A., Hill-Cawthorne, G., et al. (2015). Rapid determination of anti-tuberculosis drug resistance from whole-genome sequences. *Genome Med.* 7:51. doi: 10.1186/s13073-015-0164-0

Dalhoff, A., Ambrose, P. G., and Mouton, J. W. (2009). A long journey from minimum inhibitory concentration testing to clinically predictive breakpoints: deterministic and probabilistic approaches in deriving breakpoints. *Infection* 37, 296–305. doi: 10.1007/s15010-009-7108-9

Feuerriegel, S., Schleusener, V., Beckert, P., Kohl, T. A., Miotto, P., Cirillo, D. M., et al. (2015). PhyResSE: a web tool delineating *Mycobacterium tuberculosis* antibiotic resistance and lineage from whole-genome sequencing data. *J. Clin. Microbiol.* 53, 1908–1914. doi: 10.1128/JCM.00025-15

Garrison, E., and Marth, G. (2012). Haplotype-based variant detection from short-read sequencing. *arXiv preprint arXiv:1207.3907* [q-bio.GN].

Gumbo, T. (2010). New susceptibility breakpoints for first-line antituberculosis drugs based on antimicrobial pharmacokinetic/pharmacodynamic science and population pharmacokinetic variability. *Antimicrob. Agents Chemother.* 54, 1484–1491. doi: 10.1128/AAC.01474-09

Gygli, S. M., Keller, P. M., Ballif, M., Blochliger, N., Homke, R., Reinhard, M., et al. (2019). Whole-genome sequencing for drug resistance profile prediction

in *Mycobacterium tuberculosis*. *Antimicrob. Agents Chemother.* 63:e02175-18. doi: 10.1128/AAC.02175-18

Hemanth Kumar, A. K., Kannan, T., Chandrasekaran, V., Sudha, V., Vijayakumar, A., Ramesh, K., et al. (2016). Pharmacokinetics of thrice-weekly rifampicin, isoniazid and pyrazinamide in adult tuberculosis patients in India. *Int. J. Tuberc. Lung Dis.* 20, 1236–1241. doi: 10.5588/ijtld.16.0048

Jabbar, A., Phelan, J. E., de Sessions, P. F., Khan, T. A., Rahman, H., Khan, S. N., et al. (2019). Whole genome sequencing of drug resistant *Mycobacterium tuberculosis* isolates from a high burden tuberculosis region of North West Pakistan. *Sci. Rep.* 9:14996. doi: 10.1038/s41598-019-51562-6

Jamshidi, S., Sutton, J. M., and Rahman, K. M. (2018). Mapping the dynamic functions and structural features of acrb efflux pump transporter using accelerated molecular dynamics simulations. *Sci. Rep.* 8:10470. doi: 10.1038/s41598-018-28531-6

Joshi, K. R., Dhiman, H., and Scaria, V. (2014). Tbvar: a comprehensive genome variation resource for *Mycobacterium tuberculosis*. *Database.* 2014:bat083. doi: 10.1093/database/bat083

Jureen, P., Angeby, K., Sturegard, E., Chryssanthou, E., Giske, C. G., Werngren, J., et al. (2010). Wild-type MIC distributions for aminoglycoside and cyclic polypeptide antibiotics used for treatment of *Mycobacterium tuberculosis* infections. *J. Clin. Microbiol.* 48, 1853–1858. doi: 10.1128/JCM.00240-10

Kim, S. J. (2005). Drug-susceptibility testing in tuberculosis: methods and reliability of results. *Eur. Respir J.* 25, 564–569. doi: 10.1183/09031936.05.00111304

Koboldt, D. C., Larson, D. E., and Wilson, R. K. (2013). Using varscan 2 for germline variant calling and somatic mutation detection. *Curr. Protoc. Bioinformatics.* 44, 15.4.1–17. doi: 10.1002/0471250953.bi1504s44

Langmead, B., and Salzberg, S. L. (2012). Fast gapped-read alignment with Bowtie 2. *Nat. Methods.* 9, 357–359. doi: 10.1038/nmeth.1923

Leandro, A. C., Rocha, M. A., Lamoglia-Souza, A., VandeBerg, J. L., Rolla, V. C., and Bonecini-Almeida, M. D. G. (2013). No association of IFNG+874T/A SNP and NOS2A-954G/C SNP variants with nitric oxide radical serum levels or susceptibility to tuberculosis in a Brazilian population subset. *Biomed Res. Int.* 2013:901740. doi: 10.1155/2013/901740

Lee, J., Armstrong, D. T., Ssengooba, W., Park, J. A., Yu, Y., Mumbowa, F., et al. (2014). Sensititre MYCOTB MIC plate for testing *Mycobacterium tuberculosis* susceptibility to first- and second-line drugs. *Antimicrob. Agents Chemother.* 58, 11–18. doi: 10.1128/AAC.01209-13

Li, H., Handsaker, B., Wysoker, A., Fennell, T., Ruan, J., Homer, N., et al. (2009). The Sequence Alignment/Map format and SAMtools. *Bioinformatics* 25, 2078–2079. doi: 10.1093/bioinformatics/btp352

McKenna, A., Hanna, M., Banks, E., Sivachenko, A., Cibulskis, K., Kernytsky, A., et al. (2010). The Genome Analysis Toolkit: a MapReduce framework for analyzing next-generation DNA sequencing data. *Genome Res.* 20, 1297–1303. doi: 10.1101/gr.107524.110

Naidoo, A., Naidoo, K., McIlleron, H., Essack, S., and Padayatchi, N. (2017). A review of moxifloxacin for the treatment of drug-susceptible tuberculosis. *J. Clin. Pharmacol.* 57, 1369–1386. doi: 10.1002/jcph.968

Pasipanodya, J., Srivastava, S., and Gumbo, T. (2012). New susceptibility breakpoints and the regional variability of MIC distribution in *Mycobacterium tuberculosis* isolates. *Antimicrob. Agents Chemother.* 56:5428. doi: 10.1128/AAC.00976-12

Ramachandran, G., AgibothuKupparam, H. K., Vedhachalam, C., Thiruvengadam, K., Rajagandhi, V., Dusthackeer, A., et al. (2017). Factors influencing tuberculosis treatment outcome in adult patients treated with thrice-weekly regimens in India. *Antimicrob. Agents Chemother.* 61:e02464-16. doi: 10.1128/AAC.02464-16

Ruesen, C., Riza, A. L., Florescu, A., Chaidir, L., Editoiu, C., Aalders, N., et al. (2018). Linking minimum inhibitory concentrations to whole genome sequence-predicted drug resistance in *Mycobacterium tuberculosis* strains from Romania. *Sci. Rep.* 8:9676. doi: 10.1038/s41598-018-27962-5

Satta, G., Lipman, M., Smith, G. P., Arnold, C., Kon, O. M., and McHugh, T. D. (2017). *Mycobacterium tuberculosis* and whole-genome sequencing: how close are we to unleashing its full potential? *Clin. Microbiol. Infect.* 24, 604–609. doi: 10.1016/j.cmi.2017.10.030

Schon, T., Jureen, P., Giske, C. G., Chryssanthou, E., Sturegard, E., Werngren, J., et al. (2009). Evaluation of wild-type MIC distributions as a tool for determination of clinical breakpoints for *Mycobacterium tuberculosis*. *J. Antimicrob. Chemother.* 64, 786–793. doi: 10.1093/jac/dkp262

Somasundaram, S., and Paramasivan, N. C. (2006). Susceptibility of *Mycobacterium tuberculosis* strains to gatifloxacin and moxifloxacin by different methods. *Chemotherapy* 52, 190–195. doi: 10.1159/000093486

Steiner, A., Stucki, D., Coscolla, M., Borrell, S., and Gagneux, S. (2014). KvarQ: targeted and direct variant calling from fastq reads of bacterial genomes. *BMC Genomics* 15:881. doi: 10.1186/1471-2164-15-881

Werngren, J., Sturegard, E., Jureen, P., Angeby, K., Hoffner, S., and Schon, T. (2012). Reevaluation of the critical concentration for drug susceptibility testing of *Mycobacteriumtuberculosis* against pyrazinamide using wild-type MIC distributions and pncA gene sequencing. *Antimicrob. Agents Chemother.* 56, 1253–1257. doi: 10.1128/AAC.05894-11

World Health Organization (2007). *The Use of Liquid Medium for Culture and Drug Susceptibility Testing (DST) in Low- and Medium-income Settings: Summary of the Expert Group Meeting on the Use of Liquid Culture Systems*, 1–14.

World Health Organization (2012). *Global TB Programme*. Updated interim critical concentrations for first-line and second-line, DST.

World Health Organization (2018). *Global Tuberculosis Report*. Geneva: World Health Organization. Avaliable online at: https://www.who.int/tb/publications/global_report/en/ (accessed December 2, 2019).

World Health Organization Technical Report (2018). *Technical Report on Critical Concentrations for Drug Susceptibility Testing of Medicines Used in the Treatment of Drug-Resistant Tuberculosis*.

Zheng, X., Levine, D., Shen, J., Gogarten, S. M., Laurie, C., and Weir, B. S. (2012). A high-performance computing toolset for relatedness and principal component analysis of SNP data. *Bioinformatics* 28, 3326–3328. doi: 10.1093/bioinformatics/bts606

Conflict of Interest: The authors declare that the research was conducted in the absence of any commercial or financial relationships that could be construed as a potential conflict of interest.

frontiers in Microbiology

ORIGINAL RESEARCH
published: 15 July 2020
doi: 10.3389/fmicb.2020.01444

Genomic Analysis Identifies Mutations Concerning Drug-Resistance and Beijing Genotype in Multidrug-Resistant *Mycobacterium tuberculosis* Isolated From China

Li Wan[1,2], Haican Liu[2], Machao Li[2], Yi Jiang[2], Xiuqin Zhao[2], Zhiguang Liu[2], Kanglin Wan[2], Guilian Li[2] and Cha-xiang Guan[1]**

[1] Department of Physiology, Xiangya School of Medicine, Central South University, Changsha, China, [2] State Key Laboratory for Infectious Disease Prevention and Control, Collaborative Innovation Center for Diagnosis and Treatment of Infectious Diseases, National Institute for Communicable Disease Control and Prevention, Chinese Center for Disease Control and Prevention, Beijing, China

Development of modern genomics provides us an effective method to understand the molecular mechanism of drug resistance and diagnose drug-resistant *Mycobacterium tuberculosis*. In this study, mutations in 18 genes or intergenic regions acquired by whole-genome sequencing (WGS) of 183 clinical *M. tuberculosis* strains, including 137 multidrug-resistant and 46 pan-susceptible isolates from China, were identified and used to analyze their associations with resistance of isoniazid, rifampin, ethambutol, and streptomycin. Using the proportional method as the gold standard method, the accuracy values of WGS to predict resistance were calculated. The association between synonymous or lineage definition mutations with different genotypes were also analyzed. The results show that, compared to the phenotypic proportional method, the sensitivity and specificity of WGS for resistance detection were 94.2 and 100.0% for rifampicin (based on mutations in *rpoB*), 90.5 and 97.8% for isoniazid (*katG*), 83.0 and 97.8% for streptomycin (*rpsL* combined with *rrs* 530 loop and 912 loop), and 90.9 and 65.1% for ethambutol (*embB*), respectively. WGS data also showed that mutations in the *inhA* promoter increased only 2.2% sensitivity for INH based on mutations in *katG*. Synonymous mutation *rpoB* A1075A was confirmed to be associated with the Beijing genotype. This study confirmed that mutations in *rpoB*, *katG*, *rrs* 530 loop and 912 loop, and *rpsL* were excellent biomarkers for predicting rifampicin, isoniazid, and streptomycin resistance, respectively, and provided clues in clarifying the drug-resistance mechanism of *M. tuberculosis* isolates from China.

Keywords: *Mycobacterium tuberculosis*, resistance, whole-genome sequencing, mutation, Beijing genotype

OPEN ACCESS

Edited by:
Onya Opota, University of Lausanne, Switzerland

Reviewed by:
Divakar Sharma, Indian Institute of Technology Delhi, India
Gonzalo Greif, Institut Pasteur de Montevideo, Uruguay

***Correspondence:**
Guilian Li
liguilian@icdc.cn
Cha-xiang Guan
guanchaxiang@csu.edu.cn

Specialty section:
This article was submitted to Antimicrobials, Resistance and Chemotherapy, a section of the journal Frontiers in Microbiology

Received: *07 January 2020*
Accepted: *04 June 2020*
Published: *15 July 2020*

Citation:
Wan L, Liu H, Li M, Jiang Y, Zhao X, Liu Z, Wan K, Li G and Guan C-x (2020) Genomic Analysis Identifies Mutations Concerning Drug-Resistance and Beijing Genotype in Multidrug-Resistant Mycobacterium tuberculosis Isolated From China. Front. Microbiol. 11:1444. doi: 10.3389/fmicb.2020.01444

INTRODUCTION

The World Health Organization's (WHO's) target is to end the tuberculosis epidemic by 2035 (Treatment Action Group and Stop Tb Partnership, 2018). The evolution and spread of rifampicin-/multidrug-resistant tuberculosis (RR-TB/MDR-TB) poses a major obstacle to success with an estimated half a million cases worldwide in 2018 alone (United Nations General Assembly, 2018). WHO estimated that only one in three of the approximately half a million RR-TB/MDR-TB cases were enrolled in treatment with a second-line regimen (World Health Organization, 2019). Closing the gap in detection and treatment of resistant TB cases requires much higher coverage of drug susceptibility testing among people diagnosed with TB and rapid, accurate, and sensitive susceptibility testing methods.

Generally, the culture-based conventional drug sensitivity test (DST) has long been considered as the gold standard for diagnosing drug-resistant *Mycobacterium tuberculosis* although it is time-consuming, labor-intensive, and lacking sensitivity. Therefore, nucleic acid–based antibiotic susceptibility tests, which can determine the isolate's drug resistance profile within hours instead of culture-based diagnostics that require days or weeks, are increasingly considered as a diagnostic alternative. Acquired antibiotic resistance in *M. tuberculosis* mostly arises from the serial acquisition of point mutations in genes encoding drug targets or drug-activating enzymes. Many known mutations have been identified, e.g., *katG*315 and *inhA*(-15) for isoniazid (INH) resistance (Liu et al., 2018; Luo et al., 2019; Unissa et al., 2016), 81-bp of rifampicin (RMP) resistant determined region (RRDR) for RMP resistance (Li et al., 2010; Maningi et al., 2018; Luo et al., 2019), *embB*306 for ethambutol (EMB) resistance (Mokrousov et al., 2002; Campbell et al., 2011; Moure et al., 2014; Zhao et al., 2015a), and *rpsL*44 and *rpsL*88 for streptomycin (STR) resistance (Li et al., 2010; Maningi et al., 2018). Current molecular diagnostics amplify and detect known drug resistance–associated mutations, and their performance depends on the inclusion of a comprehensive catalog of these mutations. Although known mutations explain much resistance in *M. tuberculosis*, causative mutations have not been identified in 10–40% of clinically resistant isolates (Campbell et al., 2011; Zhang et al., 2014; Zhao et al., 2014a), implying the contribution of noncanonical mutations in known or unknown genes or other resistance mechanism(s). Mutations outside of RRDR in *rpoB* or mutations except the canonical mutation *katG*315 in *katG* have been reported to be associated with RMP or INH resistance, respectively (Zhao et al., 2014b; Torres et al., 2015). Maningi et al. (2018) reports that whole-genome sequencing (WGS) shows better concordance with the Lowenstein–Jensen (L-J) phenotypic assay than with Hain line probe assay in that many more mutations were found by WGS. Moreover, many genes, such as *ndh*, *efpA*, *kasA*, *iniABC* operon (for INH resistance) (Sandgren et al., 2009; Nguyen, 2016); *rpoC* (RMP) (Farhat et al., 2013; Perdigao et al., 2020); *embA*, *embC*, *ubiA* (EMB) (Plinke et al., 2010; Zhao et al., 2015a; Farhat et al., 2016); and *gidB* (STR) (Nhu et al., 2012; Spies et al., 2011; Perdigao et al., 2014), are reported to correlate with drug resistance.

Whole-genome sequencing enables the screening of known resistance-associated loci while also providing opportunities to characterize other loci as predictive of resistance or not (Farhat et al., 2013; Casali et al., 2014). In this study, we analyze the sequence polymorphisms in 18 chosen genes or regions of 183 *M. tuberculosis* isolates based on the whole-genome sequenced data. The sequences or regions were chosen on the basis of their demonstrated association with drug resistance and according to the TB Drug Resistance Database (Sandgren et al., 2009).

MATERIALS AND METHODS

Strains

We used 183 *M. tuberculosis* isolates for WGS. H37Rv (ATCC 27294), which is susceptible to the four first-line anti-tuberculosis drugs INH, RMP, EMB, and pyrazinamide (i.e., pansusceptible), was used as a reference. The isolates used for WGS were obtained from 183 adult patients with pulmonary TB from 2005 to 2009 from institutes for tuberculosis control and prevention as well as tuberculosis hospitals distributed in 11 provincial-level administration divisions (PLADs) of China; the numbers isolated from each PLAD were as follows: Beijing, 13; Fujian, 24; Guangdong, 8; Guizhou, 21; Henan, 6; Inner Mongolia, 5; Liaoning, 20; Shaanxi, 25; Shanghai, 26; Tibet, 30; and Xinjiang, 5.

Drug Susceptibility Testing and Mycobacterium Species Identification

The isolate profiles of drug susceptibility were evaluated in our laboratory by the proportional method using L-J slants with the following drug concentrations: INH, 0.2 μg/mL; RMP, 40 μg/mL; STR, 4 μg/mL; EMB, 2 μg/mL; kanamycin (KAN), 30 μg/mL; ofloxacin (OFX), 2 μg/mL; capreomycin (CAP), 40 μg/mL (World Health Organization, 2008). L-J medium containing para-nitrobenzoic acid (500 μg/mL) was used to identify *M. tuberculosis* complex species from non-tuberculosis mycobacteria, and medium containing thiophen-2-carboxylic acid hydrazide (5 μg/mL) was used to exclude *Mycobacterium bovis* (*M. bovis*) from the *M. tuberculosis* complex. This study included the *M. tuberculosis* complex but did not include *M. bovis* clinical isolates. All the strains were stored in physiological saline containing 50% glycerol at −70°C. Prior to characterizing the drug susceptibility, the strains were recovered on L-J medium for 4 weeks at 37°C. DST, mycobacterium species identification, and inactivation of strains were all performed in a Biosafety Level 2 Laboratory.

Genome Sequencing

Genomic DNA was extracted from *M. tuberculosis* colonies on L-J medium using CTAB (van Embden et al., 1993). DNA libraries (350 bp insert) were constructed with genomic DNA using kits provided by Illumina according to the manufacturer's instructions. DNA libraries were then selected to perform cluster growth and 90 bp paired-end sequencing on an Illumina HiSeq 2000 sequencer according to standard protocols. Raw reads with consecutive bases covered by fewer than five reads, duplicate

reads, and the adapter were removed; then, the rest of the reads, called clean data, from each strain were mapped to the genome of H37Rv (GenBank accession number, NC_000962.2) using SOAP2 (Li et al., 2009). An average of 5.27 million sequence reads were acquired per genome at a depth of 112× and with coverage of 99.32%. The accuracy of the sequencing was assessed by sequencing *rpoB* in a random selection of 80 isolates on an ABI Prism 3730 automated DNA sequencer (ABI, Shirley, NY, United States) as described by Zhang et al. (2013), the results show 100% consensus between the Illumina HiSeq 2000 and ABI 3730 sequencing results.

Identify Mutations in Drug Resistance–Associated Genes and Promoter Regions

Identification of resistance-causing single-nucleotide polymorphisms (SNPs) from genome-wide sequence is challenging. We focused on putative or known resistance genes and promoter regions on the basis of their demonstrated association with drug resistance and according to the TB Drug Resistance Database (Sandgren et al., 2009; **Table 1**). All mutations in these genes and promoter regions were compared with the pan-susceptible reference genome (H37Rv, accession number: NC_000962.2) at the level of SNPs in promoter regions, amino acids in genes, or insertions and deletions. In this study, we first characterized the synonymous and lineage-defining mutations that did not cause resistance, and then, we characterized the mutations associated with drug resistance. The phenotypic and genotypic results were compared to determine the specificity and sensitivity for each gene or region studied.

TABLE 1 | Eighteen candidate genes and intergenic regions linked with acquisition of drug resistance.

Drug	Genes or regions	Product
Isoniazid	*katG*	Catalase-peroxidase-peroxynitritase
	inhA coding region	NADH-dependent enoyl-acyl carrier protein reductase
	promoter of *inhA*	–
	ahpC coding region	Alkyl hydroperoxide reductase C
	oxyR-ahpC intergenic region	–
	ndh	NADH dehydrogenase
	efpA	EfpA
	kasA	Beta-ketoacyl-ACP synthase
	iniA	Rv0342
	iniC	Rv0343
	iniB	Lipoprotein LpqJ
Rifampicin	*rpoB*	DNA-directed RNA polymerase β chain
Streptomycin	*rpsL*	30S ribosomal protein S12
	rrs	16S rRNA
	gidB	Glucose-inhibited division protein B
Ethambutol	*embB*	Arabinosyltransferase B
	embC	Arabinosyltransferase C
	embA	Arabinosyltransferase A

Spoligotyping and Data Analysis

Spoligotyping was performed using 43 covalently bound oligonucleotides derived from the spacer sequences of *M. tuberculosis* H37Rv and *M. bovis* BCG P3 as previously described by Kamerbeek et al. (1997). The results in binary format were entered into an Excel spreadsheet and compared with the spoligotyping database SpolDB4.[1]

Statistical Analysis

SPSS 16.0 (SPSS Inc., Chicago, IL, Untied States) was used to perform Chi-square and Fisher's exact analysis according to the sample number and multivariate regression analysis. The difference was considered to be statistically significant when $P < 0.05$.

RESULTS

Drug Susceptibility Patterns

All isolates for WGS underwent culture-based DST to seven drugs: 46 were fully drug susceptible; 137 were resistant to both INH and RMP. Among 137 MDR strains, 100 (73.0%), 77 (56.2%), 60 (43.8%), 22 (16.1%), and 21 (15.3%) were resistant to STR, EMB, OFX, KAN, and CAP, respectively; 18% (24/137) of the MDR isolates were extensively drug resistant (XDR, MDR isolates are also resistant to both fluoroquinolone and an injectable drug). Detailed susceptibility profiles are shown in **Supplementary Table 1**.

Genotype Distribution of the *M. tuberculosis* Isolates

Among the *M. tuberculosis* isolates for WGS, 141 (77.0%) belonged to the Beijing genotype, and 42 (23.0%) were non-Beijing family, which included the T1 family (12), H3 family (3), T2 family (3), CAS family (2), Haarlem3 family (2), MANU2 family (2), CAS1-DELH1 family (1), LAM9 family (1), U family (1), and a new found genotype (12).

Synonymous Mutations in Chosen Genes and Regions

A total of 55 synonymous mutations were found and are shown in **Supplementary Table 2**. Although synonymous mutations were universally acknowledged to be unrelated with drug resistance, we found that the prevalence of *rpoB* 1075 GCT-GCC (Ala-Ala) in RMP-resistant *M. tuberculosis* was higher than that in RMP-susceptible isolates, and the prevalence of *gidB* 205 GCA-GCG (Ala-Ala) in STR-resistant isolates was higher than that in STR-susceptible isolates. Among 55 synonymous mutations, 17 were found only in interested drug–susceptible isolates, 27 were found only in interested drug–resistant isolates, and the remaining 11 were found in both interested drug–susceptible and –resistant

[1] http://www.pasteur-guadeloupe.fr:8081/SITVITDemo/index.jsp

isolates. Sixteen out of the 27 synonymous mutations were found in the 11 genes or regions related with INH resistance in INH-resistant isolates. None of the stand-alone synonymous mutations in the known genes *katG* (INH), *rpoB* (RMP), and *rpsL* (STR) was found only in isolates resistant to INH, RMP, and STR, respectively, and one stand-alone synonymous mutation 304 CTG-TTG (L-L) in the known gene *embB* was only found in one EMB-resistant isolate.

We further analyzed the associations between the 55 synonymous mutations and the Beijing genotype and found that the prevalence of *iniA* 178 GGT-GGC (Gly-Gly) and *embA* 1092 GCG-GCA (Ala-Ala) was much higher in the non-Beijing genotype than in the Beijing genotype *M. tuberculosis*, and the prevalence of *rpoB* 1075 GCT-GCC (Ala-Ala), *embA* 76 TGC-TGT (Cys-Cys), and *gidB* 205 GCA-GCG (Ala-Ala) was much higher in the Beijing genotype than in the non-Beijing genotype. Among 55 synonymous mutations, 31 were only found in Beijing genotype strains, 17 were only found in the non-Beijing genotype, and seven were found in both genotypes. The results are shown in **Supplementary Table 3**.

We then performed multivariate analysis toward the mutations of *rpoB* 1075 GCT-GCC (Ala-Ala) and *gidB* 205 GCA-GCG (Ala-Ala) based on the univariate analysis. As shown in **Table 2**, the analysis data revealed that the Beijing genotype is the high-risk factor for these two synonymous mutations, not the RMP or STR resistance.

Analysis on Mutations *katG* R463L and *gidB* E92D Known Not to Code for Resistance

In the present study, 146 and 143 out of 183 isolates carried mutations *katG* 463 CGG-CTG (Arg-Leu) and *gidB* 92 GAA-GAC (Glu-Asp), respectively. According to previous studies, both mutations are known not to be associated with resistance (Meacci et al., 2005; Via et al., 2010; Feuerriegel et al., 2014; Nebenzahl-Guimaraes et al., 2014), and *gidB*92 polymorphism (276C allele) has been reported to be associated with the Beijing lineage (Spies et al., 2011). However, statistical analysis shows that the prevalence of *katG* 463 CGG-CTG (Arg-Leu) in INH-resistant isolates are higher than that in INH-susceptible isolates, and the prevalence of *gidB* 92 GAA-GAC (Glu-Asp) in STR-resistant isolates is higher than that in STR-susceptible isolates; both *P*-values were less than 0.05 (see **Supplementary Table 4**). We also found that the prevalence of *katG* 463 CGG-CTG (Arg-Leu) and *gidB* 92 GAA-GAC (Glu-Asp) in the Beijing genotype is much higher than in the non-Beijing genotype isolates; see **Supplementary Table 5**.

Multivariate analysis toward the mutations of *katG* 463 CGG-CTG (Arg-Leu) and *gidB* 92 GAA-GAC (Glu-Asp) based on the univariate analysis shows that the Beijing genotype is the high-risk factor for both mutations, not the INH resistance or STR resistance (**Table 2**).

TABLE 2 | Multivariate analysis of drug resistance and genotypes of *M. tuberculosis* according to the four mutations.

Dependent variables (mutations)	Characteristic	Adjusted ORs (95% CI)	*P*-value
rpoB 1075 GCT-GCC (Ala-Ala)	Beijing genotype	477.6 (110.2–2069.8)	0.000
	RMP resistance	0.4 (0.1–1.9)	0.266
katG 463 CGG-CTG (Arg-Leu)	Beijing genotype	477.6 (110.2–2069.8)	0.000
	INH resistance	0.4 (0.1–1.9)	0.266
gidB 92 GAA-GAC (Glu-Asp)	Beijing genotype	453.2 (116.9–1757.5)	0.000
	STR resistance	1.6 (0.4–6.0)	0.523
gidB 205 GCA-GCG (Ala-Ala)	Beijing genotype	334.1 (90.8–1229.4)	0.000
	STR resistance	1.1 (0.3–4.0)	0.859

RMP, rifampicin; STR, streptomycin; INH, isoniazid.

Drug Resistance and Gene Mutations

Isoniazid Resistance and Mutations in Genes and Intergenic Regions

Whole-genome sequencing data shows that, respectively, among 137 INH-resistant and 46 INH-susceptible isolates, 124 and 1 carry mutations in *katG*, 28 and 0 in the *inhA* promoter, and 12 and 2 in the *oxyR-ahpC* intergenic region (**Table 3**). We found a rare high prevalence (90.5%) of the *katG* mutation in INH-resistant *M. tuberculosis*, which has never been reported in China. *katG* mutations combined with that in the *inhA* promoter only increased the sensitivity from 90.5 to 92.7% while there was no additional specificity (**Figure 1**). At the base of mutations in *katG* and the *inhA* promoter, adding the mutations in the *oxyR-ahpC* intergenic region, the sensitivity was not changed although the specificity fell from 97.8 to 93.5% as shown in **Figure 1**. The most frequent mutation site was *katG*315 (92/137, 67.2%); among the isolates that carried this mutation, only 14 combined mutations in the *inhA* promoter and/or the *oxyR-ahpC* intergenic region; among 32 INH-resistant isolates, which carried mutations in *katG* non-315, 21 combined mutations in the *inhA* promoter and/or the *oxyR-ahpC* intergenic region; among 13 INH-resistant isolates, which carried the wild-type of *katG*, three carried mutations in the *inhA* promoter and/or the *oxyR-ahpC* intergenic region, four carried mutations only in the other eight genes related to INH resistance, and there were still six INH-resistant strains with the wild-type of 11 sequenced genes that have been reported to be associated with INH resistance; see **Figure 2**. Among 28 INH-resistant isolates that carried mutations in the *inhA* promoter, 11 carried mutations of *katG*315, 14 carried mutations in *katG* but not in codon 315, and three carried wild-type *katG*.

In the present study, a total of 29 mutation sites in *katG* except *katG315* were found in 34 INH-resistant isolates of which two were combined with the mutation of *katG*315 (**Figure 2** and **Supplementary Table 6**). We also found that 23 out of 45 isolates possessed *katG* non-315 mutations, or wild-type *katG* carried *inhA* C(-15)T and/or mutations in the region of *ahpC* from −84 to −48, which occupied 16.8% of the INH-resistant isolates. So the *inhA*(-15) and *ahpC*−84 to −48 combined with

TABLE 3 | The evaluation between whole-genome sequencing analysis of 18 drug-resistant associated genes or regions and the phenotypic drug susceptibility testing.

Drugs	Genes	Number of isolates (%*) carried mutations[&] in resistant strains	Number of isolates (%[#]) carried mutations[&] in susceptible strains	χ^2	*P*	Sensitivity[a] (%)	Specificity[b] (%)
INH	*katG*	124 (90.5)	1 (2.2)	119.2	0.000	90.5	97.8
	inhA promoter	28 (20.4)	0 (0.0)	11.1	0.001	20.4	100.0
	OxyR-ahpC intergenic region	12 (8.8)	2 (4.3)	0.4	0.514	8.8	95.7
	inhA coding region	3 (2.2)	0 (0.0)	0.1	0.733	2.2	100.0
	ahpC coding region	1 (0.7)	0 (0.0)	0.0	1.0	0.7	100.0
	ndh	18 (13.1)	5 (10.9)	0.2	0.688	13.1	89.1
	kasA	3 (2.2)	0 (0.0)	0.1	0.733	2.2	100.0
	efpA	3 (2.2)	0 (0.0)	0.1	0.733	2.2	100.0
	iniA	5 (3.6)	1 (2.2)	0.0	0.994	3.6	97.8
	iniB	32 (23.4)	12 (26.1)	0.1	0.708	23.4	73.9
	iniC	8 (5.8)	2 (4.3)	0.0	0.992	5.8	95.7
RMP	*rpoB*	129 (94.2)	0 (0.0)	146.8	0.000	94.2	100.0
STR	*rpsL*	72 (72.0)	3 (3.6)	87.70	0.000	72.0	96.4
	rrs 530 loop and 912 loop	11 (11.0)	0 (0.0)	7.86	0.005	11.0	100
	gidB	12 (12)	7 (8.4)	0.62	0.431	12.0	91.6
EMB	*embA*	7 (9.1)	9 (8.5)	0.02	0.887	9.1	91.5
	embB	70 (90.9)	37 (34.9)	57.61	0.000	90.9	65.1
	embC	4 (5.2)	9 (8.5)	0.73	0.392	5.2	91.5

*INH, isoniazid; RMP, rifampicin; STR, streptomycin; EMB, ethambutol. *Compared with the total number of isolates resistant to the interested drug: INH, 137; RFP, 137; STR, 100; EMB, 77. [&]Mutations used here did not include synonymous mutations and well-known nonsynonymous polymorphisms (katG R463L and gidB E92D) which universally acknowledged unrelated with drug resistance. [#]Compared with the total number of isolates susceptible to the interested drug: INH, 46; RFP, 46; STR, 83; EMB, 106. [a]Sensitivity = number of interested drug resistant isolates with mutation/total number of interested drug resistant isolates. [b]Specificity = number of interested drug susceptible isolates without mutation/total number of interested drug susceptible isolates.*

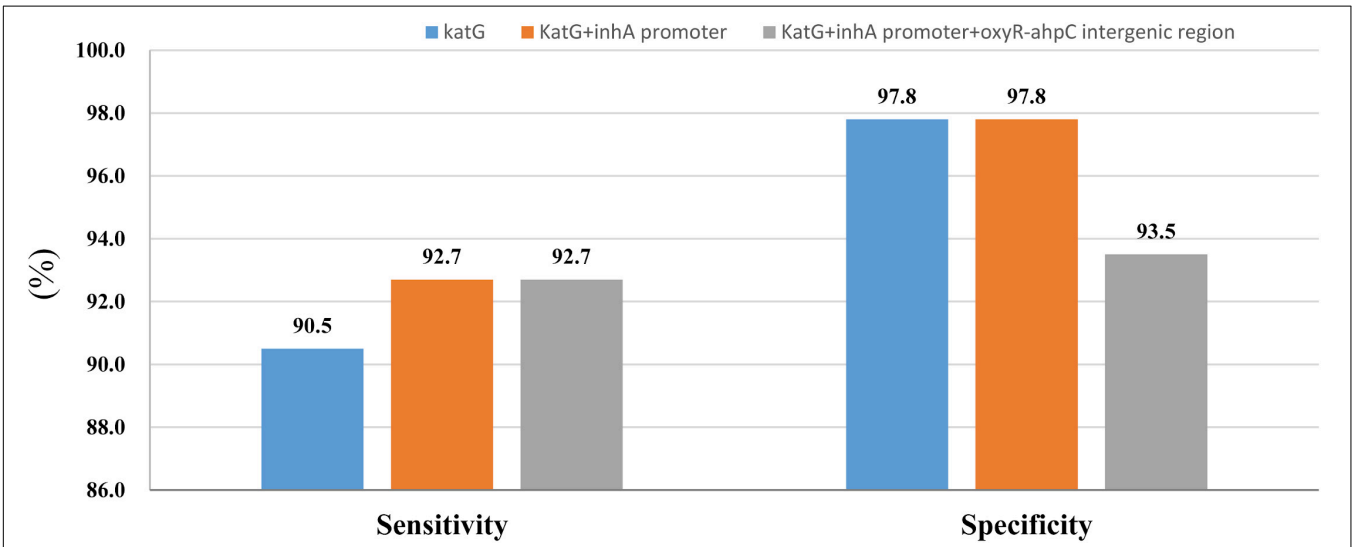

FIGURE 1 | Sensitivity and specificity of sequencing of *katG* combined with *inhA* promoter and *oxyR-ahpC* intergenic region for isoniazid resistance and susceptibility diagnoses.

*katG*315 can make a preferable set for INH-resistance diagnoses, and the mutation sites in *katG* except 315 were scattered, which made these codons have less diagnostic value when used in gene chip, line/dot-blot hybridization or multiplex fluorescence melting curve analyses.

Besides *katG*, the *inhA* promoter, and *oxyR-ahpC* intergenic region, eight genes (coding regions) were also included to clarify the mechanism of INH resistance. The strain numbers that carried mutations in eight studied genes (coding regions) in INH-resistant and -susceptible isolates were as follows, respectively: *inhA* coding region, 3 and 0; *ahpC* coding region, 1 and 0; *ndh*, 18 and 5; *kasA*, 3 and 0; *efpA*, 3 and 0; *iniA*, 5 and 1; *iniB*, 32 and 12; *iniC*, 8 and 2 (**Table 3**). Low mutation prevalence of these genes in INH-resistant strains and mutations has even been found in

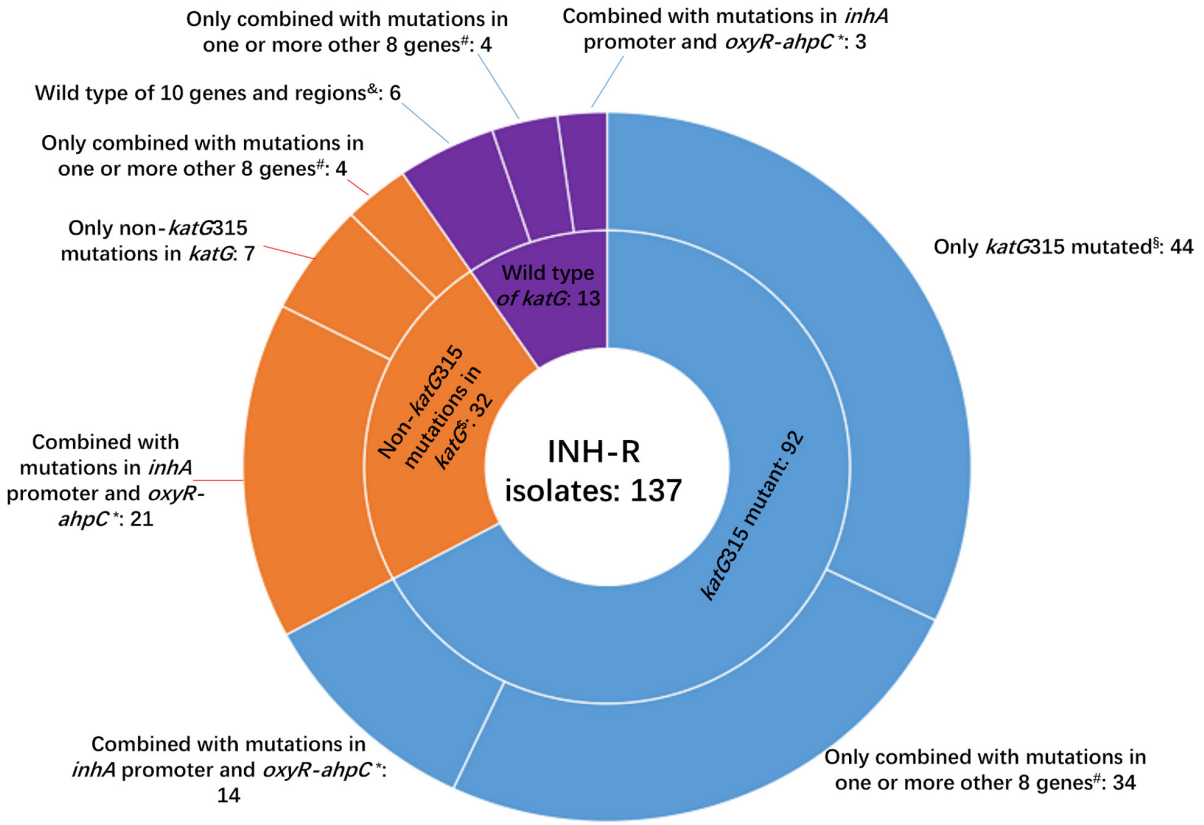

FIGURE 2 | Number of isolates carrying *katG* mutations combined with mutations in another 10 genes or intergenic regions among 137 MDR *M. tuberculosis*. INH-R, isoniazid resistant; *this group included isoniazid-resistant isolates that also carried mutations in *ahpC* coding region, *inhA* coding region, *ndh*, *efpA*, *kasA*, *iniA*, *iniB*, and/or *iniC*. #Eight genes included *ahpC* coding region, *inhA* coding region, *ndh*, *efpA*, *kasA*, *iniA*, *iniB*, and *iniC*; §two isolates that had mutations of *katG*315 and other substitutes in *katG* were not included in this group. § This group included two isolates that had mutations of *katG*315 and other substitutes in *katG*; &10 genes and regions included *inhA* promoter, *oxyR-ahpC* intergenic region, *ahpC* coding region, *inhA* coding region, *ndh*, *efpA*, *kasA*, *iniA*, *iniB*, and *iniC*.

INH-susceptible strains, which made the associations confused between these genes and INH resistance.

As shown in **Table 4**, we found 18 novel mutations, which included 10 in the gene *katG*, three in the *oxyR-ahpC* intergenic region, one in the *ahpC* coding region, two in the *kasA* gene, and four in the *efpA* gene.

Rifampicin Resistance and *rpoB* Mutations

The whole *rpoB* sequence of 183 *M. tuberculosis* was analyzed. Altogether, 94.2% (129/137) of the RMP-resistant isolates harbored at least one mutation within *rpoB*, and other eight isolates lacked such a mutation (**Supplementary Table 7**). Eighty-nine isolates (65%) had a single mutation, and 48 (35%) had two or more mutations each. When all of the mutations were considered, regardless of single, double, or more, a total of 55 genotype patterns were identified, and 127 out of 137 RMP-resistant *M. tuberculosis* isolates carried mutations in the 81-bp RRDR of the *rpoB gene*. The most frequently mutated codons were 450 (*Escherichia coli* 531), 445 (*E. coli* 526), and 435 (*E. coli* 516) with mutation frequencies of 51.1% (70/137 isolates), 23.4% (32/137 isolates), and 12.4% (17/137 isolates) (**Table 5**). An independent and novel mutation was detected in *rpoB*: 675 GGC-GAC (Gly-Glu), which was only found in an RMP-resistant isolate. In contrast, none of 46 susceptible isolates possessed a nonsynonymous mutation within the whole sequence of the *rpoB* gene.

Streptomycin Resistance and Mutations in *rpsL*, *rrs*, and *gidB*

Previous studies show that mutations in loop 530 and loop 912 of *rrs* are associated with STR resistance (Finken et al., 1993; Sreevatsan et al., 1996; Li et al., 2010), so we only analyzed the mutations in these two regions of *rrs* and the whole sequence of *rpsL* and *gidB* in this study.

The WGS data shows that 72, 11, and 12 out of 100 STR-resistant isolates carried mutations in *rpsL*, *rrs* 530 loop, or 912 loop and *gidB*, respectively; in contrast, 3, 0, and 7 out of 83 STR-susceptible isolates carried, respectively (**Table 3**). None of the STR-resistant isolates were found to carry mutations simultaneously in both *rpsL* and *rrs* 530 loop or 912 loop. The sensitivity and susceptibility of mutations in *rpsL* combined with *rrs* 530 loop and 912 loop were 83.0% (83/100) and 92.8% (77/83). We also found that, among 83 STR-susceptible isolates, eight

TABLE 4 | Novel mutations occurred in genes and regions associated with isoniazid resistance and found only in phenotypic isoniazid resistant *M. tuberculosis*.

Genes	Codon change(s)	Amino acid/ nucleotide changes	Combined mutations in *katG*, *inhA* promoter or *oxyR-ahpC* intergenic region	Number of INH resistant isolates*
KatG	TGG-AGG	Trp90Arg	*ahpC* G(-48)A	1
	CTG-CGG	Leu587Arg	*katG* Tyr155Cys and *ahpC* C(-72)T	1[a]
	GAC-GCC	Asp189Ala	none	1
	GAC-GGC	Asp419Gly	*katG* Pro232Ser	1
			ahpC (-47) insert T	1[b]
	CCG-TCG	Pro235Ser	*katG* Ser302Arg	1
	GCC-ACC	Ala649Thr	*katG* Ser315Thr	1
	ACT-CCT	Thr380Pro	*inhA* C(-15)T	1
	–	Nucleotide positions 861-866 deleted ACCCGA	None	1
	–	Nucleotide positions 86–88 deleted CC	*inhA* C(-15)T	1
	–	nucleotide position 956 deleted T	*ahpC* C(-81)T	1[c]
oxyR-ahpC intergenic region	–	(-72) C-T	*katG* Tyr155Cys and Leu587Arg	1[a]
			katG Gly169Ser and *inhA* C(-15)T	1
			katG Leu378Pro	1
	–	(-47) insert T	*katG* Asp419Gly	1[b]
	–	C(-81)T	nucleotide position 1735 deleted A in *katG*	1
			nucleotide position 956 deleted T in *katG*	1[c]
ahpC coding region	AGC-AGA	Ser148Arg	*katG* Ser315Thr and *inhA* C(-8)T	1
kasA	GTT-ATT	V142I	*katG* Ser315Thr	1
	CAC-TAC	H253Y	*katG* Ser315Thr	2
efpA	ACA-CCA	T7P	*katG* Ser315Thr	1[d]
	GCC-GAC	A227D	*katG* Ser315Thr	1[d]
	CTG-ATG	L275M	none	1
	ATC-GTC	I313V	*katG* Ser315Thr	1

**Identical letters in this column means that these mutations were occurred in the same isoniazid resistant isolates.*

TABLE 5 | Mutation frequency of codons of *rpoB* 81-bp rifampicin resistance determined region among 137 MDR isolates from China.

M. tuberculosis H37Rv codon number	*E. coli* codon number	Number (%) of rifampicin resistant isolates	Number of isolates without other *rpoB* mutation	Number of isolates combined with other *rpoB* mutations*
450	531	70 (51.1)	56	14
445	526	32 (23.4)	13	19
435	516	17 (12.4)	6	11
452	533	8 (5.8)	3	5
430	511	6 (4.4)	0	6
428	509	3 (2.2)	0	3
441	522	2 (1.5)	1	1
427	508	1 (0.7)	0	1
429	510	1 (0.7)	0	1
431	512	1 (0.7)	0	1
437	518	1 (0.7)	0	1
438	519	1 (0.7)	0	1

**Other rpoB mutations included the mutations which were in or outside of the rifampicin resistance determined region of rpoB.*

carried mutations in *rrs* outside of the 530 loop or 912 loop: one carried a mutation with nucleotides in positions 334–344 deleted, four carried mutations with nucleotides in positions 388–394 deleted, one carried a mutation of 555 A-T, and two carried mutations with 846 C-T and 1017 G-C. Among these eight isolates, seven were susceptible to INH, RMP, STR, EMB, CPM, KAN, and OFX.

As shown in **Table 6**, for *rpsL*, the most frequently mutated codons were 43 and 88 with mutation frequencies of 50.0% (50/100 isolates) and 19.0% (19/100 isolates), respectively. For the 530 loop and 912 loop, the most frequently mutated positions were 515, 518, and 888 with mutation frequencies of 8.0% (8/100 isolates), 2.0% (2/100 isolates), and 1.0% (1/100 isolates), respectively. In the present study, no isolate was found to carry

TABLE 6 | Mutation characterizations of *rpsL* and *rrs 530 loop and 912 loop* among 100 streptomycin resistant *M. tuberculosis* from China.

Genes	Mutations	Frequency (Number of isolates)	Relative frequency[a] (%)
rpsL	43AAG-AGG(Lys-Arg)	53	53.0
	88AAG-AGG(Lys-Arg)	19	19.0
rrs 530 loop and 912 loop	515A-C	8	8.0
	518C-T	2	2.0
	888G-T	1	1.0

[a]*Compared with the total number of isolates resistant to streptomycin.*

mutations in *rpsL* combined with *rrs* 530 loop or 912 loop although one STR-resistant isolate was found to carry mutations of *rpsL* Lys88Arg and *rrs* 38 G-A. The mutation results of *gidB* were confused as shown in **Table 3** and **Supplementary Table 8**; both STR-resistant and susceptible isolates carried mutations, and the mutated codons were scattered throughout the gene.

Ethambutol Resistance and Mutations in *embB, embA*, and *embC*

Known mechanisms of EMB resistance are caused by mutations in the *embCAB* operon, especially in *embB*. The whole sequences of *embA, embB,* and *embC* were analyzed in this study. The results show that, among 77 EMB-resistant isolates, there were 7, 70, and 4 carried mutations in *embA*, *embB*, and *embC*, respectively, and among 106 EMB-susceptible isolates, there were 9, 37, and 9 carried mutations in *embA*, *embB*, and *embC*, respectively (**Table 3**).

The most predominant mutation in *embB* occurred at codon 306 (45, 58.4%), where the codon ATG (Met) was replaced with GTG (Val, 26, 33.8%), ATA (Ile, 11, 14.3%), ATC (Ile, 4, 5.2%), CTG (Leu, 2, 2.6%), ATT (Ile, 1, 1.3%), and GTA (Val,1, 1.3%), respectively. Mutation of *embB* Gly406 was the next most predominant mutation (9, 11.7%). Among the EMB-susceptible isolates, mutations in Met306 and Gly406 were also the most predominant in *embB*. As shown in **Supplementary Table 9**, among the EMB-resistant isolates, all of the mutations in *embA* or *embC* combined with mutations in *embB* and the mutated codons scattered in *embA* and *embC*.

DISCUSSION

The present study is the first to comprehensively analyze the whole sequences of 18 drug resistance–associated genes or intergenic regions of 183 *M. tuberculosis* isolates, which include MDR-TB and XDR-TB isolates from 11 provinces of China. The results suggest that sequencing the whole sequence of four genes can now characterize profiles of resistance to INH, RMP, and STR with an acceptable degree of accuracy sufficient for clinical use. Furthermore, more drug resistance–associated loci and Beijing genotype–associated loci were found in our research.

Compared to the molecular assays of DST, such as line-probe arrays, PCR methods based on TaqMan probes, or melting curves (Boehme et al., 2010; Chen et al., 2014; Zhao et al., 2015b; World Health Organization, 2016; Makhado et al., 2018; Cao et al., 2019), WGS displays better performance to predict drug resistance according to the limited known mutations as well as a big catalog of mutations in various genes. However, among the mutations found by WGS, synonymous mutations, mutations of lineage markers, and some well-known nonsynonymous polymorphisms (e.g., *katG* R463L, gyrA S95T) (Feuerriegel et al., 2014; Zhao et al., 2014b), which are universally acknowledged to be unrelated with drug resistance, must be excluded before predicting resistance. In the present study, we found that both *gidB* E92D and *katG* R463L occurred in almost all of the Beijing genotype strains although they sparsely occurred in strains with CAS, MANU, and new genotypes. As reported by previous studies (Jagielski et al., 2014; Sun et al., 2016), we also found that the nonsynonymous mutations *gidB* E92D and the synonymous mutation *gidB* A205A were associated with the Beijing genotype. The synonymous mutations *rpoB* A1075A and *embA* C76C were associated with the Beijing genotype, and *iniA* G178G and *embB* A1092A were associated with the non-Beijing genotype, which were first reported by us. The remaining 50 synonymous mutations were not found to have statistics association with drug resistance or genotypes.

It is well known that the mechanism of action of INH, which has a simple chemical structure, is very complex, and several bactericidal strategies have been reported (Timmins and Deretic, 2006). Consequently, several genes in multiple biosynthetic networks and pathways involved in INH action have been reported to play a role in INH resistance (Unissa et al., 2016). Mutations in the *katG* gene are the major contributors for INH resistance, followed by *inhA*, *ahpC*, *kasA*, *ndh*, *iniABC*, *efpA*, *fadE*, *furA*, *Rv1592c*, and *Rv1772* (Unissa et al., 2016). In the present study, There were 90.5% INH-resistant isolates that carried mutations in *katG*, which was higher than the 86.2% reported by Liu et al. (2018) and the 74.5% reported by Luo et al. (2019). Liu et al. (2018) reported that 47.1% (16/34) INH-resistant isolates had *inhA* promoter mutations combined with a mutation in *katG*, which was far lower than the 89.3% (25/28) found in our study. One explanation may be that they only sequenced 518 bp of *katG* while we analyzed the whole sequence of *katG*. In the present study, 29 additional mutations except *katG*315 were found in *katG*, of which 10 were novel mutations, and only three novel mutations combined with *katG*315 or *inhA*(-15) mutations. All of these novel mutations were found only in phenotypic INH-resistant isolates, suggesting that these mutations were resistance-associated but needed to be further verified by site-directed mutagenesis or other experiments. Many non-*kat*G315 mutations in the *katG* gene, e.g., Y95C, P131T, D142G, A162V, T306P, Y64S, F483L, and A541D, have been confirmed causing INH resistance, and *katG* R385W and D387G did not play a role in INH resistance by in vitro mutagenesis experiments (Torres et al., 2015).

In the present study, the mutation rates in *inhA* and *ahpC* coding regions, *kasA* and *efpA* in INH-resistant isolates were low. To make sure these mutations are associated with INH resistance, more studies for the phenotypic effect of these mutations are required. Another four genes (*ndh*, *iniA*, *iniB*, and *iniC*) show similar mutation frequency in both INH-resistant

and -susceptible *M. tuberculosis*. The total mutation frequency of *ndh*, *iniA*, *iniB*, and *iniC* were 12.6% (23/183), 3.3% (6/183), 24% (44/183), and 5.5% (10/183), respectively. The mutation rate of *ndh* in INH-resistant isolates was higher than that reported by Islam et al. (13.1 vs. 2.9%) (Islam et al., 2019). Many reports have shown that isolates with mutations in *iniABC* had mutations in other genes as well (Ramaswamy et al., 2003), which was similar to our findings. However, the high mutation frequency of *iniABC* among clinical isolates in our study has never been reported. Previous studies have shown that IniA, IniB, and IniC were proteins that can be induced by isoniazid (Colangeli et al., 2005; Unissa et al., 2016). We speculated that there was a joint mechanism between efflux pumps and acquired mutations, e.g., *iniABC* and *katG*, and the accumulation of mutations under the pressure of drug selection may contribute to the appearance of INH resistance. Such knowledge of other genes (apart from *katG*) aids in developing better means to diagnose and prevent the transmission of INH-resistant tuberculosis.

Previous studies show that mutations in RRDR of *rpoB* account for 90% or higher RMP resistance (Li et al., 2010; Zhao et al., 2014b; Luo et al., 2019). We found 92.7% of RMP-resistant isolates carried mutations in this area, which is concordant with previous studies (Li et al., 2010; Zhao et al., 2014b; Luo et al., 2019). Only two RMP isolates carried mutations outside of RRDR: one carried a novel independent mutation of 675 GGC-GAC (Gly-Glu); the other isolate carried two substitutions of 170 GTC-TTC (Val-Phe) and 920 ATG-GTG (Met-Val). The most common mutations of the *rpoB* gene were in codons 450 (*E. coli* 531), 435 (*E. coli* 526), and 445 (*E. coli* 516) (**Table 5**); the results are consistent with other studies performed in China and other countries that reported the same trends (Li et al., 2010; Maningi et al., 2018; Luo et al., 2019). However, data from WGS in the present study reveal that 40 additional mutations outside of the RRDR region of *rpoB* are found in RMP-resistant phenotypes, and most of them are shown in the form of joint mutations with codons in RRDR, which may explain why isolates carrying the same mutation patterns in RRDR show different minimum inhibitory concentrations against RMP. Mutations in *rpoB* cannot answer the 5.8% RMP resistance in the present study. Previous studies show that substitutions in *rpoC* were frequent in RMP-resistant isolates; however, most *rpoC* substitutions combined with mutations in *rpoB* and are recognized as a modification or compensation for the phenotypes of mutations in the *rpoB* (Farhat et al., 2013; Perdigao et al., 2020).

Resistance to STR is due mostly to mutations in the *rpsL*, followed by mutations in *rrs* 530 loop or 912 loop. Only two mutations, Lys43Arg and Lys88Arg in *rpsL*, were found in STR-resistant isolates, similar to the data from other areas in China (Li et al., 2010) and South Africa (Maningi et al., 2018). The most common mutations of the *rrs* were A515C, C518T, and G888T, which are located in the *rrs* 530 loop or 912 loop. Eight out of 83 STR-susceptible isolates carried mutations outside of the *rrs* 530 loop or 912 loop, suggesting that these mutations are not related to STR resistance. Recently, mutations in *gidB* were reported to cause STR resistance (Perdigao et al., 2014; Verma et al., 2014). *gidB* mutations were found in both STR-resistant and -susceptible strains in the present study, consistent with data from previous studies (Nhu et al., 2012; Spies et al., 2011). Among 17 STR-resistant isolates without mutations in the *rpsL* or *rrs* 530 loop or 912 loop, seven carried *gidB* mutations found in six codons, of which one mutation (K163stop codon) was found in two STR-resistant isolates, and one mutation (nucleotide 120 C deleted) was also found in three STR-susceptible isolates. The results suggest that mutations in *gidB* do not help to explain STR resistance in isolates without the *rpsL* or *rrs* 530 loop and 912 loop mutations. The overexpressed proteins in STR-resistant isolates identified by Sharma and Bisht (2017b) are assumed to be responsible for STR resistance; however, the corresponding genes were not analyzed in the present study.

Resistance to EMB is mostly attributed to mutations in codon 306 in *embB,* accounting for 48.3–70.6% resistant isolates (Mokrousov et al., 2002; Campbell et al., 2011; Moure et al., 2014; Zhao et al., 2015a). In the present study, 58.4% EMB-resistant isolates carried mutations of *embB*306, in line with previous studies (Mokrousov et al., 2002; Campbell et al., 2011; Moure et al., 2014; Zhao et al., 2015a). Mutations of *embB*406 were found in 11.7% EMB-resistant isolates. WGS data from the present study found 19 more mutations besides the two canonical mutations in 16 EMB-resistant isolates, of which four isolates had double noncanonical mutations and one combined with *embB* M306I. *embB* mutations were found in 90.9% EMB-resistant isolates while previous studies ranged from 38.2 to 89.9% (Li et al., 2010; Campbell et al., 2011; Moure et al., 2014; Zhao et al., 2015a). However, 34.9% of EMB-susceptible isolates also carried mutations in *embB*, which is much higher that a previous study (6.5%) (CRyPTIC Consortium and the 100,000 Genomes Project et al., 2018). One explanation may be that previous studies showed that the conventional DST method for EMB resistance was an imperfect standard, particularly for isolates with *embB* mutations (Zhang et al., 2009; Walker et al., 2015; Schon et al., 2017). A previous study in our laboratory shows that, using the EMB concentration with 1.6 μg/mL instead of 2.0 μg/mL in L-J slants by the proportional method, 23 out of 28 EMB-susceptible isolates that carried *emb*306 mutations could be successfully recognized as EMB-resistant isolates while the susceptibility patterns of 26 EMB susceptible isolates with wild-type *embB* were not affected (Zhang et al., 2009). A recent study shows that *embB* mutations are also associated with INH resistance in EMB-susceptible isolates (Wan et al., 2020) and another study shows that the *embB* M306I and M306V mutations are significantly associated with INH resistance in both EMB-resistant and -susceptible strains (Farhat et al., 2016). We speculate that the ambiguous relationship between mutations in *embB* and EMB or INH resistance may also lower the specificity of *embB* for predicting EMB resistance.

Mutations in *embC* and *embA*, which are suggested to be involved in EMB resistance development (Plinke et al., 2010; Zhao et al., 2015a; Farhat et al., 2016) were also analyzed in the present study; all of the isolates carried mutations in *embC* or *embA* combined with mutations in *embB*, and the prevalence of mutations in these two genes among EMB-resistant and

-susceptible isolates were comparable. Therefore, 9.1% EMB resistance cannot be explained by *embC*, *embA* and *embB* in the present study. Farhat et al. (2016) finds univariate associations between *embA* N54D or *iniB* A70T and EMB resistance; however, no isolates carried these two mutations in the present study. Zhao et al. (2015a) reports that the mutations in the *embA* upstream region showed significant correlation with EMB resistance; however, this region was not included in the present study. Mutations in *ubiA* except a lineage-specific mutation E149D are reported to correlate with high-level EMB resistance and responsible for 3.2–6.4% EMB resistance (He et al., 2015; Xu et al., 2015; Tulyaprawat et al., 2019).

The WHO target product profiles for new molecular assays for *M. tuberculosis* require more than 90% sensitivity and 95% specificity (World health organization, 2014). Our findings show the predicted resistance to rifampicin and isoniazid exceeded 90% sensitivity and 95% specificity by WGS and analyzing *rpoB* (RMP) and *katG* (INH) (**Table 3**). In the present study, the additional mutation loci found in *katG* except in codon 315 made the mutations in the *inhA* promoter and *oxyR-ahpC* less meaningful for predicting INH resistance for that mutation in the latter two regions increased only 2.7% sensitivity by WGS. Although several molecular DSTs for INH resistance testing are recommended by WHO, several reports show that the calculated sensitivity among clinical isolates is far lower 90% (Li et al., 2015; Javed et al., 2016, 2018; World Health Organization, 2016; Maningi et al., 2018). According to the standard (World health organization, 2014) and the actual situations in clinical practice of new molecular DST assays (Li et al., 2015; Javed et al., 2016, 2018; World Health Organization, 2016; Maningi et al., 2018), the sensitivity for STR by WGS in the present study was recognized to achieve to an acceptable degree (using *rpsL* and *rrs* 530 loop and 912 loop, 83%), and the specificity was excellent (97.8%) while the sensitivity of *embB* for predicting EMB resistance was excellent (90.9%), but the specificity (65.1%) was far lower than the standard, which requires more than 95% (World health organization, 2014).

The results in the present study show that the sensitivity of drug resistance-associated genes or intergenic regions, whether alone or combined, could not predict 100% of the interested drug resistance, which is similar to that reported by most studies (Li et al., 2010; Farhat et al., 2016; Miotto et al., 2017; Shea et al., 2017). For the gap between genotypic and phenotypic resistance, one most fundamental cause may be that current sequencing technologies have varying capabilities to detect low frequencies (<20%) of resistant strains mixed with susceptible strains relative to phenotypic testing that can detect resistant strains making up only 1% of the total population (Canetti et al., 1969; Do and Dobrovic, 2009; Oh et al., 2010; Miotto et al., 2017). Second, breakpoint artifacts (i.e., inappropriately high critical concentrations) can be a major source of misclassification of phenotypes (Miotto et al., 2017), e.g., the threshold value for EMB resistance used in L-J medium mentioned in Zhang et al.'s (2009) report. Third, synonymous mutations are universally acknowledged to be unrelated with drug resistance as they do not cause any change in the structure of the protein (Torres et al., 2015), so synonymous mutations are excluded in the present study; however, drug-resistant strains are more likely to carry synonymous mutations although no statistical differences were found for most of loci (**Supplementary Table 5**), which cut down the sensitivity of sequencing. Previous studies show that these mutations can sometimes confer resistance (Safi et al., 2013; Van Deun et al., 2013). Fourth, predicting drug resistance based on WGS data relies on the knowledge of drug-resistance mechanisms; however, drug-resistance mechanisms have not been understood clearly, which results in WGS mispredicting resistance or susceptibility according to including mutations or without mutations, respectively. Previous studies (Li et al., 2010; Farhat et al., 2016; Miotto et al., 2017; Shea et al., 2017) as well as the present study report certain phenotypically susceptible isolates carried mutations while phenotypically resistant isolates show wild types in interested genes, especially in noncanonical genes associated with resistance. Applied proteomics and bioinformatics analysis (such as molecular docking, pupylation, and protein–protein interaction) on uncharacterized and hypothetical proteins in *M. tuberculosis* might give a clue for the novel mechanism of drug resistance (Sharma and Bisht, 2017a,b; Sharma et al., 2018).

CONCLUSION

The data in this study raise our understanding of the molecular determinants of resistance to INH, RMP, EMB, and STR; high sensitivities and specificities of mutations in the genes of *katG* (INH), *rpoB* (RMP), *rpsL* (STR), and *rrs* 530 loop and 912 loop (STR) provide us a good choice to predict INH, RMP, and STR resistance by WGS or target region sequencing in the future. Further, the results provide clues in clarifying the drug-resistance mechanisms of *M. tuberculosis* isolates from China.

DATA AVAILABILITY STATEMENT

The datasets generated for this study can be found in the NCBI with accession numbers SRA065095 and PRJNA633954.

ETHICS STATEMENT

This study was approved by the ethics committee of the National Institute for Communicable Disease Control and Prevention, Chinese Center for Disease Control and Prevention. The patients with TB were included in the present research only after we received informed written consent from themselves or from their parents/guardians in cases in which the patient was a child (18 years of age). An assent was also obtained from participants between 14 and 18 years of age.

AUTHOR CONTRIBUTIONS

GL designed and conducted this study. LW and GL wrote the first drafts of the manuscript. LW, HL, and ML sequenced the isolates and performed molecular characterization. YJ, XZ, and ZL performed drug susceptibility testing and spoligotyping. KW collected *M. tuberculosis* strains and provided oversight for sequencing and bioinformatics support. C-XG provided key manuscript edits. All authors commented on the manuscript draft and read and approved the final manuscript.

FUNDING

This work was financially supported by projects (2018ZX10103001-003-012) of the National Key Programs of Mega Infectious Diseases from the Ministry of Science and Technology, People's Republic of China, grant (2017zzts069) from Fundamental Research Funds for the Central Universities of Central South University, and the grant (81670014) from National Natural Science Foundation of China.

ACKNOWLEDGMENTS

We thank the staff of Beijing, Fujian, Guangdong, Guizhou, Heilongjiang, Henan, Inner Mongolia, Liaoning, Shaanxi, Shanghai, Tibet, and Xinjiang for supplying strains.

SUPPLEMENTARY MATERIAL

The Supplementary Material for this article can be found online at: https://www.frontiersin.org/articles/10.3389/fmicb.2020.01444/full#supplementary-material

Table S1 | Drug susceptibility patterns of 183 clinical *M. tuberculosis* for whole-genome sequencing.

Table S2 | Synonymous mutations in 183 *M. tuberculosis* and their associations with drug resistance.

Table S3 | Associations between synonymous mutations and Beijing genotype of 183 *M. tuberculosis* clinical isolates.

Table S4 | Associations between mutations *katG*463 or *gidB*92 and drug resistance in 183 *M. Tuberculosis*.

Table S5 | Associations between mutations *katG*463 or *gidB*92 and Beijing genotype in 183 *M. Tuberculosis*.

Table S6 | Characterizations of *katG* mutations and its combination mutations with other 10 genes or regions associated with isoniazid resistance among 137 multi-drug resistant isolates.

Table S7 | Mutation characterizations of *rpoB* among 137 MDR isolates from China.

Table S8 | Mutation characterizations of *gidB* among 100 streptomycin resistant isolates and 83 streptomycin susceptible isolates from China.

Table S9 | Mutation characterizations of *embABC* among 77 ethambutol resistant isolates and 106 ethambutol susceptible isolates from China.

REFERENCES

Boehme, C. C., Nabeta, P., Hillemann, D., Nicol, M. P., Shenai, S., Krapp, F., et al. (2010). Rapid molecular detection of tuberculosis and rifampin resistance. *N. Engl. J. Med.* 363, 1005–1015. doi: 10.1056/NEJMoa0907847

Campbell, P. J., Morlock, G. P., Sikes, R. D., Dalton, T. L., Metchock, B., Starks, A. M., et al. (2011). Molecular detection of mutations associated with first- and second-line drug resistance compared with conventional drug susceptibility testing of *Mycobacterium tuberculosis*. *Antimicrob. Agents Chemother.* 55, 2032–2041. doi: 10.1128/AAC.01550-10

Canetti, G., Fox, W., Khomenko, A., Mahler, H. T., Menon, N. K., Mitchison, D. A., et al. (1969). Advances in techniques of testing mycobacterial drug sensitivity, and the use of sensitivity tests in tuberculosis control programmes. *Bull. World Health Organ.* 41, 21–43.

Cao, Y., Parmar, H., Simmons, A. M., Kale, D., Tong, K., Lieu, D., et al. (2019). Automatic identification of individual rpoB gene mutations responsible for rifampin resistance in mycobacterium tuberculosis by use of melting temperature signatures generated by the Xpert MTB/RIF ultra assay. *J. Clin. Microbiol.* 58, 907–919. doi: 10.1128/JCM.00907-19

Casali, N., Nikolayevskyy, V., Balabanova, Y., Harris, S. R., Ignatyeva, O., Kontsevaya, I., et al. (2014). Evolution and transmission of drug-resistant tuberculosis in a Russian population. *Nat. Genet.* 46, 279–286. doi: 10.1038/ng.2878

Chen, C., Kong, W., Zhu, L., Zhou, Y., Peng, H., Shao, Y., et al. (2014). Evaluation of the GenoType((R)) MTBDRplus line probe assay on sputum-positive samples in routine settings in China. *Int. J. Tuberc. Lung. Dis.* 18, 1034–1039. doi: 10.5588/ijtld.13.0857

Colangeli, R., Helb, D., Sridharan, S., Sun, J., Varma-Basil, M., Hazbon, M. H., et al. (2005). The *Mycobacterium tuberculosis* iniA gene is essential for activity of an efflux pump that confers drug tolerance to both isoniazid and ethambutol. *Mol. Microbiol.* 55, 1829–1840. doi: 10.1111/j.1365-2958.2005.04510.x

CRyPTIC Consortium and the 100,000 Genomes Project, Allix-Beguec, C., Arandjelovic, I., Bi, L., Beckert, P., Bonnet, M., et al. (2018). Prediction of susceptibility to first-line tuberculosis drugs by DNA sequencing. *N. Engl. J. Med.* 379, 1403–1415. doi: 10.1056/NEJMoa1800474

Do, H., and Dobrovic, A. (2009). Limited copy number-high resolution melting (LCN-HRM) enables the detection and identification by sequencing of low level mutations in cancer biopsies. *Mol. Cancer* 8:82. doi: 10.1186/1476-4598-8-82

Farhat, M. R., Shapiro, B. J., Kieser, K. J., Sultana, R., Jacobson, K. R., Victor, T. C., et al. (2013). Genomic analysis identifies targets of convergent positive selection in drug-resistant *Mycobacterium tuberculosis*. *Nat. Genet.* 45, 1183–1189. doi: 10.1038/ng.2747

Farhat, M. R., Sultana, R., Iartchouk, O., Bozeman, S., Galagan, J., Sisk, P., et al. (2016). Genetic determinants of drug resistance in *Mycobacterium tuberculosis* and their diagnostic value. *Am. J. Respir. Crit. Care Med.* 194, 621–630. doi: 10.1164/rccm.201510-2091OC

Feuerriegel, S., Koser, C. U., and Niemann, S. (2014). Phylogenetic polymorphisms in antibiotic resistance genes of the *Mycobacterium tuberculosis* complex. *J. Antimicrob. Chemother.* 69, 1205–1210. doi: 10.1093/jac/dkt535

Finken, M., Kirschner, P., Meier, A., Wrede, A., and Bottger, E. C. (1993). Molecular basis of streptomycin resistance in *Mycobacterium tuberculosis*: alterations of the ribosomal protein S12 gene and point mutations within a functional 16S ribosomal RNA pseudoknot. *Mol. Microbiol.* 9, 1239–1246. doi: 10.1111/j.1365-2958.1993.tb01253.x

He, L., Wang, X., Cui, P., Jin, J., Chen, J., Zhang, W., et al. (2015). ubiA (Rv3806c) encoding DPPR synthase involved in cell wall synthesis is associated with ethambutol resistance in *Mycobacterium tuberculosis*. *Tuberculosis (Edinb)* 95, 149–154. doi: 10.1016/j.tube.2014.12.002

Islam, M. M., Tan, Y., Hameed, H. M. A., Liu, Z., Chhotaray, C., Liu, Y., et al. (2019). Detection of novel mutations associated with independent resistance and cross-resistance to isoniazid and prothionamide in *Mycobacterium tuberculosis* clinical isolates. *Clin. Microbiol. Infect.* 25, 1041.e1–1041.e7. doi: 10.1016/j.cmi.2018.12.008

Jagielski, T., Ignatowska, H., Bakula, Z., Dziewit, L., Napiorkowska, A., Augustynowicz-Kopec, E., et al. (2014). Screening for streptomycin resistance-conferring mutations in *Mycobacterium tuberculosis* clinical isolates from Poland. *PLoS One* 9:e100078. doi: 10.1371/journal.pone.0100078

Javed, H., Bakula, Z., Plen, M., Hashmi, H. J., Tahir, Z., Jamil, N., et al. (2018). Evaluation of genotype MTBDRplus and MTBDRsl assays for rapid detection

of drug resistance in extensively drug-resistant *Mycobacterium tuberculosis* isolates in Pakistan. *Front. Microbiol.* 9:2265. doi: 10.3389/fmicb.2018.02265

Javed, H., Jamil, N., Jagielski, T., Bakula, Z., and Tahir, Z. (2016). Evaluation of genotype MTBDRplus assay for rapid detection of isoniazid and rifampicin resistance in *Mycobacterium tuberculosis* clinical isolates from Pakistan. *Int. J. Mycobacteriol.* 5(Suppl 1), S147–S148. doi: 10.1016/j.ijmyco.2016.11.010

Kamerbeek, J., Schouls, L., Kolk, A., van Agterveld, M., van Soolingen, D., Kuijper, S., et al. (1997). Simultaneous detection and strain differentiation of *Mycobacterium tuberculosis* for diagnosis and epidemiology. *J. Clin. Microbiol.* 35, 907–914. doi: 10.1128/jcm.35.4.907-914.1997

Li, G. L., Zhao, D. F., Xie, T., Ju, H. F., Mu, C., Zhao, H., et al. (2010). Molecular characterization of drug-resistant Beijing family isolates of *Mycobacterium tuberculosis* from Tianjin, China. *Biomed. Environ. Sci.* 23, 188–193. doi: 10.1016/S0895-3988(10)60051-7

Li, Q., Dong, H. Y., Pang, Y., Xia, H., Ou, X. C., Zhang, Z. Y., et al. (2015). Multicenter evaluation of the molecular line probe assay for multidrug resistant *Mycobacterium Tuberculosis* detection in China. *Biomed. Environ. Sci.* 28, 464–467. doi: 10.3967/bes2015.066

Li, R., Yu, C., Li, Y., Lam, T. W., Yiu, S. M., Kristiansen, K., et al. (2009). SOAP2: an improved ultrafast tool for short read alignment. *Bioinformatics* 25, 1966–1967. doi: 10.1093/bioinformatics/btp336

Liu, L., Jiang, F., Chen, L., Zhao, B., Dong, J., Sun, L., et al. (2018). The impact of combined gene mutations in *inhA* and *ahpC* genes on high levels of isoniazid resistance amongst *katG* non-315 in multidrug-resistant tuberculosis isolates from China. *Emerg. Microbes Infect.* 7:183. doi: 10.1038/s41426-018-0184-0

Luo, D., Chen, Q., Xiong, G., Peng, Y., Liu, T., Chen, X., et al. (2019). Prevalence and molecular characterization of multidrug-resistant *M. tuberculosis* in Jiangxi province, China. *Sci. Rep.* 9:7315. doi: 10.1038/s41598-019-43547-2

Makhado, N. A., Matabane, E., Faccin, M., Pincon, C., Jouet, A., Boutachkourt, F., et al. (2018). Outbreak of multidrug-resistant tuberculosis in South Africa undetected by WHO-endorsed commercial tests: an observational study. *Lancet Infect. Dis.* 18, 1350–1359. doi: 10.1016/S1473-3099(18)30496-1

Maningi, N. E., Daum, L. T., Rodriguez, J. D., Said, H. M., Peters, R. P. H., Sekyere, J. O., et al. (2018). Multi- and extensively drug resistant *Mycobacterium tuberculosis* in South Africa: a molecular analysis of historical isolates. *J. Clin. Microbiol.* 56:e01214-17. doi: 10.1128/JCM.01214-17

Meacci, F., Orru, G., Iona, E., Giannoni, F., Piersimoni, C., Pozzi, G., et al. (2005). Drug resistance evolution of a *Mycobacterium tuberculosis* strain from a noncompliant patient. *J. Clin. Microbiol.* 43, 3114–3120. doi: 10.1128/JCM.43.7.3114-3120.2005

Miotto, P., Tessema, B., Tagliani, E., Chindelevitch, L., Starks, A. M., Emerson, C., et al. (2017). A standardised method for interpreting the association between mutations and phenotypic drug resistance in *Mycobacterium tuberculosis*. *Eur. Respir. J.* 50, 1701354. doi: 10.1183/13993003.01354-2017

Mokrousov, I., Otten, T., Vyshnevskiy, B., and Narvskaya, O. (2002). Detection of *embB*306 mutations in ethambutol-susceptible clinical isolates of *Mycobacterium tuberculosis* from Northwestern Russia: implications for genotypic resistance testing. *J. Clin. Microbiol.* 40, 3810–3813. doi: 10.1128/jcm.40.10.3810-3813.2002

Moure, R., Espanol, M., Tudo, G., Vicente, E., Coll, P., Gonzalez-Martin, J., et al. (2014). Characterization of the *embB* gene in *Mycobacterium tuberculosis* isolates from Barcelona and rapid detection of main mutations related to ethambutol resistance using a low-density DNA array. *J. Antimicrob. Chemother.* 69, 947–954. doi: 10.1093/jac/dkt448

Nebenzahl-Guimaraes, H., Jacobson, K. R., Farhat, M. R., and Murray, M. B. (2014). Systematic review of allelic exchange experiments aimed at identifying mutations that confer drug resistance in *Mycobacterium tuberculosis*. *J. Antimicrob. Chemother.* 69, 331–342. doi: 10.1093/jac/dkt358

Nguyen, L. (2016). Antibiotic resistance mechanisms in *M. tuberculosis*: an update. *Arch. Toxicol.* 90, 1585–1604. doi: 10.1007/s00204-016-1727-6

Nhu, N. T., Lan, N. T., Phuong, N. T., Chau, N., Farrar, J., and Caws, M. (2012). Association of streptomycin resistance mutations with level of drug resistance and *Mycobacterium tuberculosis* genotypes. *Int. J. Tuberc. Lung. Dis.* 16, 527–531. doi: 10.5588/ijtld.11.0202

Oh, J. E., Lim, H. S., An, C. H., Jeong, E. G., Han, J. Y., Lee, S. H., et al. (2010). Detection of low-level KRAS mutations using PNA-mediated asymmetric PCR clamping and melting curve analysis with unlabeled probes. *J. Mol. Diagn.* 12, 418–424. doi: 10.2353/jmoldx.2010.090146

Perdigao, J., Gomes, P., Miranda, A., Maltez, F., Machado, D., Silva, C., et al. (2020). Using genomics to understand the origin and dispersion of multidrug and extensively drug resistant tuberculosis in Portugal. *Sci. Rep.* 10:2600. doi: 10.1038/s41598-020-59558-3

Perdigao, J., Macedo, R., Machado, D., Silva, C., Jordao, L., Couto, I., et al. (2014). GidB mutation as a phylogenetic marker for Q1 cluster *Mycobacterium tuberculosis* isolates and intermediate-level streptomycin resistance determinant in Lisbon, Portugal. *Clin. Microbiol. Infect.* 20, O278–O284. doi: 10.1111/1469-0691.12392

Plinke, C., Cox, H. S., Zarkua, N., Karimovich, H. A., Braker, K., Diel, R., et al. (2010). *embCAB* sequence variation among ethambutol-resistant *Mycobacterium tuberculosis* isolates without embB306 mutation. *J. Antimicrob. Chemother.* 65, 1359–1367. doi: 10.1093/jac/dkq120

Ramaswamy, S. V., Reich, R., Dou, S. J., Jasperse, L., Pan, X., Wanger, A., et al. (2003). Single nucleotide polymorphisms in genes associated with isoniazid resistance in *Mycobacterium tuberculosis*. *Antimicrob. Agents Chemother.* 47, 1241–1250. doi: 10.1128/aac.47.4.1241-1250.2003

Safi, H., Lingaraju, S., Amin, A., Kim, S., Jones, M., Holmes, M., et al. (2013). Evolution of high-level ethambutol-resistant tuberculosis through interacting mutations in decaprenylphosphoryl-beta-D-arabinose biosynthetic and utilization pathway genes. *Nat. Genet.* 45, 1190–1197. doi: 10.1038/ng.2743

Sandgren, A., Strong, M., Muthukrishnan, P., Weiner, B. K., Church, G. M., and Murray, M. B. (2009). Tuberculosis drug resistance mutation database. *PLoS Med.* 6:e2. doi: 10.1371/journal.pmed.1000002

Schon, T., Miotto, P., Koser, C. U., Viveiros, M., Bottger, E., and Cambau, E. (2017). *Mycobacterium tuberculosis* drug-resistance testing: challenges, recent developments and perspectives. *Clin. Microbiol. Infect.* 23, 154–160. doi: 10.1016/j.cmi.2016.10.022

Sharma, D., and Bisht, D. (2017a). *M. tuberculosis* hypothetical proteins and proteins of unknown function: hope for exploring novel resistance mechanisms as well as future target of drug resistance. *Front. Microbiol.* 8:465. doi: 10.3389/fmicb.2017.00465

Sharma, D., and Bisht, D. (2017b). Secretory proteome analysis of streptomycin-resistant *Mycobacterium tuberculosis* clinical isolates. *SLAS Discov.* 22, 1229–1238. doi: 10.1177/2472555217698428

Sharma, D., Bisht, D., and Khan, A. U. (2018). Potential alternative strategy against drug resistant tuberculosis: a proteomics prospect. *Proteomes* 6:26. doi: 10.3390/proteomes6020026

Shea, J., Halse, T. A., Lapierre, P., Shudt, M., Kohlerschmidt, D., Van Roey, P., et al. (2017). Comprehensive whole-genome sequencing and reporting of drug resistance profiles on clinical cases of *Mycobacterium tuberculosis* in New York state. *J. Clin. Microbiol.* 55, 1871–1882. doi: 10.1128/JCM.00298-17

Spies, F. S., Ribeiro, A. W., Ramos, D. F., Ribeiro, M. O., Martin, A., Palomino, J. C., et al. (2011). Streptomycin resistance and lineage-specific polymorphisms in *Mycobacterium tuberculosis gidB* gene. *J. Clin. Microbiol.* 49, 2625–2630. doi: 10.1128/JCM.00168-11

Sreevatsan, S., Pan, X., Stockbauer, K. E., Williams, D. L., Kreiswirth, B. N., and Musser, J. M. (1996). Characterization of *rpsL* and *rrs* mutations in streptomycin-resistant *Mycobacterium tuberculosis* isolates from diverse geographic localities. *Antimicrob. Agents Chemother.* 40, 1024–1026. doi: 10.1128/aac.40.4.1024

Sun, H., Zhang, C., Xiang, L., Pi, R., Guo, Z., Zheng, C., et al. (2016). Characterization of mutations in streptomycin-resistant *Mycobacterium tuberculosis* isolates in Sichuan, China and the association between Beijing-lineage and dual-mutation in *gidB*. *Tuberculosis (Edinb)* 96, 102–106. doi: 10.1016/j.tube.2015.09.004

Timmins, G. S., and Deretic, V. (2006). Mechanisms of action of isoniazid. *Mol. Microbiol.* 62, 1220–1227. doi: 10.1111/j.1365-2958.2006.05467.x

Torres, J. N., Paul, L. V., Rodwell, T. C., Victor, T. C., Amallraja, A. M., Elghraoui, A., et al. (2015). Novel *katG* mutations causing isoniazid resistance in clinical *M. tuberculosis* isolates. *Emerg. Microbes Infect.* 4:e42. doi: 10.1038/emi.2015.42

Treatment Action Group and Stop Tb Partnership, (2018). *Tuberculosis Research Funding Trends 2005–2017*. New York, NY: Treatment Action Group.

Tulyaprawat, O., Chaiprasert, A., Chongtrakool, P., Suwannakarn, K., and Ngamskulrungroj, P. (2019). Association of *ubiA* mutations and high-level of

ethambutol resistance among *Mycobacterium tuberculosis* Thai clinical isolates. *Tuberculosis (Edinb)* 114, 42–46. doi: 10.1016/j.tube.2018.11.006

Unissa, A. N., Subbian, S., Hanna, L. E., and Selvakumar, N. (2016). Overview on mechanisms of isoniazid action and resistance in *Mycobacterium tuberculosis*. *Infect. Genet. Evol.* 45, 474–492. doi: 10.1016/j.meegid.2016.09.004

United Nations General Assembly (2018). *Resolution 73/3: Political Declaration of the High-Level Meeting of the General Assembly on the Fight Against Tuberculosis*. New York, NY: United Nations General Assembly.

Van Deun, A., Aung, K. J., Bola, V., Lebeke, R., Hossain, M. A., de Rijk, W. B., et al. (2013). Rifampin drug resistance tests for tuberculosis: challenging the gold standard. *J. Clin. Microbiol.* 51, 2633–2640. doi: 10.1128/JCM.00553-13

van Embden, J. D., Cave, M. D., Crawford, J. T., Dale, J. W., Eisenach, K. D., Gicquel, B., et al. (1993). Strain identification of *Mycobacterium tuberculosis* by DNA fingerprinting: recommendations for a standardized methodology. *J. Clin. Microbiol.* 31, 406–409. doi: 10.1128/jcm.31.2.406-409.1993

Verma, J. S., Gupta, Y., Nair, D., Manzoor, N., Rautela, R. S., Rai, A., et al. (2014). Evaluation of *gidB* alterations responsible for streptomycin resistance in *Mycobacterium tuberculosis*. *J. Antimicrob. Chemother.* 69, 2935–2941. doi: 10.1093/jac/dku273

Via, L. E., Cho, S. N., Hwang, S., Bang, H., Park, S. K., Kang, H. S., et al. (2010). Polymorphisms associated with resistance and cross-resistance to aminoglycosides and capreomycin in *Mycobacterium tuberculosis* isolates from South Korean Patients with drug-resistant tuberculosis. *J. Clin. Microbiol.* 48, 402–411. doi: 10.1128/JCM.01476-09

Walker, T. M., Kohl, T. A., Omar, S. V., Hedge, J., Del Ojo, Elias, C., et al. (2015). Whole-genome sequencing for prediction of *Mycobacterium tuberculosis* drug susceptibility and resistance: a retrospective cohort study. *Lancet Infect. Dis.* 15, 1193–1202. doi: 10.1016/S1473-3099(15)00062-6

Wan, L., Guo, Q., Wei, J.-H., Liu, H.-C., Li, M.-C., Jiang, Y., et al. (2020). Accuracy of a reverse dot blot hybridization assay for simultaneous detection of the resistance of four anti-tuberculosis drugs in *Mycobacterium tuberculosis* isolated from China. *Infect. Dis. Poverty* 9:38. doi: 10.1186/s40249-020-00652-z

World Health Organization (2008). *Policy Guidance on Drug-Susceptibility Testing (DST) of Second-line Antituberculosis Drugs (WHO/HTM/TB/2008.392)*. Geneva: World Health Organization.

World health organization (2014). *High-Priority Target Product Profiles for New Tuberculosis Diagnostics: Report of a Consensus Meeting*. Geneva: World Health Organization.

World Health Organization (2016). *The Use of Molecular Line Probe Assays for the Detection of Resistance to Isoniazid and Rifampicin, Policy Update*. Geneva: World Health Organization.

World Health Organization (2019). *Global Tuberculosis Report 2019*. Geneva: World Health Organization.

Xu, Y., Jia, H., Huang, H., Sun, Z., and Zhang, Z. (2015). Mutations found in *embCAB*, *embR*, and *ubiA* genes of ethambutol-sensitive and -resistant *Mycobacterium tuberculosis* clinical isolates from China. *Biomed. Res. Int.* 2015:951706. doi: 10.1155/2015/951706

Zhang, H., Li, D., Zhao, L., Fleming, J., Lin, N., Wang, T., et al. (2013). Genome sequencing of 161 *Mycobacterium tuberculosis* isolates from China identifies genes and intergenic regions associated with drug resistance. *Nat. Genet.* 45, 1255–1260. doi: 10.1038/ng.2735

Zhang, N., Zhao, X. Q., and Wan, K. L. (2009). Preliminary study on the appropriate concentrations of drug used in the drug-susceptibility test to detect the Ethambutol-resistant isolates of *Mycobacterium tuberculosis*. *Chin. J. Zoonoses* 25, 1049–1053. doi: 10.3969/j.issn.1002-2694.2009.11.005

Zhang, Z., Liu, M., Wang, Y., Pang, Y., Kam, K. M., and Zhao, Y. (2014). Molecular and phenotypic characterization of multidrug-resistant *Mycobacterium tuberculosis* isolates resistant to kanamycin, amikacin, and capreomycin in China. *Eur. J. Clin. Microbiol. Infect. Dis.* 33, 1959–1966. doi: 10.1007/s10096-014-2144-5

Zhao, L. L., Chen, Y., Chen, Z. N., Liu, H. C., Hu, P. L., Sun, Q., et al. (2014a). Prevalence and molecular characteristics of drug-resistant *Mycobacterium tuberculosis* in Hunan, China. *Antimicrob. Agents Chemother.* 58, 3475–3480. doi: 10.1128/AAC.02426-14

Zhao, L. L., Chen, Y., Liu, H. C., Xia, Q., Wu, X. C., Sun, Q., et al. (2014b). Molecular characterization of multidrug-resistant *Mycobacterium tuberculosis* isolates from China. *Antimicrob. Agents Chemother.* 58, 1997–2005. doi: 10.1128/AAC.01792-13

Zhao, L. L., Sun, Q., Liu, H. C., Wu, X. C., Xiao, T. Y., Zhao, X. Q., et al. (2015a). Analysis of *embCAB* mutations associated with ethambutol resistance in multidrug-resistant *Mycobacterium tuberculosis* isolates from China. *Antimicrob. Agents Chemother.* 59, 2045–2050. doi: 10.1128/AAC.04933-14

Zhao, Y., Li, G., Sun, C., Li, C., Wang, X., Liu, H., et al. (2015b). Locked nucleic acid probe-based real-time PCR assay for the rapid detection of rifampin-resistant *Mycobacterium tuberculosis*. *PLoS One* 10:e0143444. doi: 10.1371/journal.pone.0143444

Conflict of Interest: The authors declare that the research was conducted in the absence of any commercial or financial relationships that could be construed as a potential conflict of interest.

frontiers in Public Health

ORIGINAL RESEARCH
published: 27 August 2020
doi: 10.3389/fpubh.2020.00455

Extensive Homoplasy but No Evidence of Convergent Evolution of Repeat Numbers at MIRU Loci in Modern *Mycobacterium tuberculosis* Lineages

Alexander C. Outhred[1,2,3], Ulziijargal Gurjav[4], Peter Jelfs[3,5], Nadine McCallum[6], Qinning Wang[3], Grant A. Hill-Cawthorne[1,7], Ben J. Marais[1,2] and Vitali Sintchenko[1,3,5]*

[1] Marie Bashir Institute for Infectious Diseases and Biosecurity, The University of Sydney, Sydney, NSW, Australia, [2] Children's Hospital at Westmead, Sydney, NSW, Australia, [3] Center for Infectious Diseases and Microbiology—Public Health, Westmead Hospital, Sydney, NSW, Australia, [4] Department of Microbiology and Immunology, Mongolian National University of Medical Sciences, Ulaanbaatar, Mongolia, [5] NSW Mycobacterium Reference Laboratory, Center for Infectious Diseases and Microbiology Laboratory Services, Institute of Clinical Pathology and Medical Research—NSW Health Pathology, Sydney, NSW, Australia, [6] Deep Seq Lab, Queen's Medical Center, University of Nottingham, Nottingham, United Kingdom, [7] School of Public Health, University of Sydney, Sydney, NSW, Australia

OPEN ACCESS

Edited by:
Onya Opota,
University of Lausanne, Switzerland

Reviewed by:
Diana Machado,
New University of Lisbon, Portugal
Liliana Kokusanilwa Rutaihwa,
Swiss Tropical and Public Health Institute (Swiss TPH), Switzerland

***Correspondence:**
Alexander C. Outhred
alexander.outhred@health.nsw.gov.au

Specialty section:
This article was submitted to Infectious Diseases - Surveillance, Prevention and Treatment, a section of the journal Frontiers in Public Health

Received: 13 October 2019
Accepted: 22 July 2020
Published: 27 August 2020

Citation:
Outhred AC, Gurjav U, Jelfs P, McCallum N, Wang Q, Hill-Cawthorne GA, Marais BJ and Sintchenko V (2020) Extensive Homoplasy but No Evidence of Convergent Evolution of Repeat Numbers at MIRU Loci in Modern Mycobacterium tuberculosis Lineages. Front. Public Health 8:455. doi: 10.3389/fpubh.2020.00455

More human deaths have been attributable to *Mycobacterium tuberculosis* than any other pathogen, and the epidemic is sustained by ongoing transmission. Various typing schemes have been developed to identify strain-specific differences and track transmission dynamics in affected communities, with recent introduction of whole genome sequencing providing the most accurate assessment. Mycobacterial interspersed repetitive unit (MIRU) typing is a family of variable number tandem repeat schemes that have been widely used to study the molecular epidemiology of *M. tuberculosis*. MIRU typing was used in most well-resourced settings to perform routine molecular epidemiology. Instances of MIRU homoplasy have been observed in comparison with sequence-based phylogenies, limiting its discriminatory value. A fundamental question is whether the observed homoplasy arises purely through stochastic processes, or whether there is evidence of natural selection. We compared repeat numbers at 24 MIRU loci with a whole genome sequence-based phylogeny of 245 isolates representing three modern *M. tuberculosis* lineages. This analysis demonstrated extensive homoplasy of repeat numbers, but did not detect any evidence of natural selection of repeat numbers, at least since the ancestral branching of the three modern lineages of *M. tuberculosis*. In addition, we observed good sensitivity but poor specificity and positive predictive values of MIRU-24 to detect clusters of recent transmission, as defined by whole-genome single nucleotide polymorphism analysis. These findings provide mechanistic insight, and support a transition away from VNTR-based typing toward sequence-based typing schemes for both research and public health purposes.

Keywords: *Mycobacterium tuberculosis*, homoplasy, convergent evolution, MIRU, VNTR, phylogeny, sensitivity, specificity

INTRODUCTION

Mycobacterial Interspersed Repetitive Unit (MIRU) typing (1–3) has been widely used to identify epidemiological clusters and potential laboratory contamination incidents involving *Mycobacterium tuberculosis* complex. MIRU is based on measuring the length of variable number tandem repeat (VNTR) loci in the *M. tuberculosis* genome, which is conceptually the same as subtyping of other bacterial genera by multiple locus VNTR analysis (MLVA). Different sets of loci can be used for analysis, and common variants include 12-locus MIRU (i.e., MIRU-12), 15- and 24-locus MIRU (MIRU-24). The increased discrimination provided by a greater number of informative loci needs to be balanced against the cost and complexity of the test. MIRU-24 is widely regarded as a well-standardized strain typing method that provides adequate discrimination for the majority of *M. tuberculosis* strains.

Australia has a low incidence of tuberculosis (5–6/100,000 population), that can be sub-classified into pre-elimination rates among people of non-Indigenous origin born in Australia (∼1/100,000 population), with higher rates (∼20/100,000 population) in individuals born overseas (4). A strong majority (>80%) of tuberculosis cases are overseas-born, implying a very low rate of *M. tuberculosis* transmission within Australia. By comparison, incidence rates of tuberculosis in England are somewhat higher but broadly similar [in overseas-born individuals, ∼40/100,000, and in local-born individuals, ∼3/100,000 (5)]. To help investigate potential local transmission, the largest MIRU-24 clusters identified in the state of New South Wales (NSW) over a 5-year period (2009–2013) were subjected to whole-genome sequencing (6). These MIRU-24 clusters were the two largest Lineage 1 ("Indo-Oceanic" or EAI) and two largest Lineage 2 (East Asian or "Beijing") clusters. Excluding three isolates related to laboratory cross-contamination, whole-genome sequencing reduced the estimated number of secondary cases from 23 isolates in four transmission chains to one isolate in one chain. These results, along with other recent reports (7–9), reveal important limitations in the value of MIRU-24 to identify likely transmission events and guide public health responses in low-transmission settings where the vast majority of *M. tuberculosis* strains are imported. Although MIRU-24 has been widely used in research and public health contexts to help understand *M. tuberculosis* transmission dynamics and to characterize relapse vs. reinfection events, it is limited by false-positive and false-negative clustering. Relaxing the cluster definition to include isolates with differences at one or two MIRU loci has been widely used to reduce false-negative clustering, but worsens false-positive clustering. Mathematical modeling suggests that homoplasy of repeat loci can partially explain false-positive MIRU clustering (10).

Homoplasy occurs when an identical characteristic arises in unrelated clades; in other words, a trait is shared for reasons other than descent from a common ancestor. Homoplasy can arise as a result of horizontal gene transfer, but this is rare in *M. tuberculosis*. More typically, homoplasy arises through stochastic processes, and can also be amplified by natural selection (convergent evolution, where certain traits have higher fitness). In *M. tuberculosis,* selection of mutations conferring drug resistance provides clear evidence of homoplasy through convergent evolution; for example, the p.Ser315Thr mutation in the *katG* gene has evolved numerous times in unrelated clades under isoniazid-induced selective pressure (11, 12). The Retention Index gives a value between 0 and 1 representing the homoplasy of a trait with reference to a phylogenetic tree; this index is the complement of the fraction of possible homoplasy that is present in the tree, so that a value of zero indicates maximal homoplasy, and a value of one indicates absence of homoplasy (13).

The discriminatory power of strain typing methods is best understood by considering mathematical indices of diversity, such as the Simpson index (14, 15). *M. tuberculosis* isolates derived from settings with low rates of *M. tuberculosis* transmission where unlinked cases of tuberculosis dominate, such as Australia and the United Kingdom, capture diverse *M. tuberculosis* sub-lineages. A diverse phylogeny provides an opportunity to assess the potential for MIRU to capture the underlying diversity, to measure the reduction in observed diversity resulting from MIRU homoplasy, and to detect evolutionary signals contributing toward MIRU homoplasy.

MIRU homoplasy has been observed numerous times previously (16–18) and simulated with a detailed model (17). The first thorough sequence-based assessment graphically depicted homoplasy in a multi-locus sequence analysis phylogeny of 97 Lineage 1–6 strains, and compared the maximum likelihoods of sequence-based and VNTR-based trees (16). In another instance comparing sequence- and VNTR-based phylogenies, a VNTR-based minimum spanning tree was accepted as the reference phylogeny and homoplasy of a SNP and an *IS6110* insertion site was described (19). In some reports it has been stated that the observed homoplasy is the result of convergent evolution (16, 18), however there has been no previous quantification of homoplasy across repeat loci in reference to a whole genome phylogeny, and no formal testing for a phylogenetic signal of convergent evolution as a driver of MIRU homoplasy.

The aim of this study was to quantify the extent and impact of MIRU locus homoplasy in modern phylogenetic lineages of *M. tuberculosis* on the potential public health utility of MIRU typing, and to test whether homoplasy can be attributed to convergent evolution. To test for a phylogenetic signal, we treated the number of repeats at MIRU loci as a trait or characteristic undergoing evolution along branches of the phylogenetic tree, regarding number of repeats at a MIRU locus as an ordinal trait. Ordinal traits are commonly treated as "pseudo-continuous" traits (20, 21); treating repeat number as a pseudo-continuous trait enables the use of Brownian motion and Ornstein–Uhlenbeck models of evolution along branches (22, 23). Brownian motion is the standard model of continuous trait evolution along branches by purely stochastic processes in the absence of natural selection. Ornstein-Uhlenbeck models add a parameter to the Brownian motion model that enables estimation of selective pressure in a manner that is biologically plausible, and can enable the detection of changes in selective pressure in different clades of a tree (24, 25). Most alternate measures to detect phylogenetic signal, such as Pagel's λ, have

more difficult interpretation as there is no underlying biological basis (e.g., [*http://www.carlboettiger.info/2013/10/11/is-it-time-to-retire-pagels-lambda.html*], accessed 16-Nov-2018).

MATERIALS AND METHODS

Selection of Isolates

M. tuberculosis strains from patients diagnosed between 2009 and 2013 and characterized by the NSW Mycobacterium Reference Laboratory (MRL) underwent MIRU-24 typing as described previously (6, 26, 27); a subset of 30 isolates was sequenced using the Ion Torrent platform and the Ion 318 kit (Thermo Fisher). A literature search was performed for publications reporting *M. tuberculosis* isolates with publicly available whole-genome sequencing data and MIRU-24 data; two papers were identified (28, 29). Merker et al. (29) generated a worldwide phylogenetic analysis of Beijing strains (Lineage 2). Walker et al. (28) analyzed UK strains, including MIRU-matched community clusters of *M. tuberculosis*. We combined these publicly available datasets with findings from the two largest MIRU-24 Beijing strain clusters identified at the NSW MRL from 2009 to 2013 (6).

Figure 1 shows the selection process for community *M. tuberculosis* isolates eligible for inclusion. Isolates without corresponding WGS data and complete MIRU-24 were excluded. Isolates that were not members of Lineage 2, 3, or 4 were excluded, as the number with complete sequence and MIRU-24 data was too small for reliable analysis. Isolates with strong *a priori* basis to assume identity were excluded (e.g., suspected laboratory cross-contamination, or isolates with same MIRU-24 from the same patient; however neither community nor household MIRU-24 clusters were excluded). The 17 NSW MRL isolates that met all criteria for inclusion comprised one 8-member and one 9-member MIRU-24 cluster. The final set of isolates and their origin is shown in **Supplementary Table S1**.

MIRU Typing of Isolates

Linked MIRU-24 and whole-genome sequencing data for isolates in these three datasets enabled a comparison of MIRU-24 evolution with the whole-genome sequencing phylogeny of a global strain collection. The order of MIRU loci adopted for the concatenated MIRU-24 string was 154, 580, 960, 1644, 2059, 2531, 2687, 2996, 3007, 3192, 4348, 802, 424, 577, 1955, 2163b, 2165, 2347, 2401, 2461, 3171, 3690, 4052, and 4156.

Sequencing Data Analysis

FASTQ files corresponding to 110 eligible isolates from the Merker (29) collection were downloaded from the European Nucleotide Archive (ENA), together with MIRU-24 data in the supporting information. FASTQ files corresponding to 132 eligible isolates from the Walker (28) collection were downloaded from ENA, together with MIRU-24 data in the supporting information. Together with 18 isolates from NSW, FASTQ files from 260 isolates were trimmed of library and sequencing adaptors using *trimadap* [https://github.com/lh3/trimadap]. FASTQ files from the Ion Torrent platform, used to sequence clustered Lineage 2 strains identified in NSW, underwent quality-score-preserving error correction using *muffinec* (30). FASTQ files from Illumina platforms underwent error correction using *bfc* (31). A reference sequence for mapping was derived from NC_000962.3 by substituting gaps for repetitive elements (all elements annotated as PE/PPE/PGRS and *cysA* genes, insertion sequences, transposases and prophage components, replacing 6.3% of the H37Rv genome with gaps). Mapping of error-corrected reads against this reference sequence was performed using the *mem* algorithm of *bwa* (32). Duplicates were marked using *samblaster* (33). Libraries with mean genome coverage below 20 were excluded. Variants were called from a merged BAM file using *freebayes* (34), specifying a haploid genome and requiring 90% of reads to support each called variant. The resulting VCF file was filtered for variants that were high confidence [QUAL $>$ 200 and ODDS $>$ 19, where ODDS represents the marginal likelihood ratio of the called variant (34)], informative (each variant called for at least 1 sample but not for all samples), and categorized as a SNP (CIGAR $=$ 1X). Variants were annotated using *snpEff* (35). SNPs within 150 nucleotides of the genes *gyrA*, *katG*, *pncA*, *rpoB*, *inhA*, *fabG1*, *ahpC*, *embA*, *embB*, *gid*, *eis*, *ndh*, *rpsA*, *rpsL*, *rrs*, and *tlyA* were considered potentially homoplasious (potentially selected through drug exposure) and were excluded from further analysis. The remaining SNP variants for each sample were patched into the reference genome using *vcf2fasta* [https://github.com/vcflib/vcflib].

A Bayesian inference phylogeny was generated from the concatenated alignment of 245 whole genomes using *mrbayes* (36), with the "mixed" model of nucleotide substitutions and a gamma distribution of substitution rates (approximated in four categories). Tip dates were not used, as it was assumed that time since the most recent common ancestor (MRCA) was much greater than the difference between *M. tuberculosis* isolation dates in the current study.

Comparison of MIRU Data With Whole Genome Phylogeny

MIRU-24 and SNP-based phylogenies of *M. tuberculosis* were examined in order to explore potential homoplasy in MIRU loci, focusing on strains from Lineages 2, 3, and 4 of *M. tuberculosis*. The distance between genomes of *M. tuberculosis* was measured by patristic distance. Higher mean patristic distance (MPD) is associated with descent from more ancestral strains; in other words, for a leaf with high MPD the branches leading toward it are long with few near neighbors. Nearest taxon distance (NTD) is a property of leaves and refers to the total substitution distance between a leaf and its nearest neighbor. Calculation of these distances from the *mrbayes* tree was performed using *DendroPy* (37). Further statistical analysis of MIRU-24 parameters and the phylogenetic tree was performed using *R* modules *ape*, *bayou*, *phangorn*, *phylobase*, *phytools*, and *vegan* (25, 38–40). Phylogenetic trees were visualized using *R ggtree* (41).

A distance between isolates (NTD) of $<$10 substitutions was arbitrarily chosen as consistent with recent transmission; this is roughly equivalent to 14–32 years of bacterial evolution (or 7–16 years on each branch of a symmetrical pair) based on

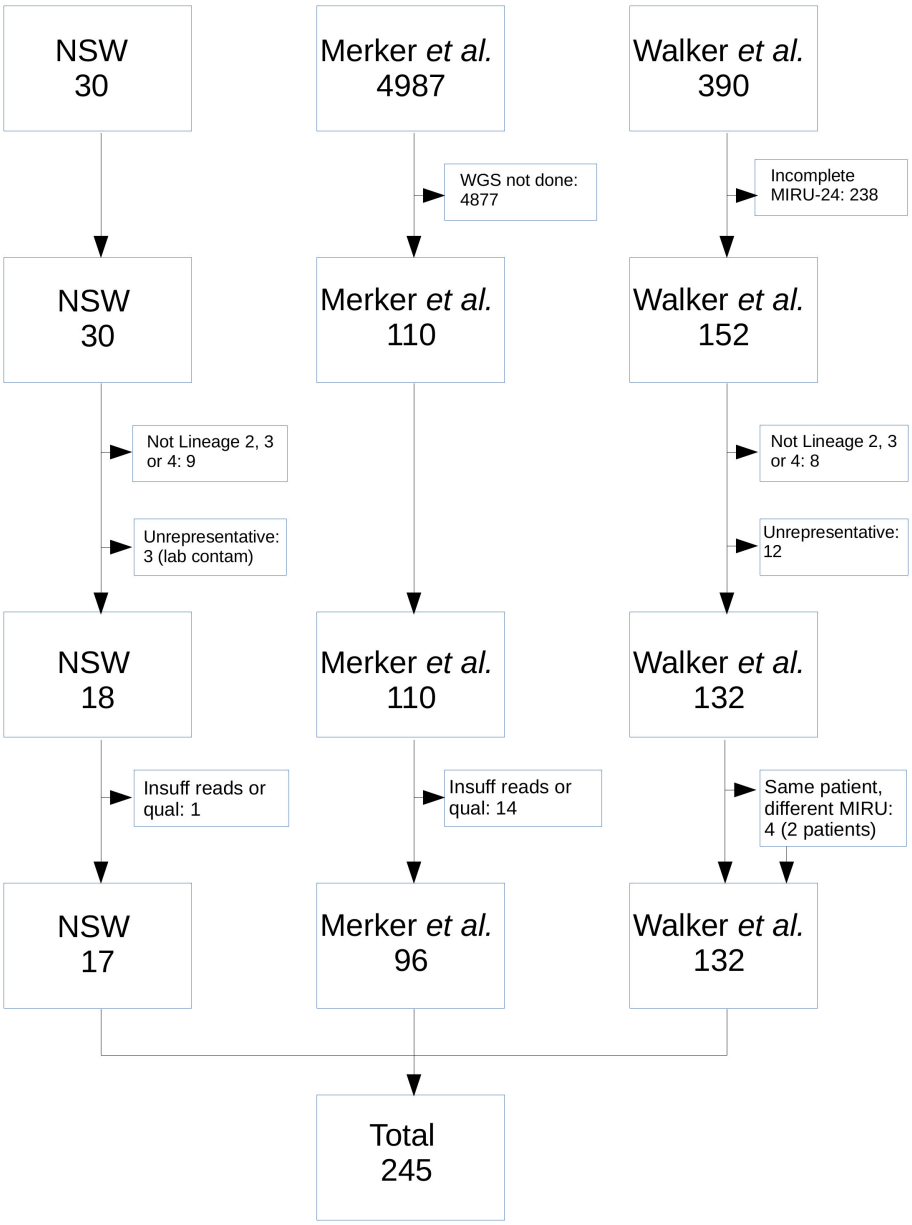

FIGURE 1 | Flow diagram of *M. tuberculosis* isolates from the NSW, Merker, and Walker collections included in the analysis. From NSW, nine isolates were excluded as they were not from Lineage 2, 3, or 4; 3 were excluded as they arose as a result of probable laboratory cross-contamination incidents in referring laboratories; 1 was excluded due to insufficient read number and quality. From the Merker collection, 4,877 were excluded because WGS was not performed; 14 were excluded due to insufficient number or quality of reads. From the Walker collection, 238 were excluded because MIRU-24 was not completely ascertained; 8 were excluded as they were not from Lineage 2, 3, or 4; 12 were excluded due to high *a priori* probability that isolates were identical (e.g., same patient and same MIRU-24). An additional four isolates from two patients in the Walker collection were retained in the analysis (i.e., same patient but different MIRU-24).

recent estimates of the *M. tuberculosis* molecular clock (28, 42–44), and hence does not necessarily indicate direct transmission between patients.

RESULTS

In total, we assessed the MIRU-24 profiles and SNP-based phylogeny of 245 isolates; 17 were derived from two MIRU-24 clusters identified in NSW Australia, 132 from the Walker collection of United Kingdom community MIRU-24 clusters, and 96 from a global collection of Lineage 2 strains, as shown in **Figure 1**. Fourteen of the 110 eligible isolates from the Merker collection were excluded from further analysis due to short read length (50 bp) or insufficient number of reads after *bfc* error correction. Four of 21 isolates from the NSW MRL were excluded from further analysis, one due to insufficient number of reads after *muffinec* error correction and three that represented likely laboratory cross-contamination. Of the 245 isolates, 118 (48%)

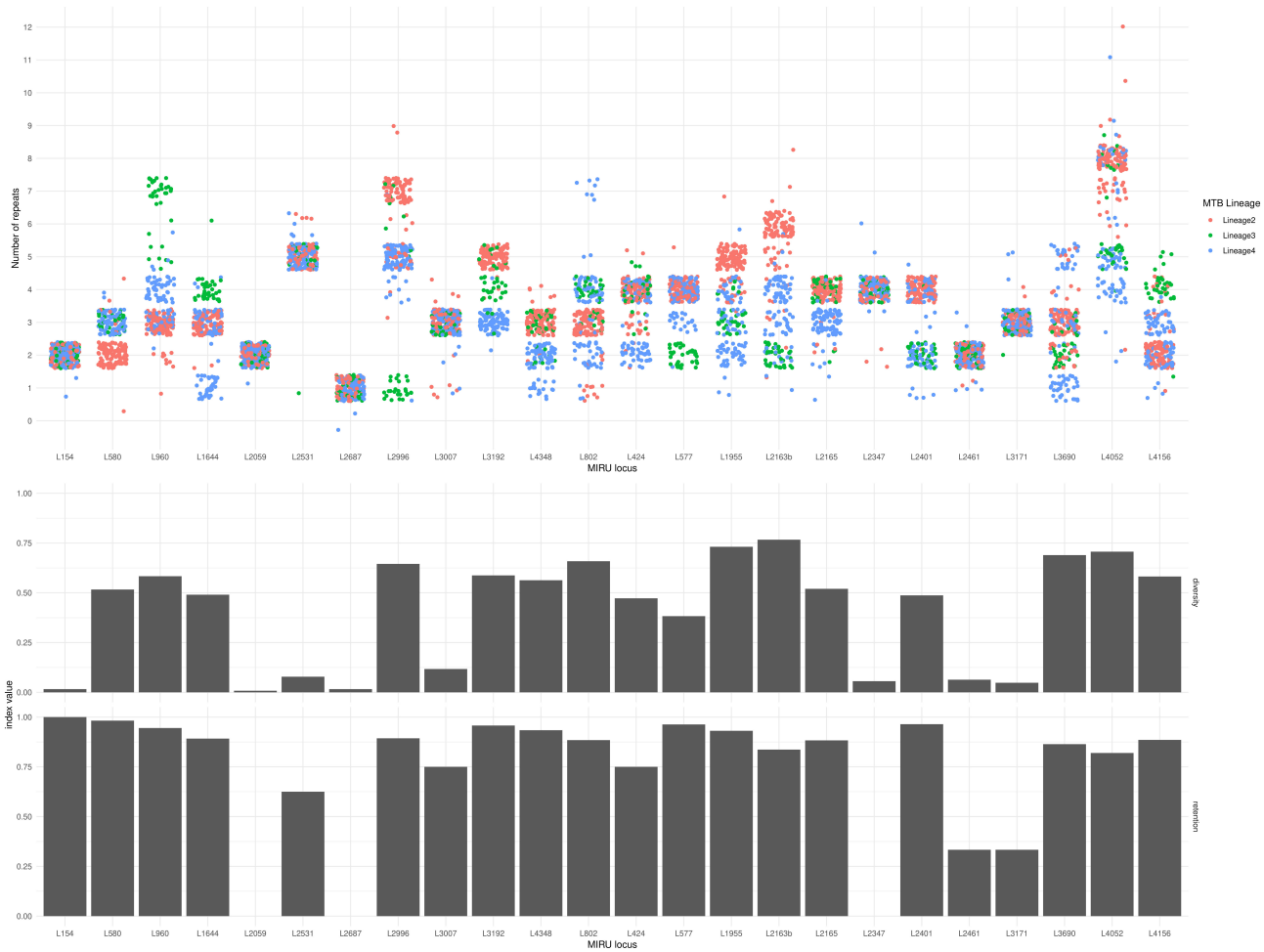

FIGURE 2 | MIRU locus, number of repeats, diversity index, and retention index for 245 Lineage 2, 3, and 4 *M. tuberculosis* isolates. In the top panel, each circle represents the number of repeats (*y*-axis) at each MIRU locus (*x*-axis) of one of the 245 isolates. Jitter has been applied in horizontal and vertical axes to reduce overlap. Circles are color-coded by Lineage. The middle panel shows the Simpson diversity index of each MIRU locus (0 represents complete absence of diversity, and 1 represents complete diversity). The bottom panel shows the retention index of each MIRU locus (0 represents complete homoplasy, and 1 represents complete absence of homoplasy). Note that loci 2347 and 2687 have retention indices of zero, and locus 2059 has an undefined retention index due to only a single instance of variation in this phylogeny.

were from Lineage 2, 35 (14%) from Lineage 3 and 92 (38%) from Lineage 4. From a total of 10,965 SNPs, 115 (1%) were excluded from analysis as potentially homoplasious (in genes where resistance-associated SNPs are believed to occur); 37 of these 115 SNPs were synonymous and 58 were present in more than one isolate. The median number of isolates possessing one of these 115 SNPs was two, suggesting that the impact of their exclusion on the phylogeny is minimal and that few of these 115 SNPs were truly homoplasious.

The Simpson diversity index for individual MIRU-24 loci ranged from 0.008 to 0.77 (median 0.50, with eight loci below 0.2). The Simpson index for the complete MIRU-24 was 0.96. In this dataset from lineages 2, 3, and 4, four loci could account for almost all of the total MIRU-24 diversity (Simpson index 0.94 using loci 1955, 2163b, 3690, and 4052). Other data transformations could preserve comparable diversity (e.g., Simpson index 0.92 for the sum total number of repeats across all 24 loci). **Figure 2** shows the distribution of repeat numbers by MIRU locus, and shows the corresponding Simpson diversity and retention indexes. The number of repeats was variable in 10 or fewer of the 245 strains at 7 MIRU loci. For MIRU loci with Simpson diversity >0.1, the retention index (using the whole genome phylogeny as reference) ranged from 0.75 (locus 424) to 0.98 (locus 580). The four MIRU loci with highest Simpson diversity (1955, 2163b [QUB-116], 3690 [VNTR-52], and 4052 [QUB-26]) had retention indices of 0.93, 0.84, 0.86, and 0.82. The lower retention indices of loci 2163b and 4052 indicate a higher degree of homoplasy. In this Lineage 2, 3, and 4 dataset, MIRU locus 2163b had the highest Simpson diversity but one

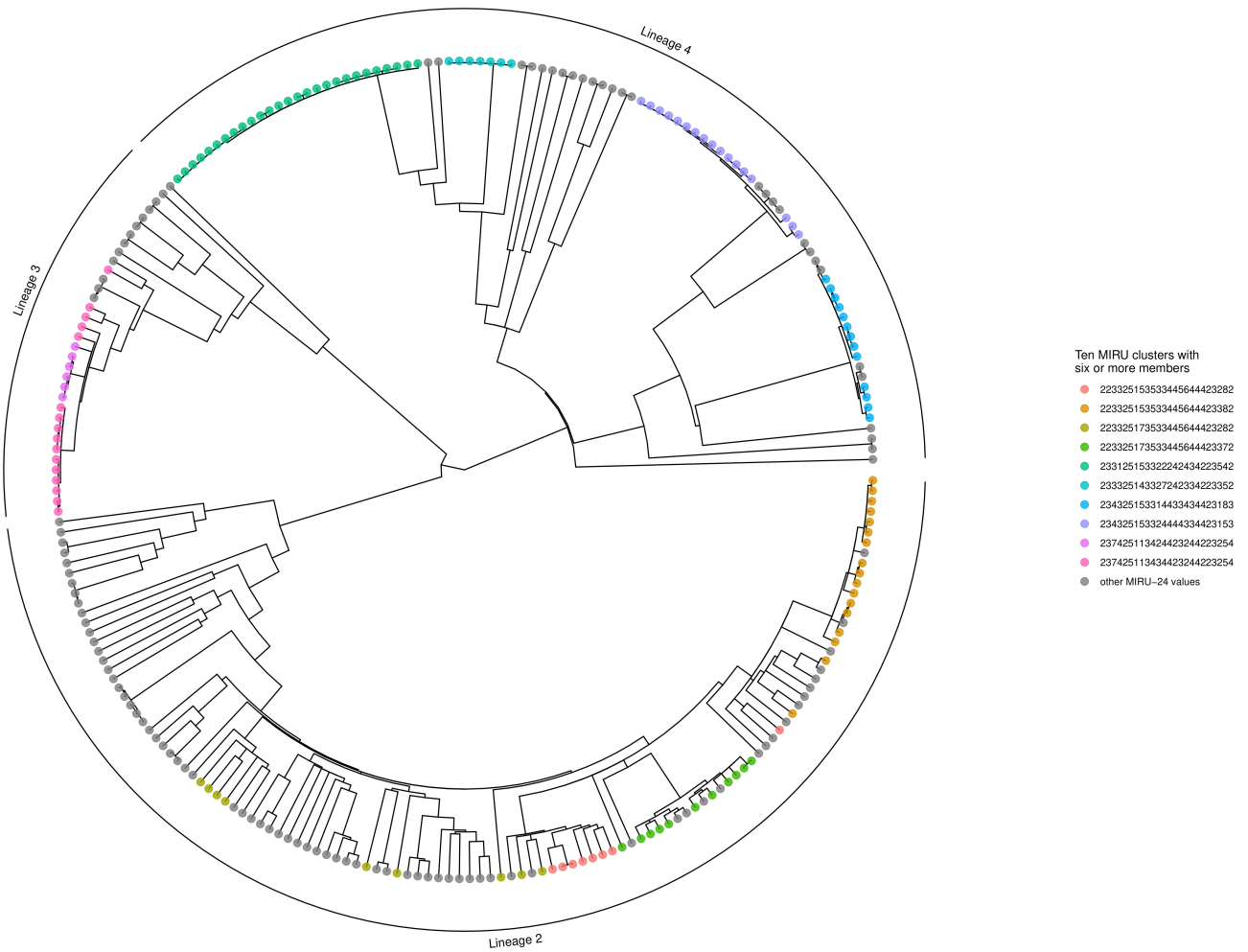

FIGURE 3 | Phylogenetic tree showing MIRU clusters with six or more members. The phylogenetic tree is ultrametric and was generated using Bayesian inference of whole genomes with substituted SNPs (n = 10,850) and a uniform clock (scale not shown; the height of the tree from root to tips is ~410 substitutions). Segments of the tree corresponding to Lineages 2, 3, and 4 are labeled with an outer arc. Isolates corresponding to the 10 largest MIRU-24 clusters are labeled with colored circles at the tips. Instances of repeat number homoplasy that affect the complete MIRU-24 are present in Lineage 2. The tree was generated using *R ggtree* (41).

of the lowest retention indices. Locus 1955 had high diversity and also a relatively high retention index, but other loci were less informative.

The Bayesian inference phylogeny, with tips color-coded according to membership of the 10 largest MIRU-24 clusters (containing six or more members), is shown as **Figure 3** (a corresponding figure with tips labeled by sample name is available as **Supplementary Image 1**). The MPD across all tips of the tree was 604 substitutions. The mean nearest taxon distance (MNTD) was 52 substitutions. Capturing diversity of a phylogenetic tree in a single index (comparable with Simpson diversity for MIRU) is difficult, but summary values derived from the tree for each tip—MPD, NTD, and median taxon distance—produced Simpson indices of 0.99, 0.99, and 0.97, respectively; these summary values encompass a higher diversity than MIRU-24.

MIRU-24 and SNP Clusters

One 8-member and one 9-member MIRU cluster among the 17 NSW isolates were identified using an identical MIRU-24 match as the cluster definition. From the Merker collection, one 17-member and one 11-member cluster were identified. In the Walker collection, there were one 27-member, one 17-member, one 16-member, one 13-member, one 7-member, and one 6-member clusters. The remaining 114 isolates were MIRU-24 singletons (68 isolates), pairs (22 isolates), or members of MIRU-24 clusters with three to five members (24 isolates). Extending a MIRU-24 cluster to include isolates with up to one mismatched locus produced a cluster with 50 strains; including up to two mismatched loci (28) produced a cluster with 77 strains. These relaxed cluster definitions were considered unhelpful and not analyzed further.

The distance tree revealed 138 isolates that were <10 substitutions from their nearest taxon, consistent with a recent

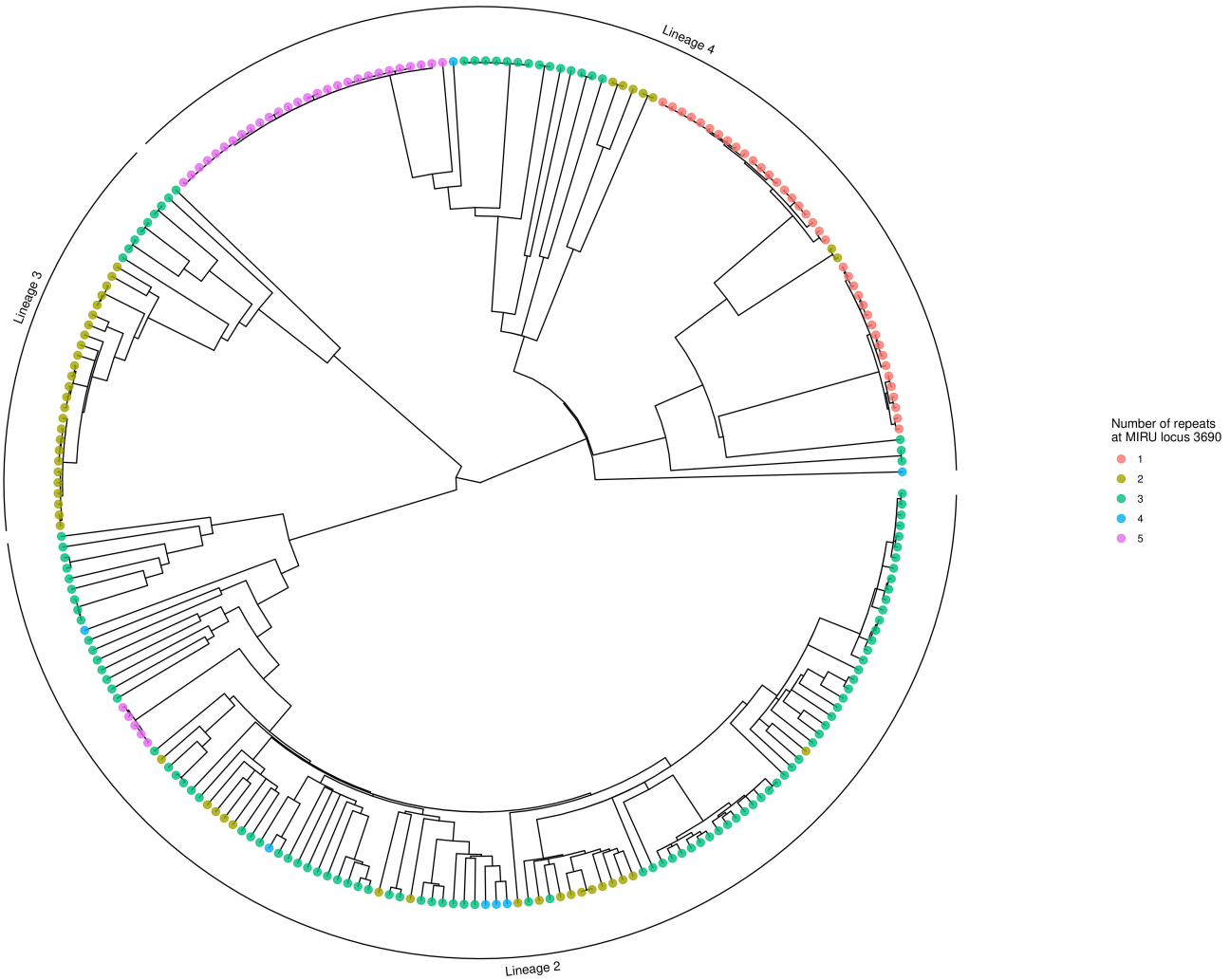

FIGURE 4 | Phylogenetic tree showing number of repeats at locus 3690. The tree is identical to that shown in **Figure 3**, except tips are colored to designate the number of repeats at locus 3690 for each isolate. Numerous instances of homoplasy are seen in Lineages 2 and 4. The tree was generated using *R ggtree* (41).

shared ancestor (shown in **Supplementary Image 2**). These were distributed in 30 SNP-clusters; 30 isolates in 9 SNP-clusters were from Lineage 2, 25 isolates in 6 SNP-clusters were from Lineage 3, and 83 isolates in 15 SNP-clusters were from Lineage 4. One of these SNP-clusters, the pair Mtb_4212 and Mtb_4878, was identified in NSW isolates; the two patients involved had no known direct contact, but had similar demographics and both had recently migrated to Australia from Nepal.

Out of 138 isolates that were members of a SNP-cluster, MIRU-24 profiles were identical within each SNP-cluster in all but seven instances (where only the first mismatched isolate of a second MIRU-24 cluster within a SNP-cluster was counted as an instance; see **Figure 3** and **Supplementary Table S2**). Across these seven instances, all differed at only a single MIRU locus (424, 2163b, 3171, 3192, or 4052), the median difference at that MIRU locus was two repeats, and the median number of substitutions separating isolates with different MIRU-24 profiles was 2, indicating recent common ancestry despite different MIRU-24 profiles.

The true positive rate or sensitivity of identical MIRU-24 for detection of recent transmission (defined as <10 SNPs) was 95% (131/138, 95% CI: 90–98%), with seven instances where SNP-clustered isolates were misclassified by MIRU-24 (see **Supplementary Table S2**). The true negative rate or specificity of MIRU-24 was 47% (50/107, 95% CI: 38–56%). In this selected group of isolates, the prevalence of recent transmission by SNP clustering was 56% (138/245), the positive predictive value of an identical MIRU-24 for detecting recent transmission was 72% (127/177, 95% CI: 65–78%), and the negative predictive value was 84% (57/68, 95% CI: 73–91%).

The Simpson diversity index for MIRU remained reassuringly high (0.96). However, by MIRU-24, 177 isolates were clustered, vs. 138 isolates by the permissive criterion of substitution distance <10. This represents a reduction in potential secondary

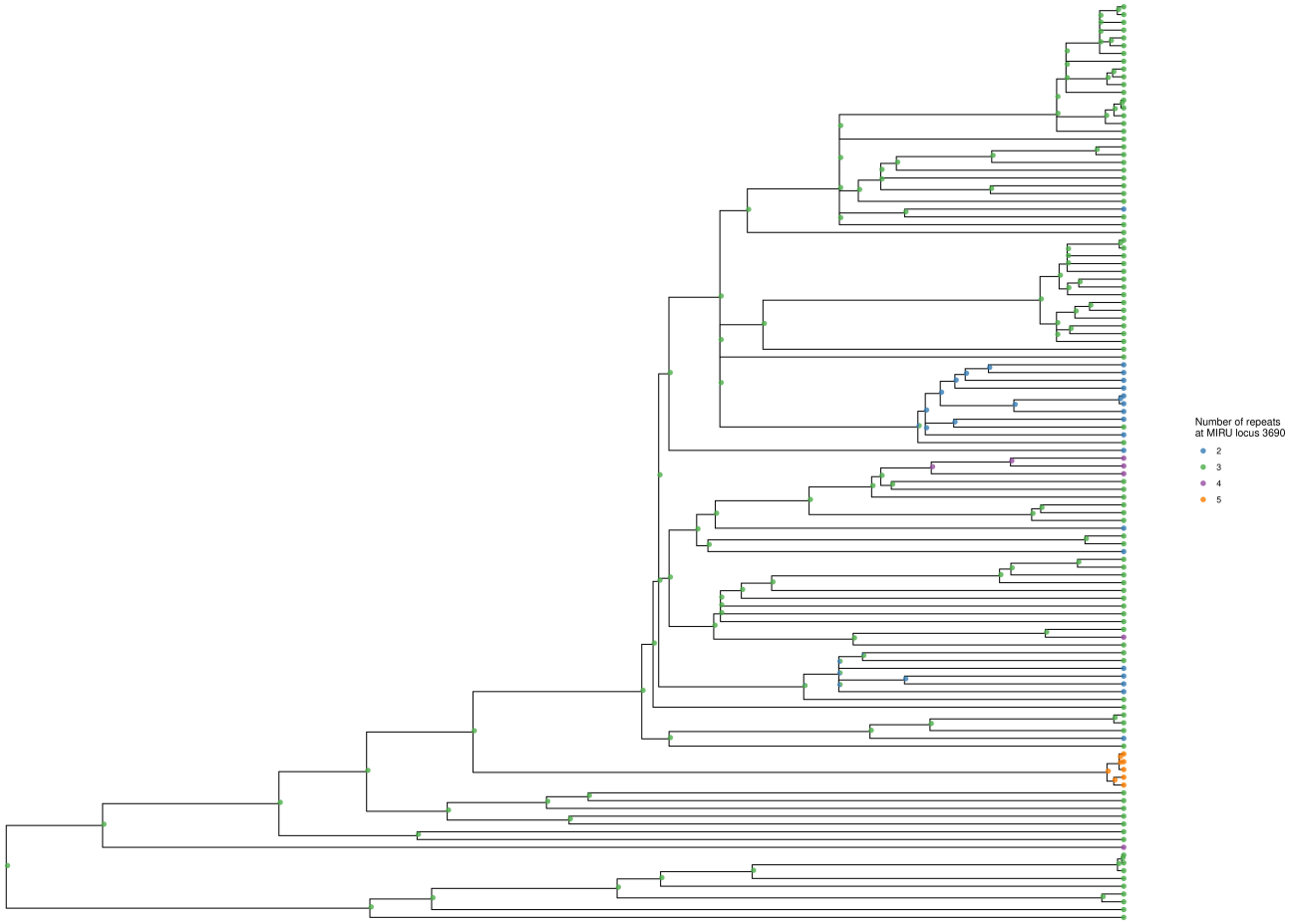

FIGURE 5 | Ancestral state reconstruction for locus 3690, shown for Lineage 2 subtree. The tree corresponds to the Lineage 2 subtree from **Figures 3**, **4**. Tips are colored to designate the number of repeats at locus 3690 for each isolate. Internal nodes show the ancestral state likelihoods, generated using the maximum likelihood method of *R phytools*::*rerootingMethod* (38), and displayed as a pie chart with the same color scheme as the tips. The tree was generated using *R ggtree* (41).

cases from 149 isolates in 28 clusters with MIRU, to 108 isolates in 30 clusters with SNP typing (of which 13 isolates in seven SNP clusters had the "wrong" MIRU-24). In other words, 32% (48/149) of potential secondary cases by MIRU-24 were "false positives," using a permissive standard for recent transmission.

MIRU Homoplasy

Using locus 3690 as a representative example, **Figure 4** shows the number of repeats for each isolate in comparison to the phylogeny. For this locus, there is extensive homoplasy affecting lineages 2 and 4. Locus 3690 is not exceptional; all 20 loci with a retention index other than one demonstrate homoplasy. Treating the number of repeats at each MIRU locus as a discrete trait or characteristic, the *R* package *phytools* (38) was used to model the ancestral states (i.e., number of repeats) for MIRU loci using a maximum likelihood algorithm. Focusing on Lineage 2 for clarity, the most likely number of repeats at internal nodes of the tree for representative MIRU locus 3690 are displayed in **Figure 5**. This demonstrates at least nine instances of repeat number homoplasy at locus 3690 arising in the phylogeny of these 118 Lineage 2 isolates.

Treating the number of repeats at a MIRU locus as a continuous trait or characteristic (20, 21), the *R* package *bayou* was used to model the evolution of repeat number using a Bayesian reversible-jump MCMC model with stepping stone importance sampling to estimate marginal likelihood. This was used to compare the Brownian motion and Ornstein–Uhlenbeck models of trait evolution. MIRU-24 loci with Simpson diversity index >0.2 were individually analyzed. The simpler Brownian motion model was favored for all 16 of these loci; in other words, there was no evidence that number of repeats at any of these loci was subject to selective pressure over the branches of this phylogeny.

One possible selective pressure acting on repeat loci is genome reduction due to gene loss, as observed for *M. tuberculosis* and *M. leprae* compared to ancestral and environmental mycobacteria. In an attempt to capture small selective forces that might operate on multiple loci to favor more or fewer repeats across the chromosome, modeling of total repeats over all 24 loci as a

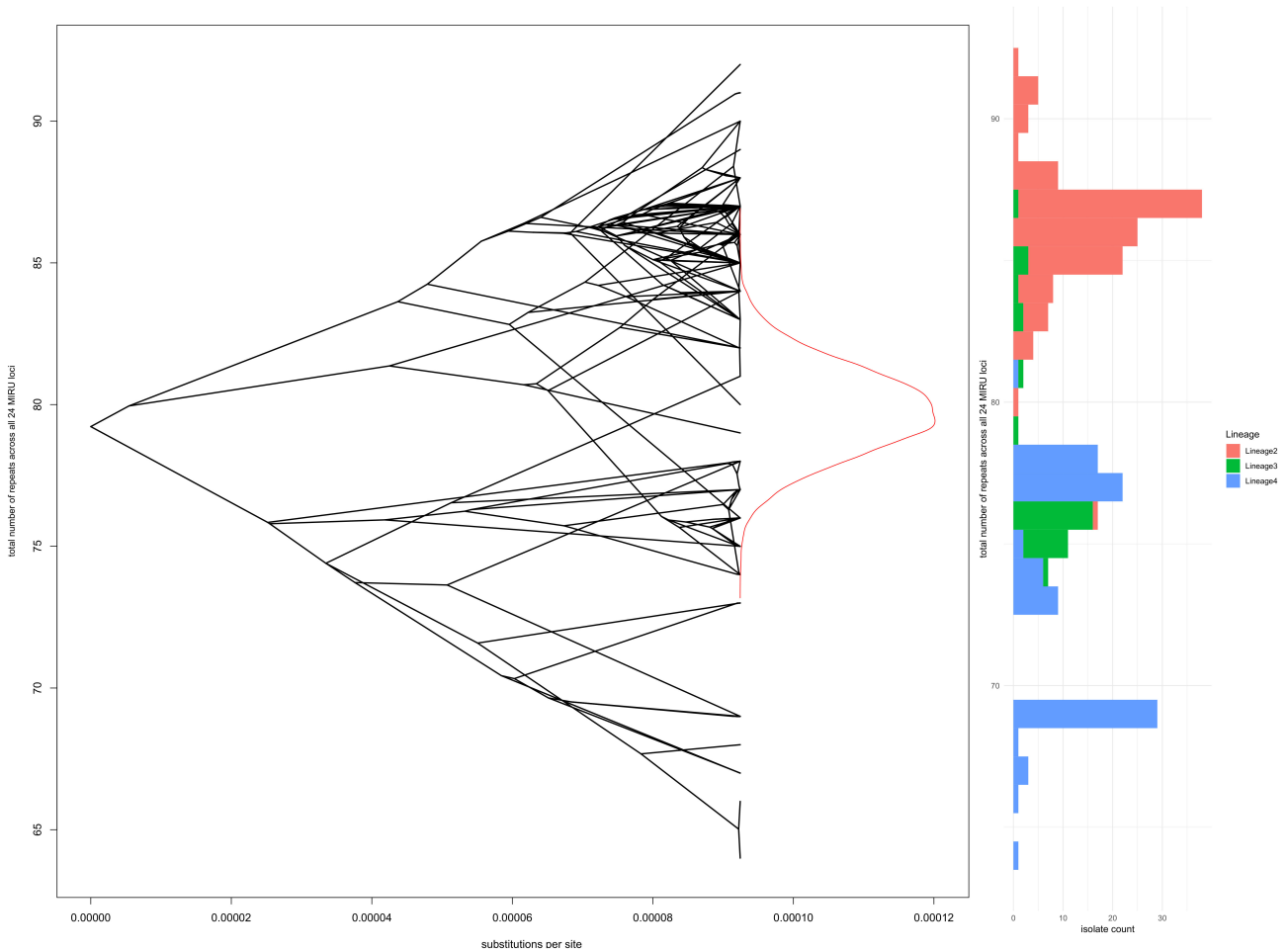

FIGURE 6 | Total number of repeats for all 24 loci in comparison to whole genome phylogeny and Lineage. The left panel shows a "phenogram," overlaying the same phylogenetic tree shown in **Figures 3**, **4** onto "trait space," where the *y*-axis represents total number of repeats. Ancestral states were modeled using *R bayou* (25), with a Brownian motion model of evolution. The Brownian motion model was favored by stepping stone marginal likelihood over the corresponding Ornstein-Uhlenbeck model. The central part of the left panel shows the MCMC sampling probability density of total number of repeats at the root node (the MRCA for Lineages 2, 3, and 4). The right panel is a histogram of total number of repeats, shaded by Lineage.

continuous trait was performed using *bayou*; again there was no evidence to reject the simplest Brownian motion model of stochastic changes in repeat number, without selective pressure. **Figure 6** shows the whole genome phylogeny overlaid on the total number of repeats at each node (reconstructed using *bayou* for internal nodes), a density plot of reconstructed total number of repeats at the root node, and a histogram of total repeats by lineage for the 245 isolates at the tips.

DISCUSSION

This analysis of *M. tuberculosis* isolates of modern lineages using genome-wide phylogeny shows evidence of extensive homoplasy of repeat number at MIRU loci. Comparison of repeat loci with genomic deletions has demonstrated fewer repeats per locus in lineages that separated later from the common ancestor of modern *M. tuberculosis* (e.g., Lineages 2-4), whilst more ancient lineages (e.g., Lineage 1) have a higher average number of repeats per locus (45). This trend was not apparent in our data; in addition we found no evidence for selective pressure operating on number of repeats at individual loci or total number of repeats across 24 loci. Stochastic variation in repeat number, without subsequent natural selection, appears to have been the dominant process since the emergence of the modern *M. tuberculosis* lineages, although weaker selective pressures operating over longer time periods cannot be excluded with confidence. It is worth noting that strains from Lineage 2, the epitome of a successful modern clade of *M. tuberculosis*, had a higher total number of repeats than other modern lineages (**Figure 6**). Within Lineage 2, the lowest total number of repeats was found amongst the "ancient Beijing" strains.

Extending the definition of a MIRU-24 cluster to include isolates with up to one MIRU locus mismatch was not helpful for detection of recent transmission in this dataset. This was clearly demonstrated for Lineage 2 isolates, where allowing one

locus mismatch produced a "super-cluster" of 50 isolates, and two mismatched loci produced a cluster of 77 isolates that was completely uninformative regarding recent transmission. One potential advantage of allowing a mismatch is that it also dilutes random homoplasious changes in repeat numbers, maintaining cluster membership; this could be valuable if the objective of MIRU-24 was classification into major clades or lineages, rather than to detect recent transmission. However, a PCR-based SNP typing scheme would be cheaper and more accurate in these scenarios.

A limitation of this analysis is underlying bias in isolate selection. Selection bias would most strongly affect the prevalence of clustering and hence the positive and negative predictive value estimates for MIRU-24 to detect recent transmission, but could also influence the analysis of homoplasy. Within the NSW and Walker datasets isolates underwent MIRU-24 routinely; however they were chosen for sequencing based on MIRU-24 properties (MIRU-24 clusters with no mismatches for the NSW isolates; up to two mismatches for the Walker isolates). In contrast, the Merker data is intended to be globally representative of Lineage 2 strains. However, it derives primarily from a culture collection at a single major reference laboratory, and the high proportion of MDR strains within the collection is typical of culturing bias in resource-limited settings. Other datasets [e.g., (46)] captured a large number of *M. tuberculosis* isolates but did not provide corresponding MIRU-24 data. In settings with a low frequency of recent transmission, or where only a small proportion of infectious patients have isolates available for molecular epidemiology, true clustering rates and the positive predictive value of MIRU-24 clustering will be correspondingly lower.

Another limitation of this analysis is the handling of potential errors in ascertainment of repeat number at MIRU loci. MIRU-24 data employed in this study were generated by reference laboratories, and have been published previously, so are likely to match or exceed real-world quality of MIRU data. The reproducibility of MIRU-24 is good (87–100%) (47–49), but each error in repeat number has potential to generate spurious homoplasy. However, it is unlikely that the same error in repeat number would co-occur in closely related isolates (as observed in these data). Any errors in MIRU ascertainment that produce a false homoplasy signal would also represent an important limitation of MIRU. Mitigation of MIRU errors would require either routine repetition of MIRU typing or relaxation of the MIRU cluster definition, which in this dataset did not retain sufficient diversity.

Our data suggest that the number of repeats at specific MIRU loci evolve at random, without evidence of selective pressure. Homoplasy of repeat numbers reduces the utility of MIRU-24. In these data, MIRU-24 showed poor specificity and modest positive and negative predictive values for the detection of recent transmission, using a permissive SNP threshold. Unless supported by independent evidence (e.g., epidemiological links), clusters detected using MIRU-24 will often be polyphyletic and unhelpful for detecting recent transmission, especially in settings with incomplete sampling, limited local transmission, or high rates of imported disease. Inclusion of additional hypervariable repeat loci (50) could help to improve specificity, but has been superseded by WGS approaches. If WGS is not yet feasible due to resource constraints, consideration should be given to the use of a hybrid scheme, for example, a small number of hypervariable loci for diversity, supplemented with an independent typing method with rare homoplasy [e.g., SNP typing (51–53) as recommended previously (16)] that has been validated in locally prevalent *M. tuberculosis* clades.

In conclusion, we found frequent homoplasy of MIRU repeats in modern *M. tuberculosis* lineages, arising through stochastic processes without natural selection. This homoplasy contributed to relatively poor specificity and low positive predictive values for the detection of recent transmission. These findings strengthen the case for transition away from MIRU-based to WGS-based methods of typing, which display much higher discrimination and rarer homoplasy, and provide important drug resistance information.

DATA AVAILABILITY STATEMENT

The datasets generated for this study can be found in the European Nucleotide Archive, PRJEB11778, PRJEB7281, and PRJEB2221.

ETHICS STATEMENT

The studies involving human participants were reviewed and approved by Human Research Ethics Committee University of Sydney. Written informed consent for participation was not required for this study in accordance with the national legislation and the institutional requirements.

AUTHOR CONTRIBUTIONS

AO, BM, and VS developed the concepts for this analysis. UG collected data and initiated the analysis of NSW MRL MIRU-24 clusters. UG, PJ, NM, and QW performed laboratory procedures including MIRU-24 and whole genome sequencing for the NSW MRL isolates. GAH-C provided expertise regarding whole genome sequencing and bioinformatic analysis. AO performed bioinformatic and statistical analyses. AO and BM drafted the initial manuscript. BM and VS supervised the research. All authors participated in manuscript revision.

FUNDING

This research was supported using internal funds of CIDM-Public Health.

SUPPLEMENTARY MATERIAL

The Supplementary Material for this article can be found online at: https://www.frontiersin.org/articles/10.3389/fpubh.2020.00455/full#supplementary-material

REFERENCES

1. Frothingham R, Meeker-O'Connell WA. Genetic diversity in the *Mycobacterium tuberculosis* complex based on variable numbers of tandem DNA repeats. *Microbiology.* (1998) 144:1189–96. doi: 10.1099/00221287-144-5-1189
2. Supply P, Mazars E, Lesjean S, Vincent V, Gicquel B, Locht C. Variable human minisatellite-like regions in the *Mycobacterium tuberculosis* genome. *Mol Microbiol.* (2000) 36:762–71. doi: 10.1046/j.1365-2958.2000.01905.x
3. Supply P, Lesjean S, Savine E, Kremer K, Soolingen D van, Locht C. Automated high-throughput genotyping for study of global epidemiology of *Mycobacterium tuberculosis* based on mycobacterial interspersed repetitive units. *J Clin Microbiol.* (2001) 39:3563–71. doi: 10.1128/JCM.39.10.3563-3571.2001
4. Toms C, Stapledon R, Coulter C, Douglas P. Tuberculosis notifications in Australia, 2014. *Commun Dis Intell Q Rep.* (2017) 41:E247–E63.
5. Tuberculosis Unit, National Infection Service, Public Health England. *Tuberculosis in England: 2018 Report* (presenting data to end of 2017) (2018).
6. Gurjav U, Outhred AC, Jelfs P, McCallum N, Wang Q, Hill-Cawthorne GA, et al. Whole genome sequencing demonstrates limited transmission within identified *Mycobacterium tuberculosis* clusters in New South Wales, Australia. *PLoS One.* (2016) 11:e0163612. doi: 10.1371/journal.pone.0163612
7. Stucki D, Ballif M, Egger M, Furrer H, Altpeter E, Battegay M, et al. Standard genotyping overestimates transmission of *Mycobacterium tuberculosis* among immigrants in a low-incidence country. *J Clin Microbiol.* (2016) 54:1862–70. doi: 10.1128/JCM.00126-16
8. Wyllie DH, Davidson JA, Grace Smith E, Rathod P, Crook DW, Peto TEA, et al. A quantitative evaluation of MIRU-VNTR typing against whole-genome sequencing for identifying *Mycobacterium tuberculosis* transmission: a prospective observational cohort study. *EBioMedicine.* (2018) 34:122–30. doi: 10.1016/j.ebiom.2018.07.019
9. Jajou R, de Neeling A, van Hunen R, de Vries G, Schimmel H, Mulder A, et al. Epidemiological links between tuberculosis cases identified twice as efficiently by whole genome sequencing than conventional molecular typing: a population-based study. *PLoS One.* (2018) 13:e0195413. doi: 10.1371/journal.pone.0195413
10. Estoup A, Jarne P, Cornuet J-M. Homoplasy and mutation model at microsatellite loci and their consequences for population genetics analysis. *Mol Ecol.* (2002) 11:1591–604. doi: 10.1046/j.1365-294X.2002.01576.x
11. Manson AL, Cohen KA, Abeel T, Desjardins CA, Armstrong DT, Barry CE, et al. Genomic analysis of globally diverse *Mycobacterium tuberculosis* strains provides insights into the emergence and spread of multidrug resistance. *Nat Genet.* (2017) 49:395–402. doi: 10.1038/ng.3767
12. Coll F, Phelan J, Hill-Cawthorne GA, Nair MB, Mallard K, Ali S, et al. Genome-wide analysis of multi- and extensively drug-resistant *Mycobacterium tuberculosis*. *Nat Genet.* (2018) 50:307–16. doi: 10.1038/s41588-017-0029-0
13. Farris JS. The retention index and the rescaled consistency index. *Cladistics.* (1989) 5:417–9. doi: 10.1111/j.1096-0031.1989.tb00573.x
14. Simpson EH. Measurement of diversity. *Nature.* (1949) 163:688.
15. Hunter PR, Gaston MA. Numerical index of the discriminatory ability of typing systems: an application of Simpson's index of diversity. *J Clin Microbiol.* (1988) 26:2465–6.
16. Comas I, Homolka S, Niemann S, Gagneux S. Genotyping of genetically monomorphic bacteria: DNA sequencing in *Mycobacterium tuberculosis* highlights the limitations of current methodologies. *PLoS One.* (2009) 4:e7815. doi: 10.1371/journal.pone.0007815
17. Reyes JF, Chan CHS, Tanaka MM. Impact of homoplasy on variable numbers of tandem repeats and spoligotypes in *Mycobacterium tuberculosis*. *Infect Genet Evol.* (2012) 12:811–18. doi: 10.1016/j.meegid.2011.05.018
18. Luo T, Yang C, Gagneux S, Gicquel B, Mei J, Gao Q. Combination of single nucleotide polymorphism and variable-number tandem repeats for genotyping a homogenous population of *Mycobacterium tuberculosis* Beijing strains in China. *J Clin Microbiol.* (2012) 50:633–9. doi: 10.1128/JCM.05539-11
19. Nakanishi N, Wada T, Arikawa K, Millet J, Rastogi N, Iwamoto T. Evolutionary robust SNPs reveal the misclassification of Mycobacterium tuberculosis Beijing family strains into sublineages. *Infect Genet Evol.* (2013) 16:174–7. doi: 10.1016/j.meegid.2013.02.007
20. Graber S, Furrer R, Isler K. *Phylogenetic comparative methods for discrete responses in evolutionary biology (Master dissertation)*. University of Zurich (2013). Available online at: https://www.zora.uzh.ch/id/eprint/152452/1/2013-Graber.pdf (accessed August 17, 2020).
21. Matthews LJ, Arnold C, Machanda Z, Nunn CL. Primate extinction risk and historical patterns of speciation and extinction in relation to body mass. *Proc Biol Sci.* (2011) 278:1256–63. doi: 10.1098/rspb.2010.1489
22. Lande R. Natural selection and random genetic drift in phenotypic evolution. *Evol Int J Org Evol.* (1976) 30:314–34. doi: 10.1111/j.1558-5646.1976.tb00911.x
23. Hansen TF. Stabilizing selection and the comparative analysis of adaptation. *Evol Int J Org Evol.* (1997) 51:1341–51. doi: 10.1111/j.1558-5646.1997.tb01457.x
24. Butler MA, King AA. Phylogenetic comparative analysis: a modeling approach for adaptive evolution. *Am Nat.* (2004) 164:683–95. doi: 10.1086/426002
25. Uyeda JC, Harmon LJ. A novel Bayesian method for inferring and interpreting the dynamics of adaptive landscapes from phylogenetic comparative data. *Syst Biol.* (2014) 63:902–18. doi: 10.1093/sysbio/syu057
26. Gurjav U, Jelfs P, McCallum N, Marais BJ, Sintchenko V. Temporal dynamics of *Mycobacterium tuberculosis* genotypes in New South Wales, Australia. *BMC Infect Dis.* (2014) 14:455. doi: 10.1186/1471-2334-14-455
27. Supply P, Allix C, Lesjean S, Cardoso-Oelemann M, Rüsch-Gerdes S, Willery E, et al. Proposal for standardization of optimized mycobacterial interspersed repetitive unit-variable-number tandem repeat typing of *Mycobacterium tuberculosis*. *J Clin Microbiol.* (2006) 44:4498–10. doi: 10.1128/JCM.01392-06
28. Walker TM, Ip CL, Harrell RH, Evans JT, Kapatai G, Dedicoat MJ, et al. Whole-genome sequencing to delineate *Mycobacterium tuberculosis* outbreaks: a retrospective observational study. *Lancet Infect Dis.* (2013) 13:137–46. doi: 10.1016/S1473-3099(12)70277-3
29. Merker M, Blin C, Mona S, Duforet-Frebourg N, Lecher S, Willery E, et al. Evolutionary history and global spread of the *Mycobacterium tuberculosis* Beijing lineage. *Nat Genet.* (2015) 47:242–9. doi: 10.1038/ng.3195
30. Alic AS, Tomas A, Medina I, Blanquer I. MuffinEc: Error correction for *de novo* assembly via greedy partitioning and sequence alignment. *Inf Sci.* (2016) 329:206–19. doi: 10.1016/j.ins.2015.09.012
31. Li H. BFC: correcting Illumina sequencing errors. *Bioinformatics.* (2015) 31:2885–7. doi: 10.1093/bioinformatics/btv290
32. Li H. Aligning sequence reads, clone sequences and assembly contigs with BWA-MEM. *ArXiv:1303.3997 Q-Bio.* (2013).
33. Faust GG, Hall IM. SAMBLASTER: fast duplicate marking and structural variant read extraction. *Bioinformatics.* (2014) 30:2503–5. doi: 10.1093/bioinformatics/btu314
34. Garrison E, Marth G. Haplotype-based variant detection from short-read sequencing. *ArXiv12073907 Q-Bio.* (2012).
35. Cingolani P, Platts A, Wang LL, Coon M, Nguyen T, Wang L, et al. A program for annotating and predicting the effects of single nucleotide polymorphisms, SnpEff: SNPs in the genome of *Drosophila melanogaster* strain w1118; iso-2; iso-3. *Fly (Austin).* (2012) 6:80–92. doi: 10.4161/fly.19695
36. Ronquist F, Teslenko M, van der Mark P, Ayres DL, Darling A, Höhna S, et al. MrBayes 3.2: efficient Bayesian phylogenetic inference and model choice across a large model space. *Syst Biol.* (2012) 61:539–42. doi: 10.1093/sysbio/sys029
37. Sukumaran J, Holder MT. DendroPy: a Python library for phylogenetic computing. *Bioinforma Oxf Engl.* (2010) 26:1569–71. doi: 10.1093/bioinformatics/btq228
38. Revell LJ. phytools: an R package for phylogenetic comparative biology (and other things): phytools: R package. *Methods Ecol Evol.* (2012) 3:217–23. doi: 10.1111/j.2041-210X.2011.00169.x
39. Paradis E, Claude J, Strimmer K. APE: analyses of phylogenetics and evolution in R language. *Bioinforma Oxf Engl.* (2004) 20:289–90. doi: 10.1093/bioinformatics/btg412
40. Schliep KP. phangorn: phylogenetic analysis in R. *Bioinforma Oxf Engl.* (2011) 27:592–3. doi: 10.1093/bioinformatics/btq706
41. Yu G, Smith DK, Zhu H, Guan Y, Lam TT-Y. ggtree: an R package for visualization and annotation of phylogenetic trees with their covariates and other associated data. *Methods Ecol Evol.* (2017) 8:28–36. doi: 10.1111/2041-210X.12628

42. Ford CB, Shah RR, Maeda MK, Gagneux S, Murray MB, Cohen T, et al. *Mycobacterium tuberculosis* mutation rate estimates from different lineages predict substantial differences in the emergence of drug-resistant tuberculosis. *Nat Genet.* (2013) 45:784–90. doi: 10.1038/ng.2656
43. Ford CB, Lin PL, Chase MR, Shah RR, Iartchouk O, Galagan J, et al. Use of whole genome sequencing to estimate the mutation rate of *Mycobacterium tuberculosis* during latent infection. *Nat Genet.* (2011) 43:482–6. doi: 10.1038/ng.811
44. Outhred AC, Holmes N, Sadsad R, Martinez E, Jelfs P, Hill-Cawthorne GA, et al. Identifying likely transmission pathways within a 10-year community outbreak of tuberculosis by high-depth whole genome sequencing. *PLoS One.* (2016) 11:e0150550. doi: 10.1371/journal.pone.0150550
45. Arnold C, Thorne N, Underwood A, Baster K, Gharbia S. Evolution of short sequence repeats in *Mycobacterium tuberculosis*. *FEMS Microbiol Lett.* (2006) 256:340–6. doi: 10.1111/j.1574-6968.2006.00142.x
46. Stucki D, Brites D, Jeljeli L, Coscolla M, Liu Q, Trauner A, et al. *Mycobacterium tuberculosis* lineage 4 comprises globally distributed and geographically restricted sublineages. *Nat Genet.* (2016) 48:1535–43. doi: 10.1038/ng.3704
47. Kremer K, Arnold C, Cataldi A, Gutierrez MC, Haas WH, Panaiotov S, et al. Discriminatory power and reproducibility of novel DNA typing methods for *Mycobacterium tuberculosis* complex strains. *J Clin Microbiol.* (2005) 43:5628–38. doi: 10.1128/JCM.43.11.5628-5638.2005
48. Cowan LS, Hooks DP, Christianson S, Sharma MK, Alexander DC, Guthrie JL, et al. Evaluation of mycobacterial interspersed repetitive-unit-variable-number tandem-repeat genotyping as performed in laboratories in Canada, France, and the United States. *J Clin Microbiol.* (2012) 50:1830–1. doi: 10.1128/JCM.00168-12
49. Nikolayevskyy V, Trovato A, Broda A, Borroni E, Cirillo D, Drobniewski F. MIRU-VNTR genotyping of *Mycobacterium tuberculosis* strains using QIAxcel technology: a multicentre evaluation study. *PLoS One.* (2016) 11:e0149435. doi: 10.1371/journal.pone.0149435
50. Allix-Béguec C, Wahl C, Hanekom M, Nikolayevskyy V, Drobniewski F, Maeda S, et al. Proposal of a consensus set of hypervariable mycobacterial interspersed repetitive-unit–variable-number tandem-repeat loci for subtyping of *Mycobacterium tuberculosis* Beijing isolates. *J Clin Microbiol.* (2014) 52:164–72. doi: 10.1128/JCM.02519-13
51. Stucki D, Malla B, Hostettler S, Huna T, Feldmann J, Yeboah-Manu D, et al. Two new rapid SNP-typing methods for classifying *Mycobacterium tuberculosis* complex into the main phylogenetic lineages. *PLoS One.* (2012) 7:e41253. doi: 10.1371/journal.pone.0041253
52. Homolka S, Projahn M, Feuerriegel S, Ubben T, Diel R, Nübel U, et al. High resolution discrimination of clinical *Mycobacterium tuberculosis* complex strains based on single nucleotide polymorphisms. *PLoS One.* (2012) 7:e39855. doi: 10.1371/journal.pone.0039855
53. Coll F, Preston M, Guerra-Assunção JA, Hill-Cawthorne G, Harris D, Perdigão J, et al. PolyTB: a genomic variation map for *Mycobacterium tuberculosis*. *Tuberculosis.* (2014) 94:346–54. doi: 10.1016/j.tube.2014.02.005

Conflict of Interest: The authors declare that the research was conducted in the absence of any commercial or financial relationships that could be construed as a potential conflict of interest.

frontiers in Public Health

BRIEF RESEARCH REPORT
published: 04 September 2020
doi: 10.3389/fpubh.2020.00443

Management of Tuberculosis: Are the Practices Homogeneous in High-Income Countries?

Frédéric Méchaï[1], Hugues Cordel[1], Lorenzo Guglielmetti[2,3], Alexandra Aubry[2,3], Mateja Jankovic[4], Miguel Viveiros[5], Miguel Santin[6], Delia Goletti[7] and Emmanuelle Cambau[2,8] on behalf of the ESGMYC group[†]*

[1] APHP, Infectious Disease Unit, Avicenne Hospital, Université Paris 13, IAME, INSERM, Bobigny, France, [2] APHP, Groupe Hospitalier Universitaire Sorbonne Université, Hôpital Pitié-Salpêtrière, Centre National de Référence des Mycobactéries et de la Résistance des Mycobactéries aux Antituberculeux, Paris, France, [3] Sorbonne Université, INSERM, U1135, Centre d'Immunologie et des Maladies Infectieuses, Cimi-Paris, Paris, France, [4] Clinic for Lung Diseases, University of Zagreb School of Medicine and University Hospital Center Zagreb, Zagreb, Croatia, [5] Global Health and Tropical Medicine, GHTM, Instituto de Higiene e Medicina Tropical, IHMT, Universidade Nova de Lisboa, UNL, Lisboa, Portugal, [6] Service of Infectious Diseases, Tuberculosis Unit, Bellvitge University Hospital-IDIBELL, University of Barcelona, L'Hospitalet de Llobregat, Barcelona, Spain, [7] Translational Research Unit, Department of Epidemiology and Preclinical Research, "L. Spallanzani" National Institute for Infectious Diseases (INMI), IRCCS, Rome, Italy, [8] AP-HP, Hôpital Lariboisière, Service de Bactériologie, Paris, France

OPEN ACCESS

Edited by:
Vitali Sintchenko, The University of Sydney, Australia

Reviewed by:
Florence Doucet-populaire, Université Paris-Sud, France
Jin-Gun Cho, The University of Sydney, Australia

***Correspondence:**
Frédéric Méchaï
frederic.mechai@aphp.fr

[†] *ESCMID (European society on clinical microbiology and infectious diseases) study group on mycobacterial infections*

Specialty section:
This article was submitted to Infectious Diseases - Surveillance, Prevention and Treatment, a section of the journal Frontiers in Public Health

Received: *12 November 2019*
Accepted: *20 July 2020*
Published: *04 September 2020*

Citation:
Méchaï F, Cordel H, Guglielmetti L, Aubry A, Jankovic M, Viveiros M, Santin M, Goletti D and Cambau E (2020) Management of Tuberculosis: Are the Practices Homogeneous in High-Income Countries? Front. Public Health 8:443. doi: 10.3389/fpubh.2020.00443

Objectives: To evaluate and compare practices regarding the diagnosis, isolation measures, and treatment of tuberculosis (TB) in high-income countries and mainly in Europe.

Materials and Methods: A survey was conducted from November 2018 to April 2019 within the European Society of Clinical Microbiology and Infectious Diseases Study Group for Mycobacterial Infections (ESGMYC). The practices observed were compared to the main international guidelines.

Results: Among 136 ESGMYC members, 64 (17 countries) responded to the questionnaire. In their practice, two (20.7%) or three sputum samples (79.3%) were collected for the diagnosis of pulmonary TB, alternatively induced sputum (n = 37, 67.2%), bronchoscopy (34, 58.6%), and gastric aspirates (15, 25.9%). Nucleic acid amplification tests (NAATs) were performed by 41 (64%) respondents whatever the smear result and by 47 (73%) in case of smear-positive specimens. NAAT and adenosine deaminase measurement were used for extrapulmonary TB diagnosis in 83.6 and 40.4% of cases, respectively. For isolation duration, 21 respondents (42.9%) were keeping isolation until smear negativity. An initial treatment without ethambutol was offered by 14% (n = 9) of respondents. Corticosteroid therapy, cerebrospinal fluid opening pressure testing, and repeated lumbar puncture were carried out for central nervous system TB by 79.6, 51.9, and 46.3% of the respondents, respectively. For patients with human immunodeficiency virus–TB coinfection, the preferred antiretroviral therapy included dolutegravir 50 mg twice a day (56.8%). Comparing with the recommendations of the main guidelines, the practices are not totally consistent.

Conclusion: This study shows heterogeneous practices, particularly for diagnosis, and isolation, although rapid molecular testing is implemented in most centers. More standardization might be needed.

Keywords: tuberculosis, survey, Europe, guidelines, harmonization, diagnosis, treatment

INTRODUCTION

In 2017, 10 million people were diagnosed with tuberculosis (TB) in the world (1, 2). Although the European region accounted for only 3% of all cases (3), TB remains a common infection. Despite a rate of latent TB estimated at 23% of the world population, there are very large disparities in incidence between continents and countries with an incidence of fewer than 10 per 10,000 inhabitants in Western Europe to more than 500 per 100,000 for countries such as South Africa, the Philippines, and Mozambique (2). The overall objective of the World Health Organization (WHO) by 2035 (The End TB strategy) is to reduce the number of deaths from TB by 95% (compared to 2015) and to reduce the incidence rate of TB by 90% to fewer than 10 per 100,000 people. In 2016, 58,994 cases of TB were reported in 30 European Union/European Economic Area (EU/EEA) countries (2). The decreasing notification rates observed in most countries are reassuring, but annual rates of decline are still insufficient to achieve the WHO target of TB elimination by 2050 in European low-incidence countries. Multidrug-resistant (MDR) TB was reported for 3.7% of 36,071 cases with drug susceptibility testing results and continues to be the highest (more than 10%) in the three Baltic countries. Extensively drug-resistant (XDR) TB was reported for 20.1% of 984 MDR TB cases tested for second-line drug susceptibility (4). Data on human immunodeficiency virus (HIV) coinfection remained widely incomplete in Europe. Of all TB cases with known HIV status, 4.5% were coinfected with the virus (5).

An evaluation of TB case management in the EU/EEA countries, with special focus on MDR and XDR-TB, was conducted in 2010, using a standardized survey tool in five European centers. Deviations from international standards of TB care were observed in the following areas: surveillance (no information available on patient outcomes); infection control (lack of respiratory isolation rooms/procedures and negative-pressure ventilation rooms); clinical management of TB, MDR-TB, and HIV coinfection (inadequate bacteriological diagnosis, regimen selection, and treatment duration); laboratory support; and diagnostic/treatment algorithms (6).

A response to this need of harmonization has already been initiated through the development of European Union Standards for TB Care (ESTC) in 2012 with an update in 2017. They identified key standards for the diagnosis, management, prevention, and control of TB, MDR-TB, and XDR-TB. These standards aim to support health care workers in optimizing TB case management and thus at contributing to improved TB control in the EU/EEA (7–11). In fact, after the implementation of these standards, the knowledge of appropriate TB case management in high-income countries and in particular the different European countries is scarce. The main aim of this study was therefore to verify the current good homogeneity of practices of the different actors involved in the fight against TB and to compare them with the main national or international recommendations.

TABLE 1 | Summary of the questionnaire.

Respondents	Name, country, institution, age, profession
	Medical information used for the practice
Microbiological TB diagnosis	Investigations for a suspicion of active pulmonary tuberculosis
	Management of NAAT for pulmonary TB
	Microbiological monitoring
	Management of NAAT for non-pulmonary samples
	Criteria for using ADA
	TB meningitis: diagnosis and management of corticosteroids and rifampicin
	Criteria for using IGRA and TST
Isolation practices	Kind of isolation room
	Duration of isolation and circumstances to stop isolation
	Isolation criteria of smear negative patients
	Hospital discharge criteria
TB treatment	Standard treatment of tuberculosis
	Fluoroquinolones treatment criteria
	Ethambutol if no isoniazid resistance mutation
	B6 vitamin treatment criteria
	Ophtalmology exam and ethambutol
	Drug blood levels following TB treatment
	HIV treatment in case of TB coinfection
	Management of latent TB in HIV patients
	Management of TB compliance

NAAT, Nucleic acid amplification tests.

MATERIALS AND METHODS

A survey was conducted from November 2018 to April 2019 among members of the European Society of Clinical Microbiology and Infectious Diseases (ESCMID) Study Group for Mycobacterial Infections (ESGMYC), an offshoot of the ESCMID. The questionnaire was initially sent out on November 8, 2018, with subsequent reminders, the last being sent on March 15, 2019. The online questions comprised 63 items and focused on three topics: (1) diagnosis of TB, (2) isolation and prevention of TB transmission, and (3) TB treatment (summarized in **Table 1**). Descriptive statistics were used to

TABLE 2 | Microbiological TB diagnosis: synthesis of the international recommendations and main results from the ESGMYC survey.

Diagnostic tools	IDSA/ATS/CDC 2017 (12)	NICE 2016 (14)	WHO Europe 2017 (17)	ERS/ECDC 2017 (11)	ESGMYC survey (% of respondents)
Pulmonary TB	• Three sputum specimens • Sputum volume of at least 3 ml (optimal 5–10 ml) • Both liquid and solid culture (at least one liquid culture on all specimens)	• Three sputum specimens • Preferably one early morning sample	• Three sputum specimens • Both liquid and solid culture	• At least two sputum specimens (at least one early morning) for microscopic examination • Samples can be collected on the same day • Good quality sputum • At least liquid culture • Phenotypic drug susceptibility testing (DST)	• Sputum collection in the early morning (97%) • Three samples (81%) • 3 consecutive days (58%)
Other procedures (patient unable to expectorate)	• Sputum induction rather than flexible bronchoscopy sampling • Collect post-bronchoscopy sputum specimens	• Three sputum inductions or Three gastric lavages • Induction of sputum or bronchoscopy and lavage in adults	NA	• Sputum induction • Bronchoscopy/bronchoalveolar lavage • Gastric lavage in children	• Induced sputum (66%) • Bronchoscopy (59%) • Gastric aspiration (27%)
Molecular tests (pulmonary TB)	• NAAT on the initial specimen • A rapid molecular drug susceptibility testing for rifampicin with or without isoniazid • Genotyping in regional laboratory for each mycobacterial culture-positive	• NAAT on primary specimens if clinical suspicion of TB disease and/or • HIV-positive patient, or • Rapid information about mycobacterial species would alter the person's care, or • Need for a large contact tracing initiative is being explored.	• NAAT on at least one specimen	• One sputum tested for NAAT • WHO-recommended rapid molecular assays (sputum sample) • For DST, if use of WGS, results must be confirmed by phenotypic testing.	• Systematically done (64%) • Detection of resistance mutations to rifampicin (84%), isoniazid (29%), and others drugs (7%) • Mutations sought for INH resistance were *katg* gene and *InhA* promoter (64%), or only *katG* gene (15%) • Systematically whole genome sequencing (19.4%)
Extrapulmonary TB	• Cell counts and biochemistry on fluid specimens • ADA on fluid from pleural TB, meningitis, peritoneal, or pericardial TB • Free IFN-γ on fluid from suspected pleural or peritoneal TB • Smear microscopy for suspected extrapulmonary TB • NAAT from sites of extrapulmonary TB • Histological examination	• Addition of a spontaneously produced respiratory sample • Pleural TB: ADA, sputum samples and pleural biopsy • Meningeal TB: CSF fluid analysis, ADA, and NAAT • Lymph node: biopsy (+ histology), aspirate (+ cytology), NAAT • Pericardial TB: biopsy of pericardium (+histology), pericardial fluid (+ cytology), NAAT, ADA • Disseminated TB: biopsy (lung, liver, and bone marrow), bone marrow aspirate, bronchial lavage, appropriate CSF tests, and blood culture	NA	• Tests recommended for all cases: microscopy, NAAT, and culture, histopathology	• NAAT (85%) • ADA (40%): on pleural fluid (96%), CSF (40%), and peritoneal fluid (24%)

NAAT, Nucleic acid amplification tests; WGS, whole genome sequencing; ADA, adenosine deaminase; TB, tuberculosis; IFN-γ, interferon-gamma; CSF, cerebrospinal fluid; DST, drug susceptibility testing.

analyze the results of the survey. The data were analyzed using STATA 10.0 (StataCorp LP, College Station, TX, USA). Paris-Seine-Saint-Denis University Hospitals Committee review waived the requirement for ethical approval for this study because of absence of interventional research on the human person, in accordance with the national legislation and the institutional requirements.

In a second step, in order to understand the differences in the management of TB in high-income countries, we compared the participants' responses to the main principles of TB management according to the following international recommendations: Infectious Disease Society of America/Centers for Disease Control/American Thoracic Society (IDSA/CDC/ATS) guidelines (12, 13), National Institute for Health and Care Excellence (NICE) guidelines (14), ERS/ECDC (European Respiratory Society/European Centers for Disease Control) guidelines (11), WHO (15), and the recommendations of the French Hospital Hygiene Society (16). These are summarized in **Tables 2–4** for comparing the proposals of each academic society.

RESULTS

Respondents

Among 136 ESGMYC members, 64 (47.1%) responded to the questionnaire representing 14 European countries (Albania, Croatia, Denmark, Germany, Greece, France, Italy, Netherlands, Norway, Romania, Spain, Sweden, Switzerland, Turkey, and the United Kingdom), with 1–13 per country, and 3 non-European countries (New Zealand, Singapore, and Australia; **Figure 1**). Median age was 44 years (interquartile range = 38–51 years). The participants were working in an infectious diseases (67%, $n = 43/64$) or clinical microbiology (30%, $n = 19/64$) department. Sources of medical information for their practice were national guidelines alone for 8% ($n = 5/64$) of them, international guidelines only for 11% ($n = 7/64$), and an association of both for 64% ($n = 41/64$). TB specialist opinion was consulted, alone or together with other sources, by 50% ($n = 32/64$) of respondents. Among international recommendations, the main source was the WHO guidelines for 34% of respondents ($n = 15/44$).

Microbiological TB Diagnosis

For the microbiological diagnosis of pulmonary TB, 97% ($n = 62/64$) of respondents used to collect at least one sputum in the early morning on an empty stomach, with 19% ($n = 12/64$) and 81% collecting two or three samples, respectively. The two remaining responders collected induced or spontaneous sputum at admission or randomly timed sputum sample. Multiple samples are usually taken during 3 consecutive days (58%, $n = 37/64$), or 2 (33%, $n = 21/64$) or within the same day (17%, $n = 11/64$). If the patient could not produce sputum, the alternatives were induced sputum (66%, $n = 42/64$), bronchoscopy aspirate (59%, $n = 38/64$), and gastric aspiration (27%, $n = 17/64$).

A rapid molecular test was performed systematically by 41/64 (64%) respondents, on one (31%, $n = 14/45$) or multiple respiratory specimens (33%, $n = 15/45$). In case of strong suspicion of pulmonary TB with negative sputum smears, 16/64 (25%) respondents would start treatment, 11/64 (17%) would wait for the culture result before starting, and 44/64 (78.6%) would perform additional diagnostic tests, namely, rapid molecular tests (66%), or bronchoscopy aspirate testing (61.3%). In case of positive sputum smear, a rapid molecular test was performed to detect mutations conferring resistance to rifampicin by 84% ($n = 52/64$), to isoniazid by 29% ($n = 18/62$), and to other drugs by 7% ($n = 4/62$), whereas 10 (16%) did not perform any rapid molecular test. Regarding the type of mutation sought for isoniazid resistance, among the 26 microbiologists who gave an answer, 17 (65%) perform rapid molecular tests to detect mutations in both *katG* gene and the *inhA* promoter, and four only in the *katG* gene (15%). Eight respondents (31%) were looking for genotypic resistance to other drugs besides rifampicin and isoniazid, with five of them performing whole-genome sequencing.

In the case of positive culture, of 61 respondents, 38 (62%) were asking for molecular detection of rifampicin resistance mutation, 24 (39%) for an isoniazid resistance mutation, and 9 (15%) for resistance mutations to other drugs, whereas 23 (38%) were not looking for genotypic resistance.

For the diagnosis of extrapulmonary TB, nucleic acid amplification test (NAAT), and measurement of adenosine deaminase (ADA) were performed in 85% ($n = 52/61$ responses) and 40% ($n = 25/62$ responses) of cases, respectively. ADA was performed mainly for the diagnosis of pleural effusion (96%, $n = 24/25$), but also on the cerebrospinal fluid (CSF) (40%, $n = 10/25$) in case of suspicion of TB meningitis and on peritoneal fluid (24%, $n = 6/25$). Sputum smear was repeated after 2 and 6 months of treatment by 53/63 (83%) and 37/63 (58%) participants, respectively. Overall, interferon-γ release assays (IGRAs) and tuberculin skin testing (TST) were performed by 31% ($n = 20/64$) and 23% ($n = 15/64$) of respondents, respectively, even for the diagnosis of active TB.

Isolation Practices

Overall, 23% ($n = 15/63$) of respondents used a conventional single room to isolate pulmonary TB patients, whereas 77% ($n = 50/63$) reported using a negative-pressure room whatever the drug susceptibility profile of the strain. Regarding the duration of isolation for pulmonary TB with smear-positive sputum, 23/64 (36%) respondents adopted a standardized duration of 2 to 3 weeks, whereas 23/64 (36%) reported waiting for the sputum smear-negative conversion. In case of patients hospitalized with a suspicion of pulmonary TB but negative sputum smears and pending culture results, 18/64 (28%) of the respondents did not isolate the patient. Patients with a positive sputum smear were allowed to leave the hospital by 75% ($n = 48/64$) of respondents, in the following cases: if they agreed to wear a mask ($n = 31/48$, 65%), if there were no other people at home ($n = 39/48$, 81%), and in the absence of children ($n = 29/48$, 60%) or of immunocompromised individuals ($n = 36/48$, 75%) at home.

TB Treatment

A majority of respondents (81%, $n = 52/64$) used the standard first-line treatment with isoniazid, rifampicin, pyrazinamide,

TABLE 3 | Isolation measures recommended for pulmonary tuberculosis patients in healthcare settings: synthesis of international recommendations and ESGMYC survey main results.

Isolation measures	SF2H* 2013 (16)	ATS/CDC/IDSA 2005 (18)	NICE 2016 (14)	ERS/ECDC 2017 (11)	ESGMYC Survey (% of respondents)
Smear-positive pulmonary TB cases	Up to 2 weeks if: • No suspicion of resistance • Decrease of cough intensity • Low initial smear grade • No immunocompromised patients in the same ward	Isolation until: • Patient under standard multi drug anti TB therapy, • Clinical improvement and • Three consecutive AFB-negative smear results of sputum specimens	Up to 2 weeks if: • (Complete) adherence to treatment • Resolution of cough • Improvement on treatment • Low initial smear grade (2 or less) • No cavitation • No laryngeal TB	Until: Bacteriological conversion (negative sputum smear)	Duration: • Standardized duration of 2–3 weeks (36%) • Until bacteriological conversion (36%)
Smear negative tuberculosis cases, suspicion of pulmonary TB	Isolation until culture results are available	NA	NA	NA	No isolation (28%)
Type of room for hospitalization	NA	NA	Single room/negative pressure room for patients at high risk of MDR-TB	Negative pressure ventilation room	Negative pressure room (77%)
Type of ward	NA	NA	No admission in wards with immunocompromised patients	NA	NA
Conditions of discharge from hospital	NA	Non infectiousness if: • Negligible likelihood of MDR TB • Anti TB therapy for 2–3 weeks • Complete adherence to treatment • Clinical improvement (reduction of cough, or of the grade of the sputum AFB smear result • Close contacts identified	• No continuing clinical or public health need for admission • unlikely to be rifampicin resistant • To avoid congregate settlings in the first 2 weeks of treatment	NA	To leave the hospital in case of positive smear sputum (75%) pending of conditions • Mask (65%) • No other people at home (81%) • Absence of children at home (60%) or • No immunocompromised people (75%) at home

MDR-TB, multidrug-resistant tuberculosis.
**French Society of Hospital Hygiene.*

TABLE 4 | Drug-susceptible tuberculosis treatment: synthesis of international recommendations and ESGMYC survey main results.

Treatment scheme	IDSA/ATS/CDC 2017 (13)	NICE 2016 (14)	WHO 2010/2017 (15)	ERS/ECDC 2017 (11)	ESGMYC survey (% of respondents)
Intensive phase	• INH/RIF/PZA/EMB • Stop EMB if susceptibility to RIF and INH	INH/RIF/PZA/EMB for 2 months	INH/RIF/PZA/EMB for 2 months	INH/RIF/PZA/EMB for 2 months	• INH/RIF/PZA/EMB (81%) • Tritherapy without ethambutol (14%)
Continuation phase	INH/RIF	INH/RIF for 4 months	INH/RIF for 4 months	INH/RIF for 4 months	NA
Doses	• Intensive phase: 7 days/week for 56 doses or 5 days/week for 40 doses* • Continuation phase: 7 days/week for 126 doses or 5 days/week for 90 doses**	• Fixed-dose combination tablet • Dosing regimens of fewer than three times per week are not recommended • Daily dosing schedule is recommended	• Fixed-dose combination tablet • Daily dosing schedule is recommended	• Daily dosing schedule is recommended	NA
Adjunctive pyridoxine	To all persons at risk of neuropathy***	During all the treatment	NA	NA	Systematically for 89% of respondents
HIV co-infection	• 6 months treatment duration • 9 months if no antiretroviral therapy • Caution with drug–drug interactions	• 6 months duration • Caution with drug–drug interactions	• 6 months duration • Start of antiretroviral treatment within 8 weeks (within the first 2 weeks if CD4 counts <50 cells/mm^3)	Delay between the initiation of TB therapy and the start of antiretroviral treatment of at least 14 days	• Associated antiretroviral therapy: dolutegravir 50 mg bid (60%), efavirenz 600 mg daily (35%), a protease inhibitor with rifabutin (17%), raltegravir 800 mg bid (15%), raltegravir 400 mg bid (13%), and efavirenz 800 mg daily (6%). • Preventive treatment for all HIV-positive patients with latent TB infection (100%)
Adjunctive corticosteroids	• TB pericarditis: not to be used routinely (if large effusions, high levels of inflammatory cells or markers, early signs of constriction) • Central nervous system TB: dexamethasone or prednisolone for 6–8 weeks	• Central nervous system TB and active pericardial TB: dexamethasone (CNS) or prednisolone (CNS, pericardial)	• TB meningitis: dexamethasone or prednisone first 6–8 weeks • TB pericarditis: initial adjuvant corticosteroid therapy may be used (conditional recommendation)	• TB meningitis: dexamethasone or prednisone during the first 6–8 weeks of treatment • TB pericarditis • Renal TB: to prevent ureteric stenosis • Spinal TB: if spinal cord compression	• Use of corticosteroids for neuro-meningeal TB (80%) • Duration of treatment with corticosteroids from 2 (10%) to 12 weeks (5%)
Adjunctive surgery	NA	• Central nervous system TB with raised intracranial pressure • Spinal TB with spinal instability or spinal cord compression	NA	NA	NA
Tuberculosis of the central nervous system	• INH/RIF/PZA/EMB for 2 months then INH/RIF 7–10 months • Repeated lumbar punctures	INH/RIF/PZA/EMB for 2 months (with pyridoxine) then INH/RIF 10 months (with pyridoxine)	NA	NA	• Measurement of CSF pressure (51%) • Repeated lumbar punctures (46%)
Culture negative tuberculosis	• Bronchoscopy with bronchoalveolar lavage and biopsy • Start treatment • Duration 4 months if clinical or radiographic response after 2 months of intensive phase therapy	Start treatment without waiting for culture results if life-threatening disease	NA	NA	NA

(Continued)

TABLE 4 | Continued

Treatment scheme	IDSA/ATS/CDC 2017 (13)	NICE 2016 (14)	WHO 2010/2017 (15)	ERS/ECDC 2017 (11)	ESGMYC survey (% of respondents)
Response to therapy	NA	NA	Follow up smear microscopy at time of completion of the intensive phase and 5–6 months if initial smear positive	Follow up smear microscopy and culture at least at time of completion of the intensive phase	Sputum smear repeated after: • 2 months (83%) • 6 months (58%) of treatment
Optic neuritis	Visual acuity and color discrimination tests monthly during EMB use	NA	NA	NA	Ophthalmology assessment during the first 2 months of ethambutol treatment (50%)
Therapeutic Drug Monitoring	• Suspicion of drug malabsorption, drug underdosing, and clinically important drug-drug interactions • Delayed sputum conversion or treatment failure • Reduced renal function • Treatment for drug-resistant tuberculosis	NA	NA	Therapeutic drug monitoring if poor response to treatment (underdosing or malabsorption)	Therapeutic drug monitoring for rifampicin and isoniazid: • Never (50%) • Routinely (17%) • Only in specific cases (23%)
Management of IRIS	• Mild IRIS: TB and HIV treatment continued, and anti-inflammatory drugs • Severe IRIS: drainage for pleural effusions or abscesses, corticosteroids (2–4 weeks of treatment with subsequent tapering over a period of 6–12 weeks or longer)	NA	NA	NA	NA
Recurrence	• Retreatment using the standard intensive phase regimen • Rapid molecular tests to detect resistance	NA	• Drug-susceptibility testing before the start of treatment • Rapid molecular tests if possible	NA	NA
Adherence	Suggest using DOT	NA	• Health education and counseling (adherence interventions) • DOT (or VOT: Video observed Treatment)	NA	Interpreter use (56%) Nurse specialized in therapeutic education (48%) Systematic DOT (47%) Hospitalization for the full duration of treatment (28%) DOT at home with a nurse (61%)

INH, isoniazid; RIF, rifampicin; PZA, pyrazinamide; EMB, ethambutol; TB, tuberculosis; CNS, central nervous system; IRIS, immune reconstitution inflammatory syndrome; DOT, directly-observed therapy.

**Preferred regimen.*

***Extend the continuation phase for patients with cavitation on the initial chest radiography and patients who have culture positive after completion of 2 months of therapy.*

****Pregnant women; breastfeeding infants; persons infected with human immunodeficiency virus [HIV]; patients with diabetes, alcoholism, malnutrition, or chronic renal failure; or those who are of advanced age.*

FIGURE 1 | Europe map presenting the number of respondents per country.

and ethambutol for 2 months, followed by 4 months of treatment with isoniazid and rifampicin; but 14% (n = 9/64) of respondents offered an initial treatment without ethambutol. Fluoroquinolones were never prescribed as part of first-line treatment by 29/61 (45%) of respondents; conversely, 5/61 (8%) and 26/61 (41%), respectively, used them under certain conditions such as bone TB or suspicion of resistance to isoniazid. Overall, 30% (n = 19/63) of respondents reported to discontinue ethambutol treatment in the absence of mutations conferring resistance to isoniazid. Among respondents, 89% (n = 57/63) systematically gave B_6 vitamin therapy. With regard to treatment monitoring, 50% (n = 32/62) of respondents performed an ophthalmology assessment during the first 2 months of ethambutol treatment. Overall, 50% (n = 32/64) of respondents never performed therapeutic drug monitoring for rifampicin and isoniazid, 17% (n = 11/64) routinely performed it, and 23% (n = 15/64) performed it only in specific cases (i.e., HIV infection, overweight, renal insufficiency). For neuromeningeal TB cases, 80% (43/54) of respondents added corticosteroids to the TB treatment for a variable duration, from 2 (10%, n = 4/40 respondents) to 12 weeks (5%, n = 2/40). The measurement of CSF pressure and repeated lumbar punctures were performed by 51% and 46% of the 59 respondents, respectively. In case of HIV coinfection, the most frequently used antiretroviral drugs were dolutegravir 50 mg twice a day (BID) (60%, n = 29/48 respondents), efavirenz 600 mg daily (35%, n = 17/48), a protease inhibitor with rifabutin (17%, n = 8/48), raltegravir 800 mg BID (15%, n = 7/48), raltegravir 400 mg BID (13%, n = 6/48), and efavirenz 800 mg daily (6%, n = 3/48). All respondents offered preventive treatment to HIV-positive patients with latent TB infection, using the following: isoniazid for 6 months (84%, n = 43/51 respondents), isoniazid and rifampicin for 3 months

(24%, $n = 12/51$), rifampicin for 3–4 months (24%, $n = 12/51$), or isoniazid plus rifapentine for 3 months (4%, $n = 2/51$). To optimize adherence and treatment support, clinicians used an interpreter (56%, $n = 36/64$), a nurse specialized in therapeutic education (48%, $n = 31/64$), systematic Directly Observed Therapy (DOT) (47%, $n = 30/64$), or hospitalization for the full duration of treatment (28%, $n = 18/64$). As an alternative to hospitalization, 39/64 (61%) offered a DOT at home with a nurse.

DISCUSSION

TB continues to be a priority public health challenge in high-income countries. While EU/EEA countries adopted the key principles of TB control and elimination through the Europe-specific consensus-based documents born within the Wolfheze initiative and subsequent documents, a uniform set of guidelines summarizing essential standards to guide European clinicians and health care workers was developed only in 2012 (7, 8). Both International Standards for Tuberculosis Control (ISTC) and ESTC prescribe a widely accepted level of TB care, to guide all health care providers and clinicians, both public and private, in achieving optimal standards in managing individuals who have active TB, latent TB infection, or signs and symptoms compatible with the disease. The standards are designed to complement existing national or international guidelines and are consistent with the WHO definitions and recommendations (15, 17).

Our survey of TB management shows that practical attitudes currently can differ in some respects.

Regarding the diagnosis of TB, the practices are relatively consensual with the continued use of sputum examination, although the modalities may differ in number or timeframe (19). It should be noted, however, that 13.8% of participants performed only one sputum examination, whereas the guidelines always recommend performing at least two sputum smears (**Table 1**). Alternative examinations when patients were unable to provide a sputum sample vary according to the centers with equally heterogeneous guidelines: IDSA/ATS/CDC recommendations favor sputum induction compared to bronchoscopy. NICE guidelines are the only ones to propose gastric lavage, whereas 25.9% of respondents use it in clinical practice (**Table 1**) (20, 21). We observed that almost all centers use NAAT, although these tests are not yet carried out systematically for the diagnosis of TB (only 62.1% of respondents) as recommended by the guidelines (19, 22, 23). Despite recommendations to look for mutations conferring resistance to rifampicin and isoniazid, 16% of participants did not perform rapid molecular detection testing for rifampicin resistance in case of smear-positive patients (24, 25). For extrapulmonary TB, a majority of participants (86.3%) in the survey performed several rapid molecular tests as recommended by international guidelines. In contrast, the measurement of ADA was not universally used (40%), and it was mainly confined to pleural fluid. This recommendation is not consistent across all guidelines, because the ADA is used only for the ATS/ IDSA/CDC and NICE guidelines for pleural fluid, peritoneal fluid, and CSF. The monitoring of sputum smear microscopy and sputum culture is only recommended in the ERS/ECDC and WHO guidelines at least at the end of completion of intensive phase and actually performed after 2 months of treatment by most participants (82.5%). Finally, it should be noted that almost a third and a quarter of the responders, respectively, used IGRA and TST tests for diagnosis, whereas this is not recommended in most guidelines. These tests cannot effectively differentiate active and latent TB, even though a phlyctenular TST could predict rather an active TB (26).

Concerning the prevention of the risk of transmission of TB, the ERS/ECDC and NICE guidelines clearly specify the need to isolate the patient in a negative-pressure chamber, whereas 22% of the participants did not (14, 18). The isolation duration of contagious patients remains controversial, with 36% of respondents having adopted standardized isolation duration of 2–3 weeks, like the guidelines of NICE and the French Hospital Hygiene Society (14, 16); 43% prefer to wait for sputum smear conversion, as recommended by WHO and ATS/IDSA/CDC guidelines (13, 15). It should be noted that the conditions for patients discharged from health care facilities remains poorly studied, and this lack of evidence is reflected in the international recommendations from academic societies.

Regarding the treatment of TB, the initial treatment with four drugs is highly consensual between the respondents and the different recommendations; however, 14% still prescribed an initial treatment with only three drugs (respondents from different countries). The role of rapid molecular tests for resistance to isoniazid in guiding the withdrawal of ethambutol from the intensive phase treatment is yet unclear. The role of fluoroquinolones in first-line treatment, pyridoxine prophylaxis, CSF pressure measurement, and therapeutic drug monitoring should be better defined with additional studies. Similarly, monthly ophthalmologic monitoring of ethambutol patients is recommended only by the North American ATS/IDSA/CDC guidelines (13). On the other hand, the use of corticosteroids in the treatment of central nervous system TB is well established in the literature and among the various guidelines, whereas 20% of the participants in our survey did not routinely prescribe corticosteroids. Among HIV-positive patients, it is well established that the duration of TB treatment should be identical to that of HIV-negative patients. The importance of managing drug–drug interactions is also well emphasized in the different guidelines, although there is no clear recommendation on which antiretrovirals should be used in combination with rifampicin. Counseling is mostly developed in WHO guidelines, which target low-resource countries. The collaboration of the interpreter and the nurse in therapeutic education is still infrequent for the stakeholders of our study: 57 and 50%, respectively, whereas most European countries report increasing TB rates among newly arrived migrants (27, 28).

Analysis of Differences in Practice

It is difficult to analyze the variability of practices observed between the different respondents. There may be variability between countries due to different local recommendations but also a disparity of human or economic resources. The

availability of medications, funding of TB programs, laboratory practice, staff availability, and TB epidemiology can differ between countries, but this phenomenon is probably lower in high-resource European countries than on other continents. Furthermore, in our survey, 7% of respondents used only local recommendations for TB care management, whereas 78% also relied on international recommendations, which should also limit the variability between countries. It must also be emphasized that interindividual variability within the same country is possible. Although the respondents are among the TB experts for each country, their management practice cannot be fully representative of their respective countries. For instance, the practice survey conducted in France in 2013 with specialists in infectious diseases, pneumology, and internal medicine showed that different doctors often had very different habits concerning the treatment of TB or the isolation of active TB (29). Finally, the heterogeneity of practices can also be partially explained by the heterogeneity between the different national or international recommendations, as we have seen above. This lack of consistency across the different guidelines, as it is the case, for example, with regard to isolation practices, can be confusing for the clinician.

The ISTC defined the essential level of care for managing patients who have or are presumed to have TB or are at increased risk of developing the disease. In a high-resource setting, such as the EU/EEA, higher standards of care can be attained with regard to TB diagnosis, prevention, and treatment. On this basis, the ESTC was published in 2012 as standards specifically tailored to the European setting. Since the publication of the ESTC, new scientific evidence has become available, and therefore, the standards were reviewed and updated in 2017. Despite these new standards tailored to the EU setting, the harmonization of practices needs to be further improved. This is conditioned by a better standardization of national and international recommendations, a wider communication with people in charge of TB, and complementary studies to increase the level of evidence on controversial aspects of TB care. If we take the example of the joint ERS and ESCMID guidelines on the management of infections due to nontuberculous mycobacteria, which are being updated, collaboration between the various European academic societies would probably be beneficial.

Our study has several limitations. First, our sample is too small to be representative. Second, the responders were selected within the ESGMYC group, with mainly microbiologists and infectious disease specialists. Therefore, this sample does not include a lot of pulmonary physicians, although they are also very involved in TB care. Third, as mentioned above, the management practice of the responders could not be fully representative of their respective countries. Nevertheless, we think that this survey gives an interesting overview of different practices in Europe and highlights a heterogeneity in the management of TB that should be confirmed by a study with larger sample. In conclusion, WHO's international recommendations for TB management are focused on countries with high incidence. Recommendations that are more adapted to the European socioeconomic and epidemiological context have also been developed under the auspices of the ERS and the ECDC. This study shows that the management of TB is probably still heterogeneous within high-income countries, in particular for the prevention of transmission and the treatment. Concerning microbiological diagnosis, the practices seem to be better standardized, as rapid molecular testing takes an important role across most European centers. With the main objective of control and eventual elimination of TB, it seems necessary to better harmonize and disseminate the recommendations for the management of TB in Europe. European scholarly societies, and in particular ESCMID, should play a prominent role.

DATA AVAILABILITY STATEMENT

The datasets analyzed in this article are not publicly available. Requests to access the datasets should be directed to frederic.mechai@aphp.fr.

AUTHOR CONTRIBUTIONS

All authors participated in the writing and editing of the article, the analysis of the data as well as the dissemination that the investigation at the origin of this work.

FUNDING

This work was supported by ESGMYC funding (ESCMID).

ACKNOWLEDGMENTS

ESGMYC Group

Alexander Eliza, Andresen David, Anibarro Luis, Armstrong Mark, Balas Iulia, Bradbury Ross, Burke Andrew, Calcagno Andrea, Chew Rusheng, Choong Keat, Cirillo Daniella, Comelli Agnese, Davis Joshua, Del Bravo Paola, Denholm Justin, Di Carlo Paola, Edmond Tess, Esteban Jaime, Faliero Domenico, García-Gasalla Mercedes, Garcia-Goez Jofer, Giordani Maria Teresa, Goic-Barisic Ivana, Gonzalez-Galan Verónica, Gray Thimoty, Grimwade Kate, Hasan Tasnim, Huang Khai, Iulia Balas, Jenkin Grant, Khatami Ameneh, Kocagoz Tanil, Lim Lyn-li, Mahony Andrew, Maurer Florian, Mazzarelli Antonio, Motta Ilaria, Oman Kimberly, Onya Opota, Ozturk-Engin Derya, Papaventsis Dimitrios, Paues Jakob, Pham David, Pickles Robert, Puca Edmond, Rajakaruna Gawri, Riccardi Niccolo, Saralardo, Sanchez Francesca, Syre Heidi, Tafaj Silva, Thomas Schön, Tiberi Simon, Timothy Gray, Wang Dingyuan Alvin, Wejse Christian, Whitmore Timothy, Woolley Ian, Van Ingen Jakko, Veziris Nicolas, Yograjsinh Sagar, Mohamad-Ali Trad.

SUPPLEMENTARY MATERIAL

The Supplementary Material for this article can be found online at: https://www.frontiersin.org/articles/10.3389/fpubh.2020.00443/full#supplementary-material

REFERENCES

1. Furin J, Cox H, Pai M. Tuberculosis. *Lancet.* (2019) 393:1642–56. doi: 10.1016/S0140-6736(19)30308-3
2. *WHO/Global Tuberculosis Report 2018.*
3. European Centre for Disease Prevention and Control/WHO Regional Office for Europe. *Tuberculosis Surveillance and Monitoring in Europe 2018-2016 Data*. Stockholm, European Centre for Disease Prevention and Control (2018). Available online at: https://ecdc.europa.eu/sites/portal/files/documents/ecdc-tuberculosis-surveillance-monitoring-Europe-2018-19mar2018.pdf
4. World Health Organization Regional Office for Europe. *Roadmap to Implement the Tuberculosis Action Plan for the European Region 2016-2020. Towards Ending Tuberculosis and Multidrug-Resistant Tuberculosis.* Copenhagen, WHO Regional Office for Europe, 2016.
5. Van der Werf MJ, Kodmon C, Zucs P, Hollo V, Amato-Gauci AJ, Pharris A. Tuberculosis and HIV coinfection in Europe: looking at one reality from two angles. *AIDS.* (2016) 30:2845–53. doi: 10.1097/QAD.0000000000001252
6. Sotgiu G, Centis R, D'ambrosio L, De Lorenzo S, D'Arcy Richardson M, Lange C et al. Development of a standardized tool to survey MDR-/XDR-TB case management in Europe. *Eur Resp J.* (2010) 36:208–11. doi: 10.1183/09031936.00186409
7. Migliori GB, Sotgiu G, Blasi F, Zumla A, Loddenkemper R, Raviglione MC, et al. Towards the development of EU/EEA Standards for Tuberculosis Care (ESTC). *Eur Respir J.* (2011) 38:493–5. doi: 10.1183/09031936.00094211
8. Migliori GB1, Zellweger JP, Abubakar I, Ibraim E, Caminero JA, De Vries G, et al. European union standards for tuberculosis care. *Eur Respir J.* (2012) 39:807–19. doi: 10.1183/09031936.00203811
9. van der Werf MJ, Sandgren A, D'Ambrosio L, Blasi F, Migliori GB. The European Union standards for tuberculosis care: do they need an update? *Eur Respir J.* (2014) 43:933–42. doi: 10.1183/09031936.00216613
10. Lonnroth K, Migliori GB, Abubakar I, D'Ambrosio L, de Vries G, Diel R. Towards tuberculosis elimination: an action framework for low-incidence countries. *Eur Respir J.* (2015) 45:928–52. doi: 10.1183/09031936.00214014
11. Migliori GB, Sotgiu G, Rosales-Klintz S, Centis R, D'Ambrosio L, Abubakar I, et al. ERS/ECDC Statement: European Union standards for tuberculosis care, 2017 update. *Eur Respir J.* (2018) 51:1702678 doi: 10.1183/13993003.02678-2017
12. Lewinsohn DM, Leonard MK, LoBue PA, Cohn DL, Daley CL, Desmond E, et al. Official American Thoracic Society/Infectious Diseases Society of America/Centers for Disease Control and Prevention Clinical Practice Guidelines: diagnosis of tuberculosis in adults and children. *Clin Infect Dis.* (2017) 64:e1–e33. doi: 10.1093/cid/ciw694
13. Nahid P, Dorman SE, Alipanah N, Barry PM, Brozek JL, Cattamanchi A, et al. Official American Thoracic Society/Centers for Disease Control and Prevention/Infectious Diseases Society of America Clinical Practice Guidelines: treatment of drug-susceptible tuberculosis. *Clin Infect Dis.* (2016) 63:e147–e95. doi: 10.1093/cid/ciw376
14. National Institute for Health and Care Excellence. *Tuberculosis (NG33).* London, NICE (2016).
15. World Health Organization. *Guidelines for Treatment of Drug-Susceptible Tuberculosis and Patient Care, 2017 Update*. Geneva: World Health Organization (2017).
16. Recommendations Nationales. *Prévention de la Transmission Croisée par Voie Respiratoire Air ou Gouttelettes*. Vol. 20. Société Française d'Hygiène Hospitalière (SF2H) (2013).
17. World Health Organization Regional Office for Europe. *Algorithm for Laboratory Diagnosis and Treatment-Monitoring of Pulmonary Tuberculosis and Drug-Resistant Tuberculosis Using state-of-the-Art Rapid Molecular Diagnostic Technologies*. Expert opinion of the European Tuberculosis Laboratory Initiative core group members for the WHO European Region. Copenhagen, WHO Regional Office for Europe (2017).
18. Jensen PA, Lambert LA, Iademarco MF, Ridzon R. Guidelines for preventing the transmission of *Mycobacterium tuberculosis* in health-care settings, 2005. *MMWR Recomm Rep.* (2005) 54:1–141.
19. European Centre for Disease Prevention and Control. *Handbook on TB Laboratory Diagnostic Methods for the European Union.* Stockholm, ECDC (2016).
20. Datta S, Shah L, Gilman RH, Evans CA. Comparison of sputum collection methods for tuberculosis diagnosis: a systematic review and pairwise and network meta-analysis. *Lancet Glob Health.* (2017) 5:e760–e71. doi: 10.1016/S2214-109X(17)30201-2
21. Schoch OD, Rieder P, Tueller C, Alpeter E, Zellweger JP, Rieder HL. Diagnostic yield of sputum, induced sputum, and bronchoscopy after radiologic tuberculosis screening. *Am J Respir Crit Care Med.* (2007) 175:80–6. doi: 10.1164/rccm.200608-1092OC
22. Boehme CC, Nabeta P, Hillemann D, Nicol MP, Shenai S, Krapp F et al. Rapid molecular detection of tuberculosis and rifampin resistance. *N Engl J Med.* (2010) 363:1005–15. doi: 10.1056/NEJMoa0907847
23. Nathavitharana RR, Cudahy PG, Schumacher SG, Steingart KR, Pai M, Denkinger CM. Accuracy of line probe assays for the diagnosis of pulmonary and multidrug-resistant tuberculosis: a systematic review and meta-analysis. *Eur Respir J.* (2017) 49:1601075. doi: 10.1183/13993003.01075-2016
24. Pankhurst LJ, Del Ojo Elias C, Votintseva AA, Walker TM, Cole K, Davies J, et al. Rapid, comprehensive, and affordable mycobacterial diagnosis with whole-genome sequencing: a prospective study. *Lancet Respir Med.* (2016) 4:49–58. doi: 10.1016/S2213-2600(15)00466-X
25. Walker TM, Cruz ALG, Peto TE, Smith EG, Esmail H, Crook DW, et al. Tuberculosis is changing. *Lancet Infect Dis.* (2017) 17:359–61. doi: 10.1016/S1473-3099(17)30123-8
26. Cao D, Zhang Z, Yang Z, Ma S, Sun Z, Duan H, et al. The association between tuberculin test and active tuberculosis risk of college students in Beijing, China: a retrospective cohort study. *BMC Infect Dis.* (2019) 19:619. doi: 10.1186/s12879-019-4238-2
27. Munro SA, Lewin SA, Smith HJ, Engel ME, Fretheim A, Volmink J, et al. Patient adherence to tuberculosis treatment: a systematic review of qualitative research. *PLoS Med.* (2007) 4:e238. doi: 10.1371/journal.pmed.0040238
28. Volmink J, Matchaba P, Garner P. Directly observed therapy and treatment adherence. *Lancet.* (2000) 355:1345–50. doi: 10.1016/S0140-6736(00)02124-3
29. Méchaï F, Figoni J, Wyplosz B, Aoun O, Bouchaud O, Robert J. Survey of French physician practices in treatment and control of transmission of smear-positive tuberculosis. *Int J Tuberc Lung Dis.* (2015) 19:205–9. doi: 10.5588/ijtld.14.0470

Conflict of Interest: The authors declare that the research was conducted in the absence of any commercial or financial relationships that could be construed as a potential conflict of interest.

Advantages of publishing in Frontiers

OPEN ACCESS
Articles are free to read for greatest visibility and readership

FAST PUBLICATION
Around 90 days from submission to decision

HIGH QUALITY PEER-REVIEW
Rigorous, collaborative, and constructive peer-review

TRANSPARENT PEER-REVIEW
Editors and reviewers acknowledged by name on published articles

Frontiers
Avenue du Tribunal-Fédéral 34
1005 Lausanne | Switzerland

Visit us: www.frontiersin.org
Contact us: frontiersin.org/about/contact

REPRODUCIBILITY OF RESEARCH
Support open data and methods to enhance research reproducibility

DIGITAL PUBLISHING
Articles designed for optimal readership across devices

FOLLOW US
@frontiersin

IMPACT METRICS
Advanced article metrics track visibility across digital media

EXTENSIVE PROMOTION
Marketing and promotion of impactful research

LOOP RESEARCH NETWORK
Our network increases your article's readership